



MINISTERO DELL'ISTRUZIONE,  
DELL'UNIVERSITÀ E DELLA RICERCA

Department of Sciences



International Ph.D.  
Applied Biology & Environmental Safeguard



*Università degli Studi della Basilicata*

Ph.D. Program

*“Applied Biology and Environmental Safeguard”*

Scientific Disciplinary Sector

“AGR/11”

***Characterization of antimicrobial peptides deriving from insects  
and their application in the biomedical field***

*Ph.D. Coordinator*

Prof. Patrizia Falabella

*Ph.D. Candidate*

Dr. Antonio Moretta

*Tutor*

Prof. Patrizia Falabella

**CYCLE XXXIII**

*To my family,  
for their endless support.*

*“And once the storm is over,  
you won’t remember how you  
made it through, how you  
managed to survive.  
You won’t even be sure,  
whether the storm is really over.  
But one thing is certain.  
When you come out of the storm,  
you won’t be the same person who walked in.  
That’s what this storm’s all about.”*

*Haruki Murakami*

# Summary

<b>ABSTRACT</b> .....	7
<b>1. INTRODUCTION</b> .....	9
1.1. Insects Immune Response .....	10
1.2. Antimicrobial Peptides (AMPs) .....	12
1.2.1. Defensins (Cysteine-rich AMPs).....	14
1.2.2. Cecropins ( $\alpha$ -helical AMPs).....	16
1.2.3. Attacins.....	17
1.2.4. Proline-rich peptides.....	18
1.2.5. Glycine-rich peptides.....	18
1.3. Antimicrobial peptides function .....	19
1.3.1. Antibacterial peptides .....	19
1.3.2. Anticancer peptides .....	19
1.3.3. Antiviral peptides .....	20
1.3.4. Antifungal peptides.....	21
1.3.5. Antibiofilm peptides .....	21
1.4. Signaling Pathways activating AMPs genes in insects.....	23
1.5. AMPs mechanism of action.....	26
1.6. Sources of AMPs .....	29
1.6.1 Microorganisms as source of AMPs.....	30
1.6.2. Plants as source of AMPs .....	31
1.6.3. Animals as source of AMPs .....	32
1.7. Insects as natural sources of antimicrobials.....	33
1.8. <i>Hermetia illucens</i> insect .....	35
<b>2. AIM OF THE RESEARCH ACTIVITIES</b> .....	38
<b>3. MATERIALS &amp; METHODS</b> .....	40
3.1. <i>Hermetia Illucens</i> rearing and RNA isolation .....	40
3.2. RNA-Seq, de novo larvae and combined male and female adults' transcriptomes assembly and gene identification .....	40
3.3. Identification of antimicrobial peptides (AMPs) genes.....	41
3.4. Study of the nucleotide sequences and translation into amino acid frames.....	41
3.5. <i>In silico</i> prediction of the biological activity of the identified peptides and their physio-chemical properties .....	42
3.6. Molecular Modeling of the identified peptides. ....	43
3.7. Molecular cloning in TOPO – VECTOR plasmid.....	45
3.8. Double digestion and dephosphorylation of the pGEX-4T1 expression plasmid .....	46
3.9. Molecular Cloning in pGEX-4T1 expression plasmid .....	47

3.10.	Heterologous expression and purification of the recombinant products by affinity chromatography.....	48
3.11.	Hill_BB_C15867 and Hill_BB_C2519 primary structure validation through <i>in situ</i> hydrolysis and MALDI-TOF Mass Spectrometry analysis.....	49
3.12.	Determination of the Minimum Inhibitory Concentration (MIC) of the C15867 peptide.....	51
3.13.	Molecular docking analysis for the <i>in silico</i> evaluation of the C15867 peptide interaction with FtsZ protein and Lipopolysaccharide (LPS) targets. ....	51
3.14.	Evaluation of the antimicrobial activity of the C6571, C46948, C16634 and C7985 peptides.....	52
3.15.	Chemical Synthesis on Solid Phase (CSSP).....	52
3.16.	<i>Hermetia illucens</i> larvae infection, hemolymph collection and protein/peptide separation.....	55
3.17.	Evaluation of the hemolymph antibacterial activity through Microdilution Assay and Bioautography (SDS gel overlay method) experiment.....	55
3.17.	Hemolymph analysis performed at the Technische Hochschule Mittelhessen University of Applied Sciences, Gießen, Germany.....	56
<b>4.</b>	<b>RESULTS</b> .....	<b>57</b>
4.1.	Transcriptomes analysis for the identification of AMPs and functional annotation. ....	57
4.2.	Sequences study for the identification of the mature active peptide. ....	61
4.3.	Bioinformatic analyzes for the prediction of AMPs biological activity. ....	81
4.4.	<i>In silico</i> calculation of the physio-chemical properties and amino acid composition. ....	95
4.5.	Molecular Modelling for the secondary and tertiary structures and <i>in silico</i> analysis for the disulfide bonds formation.....	107
4.6.	Molecular cloning in TOPO – VECTOR plasmid.....	139
4.7.	Molecular cloning in pGEX-4T1 expression plasmid. ....	142
4.8.	Heterologous expression and purification of the C15867 and C2519 peptides.....	148
4.9.	Minimum Inhibitory Concentration (MIC) of the C15867 peptide.....	153
4.10.	Molecular Docking analysis for the <i>in silico</i> evaluation of the C15867 peptide interaction with the FtsZ protein and Lipopolysaccharide (LPS) targets. ....	153
4.11.	Antibacterial activity of C6571, C46948, C16634 and C7985 peptides. ....	159
4.12.	Chemical Synthesis on Solid Phase of the C12927, and C4669 peptides. ....	160
4.13.	Isolation of putative antimicrobial peptides from <i>Hermetia illucens</i> larvae plasma. ....	163
4.14.	Evaluation of the antibacterial activity of the plasma extracted from the infected and not infected larvae of <i>Hermetia illucens</i> .....	164
4.15.	Hemolymph analysis performed at the Technische Hochschule Mittelhessen University of Applied Sciences, Gießen, Germany.....	168
4.16.	Evaluation of the antibacterial activity of the collected fractions. ....	175
<b>5.</b>	<b>DISCUSSION</b> .....	<b>183</b>
<b>6.</b>	<b>BIBLIOGRAPHY</b> .....	<b>187</b>
<b>7.</b>	<b>APPENDIX</b> .....	<b>209</b>
<b>8.</b>	<b>PUBLICATIONS</b> .....	<b>215</b>



## ABSTRACT

Antibiotics are the current drugs used to treat pathogenic bacteria, but their prolonged use contributes to the development and spread of drug-resistant microorganisms. The antibiotic resistance issue led to the need to find new alternative molecules, which should be less prone to bacterial resistance. Antimicrobial peptides (AMPs) aroused great interest as potential next-generation antibiotics. AMPs are involved in several defence-related processes such as the binding and neutralization of endotoxins, the modulation of the immune responses to infection and the killing of pathogens. Antimicrobial peptides are small molecules with an amino acid composition ranging from 10 to 100 residues and are biosynthesized by all living organisms but it is known that the class of insects represents the largest source of these molecules. This aspect is related to insect's biodiversity and their ability to live in hostile environments rich of pathogens. Most insect AMPs are cationic molecules due to the presence of basic residues and according to their amino acid sequences and structures, they can be classified in four different groups: cysteine-rich peptides (e.g., defensins), the  $\alpha$ -helical peptides (e.g., cecropins), glycine-rich proteins (e.g., attacins) and proline-rich peptides (e.g., drosocins). Insect AMPs have demonstrated to be useful in several applications concerning the pharmaceutical as well as the agricultural fields. Moreover, insect AMPs aroused great interest for their biomedical application thanks to the increasing number of peptides that can inhibit human pathogens. For this reason, this Ph.D. project aimed to the identification of antimicrobial peptides deriving from insects, particularly from the Black Soldier Fly *Hermetia illucens* (L.) (Diptera: Stratiomyidae). Through a combination of transcriptomics and bioinformatics analysis, 57 antimicrobial peptides have been identified from *H. illucens* insect. Through an *in silico* analysis, the biological activity have been predicted and the physio-chemical properties have been calculated for all the identified peptides. Based on the bioinformatics results, the *in vitro* production of the most promising sequences has been performed through molecular cloning strategies in order to evaluate the antibacterial activity *in vitro*. Particularly, some of the identified peptides (C16571, C46948, C16634, and C7985) showed the ability to inhibit *E. coli* growth at a concentration value of 3  $\mu$ M. For the C15867 peptide, recombinantly produced and expressed, a MIC (Minimum Inhibitory Concentration) value of 18  $\mu$ M has been determined. Moreover, an *in vivo* approach was carried out for the identification of antimicrobial peptides by extracting the hemolymph from the *H. illucens* larvae, recovering then the peptides fraction from the larvae's plasma and its antibacterial activity has been evaluated against both Gram-positive and Gram-negative bacteria. The performed analysis showed that a small amount

(7.5/15  $\mu\text{L}$ ) of the peptide fraction recovered from the larvae's plasma was able to inhibit the cell growth of different bacterial strains.



# 1. INTRODUCTION

Due to the overuse of the first-line maintenance therapies, but also considering the lack of availability of new molecules [1, 2], the elaboration of an unconventional pharmacological management with new-emerging antibacterial substitutes represents nowadays a concrete perspective. Multi-drug resistant pathogens, such as ESKAPE pathogens (i.e., *Enterococcus faecium*, *Staphylococcus aureus*, *Klebsiella pneumoniae*, *Acinetobacter baumannii*, *Pseudomonas aeruginosa*, and *Enterobacter* species), have been considered practically resistant to all common antibiotics. ESKAPE pathogens have also played an important role towards the growth of nosocomial infection [3-6].

Several clinical complications such as chronic skin and soft tissues infections (SSTIs) e.g., ulcers and diabetic foot infections, together with post-surgical infections, burn wounds, could tend to a progressive worsening of the clinical outcome whether the impaired sites might involve the presence of antibiotic-resistant pathogens. Likewise, the Gram-negative bacterium *A. baumannii* has been reported as responsible of a variety of infections as well, including wound, skin, and urinary tract infections, pneumonia, and bacteremia [7].

Furthermore, infections of the lower respiratory tract due to bronchiectasis represents an increasingly widespread chronic respiratory disease, associated with not only cystic fibrosis (CF) lung disease, but also associated to chronic obstructive pulmonary disease (COPD). Generally, the stasis of the secretions of the airways leads to a worsening of the lung functions that establish consequently the development of recalcitrant bacterial infections. Hence, because of the well-known ability to resist common antimicrobials, lung infections associated with bronchiectasis lead in most cases to respiratory failure and death. The clinical course of bronchiectasis can face therefore a progression of the health-condition worsening due to the establishment of a cycle of infection and inflammation. In addition, a reduced quality of life and an increase in healthcare costs can worsen the patient compliance. Moreover, during infection management the ability of bacteria to persist to the combined actions of host immune responses and drugs can represent also a further issue [8].

Therefore, along with the irresponsible use of antibiotics, the related resistance issue towards the most common used molecules represent a global concern and the aim to find alternative drugs has been demonstrated to be a real challenge as well [9].

## 1.1. Insects Immune Response

Considering over one million of described species, insects represent the largest class of organisms, thanks to their ability to adapt to recurrent changes and their resistance to a broad spectrum of pathogens [10, 11]. This resistance skill is related to their immune system which is based exclusively on the innate immune response, which allows a general and fast response to invading organisms [12 – 15]. The first protection is represented by physical barriers such as the cuticle, the intestinal wall and the tracheas, which prevent the pathogens from enter the hemocelic cavity [15]. Insects immune response consists on a cellular and humoral immunity (Figure 1).

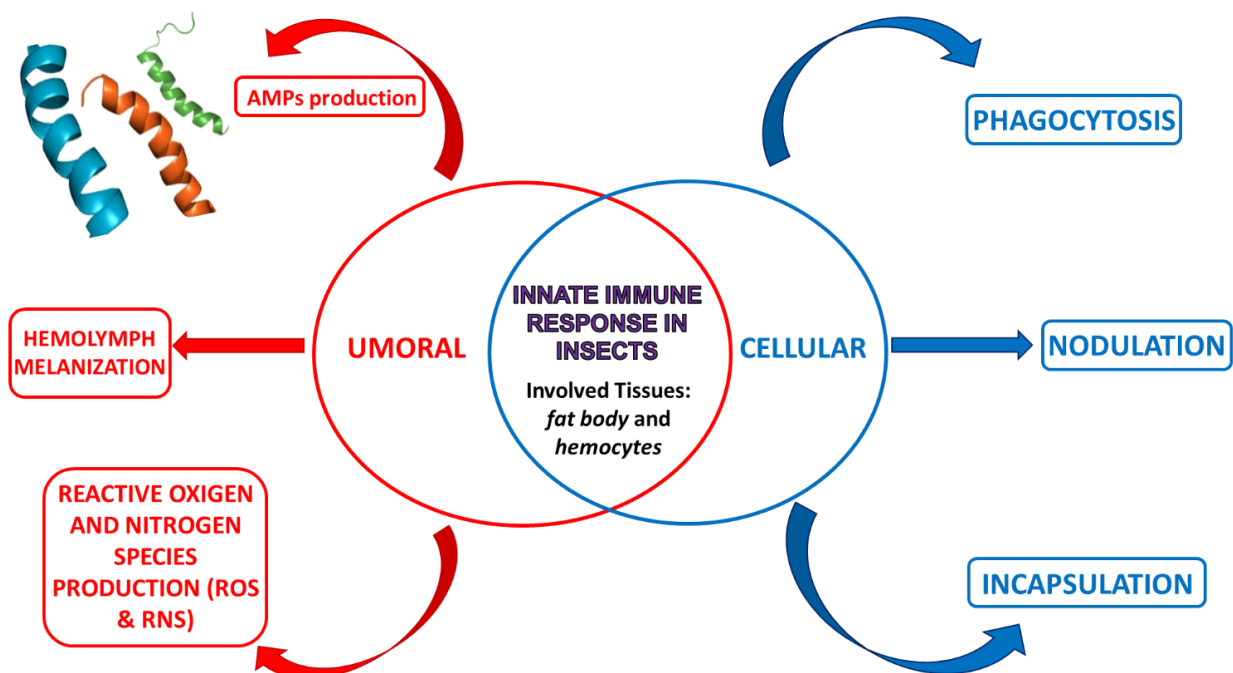


**Figure 1.** Insects Innate Immune Response can be Umoral or Cellular. *Umoral Immunity* consists on Antimicrobial Peptides production by the fat body and/or hemocytes; Hemolymph Melanization and Production of the Reactive Oxygen and Nitrogen Species. *Cellular Immunity*, instead, consists on Phagocytosis, Nodulation and Encapsulation. Phagocytosis determines the internalization of foreign agents from the hemocytes and the transport of the phagocyte material into the phagosomes where it is degraded. Nodulation occurs when bacteria are too much to be incorporated by a single hemocyte. Indeed, several hemocytes together recognize and surround foreign agents. In the encapsulation process, hemocytes create a capsule made up of several cell layers that undergoes melanization. Inside the capsule, the pathogenic organism is killed by asphyxiation and/or production of cytotoxic free radicals.

Several functionality aspects and processes are involved in the humoral immunity organization of insects. The cellular immune responses are mediated by hemocytes, which are cells that circulate in the insect hemolymph involved in cell-mediated immunity and involve several abilities such as phagocytosis, nodulation, encapsulation, and melanization. In most species of different orders, such as Lepidoptera, Diptera (except *Drosophila*), Orthoptera, Blattoidei, Coleoptera, Hymenoptera, Hemiptera, and Collemboli, the hemocytes are differentiated into granulocytes, plasmatocytes, spherulocytes, and oenocitoids [16, 17]. In Lepidoptera, granulocytes and plasmatocytes, which represent more than 50% of the circulating hemocytes, show adhesion properties. Besides, the spherulocytes, which carry cuticle components [13], and the oenocitoids, containing precursors of the activation cascade of the phenoloxidase, they are non-adhesive cells. Plasmatocytes are also involved in the production of antimicrobial peptides (AMPs) and in the release of components of the extracellular matrix [13]. Phagocytosis determines the recognition and internalization of foreign agents from the hemocytes and the transport of the phagocyte material into the phagosomes where it is completely degraded [16]. Nodulation represents a process that activates when bacteria are present in a larger number to be phagocyted by a single hemocyte. During nodulation process, several kinds of hemocytes recognize and surround microorganisms, forming thus complexes that may or may not undergo melanization [18]. In the encapsulation process, hemocytes adhere to surfaces, including larger targets, and consequently form a capsule made up of several cell layers that undergoes melanization. Inside the capsule, the pathogenic organism is killed by asphyxiation and / or production of cytotoxic-free radicals [18]. Hematopoiesis represents the mechanism by which hemocytes are replaced by new cells at the end of their life-cycle or to substitute damaged ones. Moreover, hemocytes are continuously synthesized, although this process is strongly influenced by different microenvironmental factors, such as stress, wounds, or infections [17, 19]. The activation of the insect's immune response is triggered only when the exogen agent is recognized, identifying specific and preserved molecules located on the pathogen surface, defined as pathogen-associated molecular patterns (PAMPs) [20]. PAMPs are molecular components potentially present in all microorganisms but absent in higher organisms. Examples of PAMPs comprise Gram-positive lipoteichoic acid and peptidoglycan, Gram-negative bacteria lipopolysaccharide (LPS), and fungi  $\beta$ -1,3-glucan [21]. These non-self-molecules are recognized by specific receptors (named pattern recognition proteins, PRPs), which can be both humoral and cellular. Immunolectins, peptidoglycan recognition proteins (PGRPs), and Gram-negative binding proteins (GNBPs) are circulating proteins in the hemolymph capable of recognizing specific antigens [15]. PGRP-LC and integrins, on the other hand, are receptors found on the surface of immune cells, which respectively recognize surface components of Gram-negative bacteria and the RGD motif (Arg-Gly-Asp) [11, 15]. The latter is

found in the proteins of the extracellular matrix and in some soluble proteins such as collagen, fibronectin, and laminin. The binding of integrins to the RGD motif, for example, represents the first step for the recognition of the exogen agent. Furthermore, it is involved in bacterial phagocytosis or in the encapsulation process [15]. When the receptors, both humoral and cellular, bind the molecules associated with the pathogens, specific immune responses are triggered based on the type of invader [13 – 15]. The humoral immune response includes also the production of AMPs, the enzymatic cascade that regulates the activation of hemolymph coagulation, melanization, and the production of reactive oxygen as well as nitrogen species (often indicated as ROS and RNS, respectively) [22].

## 1.2. Antimicrobial Peptides (AMPs)

In 1922, Alexander Fleming identified lysozyme from nasal mucus [23], which was considered the first human antimicrobial protein. This discovery was overshadowed when in 1928, Fleming discovered penicillin, which, together with streptomycin, in 1943, led to the beginning of the so-called *Golden Age of Antibiotics*. In the 1940s, along with Howard Florey and Ernst Chain, he brought the therapeutic use of penicillin to fruition, which allowed these scientists to be awarded the Nobel Prize for Medicine in 1945. With the advent of the *Golden Age of Antibiotics*, there was a loss of interest in the therapeutic potential of natural antimicrobial peptides (AMPs), such as lysozyme [24, 25]. However, in the 1960s, due to the increase in the number of multidrug-resistant microbial pathogens, the attention of the scientific community turned to the study of antimicrobial peptides [26 - 29].

Since the discovery of the first groups of AMPs, the magainins from the skin of the African clawed frog *Xenopus laevis* by Zasloff et al. [30 - 32] and the first antimicrobial peptides isolated from the insect *Hyalophora cecropia* by Boman [33], an ever-increasing number of AMPs have been identified and studied. Cationic AMPs are the largest group even if anionic peptides have also been identified in vertebrates, invertebrates, and plants [34].

Considering the huge number of insect species and the vast variety of ways they can interact with the environment through chemistry, it is clear that insects can have a significant potential as a source of new antimicrobial molecules [35]. Although it is possible to find smaller or larger peptides in nature, AMPs are small molecules whose amino acid composition ranges from 10 to 100 amino acids [36].

AMPs are involved in several defence-related processes such as the binding and neutralization of endotoxins, the modulation of the immune responses to infection and the killing of pathogens [37]. The first insect AMP, cecropin, was identified in 1980 from the pupae of *Hyalophora cecropia* [38, 39] and since then, a high number of new peptides deriving from insects has been identified, which show a wide range of antibacterial, antiviral, anticancer, and antifungal activity [40 - 42]. The identification of new AMPs increased thanks to the published insect genome and transcriptome datasets and to proteomics and mass spectrometry methodologies for the analysis of insect hemolymph extracted from bacteria-induced larvae [43]. In literature, AMPs usability has reached a high interest as a promising alternative to replace or support the old antimicrobial approach. 3180 AMPs have been obtained from six kingdoms, among which bacteria (i.e., 355 bacteriocins), 20 from fungi, 352 from plants, and 2356 from animal sources (<http://aps.unmc.edu/AP/>). So far, the Antimicrobial Peptide Database is currently reporting 311 out of the 3180 insects-derived AMPs (“APD3 Website”). The genomic, transcriptomic and proteomic datasets can also contribute to the growth of these numbers when referred to insects as well, with the aim to obtain a beneficial and a consistent identification of new putative AMPs [43]. Typically, antimicrobial peptides are amphiphilic molecules with both hydrophobic and hydrophilic parts, as shown in Figure 2.

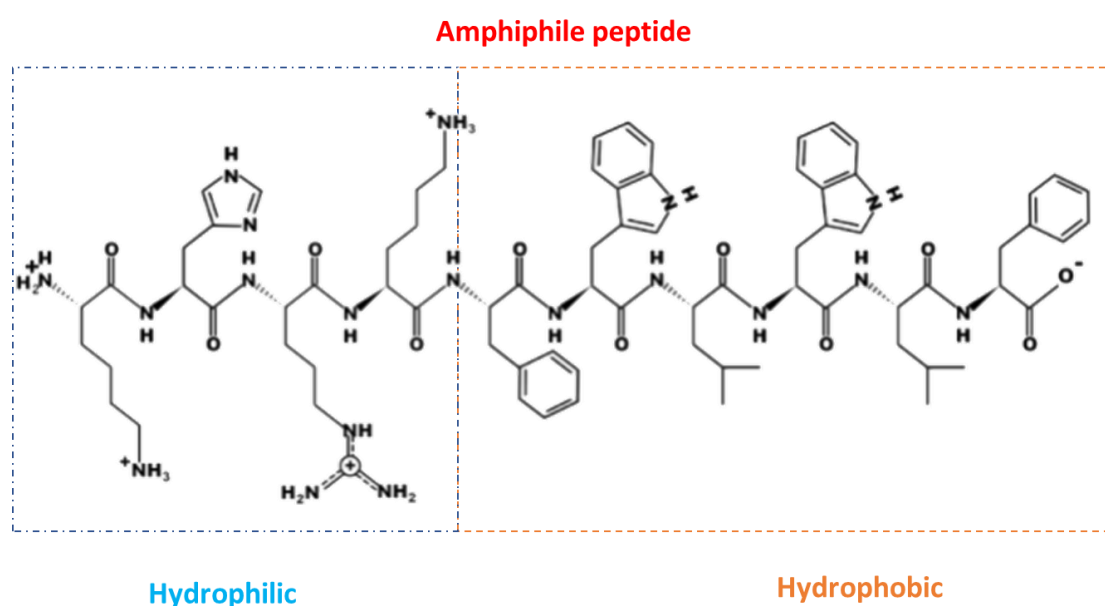


**Figure 2.** Antimicrobial peptides are amphiphile molecules containing both a hydrophilic (light blue box) region and a hydrophobic one (light yellow box).

Most insect AMPs are cationic molecules due to the presence of basic residues with biological activity against bacteria. According to their amino acid sequences and structures, AMPs can be classified in four different groups: cysteine-rich peptides (e.g., defensins), the  $\alpha$ -helical peptides (e.g., cecropins), glycine-rich proteins (e.g., attacins) and proline-rich peptides (e.g., drosocins) [44, 45].

### 1.2.1. Defensins (Cysteine-rich AMPs).

Defensins are small peptides with a cationic nature due to the presence of basic amino acids, particularly arginine [46]. They consist on 34–51 residues and contain six conserved cysteine which form three intramolecular disulfide bridges. Insect defensins have been identified in several insect orders such as *Hemiptera*, *Coleoptera*, *Diptera*, *Hymenoptera*, *Lepidoptera*, but also in the ancient order of *Odonata*, suggesting that they might derive from a common ancestor gene [47]. From a structural point of view, defensins show an N-terminal loop, an  $\alpha$ -helix, followed by an antiparallel  $\beta$ -sheet, as shown in Figure 3 for the defensin lucifensin (2LLD, PDB code) from *Lucilia sericata* (ATCDLLSGTGVKHSACAAHCLLRGNRGGYCNGRAICVCRN) [48, 49].

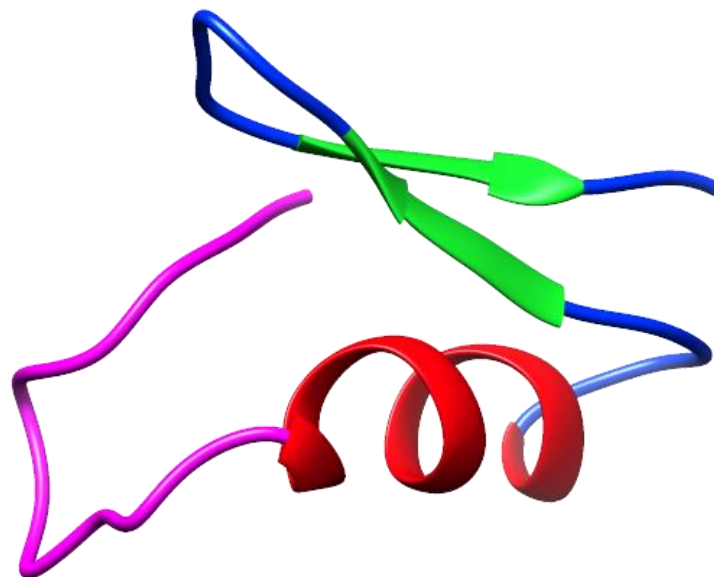


**Figure 3.** Structural representation of lucifensin, a defensin antimicrobial peptide deriving from *Lucilica sericata*, obtained from the Protein Data Bank [50]. In magenta is shown the N-terminal loop; in red the  $\alpha$ -helix region and in green the antiparallel  $\beta$ -sheet. The image has been generated with UCSF CHIMERA software [51].

Two intramolecular disulfide bonds connect the  $\beta$ -sheet and the  $\alpha$ -helix, forming a cysteine-stabilized alpha beta (CS $\alpha\beta$ ) structure [49]. In insect defensins, cysteins are linked as Cys1 – Cys4, Cys2 – Cys5 and Cys3 – Cys6 [52]. For example, Defensin A sequence from *Protophormia terraenovae* is shown in Figure 4 and Figure 5.

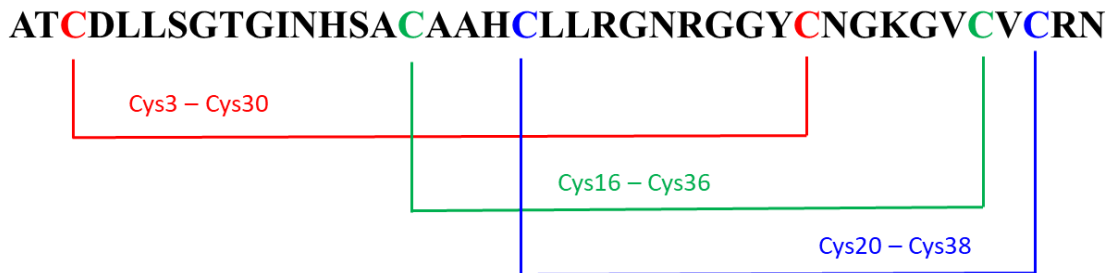


**Figure 4.** Disulfide bonds formation between cysteins in insect Defensins A from *Protophormia terraenovae*.

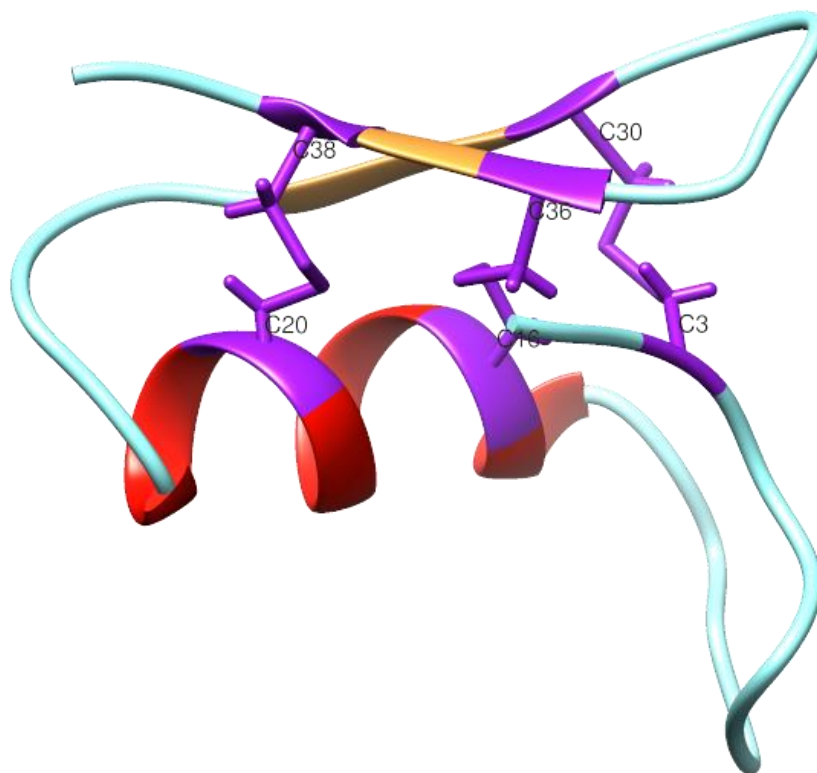


**Figure 5.** Structural representation of disulfide bonds in lucifensin. In cyan is shown the loop, in red the  $\alpha$ -helix region, in orange the antiparallel  $\beta$ -sheet while in purple the cysteine residues, and the disulfide bonds. The image has been generated using UCSF CHIMERA software [51].

Insect defensins are particularly active against Gram-positive bacteria such as *S. aureus*, *Bacillus subtilis*, *Micrococcus luteus*, and *Bacillus megaterium*. Nevertheless, some of them also have shown antimicrobial activity against Gram-negative bacteria such as *Escherichia coli* [53, 54].

### 1.2.2. Cecropins ( $\alpha$ -helical AMPs).

AMPs belonging to cecropins family represent the most abundant linear  $\alpha$ -helical AMPs in insects [39]. They were isolated for the first time from hemolymph of the lepidopteran *Hyalophora cecropia*. The antimicrobial activity of cecropins has been evaluated against several Gram-negative and Gram-positive bacteria [55]. Before maturation, insect cecropins are composed by a range between 58 to 79 amino acid. The active forms contain between 34 and 55 residues, demonstrated most active against Gram-negative bacteria, whereas, to a lesser extent, against Gram-positive bacteria [56]. It has been also demonstrated that some cecropins have exhibited (i) antifungal activity, (ii) a low toxicity against normal mammalian cells, and (iii) a weak, or absent in some cases, hemolytic effect against mammalian erythrocytes [57]. Moreover, most cecropins peptides undergo amidation of the C-terminal, which is a post-translational modification that increases the antimicrobial activity [40]. Circular dichroism analyses demonstrated that in aqueous solution cecropins assume a random coiled structure. However, upon the interaction with microbial membranes, cecropins adopt an  $\alpha$ -helical conformation [58, 59]. In Figure 6 (6a and 6b) the structures of papiliocin (2LA2, PDB code) from *Papilio xuthus*, and GK cecropin-like peptide (2MMM, PDB code) from *Aedes aegypti*, respectively are shown.

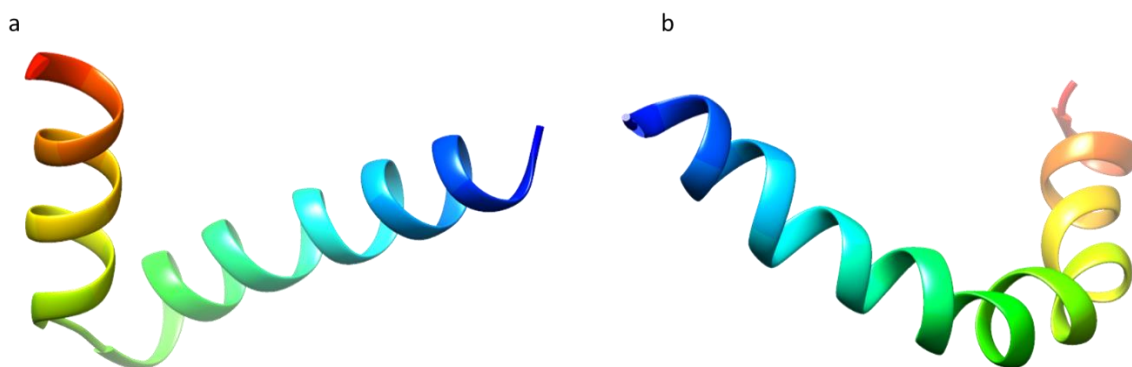


**Figure 6.** Structural representation of the (a) papiliocin deriving from *Papilio xuthus* insect and the GK cecropin-like peptide from *Aedes aegypti*, obtained from the Protein Data Bank [50]. Image generated with UCSF CHIMERA software [51].



Several insect cecropins have been studied so far from both a structural and a biological point of view, evaluating the activity *in vitro*. For example, cecropin A has a stabilized  $\alpha$ -helical structure whose mechanism of action is not very clear yet [60]. It can reduce both NADP<sup>+</sup> and glutathione levels to induce oxidative stress by forming ROS [61].

It has been demonstrated that cecropin A shows activity against the fungus *Beauveria bassiana* in silkworm larvae [62]. Instead, cecropin B is a linear cationic peptide that shows the highest antibacterial activity among the cecropins family [63]. It has been reported that cecropin B reduced the lethality of *Escherichia coli* load and plasma endotoxin and exhibited antifungal activity against *Candida albicans* [58, 64]. Some cecropins also showed anti-inflammatory activity [65, 66]. Inflammation is a protective response by an organism which takes place upon a pathogen infection, also involved in the initiation of reparative processes [67].

### 1.2.3. Attacins

Attacins are glycine-rich proteins first purified from the hemolymph of *H. cecropia* bacteria-immunized pupae. Attacins are produced as pre-pro-proteins with a signal peptide, a pro-peptide, an N-terminal attacin domain and two glycine-rich domains, called G1 and G2 domains [68].

They can be divided in two groups: The acidic attacins (i.e., attacin E, and F), and basic attacins (i.e., attacins A–D) [55]. Even though attacins are encoded by two different genes [69] and have been identified in lepidopteran and dipteran species [70, 71], they show high similarity in the amino acid sequences.

They are mostly active against Gram-negative bacteria, particularly *E. coli* and some Gram-positive bacteria, such as the attacin peptide from *Spodoptera exigua*, which is active against *E. coli* and *Pseudomonas cichorii*, and Gram-positive *Bacillus subtilis* and *Listeria monocytogenes* [72, 73].

#### 1.2.4. Proline-rich peptides

Lebocins are proline-rich peptides first isolated from the hemolymph of *Bombix mori* immunized with *E. coli* [74]. Lebocins showed antimicrobial action against Gram-positive and Gram-negative bacteria, as well as against some fungi. Lebocins, identified in *B. mori*, require the O-glycosylation for the full activity. They have also demonstrated active against *Acinetobacter sp.* and *E. coli* [74]. In insects, others proline-rich AMPs have been identified, such as drosocin, produced by *D. melanogaster*. Drosocin is an O-glycosylated 19 amino acids peptide and shows a significant sequence homology with Apidaecin IB peptide [75, 76]. Apidaecins are involved in the honeybee humoral defence against microbial invasion [76].

Moreover, a 26 residues proline-rich immune-inducible linear peptide called metchnikowin, has been identified in *D. melanogaster*, by Metchnikowin and colleagues [77]. However, this peptide has demonstrated not active against Gram-negative bacteria, whereas it has exhibited antimicrobial activity against Gram-positive bacteria and fungi. Concerning the antifungal activity, metchnikowin interacts with the fungal enzyme (1,3)-glucanosyltransferase Gel1 (FgBGT). This enzyme is involved in fungal cell wall synthesis and targets also the iron-sulfur subunit (SdhB) of succinate-coenzyme Q reductase [78].

#### 1.2.5. Glycine-rich peptides

Gloverins are glycine-rich peptides identified in the *Lepidoptera* insect order and synthesized as pre-pro-proteins [79]. They are basic molecules and, in aqueous solution, they adopt a random coil structure, assuming an  $\alpha$ -helical structure in a hydrophobic environment [80]. The first gloverin peptide has been purified from the hemolymph of *Hyalophora gloveri* pupae [80]. Furthermore, gloverin peptides are mostly active against Gram-negative bacteria, particularly *E. coli*, but some other exhibit antimicrobial activity against Gram-positive bacteria, fungi, and viruses [79, 81]. Gloverin peptide identified in *Manduca sexta*, although exhibited activity against the Gram-positive bacteria *Bacillus cereus*, *Saccharomyces cerevisiae*, and *Cryptococcus neoformans* it was, however, not active against *E. coli* [79].

Another class of glycine-rich peptides comprises dipterocins. Dipterocins A–C have been isolated from immunized larvae of *Phormia terranova*, whereas some other have also been identified in *Sarcophaga peregrina* and in *Drosophila melanogaster* [82 - 84]. Prolixicin, a 21 amino acids peptide, belongs to this peptide family, which has been isolated from *Rhodnius prolixus*. It can be produced by midgut tissues after the hemolymph bacterial infection [85].

### 1.3. Antimicrobial peptides function

Antimicrobial peptides can exert different functions such as antibacterial, anticancer, antiviral, antifungal, and antibiofilm activities, as describes in the following paragraphs.

#### 1.3.1. Antibacterial peptides

Antibacterial peptides are among the most studied and are characterized by both hydrophobic and hydrophilic domains. Most of them are cationic and this positive net charge allows these peptides to interact with the negatively charged bacterial membranes [86]. Their mechanism of action has been widely studied. AMPs can lead to bacterial cell death through both membranolytic [87–89] and non-membranolytic mechanisms, interacting with intracellular targets, such as DNA, RNA, and proteins [37, 90, 91, 92]. Both Gram-negative and Gram-positive bacteria have molecules on the outer membrane that confer a negative net charge, allowing the electrostatic interaction with cationic peptides [93]. Then, the AMPs accumulate at the surface and, once a certain concentration is reached, they assemble on the bacterial membrane [94]. A very high number of antimicrobial peptides have been found that are also active against cancer cell lines, viruses and fungi.

#### 1.3.2. Anticancer peptides

Antimicrobial peptides with anticancer activity, also called anticancer peptides (ACPs), are  $\alpha$ -helical or  $\beta$ -sheet peptides and can be divided into two groups. Peptides, such as insect cecropins and frog skin magainins, belong to the first group, characterized by peptides active against both bacteria and cancer cells but not against normal mammalian cells [95 – 97]. Peptides toxic to bacteria and both normal and cancer cells, including the bee venom melittin, insect defensins, and the human LL-37 peptide [98, 99], belong to the second group. ACPs can lead to cancer cells' death by membranolytic or non-membranolytic mechanisms according to the peptide characteristics and the peculiar target membrane features [100]. Cancer cells differ from normal mammalian cells due to their membrane net negative charge, which is conferred by anionic molecules, such as the phospholipids phosphatidylserine (PS), heparin sulfate, O-glycosylated mucins, and sialylated gangliosides. Differently, mammalian cell membranes are endowed with a zwitterionic character due to the molecules normally present on their membranes [101, 102]. In healthy cells, the phosphatidylserine

molecules are in the plasma membrane's inner-leaflet, while in cancer cells, the asymmetry between inner and outer membrane leaflets is lost, leading to the presence of PS in the outer leaflet [103, 104]. The negative net charge exposed on the cancer outer membrane makes them similar to the bacterial membranes, suggesting that AMPs and ACPs might share similar molecular principles for selectivity and activity [105]. Dermaseptin B2 and B3 have been reported to be active against the proliferation of human prostate, mammary, and lymphoma cancer cells [105]. A study conducted by Lin et al. on the cytotoxic effect of epinecidin-1 on normal and cancer cells showed that this peptide could inhibit the growth of both tumor and normal cell lines. It was also demonstrated that epinecidin-1 induces cytotoxic effects and membrane lysis, perturbing the cancer cell membrane. In addition, this peptide inhibits necrosis in HT1080 cells (highly aggressive fibrosarcoma cell line) by downregulating the necrosis-related genes [106].

### 1.3.3. Antiviral peptides

Because of the emerging resistance of viruses and the limited efficiency of commonly used drugs, antiviral peptides represent good candidates as putative therapeutic agents [107]. Antiviral agents can act at different stages, by inhibiting the activity of viral reverse transcriptase or the pre-integration complex or avoiding the transport of circular viral DNA to the nucleus. Alternatively, they can inhibit the action of viral integrase, impairing viral DNA to integrate into the cellular chromosome. In addition, antiviral compounds may inhibit the viral proteases by blocking the retroviral morphogenesis because, after transcription, the proviral DNA is translated into a polyprotein that requires the activity of viral proteases to generate the proteins needed to assemble the viral capsid [108]. It has been demonstrated that both enveloped RNA and DNA viruses can be targeted by antiviral peptides [109]. AMPs can cause membrane instability by integrating into viral envelopes, thus preventing the viruses from infecting host cells [110]. Melittin, in addition to anticancer activity, has also been reported to have inhibitory activity against enveloped viruses, such as Junin virus (JV), HIV-1, and HSV-2. Melittin was suggested to suppress HSV-1 syncytial mutant-mediated cell fusion, very likely by interfering with the activity of Na<sup>+</sup> K<sup>+</sup> ATPase, a cellular enzyme involved in the membrane fusion process [111]. Some antiviral AMPs can prevent viral particles from entering the host cells by binding specific receptors on mammalian cells. For example, some  $\alpha$ -helical cationic peptides, such as lactoferrin, can prevent HSV infections by binding to heparan sulfate molecules needed for the attachment of HSV viral particles to the host cell surface, thus blocking virus–receptor interactions [112, 113].

#### 1.3.4. Antifungal peptides

According to their mechanism of action and origin, antifungal peptides can be grouped into membrane-traversing peptides, which can lead to pore formation or act on  $\beta$ -glucan or chitin synthesis, and non-membrane-traversing peptides that interact with the cell membrane and cause cell lysis [114]. Antifungal peptides can lead to fungi death through different mechanisms of action, including inhibition of DNA, RNA, and protein synthesis; induction of apoptotic mechanisms; permeabilization of membranes; inhibition of cell wall synthesis and enzyme activity; or repression of protein folding and metabolic turnover [115, 116].

#### 1.3.5. Antibiofilm peptides

The antibiofilm activity of antimicrobial peptides has been less studied than their anti-microorganism capabilities. Moreover, the assessment of a specific ability to impair biofilm formation well apart from their antimicrobial activity is quite difficult to achieve. An AMP can be considered to be antibiofilm if the minimum biofilm inhibitory concentration (MBIC) is below the minimum inhibitory concentration (MIC), with a distinct activity compared to the direct killing antimicrobial capability. Eradication of preformed biofilms is much more difficult than inhibition [117], and the minimum biofilm eradication concentration (MBEC), i.e., the minimum concentration of an antimicrobial agent required to eliminate pre-formed biofilms, is generally larger than MBIC. In all cases, it is fundamental to being able to distinguish between dead and living cells. Recently, Raheem and Straus [118] described many biological assays and biophysical methods and techniques to define the specific antibacterial and antibiofilm functions' peptides. For all these reasons, few peptides endowed with real antibiofilm activity have been identified so far. Antibiofilm peptides were demonstrated to affect biofilm formation or degradation at different stages and with different mechanisms of action, including inhibition of biofilm formation and adhesion, downregulation and killing of pre-formed biofilm [119, 120] (Figure 7).

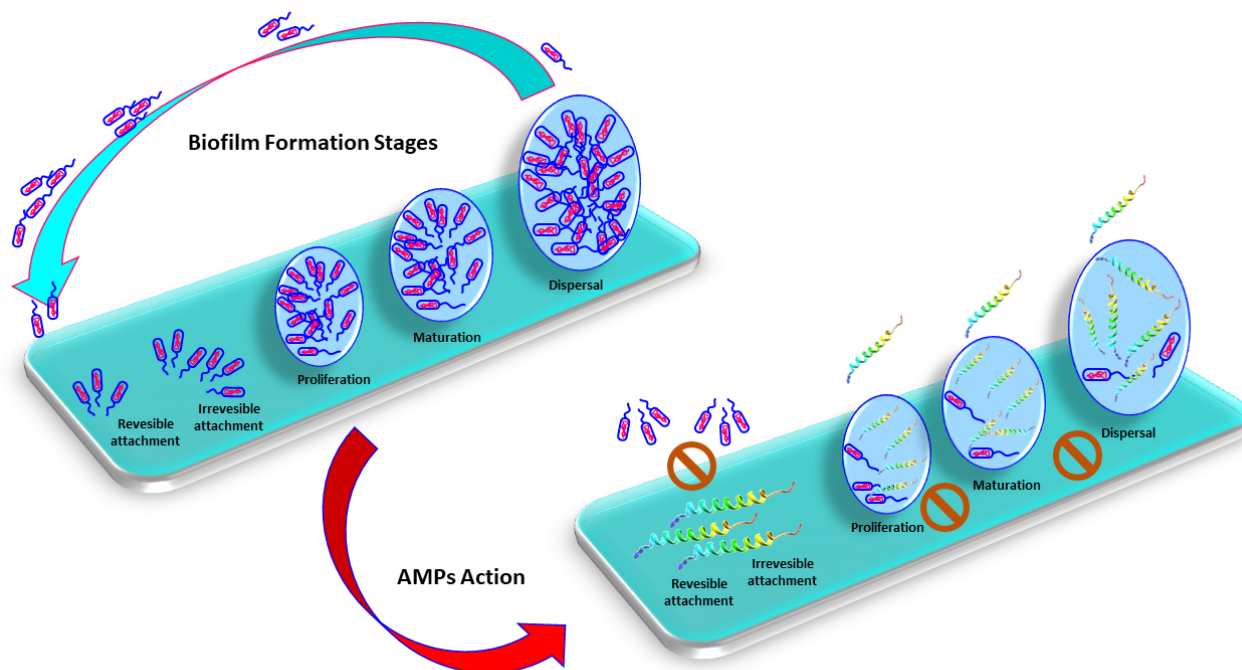


**Figure 7.** Biofilm formation consists on attachment, proliferation, mutation and detachment stages, which can be inhibited by antimicrobial peptides.

Antimicrobial peptides can also lead to the degradation of the extracellular polymeric matrix of bacterial biofilms. Hecpudin 20 can reduce the extracellular matrix mass of *Staphylococcus epidermidis* and alter its biofilm architecture by targeting the polysaccharide intercellular adhesin (PIA) [121]. Antibiofilm peptides can also target a stringent stress response in both Gram-negative and Gram-positive bacteria or downregulate genes involved in biofilm formation and the transportation of binding proteins [122]. Biofilm formation in staphylococci depends on the synthesis of the polysaccharide intracellular adhesin (PIA), which is encoded by the *icaADBC* locus. Human  $\beta$ -defensin 3 was shown to be able to reduce the expression of the *icaA*, *IcaR*, and *icaD* genes of *S. epidermidis* ATCC 35,984, leading to a reduction of biofilm formation [123]. Another peptide known as CRAMP is able to inhibit fungal biofilm formation [124], but surprisingly, it was demonstrated that AS10, a CRAMP shorter fragment, was able to inhibit biofilm growth of *Candida albicans*, *E. coli*, and *P. aeruginosa* [125]. Moreover, IDR-1018 showed antibiofilm activity against several Gram-positive and Gram-negative pathogens [126]. De la Fuente-Núñez et al. studied two synthetic peptides DJK-5 and DJK-6 based on properties associated with IDR-1018, which showed a broad spectrum of antibiofilm activity and the ability to eradicate pre-existing biofilms [127]. Mataraci and Dosler designed the CAMA peptide, a hybrid peptide (cecropin (1-7)–melittin A (2-9) amide) containing the N-terminal region of cecropin A and the N-terminal portion of melittin A.

Interestingly, this peptide was able to inhibit methicillin-resistant *Staphylococcus aureus* (MRSA) biofilm formation [128].

#### 1.4. Signaling Pathways activating AMPs genes in insects

After detection of microorganisms by Pattern-Recognition Receptors (PRRs), several signaling molecules are activated. Afterwards, signaling pathways involved in humoral immune responses follow, leading to the release of AMPs by the body fat [13]. These pathways are the Toll, the Immune Deficiency (Imd), and the JAK-STAT pathways (Figure 8), which have been well described in *D. melanogaster* [129 - 131].

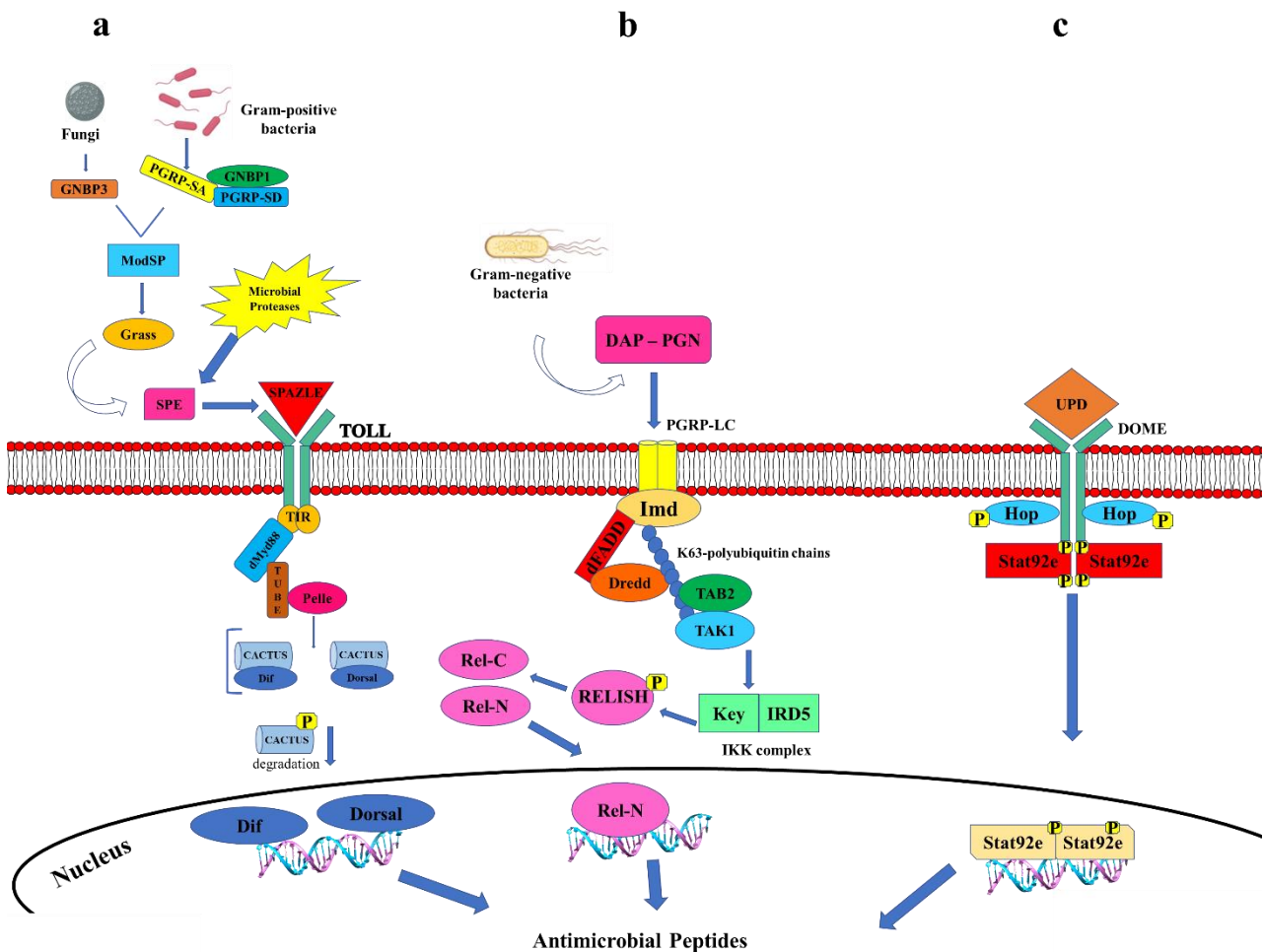


**Figure 8.** Schematic representation of Toll (a), Imd (b), and JAK-STAT (c) signaling pathways. In insects, the Toll pathway is mainly involved in fungi and Gram-positive bacteria detection. Pathogen recognition peptidoglycan recognition proteins (PGRP) activate a serine proteases cascade, involving ModSP and Grass proteins, which in turn, cleaving the inactive form of Spätzle protein, switch on the molecule. These

interactions initiate protease cascades. Spätzle activates the dimer Toll receptor, which, in turn recruits cytoplasmic proteins (dMyD88, Tube, and Pelle) involved in the activation of Cactus signaling. In normal cellular condition, Cactus protein is coupled with the Nuclear Factor kappa B (NF- $\kappa$ B) transcription factors Dorsal-related immunity factor (DIF) and Dorsal, but following the Toll pathway activation, it is phosphorylated, detached from DIF and Dorsal and degraded. Then, both DIF and Dorsal can translocate in the nucleus and induce the transcriptional regulation of specific AMP genes (A). The insect Imd signaling pathway is activated following the binding between PGRP-LC and meso-diaminopimelic acid (DAP)-type peptidoglycan of Gram-negative and some Gram-positive bacteria. The Imd protein is activated following the cleavage by the Fas-associated death domain (FADD) and the death related ced-3/Nedd2-like caspase (DREDD). The K63-polyubiquitin chains help to link this complex with TAK1 and TAB2 proteins that, in turn, act on the IKK complex, which phosphorylates the NF- $\kappa$ B-like nuclear factor Relish. Consequently, TAK1 and TAB2 proteins are activated, that in turn, act on the IKK complex, composed of Immune Response Deficient 5 (IRD5) and Kenny (Key). This activated complex cleaves Relish. In this way, the Rel DNA-binding domain is released from the C-terminal ankyrin-repeat/I $\kappa$ B-like domain, and translocates to the nucleus inducing specific AMP genes transcription (B). In insect, JAK/STAT pathway is activated when the cytokine receptor, Domeless (Dome), bind the Unpaired (Upd) cytokines which induces the JAK tyrosine kinase Hopscotch (Hop) to phosphorylate itself and the Dome cytoplasmic component. Simultaneously, the signal transducer and activator of transcription at 92E (Stat92e) bind to the phospho tyrosines on Dome, and they are phosphorylated by Hop. Phosphorylated Stat92e separates itself from the receptor, dimerize and relocate into the nucleus, where it induces the transcription of Thioester-containing protein genes (Teps) and Turandot (Tot) genes. Proteins derived from the transcription of these genes are involved in phagocytosis and melanization processes.

The Toll pathway involves signaling to nuclear factor  $\kappa$ B (NF- $\kappa$ B) [129, 132]. The cleaved extracellular cytokine-like polypeptide, called Spätzle, formed through the cleavage of proSpätzle by serine protease cascades, has demonstrated crucial to activate the transmembrane receptor Toll [133]. Consequently, it has suggested that the Toll pathway requires PRRs.

Furthermore, the Toll activation is mediated by peptidoglycan recognition protein (PGRPs), Gram-negative binding protein (GNBP) 1 in the case of Gram-positive bacterial infection, whereas Toll activation is mediated by GNBP 3 in the case of fungal infections [134, 135]. Toll signaling is activated when Spätzle binds the Toll receptor. The dimerization of the intracytoplasmic TIR domains consequently starts, leading then to the binding of the adaptor protein MyD88 [129]. This protein binds the adaptor protein Tube, which recruits the protein kinase Pelle for its autophosphorylation



and phosphorylation and degradation of an I $\kappa$ B inhibitor, Cactus. The NF- $\kappa$ B transcription factors Dorsal or Dif are then translocated into the nucleus where they activate the transcription of AMPs [136].

The Imd signaling pathway is activated when the receptors peptidoglycan recognition protein PGRP-LC binds meso-diaminopimelic acid (DAP)-type peptidoglycan [137]. Imd binds to the Fas-associated protein with death domain (FADD), while the caspase called DREDD (FADD-death-related ced-3/Nedd2-like protein) is recruited to cleave the Imd protein, which is then activated by K63-ubiquitination [138, 139]. The K63-polyubiquitin chains recruit TAK1 (transforming growth factor beta (TGF- $\beta$ )-activated kinase 1), which activates the IKK complex involved in the phosphorylation of the NF- $\kappa$ B-like nuclear factor Relish. After Relish cleavage and phosphorylation, it reaches the nucleus where it activates transcription of specific AMPs [140].

In the Janus kinase-signal transducer and activator of transcription (JAK-STAT), JAKs are activated after the binding of a cytokine to its receptors and phosphorylate specific tyrosine residues on the cytoplasmic part of the receptor and these residues then bind to STAT molecules [141]. The STAT tyrosine residues are then phosphorylated by JAKs, leading to dimers formation and to the translocation into the nucleus, where they bind the promoters of their target genes [142]. In *Drosophila melanogaster*, the JAK-STAT pathway ligands consist of three cytokine-like proteins called unpaired (upd), upd2 and upd3 [143]. The Dome receptor [144] binds to a single JAK molecule, hopscotch (hop) [145], and one STAT transcription factor, Stat92E for the induction of immune response genes [146].

However, the humoral immune response in *D. Melanogaster* is principally controlled by the Toll and Imd pathways leading to the production of AMPs [129].

## 1.5. AMPs mechanism of action

Most insect AMPs show a positive net charge which allows the interaction with the negatively charged molecules exposed on the bacterial cell surfaces i.e., LPS of Gram-negative and teichoic acids of Gram-positive bacteria, respectively. Then, the electrostatic attraction is the first interaction that occurs between peptides and cell membranes [45, 147]. Hence, AMPs can generate an unbalancing of ion flows across the membrane (i.e., depolarization) and consequently produce a permeabilization of the bacteria [148]. In contrast to bacterial cell membranes, human cell membranes are rich in zwitterionic phospholipids with a neutral net charge such as phosphatidylcholine, phosphatidylethanolamine (PE), and sphingomyelin. AMPs can self-assemble into the bacterial membrane and after reaching the onset concentrations the formation pores, cell membrane and cell death can be induced. As also demonstrated for other peptides deriving from different organisms, insect AMPs can act through a membranolytic mechanism leading to pore formation on the bacterial membranes and through a non-membranolytic one [37]. In the non-membranolytic mechanism, AMPs lead to bacterial death by interacting with intracellular targets (Figure 9), as observed, for example, for the Temporin – L peptide deriving from *Rana temporaria*. It inhibits cell division by binding the FtsZ protein that is the key protein of the divisome complex and is essential in Z-ring formation in *E. coli* [149]. Insect proline-rich peptides are also able to bind intracellular targets such as the chaperone DnaK or with the protein synthesis apparatus [150].

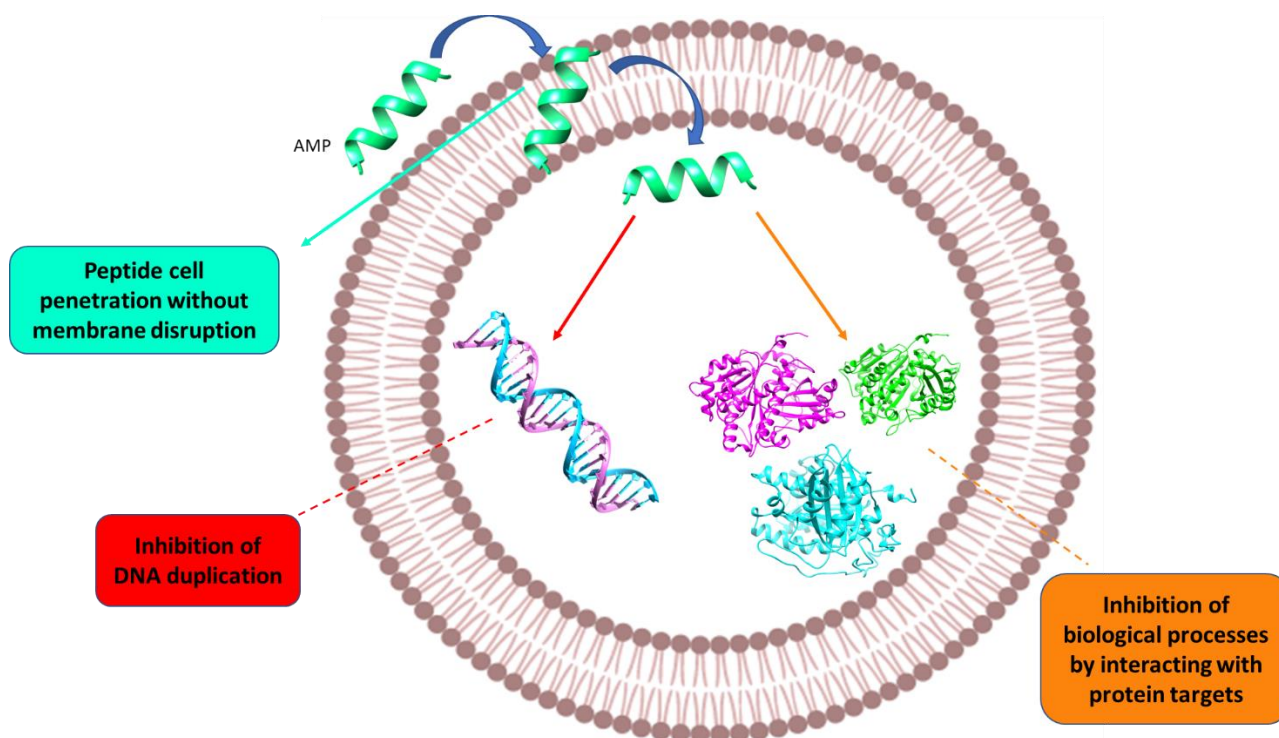


**Figure 9.** Schematic representation of AMPs non-membranolytic mechanism. In this case, AMPs can penetrate the bacterial cell, without leading to membrane disintegration, causing bacterial death by interacting with intracellular targets, including DNA and proteins involved in cellular division or protein synthesis.

Insect defensins may lead to bacterial death through the formation of channels in the bacterial cytoplasmic membrane or can interact with phospholipid to induce microheterogeneity in the lipid membrane [151, 152]. Moreover, LPS could represent a barrier for the antibacterial activity of insect defensins. Indeed, it has been demonstrated that *E. coli* strains with mutants of LPS are more sensitive to insect defensins [153].

Several studies have been performed to understand cecropins mechanism of action and to identify the functions of specific residues. Most mature cecropins have a tryptophan residue in the first or second positions, which confers antimicrobial activity to the peptide [14, 16, 147, 152]. It has been demonstrated that the Trp2 and Phe5 residues in papiliocin peptide, identified in *Papilio xuthus*, are essential for the peptide interaction with LPS in the outer membrane and then for the permeabilization into the inner membrane in Gram-negative bacteria [154].

Although cecropins do not interact with specific receptors, several mechanisms have specifically explained how pore formation can be achieved. With high peptide concentrations, they act through a membranolytic mechanism (Figure 10) known as carpet model that leads to the membrane disruption by micelles formation.

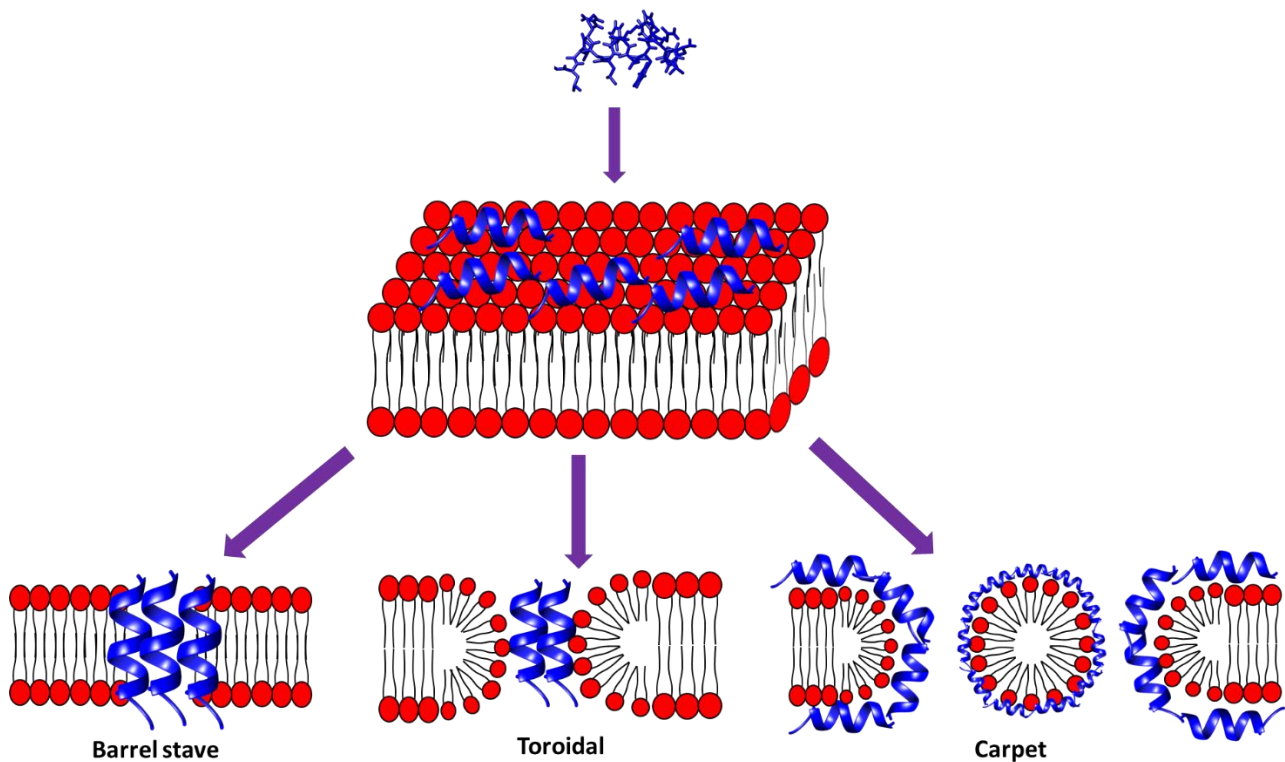


**Figure 10.** Schematic representation of AMP interaction with the bacterial membrane. Membranolytic mechanisms begin with adsorption of AMP on target cell membrane (a). In the barrel-stave model peptides permeate through the bilayer (b); in the toroidal pore mechanism, peptides interact with the head groups of the lipids, induce the bilayer curvature and perpendicularly insert into the membrane bilayer (c); in the carpet model, peptides cover all the membrane the membrane, the peptide non-polar side chains bind the membrane hydrophobic core while the polar residues with the lipid phosphates, forming micelles with the fragmented membrane (d).

In particular, the interaction via the carpet mechanism assumes that peptides cover the membrane and interact only with the lipid head groups. They associate with the bacterial membrane and then the peptide non-polar side chains fit in the membrane hydrophobic core while the polar residues interact with the lipid phosphates [155]. At low peptide concentrations, cecropins can form channels or pores into the membrane [58, 155, 156].

The toroidal pore mechanism, considered as a part of the previous mechanism, consists of a peptide insertion, perpendicularly into the bacterial membrane bilayer, a subsequent interaction with the head groups of the lipids to finally induce the bilayer curvature. The detergent-like mechanism is based on the peptide interaction related to the carpet model mechanism, leading to micelles with the fragmented membrane [157]. Instead, the barrel-stave pore formation suggests that the peptides permeate through the bilayer [158]. It has been observed that cecropins identified in *H. cecropia* form a barrel (barrel-stave model), which penetrate the bacterial membrane. Concerning peptides shorter than 22 residues

they however act through a toroidal-pore model, in which the pore is composed by both lipids and peptides [155].

Furthermore, several studies described the ability of AMPs to overpass the membrane avoiding significant permeabilization but using a specifically interaction with bacterial PE, present at higher concentration onto the bacterial membranes [148]. In eukaryotic membranes the anionic lipids (e.g., phosphatidylserine) are only located in the inner leaflet, whereas, the outer leaflet is mainly composed of lipids with no net charge. Nonetheless, it's widely accepted that AMPs can target the inhibition of several functions of the bacterial cytoplasm, including the synthesis of nucleic acids, proteins, enzymes, and cell wall. The interfering process with bacterial biosynthetic pathways allows, therefore, significant difficulty in developing resistance towards AMPs [159, 160]. Regarding attacins peptides, they can inhibit *E. coli* cells growth by inhibiting the synthesis of several bacterial porins, which are outer membrane proteins such as OmpA, OmpC and OmpF by binding to LPS without penetrating the inner membrane or cytoplasm [72].

Moreover, a well-known peptide, called melittin, is a 26 residues peptide toxin identified in bee venom and is effective against bacteria [161, 162]. It has a strong antibacterial activity against several bacteria and binds to membrane surfaces leading to pores formation and then to cell lysis [163].

On the other hand, negatively charged AMPs, as daptomycin (DAP), have received less research attention as in many cases the antimicrobial action of these peptides has demonstrated unclear. To explain the bactericidal effect against Gram-positive bacteria, several authors have reported the interaction of DAP with negatively charged sections of microbial membranes, i.e., phosphatidylglycerol, facilitated by cationic salt bridges with calcium that consequently provoke the membrane oligomerization [163].

## 1.6. Sources of AMPs

The survival of organisms in the world, where pathogens are widely distributed, solely depends on the defence mechanisms of the host. The inborn immunity of organisms involves endogenic peptides which supply a quick and viable method for safeguard against microbial attacks [164]. AMPs are universal and essential components of the defence systems of all types of life forms, varying from bacteria to plants and invertebrate and vertebrate species, including mammals [164, 165]. They are naturally produced in the body of both lower and higher organisms and their production is cell specific and may be constitutive or inducible in response to pathogenic challenges [164]. In multicellular organisms, AMPs are mostly localized to specific sites that are normally more exposed to microbes,

such as the skin and mucosa epithelia [165]. The primary role of these defence peptides is the killing of invading pathogens; however, in higher organisms they act also as modulators of the innate immune response [165]. AMPs are commonly classified according to their sources, which are represented by microorganisms, plants and animals.

#### 1.6.1 Microorganisms as source of AMPs

Bacteria and fungi are reservoirs of AMPs [166]. Among the numerous AMPs, the first isolated and characterized were those produced by bacteria [165]. AMPs from bacteria are not produced for the purpose to protect against infections, but rather as a competition strategy [165]. With their activity they kill other microbes, which compete with them for nutrients in the same niches, ensuring the survival of individual bacterial cells [165]. Bacterial AMPs, also called bacteriocins, are represented by a heterogeneous family of small ribosomally synthesized molecules with strong antimicrobial activity at specific concentrations [167]. These molecules, produced by Gram-positive and Gram-negative bacteria, are effective against many pathogenic bacteria and are extraordinary mighty compared to their eukaryotic counterparts [165, 167]. Bacteriocins were recently classified into two groups: lanthionine containing (lantibiotics) and non-lanthionine containing. Lantibiotics, which include the unusual amino acid lanthionine in their sequence, require posttranslational modifications to acquire their active forms [165]. Nisin, produced by *Lactococcus lactis*, is the main representative of the lantibiotics group and it is extensively studied being used as food preservative [167]. Nisin is the only bacteriocin legally approved as biopreservative and is used in the dairy industry to control contamination from *Listeria* strains [167]. AMPs isolated from *Pseudomonas spp* have displayed activity against several bacterial species, such as *Staphylococcus aureus*, *E. coli*, *Salmonella*, *Shigella* [168]. Mersacidin isolated by *Bacillus spp* shows bactericidal activity against Methicillin-resistant *S. aureus* (MRSA) that is equivalent to that of vancomycin [165].

Moreover, host-microbiota crosstalk is based on AMPs secretion by phagocytic cells, epithelial cells and microbiota of the human gut, skin, oral cavity; these peptides contribute to microbial and ecological balance [169]. An example of these human microbiota peptides is the thiopeptide lactocillin that is produced by the vaginal commensal *Lactobacillus gasseri* and acts against Gram-positive bacteria, including *S. aureus* and *Gardnerella vaginalis* [169].

Several filamentous fungi produce AMPs which are similar to plants and animals defensins. Examples of cysteine-rich defensin-like AMPs in ascomycetes are AFP from *Aspergillus giganteus*,

PAF from *Penicillium chrysogenum*, ANAFP from *Aspergillus niger*, AcAFP and AcAMP from *Aspergillus clavatus* [170, 171]. All these fungal peptides have antifungal activity against filamentous ascomycetes, including opportunistic animal and plant pathogens, such as *Aspergillus fumigatus*, *Fusarium sp.*, and *Botrytis sp.* [171].

#### 1.6.2. Plants as source of AMPs

Bioactive peptides from plants are essential components of their defence mechanisms, with extraordinary physiological importance, proving fast protection against bacterial and fungal infections [165, 172, 173]. Plant AMPs not only display microbicide activities but also are involved in cellular signalling [172]. Several active peptides have been extracted and isolated from roots, flowers, seeds, stems and leaves of plants and are classified on the basis of their amino acids sequence, identity and the position and number of cysteine residues involved in the disulfide bridges formation [173]. Ten families of plant AMPs have been described [173] and the best-studied groups are defensins, thionins and shakins [165, 174]. The first plant-derived AMP is purothionin, which displays activity against *Corynebacterium fascians*, *Pseudomonas solanacearum*, *Corynebacterium poinsettiae* [172]. Plants defensins are cysteine-rich AMPs, with four disulphide bridges and a globular structure [172]; they are basic peptides, composed by 45 to 54 amino acid residues, ubiquitous in the plant kingdom, displaying activities against bacteria and fungi. The PvD1 peptide is a defensin from *Phaseolus vulgaris*, which inhibits growth of yeasts, such as *Candida albicans*, *Candida tropicalis* and *Saccharomyces cerevisiae* [172]. Thionins, composed by 45 to 47 amino acids, are basic peptides found in several plant tissues, which are toxic to bacteria and phytopathogenic fungi [173]. Shakins are small peptides with 12 cysteines residues forming six disulphide bridges, useful for their biological activity [174]. Shakin-Z from *Zizipus jujuba*, composed by 31 amino acids, is more toxic for fungi than bacteria [174].

### 1.6.3. Animals as source of AMPs

Animal AMPs are produced at the sites that are constantly exposed to microbes, such as skin cells and mucosal epithelial cells [174]. Various AMPs have been isolated from invertebrates and many vertebrate species (including fish, amphibians and mammals).

In invertebrates the innate immune system is extremely efficient since they lack of adaptive immune system, and in this regard, AMPs play a key role in protection against foreign microbial attacks [165]. Invertebrates can produce a wide range of proteins and peptides which are found in phagocytes, in epithelial cells and in hemolymph (plasma and hemocytes) [165]. The  $\beta$ -hairpin-like peptidestachyplexin and polyphemusin (from horseshoe crab), melittin (from bee venom) and  $\alpha$ -helical cecropin (from fly hemolymph) are some examples of invertebrate AMPs [165].

More than 200 AMPs have been isolated in insects [175]. The number of these bioactive molecules varies between species, for example, *Hermetia illucens* and *Harmonia axyridis* produce up to 50 AMPs, while other species, such as *Acyrtosiphon pisum*, do not have these peptides [165, 176 - 178]. AMPs are produced mainly in the fat body and blood cells of insects and then are secreted into the hemolymph [164, 165].

Amphibians, especially frogs, are a rich source of antimicrobial peptides. Most of the amphibian AMPs are isolated from the frog skin. These biologically active molecules are released from cutaneous glands and excreted towards the skin surface following stimulations [179]. The prototypic amphibian antimicrobial peptide and the most famous AMP from frogs is the  $\alpha$ -helical magainin [165, 166], which is active against yeasts, fungi, bacteria and viruses [188]. Esculentins, nigrocin, brevinins, temporins are some of the best characterized peptides produced by frogs of the genus *Rana* [179]. The basic esculentin-1 peptide, composed by 46 amino acid residues and a disulphide bridge, exhibits strong activity against several human pathogens, such as *C. albicans*, *Pseudomonas aeruginosa*, *E. coli* and *S. aureus* [179]. Amphibians can protect themselves from ingested pathogens since AMPs are produced also in the mucosa of the stomach. The Asian toad peptide buforin and buforin II are the best characterized examples in this regard [166].

Mammalian AMPs have been identified in humans, cattle, sheep and other vertebrates [164]. Some AMPs from mammals have a second major function inducing chemoattraction and activation of host cells to engage in innate host defence [180]. AMPs can be stored in phagocytes and epithelial cells and they can be released extracellularly by degranulation in response to different stimuli, becoming available at the site of infection [180]. For example, cathelicidins are stored within granules



of circulating immune cells as inactive propeptides [165]. Cathelicidins and defensins are the main AMPs found in mammals. Cathelicidin family comprises heterogeneous peptides which share the N-terminal pro-region but show a variable antibacterial peptide in the C-terminal region, displaying different structures, with  $\beta$ -hairpin,  $\alpha$ -helical, arginine and proline-rich peptides represented [165]. This structural diversity reflects cathelicidin different functions and their diverse spectrum of antimicrobial and immunomodulatory activities [165]. These peptides have been found in several mammalian species, such as humans, horses, rabbits, sheep and mice. The  $\alpha$ -helical BMAP-28 is a bovine AMP of the cathelicidin family which is able to permeabilize the membranes of several bacteria and fungi at a moderate concentration in vitro [165]. Only one cathelicidin, the hCAP18, is produced in humans, which has been isolated from specific granules of neutrophil granulocytes. A second group of mammalian AMPs is the defensins, which require proteolytic processing to acquire their active form [165]. More than 50 defensins have been identified in mammalian species; some of them are stored in granules of macrophages, neutrophils and Paneth cells, while others are produced by mucosal epithelial cells and keratinocytes [180]. The expression of some defensins is constitutive, such as for human  $\beta$ -defensin-1, or inducible, such as for hBD2, whose expression is induced by exposure to bacteria or microbial components, as LPS [165].

#### 1.7. Insects as natural sources of antimicrobials

Considering over one million described species, insects represent the largest class of organisms, due to their ability to adapt to recurrent changes and their resistance to a broad spectrum of pathogens [181, 182]. This resistance skill is related to their immune system, based exclusively on the innate immune response, which allows a broad and fast response to invading organisms [183 - 186]. With the aim to prevent the entrance of pathogens within the hemocoel cavity, the first protection is represented by physical barriers such as the cuticle, the intestinal wall, and the tracheas (Figure 11) [186, 187].

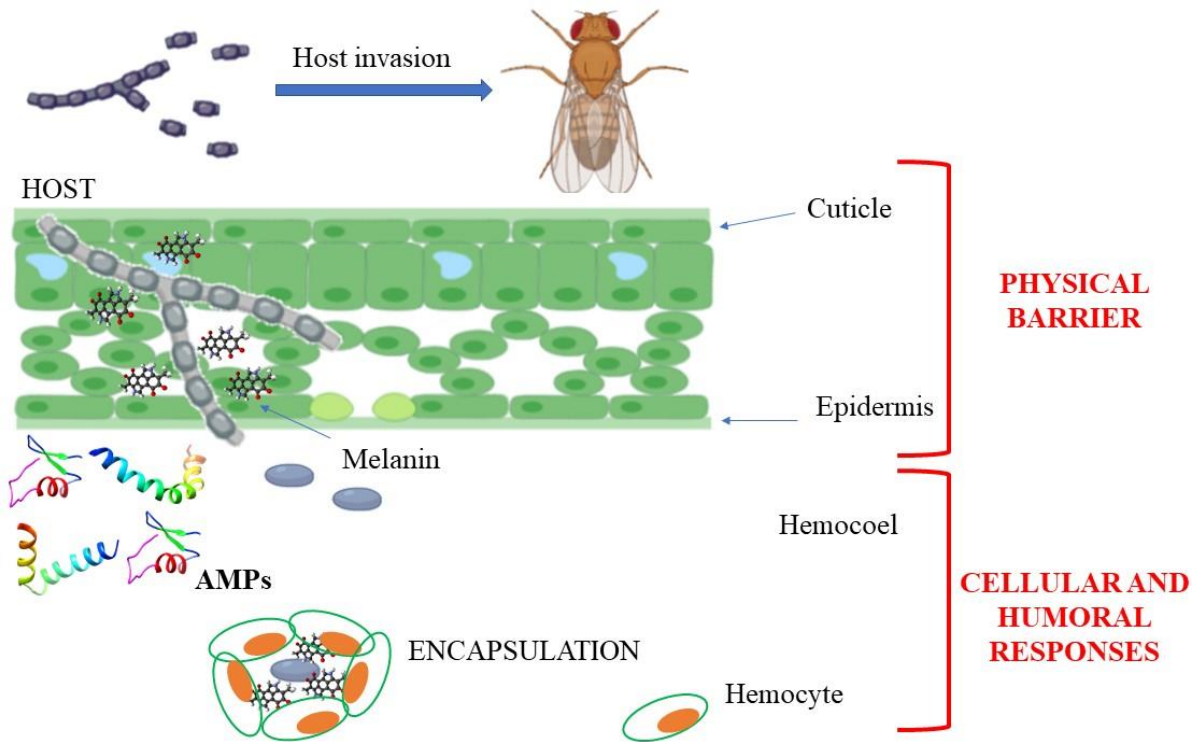


**Figure 11.** Schematic representation of insect immunity system. The first protections against the host invasion are physical barriers, including cuticle and epidermis. When pathogens succeed in overcoming these barriers, cellular and humoral immune responses are triggered, involving melanization, AMP production, and/or reaction mediated by hemocytes. Adapted from Lu and St. Leger, 2016.

In recent years, an increasing number of insect AMPs have been proving useful in several applications concerning the pharmaceutical as well as the agricultural fields. Moreover, insect AMPs aroused great interest for their biomedical application thanks to the growing number of identified peptides that can inhibit human pathogens. AMPs susceptible pathogen bacteria include multidrug-resistant *E. coli*, *K. pneumoniae*, *Bacillus coagulans*, *Citrobacter freundii*, *Francisella tularensis*, *Streptococcus sanguinis*, and *S. aureus* [188 - 191]. Besides, some insect AMPs can also inhibit virus replication such as the two alloferons from the blowfly *Calliphora vicina*. These compounds have been demonstrated to be active against both human influenza viruses A and B [192]. Furthermore, melittin, peptide derivative from *Apis mellifera*, shows antiviral activity against herpes simplex virus 1 (HSV-1) [193]. Several fungi are also susceptible to insect AMPs including *Pichia pastoris*, *Aspergillus fumigatus*, *Cryptococcus neoformans*, *Botrytis cinerea*, *Fusarium spp.*, *Neurospora crassa* and *Trichoderma viridae* [194 - 196]. Given the increasing bacterial resistance to antibiotics, there is a great interest in verifying AMPs suitability for the treatment of recalcitrant bacterial infections and killing of resistant bacteria. Indeed, several reports have highlighted that insect-derived AMPs can

represent good candidates as alternatives to conventional antibiotics [197-199]. However, the treatments to inhibit pathogenic infections by using cecropins, positively charged AMPs originally isolated from insects, for example, have suffered from some limitations. Indeed, they represent a target of human elastase produced by neutrophils, which are recruited during infections, or can be subjected to protease degradation [200, 201].

Several techniques have been exploited so far such as chemical synthesis and recombinant DNA technologies for the production in heterologous cell systems. However, the chemical synthesis seems to be the best way to produce low molecular peptides, allowing some molecular modifications, such as C-terminus amidation, into the peptide sequences or to substitute natural amino acids with the D-enantiomers [202] to make them more resistant to degradation.

Insect AMPs represent a highly promising alternative to overcome medical problems associated with antibiotic resistance. Indeed, several studies have been performed using insect cecropins in the functionalization of biomaterials used in biomedicine, such as hydrogels and polyurethane surfaces [203, 204]. Moreover, cecropin expression in transgenic plants can confer resistance to bacterial and fungal pathogens [205, 206]. Transgenic expression of an insect cecropin (sarcotoxin-IA) and defensin (*Galleria mellonella* named gallerimycin) in tobacco also confers resistance to fungi [207]. As mentioned above several strategies have been developed to overcome AMPs proteolytic degradation issue, such as the substitution of specific residues [208] with the aim to inhibit proteolytic degradation or the substitution of the amino acids L-enantiomers with D-residues [209]. Another strategy to limit the enzymatic degradation is the use of nanotechnology strategies, exploiting nanoparticles to develop new formulations for AMPs delivery [210].

### 1.8. *Hermetia illucens* insect

The insect *Hermetia illucens* (L.) (Diptera: Stratiomyidae), also known as Black Soldier Fly (BSF), is a non-pest insect distributed throughout warm temperate regions and the tropics (Figure 12). The family Stratiomyidae contains 260 known species. In the southeastern United States is abundant during late spring and early fall and has three generation per year in Georgia [211]. *H. illucens* has several sexually dimorphic traits such as features on the head, body size, abdominal spots and the shape of their abdominal terminalia to differentiate sex. Females have more whitish hairs than males on their face and only four black frontal tubercles [212].

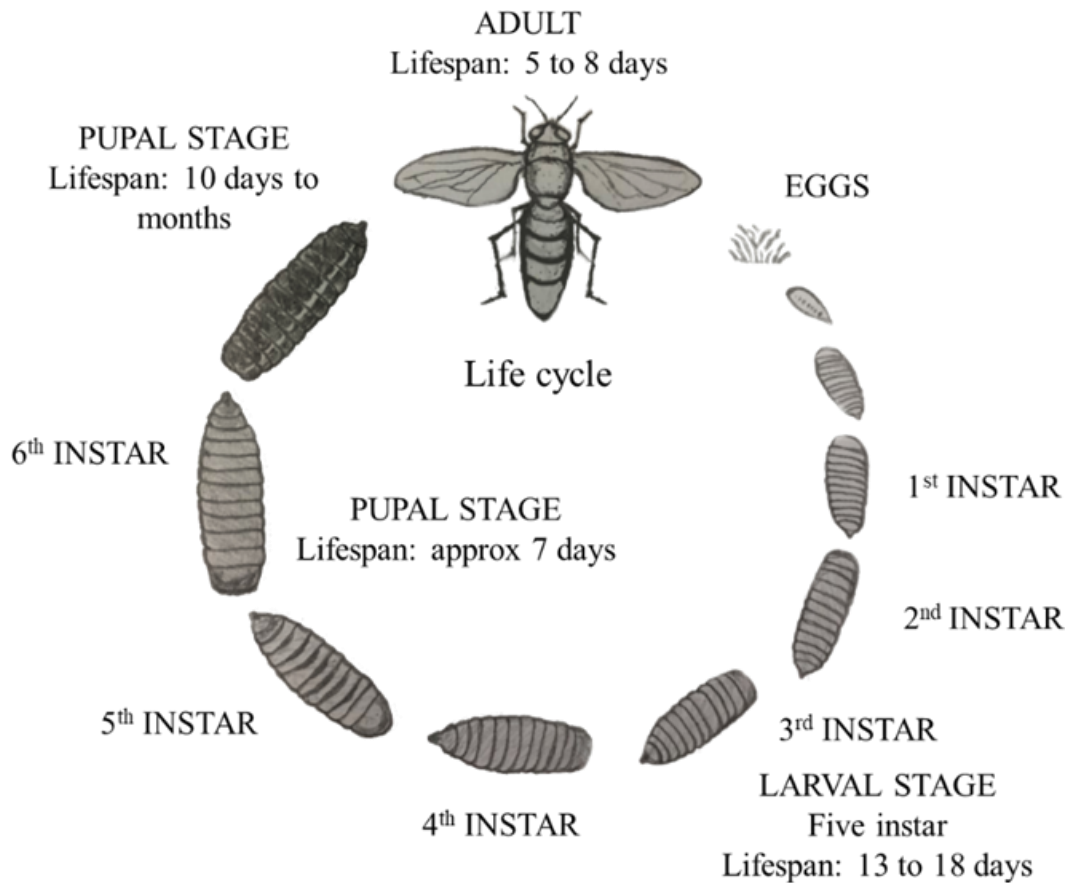


**Figure 12.** *Hermetia illucens* (L.) (Diptera: Stratiomyidae) life cycle.

As adults, the average wing length of males is 14.24 mm while females average 14.67 mm. Black soldier fly adults can reach 6 mm in width and 27 mm in length [213]. The larval stages are dull, whitish with a small, projecting head containing chewing mouthparts. Larvae pass through six instars and require approximately 14 days to complete development [212]. *H. illucens* adults are black or blue in color, their length ranges from 15 to 20 mm and live for about 5-8 days [214]. The antennae are elongated with three segments and the end of each leg is white [212, 215]. The only BSF larvae activity is eating; they feed decaying organic material and, after they are ready to pupate, move to a dry and hidden area to go through transformations [216]. BSF, unlike other Diptera such as *Musca domestica* (L.) (Diptera: Muscidae), *Calliphora vomitoria* (L.) (Diptera: Calliphoridae) or *Chrysomya spp.* (Robineau-Desvoidy) (Diptera: Calliphoridae), is non-pest fly, because even if larvae fed on decomposing organic matter, adult fly does not take up any of this food: they can survive with reserves collected during larval stages [217]. Males try to find spots in the lekking area when it is time to mate, and females do not mate with males that have no territory on which to mate [216]. *H. illucens* is not extremely competitive, in fact if another male comes in the area, the two will fight only if a female is coming and the winner will take the territory [216]. After mating, females lay their eggs on cracks

and crevices [217]. Light affects mating because direct sunlight fosters mating, in fact *H. illucens* does not mate on rainy or snowy days because the light level is low [218]. After larva stage, they will become a prepupae, which is the last larval stage before pupating. As a prepupa, they turn black from releasing melanin that increases skin durability [216]. At all stages, the black soldier fly can live in a range of temperatures between 27-30 °C. After oviposition, the eggs take about 3-4 days at 27 °C to hatch, the larval stage takes two weeks, and the pupal stage takes two weeks, but this time can increase to four months in cases of limited resources [219]. The larval stages of the black soldier fly are able to compete with other infesting flies (such as *Musca domestica*) by massively feeding on the food substrate, thus subtracting resources [219]. The main predators of *H. illucens* as both larvae and adults are Diptera including Empididae, Ephydriidae, Tendipedidae and Dolichopodidae; Hymenoptera are parasitoids of *H. illucens* eggs, larvae and pupae. Non-insect predators include spiders and leeches which only eat larvae [220]. In addition, frogs are also predators of adult males because males go near water during mating season [220]. There is a mutualistic relationship between some species of fungi and *H. illucens* which put their eggs on dead fungi, giving them a food source. When the eggs grow into larva, they eat the dead fungi and other plants in the area. When the adults die, they make the soil more nutritious for fungi [221].

## 2. AIM OF THE RESEARCH ACTIVITIES

The Ph.D. project aimed to the identification of antimicrobial peptides from insects, especially the Black Soldier Fly (BSF) *Hermetia illucens*, through a transcriptomic and bioinformatic combination approach, their production and characterization from a functional point of view. Particularly, the identified genes encoding for putative antimicrobial peptides in both larvae and adults *H. illucens* transcriptomes, were translated into the amino acid sequences and bioinformatically analysed in order to predict their antibacterial, anticancer, antiviral, and antifungal activity. Moreover, physio-chemical properties, such as molecular weight, total net charge, hydrophobic ratio, and Boman index were *in silico* calculated and all the identified peptides were computationally modelled in order to predict their secondary and tertiary structure. The most promising sequences were selected for the recombinant production through the molecular cloning strategy, for the higher molecular weight AMPs, while the chemical synthesis on solid phase has been exploited for the lower molecular weight peptides. The produced AMPs were functionally characterized by evaluating their antibacterial activity against different bacterial strains. Furthermore, a more *in vivo* approach was applied with the aim to extract putative antimicrobial peptides directly from *H. illucens* larvae and evaluating their antibacterial activity.

*FROM THE IN SILICO  
IDENTIFICATION TO  
THE IN VITRO  
PRODUCTION*

### 3. MATERIALS & METHODS

#### 3.1. *Hermetia Illucens* rearing and RNA isolation

*Hermetia illucens* larvae were reared on different diets in order to minimize the possible effect of a specific substrate on the peptides' expression, according to the protocol adopted by Vogel et al., 2018 [222]. The adults were reared in an environmental chamber under controlled conditions: temperature  $27 \pm 1.0$  °C, humidity  $70\% \pm 5\%$ , and a photoperiod of 12:12 h [L:D]. The total RNA was extracted from larvae and adults' total body, using TRI Reagent following the manufacturer's instructions (Sigma, St. Louis, Missouri, USA). A DNase (Turbo DNase, Ambion Austin, Texas, USA) treatment was carried out to eliminate any contaminating DNA. After the DNase enzyme removal, the RNA was further purified using the RNeasy MinElute Clean up Kit (Qiagen, Venlo, Netherlands) following the manufacturer's protocol, and eluted in 20  $\mu$ L of RNA Storage Solution (Ambion Austin, Texas, USA). The RNA integrity was verified on an Agilent 2100 Bioanalyzer using the RNA Nano chips (Agilent Technologies, Palo Alto, CA) and the RNA quantity was determined by a Nanodrop ND1000 spectrophotometer.

#### 3.2. RNA-Seq, de novo larvae and combined male and female adults' transcriptomes assembly and gene identification

The transcriptome sequencing of all RNA samples was performed with a poly(A)+ enriched mRNA fragmented to an average of 150 nucleotides. The sequencing was carried out by the Max Planck Genome Center (<http://mpgc.mpipz.mpg.de/home/>) using standard TruSeq procedures on an Illumina HiSeq2500 sequencer. The de novo transcriptomes' assembly was carried out using a CLC Genomics Workbench v7.1 (<http://www.clcbio.com>) which is designed to assemble large transcriptomes using sequences from short-read sequencing platforms. All obtained sequences (contigs) were used as queries for a BLASTX search [223 - 229] in the 'National Center for Biotechnology Information' (NCBI) non-redundant (nr) database, considering all hits with an E-value cut-off of  $10^{-5}$ . The transcriptomes were annotated using BLAST, Gene Ontology, and InterProScan searches using Blast2GO PRO v2.6.1 ([www.blast2go.de](http://www.blast2go.de)) [230]. To optimize the annotation of the obtained data, GO slim was used, a subset of GO terms that provides a higher level of annotations and allows a more global view of the result. Candidate AMP genes were identified through an established reference set of insect-derived AMPs and lysozymes, and additional filtering steps to avoid interpreting incomplete genes or allelic variants as further AMP genes [220].



### 3.3. Identification of antimicrobial peptides (AMPs) genes.

The Basic Local Alignment Search Tool Protein (tblastn) program was performed, with available sequences of AMPs from different insect species as “query” to identify candidate unigenes encoding putative AMPs in *Hermetia illucens*. All candidate peptides were 68, manually checked with the Blastx software from the National Center for Biotechnology Information (NCBI). The abundance in the expression level of each "unique" nucleotide sequences (contigs) was calculated on the basis of the reads per kilobase per million mapped reads method (RPKM) [231], following the formula:

$$\text{RPKM (A)} = (10,00,000 \times C \times 1000) / (N \times L)$$

where RPKM (A) is the abundance of gene A, C is the number of reads that uniquely align to gene A, N is the total number of reads that uniquely align to all genes and L is the number of bases in the gene A. In calculating the abundance of gene expression, the RPKM method is able to remove the influence of different gene lengths and sequencing discrepancy.

### 3.4. Study of the nucleotide sequences and translation into amino acid frames

The nucleotide sequences of the identified AMPs have been analyzed through the Prop 1.0 Server [232] in order to identify the signal peptide and the eventually present pro-peptide. Through the Translate tool – ExPASy [233], each sequence was then translated into the 6 FRAMES amino acid sequence, finding the start methionine (ATG codon) and the STOP codon as well. In this way, has been also possible to determine the sequences completeness at both 3' and 5' ends. The Translate tool – ExPASy gives the results high lining in red all the putative amino acid sequences. To choose the right one, for each peptide, it was chosen the longer sequence with a stop codon before the start methionine and a stop codon at the end of the sequence, in order to be sure that the chosen sequence is complete at both N and C terminal. These analyses allowed the final identification of the mature active peptides.

### 3.5. *In silico* prediction of the biological activity of the identified peptides and their physio-chemical properties.

Through a bioinformatic approach, all the identified putative antimicrobial peptides were analyzed in order to predict their antimicrobial, anticancer, antiviral and antifungal activity. Four Machine-Learning Algorithms, available on the CAMP (Collection of Antimicrobial Peptides) database [234, 235], (i) Support Vector Machine (SVM), (ii) Discriminant Analysis (DA), (iii) Artificial Neural Network (ANN) and (iiii) Random Forest (RF), were used in order to predict their antimicrobial activity. The results were returned in the form of a numerical score, except the ANN that indicates its prediction results as AMP (Antimicrobial) or NAMP (Not-Antimicrobial). All sequences that show a positive result with all four statistical methods, are considered as antimicrobial. The iACP tool [236 - 240] was used to predict the anticancer activity of the same sequences, providing the results in a numerical form. The prediction of the antiviral activity was performed *in silico* with the online server AVPpred [241]. It exploits four different models: (i) the AVP motif, which returns the result as YES or NO; (ii) the Alignment model, which gives the result in the form AVP or Not-AVP; (iii) the Composition model and the (iiii) the Physico-chemical model, which return their results in a numerical form (percentage). The overall result is expressed with a YES, if the peptide results have a putative antiviral activity, and with a NO, if otherwise. The Antifp server was used to predict the antifungal activity, and provides the result as a numerical score [242]. For this analysis, a threshold of 0.5 was used. The corresponding chemo-physical properties of the identified peptides, such as peptide length, molecular weight, total hydrophobic ratio, total net charge, isoelectric point, and the Boman Index, were determined by the Antimicrobial Peptide Database Calculator and Predictor (APD3) [243 - 245] and the Compute pI/Mw tool – ExPASy [246, 247].

### 3.6. Molecular Modeling of the identified peptides.

The secondary and tertiary structures were predicted through the I-TASSER server [248 - 250]. The server first tries to retrieve template proteins of similar folds from the PDB library by LOMETS [251, 252], a locally installed meta-threading approach. Then, in the second step, the continuous fragments excised from the PDB templates are reassembled into full-length models by replica-exchange Monte Carlo simulations with the threading unaligned regions (mainly loops) built by *ab initio* modeling. In cases where no appropriate template is identified by LOMETS tool, I-TASSER will build the whole structures by *ab initio* modeling. The low free-energy states are identified by SPICKER [253] tool through clustering the simulation decoys. In Figure 13 a schematic representation of the I-TASSER protocol is shown.

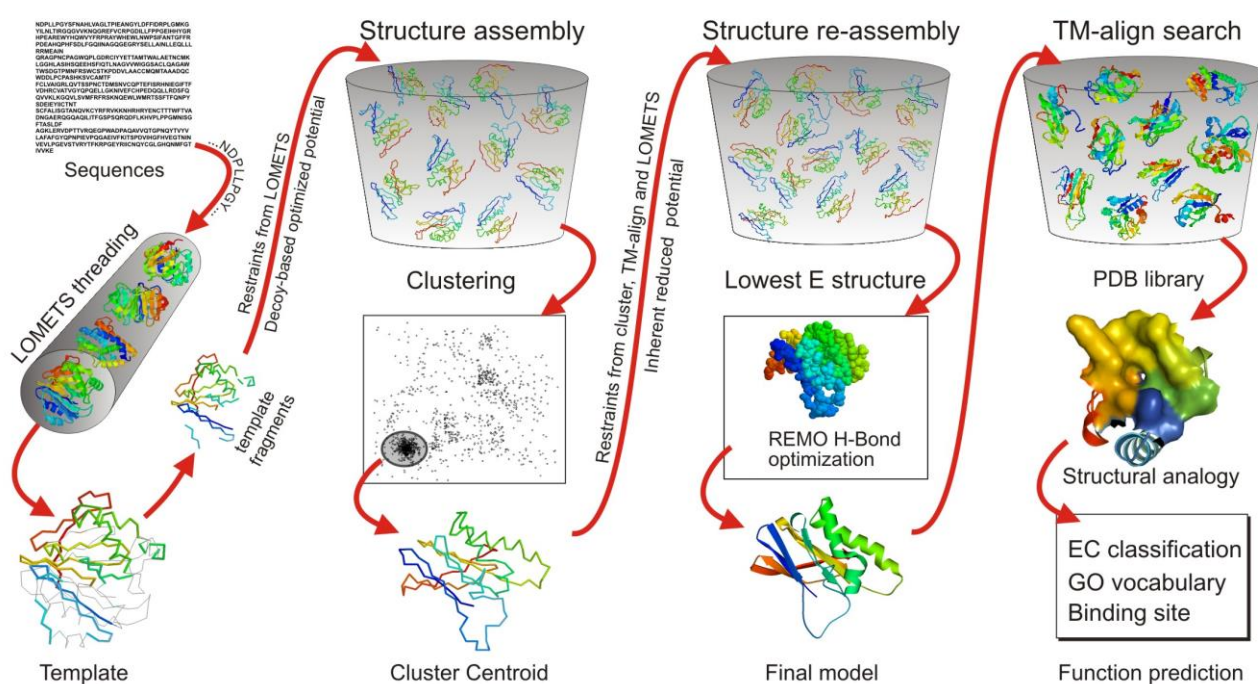


**Figure 13.** I-TASSER protocol for protein structure and function prediction. Figure adapted from Roy et al., 2011 [248].

In the third step, the fragment assembly simulation is performed again starting from the SPICKER cluster centroids, where the spatial restrains collected from both the LOMETS templates and the PDB structures by TM-align are used to guide the simulations. The purpose of the second iteration is to remove the steric clash as well as to refine the global topology of the cluster centroids. The decoys generated in the second simulations are then clustered and the lowest energy structures are selected.

The final full-atomic models are obtained by REMO which builds the atomic details from the selected I-TASSER decoys through the optimization of the hydrogen-bonding network (see Figure 13).

For each target, I-TASSER generates an ensemble of structural conformations, called decoys. To select the final models, I-TASSER uses the SPICKER program to cluster all the decoys based on the pair-wise structure similarity, and reports up to five models which corresponds to the five largest structure clusters. The confidence of each model is quantitatively measured by C-score that is calculated based on the significance of threading template alignments and the convergence parameters of the structure assembly simulations. C-score is typically in the range from -5 to +2, where a C-score of higher value signifies a model with a high confidence and vice-versa. TM-score and RMSD are estimated based on C-score and protein length following the correlation observed between these qualities. Since the top 5 models are ranked by the cluster size, it is possible that the lower-rank models have a higher C-score in rare cases. Although the first model has a better quality in most cases, it is also possible that the lower-rank models have a better quality than the higher-rank models as seen in our benchmark tests. If the I-TASSER simulations converge, it is possible to have less than 5 clusters generated. This is usually an indication that the models have a good quality because of the converged simulations.

The output of the I-TASSER server include:

- Up to five full-length atomic models (ranked based on cluster density)
- Estimated accuracy of the predicted models (including a confidence score of all models, and predicted TM-score and RMSD for the first model)
- GIF images of the predicted models
- Predicted secondary structures

Then, once obtained the peptides models in the .pdb format, they have been visualized through the molecular graphics software UCSF CHIMERA [51].

Moreover, in order to verify the correct formation of disulfide bridges for defensins and other cysteine-containing peptides, according to the scheme Cys1 - Cys4, Cys2 - Cys5 and Cys3 - Cys6, typical for insect's cysteine-rich peptides, the sequences were analyzed using the DISULFIND server [254 - 257].

### 3.7. Molecular cloning in TOPO – VECTOR plasmid

To generate Hill\_BB\_C15867, Hill\_BB\_C13792, Hill\_BB\_C10649 and Hill\_BB\_C2519 gene inserts starting from 1  $\mu$ L of template cDNA in a final volume of 50  $\mu$ L with sterile water, was carried out a reaction containing: 5  $\mu$ L Buffer #1 for KOD DNA Polymerase (10X); 5  $\mu$ L dNTPs (2 mM); 3  $\mu$ L MgCl<sub>2</sub> (25 mM); 2  $\mu$ L forward and 2  $\mu$ L reverse primers (10  $\mu$ M each); 0.4  $\mu$ L KOD DNA Polymerase (2.5 U/ $\mu$ L) (Merck Millipore, #71085). The reaction was incubated as shown in Table 2. Finished reactions were directly checked on agarose (1.2% w/v) gel electrophoresis (Appendix A1), with 0.06  $\mu$ g/ $\mu$ L of 1 Kb Plus DNA Ladder (Invitrogen, #10787018) using TAE 1X running buffer (Appendix A2).

**Table 1. Program for High Fidelity PCR of Hill\_BB\_C15867, Hill\_BB\_C13792, Hill\_BB\_C10649 and Hill\_BB\_C2519 contigs.**

<b>STEP</b>	<b>TEMPERATURE</b>	<b>TIME</b>
-------------	--------------------	-------------

<b>STEP</b>	<b>TEMPERATURE</b>	<b>TIME</b>
1: Initial Denaturation	98 °C	2 min
2: Denaturation	98 °C	20 sec
3: Annealing	58 °C	30 sec
2 – 3	Repeat for 30 cycles	
4: Stop	4 °C	hold

TOP10 chemically competent *E. coli* cells were used according to the procedure outlined in the manual (Invitrogen, K450001). Once the Hill\_BB\_C15867, Hill\_BB\_C13792, Hill\_BB\_C10649 and Hill\_BB\_C2519 PCR fragments have been extracted from agarose gel (Appendix A3) and ligated in pCR<sup>TM</sup>II-TOPO® vectors, the constructs were then transformed with heat shock process into 50  $\mu$ L of competent TOP10 cells (efficiency: 1x10<sup>7</sup> cfu/ $\mu$ g plasmid DNA) and let them grow in 37 °C shaking incubator, for 1 hour at 225 rpm. Once grown, the cell culture has been spread onto the top of poured 50 mL LB-Agar (1.5%) (Appendix A4), supplemented with Ampicillin (50  $\mu$ g/mL), previously preheated (37 °C for 30 min), after spreading 40  $\mu$ L X-gal (40  $\mu$ g/ $\mu$ L) (Appendix A5). The plate was then incubated at 37°C for 24 hours. This subcloning into pCR<sup>TM</sup>II-TOPO® vector allowed to obtain positive colonies selected by a blue/white screening. White colonies indicated the entry of

PCR fragment in the multiple cloning site incorporated in the pCR<sup>TM</sup>II-TOPO<sup>®</sup> vector. A white colony and one blue colony were picked for each recombinant product, re-inoculated into 5 mL of LB medium (Appendix A6), added with Ampicillin (50 µg/mL) and grown overnight at 37 °C. The identification of transformed *E. coli* colonies with the recombinant plasmids have been confirmed with miniprep procedures (FastPlasmid Mini Kit, 5 PRIME), and their subsequent hydrolysis with restriction enzymes for fragment length confirmation. The plasmids were sent to the Macrogen Europe (The Netherlands) to be sequenced, using forward Hill\_BB\_C15867, Hill\_BB\_C13792, Hill\_BB\_C10649 and Hill\_BB\_C2519 primers, which bound insert gene in the pCR<sup>TM</sup>II-TOPO<sup>®</sup> vector. From the same cell cultures, a midi-prep was performed, according to the manufacturer's instructions (PureLink<sup>TM</sup> HiPure Plasmid Midiprep Kit, Invitrogen K210004) and 10 µg of the recombinant products were digested in order to obtain a consistent amount of Hill\_BB\_C15867, Hill\_BB\_C13792, Hill\_BB\_C10649 and Hill\_BB\_C2519 for the subsequent cloning experiments in pGEX-4T1 expression vector (Novagen, #69744-3).

### 3.8. Double digestion and dephosphorylation of the pGEX-4T1 expression plasmid

For pGEX-4T1 plasmid double digestion, a reaction volume of 60 µL containing 15 µg of pGEX-4T1 plasmid, 60 U of EcoRI (20 U/µL), 6 µL NEBuffer EcoRI (10X) (New England Biolabs, MA, USA) was incubated at 37°C for 3 hours. EcoRI hydrolysis was then inactivated by incubation at 65°C for 15 min. Subsequently, the EcoRI-digested plasmid was purified with Quantum Prep Freeze N Squeeze DNA Gel Extraction Spin Columns (Bio-Rad, Hercules, CA, USA) and precipitated overnight at – 20 °C with 0.1 volume of 3M sodium acetate and 3 volumes of ethanol 96%. DNA recovered by precipitation (spin at 16000 rcf for 15 min at 4°C and two washes with ethanol 70%), was then digested as above with 60 U of BamHI (20 U/µL), supplemented with 0.06 µL BSA (100X) (New England Biolabs, MA, USA) and the reaction was incubated at 37°C for other 3 hours. The EcoRI/BamHI-digested plasmid, finally, has been deproteinized by extraction with phenol – chloroform - isoamyl alcohol (25:24:1) (Fisher Chemical #108-95-2, Carlo Erba Reagents #67-66- 3, Sigma #123-51-3) and precipitated as above. To ensure that a small amount of EcoRI- or BamHI digested plasmid does not re-circularize during subsequent ligation, the cloning workflow also has provided a dephosphorylation step. The use of an alkaline phosphatase to remove the terminal 5'-phosphate groups, usually reduces the occurrence of vector re-closure by intramolecular ligation, if the double digestion has not occurred correctly and the plasmid is cut only by an enzyme that creates compatible ends. The linearized plasmid has been dephosphorylated with 20 units of Calf Intestinal

Phosphatase (CIP, New England Biolabs, MA, USA) in a final volume of 20  $\mu$ L for 30 min at 37°C according to the manufacturer's protocol (NEB #M0290).

### 3.9. Molecular Cloning in pGEX-4T1 expression plasmid

The recombinant products (inserts cloned in TOPO-VECTOR) have been enzymatically hydrolyzed with BamHI and EcoRI (New England Biolabs, MA, USA) restriction enzymes in order to recover the genes of interest and clone them in pGEX – 4T1 expression plasmid. This vector allows the production of the antimicrobial peptides as fusion product with Glutathion S – transferase (GST) tag. Since that the GST protein has a higher molecular weight than the antimicrobial peptides, it will cover the peptides' antimicrobial activity allowing their heterologous expression in bacteria and it can be exploited for the next purification step. Fragment corresponding to the peptides' genes were purified using Quantum Prep Freeze N-Squeeze DNA Gel Extraction Spin Columns (Bio-Rad, Hercules, CA, USA) according to manufacture protocol and subsequently used for ligation reaction. Ligation reaction was performed according to a molarity equation (Sambrook et al., 1989) and using a 1:3 ratio of insert, 1  $\mu$ L Ligase buffer (10X), 2  $\mu$ L T4 DNA Ligase (400000 U/mL) (New England Biolabs, MA, USA). The incubation was carried out at 16 °C in a water bath over-night and, then the enzyme was inactivated at 65°C for 10 min. The total volume of ligation reaction mixture was used to transform *Escherichia coli* DH5- $\alpha$  chemically competent cells (Appendix A7). This final transformation process has allowed the recombinant product plasmid to take up into chemically competent cells for propagation and storage. After ligation reaction, positive screening was conducted through miniprep procedure (FastPlasmid Mini Kit, 5 PRIME) (Appendix A8) of suspected positive clones and were sent to Macrogen Europe (Amsterdam, The Netherlands) for sequencing, to ensure the peptides' sequences were not affected by mutations, using the forward Hill\_BB\_C15867, Hill\_BB\_C13792, Hill\_BB\_C10649 and Hill\_BB\_C2519 primers, which bound insert gene in the pGEX – 4T1 plasmid.

### 3.10. Heterologous expression and purification of the recombinant products by affinity chromatography.

The recombinant products were used to transform *Escherichia coli* DH5 $\alpha$  cells and the single colony of each transformation, grown on agar plate containing ampicillin, was used to perform a midi-prep, according to the manufacturer's instructions (PureLink™ HiPure Plasmid Midiprep Kit, Invitrogen K210004) (Appendix A9).

Quantitative evaluation of midi-preps was carried out by analyzing 1  $\mu$ L of each sample with the NanoDrop® 1000 Spectrophotometer.

Midi-preps were subsequently used for *Escherichia coli* BL21 (DE3) cells transformation to perform the expression of the recombinant products.

For the fusion protein production, IPTG (Isopropyl  $\beta$ -D-1-thiogalactopyranoside) (ThermoFisher, 15529019) (Appendix A10) 0.4 mM as inducer has been used once the bacterial culture had reached a value of OD<sub>600nm</sub>=0.6 corresponding to the exponential growth phase. The cells were then incubated at 37 °C for 3h and subsequently recovered by centrifugation at 5000 rpm for 20 mins. The obtained pellet was resuspended in *Lysis Buffer* (Na<sub>2</sub>HPO<sub>4</sub> 0.01 M, NaCl 0.15 M, DTT 5 mM, Lysozyme 5mg/mL and e PMSF 1 mM, pH 7.4).

The resuspended pellet was sonicated for 20 min in 30-second pulse mode (to dissipate heat) using an MS-72 probe which amplifies the vibration produced by the converter with an amplitude value of 20%. The lysate cells were incubated in static at 25 °C for 30 min with Triton 1% and then centrifuged at 15000 rpm for 1 h and the supernatant has been recovered to be purified through affinity chromatography with an FPLC system. The produced peptides were analysed through SDS-PAGE in order to verify that the heterologous expression had taken place correctly. In collaboration with Prof. Pietro Pucci from the University of Naples, the purification of the Hill\_BB\_C15867 and Hill\_BB\_C2519 recombinant products was carried out. The chromatographic system and the GStrap column were washed with 1 mL ddH<sub>2</sub>O and then equilibrated with a 0.5 mL/min flux with *Binding Buffer* (Na<sub>2</sub>HPO<sub>4</sub> 0.01 M, NaCl 0.15 M, DTT 5mM, pH 7.4). The elution was performed with a 1 ml/min flux and 100% of gradient of the *Elution Buffer* (Tris 25 mM, NaCl 150 mM, DTT 5 mM, Glutathione 10 mM, pH 8.0). The chromatographic samples were analysed through SDS-PAGE (Appendix A11) in order verify that the purification had taken place correctly. The purification of the Hill\_BB\_C13792 and Hill\_BB\_C10649 recombinant products is ongoing in collaboration with Prof. Pietro Pucci from the University of Naples.



### 3.11. Hill\_BB\_C15867 and Hill\_BB\_C2519 primary structure validation through *in situ* hydrolysis and MALDI-TOF Mass Spectrometry analysis.

From the obtained SDS-PAGE gel it was possible to excise the protein band of interest and perform an *in situ* hydrolysis protocol - in collaboration with Prof. Pietro Pucci from the University of Naples - which allows to carry out the proteolysis of the proteins immobilized in the meshes of the polyacrylamide gel. What is obtained is a mixture of peptides to be analyzed by MALDI-TOF mass spectrometry and to obtain the protein sequence.

The band, reduced to a smaller size, was subsequently destained by alternating phases of dehydration and rehydration: the band was covered with an appropriate volume of acetonitrile, shaking the tube to allow rapid dehydration and removal of the low molecular weight components. The supernatant was then removed and Ammonium Bicarbonate ( $\text{NH}_4\text{HCO}_3$ ) 0.1 M was added, which was then removed and the cycles of dehydration and rehydration were repeated until the band was completely destained. The reduction of the disulfide bridges and the subsequent alkylation of the cysteines is necessary to avoid, during the hydrolysis, the occurrence of secondary reactions by blocking the nucleophilic -SH groups. Therefore, the dehydrated band was coated with a 10 mM DTT solution in 0.1 M  $\text{NH}_4\text{HCO}_3$  and incubated at 56 ° C for 45 minutes. Then the liquid was removed, quickly adding acetonitrile to block the reactivity of the free cysteines. To induce alkylation, 100  $\mu\text{L}$  of 55 mM iodoacetamide solution in 0.1mM  $\text{NH}_4\text{HCO}_3$  was added, incubating the reaction in the dark and at room temperature for 30 minutes. The supernatant was removed, dehydrating with acetonitrile, rehydrating with 0.1M  $\text{NH}_4\text{HCO}_3$  and dehydrating again to completely remove the alkylating agent. The band, once dehydrated, was incubated at 4 ° C for two hours with a 10 ng/mL trypsin solution in 10 mM  $\text{NH}_4\text{HCO}_3$ . In order to remove any autoproteolytic products of trypsin, the supernatant was removed, 10 mM  $\text{NH}_4\text{HCO}_3$  was added, covering the band, and then the sample was incubated at 37 ° C for 16 hours. Hydrolysis allows to obtain peptides able to go out from the gel meshes and transferring them into solution: therefore, after 16 hours, the supernatant was recovered, carrying out subsequent hydration and dehydration steps, alternating the addition of 120  $\mu\text{L}$  of acetonitrile and 100  $\mu\text{L}$  of 0.1% formic acid, to recover the peptides still present within the band. Finally, the collected solutions were pooled and dried using Speed Vac system. The dried peptides have been then dissolved in 0.1% formic acid and analysed by MALDI-TOF mass spectrometry.

Matrix-assisted laser ionization mass spectrometry with time-of-flight analyzer (MALDI-TOF) is based on a desorption/ionization method that allows to study in a simple and highly productive way non-volatile molecules such as proteins and nucleic acids with high masses up to the order of magnitude of 500000 Da. MALDI ionization technology is based on the molecules' excitation with a laser beam to produce their vaporization and ionization. In the source the sample is dissolved in a matrix, therefore the biological molecules are not directly excited by the photons of the incident light and therefore do not undergo chemical modifications of any kind, with the exception of a protonation process. A small volume of the sample-matrix mixture (1-2  $\mu\text{L}$ ) is deposited in one of the MALDI plate wells. The matrix used is the  $\alpha$ -cyano 4-hydroxycinnamic acid 10 mg/mL, dissolved in 70% ACN (acetonitrile). After the evaporation of the solvent, when the sample-matrix mixture contained in each well have co-crystallized, the target is placed in the MALDI source, in which the vacuum is set and the wells, in sequence, are hit by a pulsed laser beam ( $\lambda = 337 \text{ nm}$ ).

The energy absorbed by the molecules of the matrix is enough to bring them into the vapor phase. In this process of the matrix vaporization also the solute molecules are entrained in the vapor phase: the ions generated are then subjected to a strong electric field (20 - 25 kV) which accelerates them towards a grid, after which they enter the analyzer. The TOF (time-of-flight) analyzer is based on a very simple principle: the ions speeds after the acceleration undergo in the ionization chamber are different because of the different  $m/z$  ratios, therefore, the time taken by each to cross the analyzer varies (flight time): all have the same kinetic energy, but lighter ions will take shorter times, while heavier ions will correspond to longer times. The detector allows to quantify the ionic current, transferring the signal to the data processing system, which returns the characteristic mass spectrum of the substance or mixture of substances to the interface.



O1)C(CO)O)O)O)C(=O)O)C(=O)O)C(=O)O)OP(=O)(O)O)OC(=O)CC(CCCCCCCCCC)OC(=O)CCCCCCCCCCCC)NC(=O)CC(CCCCCCCCCC)OC(=O)CCCCCCCCCCCC)CP(=O)(O)O.

The molecular docking analysis has been performed through the PatchDock Server [258] and the peptide-ligand complex has been refined through the FireDock Server [259]. The interactions occurring at the peptide-ligand interface have been evaluated and identified through the PLIP (Protein Ligand Interaction Profiler) Server [266].

### 3.14. Evaluation of the antimicrobial activity of the C6571, C46948, C16634 and C7985 peptides.

According to the prediction scores calculated through the bioinformatics analyses and sequences lengths, four peptides, among the most promising, were selected and purchased from Bio-Fab company. In order to evaluate their antibacterial activity, the cell proliferation was assessed by determining the number of actively dividing cells through colonies count. With the aim to assess cell viability, *E. coli* (BL21) growth starting from 0.08 OD/mL was incubated at 37 °C and monitored every 20 minutes by measuring the optical density ( $\lambda = 600$  nm). Moreover, every 20 minutes an aliquot was subjected to serial dilutions, transferred to solid culture medium (LB – agar) and the plates incubated at 37 °C for 16 h. Then, colonies count was performed for each plate.

### 3.15. Chemical Synthesis on Solid Phase (CSSP)

At the Technische Hochschule Mittelhessen University of Applied Sciences, Gießen, Germany, at the laboratory of Dr. Daniela Müller, the chemical synthesis on solid phase of three antimicrobial peptides has been performed. The AMPs corresponding to the C12927 and C4669 contigs, based on the bioinformatics predictions, were selected for the chemical synthesis.

The chemical synthesis on solid phase was carried out using a Liberty Blue microwave synthesizer with an associated UV detector. 0.2 M solutions of each amino acid were prepared, using DMF (Dimethylformamide) as solvent. Other necessary solutions are:

- Activator: solution composed of DIC (N, N'-Diisopropylcarbodiimide) (16.8 mL) and DMF (91.2 mL);
- Basic activator: OMYMA (Ethyl cyanohydroxyiminoacetate), 0.2 M, brought into solution with DMF.

- Amino acid deprotection solution: 20% Piperidine in DMF.

Once the synthesis was completed, the resin, to which the peptide chains are bound, was subjected to a washing step with DCM (Dichloromethane) and left to stir for 4h. After that, the peptide has been cleaved from the resin using a mix of chemical reagents which also has the purpose of removing the protecting groups of the amino acid side chains. This mix has the following composition: 92.5% TFA, 25% H<sub>2</sub>O, 2.5% TIS (Triisopropylsilane) and 2.5% DODT (3,6-dioxa-1,8-octanedithiol). The sample was then transferred to a thermomixer at 55 ° C and connected to a flow of N<sub>2</sub> for 15 minutes. Subsequently, 4 volumes of MTBE (Methyl-t-butyl ether) necessary for the precipitation of the peptide were added and the sample was centrifuged for 5 minutes at 5000 rpm (2 times). The recovered pellet was resuspended in H<sub>2</sub>O and 1% CH<sub>3</sub>COOH. The sample was placed at -80 ° C for 16h, lyophilized and analyzed by HPLC with a C<sub>18</sub> column (Aeris™ 2.6 μm PEPTIDE XB-C18 100 Å, Phenomenex), using water and acetonitrile as solvents performing a linear gradient from 1% to 95% ACN within 31 min and a flow rate of 0.3 mL/min.

*AN IN VIVO  
APPROACH*

### 3.16. *Hermetia illucens* larvae infection, hemolymph collection and protein/peptide separation.

Fourth and fifth-instar larvae of *H. illucens* were used for this study. Colonies of *H. illucens* were maintained under a lighting regime of 16:8 (L:D) h to mimic photoperiod at room temperature (RT,  $28 \pm 2^\circ\text{C}$ ). To induce the immunization of *H. illucens* larvae, the larvae were washed with distilled. The larvae were immunized with a fine needle dipped into *Escherichia coli* (LMG2092), as Gram-negative bacteria, and *Micrococcus flavus* (DSM1790), as Gram-positive bacteria, on a clean bench and reared at RT for 24 h. Immunized hemolymph of the larvae was collected in ice-cold tubes and in presence of 1-2 mg of ascorbic acid in order to prevent hemolymph melanization. The extracted hemolymph was then centrifuged at 10,000 rpm (using the Standard Rotor F-45-24-11) for 5 min at  $4^\circ\text{C}$ . The proteins/peptides in the hemolymph plasma from both larvae not infected, infected with *E. coli* (LMG2092) and *M. flavus* (DSM1790) were separated using 10000 Da Centrifugal filter Units (Amicon Ultra-15) by centrifuging at 4000 rpm (using the Standard Rotor F-45-24-11) for 45 minutes at room temperature. The samples were then analysed through SDS-PAGE.

### 3.17. Evaluation of the hemolymph antibacterial activity through Microdilution Assay and Bioautography (SDS gel overlay method) experiment

For the microdilution assay, performed against both *E. coli* and *M. flavus*, 30  $\mu\text{L}$  of the supernatants obtained through solvent precipitation with Methanol/Acetic Acid/Water (90:1:9 v/v) of the plasma extracted from not infected larvae and larvae infected with *E. coli* (LMG2092) and *M. flavus* (DSM1790), were serially diluted with LB medium, in a 96-well plate. 85  $\mu\text{L}$  of cell culture  $1 \times 10^6$  cells was added to the samples. The plates were incubated at  $37^\circ\text{C}$  for 24 h and the optical density at  $\lambda = 600 \text{ nm}$  was evaluated. Bioautography (SDS gel overlay method) assay was performed according to Zdybicka-Barabas et al., 2017, protocol [267]. The experiment has been performed against both *E. coli* (LMG2092) and *M. flavus* (LMG2092).

At the Eli Lilly S.P.A., Catania, Italy, a microdilution assay has been performed against *Staphylococcus aureus* (ATCC33826) and *E. coli* (a strain isolated at the University of Palermo from pecorino cheese) following the same protocol described above.

### 3.17. Hemolymph analysis performed at the Technische Hochschule Mittelhessen University of Applied Sciences, Gießen, Germany

*Hermetia illucens* larvae at V instar were provided by Prof. Andreas Vilcinskis from the Justus-Liebig-Universität, Gießen, Germany, which were reared on two different diets: Chicken Food (CF) and Cotton Pressed Cake (CPC). At the Technische Hochschule Mittelhessen University of Applied Sciences, Gießen, Germany, where I spent the period abroad provided by the doctoral program, at the Prof. Michael W. Wolff and Dr. Daniela Müller laboratories, the larvae were splitted into two groups (for larvae reared on both diets), the first one has been infected with *Micrococcus luteus* while the second was not infected, representing the negative control of the experiment. For the infection, *M. luteus* bacterium was grown at 37 °C and 1 OD/mL of the cell culture was used to infect the V instar larvae using a micro syringe and the two groups were reared at room temperature for 24 h. The hemolymph was collected in ice-cold tubes and in presence of 1-2 mg of ascorbic acid in order to prevent hemolymph melanization. The extracted hemolymph was then centrifuged at 10,000 rpm (using the Standard Rotor F-45-24-11) for 5 min at 4 °C in order to recover the plasma.

The plasma obtained from not-infected and infected larvae was analysed through High Performance Liquid Chromatography, HPLC, and Fast Protein Liquid Chromatography, FPLC. For the HPLC analysis a C<sub>18</sub> column (Aeris™ 2.6 µm PEPTIDE XB-C18 100 Å, Phenomenex) was used; water and acetonitrile as solvents and a linear gradient from 1% to 95% ACN within 31 min and a flow rate of 0.3 mL/min. For the FPLC analysis a C<sub>18</sub> column (Aeris™ 2.6 µm PEPTIDE XB-C18 100 Å, Phenomenex) was used; water and acetonitrile as solvents and a linear gradient from 1% to 66% ACN within 33 min and a flow rate of 0.3 mL/min. The obtained pics following the FPLC were collected, lyophilized, then resuspended in dH<sub>2</sub>O and all the fractions were analysed through a microdilution assay experiment for the evaluation of the antibacterial activity against *E. coli* and *M. luteus*.

For the microdilution assay, 75 µL of the hemolymph extracted from *H. illucens* larvae not infected, as control, and larvae infected with *E. coli* and *M. luteus* were subjected to serial dilution for a total of 6 dilutions. To the starting 75 µL of hemolymph were added 75 µL of LB broth. Then, from this first dilution, 75 µL were transferred into another tube containing 75 µL of LB and so on till the 6<sup>th</sup> dilution. 20 µL of each dilution were loaded on a 96-well plates containing 100 µL of *E. coli*, for one plate, and 100 µL of *M. luteus*, for the other plate. Then, the 96-well plates were incubated at 37 °C for 24 hours.



## 4. RESULTS

### 4.1. Transcriptomes analysis for the identification of AMPs and functional annotation.

The transcriptomes, deriving from different insect species - available at the Laboratory of Insect Physiology and Molecular Biology, University of Basilicata, Potenza, Italy - realized in collaboration with Prof. Heiko Vogel, from the Max Planck Genome Center in Jena, Germany, are:

- *Aphidius ervi* (combined transcriptome between males and females): 59454 "unique" nucleotide sequences (contigs);
- *Eupelmus urozonus* (transcriptome of poison glands): 16659 "unique" nucleotide sequences (contigs);
- *Heliothis virescens* (hemocyte transcriptome): 56782 "unique" nucleotide sequences (contigs);
- *Toxoneuron nigriceps* (teratocyte transcriptome): 24570 "unique" nucleotide sequences (contigs);
- *Hermetia illucens* (larvae transcriptome and combined larvae and adult transcriptome): 72481 "unique" nucleotide sequences (contigs);
- *Leptomastix dactylopii* (female transcriptome combined between antennae and bodies): 110444 "unique" nucleotide sequences (contigs);
- *Ephestia kuehniella* (combined transcriptome between larvae and adults): 65957 "unique" nucleotide sequences (contigs);
- *Megoura vicae* (combined transcriptome between antennae and bodies): 42118 "unique" nucleotide sequences (contigs);
- *Capnodis tenebrionis*: 51394 "unique" nucleotide sequences (contigs);
- *Torymus sinensis* (poison gland transcriptome): 22876 "unique" nucleotide sequences (contigs).

The sequences obtained were functionally annotated through the Blast2Go PRO v2.6.1 software ([www.blast2go.de](http://www.blast2go.de)). A similarity search was conducted in each of the available transcriptomes of sequences coding for AMPs, using known sequences of antimicrobial peptides from other insects present in the database as queries. This analysis made it possible to identify:

- 10 AMPs in *Aphidius ervi* (combined transcriptome between male and female);
- 4 AMPs in *Eupelmus urozonus* (transcriptome of poison glands);

- 13 AMPs in *Heliothis virescens* (hemocyte transcriptome);
- 7 AMPs in *Toxoneuron nigriceps* (teratocyte transcriptome);
- 68 AMPs in *Hermetia illucens* (transcriptome of larvae and combined transcriptome of larvae and adults);
- 10 AMPs in *Leptomastix dactylopii* (female transcriptome combined between antennae and bodies);
- 19 AMPs in *Ephestia kuehniella* (combined transcriptome between larvae and adults);
- 5 AMPs in *Megoura viciae* (combined transcriptome between antennae and bodies);
- 17 AMPs in *Capnodis tenebrionis*;
- 5 AMPs in *Torymus sinensis* (transcriptome of poison glands).

The high number of antimicrobial peptides identified in the transcriptome of the insect *Hermetia illucens* is to be associated with the extraordinary ability of the latter to survive in hostile environments, characterized by high microbial load. For this reason, this project focuses on the antimicrobial peptides identified in the *Hermetia illucens* insect.

The identified peptides belong mainly to the defensin class. Figure 14 shows a schematic representation of the classes of peptides identified and the respective percentage, while table 2 shows the contigs and the respective class of belonging:

- 3% Diptericins;
- 5% Knottin - like;
- 18% Lysozyme;
- 2% Stomoxyn - like;
- 3% Alo-like;
- 7% Attacins;
- 18% Cecropins;
- 44% Defensins.

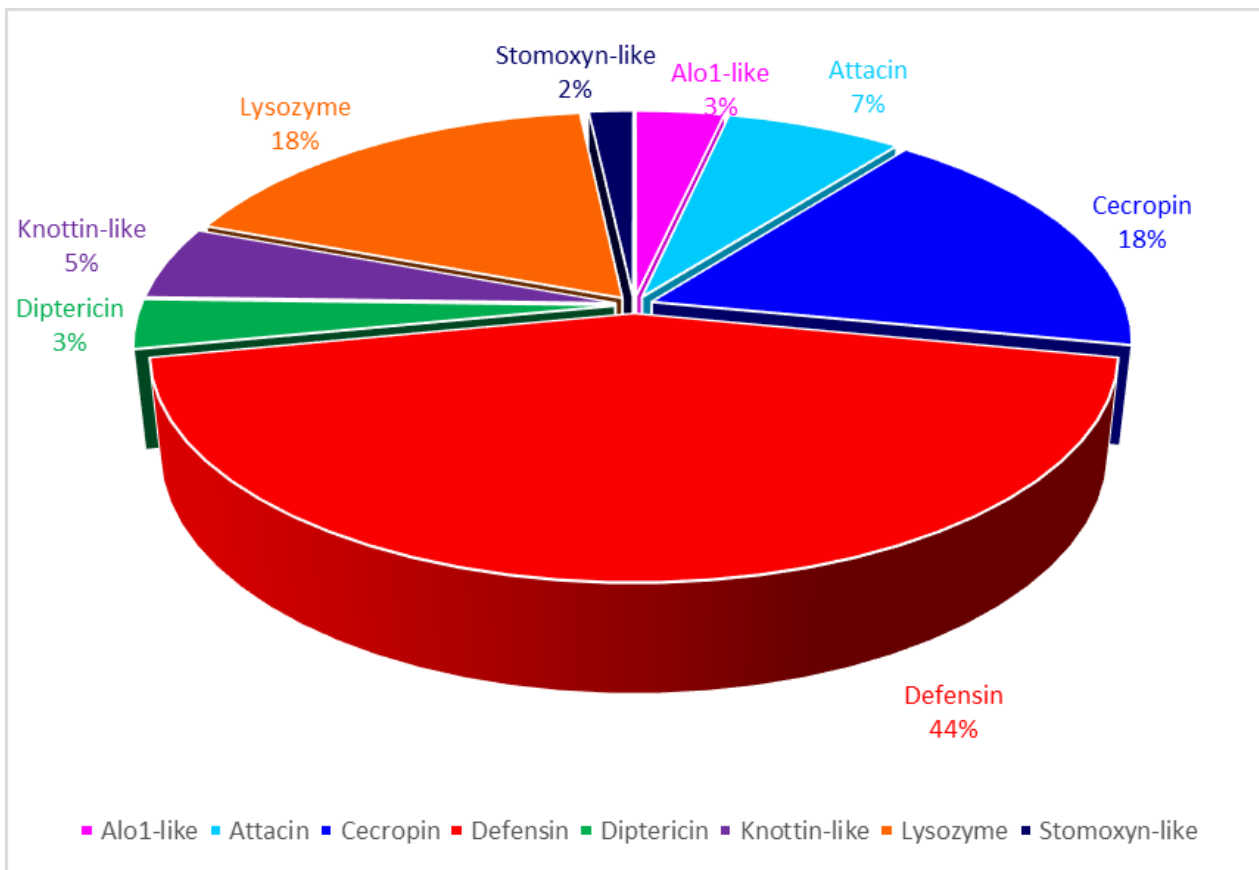


**Figure 14.** Graphic representation of the identified AMP classes from larvae and adult transcriptomes. The pie chart shows that the largest number of identified peptides belongs to the class of defensins.

**Table 2.** AMPs identified classes.

PEPTIDE	CLASS
Hill_BB_C14202	Lysozyme
Hill_BB_C3566	Lysozyme
Hill_BB_C1152	Lysozyme
Hill_BB_C1153	Lysozyme
Hill_BB_C2676	Lysozyme
Hill_BB_C269	Lysozyme
Hill_BB_C1169	Lysozyme
Hill_BB_C779	Lysozyme
Hill_LB_C36111	Lysozyme
Hill_LB_C12085	Lysozyme

---

Hill_BB_C1290	Diptericin
Hill_BB_C1827	Defensin
Hill_BB_C5878	Defensin
Hill_BB_C13793	Defensin
NHill_AD_C73537	Cecropin
NHill_AD_C16493	Cecropin
NHill_AD_C12927	Cecropin
NHill_AD_C12928	Cecropin
NHill_AD_C4669	Cecropin
Hill_BB_C3195	Cecropin
Hill_SB_C698	Cecropin
Hill_SB_C2730	Cecropin
Hill_SB_C1875	Cecropin
Hill_BB_C5151	Cecropin
Hill_BB_C390	Stromoxyn-like
NHill_AD_C53857	Alo-like
NHill_AD_C49215	Knottin-like
Hill_BB_C21232	Diptericin
Hill_LB_C16634	Knottin-like
Hill_LB_C37730	Knottin-like
Hill_BB_C46948	Knottin-like
Hill_BB_C16137	Attacin
Hill_BB_C16883	Attacin
Hill_BB_C9237	Attacin
NHill_AD_C40487	Attacin
Hill_BB_C7758	Defensin
Hill_BB_C14087	Defensin
Hill_LB_C29142	Defensin
Hill_BB_C308	Defensin
Hill_BB_C1619	Defensin
Hill_BB_C1826	Defensin

---

Hill_BB_C6571	Defensin
Hill_BB_C7081	Defensin
Hill_BB_C7985	Defensin
Hill_BB_C7176	Defensin
Hill_BB_C2519	Defensin
Hill_BB_C8473	Defensin
Hill_BB_C34351	Defensin
Hill_BB_C4683	Defensin
Hill_BB_C4977	Defensin
Hill_BB_C13326	Defensin
Hill_BB_C7171	Defensin
Hill_BB_C10649	Defensin
Hill_BB_C13792	Defensin
Hill_BB_C15867	Defensin
NHill_AD_C69719	Defensin

#### 4.2. Sequences study for the identification of the mature active peptide.

Antimicrobial peptides are naturally produced in presence of a signal peptide and, eventually, a pro-peptide as well. All the nucleotide sequences have been analysed in order to identify the start methionine, the signal peptide, the pro-peptide and the stop codon, in order to recover only the mature and active peptide sequences, as shown below. In yellow is highlighted the start codon, in green the signal peptide, in light blue the pro-peptide, in magenta the mature active peptide and in red the stop codon.

##### C15867

TTGCACGGGAATTCCGTGATGAGTCTTATCAGCGGACGATAGAAAGCAATGCGAAAAT  
 ATTTAAACCACGGCAAGCATGAAGCCGGCCATCATTTTCGTGAGTTAGTTATCGAGAGT  
 ACATTTCCAGCTTCGCTGTCTTCCTGATTCTTCATCGCCGCGTCAAGATGCATTCCTGTA  
 CCCTGGTCTTTGGTCTTGTTATCCTGGCTGCAATCGTTGGCGTTAATCATTTTCCTGCAG  
 ATCTGGATCCGATCAACAGCGAATTGGACGTTTTTCCATCTGCCCAAATTGAAGGAGA  
 GCTCATTCGTCATAAGCGAGTACCTGTGATCTTCTAAAACCTTTCTTTGGTCGCGCCC  
 CTTGCATGATGCATTGTATTTTGCGGTTTAAAAAGCGTACTGGATTCTGTAGTAGACAA

AACGTTTGCCTGTGCAGATAAAATGTTAACGGAGAATTCAGAGATTATTTAGATTAT  
TTTGTTAATTTATTTATAAATAATATATAAAACAATAAATTGTTAAAATATATTCCTATT  
GGAAAT

**C2519**

CCAGCTTTTCTTTTCTTCAATTTAAAGTTTTATTCTGAATCTAAAAGTCAAAATGCGTTC  
TATTCTCGTCTTGGGTTTAATTGTTGCCGCTTTTGCCGCTACACCTCAGCACAAACCTTA  
TCAGTTACAATACGAGGAAGATGGTCCTGGATACGCACTGGAACCTCCCTAGCGAAGAA  
GAAGGACTTCCTAGCCAAGTAGTGGAACAACATTACCGGGCGAAACGTGCAACCTGTG  
ACCTCTTGAGTCCCTTCAAAGTGGGTGATGCTGCCTGCGCACTTCATTGTATTGCCATG  
GGACGACGAGGAGGCTGGTGCGATGGTCGAGCCGTTGTAATTGCAGACGCATACTA  
AAGTGATTGTACTAATAGAGCTCTAGTTTGTATTTATTCACAAAATTTTATTATT  
TATCAATTGTTGATTGCTGTTTTGAATAAATTGTTGTTTTAGTTCTGGAAAATAAATTT  
TTGTTATGGTTGTGCAAAAGAAAAGA

**C8473**

GTGCTCTCCGATCTGAAAACGACAACCAATCCAGCACTAATTAAGCTCCAGCTTTTTT  
CTGAATCTAGAAGTCAAAATGCGTTCATTCTCGTCTTGGGTTTAATTGTTGCCGCTTT  
GCCGTCTACACCTCAGCACAAACCCTATCAGTTACAATACGAGGAAGATGGTCCTGAAT  
ATGCACTGGAACCTCCCTATTGAAGAAGAAGAACTTCCTAGCCAGGTAGTGGAGCAGCA  
TTATCGGGCAAACGTGCAACCTGTGACCTCTTGAGCCCTTCGGCGTGGGTGATGCCG  
CCTGCGCAGTTCATTGTATTGCCATGGGACGTGCGGGAGGTTGGTGCGATGATCGAGC  
CGTTTGAATTGCAGACGCATACTAAAGTGCTTGTACTAATTTTATTAATTTATC  
AATTGTTGATTGTTGTTTTGAATAAATTGTTGTTTTAATTCTGGAAAAGAAAAAAGAT

**C13792**

AGTGGCTTATCATCCGTGGCGGGGCACATTCGAGTTTGAGCTGCTTAGTATACGCATCT  
TCTAGCCAAGTTGTTACTGTTTTAAATATAAAATGTTTTGTAAAATTTGCCGGTATTTCC  
TAATCTTAATAATTCTTTCGATTGGTTTGCAACAATAAACGAAGTTAGTGCAAGCAA  
TCAAGTGATCCAGAGTCAGCGTTGTAATCAGATATTCACCCAAGGTTTAGGGCAGAGC  
TTCTTGCGATTATCTTAGCGGTTTGGGATTTCGGCGAAGACGCTGCAACACGGATTGT  
ATTGCAAAAAGGACATAAAAAGCGGTTTTTGCCTGGACTCGTTTGTGCGTTGCAGAACCT  
ATAGTGGTTAGCCATGCAGACAATTAATTTTATAAAGATTTACCCCAATCTAAACAAC  
CTGCTGCTATTGTATGCGAAAAAGTATAGAATAAAATAATAGTAATATGTATGTAAGC  
AAAATAAAACAATCTTCAAAGATCGGAAGAGCGTCGTGTAGGGAAAGAGTGTGTCA  
GTA

C308

TTCCGATCAAAAATGAAGTTAGTAATTTTTCTTGGAGCTTTTGTAGTCATCAGTTGTGCA  
GTAGTTTCTGCAACACCCGAACCTCTTGAGGGTTTAGAGCCATTGGAAAATGCAGAAT  
CATTGGACAATCTGGGAATTGGAGAGCTTGAGAGACCCAAGCGAGTTAGTTGCTGGTT  
TGAAAACGAAAACATAAAGGCTTCAGCTTGCCAAATGAGTTGCATGTATCGAAAGGGA  
CGACGAGGTGGAATGTGTGTTAATGGAGTTTGTACCTGTTCTCCTAACATAAGTTTGGAA  
ATGTTATCTATGTGCTATAAGCAATGTATTATATGTATATCAAAAATAATTGTGA

C7081

GGAATTGAAACTTATCCATATCCAACCAAAAATGCGTTTCCTCCTCTTCGCTGCCCTTTT  
GGTGCTGTTTTCTTCTTTGTGCACCCAATGCCATCCTTCGTCTTCCTGAGAAAGCGGA  
AGATTACCAGAACAGATAGCAAACATTCCACTACATCATCGTGCCAGACGTGCCACC  
TGTGACCTAATAAGTGGTACGAAAATCGAAAATGTCGCCTGTGCTGCTCACTGCATCG  
CGATGGGGCACAAAGGAGGTTATTGCAATTCTAACCTTATCTGCATTGCCGCTAAATCA  
TCTAAATTCAGGTCCTAAATAAAAACCTATTGAAATTGCAATTCTAACCTTATCTGCA

C7176

GAATCTCGTGACTGGAGTTCAGACGTGTGCTCTTCCGATCTCAACTGCTAGAATACAGA  
TCCAGCTTCAGCTTTTTCTTCAACCCAAAGCTTTGATCTTTAACTAAAGCCAAAATGCG  
TTCCGTTCTCGTCTTGGGTTAATTGTGGCCGCTTTTGCTGTCTACACCTCAGCACAACC  
CTATCAGTTACAATACGAGGAAGATGGTCTCGATCAGGCAGTGGAACCTCCTATTGAA  
GAAGAACAACCTCCGAGTCAGGTGGTGGAGCAGCATTACCGTGCGAAACGTGCAACCT  
GTGATCTCTTGAGTCCCTTCAAAGTGGGTCATGCCGCCTGCGCACTTCATTGTATTGCTT  
TGGGACGTCGTGGAGGCTGGTGGCAGTGGTCGAGCCGTTTGTAAATTGCAGACGTAAATC  
TAGAGTGCTTGTACTTATAGGGCTCCAATTTTTTATTTATTTACCAAATTTTTGTGA  
ATTT

C34351

GTCCTAGATACGCGGATCAGTCCAGAGAACGACAATCCACAGAACACAGATTAAGCTC  
CAGCTTCTTCTTCAATTTAAAGTTTTATTCTGAATCTCAAAGTCAAAAATGCGTTCTATT  
TCGTCTTGGGTTAATTGTTGCCGCTTTGCCGTCTACACCTCAGCGCAACCCTATCAGT  
TACAATACGAGGAAGATGGTCTAGATACGCACTGGAACCTCCCATTGAAGAAGAAGC  
GCTTCTGGCCAGGTGGTGGAGCAGCATTACCGGACGAAACGTGCAATGTGTGATTTA  
TTGAGTGGCTTGAACATGGGTCGTAGCGTGTGCGCAATGCGTTGTATCCTTAAGGGAC  
ATCGCGGAGGCTGGTGGCAGTGGTCAAGGCGTTTGTAAATTGCAGAGTTAAATCTAAAGT

GCTTGTACTACTTGTTTGTGAACTTATCAATTATTAATTGTTATTGTGAATAAAAATTC  
TAAATTCGTA

**C4683**

TCGAGTATTTGGAAGATTCCCAAGGATCAATCAAGCTCCAGACTCTGATTAGCTACCAC  
ACGTCACAGTGAATACTCCATTCAAATCAAAAATGAAATTCGCTCTGCTCTTTGCCGTTT  
TTGCTGTTATCTGTTCAATGGCGCTAGCCAGGCCCGACAATATCGAGTATTTGGAAGAT  
TCCCAAGTTGCAGAATTGGTTCGTCATAAGCGTTTGTCTGTCTGTTTCGAAAATGAAGC  
GATTCGGCTCTTGCCTGTGGAGCTAGCTGCATTACACGGAAAGGACGTCGAGGAGGA  
TGGTGTTCGAATGGAGTTTGCCACTGCACACCTAATTAACATTTGTTATTTATTTATTAA  
TTAAATTTTGTGGGAATTGTTTTACTAAAAATAAAAATTCAGTTTTATGACTAAAACA  
GATCGGAA

**C4977**

CTAATTTCAAAGCGCAAATGCTTAGTTGCAAAATGAAGCTCATCATCGTTCTCGGAGTT  
TTGGCTGCTGTCTGCTGTGCAACCACTTTCGCTAGGCCCTGAGTACTTGGAGCTGGAAGG  
ATTGGAGCAATTGGAAAATGCAGAACCTAGCTCCAATGTAGAAGTTAGAGAATTGGTG  
AGACACAAACGGCTAAGCTGCTGGTTCGAAAATGAGGACATAAAGGCCACAGCCTGC  
GCAATGAGCTGTATATATCGAAAGGGACGAAAAGGTGGACGATGTGAAAATGGAATA  
TGTAGATGTACCCCAATTAAATATCTGCAATTGTGACTGACTGTGTTGTTGAAAAGAT  
TATGTTTACTTAAATAAATTATTATTCAAACCTTCAAATCACATTGTTTACTCATTGAAT  
ATAATATAACACTAATGGTTTTGCAATGCATGGACTGATGAATTTTGGTTACACAAGCT  
GAACCCTACAGA

**C7171**

AAGGTGCACCTATCTTTACCCAGATCAGTTCAGGAATTGAACTTATCCATATCCAAA  
CAAAAATGCGTTTACTCCTCTTCGCTGTCTTTTACGCGCTGTTTTCTTCTTTGTGTACCA  
GATCCCATCCTTCATCTTCCCTGAGAAAGTGGAAGATTTACCAGGACAGGTAGCAAACA  
TTCCAGTACATCATCGTGCCAGACGTACCACCTGTGACCTAATAAGTGGTACGAAAAT  
CGAAAATATCGCCTGTGCTGCTCATTGCATCGCGATGGGGCACAAGGAGGTTATTGC  
AATTCTAACCTTATCTGCATTTGCCGCTAAATCATCTAAATCCAGATCCTAAATAAAAAC  
TATTGAAATT

**49430**



TTTGGCGGTGATCAGTCGTTTCTGAAGTGTACCGTTAATAATGAAATTCCTAGCTTCT  
CTCATTGTCATCCTCGCCGTTCTTGTTGTGGCCCTTGCTGCTCCTCAATTCGGAGGGCAA  
ATTGGCGGTTTCGGAGGAGGTGGTTTTGGCGGTGGTGGTTTTGGTCCAGGTGGTGGTTT  
CCGTCCGGGTGGTGTGCTGAATTCCAAGAATCGTCATCATCAGTAAATGTTGAAAGA  
GAAACCTTCGATCAAGGCGGTTTCGAGATCTCAGATTCATCTGTCACTTCTTCATCTGT  
CTCAGAATCATTCCGTGATTAAACTATACTCTTAATATTAATTTAGATAATACTGAA  
TTAGAAAATAAATGTGTTTCC

#### C10074

GAAGAAAAGATCTTCTCAAGACAAGTTAATAAAGTGTAAAGTTTAATTGAATCAACCA  
AATCTTCAAGTATGTTGTTCAAAGTGCTCATTATTTTCGGTGTGTTCTCTGCGGGGCTTA  
CGTTTTTCGCTGCCGCAAACAATATTGCCGATGATGATTCCAAGAGGTGCAAAGGTA  
TTCATCGAGAATTATTGACCCGGGCAGTCAGTTCTTGATCCGTGGAGAGGATTTAGATG  
ACATTTTTGAGCCGAGAGAGGAAGAAGGTTTACCTGAAGATGTAATTCGAGCCAGAAG  
ATCACCGCAAGATGGACGTCGCGGTTCTGCTAGTGTACAGTAAATAATGAAAGCAGG  
CGGGGAAGTGTACGAGCTGATCTCAACGCTAGACTTTGGGAGGGTAACAATAGAA  
GGTCAAGTTTGGATGCTAATGCTTACTATCAACGACATTTTCGGTGGACCCATGGGCACC  
GGACGACCAGATGCTGGAGTTGGATTGAACTTTCGACATCGGTTCTAGATAGCATCGC  
GTAGCAGTAGCAGTAGTAATCATCATTTAATT

#### C12927

CCGGCTATCATCCTCAGTCATTTCTTTCAAGTAGGAAGACTATCAAAATATTTACGAAA  
CCAACATGAATTTTCGCTAAACTTTTCGTTGTCTTTGCGATTGTTCTTGTCGCCTTCTCTG  
GTCAAAGTGAAGCTGGTTGGTGGAAAGAGGGTTTTCAAGCCAGTGGAAAACTTGGCCA  
ACGAGTTCGTGATGCCGGTATTCAAGGACTCGAAATTGCACAACAAGGAGCCAATGTT  
CTGGCAACAGCCCAGGTGGACCACCACAGCAAGGATAATTATTATAAATTATTTTTCT  
TTGTATTTATATTTCTTTTATTTATTGAACTTAAGTATTTAAAACCAGACAAAGGATAATT  
TGGAAAATAAAATATGTAAAAAATTATTGATTTTCAAGAACTTTGGAACATTAGGGGA  
ATATTCATAACCCACCAAACAACACTACATATAGTATGTATGTTTTCTCATAGATGTT  
TGTATCCATCAAACTCTTTCAAATTGACTGACCAGAAGAAAAATATAGCAGTTGGGC

#### C12928

GCGGGTTCAGTTTGAATCTTCAAGTAGCTCATCTCAACTCATTCAACAATCAATTGACA  
ACCAAATTAACAAA **ATGA**AATTCACAAAGCTTTTCGTTGTTTTCACTATTCTTATTGTG  
**GCGTTCTTTGGTCAAAGTGAAGCTGGT**TGGTGGAAAGAGAGTCTTCAAGCCAGTGGAAC  
GACTTGGTCAAAGAGTTCGTGACGCTGGTATTCAAGGACTCCAAATTGCCCAACAAGG  
**AGCCAATGTTTTGGCAACGGTTCGAGGTGGACCACCCAACAAGGA** **TAA**CTGGAATGC  
AGAGTGCAATTAATTTTTTCGAATTTGTATTAATTTATGATATTTAATTTATTTATTGGA  
AAGTGTGAGACAGAAGAAGTTTGGAAAATAAACTTTGGTGTGATTTGTGAAAACGAAA  
AA

### C4669

CGATACTCTTGGGCGGATTGTGTAGAGTCTTTATCGTTTGTGAGATAAGAAAATTTTCT  
CAATACTGAATAGCGGTAGGATCGCGAGGGCAGCCACATTGTATTTAGAGGGTCGGC  
ATTCTGTTCCCGTGCGGTAAACCAAATCACGACATGCAAGCGAAGGAAAAAGTCGGTC  
AAAGAGTTCNNATAAAAGCTCAATATGGATGCAAAAACCGCATCACTCCCGTGTCTTCT  
AAGCATTTCAGTTCGAGTCTTTGCATAATCTGTGAAGCTGAAAAACAAA **ATGA**AATTC  
**TTAAGATTTTATTTGCTTTCACCATTCTTATTGTTGCTTTCGCTGGACAAAGTGAGGCT** **A**  
**GTTGGTTCAAAAAGTGTTCAAGCCAGTGGAAAAAGTCGGTCAAAGAGTTCGTGATGC**  
**TGGAATTCAAGGAGTAGCCATAGCCAGCAAGGAGCTAATGTTTTAGCTACGGCTCGA**  
**GGAGGACCACCGCAT** **TAA**TGACTGAAACTAACGGGTTCAAGGATTCATATTTGGTTAT  
GTTTGCTAACTTGGATGTTTCACATAACAAATTCATTTGATATGAATAAAAAGGAATAA  
TAATAATAAAAATAATAAATTGTATAAGAAAAAAAAAAAAAAAAA

### C3195

ATAAGTTACAAATGAACGTAAAAACAGCAGCACCTCAGGATTGCTCCAAGTTCCGACA  
AAGGTGTCTTGAATTGATTCATCCGCGTTGAAAACGTGTGCGCCGAATTCGGGGCTTTTT  
AAAATACTCCCCATTATCGCAAACAGTCTTTAAACACGACCGGTGTCATTATCTACGTT  
TATTTGCAACTTTCTATAAAAACGTGCTGCCGGTGCACAAACGGTATCAGTTCAATATC  
AACTTTTCGAGTATATCAAGATAGCTCAAGCTAATTCCAAATCTCTAACAGAAATCAA  
**AATGA**AATTCACTAAACTTTTCGTTGTCTTACCATTCTTATCGTTGCTTTTGCTGGCCA  
**AAGTGAAGCT**GGCTGGTGGAAAGAAAGTCTTCAAGCCTGTGGAGAACTTGGTCAACGA  
**GTTCCGGATGCTGGAATTCAAGGAATCGCAATTGCCAACAAGGAGCCAATGTGTTGG**  
**CTACGGTTCGAGGTGGACCACCACAA** **TAA**TTGCCATTAAAGAATATAGTTGTTCCCTATT  
TATTCAACTTAATATTACAATAAATTATTTATTTAGCAAAAATTTAAAAAAAAAAAAAAAAA  
AAA

C16493

GCAGCGAGTCATAAAGCAAGTGGAACAATCTGATCAAACAGGACGCCATGCAGGTGT  
GAGCGGAATCAGCATCAGTTCAGCATTTTATTAGCAATCGTCGCTTTC AAGCAGACAA  
ACAATCAAATAACATTCAAAGTCAAAAATGAATTTCACTAAGCTTTTCGTTGTTTCGCT  
GTTGTCCTTGTTCCTTCGCCGGTCAAAGTGAAGCTGGTTGGTGAAGAGGGTCTTCAA  
GCCAGTGGAAAAATTTGGTCAACGAGTTCGTGATGCTGGTGTTCAGGGAATCGCAATT  
GCTCAACAAGGAGCCAATGTTCTGGCAACCGCTCGAGGTGGACCACCACAACAAGGAT  
AATTGTGATAGATTAGCTTAACTGTTCTAAATGTTATTTATTCTCTATAATTTATTATT  
GAACGACAAAATGAAAACCTCGAAAAATAAACTTGGTTTATGAAAATGAAA

C53857

GCCTTATCTTCTGTTTGGACTTTTATAGATCAATCTATTTGTCAACATGAAGTTCTTTTC  
CCTCTTTTTCATCGTTATCTTCGCCATCCTTGGACTGCAACAGGCCGCCATGGCATGCAT  
CAACAATGGCGACGGTTGCCAACCTGATGGTCGTCAAGGAAACTGTTGTTTCAGGATAT  
TGTCACAAGGAACCAGGATGGGTTACTGGTTACTGCCGCTAGATTTATGCTTTATTGGC  
ATTGCAAGAGAAGATATATCCTTCTATTATCACTACTGTGCAGAAATCGATAAATTTCT  
GCATTATTAACGCAGTAATCCGATTAACATTTGATGTAACATTGAAATTGTTAATGCTT  
TTATTCTTGCAAGATTTATTAACACATGTAATATTTAAA

C16137

TACTTTCTCTAGAATGAATATCCAGGGTAATGCAGTTTCCAATCCCGCTGGAGGACAGG  
ATGTGACCGTAACTGCTGGCAAGCAATTTGGTCCGACAATGCGAATATCACAGCTGG  
AGGTTTTGCTGGGGGTAACTCTACGCGGGCCACCAAATGCTGGAGTTTTTGCAAGT  
GCTAATGCCAATGGTCACAGTCTATCGGTTTCAAAAACCGTTGTCCTTGAATATCATC  
AACGACTTCCCATGGTGCCAGTGCAAACCTCTTCCGCAATAA

C73537

CCAGTATTAATCTTAACCCAATTCGCTTAACTACCTGAAAACCCAATCAAAAATGCA  
ATTCACAAAACTTTTGTTGTTTTACTATTCTTATTGTTGCATTTCGCTGGTCAAAGTGA  
AGCTAGTTGGTGAAGAAAGTCTTCAAGCCAGTGGAGAACTTGGTCAACGAGTCCGT

GATGCTACCATTCAGGGAATCGGAATTGCTCAGCAAGGTGCGAATGTTTTGGCAACCG  
TTGAGGTGGTCCCCACAATGA TTGTTTCATTAAATTAATATATAGTTCTATTTGTTAA  
TGTCTTGCTCTACCGTCCTGTATTTATGATAAATAAACTATGTTCTTGTTAATTAACTTA  
AAA

**C10649**

TTCATCACGCGAAGTTCAATTTAATTGGTACAAAGATAACCTCCACCTCCCATCAAAAAT  
GAAACTCGCACTATATCTCGTTATTTTTGCTGTGATTCCTCCATGGTTCTGGGT CAGTT  
TGACAATCTAGAAGATACAGGAGTTGAGGAGAAAGTTCGTCATAAGCGCCTAACCTGC  
CTATTCGACAATCGCCCCATCTCAGCATTGCGTGTGGTTCCAACCTGTGTTTCACGAAA  
AGGAAAACGTGGTGGATGGTGTGTCAATGGAGTTTGTAGATGCACC TAA ATTTCTGAA  
ATTCCCCTGAACATTTTATTGTAATCAACATTAAGTATTTATCAAATTTTGTGTTTC

**C5878**

TCCATCAATTAAGTTCAAATTTTTGTAACGAAGATAACGTTTATTTTATATCAAAAATGA  
AAATCGCAATAGTCCTCGCTATTTTTGCTGTTATTTGCTCGATGGCCTTGCA AGGCCTG  
AAGGTTTGGAGGATGTAGAAGATTCAGAAGTTGTGGAGTTAGTTCGTCATAAGCGTTT  
GAGCTGCCTCTTCGAGAATCAAGCCATCTCAGCGATAGCATGCGGAGCCAGCTGTATT  
ACACGGAAAGGACGACGAGGTGGATGGTGTTCGAATGGAGTGTGTAGATGTACCCCTA  
ATTAA GACTGCAGATATTTTAATATTTTTATATAATT

**C5151**

AACCCACAATCGACTACGAAACAAAATGA AATTTCTCAAAGCTTCTCATCGTCTTTACAA  
TTCTCCTGGTTGCTTTTCGCCGGTCAAAGTGAATCACGCAGTTTGTGGAAGAAACTCTTC  
AAGCCAGTGAACGAGCAGGTCAAAGAATCCGTGATGCAACCATCAAAGGCATTGTTA  
TTGCCCAACAAGGAGCAAATGTTCTGGCAACAATTCGCGGGGGTCCAGCAATCCCTCC  
CGGACAAGGT TAA GTGGATGCGTGCGAAATGAGATTAGCGGAGTTTAGATCATCTGAT  
AAACTTATAAATAAGACTGTGCGAAAATGTATAAATGTAGTATGT

**C69719**

TCTATTCTCATCCAAGCAACATCTCTTGAAAAAGCGAAACAAA ACTAAACATG GTGAA  
GAGTGCCGTATTGCTGATGATGTGCGTGGCTCTGGTGGTGATCATCTCGACTCCTGCGG  
TCGAGGCA GATGTCAGTATTGGTAGCTGTGTGTGGGGCGGCAGCAACTACGTATCAGA  
CTGCAATGGAGAATGCAAGAGGCGAGGGTATAAGGGAGGACACTGTGGCAGCTTCCT  
CAACAACATCTGCTGGTGTGAAACG TAA AGGGAATCTAAGACTGGCTGCGAG

**C2676**

GTTGATGGCACCAACAGCTTGATCAGTTTCCTTGAGTCTATCAAAGAACCAAACATTCC  
AAAATGAAGGCCTTCGCAGTCATTGCTTTCGCACTCGTCATCTCTGTTGCCAAGGCAC  
AGTTTACAGCCGTTGTGGTTTCGCTCAAACCTCTCTACTACGACTATGGCGTAACTGACA  
TGAACACCCTCGCCAACTGGGTCTGTTGGTTCAATACGAATCATCCTTCAACGATCAA  
GCTGTTGGTGCCATCAACTACAATGGAACCCAAGATTTCCGGTCTTTTCCAAATCAACAA  
TAAATATTGGTGCCAAGGAGCCGTGAGCTCATCTGACAGCTGTGGTATCGCTTGCACCT  
CACTTCTTGAAACTTGTCTGCTTCTGGAGCTGTGCCAACTTGTCTACCAACAACAA  
GGATTCAGCGCCTGGTACGGATGGCTCAACAACCTGCAATGGAACCTGCTCCAAGTGTG  
CTGACTGCTTCTAAAGTTTTGTTGAAGTTTGAATAAATAGATCGGAAGAG

**C779**

AGAACCGAACTATTCACAATGAAGCCATCGCAGTTATTGCCCTGCTCGTTCTTGTTGC  
CTGTGCCAAGGC AAGGTTTACACCCGTTGTGAAATGGCACGTATCCTCTATCACGACC  
ATGGTGTA AAAAATCTAACCACCCTTGCCAACTGGGTTTGTGTTGATTGAACACGAATCA  
GGATTCAACGATGAAGCCGTGGGTGCCCTCAACTCCAATGGAACCCGTGACTACGGTC  
TCTTCCAAATCAACAACAATACTGGTGCAAAGGAAACGTTGCTTCCAGTGACAGCTG  
TAAAATTGCCTGTACCGCTTCTCGGAAACGTTGATGCCTCCTGGAAGTGTGCTCAAC  
TCGTGTACAAGGAACAAGGATTCAAGGCCTGGTACGGATGGCTTAA

**C14202**

ATATAGTACGAATTTAGAACATCCAATGGTATTACTCCGGCATTATAAAAGCAACATG  
GATAAATCTTCAA AATTGCGATTTATCGACTTCAGTTTGGTTCTGTTCACTATCGAGTA  
AGGATGAAGTTCTGTACAGTATTCCTGTTTCTGGTTTTAACTGTGTTTGCCTCTGTGGAG  
TCTAAGCGATTCACAAAGTGTACCTTGGCGAGAGAACTGTTTCAACGTGGTATCCCCA  
AGTCTGAGCTGCCC GACTGGGTCTGCTTGGTTCGCTGGGAGAGCAACTATCAAACGAA  
TGCAATGAACAAGAATAACAGGGATGGCAGTTGGGACTATGGACTATTTCAAATCAAC  
GATAAATGGTGGTGCAAAGGACATATTAATCTCATAATGCTTGC GGTTTGTTCGTGTAA  
TGAACCTCTGAAGCACGCCCCCATTGCTTACGTCTGCGTAACGTCCCGCTATAA

C3566

AATCCGATATAAAAAGCCAAATGGCATTTCGCATCTAGATCAGTTTCAGATCGATCTTC  
GCCTAAAGATCATTCCAAAACTAGAATAGTTAAGAAATCAGTCCCGCATTACC**ATG**  
AGAACTTTAAGTCTTTGCGTTTTGTTTGTATCCTCTTTTGCGCAAGCCAAGGATTAGCG  
GCGAAGATGAGCCGGTGTGGAGTAGCTAATATGCTGCTGAAATATGGATTTCCAGGA  
AAGATTTAGCCGACTGGGTGTGTCTGATTGAACATGAGAGTTCCTTCAGGACGAACGT  
CGTCGGACCTCCAAACACAGATGGCTCACGGGATTATGGATTGTTCCAGATCAACAGC  
CGATATTGGTGCTCCGGGGATGGTCCATCGCATAACATGTGCCGTATTCCCTGCCGAAT  
GCTCCTCTCCAATGACATGACCCATTCAATCCGCTGTGCTGTAACCGTGTTCAGGAAGC  
AAGGATTAAGTGCCTGGTACGGCTGGTCTGGACATTGCCAGGGTAACGCGCCAGTGT  
GGAGAACTGCTTCAGGAGCTATAACAACCTCTATTATGGAAAA**TAG**AATAGTTTCGAA  
TATTAGGACGTAAGATAGTTACTAAGTGTTAAATAAAGTGATGTTAATAAAAGAAATA  
GCGCCTAGATTTTTGCCACGTGACCGATTAATAGACGAAACCATATTACATAATCAA  
AGATAGCACTCTGGGTCAACGTCTTATATCTTTGGTCATT

C269

ACGCTTGATATAGGAATTTGCGCGTTTCTACCAGAAGAAGCTTTAAAAGTTTTCACTAT  
TCTAGATTGTGTCTAGTTGCTCCACAGATACAAACTTCACCAGTTGGTGTGGGCGTTTG  
GTGCGCTTCAACGAACAACACCTGAGTTCTCAGAATACTTGAAGTGATCATAGCGTA  
GCCAGTCAAGGCACTGAGACTTTAACGCGGTGCTAAGTGTAGATGAAGAGACTTTAAG  
GTCGCGTTTGTTTACCGCAATTCATCGAAAGCAA**ATGGCATCAGCAAAGGTGATATA**  
**TTGTTGAAATCAATAGTGACCATCAGTCTTTTATGCGCATGGAGTGAAGCC**AAAGTTTT  
CACGCGATGCCAGCTCGCCAAAGAATAATTCGTTATGATTTCCCGAGGACATTTTTAT  
CAAATTGGGTTTGCTTAATTGAGAGCGAAAGCGGACGCAGCACTTCGAAGACGCTTCA  
GCTGCCTAATACGAGCGCCAACCTATGGTATATTCCAGATCAATAGCAAAACATGGTGC  
CGGAAAGGACGGAAAGGAGGTCTGTGCGAAATGAAATGTGAAGATTTCTTAACGAT  
GATATTTTCGGATGATGCCGTTGCGCAAAGCAAATCTACAATAGACACGGCTTCCAAG  
GTTGGCCTGGATGGGTAAATAAATGTGCGGACGTGCTTTGCCTGACGTAATAATG  
**TTAG**TCGTTAAGCACTGAAGTCAATAACAGGCTTGTTGGAATGCAGCTCTCCCATCTG  
TTGCAGTAAAAAATCTCTATATTTATATGCATATCAATTGTTGATTCAAAGAGGCACC  
CTGAAGTAGGCGGAAAGTGACATATGTATATTATACATACGCGTATTAAATTCATCATT  
TGTCGAGTTATCTGTAAAGGGCCCTTGAAATTCAGAAATAAAATTTTCAGGAATTCAAA  
AATAGTAACCAATTAATATACATATGTAGAAGAGCCAGATATGAATAAGTATTGGTAG  
TTAATTTGCGATTGTAAGTGTGCGATCGAATTTTTTTCATGTCTTTTATAAAATTTATAAG  
TCAACTTTGGTGGATTTCTTTTACAAGCAAGCATGGATCCGGATGACCCCAAAGTCTAT  
ACCTTCATTACCCATATTTTCTCTATGGTATGGTATGGCTATGTCTTCTCTTTTTCTAA  
GCCGTTCTTCCCAAGCGTAATCAACTTTACTTCAACTAAAAACAAGTCGGAAACCAG  
AAGCTCTGCATGCTTCCGGTAGGAAAGTATTCCCGTATATGCATTTACGGGGCGAACAT  
ATTAGGAGGTCTTCATAATTGAACCTATTTTATTGCATATATCTATCTAAGCTATCCTAG  
AATATTCTGCAGAAATTCCAAGAAAAAATTTGCATTCTTTTAAATTTTATGACAGGCTC  
CGGTTGGAGCGCCCAAGTTATCTACGTAATCTTCTCCGATATAGCGTATTTGTACATGC  
TCGGCGTGAACCCC

C36111

CTGGTTGCAGTCTTTAACC GCGTTCAAAGCAGACAGTGCCATTCTGCCTGCAAAAATAT  
TAACG **ATGA**AGTCTCTATCACTTCTCTCGGTAGCCATCTTACTGGTTGCAGTCTTTAACC  
**GCGTTCAAAGC** AAACAATTCAACAAATGTTCACTAGCCACGGAGCTATCTCGTCTTGGT  
GTACCAAAGTCGGAATTGCCGGATTGGGTGTGTTTAGTGCAGCACGAAAGTAACTTCA  
AGACGAATTGGATCAACAAGAAAACTCCAATGGCAGCTGGGATTTCCGGCCTATTCCA  
GATCAACGATAAGTGGTGGTGTGAAGGACACATCAGGAGTCATAAACTTGCAATGTT  
AAATGTGAAGAACTGGTGACCGAGGACATAGAGAAGGCTTTGGAATGTGCGAAAGTG  
ATCAAAAGGGAGCGGGATACAAGGCTTGGTACGGGTGGTTGAATAATTGCCAAAAC  
AAGAAACCATCAGTAGACGAATGTTTT **TAA**GGATACTCTGTAAACCCTCTCACGTTCTT  
AGTAATCTTTTTAGTAAATTAAGATAAAAATCACACTTGTGTTGCTAACAAATGTTTTA  
TTTCAAAACTAATATCTACTTCTGTTGCTAATAAAAAGCGAAAAAGGAAGGAAGCAGA  
TCGGAAGA

C309

ATATTTAGCGAACTGCGTTTGATTCACTGGAGTGCAAACACTTGAAGTGTCAA **ATGA**  
**AGTTAGTAATTTTCTTGGAGCTTTTGCGGTCATCACTTTTGCAGTTGTTTCTGCA**ACAC  
CCGAAAATCTTGAGGGTTTAGAGCCATTGGAAAATGCAGAGTCATTGGACAATCTGGG  
AATTGGAGAGCTCGAGAGACCCAAGCGA **GTTAGTTGCTGGTTTGAAAATGAAAATATA**  
AAGGCTTCAGCTTGCCAGATGAGTTGCATGTATCGAAAAGGACGACGAGGTGGAATGT  
GTGTTAATGGAGTTTGTACCTGTTCTCCTAAC **TAA**ATTTTGAAATGTTATATATGTGCAT  
ACAATCGATGTATAATATGTATATCAAATAATTGTGAATTTATAAATTAAGCTGTTTT  
TGAGGAAATAAATACTTTGTGTAGGAGAGATCGGAAGAGCGT

C1827

TTTCTTTATCAAA **ATG**GCTAGACCAACGCTCTTGGCTTTGATCTTATTAATTATAACCTT  
**TGCGGTGGTAAATTCC**AATTCAGTGGACGAAAATAATGGAAATTTCAATCAACCGGTG  
CAACAGCTTGAAACGAACCTTCCTTATGGATCACAACCTACGGGAAAAACGC **ACAA**  
CCTGCACCCATTTGAATTGCAAACTTCATTGCGTATTATACAGGAAACGTAGTGGACGT  
TGTGATCGGTTAACATTTGTAAATGTATTTC **TAA**

C13793

AGCTGCTTAGTATACGCATCTTCTGAGCAAGTTGTTATTGTTTTAAATTAATAATGTTTTG  
TAAAATTTGCCGGTATTTCTTAATCTTAATAATTCTTTTCGATTGGTTTGCAACAAATAA  
AGGAAGTTAGTACGAAGGAATCCAGTGATCCAGACTCAGCGTTGTACTCAGATATTCA  
CCCAAGGTTTAGGCGACAGCTCCCTTGCGATTATCTTAGCGGTTTGGGATTCGGCGAAG  
ATGCCTGCAATACGGATTGTATTGCAAAAGGACATAAAAAGCGGTTTTTGCCTGGACT  
CGTTTGTTCGTTGCAGAACCTTA TAG TCTGTGCAGATAATTAATTTTCATAAGATATAAC  
CCAATCTAATCGACTCTGCTGCCATTGTATGCCAGATCGGAAGAGCGTCGTGTAGGGA  
AAGAGTGTGCCTCTATGTG

### C698

ATTTACTAGCAATCGCTTTCAAGCAGAAACAATCAAATTATATTCAAAGTCAAAAATG  
AATTTCACTAAGCTTTTCGTTGTTTTTCGCTGTTGTCTTGTTCCTTCGCCGGTCAAAGT  
GAAGCTGGTTGGTGGAAAGAGGGTCTTCAAGCCAGTGGA AAAAATTTGGTCAACGAGTTC  
GTGATGCTGGTATTCAAGGAATCGAAATTGCACAACAAGGAGCCAATGTTCTGGCAAC  
CGCTCGAGGTGGACCACCACAACAAGGA TAA TTATGAGAAATTA ACTTAACCTTACCC  
AAATTTTATTTATTTATTTTAAATTATTATTAAAATCAAAAAGAACAAAATTAATGTTT  
AGAAAATAAACTGTTAT

### C2730

GTAGTTCATCTCAATCCATTCAAATCCAAATTAACAAAATGAATTCACAAAGCTTTT  
TGTGTCTTCGCCGTTGTTCTTATCGCCTTCTCCGGTCAAAGTGAAGCTGGTTGGTGGAA  
AGAGAGTTTTCAAGCCAGTGGA AAAA ACTTGGTCAACGAGTTCGTGATGCTGGTATTCA  
AGGACTCGAAATTGCACAACAAGGAGCCAATGTTCTGGCAACGGTTCGAGGTGGACCA  
CCCCAACAAGGA TAA CTGGAATGCAGAGTGCAATTAATTTTTTCGAA

### C1875

CTCAAAGTATCTCATCTCAGTTCAACCTCCAATCTATAATAACTATCAAATCCAACCAA  
AATGAACTTCACAAAGCTTTTTGTCGTATTC ACTATTCTTCTTGTTCGTTTCGCCGGACA  
AGGTGAATCAAGGAGTTTATGGAAGAAAATCTTTAAGCCAGTGGA AAAA ACTGGGTCAA  
CGAGTTCGTGATGCCGGTATTCAAGGAATCGCAATCGCTCAACAAGGGGCCAATGTTT  
TAGCCACAGTTAGAGGAGGCCACCACAA TAA TTGCTACAATAGATTAGTTACACAAA  
ATTTATTTGTACCGAA



C49215

GACGTGTGCTCTTCCGATCTTAGTAATTCAGGAAGGTACCTACGATACGCCATTAACAA  
CCAAAATGAAATTCTTCAACGTTTTCTTCATCGTTATCTTCGCCATCCTTGGACTGCAAC  
AGGCGGCCAACGCTTGTATTGCCAACGGTAATGGTTGCCAACCTGATGGACGTCAAGG  
AAACTGTTGCTCCGGCTTCTGTTACAAACAACGTGGATGGGTTGCTGGTTATTGCAGAA  
GAAGATAAATTATTATTACTAAATTATTTAATGATTAATTACGATTATTATGTTGAT  
GTTTTGGGTATTTTACAATTAAGATTTTAA

C16634

ACAAAACCAAACCTTACTTTACCCCAACAAAATGAGATCATTCAAGATTTTGTTTATTA  
CATTGTGTCCTTAATCGTGGCATCAATTGCCATTCGATCCATCGAGGATAACTCAAGAA  
AGCAAGGAAGGAATTGAAGATAGTAATGCTGGCGTTCCTGCAATCCCAAAGAACAAG  
ATCAGTTGGTGATGATGGATATTGAAGTTGGGGACGAAAATGCTGATGCAAAGGACGA  
GCCTCTTCAAAGGATAAAATGTACAGCAAGTATATGTACACAAATCTGTCCGATTTTG  
AAATATAAATGTGGATATTGTGCGAGTGCAGTCGCTGCGTATGTTTGAAGTGAACA  
TTTTTTTTTTATAAATTCATAAGAAAATAAACTTTTTTTAGATAAATTCAAAA

C37730

AAATCAAACGAGATTTCTATTACTCGTGTAGAGATTCACCTCAATTCGAGGTCTACATA  
TTTCGATTCACCGCCATTTCAAAAATGCAATTCGTAAGATTTTGCTTGTTATCTTGTCAC  
TTTCTCTGTCGGCTTTTGCTTTTGACGTGACAAGGAAAATCAATCCTGAAACCTCCGCA  
GTTGAGAGACCTGAAGTTTCTGAATATCCTGAAATTCCAAAAGGTACAAAACCTCAAG  
AGTTTGTGATGATGGACATTGAGATCGAGGAGGAAGGTGCGGATAATAGAGCCGAAA  
CGATCCAAAGGATAAAATGTGTACCGAGCCAATGCAATCAAATTTGTAGGGTTTTAGG  
AAAGAAATGTGGTTATTGCAAAAATGCATCTACATGTGTTTGTTTAGGATAAATGAT

C46948

AGGGAGCGGGGAATATACTTTAAAGTTTCAAATCAATCAATTTCTACTATACGAAGCC  
ATTTGCTTCAATTCGAGATCTACATATTTAGATTGACTTCAATTTCAAAAATGCAATTCGT  
AAACCTTTTCCTTGTGTTCTCCTCTCAATGATTCTATCAACGTTTGCTTTTGACGTGAC  
AAGGAAAACCAACCCTGAAACGTCCGTGGTTGGGGAGCCTGAAATTTCTGAACTTCCT  
GAAATTCAGAATTTCAAGAGGTTCGATGAGGAAGGTCCTGAAAAAGACAGTGAGGGA  
ATAAACCAGACGAGAAAATGTACTGCAAGTCAATGCACTCGTGTCTGCAAGAAATTAG  
GGTATAAACGCGGCTATTGCCAAAGTTCAACTAAATGTGTTTGTGTGATAAATGAT

C16883

ATGCATCGCTGATTATTGCAATTGTTGGAATCTGCTGCACTTCAACGTTGGGCCAACTA  
TCAGGATCGATTACACCCGATATGGCGGGAGGCAATAATGTTAACATCATGGCATCGA  
AATTCTTAGGAAACCCCAATCACAACATTGGTGGAGGAGTTTTTCGCATCAGGAAACAC  
ACGATCCAATACTCCATCCTTGGGAGCTTTTGAACCCTAAACCTAAAGGACCATAGTT  
TGGGGGTGTCGAAAACCATCACTCCAGGGGTAAGTGATACATTAGTCAAATGCACG  
ACTAATTATCCTGAAGACTCCTGATCATCGCGTGGATGCGAACGTTTCAATAGTCATA  
CAAGGCTGAATAATGGATTCGCATTCGATAAACGAGGCGGTAGTCTGGATTATACCCA  
CAGGGCAGGACATAGTCTTTCTTTGGGAGCCAGTCATATCCCTAAATTTGGAACGACTG  
CTGAATTAACGGGTAAAGCTAACCTCTGGAAATCACCGAGTGGTCTATCAACGTTTGA  
TTAACTGGAAGTGCATCGTGA

C40487

ACACACTCTTCCCTACACGACGCTCTTCCGATCTATTGAACTGAAGTGTTAAGGCGCT  
TACAGCAACTCGACAAATCTTCATAAGAAAAAGGAAGAAAGTACTTTCTCTAGAATGA  
ATATCCAAGGTAATGCAGTATCCAATCCCGCTGGAGGACAGGATGTGACCGTAACCGC  
TGGCAAGCAATTTGGTTCCGACAACACTAATATCACAGCTGGAGCTTTTGCCGGAGGT  
AATACTCTACGAGGACCACCAAATGCTGGAGTATTTGCAAGTGCTAATGCCAATGGTC  
ACAGTCTATCGGTTTCAAAAACCGTTGTCCCGGAGTATCATCAACCACTTCCCATGCT  
GCCAGTGCAAACCTCTTCCGCAACGATCAACACAATGTCAATGCACAAGCATTTTCCA  
GTGCAACAAAATTAATGACGGATTTCAATTCAAACAACACGGAGCAGGTCTGAATTA  
TAACAATGCTAATGGCCACGGAGCTTCCATTGGCGTGAATAAGATCCCGGTTTCGGT  
AGTTCAATGGACGTAGGAGCAAGAGCAAATATCTTCCAGAACCCAAATACTTCTTTG  
ATGTCATGGCTAATCAAGAACTCACCTGAGTGGCCCTTTTCAAGGGAAAACAACTTT  
GGTAA

C29142

GGCATGTTTGAAACCTCCGTGCAAAGAGTTCCAATTCAACCTCCCATTGGAAGATACA  
ATTCAATAGTCCTTAAAGATACTTTGTGCTTTTTAAAGAACATACAAAATGCGTGTGAC  
CGTGTGTCTATTCAGTGTCTGCTTGCCTTATTTGCAATGGTCCATTGCCAACCTTTCCA  
CGAGACGGAAGGTGACCAACAGCTGGAACCAGTCGTTGCTGAAGTAGACGATGTTGTC  
GATTTGGTAGCCATTCAGAACATACACGAGAAAAACGAGCAACCTGTGACCTGTTGA  
GCCCTTTTAAAGTTGGTCATGCCGCATGCGCTGCTCATTGTATCGCAAGGGGCAAACGA  
GGAGGATGGTGTGACAAAAGAGCTGTTTGCAACTGCCGAAAAATAGGAGTACTAT

**C1619**

TAATCTCCATCCCGCTATACAGAGCAGAATACTTTGAATTTAAAATGAAGTTTACAATT  
AATTCGCGGTTTTTCTGGCCATTGCTCCACGGTGTGGCCATGCCAAATCATATTCAA  
GGATTAGAGGATGCCGAAGATACAGGGATTTATGCCGTCGGAGAGTTGTTCGAGGATTA  
AGCGCCTGAGCTGTTTGTTCGAAAATCAGGCGGTGTCAGCAATTGCTTGTGGATCGAGT  
TGCATTGCACGGAAAGGACGCCGAGGTGGATATTGCAGAAACGGAGTCTGCGTTTGT  
CCGATAACTAATTTTGTGGAGAAAATTAATTAATTATCGAAAGTTAATTAATACTGT  
TAGTATCATTGTTCCAAGTGTTAAATTAATAAAGAGTATTTAGTGT

**C6571**

TTACATTCATATCGGTGGAGTACATTTAGCATATAAAAAGCAGACAGCAGCTCTGCTTGG  
CGATAGATAGAAAAAGTGCTTGAGTTGAACACGTCTCTTTATCGACACATTTATACT  
TCTTTATTAATAATGCTCTACACAGATATTTCTGGCTTTGGTCTTATTAGTCGCCACTTTCA  
TGGGGGTAAATTCCAGTTCAGTTGGGGAAAACAACGGCAATAACAATCTTCCTGTCGA  
CCGGCTAGAAAGCGAACCGTCCTTAAGGGTCATAAACCTACGAGAAAAACGAGCAAC  
CTGTACCAATTGGAATTGCAGAACTCAATGCATCGCTCGAGGAAAGCGTGGTGGCTAT  
TGTGTCGAGCGTAACATTTGCAAATGCACTTCTTAGTATGCTTAAGTATCTTTTATTGCA  
ATGAATCACTGAACAAATAAAAAATTAAGATCGCAGATCGGAAGAGCAC

**C7985**

AGTCGCGCTAGATAGAAAAAGTTCTTCAGTTGAACACGTTTCCTTATCAAAAACATTTT  
TCACATTTTCTTATCAAAAATGAATAAACTGGCATTCCAGGCATTGGTCTTATTAATTGT  
CATTCTCACGCTGGCGGATTGCAGTTCAGTTGAGGAAAACAACCACCAGTCATTGGAG  
CACCCAAAAGGCGAACCCCTCTTAAAGATCATAAATCTACGACAAAAAAGA TTTACCT  
GCTCTAATCTGGGCTGCAAGGCTCAGTGCATCATTCTCGGGAACCGTAGTGGAGGTTGT  
AATAGATTAGGCGTTTGCCAATGTAATTAATAATTATTGCAACATTGTTGAACTACT  
GCAAGGCTCAGTGCATCATTCT

**C13326**

GAGCTTTCGATCAACACAGTCAGTCCATTCAATAACAAATTAAACTTAACCAAATGA  
AGCTTACTTTGGTACTTGTTCGCTTTGCTGTTATCTGTTCAATGGCTTTAGCAAGACCTG  
AAAACCTGGAGAACGTAGAAGATTCTGGAGTTGTGGAGCTGGTTCGCCATAAGCGTCT  
AAGTTGTCTCTTCGAGAACCAAGCTGTCTCAGCAATAGCATGCGGAGCCAGCTGTATT  
ACAAGGAAAGGAAAACGAGGTGGATGGTGTTCATGAGTAA

C390

TTTTTTTTTTTCAAGCAGAAGACGGCATACGAGATAATGATCGGTGACTGGAGTTCAGACGTGTGCTCTTCCGATCTGGTATTAGTATCGACAGCAATTAACCAATTCAAGATGAAACTCGCCATTGTCCTTTTGGGCTTTGTAGCCCTCTCTGTCGCCGCTCCACAACAACGCGGACTCGTTGGTAACATGCTTCAGGACCAGGTTACCAATGCTCAGTCTCAATTGAGCAGCCTTCAGGACCAAGTCAGCGATTTGAAAAACAAGATCGAAACTGATGCTGCCAATGTCATCTCCGCTGCTGAGGCCAAGCTTGGACCCATGTTACCCGATTTGGAAAACGAAATTTCCAATTGATTGCCAAGGGTGAAGTTATTGCTGATTGCGCCATCAAGAACCGCGATGATTTGGCAGAATTCAAACCCATCGCTTTCAACAACCTTACCAATCTGCGTGGAAGGATTAGCTGGAGATATTGGTTCCATTCTTCTTGGTGTGAATCAGATATCGGTGCATTGGCTGGTGCATCGCCAATTTGGCTCTTATTGCTGGTGAATGCGCTGCACAAGGTGAAGCAGGAGCTGCTATCTGCGCTGGTACCAAGGCCGGACCTATTGTAGGCAATGTCCTCTCCATCGTTGGTGATGCCGTCGCTGCTATTGGAATTGCCATTGCCAGGGCTCCTGCTATTGTTGCCGATGTCGAATACTGTGCCACAATGTCGTTGCAACTACCGTTGCCACCCTTAGCAAGTTCGGCGCCGCTGTTAAGAAGTGCGCTTAAAGCCCTTT

C17624

CTGCTGTCTCTCAATCAGTTAAGTTCATCAAAATCTAATCAATTGCAAAGATGAATCTAAGTTTGTGTTCTTTGCGTATGCCTGGCAGTCGTATCAGCTGTTAATATAACCAGCTGTAGACGATCTCCGCGAGGCGTTTGAAGCTGAAGACTCTCTCTATATTCTATCTCCGACGTAGAAGCCGAACAACCTAAGACTGCCAAGAAGCTCCACATACCCCGGAAGAGGCTACCCCAGCTTGAGGAAGATACAGCAAGCGATGATTGGGAAACCGAGCAGCTGAGGCTACCAAGAAGTATTCCAAACATTGAATATCATCACCAGCATCATATAAACATAAGCGGCCACACCGTAGTCTAGATGAAGCTTTTGAAGCTGAAGATGCCTATTACATCCCAATGTCAGATGAAGAGGTTGATTCACTTCGACTTCCAAGGAGTTTGGATGAACTACAAAAACAATTGAATCGGAAGGTCTCATCGACAATGTAGAATCCGGTCTGCGCCAAACGACAGATCTTTGCACAAGGTGGAGGAAGTCCAGGAAAAGGATATGACATCTATGCCCAAGGACGAGCAAATTATGGGAGAGTCAAACCAACGAAATAGCCTTCATGGAACAGCTTCTTATAGTCAACATTTAGGTGGCCCATATGGTAACAGTCGGCCAAATGTAGGCGGTGGATTAACTTTACACATCGTTTTTGAATAACTAAAAGTAGCTATATTTAACTTTTTATTTTAATTTCTTTAATTTATTAGTATTCAAT

C7347

CCAAAATGTTGACTATATTGACCTGTACCGTGAAGGGTGTACGTTTGTATTACTTTCCAAAGTTTTTTTTGACCTTGGATACTAAGATTGAAACCAGAATGTGGGCTTCCACCTCCTTGAATATTCAATTGCCTTTTTGCACGTTGCACTGTATGGTCTGCAACAATTTCTACGT

GTTCTTCTCCATCTCCTGATAA TGCGAGGTCATCAATACTGGGCAATCTGAGAAGTTCA  
GCTTCCTCATCGCTCACTGGAACGTAGTATGCATCTTCGGTTTCAAGAAGTTGTTCAA

### C9109

CGGTCGTGCCAAACGACAGATCTTTGCACAAGGTGGAGGAAGTCCAGGAAAAGGATA  
TGACATCTATGCCCAAGGACGAGCAAAATTATGGGAGAGTCAAAACCAACGAAATAG  
CCTTCATGGAACAGCTTCTTATAGTCAACATTTAGGTGGCCCATATGGTAACAGTCGGC  
CAAATGTAGGCGGTGGATTAATTTTCACACATCGTTTTTGAATAACTAAAAGTAGCTAT  
GTTTAACTTTTTATTTCAATTTCTTTAATTTATTAGTATTCAAATAAATTCAGTATGT  
TTATA

### C11804

CCAAAATGTTGACTATATTGACCTGTACCGTGAAGGGTGTACGTTTGTATTACTTTC  
CCAAAGTTTTTTTTGGCCTTGGATAC TAAGATTA AAAACCAGAATGTGGACTTCCACCTC  
CTTGAATATTCAATTGTCTTTTTGCCCGTTGCACTGTGTGATCTGCAACAATTTCTACGT  
TTGCTTTTCCATCTTCAGATAATGCGAGGTCGTCAATAC TAGGCAATCTGAGAAGTTCA  
GCTTCCTCATCACTCACTGGAAC

### C8756

CGCACCAGCCTCCGCGTCATCCCATGGCAAACCATCAAGTACGCAAGCGGCGTGCCC  
AACTTTGAAGGGACTCAAGAGATCGCAGGTTGCACGTTTCGCTTGGTGTATGTTGCTCCA  
CCACCTGGCTAGGAAGTTCTTCTTCTTCGATGGGGAGTTCCCGTGCGTATTCAGGACCG  
TCTTCTTCGTATTGTAGCTAATATGGTTGTGCTGAGGTGTATACGGCGAAAGCGGCAAC  
AATTAAACCCAAAACGAGGACAGAACGCATTTTAACTTTTAGTTTATGAATAAAAAGTT  
TAGATTAAGAAAATGCTGGAGCTTAACTCTGTTCTCTATTGATTGTCCATTTTGTGTATT  
GATAGCTCAGGTGTATA

### C2323

GTCTGAGATTGCCCCGAAGCATTGATGATCTCCATTATCAGAATACGAAGGAGTGCA  
CGTAGAAATTGTCGCCGATGACGAAGTTCAACGTGCAAAAAGGCAACTGAACATTCAG  
GGAGGCGGAAGTCCACATTCTGGTTTCGATCTTAGTGTTCAAGGACGTGCGAAAATAT  
GGGAAAGTGATAATGGACGCAACACCCTTTATGGTACGGGTCAATATGGTCAACATTT  
GGGTGGACCCTACGGTAATTCTGAACCCAGTTTCGGTGGTGGATTAATGTTCTCACATC  
GTTTCTAAATTTATATTTCTTTGAGTGTAATTATTAGCTATGCTTGGTTTGGAGAGAAGA  
TCGGAAGAGCGTCGTGTAGGGAAAGAGTGTGTCAGTACGTGTAGA

### C7345

CACTCTTCGCTTGGCTGTAGTGTCTGCAGCCAGTGTCCAGAACCAGCTGATCTT  
CGTGAAGCTTTTGAACACTGAAGATGCCATTTACATTCCAATTTCCATTGAGGAGGCGAA

CCGGCTAAGGTTACCAAGAAGTGCTCCAAAGCTGGAAGAAGAATCTGCCTTGTCATAT  
ATTCCAGATGC TCGGGAAGCAGAAATCGCAGAACCTGCGTCTTCTCATGGTCGTGTAC  
GTCGTGATGTTGAGCAAGTTCTTGAAACCGAAGATGCATACTACGTCCCAGTGAGCGA  
TGAGGAAGCTGAAGTTCTCAGATTGCCCAGAAGTATTGATGATCTCACATTATCAGAA  
GATGGAGAGGATCATGTAGA AATTATCACAGATGACGAAGTACAACGTGCAAAGAGG  
CAATTGAATATTCAAGGAGGTGGAAGTCCTCATTCTGGTTTTGACCT TAA TGTTCAAGG  
TCGTGCAAAGATTTGGGAAAGTAACAATGGACGCAATACCCTTCACGGTACTGGTGAA  
TATAGTCAACATTTGGGTGGACCCTACGGTAATAGCCGACCCAACCTTTGGAGGTGGAT  
TAGTTTTACCCATCGCTTCTAAGTTA

### C7346

CGCTTGCTTGGCTGTAGCGTCTGCCGCCAGTATTCCAGAACCAGCTGATCTTCGTGAGG  
CTTTCGAAACTGAAGATGCTATTTACATTCCAATTTCCATTGAGGAAGCGAACCAGCTA  
AGGTTACCAAGAAGTGCTCCAAAGCTGGAAGAAGAATCTGCCTTGTCATATATTCCAG  
ATGCTGCGGAAGCTGAAATCGCAGAACCTGCATCTTCTCATGGTCGTGTACGTCGTGAT  
GTTTCAGCAAGTTCTTGAAACCGAAGATGCATACTACGTCCCAGTAAGCGATGAGGAAG  
CTGAACTTCTCAGATTGCCCAGAAGTATTGATGATCTCGCATTATCAGAAGATGGAGA  
GGATCATGTAGAAATTATCACAGATGACGAAGTACAGCGTGAGAAAAGGCAGTTGAA  
TATTCAAGGTGGTGGAAGTCCTCATTCTGGTTTTGACCTTAATGTTCAAGGTCGTGCAA  
AGATTTGGGAAAGTAATAATGGACGCAATACTCTTCACGGTACTGGTGAATATAGTCA  
ACACTTGGGTGGACCCTATGG TAA TAGCCGACCCAACCTTTGGAGGTGGATAACTTTTCA  
CCATCGCTTCTAAGTTATTCTTTCTTTATAAATTATTAATTGTGTGT

### C11803

ACCGCTCTTCCGATCTTACCACACAGATAATAATTTATTTTCAACACGCACGATTAATA  
CCTTCCAATAAAGTATTAATTTAGAAGCG ATGTGTAAAACTAATCCACCTCCGAAGTT  
GGGTGCGCTGTTGCCGTAGGGTCCACC AAAATGTTGACTATATTGACCTGTACCGTGAA  
GGGTGTTACGTTTGTATTACTTTCCCAAAGTTTTTTTTGGCCTTGGATACTAAGGTTAA  
AACCAGAATGTGGGCTTCCACCTCCTTGAATGTTCAATTGCCTTTTTGCACGTTGCACT  
GTGTGGTTCGGCGACAATTTCTACGTGTGCTTCTCCATCTCCTGAT AATGCGAGGTCGTC  
AATACTGGGCAATCTGAGAAGTTCAGCTTCTCATCGTTCCTGGAACGTAGTATGCAC  
CTTCGGTTTCAAGAACTTGTTCAA

In Table 3 all the identified mature peptides are listed.

**Table 3.** Amino acid sequence of the identified antimicrobial peptides.

PEPTIDE	SEQUENCE
Hill_BB_C14202	KRFTKCTLARELFQRGIPKSELPDWVCLVRWESNYQTNAMKNNRD GSWDYGLFQINDKWWCKGHIKSHNACGLSCNELLKDDISKAVTCAR LIKRRQQGFRAWYGWLNHCTKVKPSIHECF
Hill_BB_C3566	AKMSRCGVANMLLKYGFPKDLADWVCLIEHESSFRTNVVGPPNTD GSRDYGLFQINSRYWCSGDGPSHNMCRIPCRMLLSNDMTHSIRCAVT VFRKQGLSAWYGWSGHCQGNAPSVENCFRSYNNLYYGK
Hill_BB_C1152	RYGFPRNQLADWICLVEWESSFRTDVAVGPPNGDGSRDWGLFQINDRY WCQSANYGNSHNICGVSCERLLSDDITTA VNCVRKIYAAHGFSGWNA WTQHCHSPSSVEHCFVESDCLPGGVSFDKHWL
Hill_BB_C1153	ASGRQFERCELARILHNRYGFPRNQLADWICLVEWESSFRTNVAVGPPN SDGSRDWGLFQINDRYWCKSSNYRNSHNMCVGSCEHLLSDDITTA VNC CVRKIYAAHGFSGWNAWTQH
Hill_BB_C2676	TVYSRCGFAQTLYYDYGVTDMNTLANWVCLVQYESSFNDQAVGAIN YNGTQDFGLFQINNKYWCQGA VSSSDSCGIACTSLLGNLSASWSCAQ LVYQQQGFSAWYGWLNNCNGTAPSVADCF
Hill_BB_C269	KVFTRCQLAKELIRYDFPRTFLSNWVCLIESESGRSTSKTLQLPNTSAN YGIFQINSKTWCRKGRKGGLCEMKCEDFLNDDISDDARCAKQIYNRH GFQGWPGWVNKCRGRALPDVLKC
Hill_BB_C1169	SNGPRDYGLFQINNQYWCQGNVKSANECHIACTSLLSDDITHALNCA KKIKAQQGFKAWYGWLNVCQKSKPSVKECF
Hill_BB_C779	KVYTRCEMARILYHDHGVKNLTTLANWVCLIEHESGFNDEAVGALNS NGTRDYGLFQINNKYWCQGNVASSDSCKIACTALLGNVDASWKAQ LVYKEQGFKAWYGW
Hill_LB_C36111	KQFNKCSLATELSRLGVPKSELPDWVCLVQHESNFKTNWINKKNSNG SWDFGLFQINDKWWCEGHIRSHNTCNVKCEELVTEDIEKALECAKVI KRERGYKAWYGWLNNCQNKKPSVDECF
Hill_LB_C12085	KTFTKCSLAKTLYAHGIPKSELPDWVCLVQHESGFRTDAVGALNSNG TRDYGLFQINNKYWCQGNVSSYNECNIACSALLSDDI
Hill_BB_C1290	QLNIQGGAKSPLSDFDLNVQGGARKYNNNGHKPLHGTEYDYNQHLGG PYGYSRPNFGGGLLFTHRFKLCSLSKLLIVC
Hill_BB_C7347	QLNIQGGGSPHSGFNLSIQGQKKLWESNNKRNTLHGTGQYSQHF
Hill_BB_C9109	QIFAQGGGSPGKGYDIYAQGRAKLWESQNQRNSLHGTASYSQHLGGP YGNRPNVGGGLIFTHRF
Hill_BB_C11804	QLNIQGGGSPHSGFNLSIQGQKKLWESNNKRNTLHGTGQYSQHF
Hill_BB_C309	VSCWFENENIKASACQMSCMYRKRRGGMCVNGVCTCSPN
Hill_BB_C1827	TTCTHLNCKLHCVLRYKRSGRCDFRNICKCI
Hill_BB_C5878	LSCLFENQAISAACGASCITRKRRGGWCSNGVCRCTPN
Hill_BB_C8756	QPYQLQYEEEDGPEYARELPIEEEEELPSQVVEQHHQAKRATCDLLSPFK VGHAACVLDGFAMGRRGGWC
Hill_BB_C13793	KESSDPDSALYSDIHPRFRRLPCDYLSGLGFGEDACNTDCIAKGHKS GFCTGLVCRCTRL
NHill_AD_C73537	GQSEASWWKKVFKPVEKLGQRVRDATIQGIGIAQQGANVLATVRGG PPQ
NHill_AD_C16493	GQSEAGWWKRVFKPVEKFGQRVRDAGVQGIAIAQQGANVLATARG GPPQQG

NHill_AD_C12927	GWWKRVFKPVEKLGQRVRDAGIQGLEIAQQGANVLATARGGPPQQG
NHill_AD_C12928	GWWKRVFKPVERLGQRVRDAGIQGLQIAQQGANVLATVRGGPPQQG
NHill_AD_C4669	SWFKKVFVKPVEKVGQRVRDAGIQGVAIAQQGANVLATARGGPPH
Hill_BB_C3195	GWWKKVFVKPVEKLGQRVRDAGIQGIAIAQQGANVLATVRGGPPQ
Hill_SB_C698	GQSEAGWWKRVFKPVEKFGQRVRDAGIQGIEIAQQGANVLATARGG PPQQG
Hill_SB_C2730	GWWKRVFKPVEKLGQRVRDAGIQGLEIAQQGANVLATVRGGPPQQG
Hill_SB_C1875	GQGESRSLWKKIFKPVKLGQRVRDAGIQGIAIAQQGANVLATVRGG PPQ
Hill_BB_C5151	GQSESRSLWKKLFPKVERAGQRIRDATIKGIVIAQQGANVLATIRGGP AIPPGQG
Hill_BB_C390	FNNLPICVEGLAGDIGSILLGVESDIGALAGAIANLALIAGECAAQGEA GAAICA
NHill_AD_C53857	CINNGDGCQPDGRQGNCCSGYCHKEPGWVTGYCR
NHill_AD_C49215	CIANGNGCQPDGRQGNCCSGFCYKQRGWVAGYCRRR
Hill_BB_C2323	QLNIQGGGSPHSGFDLSVQGRAKIWESDNGRNTLYGTGQYQHLGGP YGNSEPSFGGGLMFSHRF
Hill_BB_C7345	SIDDLTSEDGEDHVEIITDDEVQRAKR
Hill_BB_C7346	QLNIQGGGSPHSGFDLNVQGRAKIWESNNGRNTLHGTGEYSQHLGGP YGNRPNFGGGLLFTHRF
Hill_BB_C11803	QLNIQGGGSPHSGFNLSIQGQKKLWESNNKRNTLHGTGQYSQHFGGP YGNRPNFGGGLVFTHRF
Hill_BB_C21232	QLNIQGGSKSTFLILISMSKVRESNNGHETLHGTGDYNQHLGGPYGN SQPNFGGELLFTHRFKLCSLKLLIVCVFSKCRK
NHill_AD_C17624	QIFAQGGGSPGKGYDIYAQGRAKLWESQNQRNSLHGTASYSQHLGGP YGNRPNVGGGLTFTHRF
Hill_LB_C16634	IKCTASICTQICRILKYKCGYCASASRCVCLK
Hill_LB_C37730	AFAFDVTRKINPETSAYERPEVSEYPEIPKGTKLQEFVMMDIEIEEEGA DNRAETIQRIKCVPSQCNQICRVLGKKCGYCKNASTCVCLG
Hill_BB_C46948	RKCTASQCTRVCKKLGKRGYQCSSTKVC
Hill_BB_C16137	MNIQGNVSNPAGGQDVTVTAGKQFGSDNANITAGGFAGGNTLRGP PNAGVFASANANGHLSVSKTVVPGISSTTSHGASANLFR
Hill_BB_C16883	QLSGSITPDMAGGNVNIMASKFLGNPNHNIGGGVFASGNTRSNTPSL GAFGTLNLKDHSLGVSKTITPGVSDTFSQNARLILKTPDHRVDANVFN SHTRLNNGFAFDKRGSLDYTHRAGHSLSLGASHIPKFGTTAELTGKA NLWKSPSGLSTFDLTGSAS
Hill_BB_C10074	SPQDGRRGASVTVNNESSRRGTDVRADLNARLWEGNNRRSSLDANA YYQRHFGGPMGTGRPDAGVGLNFRHRF
Hill_BB_C9237	MNIQGNVSNPAGGQDVTVTAGKQFGSDNTNITAGAFAGGNTLRGPP NAGVFASANANSHLSVSKTVVPGVSATTSHAASANLFRNDQHSVNA QAFSSATKLNDFQFKQHAGLNYNANGHGASIGVKNIPGFGSSMD VGARANIFQNPNTSFDVMANSRTHLSGPFQKTNFGVSAGITRRF
	MNIQGNVSNPAGGQDVTVTAGKQFGSDNTNITAGAFAGGNTLRGPP NAGVFASANANGHLSVSKTVVPGVSSTTSHAASANLFRNDQHNVA



NHill_AD_C40487	QAFSSATKLNDFQFKQHGAGLNYNNANGHGASIGVKNKIPGFGSSMD VGARANIFQNPNTSFDVMANSRTHLSGPFQGKTNF
Hill_BB_C7758	AACDLFSALNVASSICAAHCLYLGYKGGYCDSKLVCVCR
Hill_BB_C14087	VTCDLLEPFLGPAPCMIHCVFRFRKRTGYCNSQNVVCRG
Hill_LB_C29142	ATCDLLSPFKVGHAACAAHCIARGKRGGWCDKRAVCNCRK
Hill_BB_C308	VSCWFENENIKASACQMSCMYRKRRGGMCVNGVCTCSPN
Hill_BB_C1619	LSCLFENQAVSAIACGSSCIARKGRRGGYCRNGVCVCTDN
Hill_BB_C1826	TTCTHLNCKLHCLLQRKRSGRCDFNICKCIS
Hill_BB_C6571	ATCTNWNCRQTQCIARGKRGGYCVERNICKCTS
Hill_BB_C7081	ATCDLISGTKIENVACAAHCIAMGHKGGYCNSNLICIR
Hill_BB_C7985	FTCSNLGCKAQCIILGNRSGGCNRLGVCQCN
Hill_BB_C7176	ATCDLLSPFKVGHAACALHCIALGRRGGWCDGRAVCNCR
Hill_BB_C2519	ATCDLLSPFKVGHAACALHCIAMGRRGGWCDGRAVCNCR
Hill_BB_C8473	ATCDLLSPFGVGHAACAVHCIAMGRRGGWCDGRAVCNCR
Hill_BB_C34351	AMCDLLSGLNMGRSVCAMRCILKGHRGGWCDQGVNCRV
Hill_BB_C4683	RPDNIEYLEDSQVAELVRHKRLSCLFENEAISALACGASCITRKRRGG WCSNGVCHCTPN
Hill_BB_C4977	LSCWFENEDIKATACAMSCIYRKGRKGGRCENGICRCTPN
Hill_BB_C13326	LSCLFENQAVSAIACGASCITRKGRGGWCSNGVCRCTPN
Hill_BB_C7171	TTCDLISGTKIENIACAHAHCIAMGHKGGYCNSNLICIR
Hill_BB_C10649	QFDNLEDTGVEEKVRHKRLTCLFDNRPIAFACGSNCVSRKGRGGW CVNGVCRCT
Hill_BB_C13792	KQSSDPESALYSDIHPFRRLPCDYLSGLGFEDACNTDCIAKGHKS GFCTGLVCRCTL
Hill_BB_C15867	VTCDLLKPFGRAPCMHHCILRFKRTGFCSRQNVVCR
NHill_AD_C69719	DVSIKSCVWGSNYVSDCNCECKRRRGYKGGHCGSFLNNICWCET
Hill_BB_C49430	APQFGGQIGFGGGGFGGGGFGPGGGFRPGGVAEFQESSSSVNVERET FDQGGFEISDSSVTSSSVSEFRD

#### 4.3. Bioinformatic analyzes for the prediction of AMPs biological activity.

All identified 68 sequences, encoding putative antimicrobial peptides, were analysed in silico by the four machine-learning algorithms, such as Support Vector Machine (SVM), Discriminant Analysis (DA), Artificial Neural Network (ANN), and Random Forest (RF), available on the free online CAMP

database, in order to predict their antimicrobial activity. The results are shown in Table 4. Table 5 reports the anticancer and non-anticancer scores obtained by the iACP tool. Table 6 shows the results obtained with the AVPpred server to predict the antiviral activity and with the Antifp server used to predict the antifungal activity. These analyses allowed the identification of 57 putatively active peptides, of which 13 show a putative antimicrobial activity, 22 show a putative antimicrobial and anticancer activity, 8 show an antimicrobial and an antiviral activity, 7 show an antimicrobial, an anticancer and an antiviral activity. Moreover, both the antimicrobial and antifungal activity were predicted for Hill\_BB\_C1827 and Hill\_BB\_C13792 peptides, whereas only the Hill\_BB\_C15867 peptide showed an antimicrobial, an antiviral and an antifungal activity according to the *in silico* analysis. The peptides Hill\_BB\_C46948 and Hill\_BB\_C6571 resulted as antimicrobial, anticancer and antifungal, whereas Hill\_LB\_C16634 and NHill\_AD\_C69719 peptides were positive to all activities in the prediction analysis. The remaining 11 did not show any activity according to the *in silico* investigation. In Table 6, all the predicted activities are listed.

**Table 4.** Prediction of the antimicrobial activity through the CAMP database. From left to right are shown in order: peptide contig, peptide sequence, Support Vector Machine (SVM) score, Random Forest (RF) score, Artificial Neural Network (ANN) result and the Discriminant Analysis (DA) score.

PEPTIDE	SEQUENCE	SVM	RF	ANN	DA
Hill_BB_C14202	KRFTKCTLARELFQRGIPKSELDPDWVCLV RWESNYQTNAMNKNNRDGSWDYGLFQI NDKWWCKGHIKSHNACGLSCNELLKDDI SKAVTCARLIKRRQQGFRAWYGLNHCT KVKPSIHECF	1.000	0.800	AMP	1.000
Hill_BB_C3566	AKMSRCGVANMLLKYGFPRKDLADWVC LIEHESSFRNTNVGPPNTDGSRDYGLFQIN SRYWCSGDGSPSHNMCRIPCRMLLSNDMT HSIRCAVTVFRKQGLSAWYGWSGHCQG NAPSVENCFRSYNNLYYGK	1.000	0.916	AMP	1.000
Hill_BB_C1152	RYGFPRNQLADWICLVEWESSFRDVAVG PPNGDGSRDWGLFQINDRYWCQSANYG NSHNICGVSCERLLSDDITAVNCVRKIY AAHGFSGWNAWTQHCHSPSSVEHCFVES DCLPGGVSFDKHWL	1.000	0.8045	AMP	1.000
Hill_BB_C1153	ASGRQFERCELARILHNRYGFPRNQLAD WICLVEWESSFRNTNAVGPNSDGSRDWG LFQINDRYWCKSSNYRNSHNMCGVSCEH LLSDDITAVNCVRKIYAAHGFSGWNAW TQH	1.000	0.918	AMP	1.000
Hill_BB_C2676	TVYSRCGFAQTLYDYGVTDMLANW VCLVQYESSFNDQAVGAINYNGTQDFGL FQINNKYWCQGAVSSSDSCGIACTSLGN LSASWSCAQLVYQQGFSAWYGLNNC NGTAPSVADCF	1.000	0.611	AMP	1.000
Hill_BB_C269	KVFTRCQLAKELIRYDFRPTFLSNWVCLI EESGRSTSKTLQLPNTSANYGIFQINSKT	1.000	0.8725	AMP	1.000

	WCRKGRKGGLCEMKCEDFLNDDISDDA RCAKQIYNRHGFQGWPGWVNKCRGRAL PDVLKC				
Hill_BB_C1169	SNGPRDYGLFQINNQYWCQGNVKSANEC HIACTSLSDDITHALNCAKKIKAQQGFK AWYGWLNQCQKSKPSVKECF	0.937	0.8045	AMP	0.993
Hill_BB_C779	KVYTRCEMARILYHDHGVKNLTTLANW VCLIEHESGFNDEAVGALNSNGTRDYGLF QINNKYWCKGNVASSDCKIACTALLGN VDASWKCAQLVYKEQGFKAWYGW	1.000	0.7555	AMP	1.000
Hill_LB_C36111	KQFNKCSLATELSRLGVPKSELPDWVCL VQHESNFKTNWINKKNSNGSWDFGLFQI NDKWWCEGHIRSHNTCNVKEELVTEDE EKALECAKVIKRERGYKAWYGWLNQC NKKPSVDECF	1.000	0.8235	AMP	1.000
Hill_LB_C12085	KTFTKCSLAKTLYAHGIPKSELPDWVCLV QHESGFRTDAVGALNSNGTRDYGLFQIN NKYWCKGNISSYNECNIACSALLSDDI	0.890	0.871	AMP	0.987
Hill_BB_C1290	QLNIQGGAKSPLSDFDLNVQGGARKYYN NGHKPLHGTEDYNQHLGGPYGYSRPNFG GLLFTHRFLKCSLSKLLIVC	0.581	0.5055	AMP	0.554
Hill_BB_C7347	QLNIQGGGSPHSGFNLSIQGQKKLWESNN KRNTLHGTGQYSQHF	0.307	0.374	NAMP	0.031
Hill_BB_C9109	QIFAQGGGSPGKGYDIYAQGRAKLWESQ NQRNSLHGTASYSQHLGGPYGNSRPNVG GGLIFTHR	0.351	0.6175	AMP	0.270
Hill_BB_C11804	QLNIQGGGSPHSGFNLSIQGQKKLWESNN KRNTLHGTGQYSQHF	0.307	0.374	NAMP	0.031
Hill_BB_C309	VSCWFENENIKASACQMSCMYRKRRRG GMCVNGVCTCSPN	0.827	0.6825	AMP	0.908
Hill_BB_C1827	TTCTHLNCKLHCVLRYKRSGRCDFNIC KCI	0.898	0.8805	AMP	0.995
Hill_BB_C5878	LSCLFENQAISAIACGASCITRKRRGGW CSNGVCRCTPN	0.971	0.941	AMP	0.994
Hill_BB_C8756	QPYQLQYEEDGPEYARELPIEEEELPSQV VEQHHQAKRATCDLLSPFKVGHAAACVLD GFAMGRRGGWC	0.266	0.0085	NAMP	0.037
Hill_BB_C13793	KESSDPDSALYSDIHPRFRRLPCDYLSGL FGGEDACNTDCIAKGHSFGCTGLVCRC RTL	0.503	0.5453	AMP	0.645
NHill_AD_C73537	GQSEASWWKKVFKPVEKLGQRVRDATI QGIGIAQQGANVLATVRGGPPQ	0.633	0.870	AMP	0.904
NHill_AD_C16493	GQSEAGWWKRVFKPVEKFGQRVRDAGV QGIAIAQQGANVLATARGGPPQQG	0.633	0.842	AMP	0.885
NHill_AD_C12927	GWWKRVFKPVEKLGQRVRDAGIQGLEIA QQGANVLATARGGPPQQG	0.672	0.9075	AMP	0.955
NHill_AD_C12928	GWWKRVFKPVERLGQRVRDAGIQLQIA QQGANVLATVRGGPPQQG	0.773	0.911	AMP	0.969

NHill_AD_C4669	SWFKKVFVKPVEKVGQRVRDAGIQGVAIA QQGANVLATARGGPPH	0.574	0.745	AMP	0.899
Hill_BB_C3195	GWWKKVFVKPVEKLGQRVRDAGIQGIAIA QQGANVLATVRGGPPQ	0.868	0.9945	AMP	0.988
Hill_SB_C698	GQSEAGWWKRVFVKPVEKFGQRVRDAGI QGIEIAQQGANVLATARGGPPQQG	0.558	0.718	AMP	0.770
Hill_SB_C2730	GWWKRVFKPVEKLGQRVRDAGIQGLEIA QQGANVLATVRGGPPQQG	0.700	0.9095	AMP	0.959
Hill_SB_C1875	GQGESRSLWKKIFKPVEKLGQRVRDAGI QGIAIAQQGANVLATVRGGPPQ	0.714	0.9115	AMP	0.949
Hill_BB_C5151	GQSESRSLWKKLFPVERAGQRIRDATIK GIVIAQQGANVLATIRGGPAIPPGQG	0.641	0.944	AMP	0.935
Hill_BB_C390	FNNLPICVEGLAGDIGSILLGVESDIGALA GAIANLALIAGECAAQGEAGAAICA	0.946	0.685	AMP	0.822
NHill_AD_C53857	CINNGDGCQPDGRQGNCCSGYCHKEPG WVTGYCR	0.811	0.742	AMP	0.973
NHill_AD_C49215	CIANGNGCQPDGRQGNCCSGFCYKQRG WVAGYCRRR	0.961	0.8735	AMP	0.999
Hill_BB_C2323	QLNIQGGGSPHSGFDLSVQGRAKIWESDN GRNTLYGTGQYGQHLGGPYGNSEPSFGG GLMFSHRF	0.163	0.048	NAMP	0.007
Hill_BB_C7345	SIDDLTSEDGEDHVEITDDEVQRAKR	0.456	0.1395	NAMP	0.024
Hill_BB_C7346	QLNIQGGGSPHSGFDLNVQGRAKIWESN NGRNTLHGTGEYSQHLGGPYGNSRPNFG GGLLFTHRF	0.223	0.1105	NAMP	0.019
Hill_BB_C11803	QLNIQGGGSPHSGFNLSIQGQKKLWESNN KRNTLHGTGQYSQHFGGPYGNSRPNFGG GLVFTHRF	0.278	0.3295	AMP	0.030
Hill_BB_C21232	QLNIQGGGSKSTFLILISMSKVVRESNNGHE TLHGTGDYNQHLGGPYGNSQPNFGGELL FTHRFKLCSLSKLLIVCVFSKCRK	0.749	0.8505	AMP	0.865
NHill_AD_C17624	QIFAQGGGSPGKGYDIYAQGRAKLWESQ NQRNSLHGTASYSQHLGGPYGNSRPNVG GGLTFTHRF	0.284	0.515	NAMP	0.170
Hill_LB_C16634	IKCTASICTQICRILKYKCGYCASASRCVC LK	0.992	0.913	AMP	0.999
Hill_LB_C37730	AFAFDVTRKINPETAVERPEVSEYPEIPK GTKLQEFVMMDIEIEEEGADNRAETIQRI KCVPSQCNQICRVLGKKCGYCKNASTCV CLG	0.988	0.9565	AMP	0.984
Hill_BB_C46948	RKCTASQCTRVCKKLGKRGYCSSTKC VC	0.968	0.9375	AMP	0.999
Hill_BB_C16137	MNIQGNVSNPAGGQDVTVTAGKQFGS DNANITAGGFAGGNTLRGPPNAGVFASA NANGHSLSVSKTVVPGISSTTSHGASANL FR	0.886	0.8225	AMP	0.758
Hill_BB_C16883	QLSGSITPDMAGGNVNMASKFLGNPN HNIGGGVFASGNTRSNTPSLGAFTLNLK	1.000	0.9275	AMP	1.000

	DHSLGVSKTITPGVSDTFSQNARLILKTP DHRVDANVFNSHTRLNNGFAFDKRGGSL DYTHRAGHSLSLGASHIPKFGTTAELTGK ANLWKSPSGLSTFDLTGSAS				
Hill_BB_C10074	SPQDGRRGSASVTVNNESRRGTDVRADL NARLWEGNNRRSSLDANAYYQRHFGGP MGTGRPDAGVGLNFRHRF	0.400	0.4375	NAMP	0.566
Hill_BB_C9237	MNIQGNVSNPAGGQDVTVTAGKQFGS DNTNITAGAFAGGNTLRGPPNAGVFASA NANSHLSVSKTVVPGVSATTSHAASAN LFRNDQHSVNAQAFSSATKLNDFQFKQ HGAGLNYNNANGHGASIGVKNIPGFGSS MDVGARANIFQNPNTSFDVMANSRTHLS GPFQGKTNFGVSAGITRRF	1.000	0.9505	AMP	1.000
NHill_AD_C40487	MNIQGNVSNPAGGQDVTVTAGKQFGS DNTNITAGAFAGGNTLRGPPNAGVFASA NANGHLSVSKTVVPGVSATTSHAASAN LFRNDQHNVAQAFSSATKLNDFQFKQ HGAGLNYNNANGHGASIGVKNIPGFGSS MDVGARANIFQNPNTSFDVMANSRTHLS GPFQGKTNF	1.000	0.9745	AMP	1.000
Hill_BB_C7758	AACDLFSALNVASSICAAHCLYLGYKGG YCDSKLVCVCR	0.985	0.819	AMP	0.988
Hill_BB_C14087	VTCDLLEPFLGPAPCMIHCIVRFRKRTGY CNSQNVCVCRG	0.712	0.6305	AMP	0.709
Hill_LB_C29142	ATCDLLSPFKVGHAAACAAHCIARGKRRG WCDKRAVCNCRK	0.956	0.9455	AMP	0.999
Hill_BB_C308	VSCWFENENIKASACQMSCMYRKRRRG GMCVNGVCTCSPN	0.827	0.6825	AMP	0.908
Hill_BB_C1619	LSCLFENQAVSAIACGSSCIARKGRRGGY CRNGVCVCTDN	0.972	0.900	AMP	0.972
Hill_BB_C1826	TTCTHLNCKLHCLLQRKRSRCDRFNICK CIS	0.878	0.9105	AMP	0.995
Hill_BB_C6571	ATCTNWNCRTOCIARGKRRGGYCVERNIC KCTS	0.950	0.9815	AMP	0.992
Hill_BB_C7081	ATCDLISGKTIENVACAAHCIAMGHKGG YCNSNLICICR	0.987	0.907	AMP	0.979
Hill_BB_C7985	FTCSNLGCKAQCIILGNRSGGCNRLGVCQ CN	0.991	0.9175	AMP	0.999
Hill_BB_C7176	ATCDLLSPFKVGHAAALHCIALGRRGG WCDGRAVCNCR	0.933	0.938	AMP	0.996
Hill_BB_C2519	ATCDLLSPFKVGHAAALHCIAMGRRGG WCDGRAVCNCR	0.895	0.8835	AMP	0.987
Hill_BB_C8473	ATCDLLSPFGVGHAAACAVHCIAMGRRGG WCDDRAVCNCR	0.855	0.8145	AMP	0.977
Hill_BB_C34351	AMCDLLSGLNMGRSVCAMRCILKGHRG GWCDQGVNCRV	0.816	0.6875	AMP	0.971

Hill_BB_C4683	RPDNIYELEDSQVAELVRHKRLSCLFENE AISALACGASCITRKRRGGWCSNGVCH CTPN	0.734	0.5745	AMP	0.645
Hill_BB_C4977	LSCWFENEDIKATACAMSCIYRKGRKGG RCENGICRCTPN	0.828	0.7115	AMP	0.913
Hill_BB_C13326	LSCLFENQAVSAIACGASCITRKGRGGW CSNGVCRCTPN	0.975	0.9475	AMP	0.991
Hill_BB_C7171	TTCDLISGTKIENIACAAHCIAMGHKGGY CNSNLICIR	0.981	0.8805	AMP	0.984
Hill_BB_C10649	QFDNLEDTGVEEKVRHKRLTCLFDNRPI AFACGSNCVSRKGRGGWCVNGVCRCT	0.860	0.595	AMP	0.983
Hill_BB_C13792	KQSSDPESALYSDIHPFRRLPCDYLSGL FGGEDACNTDCIAKHKSGFCTGLVCRC RTL	0.995	0.9725	AMP	0.965
Hill_BB_C15867	VTCDLLKPFGRAPCMMHCILRFKRTGF CSRQNVCVCR	0.826	0.5095	AMP	0.885
NHill_AD_C69719	DVSIGSCVWGSNYVSDCNGECKRRGYK GGHCGSFLNNICWCET	0.984	0.913	AMP	0.993
Hill_BB_C49430	APQFGGQIGGFGGGGFGGGGFGGGGFR PGGVAEFQESSSSVNVERETFDQGGFEIS DSSVTSSSVSEFRD	0.012	0.2715	NAMP	0.031

In Table 5 are reported the obtained scores for the anticancer activity prediction.

**Table 5.** Prediction of the anticancer activity through the iACP tool. From left to right are shown in order: peptide contig, peptide sequence, the anticancer and non-anticancer scores related to each sequence.

PEPTIDE	SEQUENCE	Anticancer SCORE	Non-Anticancer SCORE
Hill_BB_C14202	KRFTKCTLARELFQRGIPKSELPD WVCLVRWESNYQTNAMNKNNR DGSWDYGLFQINDKWWCKGHIK SHNACGLSCNELLKDDISKA VTC ARLIKRRQQGFRAWYGWLNHCTK VKPSIHECF	0.452542	0.547458
Hill_BB_C3566	AKMSRCGVANMLLKYGFPRKDL ADWVCLIEHESSFRTNVVGPPNT DGSRDYGLFQINSRYWCSGDGPS HNMCRIPCRMLLSNDMTHSIRCA VTVFRKQGLSAWYGWSGHCQGN APSVENCFRSYNNLYYGK	0.603649	0.396351
Hill_BB_C1152	RYGFPRNQLADWICLVEWESSFR TDAVGPPNGDGSRDWGLFQINDR YWCQSANYGNSHNICGVSCERLL SDDITTAVNCVRKIYAAHGFSGW NAWTQHCHSPSSVEHCFVESDCL PGGVSFDKHWL	0.744031	0.255969
Hill_BB_C1153	ASGRQFERCELARILHNRYGFP NQLADWICLVEWESSFRNAVGP PNSDGSRDWGLFQINDRYWCKSS NYRNSHNMCVGSCEHLLSDDITT	0.322215	0.677785

	AVNCVRKIYAAHGFSGWNAWTQH		
Hill_BB_C2676	TVYSRCGFAQTLYDYGVTDMLN TLANWVCLVQYESSFNDAQVGA NYNGTQDFGLFQINNKYWCQGA VSSSDSCGIACSTLLGNLSASWSC AQLVYQQQGFSAWYGWLNNCN GTAPSVADCF	0.508041	0.491959
Hill_BB_C269	KVFTRCQLAKELIRYDFPRTFLSN WVCLIESESGRSTSKTLQLPNTSA NYGIFQINSKTWCRKGRKGGGLCE MKCEDFLNDDISDDARCAKQIYN RHGFQGWPGWVNKCRGRALPD VLKC	0.353721	0.646279
Hill_BB_C1169	SNGPRDYGLFQINNQYWCQGNV KSANECHIACTSLSDDITHALNC AKKIKAQQGFKAWYGWLNQCQ KSKPSVKECF	0.995537	0.004463
Hill_BB_C779	KVYTRCEMARILYHDHGKLNLT TLANWVCLIEHESGFNDEAVGAL NSNGTRDYGLFQINNKYWCKGN VASSDSCKIACTALLGNVDASWK CAQLVYKEQGFKAWYGW	0.717440	0.282560
Hill_LB_C36111	KQFNKCSLATELSRLGVPKSELDP WVCLVQHESNFKTWINKKNSN GSWDFGLFQINDKWWCEGHIRSH NTCNVKCEELVTEDIEKALECAK VIKRERGYKAWYGWLNQCQNK KPSVDECF	0.644890	0.355110
Hill_LB_C12085	KTFTKCSLAKTLYAHGIPKSELDP WVCLVQHESGFRTDAVGALNSN GTRDYGLFQINNKYWCKGNISY NECNIACALLSDDI	0.500000	0.500000
Hill_BB_C1290	QLNIQGGAKSPLSDFDLNVQGGA RKYYNNGHKPLHGTEYNQHLG GPYGYSRPNFGGGLLTHRFKLC LSKLLIVC	0.878792	0.121208
Hill_BB_C7347	QLNIQGGGSPHSGFNLSIQGQKKL WESNNKRNTLHGTGQYSQHF	0.005102	0.994898
Hill_BB_C9109	QIFAQGGGSPGKGYDIYAQGRAK LWESQNQRNSLHGTASYSQHLG GPYGNRPNVGGGLIFTHRF	0.115082	0.884918
Hill_BB_C11804	QLNIQGGGSPHSGFNLSIQGQKKL WESNNKRNTLHGTGQYSQHF	0.005102	0.994898
Hill_BB_C309	VSCWFENENIKASACQMSCMYR KGRRGGMCVNGVCTCSPN	0.444002	0.555998
Hill_BB_C1827	TTCTHLNCKLHCVLYRKRSGRCD RFNICKCI	0.215222	0.784778
Hill_BB_C5878	LSCLFENQAISAIACGASCITRKG RRGGWCSNGVCRCTPN	0.724609	0.275391

Hill_BB_C8756	QPYQLQYEEDGPEYARELPIEEEE LPSQVVEQHHQAKRATCDLLSPF KVGHAACVLDGFAMGRRGGWC	0.000000	1.000000
Hill_BB_C13793	KESSDPDSALYSDIHPFRRLQPC DYLSTGLGFEDACNTDCIAKGHK SGFCTGLVCRCTL	0.051485	0.948515
NHill_AD_C73537	GQSEASWWKKVFKPVEKLGQRV RDIQIGIGIAQQGANVLATVRG GPPQ	0.508308	0.491692
NHill_AD_C16493	GQSEAGWWKRVFKPVEKFGQRV RDAGVQGIAIAQQGANVLATARG GPPQQG	0.520865	0.479135
NHill_AD_C12927	GWWKRVFKPVEKLGQRVRDAGI QGLEIAQQGANVLATARGPPQQ G	0.389374	0.610626
NHill_AD_C12928	GWWKRVFKPVERLGQRVRDAGI QGLQIAQQGANVLATVRGGPPQQ G	0.492318	0.507682
NHill_AD_C4669	SWFKKRVFKPVEKVGQRVRDAGI QGVIAIAQQGANVLATARGPPH	0.901851	0.098149
Hill_BB_C3195	GWWKRVFKPVEKLGQRVRDAGI QGIAIAQQGANVLATVRGGPPQ	0.839903	0.160097
Hill_SB_C698	GQSEAGWWKRVFKPVEKFGQRV RDAGIQGIEIAQQGANVLATARG GPPQQG	0.519633	0.480367
Hill_SB_C2730	GWWKRVFKPVEKLGQRVRDAGI QGLEIAQQGANVLATVRGGPPQQ G	0.481171	0.518829
Hill_SB_C1875	GQGESRSLWKKIFKPVEKLGQRV RDAGIQGIAIAQQGANVLATVRG GPPQ	0.702695	0.297305
Hill_BB_C5151	GQSESRSLWKKLFPVERAGQRI RDIKIGIVIAQQGANVLATIRGG PAIPPGQG	0.870751	0.129249
Hill_BB_C390	FNNLPICVEGLAGDIGSILLGVESD IGALAGAIANLALIAGECAAQGE AGAAICA	0.908553	0.091447
NHill_AD_C53857	CINNGDGCQPDGRQGNCCSGYC HKEPGWVTGYCR	0.991593	0.008407
NHill_AD_C49215	CIANGNGCQPDGRQGNCCSGFCY KQRGWVAGYCRRR	0.994731	0.005269
Hill_BB_C2323	QLNIQGGGSPHSGFDLSVQGRAKI WESDNGRNTLYGTGQYQHLGG PYGNSEPSFGGGLMFSHRF	0.071113	0.928887
Hill_BB_C7345	SIDDLTSEDGEDHVEITDDEVQ RAKR	0.014171	0.985829
Hill_BB_C7346	QLNIQGGGSPHSGFDLNVQGRAK IWESNNGRNTLHGTGEYSQHLGG PYGNSRPNFGGGLLFTHRF	0.035845	0.964155



Hill_BB_C11803	QLNIQGGGSPHSGFNLSIQGQKKL WESNNKRNTLHGTGQYSQHFGG PYGNSRPNFGGGLVFTHRF	0.066283	0.933717
Hill_BB_C21232	QLNIQGGSKSTFLILISMVRES NNGHETLHGTGDYNQHLGGPYG NSQPNFGGELLFTHRFKLSLKL LIVCVFSKCRK	0.945162	0.054838
NHill_AD_C17624	QIFAQGGGSPGKGYDIYAQGRAK LWESQNQRNSLHGTASYSQHLG GPYGNSRPNVGGGLTFTHRF	0.075412	0.924588
Hill_LB_C16634	IKCTASICTQICRILKYKCGYCAS ASRCVCLK	0.960433	0.039567
Hill_LB_C37730	AFAFDVTRKINPETAVERPEVSE YPEIPKGTKLQEFVMMDIEIEEEG ADNRAETIQRIKCVPSQCNQICRV LGKKCGYCKNASTCVCLG	0.006798	0.993202
Hill_BB_C46948	RKCTASQCTRVCCKLGYKRGYC QSSTKCVC	0.782932	0.217068
Hill_BB_C16137	MNIQGNVSNPAGGQDVTVTAG KQFGSDNANITAGGFAGGNTLRG PPNAGVFASANANGHLSVSKTV VPGISSTTSHGASANLFR	0.574294	0.425706
Hill_BB_C16883	QLSGSITPDMAGNNVIMASKF LGNPNHNIGGGVFASGNTRSNT SLGAFGTLNLKDHS LGVSKTITPG VSDTFSQARLILKTPDHRVDAN VFNSHTRLNNGFAFDKRGGLDY THRAGHSLSLGASHIPKFGTTAEL TGKANLWKS PSLSTFDLTGSAS	0.883543	0.116457
Hill_BB_C10074	SPQDGRRGASVTVNRESRRGTD VRADLNARLWEGNRRSSLDAN AYYQRHFGGPMGTGRPDAGVGL NFRHRF	0.000017	0.999983
Hill_BB_C9237	MNIQGNVSNPAGGQDVTVTAG KQFGSDNTNITAGAFAGGNTLRG PPNAGVFASANANSHLSVSKTV VPGVSATTSHAASANLFRNDQHS VNAQAFSSATKLDNGFQFKQHG AGLNYNANGHGASIGVKNKIPGF GSSMDVGARANIFQNPNTSFDVM ANSRTHLSGPFQKTNFGVSAGIT RRF	0.434155	0.565845
NHill_AD_C40487	MNIQGNVSNPAGGQDVTVTAG KQFGSDNTNITAGAFAGGNTLRG PPNAGVFASANANGHLSVSKTV VPGVSSTTSHAASANLFRNDQHN VNAQAFSSATKLDNGFQFKQHG AGLNYNANGHGASIGVKNKIPGF GSSMDVGARANIFQNPNTSFDVM ANSRTHLSGPFQKTNF	0.443017	0.556983
Hill_BB_C7758	AACDLFSALNVASSICAHCLYL GYKGGYCDSKLVVCR	0.791573	0.208427

Hill_BB_C14087	VTCDLLEPFLGPAPCMIHCIVRFR KRTGYCNSQNVCVCRG	0.391809	0.608191
Hill_LB_C29142	ATCDLLSPFKVGHAAACAAHCIAR GKRGGWCDKRAVCNCRK	0.450101	0.549899
Hill_BB_C308	VSCWFENENIKASACQMSCMYR KGRRGGMCVNGVCTCSPN	0.444002	0.555998
Hill_BB_C1619	LSCLFENQAVSAIACGSSCIARKG RRGGYCRNGVCVCTDN	0.954283	0.045717
Hill_BB_C1826	TTCTHLNCKLHCLLQKRKSRGCD RFNICKCIS	0.068550	0.931450
Hill_BB_C6571	ATCTNWNCRQTQCIARGKRGGYC VERNICKCTS	0.842113	0.157887
Hill_BB_C7081	ATCDLISGTKIENVACAAHCIAM GHKGGYCNSNLICIR	0.945143	0.054857
Hill_BB_C7985	FTCSNLGCKAQCIILGNRSGGCNR LGVCQCN	0.822369	0.177631
Hill_BB_C7176	ATCDLLSPFKVGHAAACALHCIAL GRRGGWCDGRAVCNCR	0.011073	0.988927
Hill_BB_C2519	ATCDLLSPFKVGHAAACALHCIAM GRRGGWCDGRAVCNCR	0.020927	0.979073
Hill_BB_C8473	ATCDLLSPFGVGHAAACAVHCIAM GRRGGWCDDRAVCNCR	0.165217	0.834783
Hill_BB_C34351	AMCDLLSGLNMGRSVCAMRCIL KGRGGWCDDQGVNCRV	0.029224	0.970776
Hill_BB_C4683	RPDNIEYLEDSQVAELVRHKRLS CLFENEAISALACGASCITRKGR GGWCSNGVCHCTPN	0.224878	0.775122
Hill_BB_C4977	LSCWFENEDIKATACAMSCIYRK GRKGGRCENGICRTPN	0.106600	0.893400
Hill_BB_C13326	LSCLFENQAVSAIACGASCITRK KRGWCSNGVCRCTPN	0.701191	0.298809
Hill_BB_C7171	TTCDLISGTKIENIACAAHCIAMG HKGGYCNSNLICIR	0.952388	0.047612
Hill_BB_C10649	QFDNLEDTGVEEKVRHKRLTCLF DNRPIAFACGSNCVSRKGRGG WCVNGVCRCT	0.974103	0.025897
Hill_BB_C13792	KQSSDPESALYSDIHPRFRQLPC DYLSGLGFEDACNTDCIAKGHK SGFCTGLVCRCTL	0.295265	0.704735
Hill_BB_C15867	VTCDLLKPFGRAPCMMHCILRF KKRTGFCSRQNVCVCR	0.182360	0.817640
NHill_AD_C69719	DVSIGSCVWGGSNYVSDCNCEC KRRGYKGGHCGSFLNNICWCET	0.924393	0.075607
Hill_BB_C49430	APQFGGQIGFGGGGFGGGGFGP GGGFRPGGVAEFQESSSVNVER ETFDQGGFEISDSSVTSSSVSEFR D	0.330011	0.669989

The obtained antiviral and antifungal prediction results are summarized in Table 6.

**Table 6.** Results obtained with the AVPpred server for the antiviral activity prediction and with Antifp server for the antifungal activity prediction. From left to right are shown in order: peptide contig, AVP motif model results, alignment model results, composition model results, the physio-chemical model results, the overall results for the antiviral prediction, antifungal score and prediction result for the antifungal activity.

PEPTIDE	AVPpred: ANTIVIRAL ACTIVITY PREDICTION					Antifp: ANTIFUNGAL ACTIVITY PREDICTION	
	AVP Motif (Model)	Alignment Model	Composition Model	Physio-chemical Model	Overall Prediction	SCORE	PREDICTION
Hill_BB_C14202	\	Non-AVP	53.26	64.08	YES	0.20892203	Non-Antifungal
Hill_BB_C3566	\	Non-AVP	42.65	64.08	NO	0.26737087	Non-Antifungal
Hill_BB_C1152	\	Non-AVP	31.33	64.08	NO	-0.21250625	Non-Antifungal
Hill_BB_C1153	\	Non-AVP	38.83	64.08	NO	-0.37506205	Non-Antifungal
Hill_BB_C2676	\	Non-AVP	46.61	64.08	NO	-0.17216018	Non-Antifungal
Hill_BB_C269	\	Non-AVP	52.07	64.08	YES	-0.025392142	Non-Antifungal
Hill_BB_C1169	\	Non-AVP	44.47	64.08	NO	0.072220496	Non-Antifungal
Hill_BB_C779	\	Non-AVP	41.2	64.08	NO	-0.33302841	Non-Antifungal
Hill_LB_C36111	\	Non-AVP	40.25	64.08	NO	-0.21911853	Non-Antifungal
Hill_LB_C12085	\	Non-AVP	42.31	64.08	NO	0.139426	Non-Antifungal
Hill_BB_C1290	\	Non-AVP	31.53	64.08	NO	0.11095482	Non-Antifungal
Hill_BB_C7347	\	Non-AVP	39.24	64.12	NO	-0.040857298	Non-Antifungal
Hill_BB_C9109	\	Non-AVP	23.7	64.08	NO	-0.068718526	Non-Antifungal
Hill_BB_C11804	\	Non-AVP	39.24	64.12	NO	-0.040857298	Non-Antifungal
Hill_BB_C309	\	Non-AVP	48.85	64.73	NO	0.065455296	Non-Antifungal
Hill_BB_C1827	\	Non-AVP	46.85	49.78	NO	0.73998352	Antifungal
Hill_BB_C5878	YES	Non-AVP	50.55	67.39	YES	-0.16644401	Non-Antifungal
Hill_BB_C8756	\	Non-AVP	26.31	64.08	NO	-0.34776804	Non-Antifungal
Hill_BB_C13793	\	Non-AVP	42.66	64.09	NO	0.25709331	Non-Antifungal
NHill_AD_C73537	\	Non-AVP	33.7	63.94	NO	-0.36753515	Non-Antifungal
NHill_AD_C16493	\	Non-AVP	34.66	64.07	NO	-0.43908213	Non-Antifungal
NHill_AD_C12927	\	Non-AVP	39.89	64.07	NO	-0.47185039	Non-Antifungal
NHill_AD_C12928	\	Non-AVP	40.33	64.09	NO	-0.40020762	Non-Antifungal
NHill_AD_C4669	\	Non-AVP	36.71	63.87	NO	-0.031971647	Non-Antifungal

Hill_BB_C3195	\	Non-AVP	37.43	64.08	NO	-0.24406508	Non-Antifungal
Hill_SB_C698	\	Non-AVP	33.23	64.07	NO	-0.43908213	Non-Antifungal
Hill_SB_C2730	\	Non-AVP	39.88	64.09	NO	-0.38062322	Non-Antifungal
Hill_SB_C1875	\	Non-AVP	34.95	63.96	NO	-0.22572859	Non-Antifungal
Hill_BB_C5151	\	Non-AVP	31.71	64.03	NO	-0.34876968	Non-Antifungal
Hill_BB_C390	\	Non-AVP	52.45	64.08	YES	-0.67921544	Non-Antifungal
NHill_AD_C53857	\	Non-AVP	51.96	65.69	YES	0.12385895	Non-Antifungal
NHill_AD_C49215	\	Non-AVP	46.35	65.52	NO	0.2406468	Non-Antifungal
Hill_BB_C2323	\	Non-AVP	19.92	64.08	NO	-0.10977439	Non-Antifungal
Hill_BB_C7345	\	Non-AVP	26.56	47.85	NO	-0.87408278	Non-Antifungal
Hill_BB_C7346	\	Non-AVP	23.75	64.08	NO	-0.059453989	Non-Antifungal
Hill_BB_C11803	\	Non-AVP	28.99	64.08	NO	-0.052337869	Non-Antifungal
Hill_BB_C21232	\	Non-AVP	44.14	64.08	NO	-0.070217673	Non-Antifungal
NHill_AD_C17624	\	Non-AVP	23.01	64.08	NO	-0.15660532	Non-Antifungal
Hill_LB_C16634	\	Non-AVP	53.29	64.88	YES	0.7067461	Antifungal
Hill_LB_C37730	\	Non-AVP	34.85	64.08	NO	0.38202837	Non-Antifungal
Hill_BB_C46948	\	Non-AVP	48.59	64.22	NO	0.71418843	Antifungal
Hill_BB_C16137	\	Non-AVP	28.08	64.08	NO	0.010457995	Non-Antifungal
Hill_BB_C16883	\	Non-AVP	25.14	64.08	NO	-0.52680116	Non-Antifungal
Hill_BB_C10074	\	Non-AVP	12.45	64.08	NO	-0.19881079	Non-Antifungal
Hill_BB_C9237	\	Non-AVP	28.71	64.08	NO	0.32515345	Non-Antifungal
NHill_AD_C40487	\	Non-AVP	28.54	64.08	NO	0.37181457	Non-Antifungal
Hill_BB_C7758	\	Non-AVP	61.82	64.18	YES	0.18741319	Non-Antifungal
Hill_BB_C14087	YES	Non-AVP	63.07	66.59	YES	0.10302883	Non-Antifungal
Hill_LB_C29142	\	Non-AVP	52.07	64.12	YES	0.33363813	Non-Antifungal
Hill_BB_C308	\	Non-AVP	48.85	64.73	NO	0.065455296	Non-Antifungal
Hill_BB_C1619	YES	Non-AVP	52.47	68.2	YES	-0.12761437	Non-Antifungal
Hill_BB_C1826	\	Non-AVP	46.42	49.91	NO	0.2129187	Non-Antifungal
Hill_BB_C6571	\	Non-AVP	49.54	67	NO	0.5009657	Antifungal
Hill_BB_C7081	\	Non-AVP	51.03	64.65	YES	0.35232096	Non-Antifungal
Hill_BB_C7985	\	Non-AVP	48.06	65.99	NO	0.44711187	Non-Antifungal
Hill_BB_C7176	\	Non-AVP	55.82	64.95	YES	0.27115344	Non-Antifungal
Hill_BB_C2519	\	Non-AVP	53.4	64.85	YES	0.27115344	Non-Antifungal
Hill_BB_C8473	\	Non-AVP	47.7	64.69	NO	0.21172458	Non-Antifungal
Hill_BB_C34351	\	Non-AVP	50.25	64.13	YES	0.10334371	Non-Antifungal
Hill_BB_C4683	\	Non-AVP	39.94	64.09	NO	-0.25553273	Non-Antifungal

Hill_BB_C4977	\	Non-AVP	52.52	65.92	YES	0.0078493215	Non-Antifungal
Hill_BB_C13326	YES	Non-AVP	56.26	68.51	YES	-0.21725812	Non-Antifungal
Hill_BB_C7171	\	Non-AVP	44.07	64.19	NO	0.21225639	Non-Antifungal
Hill_BB_C10649	\	Non-AVP	45.72	64.11	NO	-0.13179766	Non-Antifungal
Hill_BB_C13792	\	Non-AVP	47.38	64.08	NO	1.0166485	Antifungal
Hill_BB_C15867	\	Non-AVP	66.1	63.61	YES	0.70687492	Antifungal
NHill_AD_C69719	YES	Non-AVP	47.27	64.08	YES	0.91354184	Antifungal
Hill_BB_C49430	\	Non-AVP	33.03	64.08	NO	-0.36274044	Non-Antifungal

The bioinformatics results lead, thus, to the identification of 57 peptides, 13 of which were predicted as endowed with an antimicrobial activity, 22 with an antimicrobial and anticancer activity, 8 with an antimicrobial and antiviral activity, 2 with an antimicrobial and antifungal activity, 7 with an antimicrobial, anticancer and antiviral activity. Only one peptide was predicted as antimicrobial, antiviral and antifungal activity, whereas 2 peptides were predicted to have a putative antimicrobial, anticancer and antifungal activity. 2 peptides, corresponding to Hill\_LB\_C16634 and NHill\_AD\_C69719 contigs, resulted positive to all activity predictions (Table 7).

**Table 7.** Summary of all activities predicted for the identified peptides. The acronyms AMPs, ACPs, AVPs and AFPs represent antimicrobial, anticancer, antiviral, and antifungal, respectively.

PREDICTED ACTIVITY	PEPTIDE
AMPs	Hill_BB_C1153
	Hill_BB_C309
	Hill_BB_C13793
	NHill_AD_C12927
	NHill_AD_C12928
	Hill_SB_C2730
	Hill_LB_C37730
	Hill_BB_C9237
	NHill_AD_C40487
	Hill_BB_C308
	Hill_BB_C1826

	<p>Hill_BB_C8473</p> <p>Hill_BB_C4683</p>
<p>AMPs + ACPs</p>	<p>Hill_BB_C3566</p> <p>Hill_BB_C1152</p> <p>Hill_BB_C2676</p> <p>Hill_BB_C1169</p> <p>Hill_BB_C779</p> <p>Hill_LB_C36111</p> <p>Hill_LB_C12085</p> <p>Hill_BB_C1290</p> <p>NHill_AD_C73537</p> <p>NHill_AD_C16493</p> <p>NHill_AD_C4669</p> <p>Hill_BB_C16137</p> <p>Hill_BB_C3195</p> <p>Hill_SB_C698</p> <p>Hill_SB_C1875</p> <p>Hill_BB_C5151</p> <p>NHill_AD_C49215</p> <p>Hill_BB_C21232</p> <p>Hill_BB_C16883</p> <p>Hill_BB_C7985</p> <p>Hill_BB_C7171</p> <p>Hill_BB_C10649</p>
<p>AMPs + AVPs</p>	<p>Hill_BB_C14202</p> <p>Hill_BB_C269</p> <p>Hill_BB_C14087</p> <p>Hill_LB_C29142</p> <p>Hill_BB_C7176</p> <p>Hill_BB_C2519</p> <p>Hill_BB_C34351</p> <p>Hill_BB_C4977</p>
<p>AMPs + AFPs</p>	<p>Hill_BB_C1827</p> <p>Hill_BB_C13792</p>

AMPs + ACPs + AVPs	Hill_BB_C5878 Hill_BB_C390 NHill_AD_C53857 Hill_BB_C7758 Hill_BB_C1619 Hill_BB_C7081 Hill_BB_C13326
AMPs + AFPs + AVPs	Hill_BB_C15867
AMPs + ACPs + AFPs	Hill_BB_C46948 Hill_BB_C6571
AMPs + ACPs + AVPs + AFPs	Hill_LB_C16634 NHill_AD_C69719

#### 4.4. *In silico* calculation of the physio-chemical properties and amino acid composition.

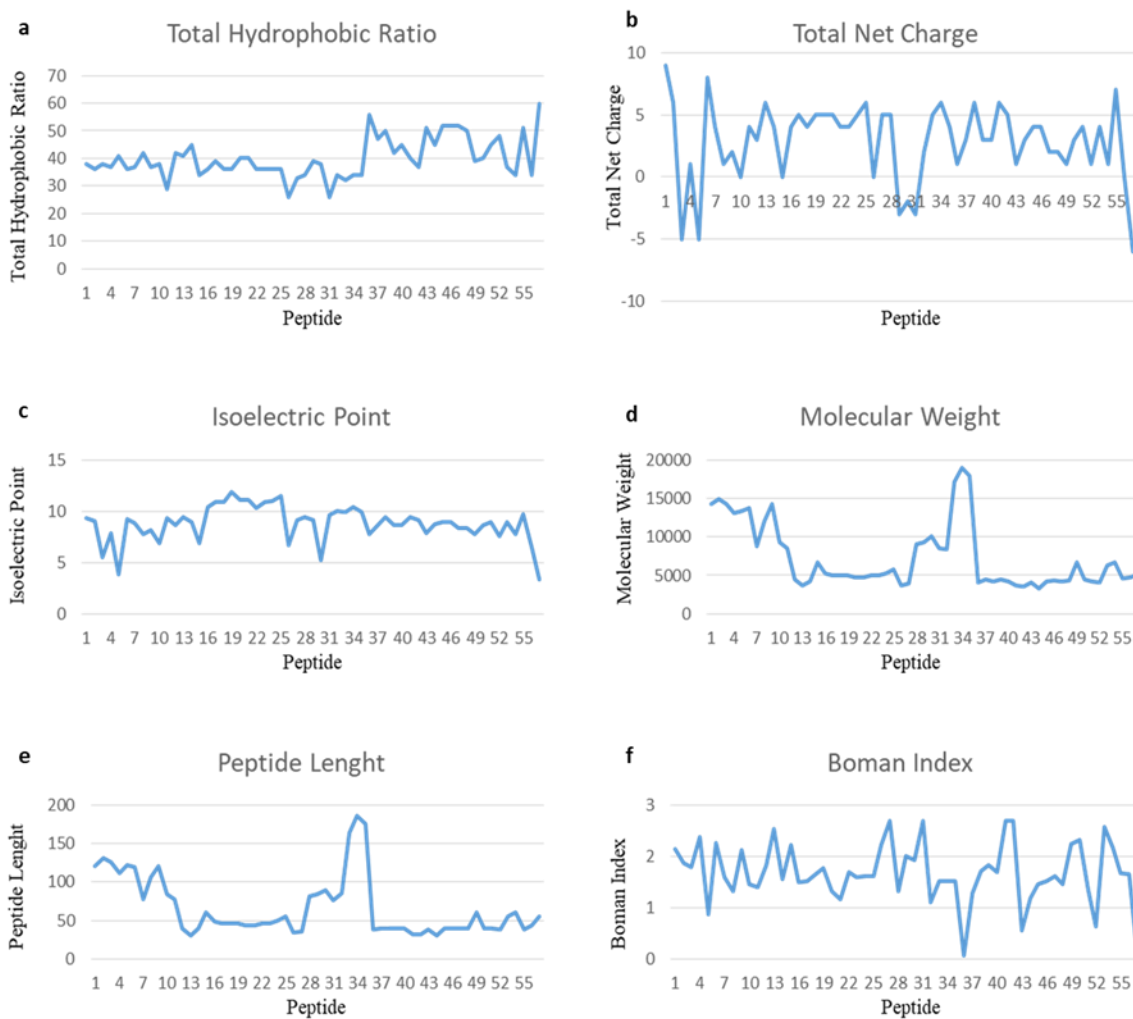
The 57 identified putatively active peptides belong to different classes of antimicrobial peptides including defensins, cecropins and attacins (Figure 1). The physicochemical properties of these peptides were evaluated with the Antimicrobial Peptide Database Calculator and Predictor APD3 (Table 8). Figure 13 shows the graphical representation of the calculated physicochemical properties of the 57 identified peptides, whereas Table 9 reports their amino acid composition and the amino acid frequency, compared to the amino acid composition of the patent AMPs available in the APD database. The highest amino acid content in all the analysed antimicrobial peptides was found for Gly, Ala, Arg, Asn, Cys, Leu, Ser residues, whereas the lowest content was found for His, Met, Trp, Tyr residues. A graphical representation of the amino acid composition of each identified peptide is shown in supplementary Figure 14. The molecular mass of the identified peptides ranges from 3,000 Da for the smallest peptide Hill\_BB\_C7985 to 19,000 Da for the largest peptide Hill\_BB\_C9237, with an average of approximately 7,000 Da. The amino acid sequences varied from a minimum value of 31 residues to a maximum of 186 residues, and an average of approximately 66 residues. The total hydrophobic ratio showed the lowest value of 26 for the peptide NHill\_AD\_C53857 and the highest of 60 for the peptide Hill\_BB\_C390, and an average value of approximately 40. The total net charge of the identified peptides ranges from -6, for the Hill\_BB\_C390 peptide to +9 for the Hill\_BB\_C14202 peptide, with an average value of +3, while the Isoelectric Point (pI) varies from 3.34 for the Hill\_BB\_C390 peptide to 11.83 for the NHill\_AD\_C12928 peptide, with an average value of 8.79.

**Table 8.** Prediction of physicochemical properties through the Antimicrobial Peptide Database Calculator and Predictor (APD3) and the Compute pI/Mw tool – ExPASy. From left to right are shown in order: peptide contig, the peptide length, the molecular weight, the total hydrophobic ratio, the total net charge, the isoelectric point (pI) and the Boman index.

Peptide	Lenght (aa)	Molecular Weight (g/mol)	Total Hydrophobic Ratio (%)	Total Net Charge	pI	Boman Index (kcal/mol)
Hill_BB_C14202	121	14282.443	38	+9	9.32	2.14
Hill_BB_C3566	131	14871.993	36	+6	8.99	1.87
Hill_BB_C1152	126	14259.799	38	-5	5.55	1.8
Hill_BB_C1153	112	13084.607	37	+1	7.84	2.37
Hill_BB_C2676	122	13394.838	41	-5	3.80	0.88
Hill_BB_C269	119	13730.8	36	+8	9.24	2.26
Hill_BB_C1169	77	8763.954	37	+4	8.80	1.59
Hill_BB_C779	107	12074.699	42	+1	7.76	1.32
Hill_LB_C36111	121	14214.145	37	+2	8.15	2.13
Hill_LB_C12085	84	9307.51	38	0	6.88	1.45
Hill_BB_C1290	77	8480.598	29	+4	9.30	1.39
Hill_BB_C309	40	4422.19	42	+3	8.67	1.83
Hill_BB_C1827	31	3686.457	41	+6	9.38	2.53
Hill_BB_C5878	40	4204.904	45	+4	8.98	1.56
Hill_BB_C13793	61	6712.597	34	0	6.88	2.22
NHill_AD_C73537	49	5259.014	36	+4	10.43	1.49
NHill_AD_C16493	51	5404.099	37	+4	10.93	1.63
NHill_AD_C12927	46	4969.69	36	+4	10.93	1.65
NHill_AD_C12928	46	5024.777	36	+5	11.83	1.78
NHill_AD_C4669	44	4670.398	40	+5	11.07	1.32
Hill_BB_C3195	44	4726.506	40	+5	11.07	1.16
Hill_SB_C698	51	5476.163	35	+3	10.26	1.78
Hill_SB_C2730	46	4997.744	36	+4	10.93	1.60
Hill_SB_C1875	50	5312.123	36	+5	11.00	1.61
Hill_BB_C5151	55	5823.746	36	+6	11.47	1.61
NHill_AD_C53857	34	3679.079	26	0	6.70	2.23
NHill_AD_C49215	36	3985.541	33	+5	9.18	2.69
Hill_BB_C21232	82	9053.427	34	+5	9.46	1.32



Hill_LB_C16634	32	3531.395	53	+6	9.18	0.75
Hill_LB_C37730	90	10059.611	38	-2	5.17	1.93
Hill_BB_C46948	30	3390.071	33	+8	9.64	2.58
Hill_BB_C16137	86	8328.081	34	+2	9.98	1.11
Hill_BB_C16883	164	17080.992	32	+5	9.89	1.51
Hill_BB_C9237	186	18942.725	34	+6	10.36	1.52
NHill_AD_C40487	176	17910.512	34	+4	9.87	1.52
Hill_BB_C7758	39	4089.842	56	+1	7.81	0.07
Hill_BB_C14087	40	4501.427	47	+3	8.69	1.28
Hill_LB_C29142	40	4275.055	50	+6	9.38	1.72
Hill_BB_C308	40	4422.19	42	+3	8.67	1.83
Hill_BB_C1619	40	4183.84	45	+3	8.69	1.7
Hill_BB_C1826	32	3752.517	40	+6	9.43	2.7
Hill_BB_C6571	32	3597.19	37	+5	9.18	2.7
Hill_BB_C7081	39	4055.809	51	+1	7.83	0.55
Hill_BB_C7985	31	3233.819	45	+3	8.70	1.18
Hill_BB_C7176	40	4259.049	52	+4	8.98	1.45
Hill_BB_C2519	40	4277.088	52	+4	8.98	1.52
Hill_BB_C8473	40	4249.98	52	+2	8.37	1.62
Hill_BB_C34351	40	4330.189	50	+2	8.36	1.46
Hill_BB_C4683	61	6736.674	39	+1	7.79	2.25
Hill_BB_C4977	40	4486.229	40	+3	8.66	2.33
Hill_BB_C13326	40	4162.859	45	+4	8.96	1.35
Hill_BB_C7171	39	4099.862	48	+1	7.54	0.64
Hill_BB_C10649	56	6263.181	37	+4	7.54	2.58
Hill_BB_C13792	61	6725.639	34	+1	7.78	2.17
Hill_BB_C15867	39	4566.65	51	+7	9.69	1.68
NHill_AD_C69719	44	4763.313	34	+1	6.71	1.66
Hill_BB_C390	55	5182.986	60	-6	4.06	-

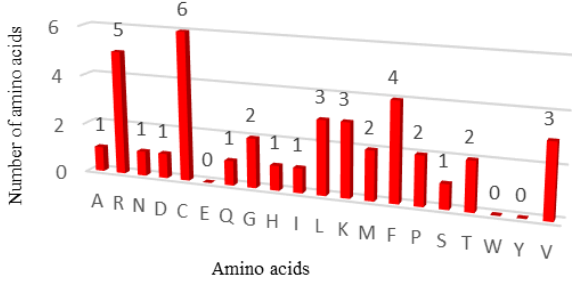
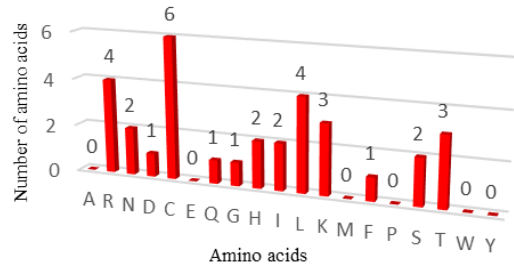
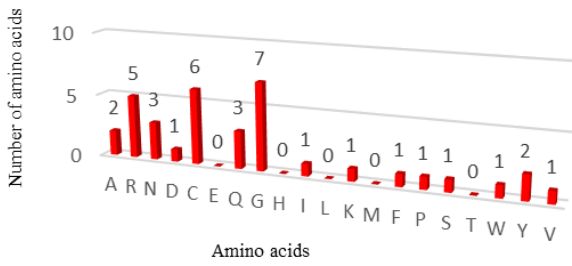
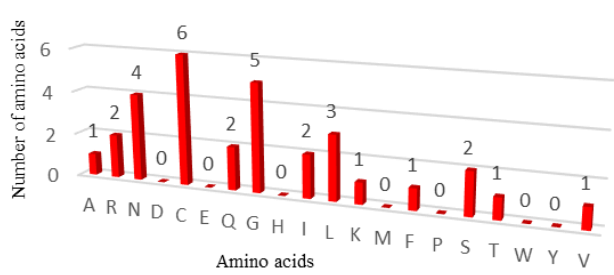
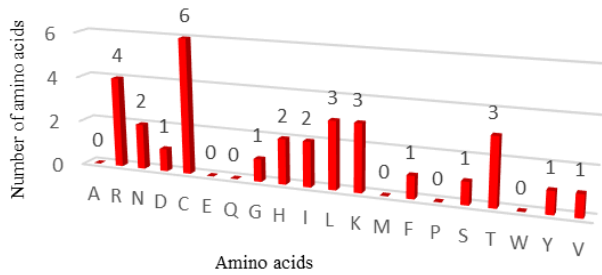
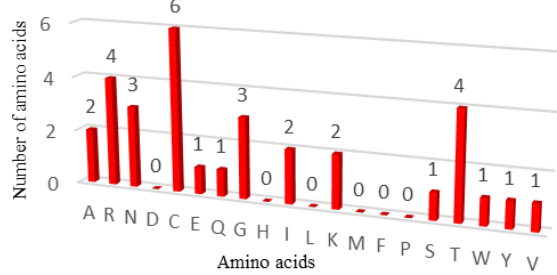


**Figure 13.** Graphical representation of the physicochemical properties of the 57 peptides with putative activity: a) Total Hydrophobic Ratio; b) Total Net Charge; c) Isoelectric Point; d) Molecular Weight; e) Peptide Length; f) Boman Index.

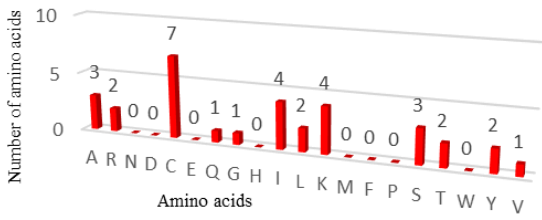
**Table 9.** Amino acid frequency and amino acid composition of the identified peptides. As it is shown, the Gly, Ala, Arg, Asn, Cys, Leu, Ser residues are the most abundant, whereas the lowest content is associated with the His, Met, Trp, Tyr residues.

<i>Amino acid composition of peptides identified in <i>Hermetia illucens</i></i>			<i>Amino acid composition of patent AMPs in the APD database</i>
<i>Amino acid three letter code? MINO ACID THREE LETTER CODE</i>	<i>Amino Acid Frequency</i>	<i>Amino Acid Composition (%)</i>	<i>Amino Acid Composition (%)</i>
Ala	297	7.98816	7.61
Arg	230	6.18612	5.81
Asn	258	6.93921	3.85
Asp	142	3.81926	2.65
Cys	262	7.04679	6.86

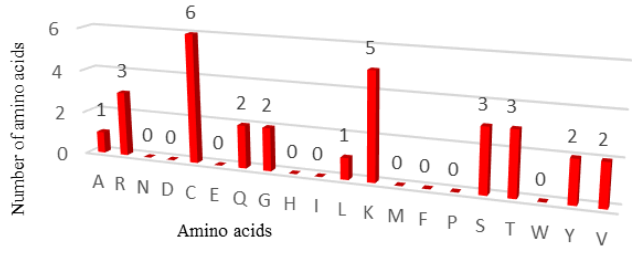
Glu	113	3.03927	2.69
Gln	166	4.46477	2.57
Gly	406	10.91985	11.56
His	89	2.39376	2.16
Ile	175	4.70683	5.93
Leu	242	6.50888	8.34
Lys	205	5.51372	9.55
Met	42	1.12964	1.25
Phe	143	3.84615	4.08
Pro	124	3.33513	4.69
Ser	270	7.26197	6.07
Thr	168	4.51856	4.51
Trp	85	2.28617	1.64
Tyr	85	2.28617	2.48
Val	216	5.80957	5.7
<b>TOTAL</b>	<b>3718</b>	<b>100</b>	<b>100</b>

**C15867****C1826****C49215****C7985****C1827****C6571**

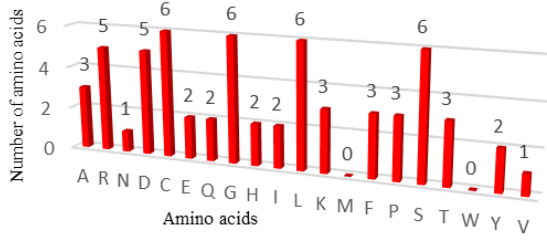
**C16643**



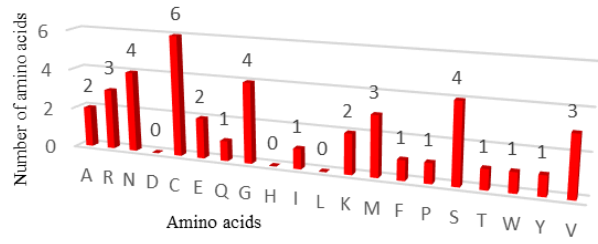
**C46948**



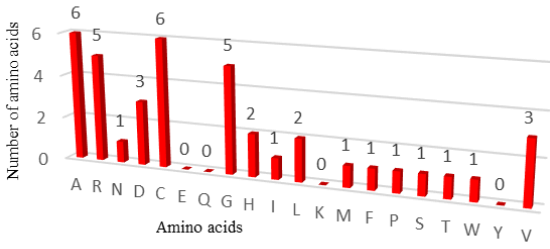
**C13792**



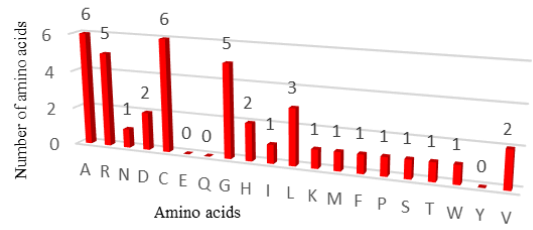
**C309**



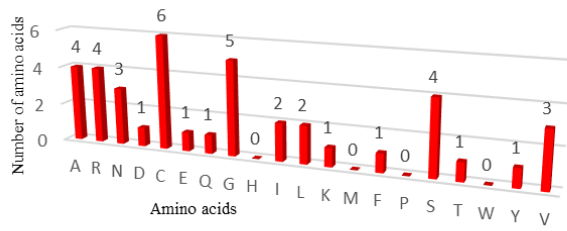
**C8473**



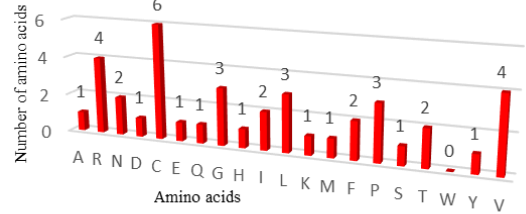
**C2519**



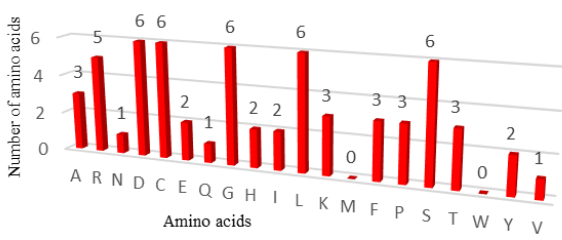
**C1619**



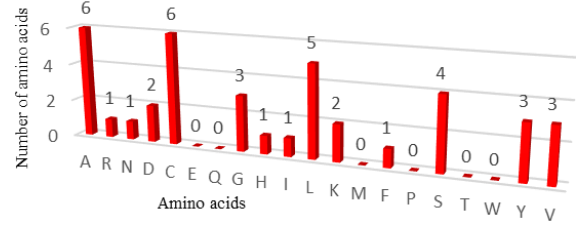
**C14087**



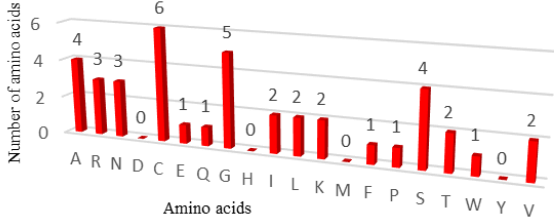
**C13793**



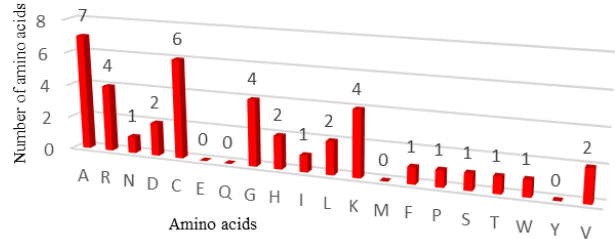
**C7758**



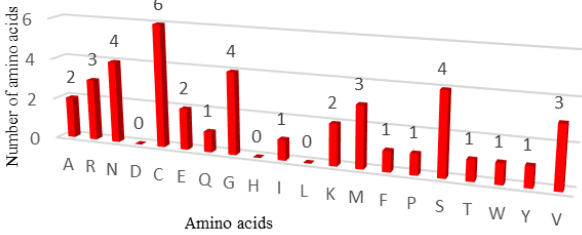
**C13326**



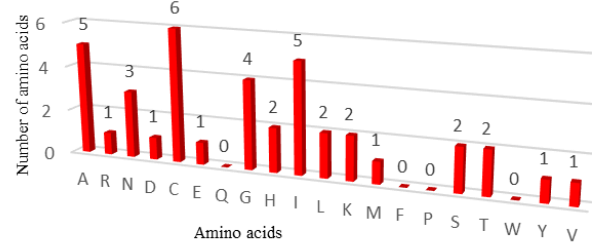
**C29142**

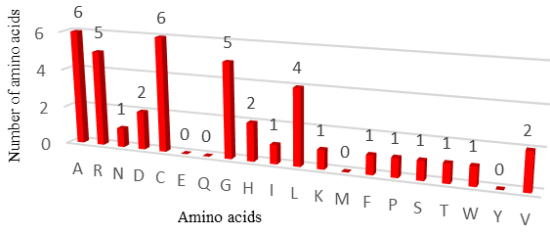
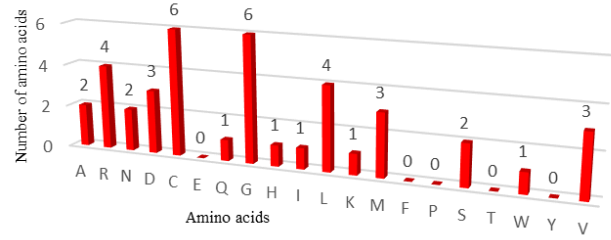
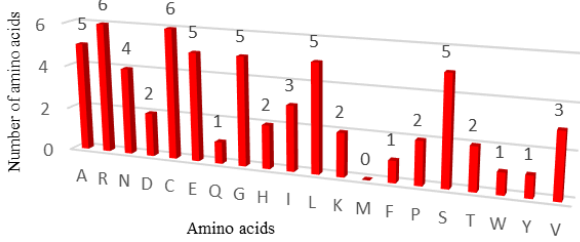
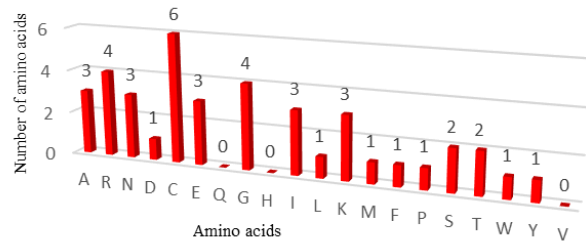
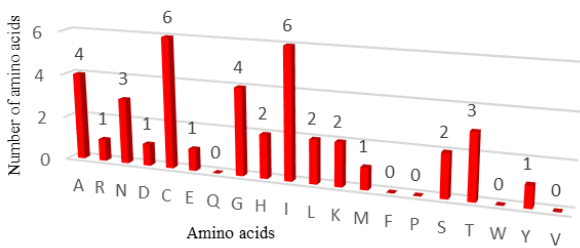
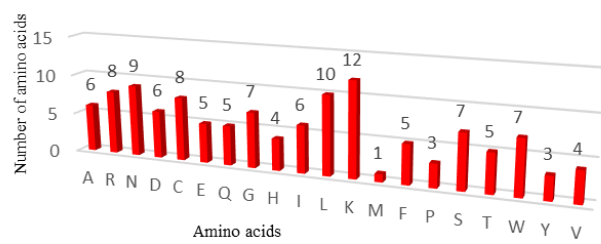
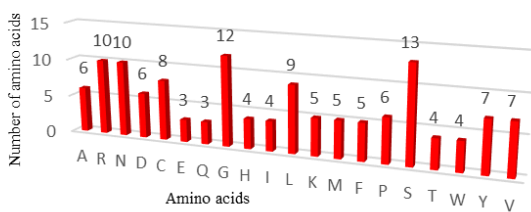
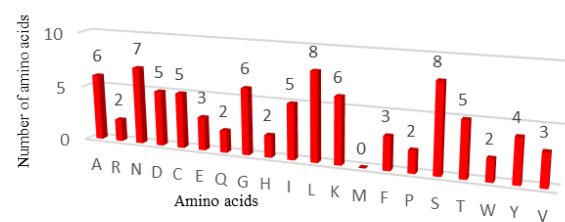
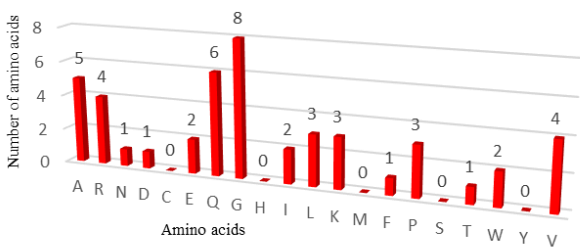
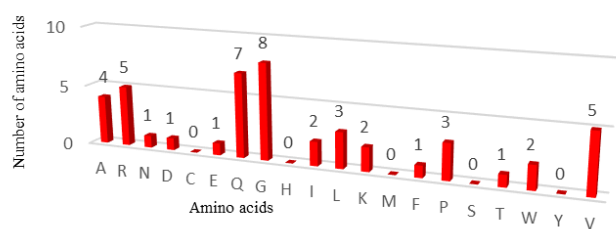


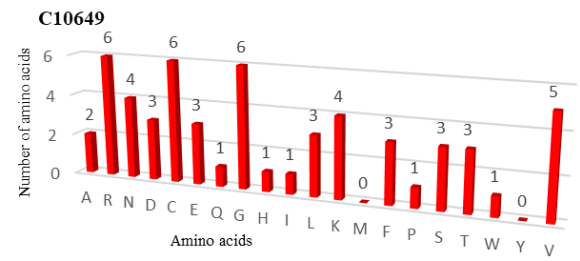
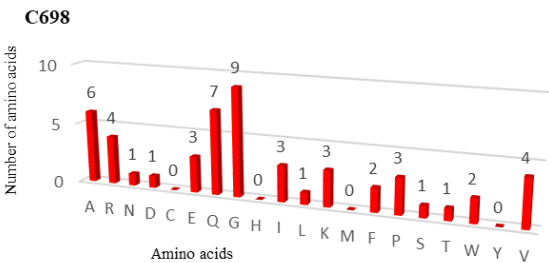
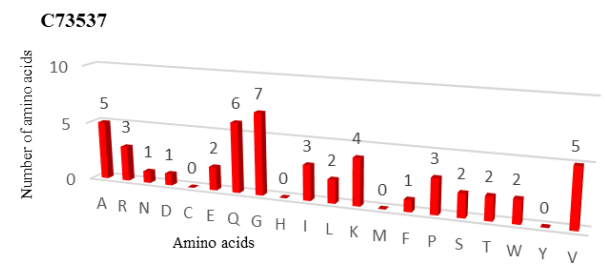
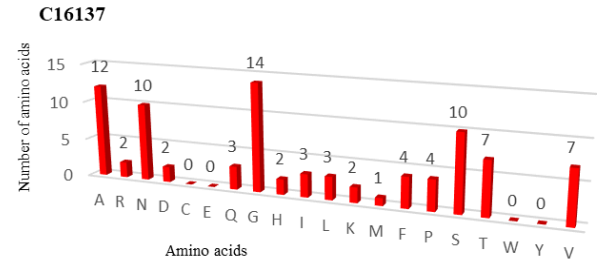
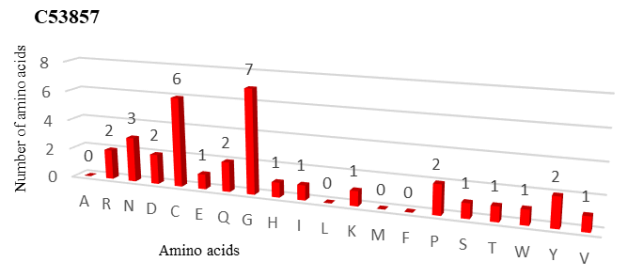
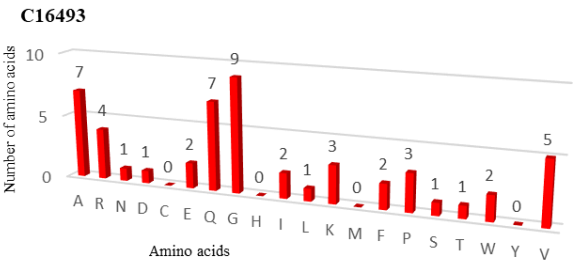
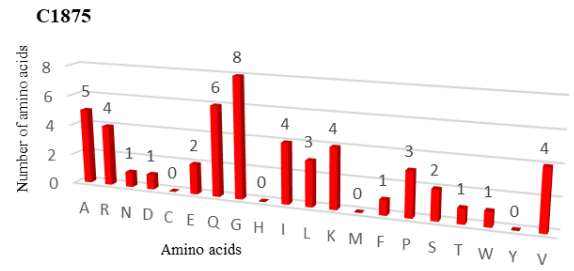
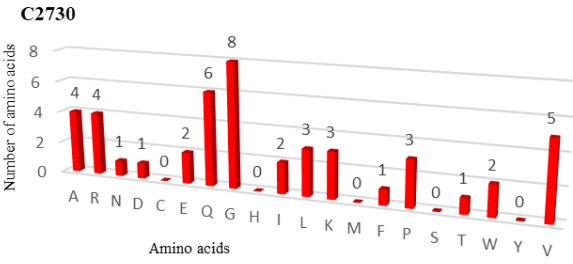
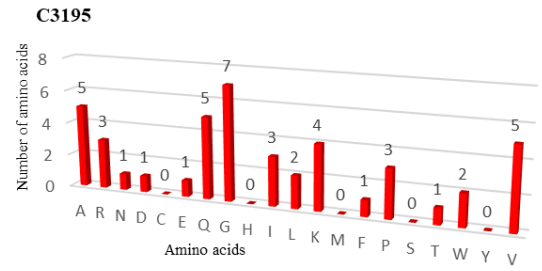
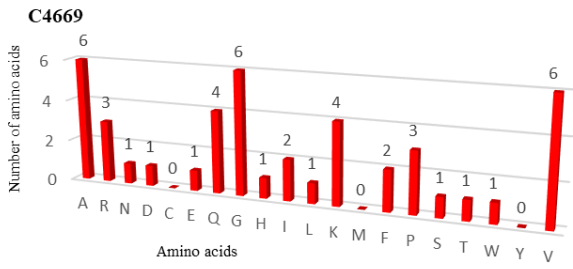
**C308**



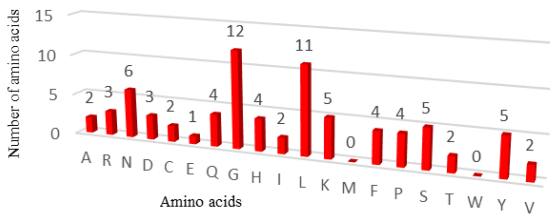
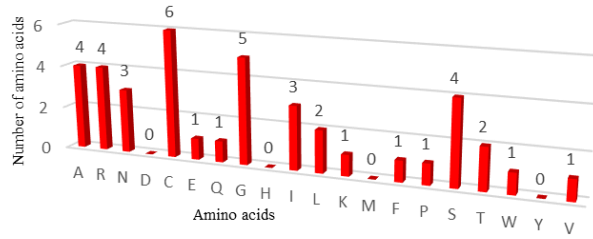
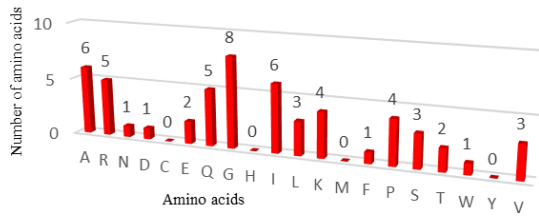
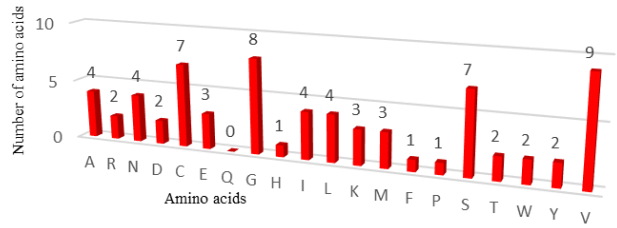
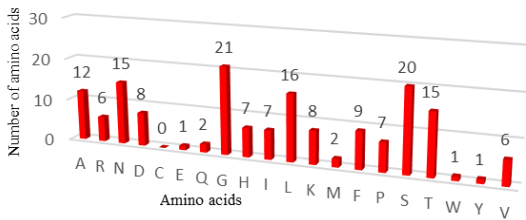
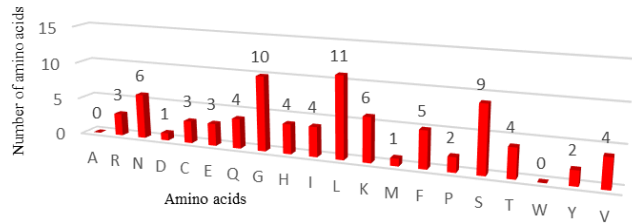
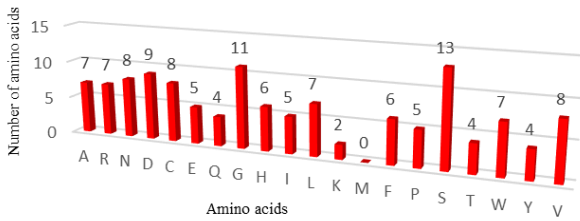
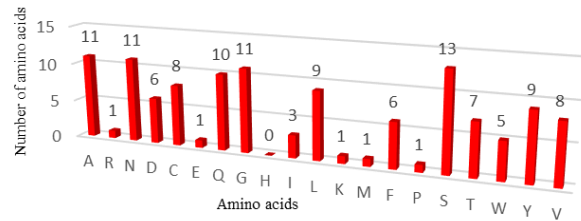
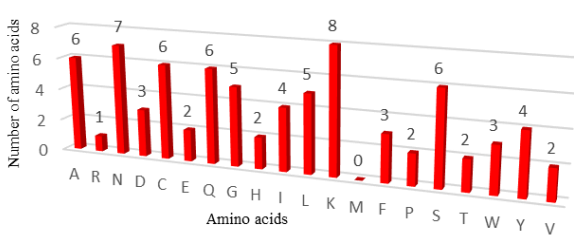
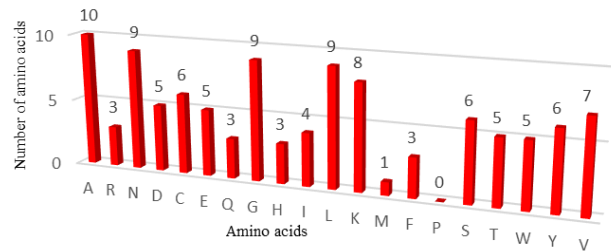
**C7081**



**C7176****C34351****C4683****C4977****C7171****C14202****C3566****C12085****C12927****C12928**





**C1290****C5878****C5151****C69719****C16883****C21232****C1152****C2676****C1169****C779**

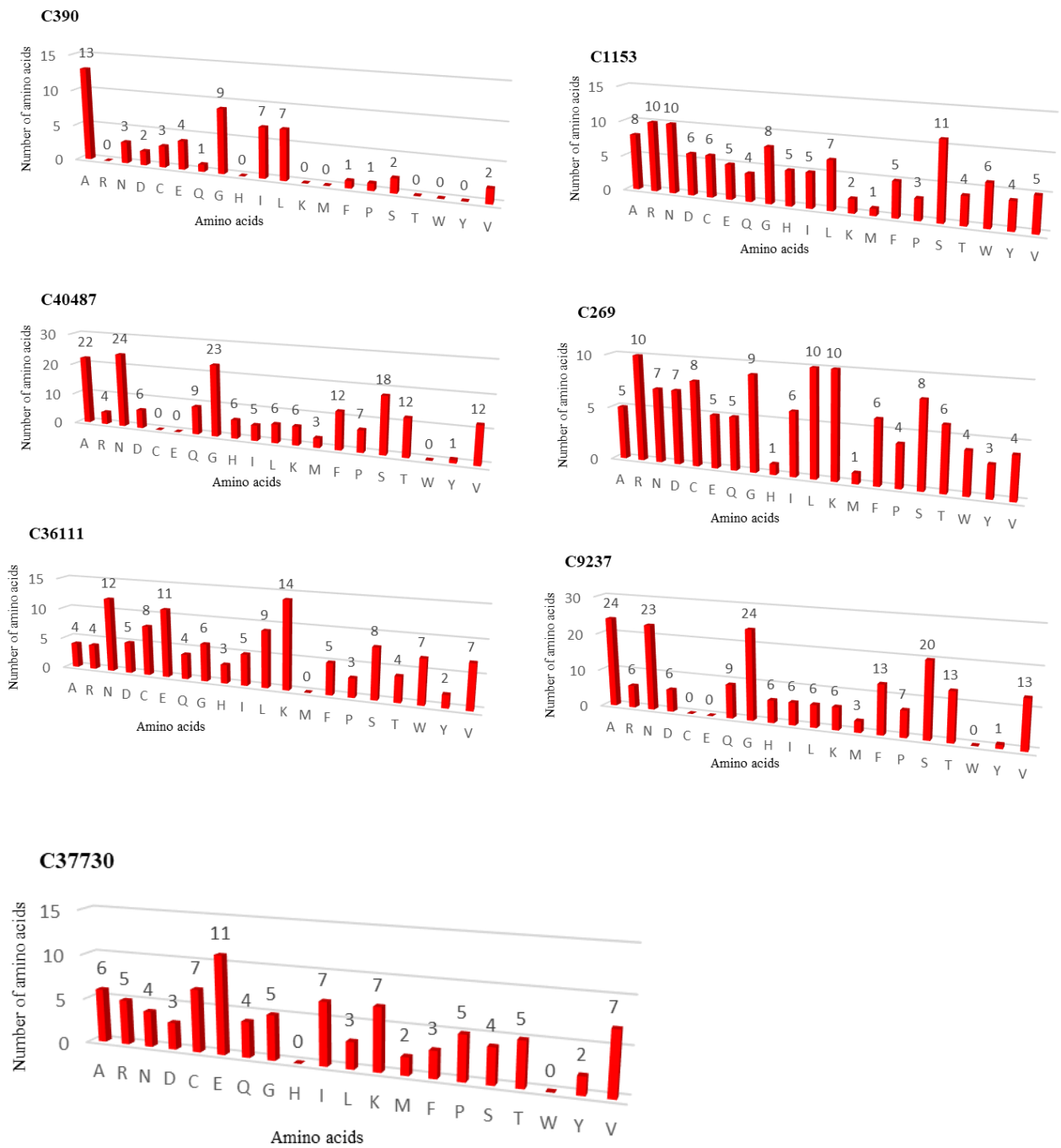


**Figure 14.** Graphic representation of the identified peptides amino acids composition.

#### 4.5. Molecular Modelling for the secondary and tertiary structures and *in silico* analysis for the disulfide bonds formation.

The identified antimicrobial peptides have been modelled using the I-TASSER server. In Table 10 are listed the C-score, TM-score and RMSD values obtained for each peptide.

**Table 10.** C-score, TM-score e RMSD obtained with the I-TASSER server.

PEPTIDE	C-score	TM-score	RMSD
NHill_AD_C49215	1.02	0.85±0.08	0.5±0.5 Å
Hill_BB_C7758	0.39	0.77±0.10	1.5±1.4Å
Hill_LB_C29142	0.38	0.76±0.10	1.6±1.4Å
Hill_BB_C7171	0.35	0.76±0.10	1.6±1.4Å
Hill_BB_C7176	0.27	0.75±0.10	1.8±1.5Å
Hill_BB_C2519	0.15	0.73±0.11	2.0±1.6Å
Hill_BB_C15867	0.14	0.73±0.11	1.9±1.6Å
Hill_BB_C7081	0.12	0.73±0.11	2.0±1.6Å
Hill_BB_C1826	-0.15	0.69±0.12	2.7±1.7Å
Hill_BB_C8473	-0.15	0.69±0.12	2.5±1.9Å
Hill_BB_C34351	-0.16	0.69±0.12	2.2±1.9Å
Hill_BB_C14087	-0.35	0.67±0.13	2.9±2.1Å
Hill_BB_C6571	-0.41	0.66±0.13	2.6±1.9Å
Hill_BB_C4977	-0.67	0.63±0.14	3.5±2.4Å
Hill_BB_C308	-0.72	0.62±0.14	3.6±2.5Å
Hill_BB_C309	-0.79	0.62±0.14	3.6±2.5Å
Hill_BB_C13326	-0.99	0.59±0.14	4.1±2.7Å
NHill_AD_C4669	-1.01	0.59±0.14	4.3±2.9Å
Hill_BB_C5878	-1.06	0.58±0.14	4.2±2.8Å
Hill_BB_C7985	-1.06	0.58±0.14	3.7±2.6Å
Hill_BB_C1619	-1.15	0.57±0.15	4.4±2.9Å
Hill_BB_C1827	-1.19	0.57±0.15	4.0±2.7Å

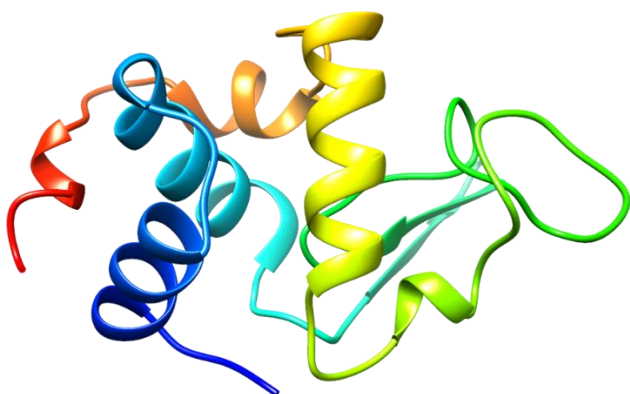
Hill_SB_C1875	-1.31	0.55±0.15	5.2±3.3Å
Hill_SB_C2730	-1.31	0.55±0.15	5.0±3.2Å
NHill_AD_C16493	-1.34	0.55±0.15	5.3±3.4Å
Hill_BB_C3195	-1.38	0.54±0.15	5.1±3.3Å
Hill_BB_C13792	-1.40	0.54±0.15	5.8±3.6Å
Hill_SB_C698	-1.41	0.54±0.15	5.4±3.5Å
NHill_AD_C12928	-1.50	0.53±0.15	5.4±3.4Å
Hill_BB_C10649	-1.59	0.52±0.15	6.0±3.7Å
NHill_AD_C12927	-1.59	0.52±0.15	5.6±3.5Å
NHill_AD_C73537	-1.72	0.51±0.15	6.0 ±3.7Å
Hill_BB_C5151	-1.81	0.50±0.15	6.4±3.9Å
Hill_BB_C4683	-1.93	0.48±0.15	6.9±4.1Å
Hill_BB_C21232	-3.60	0.32±0.11	11.6±4.5Å
Hill_BB_C309	-0.72	0.62±0.14	3.6±2.5Å
Hill_BB_C15867	0.14	0.73±0.11	1.9±1.6Å
Hill_BB_C14202	1.44	0.91±0.06	1.7±1.4Å
Hill_BB_C3566	0.28	0.75±0.10	3.9±2.7Å
Hill_BB_C1152	-0.07	0.70±0.12	4.5±3.0Å
Hill_BB_C1153	1.07	0.86±0.07	2.2±1.7Å
Hill_BB_C2676	1.16	0.87±0.07	2.2±1.7Å
Hill_BB_C269	1.18	0.88±0.07	2.1±1.7Å
Hill_BB_C1169	0.75	0.81±0.09	2.1±1.6Å
Hill_BB_C779	1.13	0.87±0.07	2.0±1.6Å
Hill_LB_C36111	1.52	0.93±0.06	1.5±1.4Å
Hill_LB_C12085	0.99	0.85±0.08	1.8±1.5Å
Hill_BB_C1290	-3.39	0.34±0.11	10.9±4.6Å
Hill_BB_C13793	-1.30	0.55±0.15	5.6±3.5Å
NHill_AD_C53857	0.95	0.84±0.08	0.5±0.5Å
Hill_LB_C16634	-0.01	0.71±0.11	1.9±1.5Å
Hill_LB_C37730	-3.89	0.30±0.09	12.6±4.3Å
Hill_BB_C46948	0.08	0.72±0.11	1.6±1.4Å
Hill_BB_C16137	-3.11	0.36±0.12	10.5±4.6Å

Hill_BB_C16883	-3.17	0.36±0.12	12.3±4.4Å
Hill_BB_C9237	-2.48	0.43±0.14	10.8±4.6Å
NHill_AD_C40487	-2.72	0.40±0.14	11.3±4.5Å
NHill_AD_C69719	1.20	0.88±0.07	0.5±0.5Å
Hill_BB_C390	-0.90	0.60±0.14	4.5±3.0Å

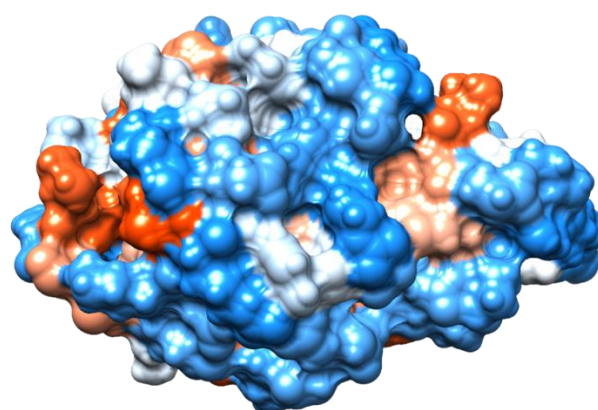
The 3D models and the hydrophobicity surfaces are shown in Figure 15.

**C269**

**a**

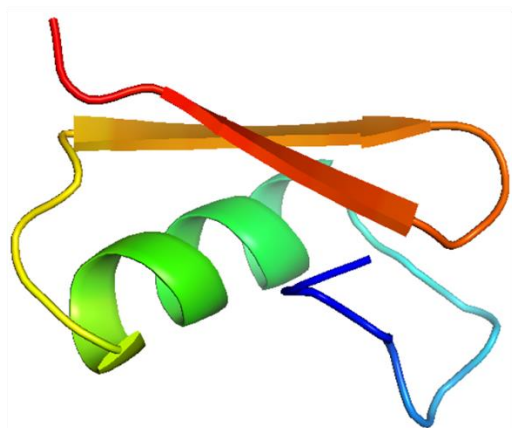


**b**

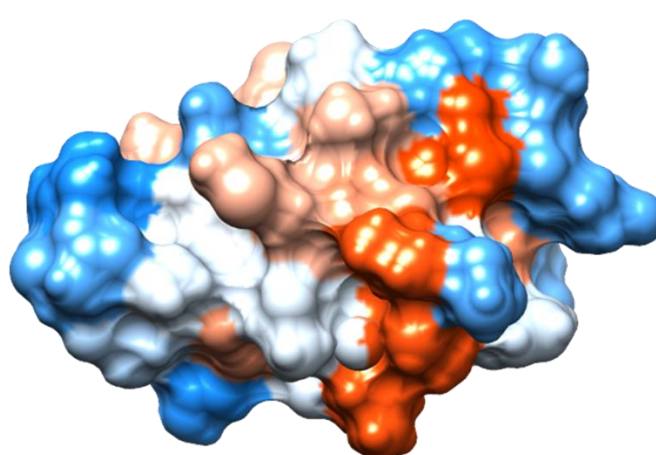


**C308**

**a**

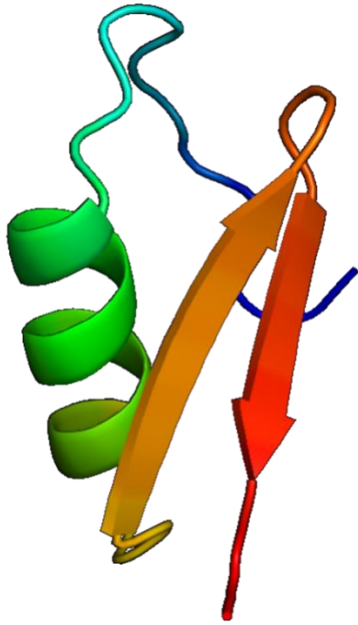


**b**

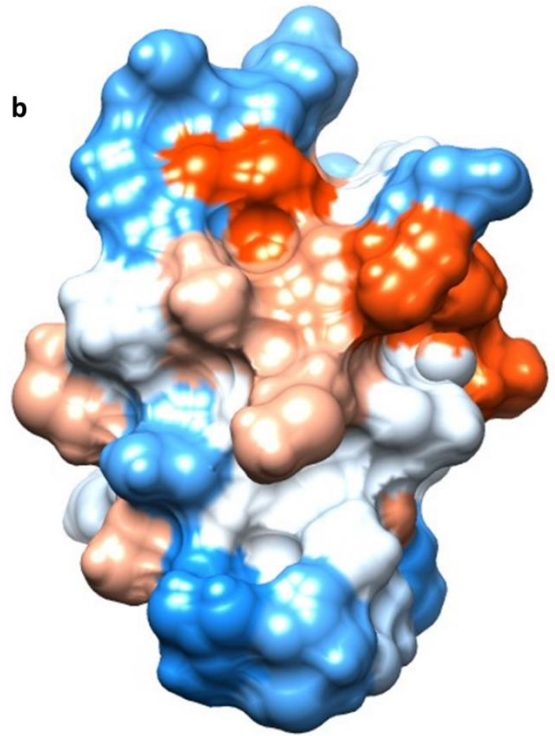


C309

a

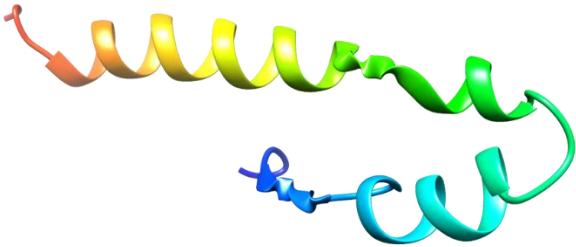


b

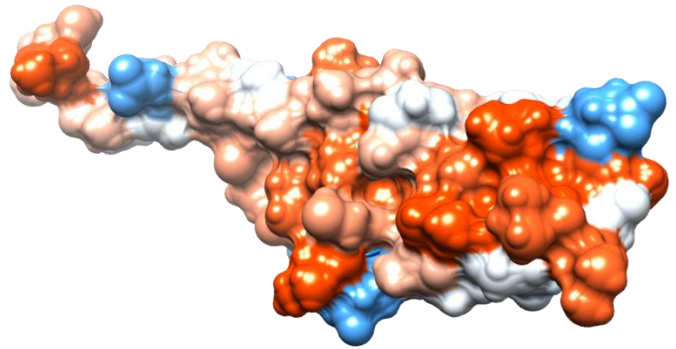


C390

a

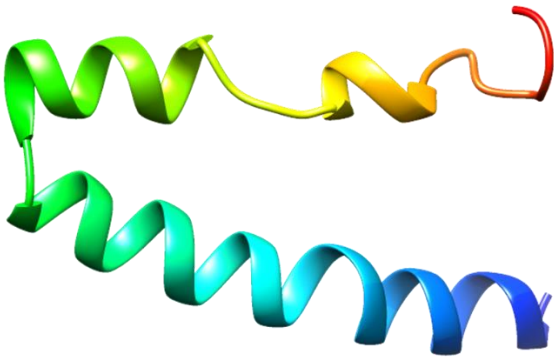


b

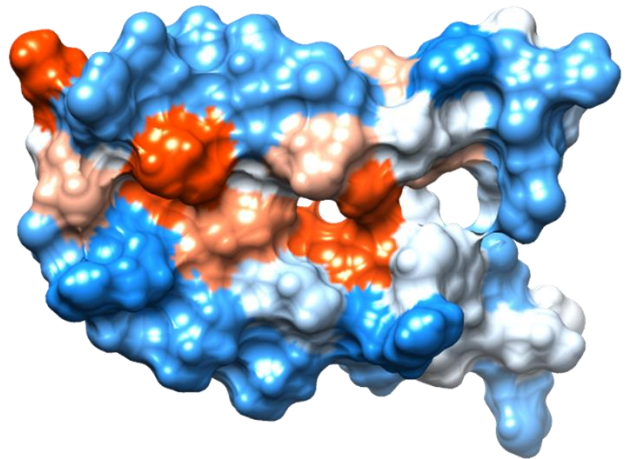


C698

a

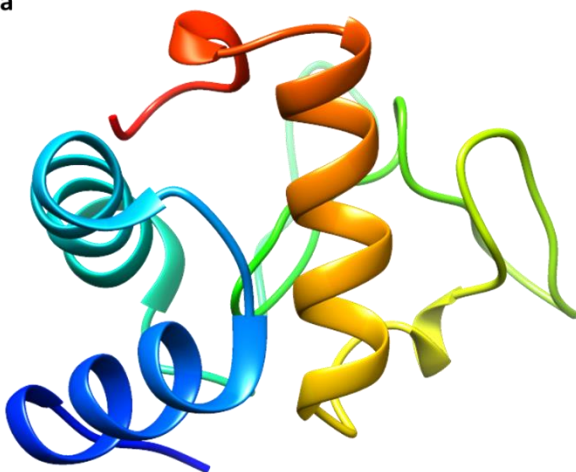


b

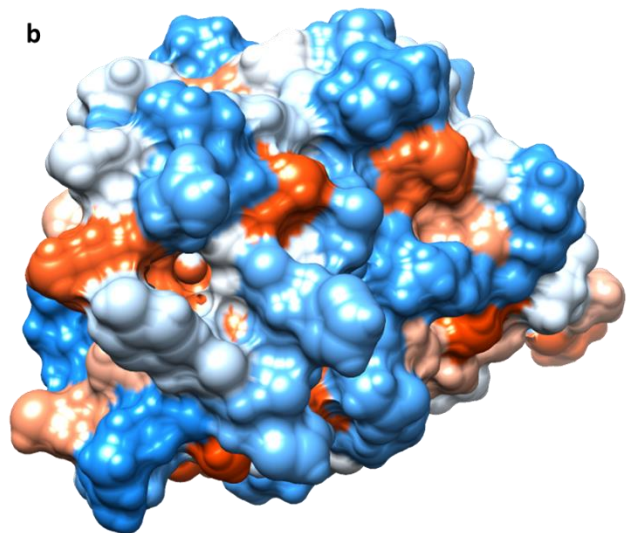


C779

a

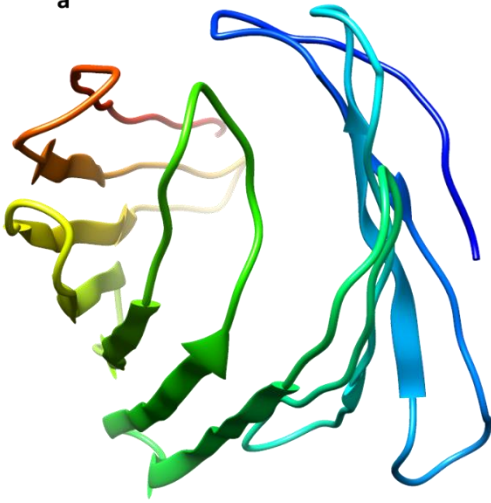


b

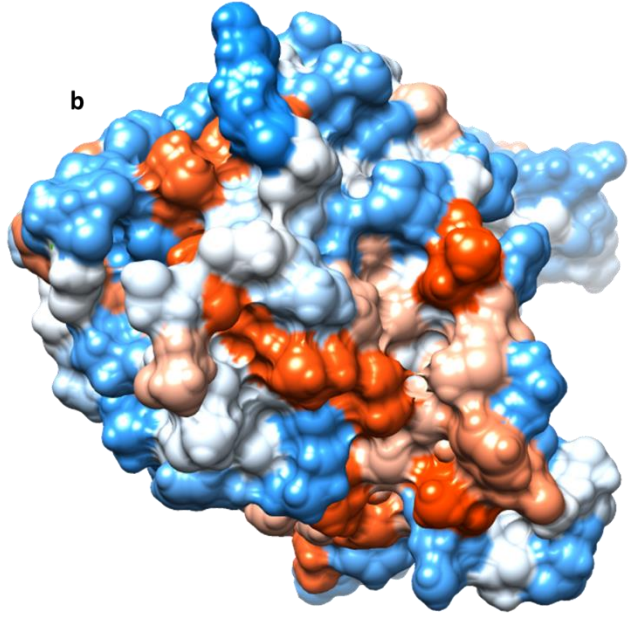


C9237

a

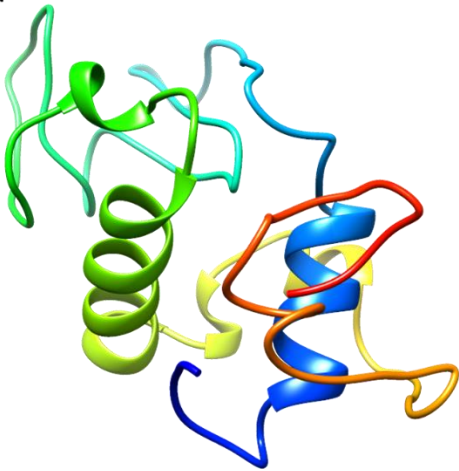


b

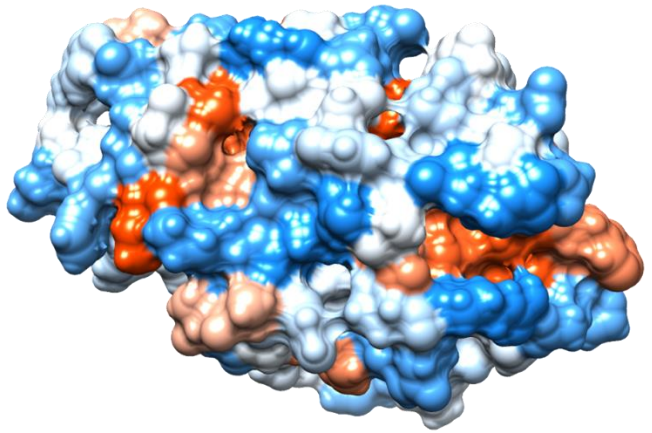


C1152

a



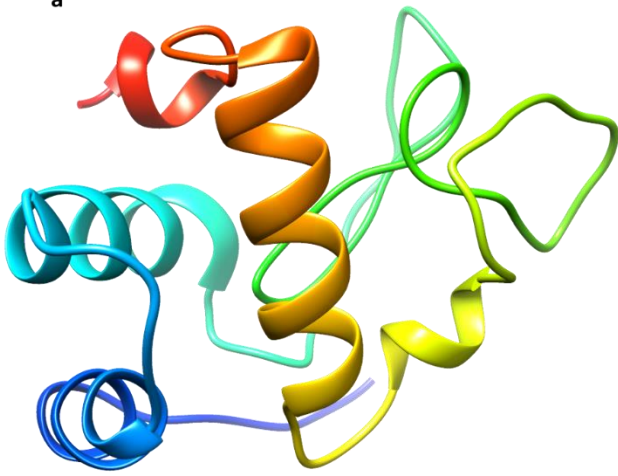
b



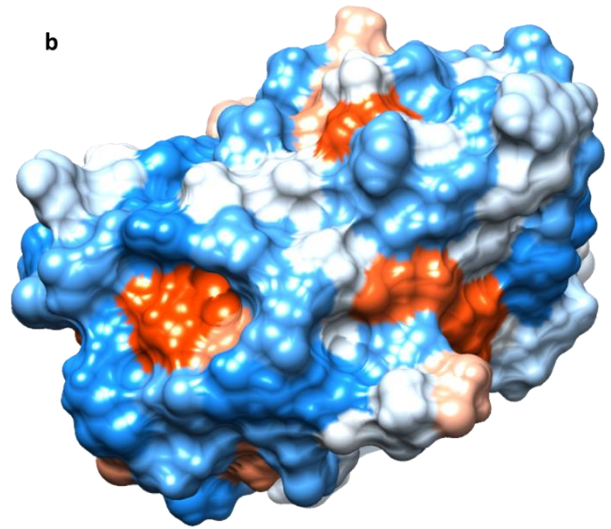


C1153

a

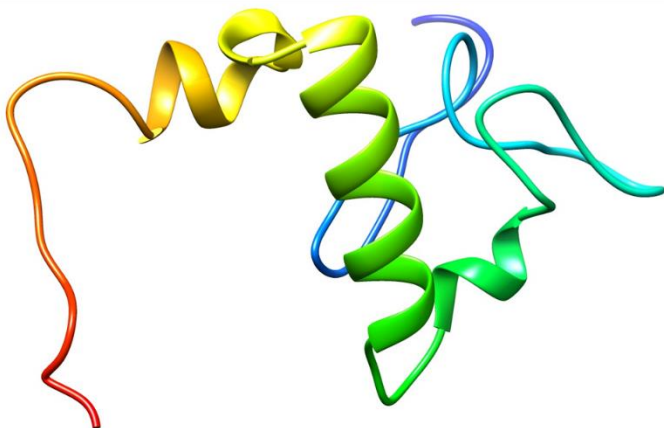


b

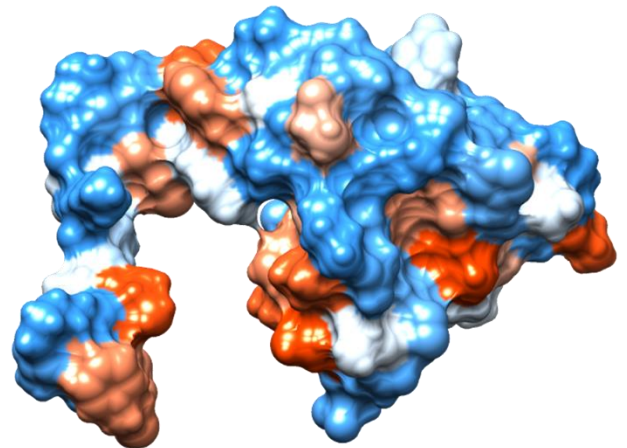


C1169

a



b

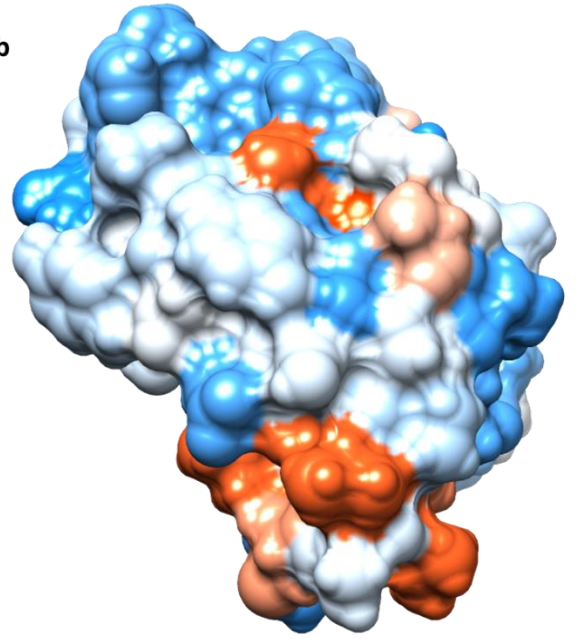


C1290

a

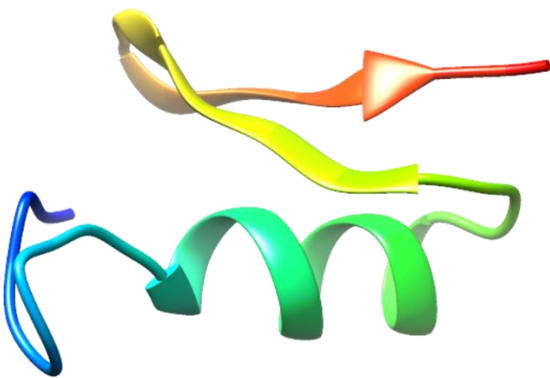


b

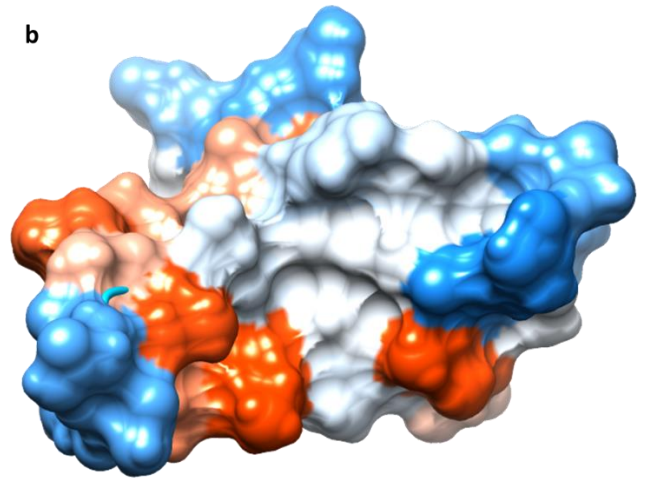


C1619

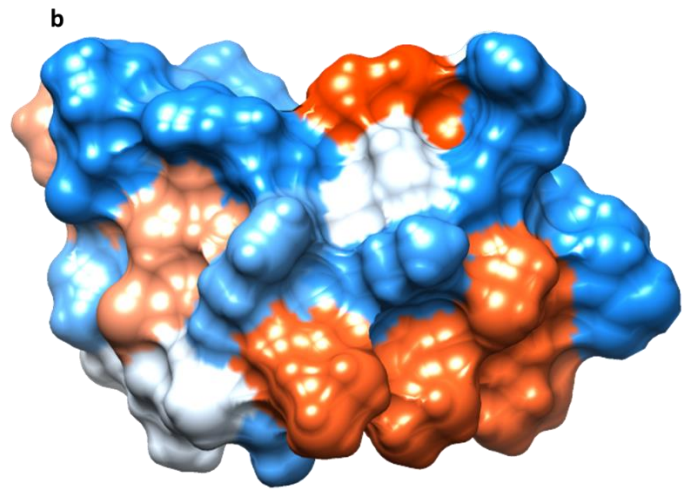
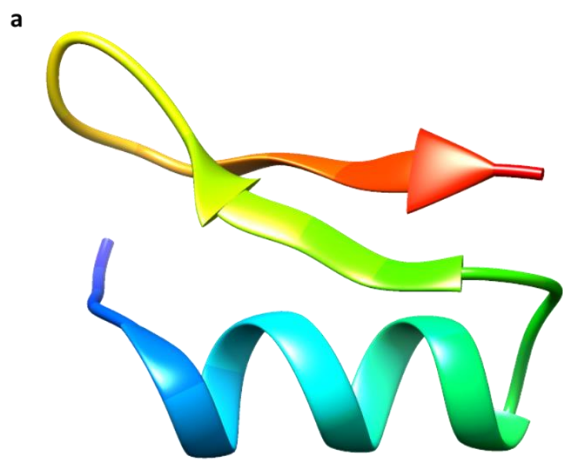
a



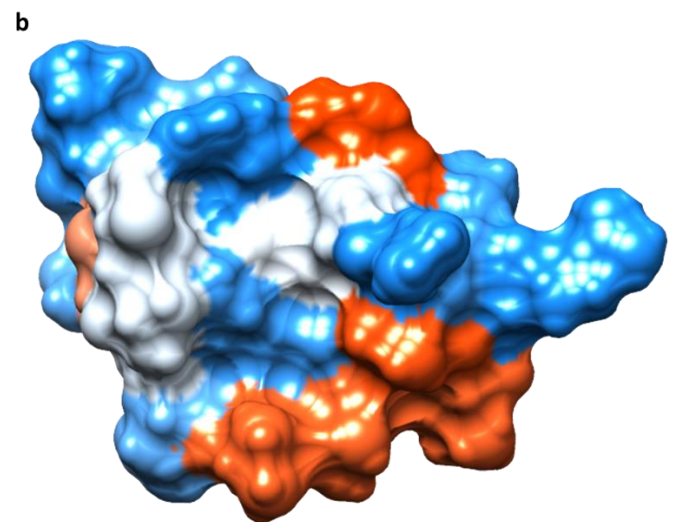
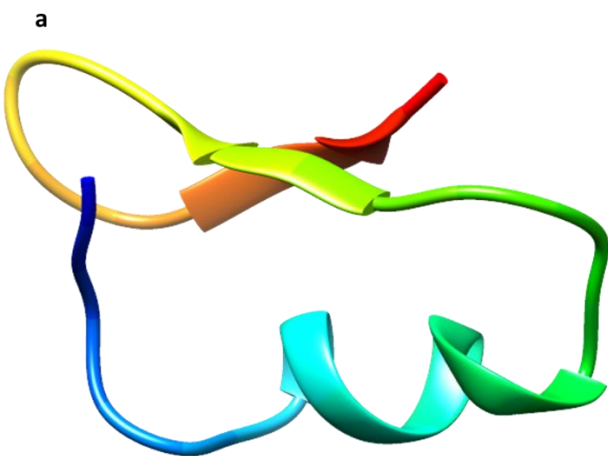
b



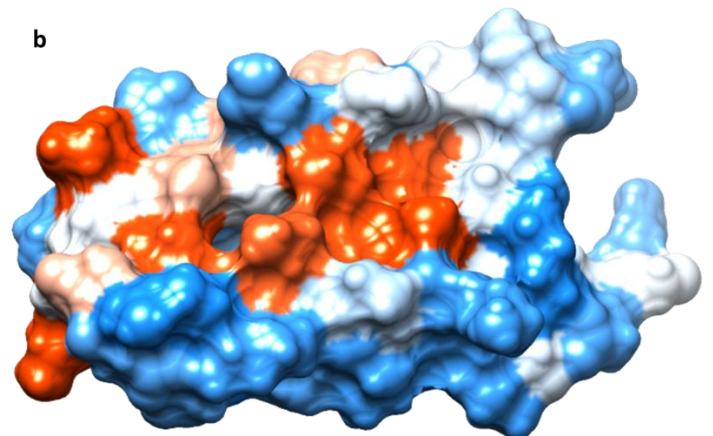
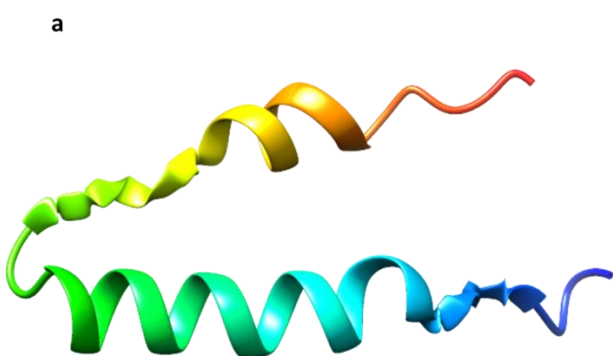
C1826



C1827

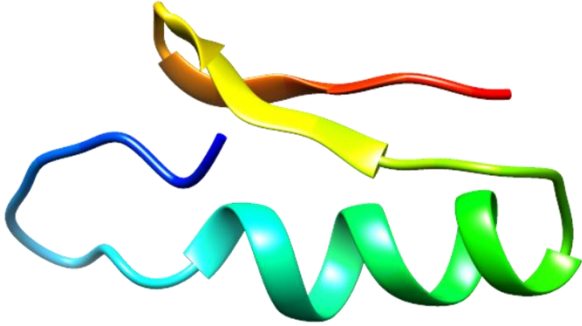


C1875

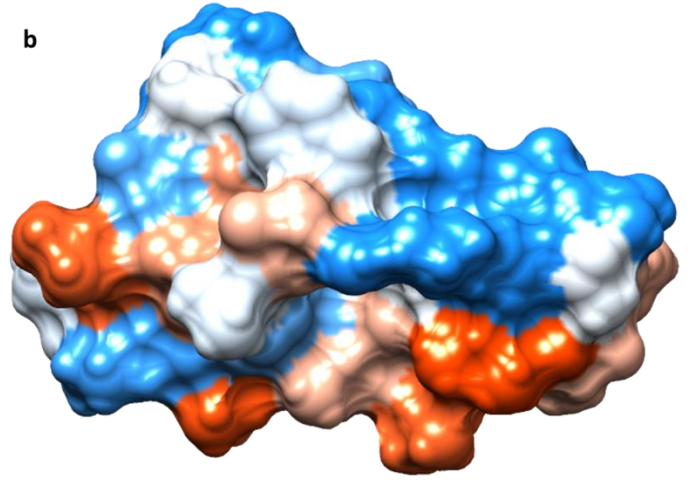


C2519

a

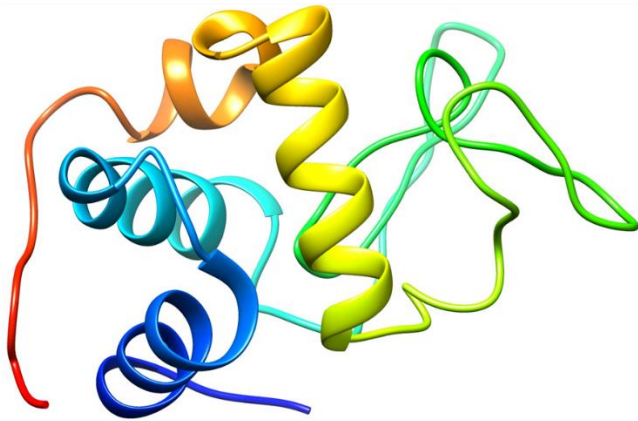


b

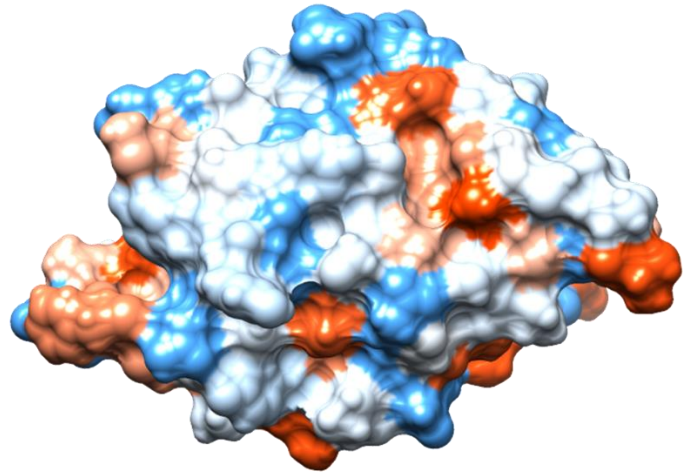


C2676

a

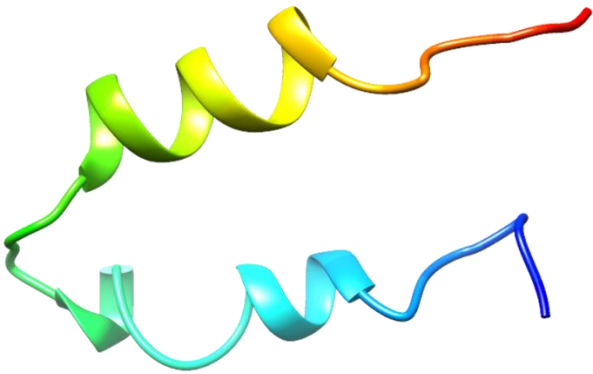


b

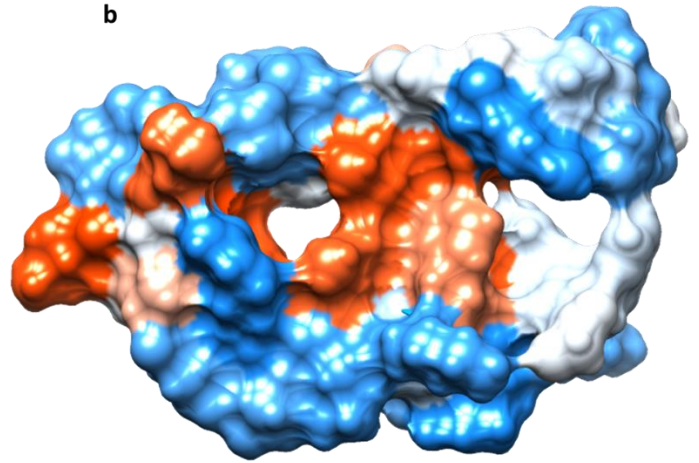


C2730

a

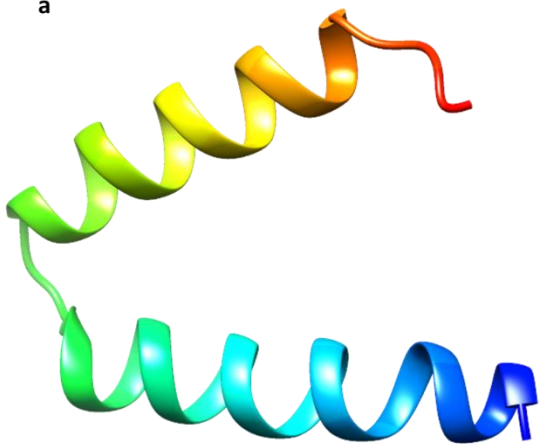


b

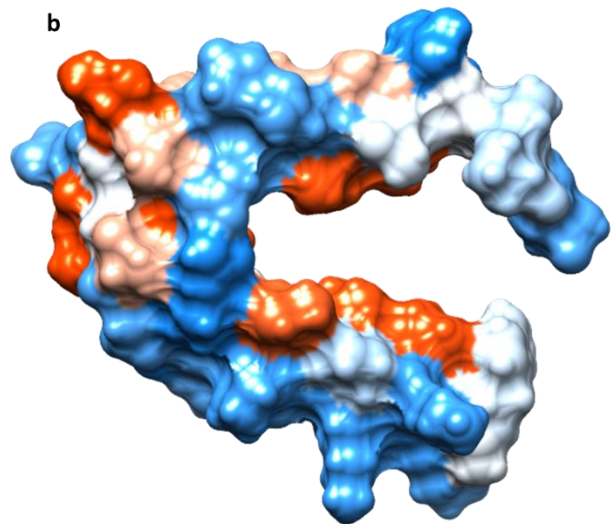


C3195

a

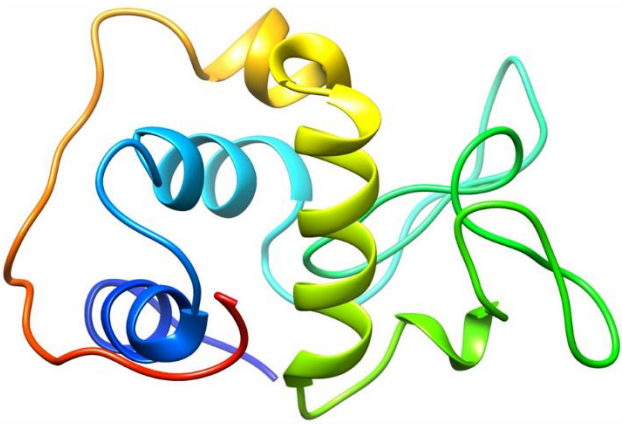


b

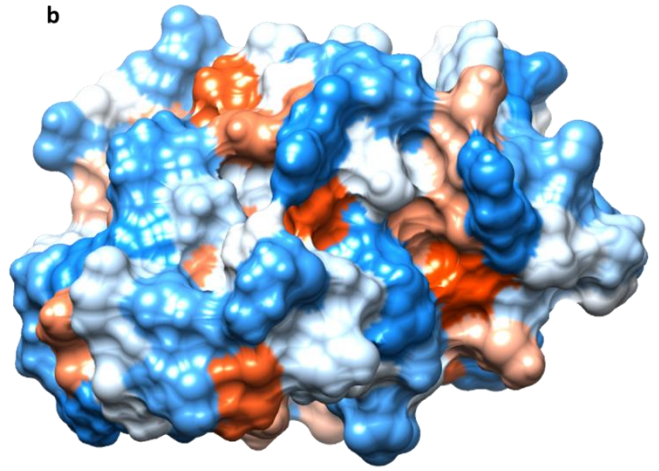


C3566

a



b

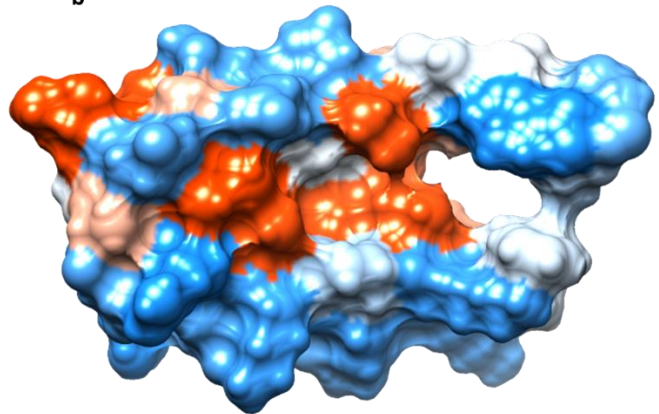


C4669

a

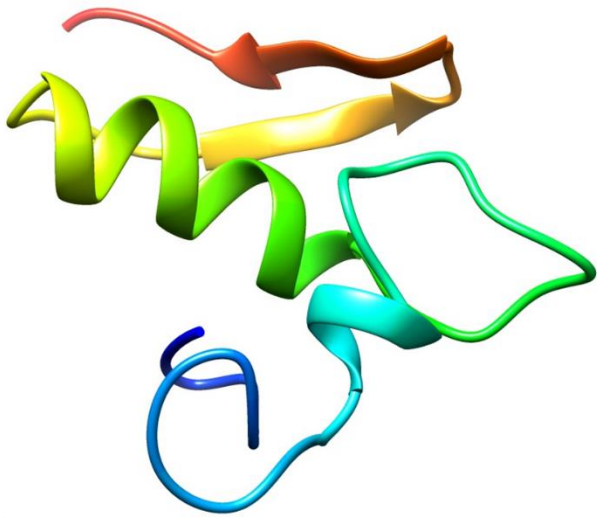


b

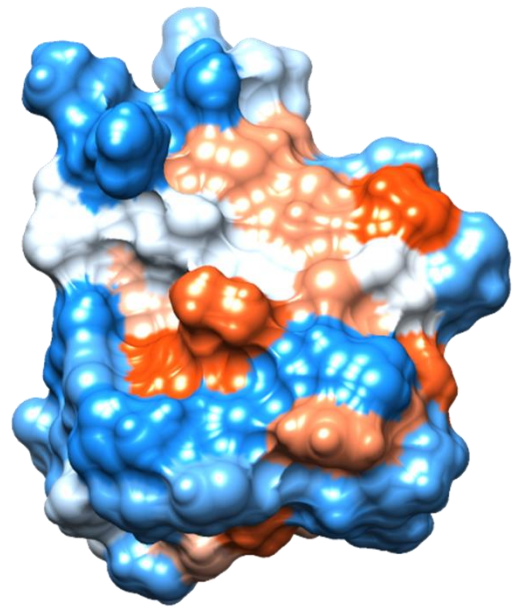


C4683

a

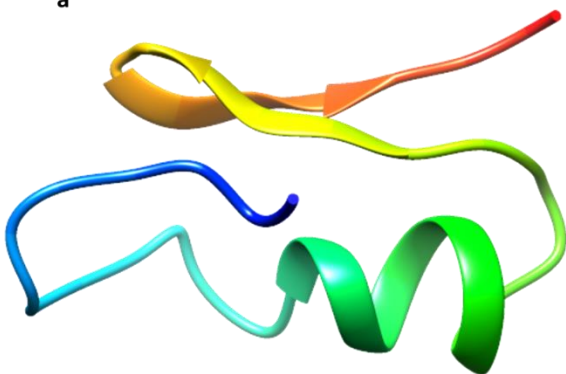


b

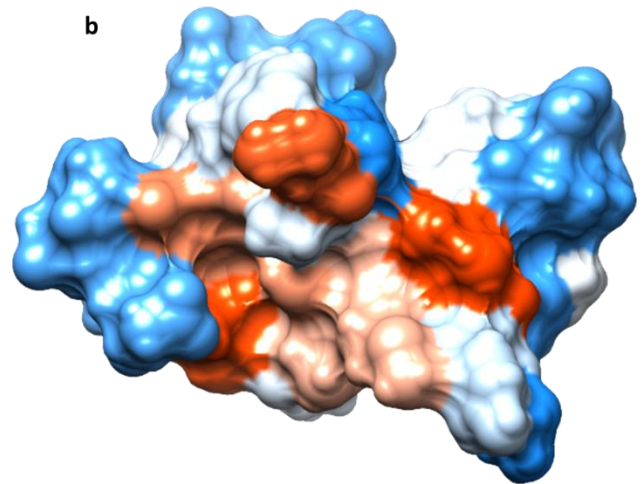


C4977

a

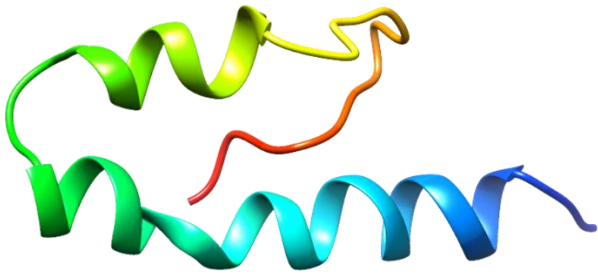


b

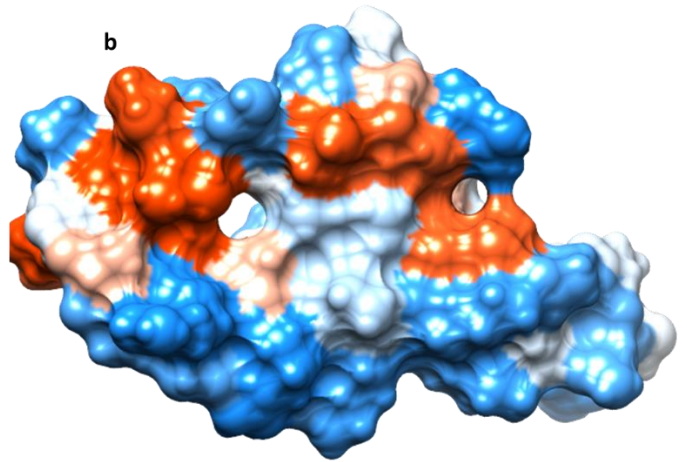


C5151

a

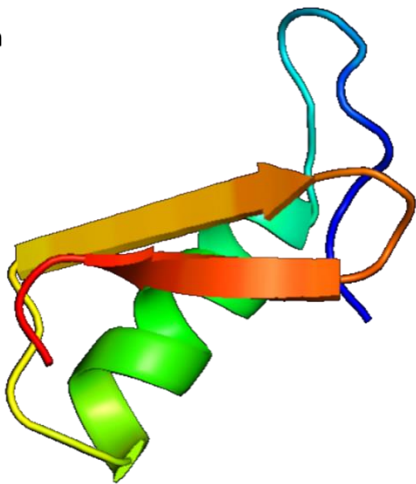


b

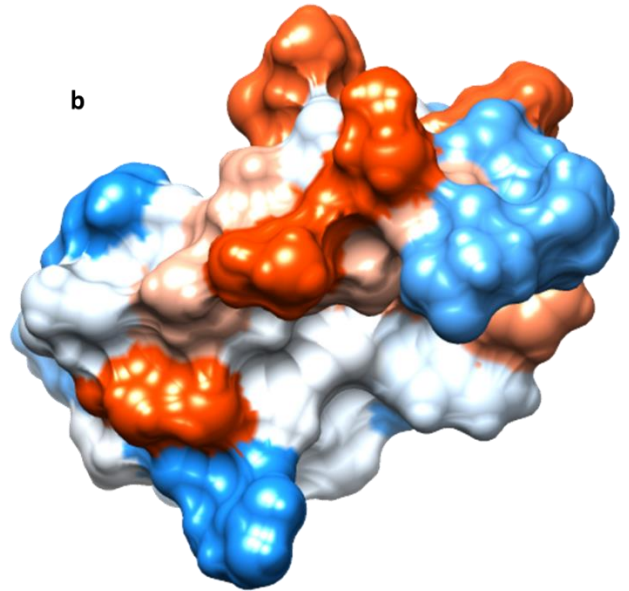


C5878

a



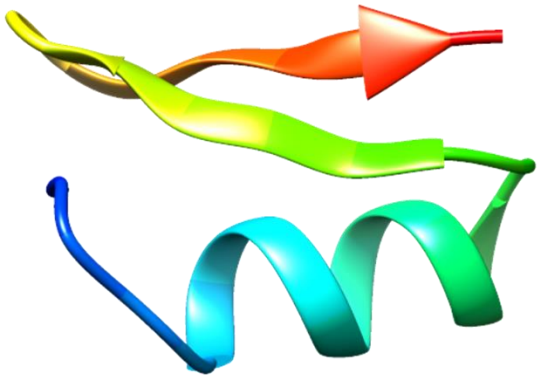
b



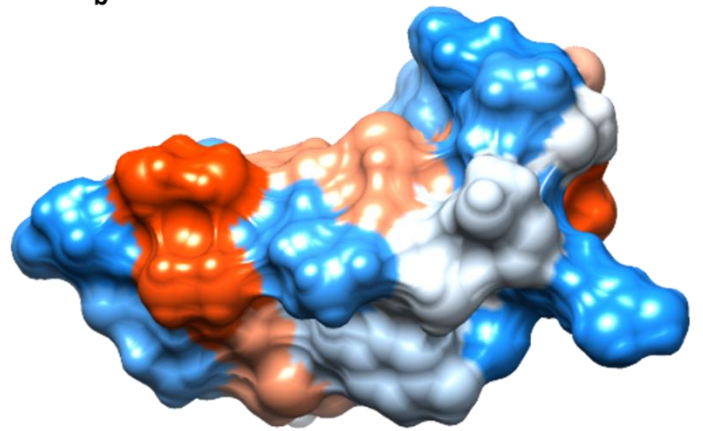


C6571

a

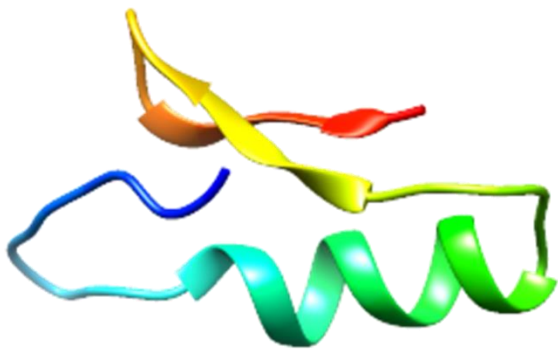


b

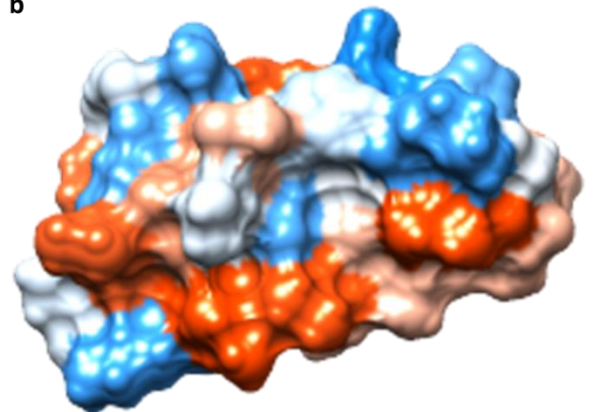


C7081

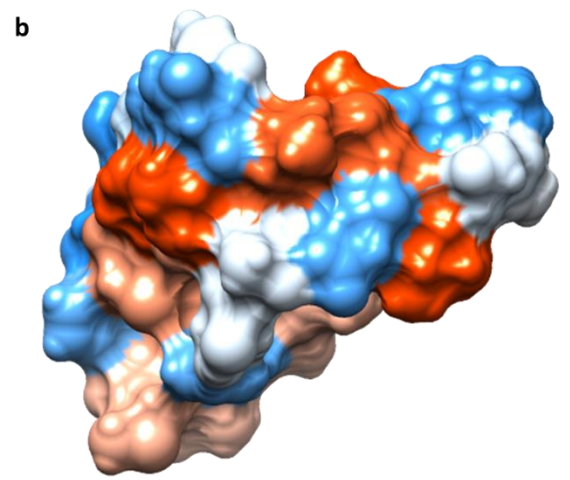
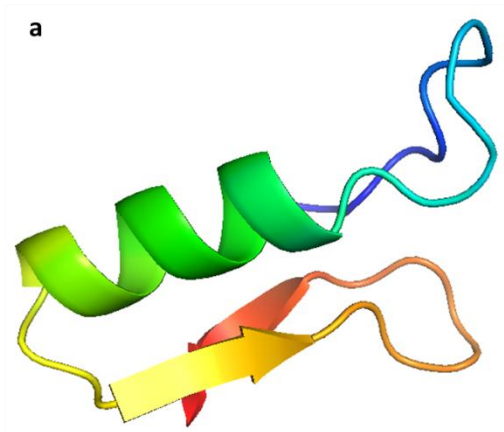
a



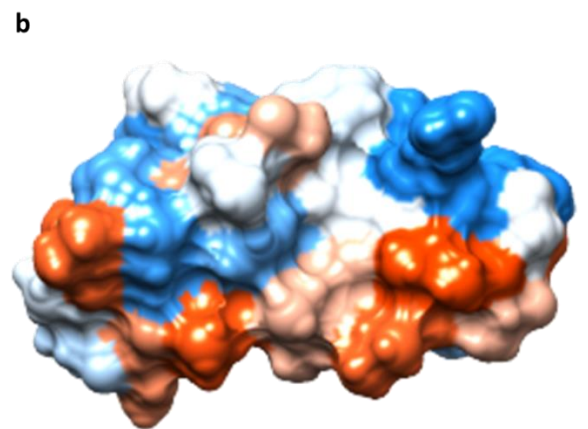
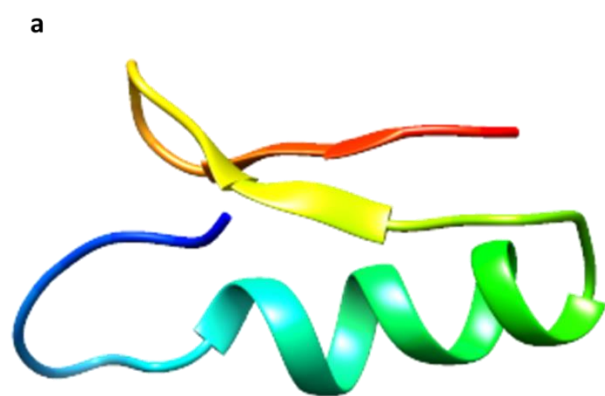
b



C7171

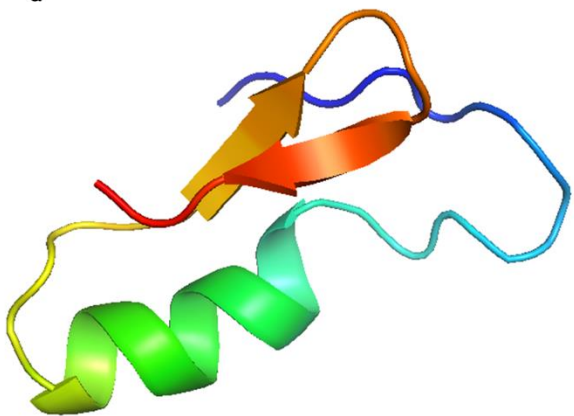


C7176

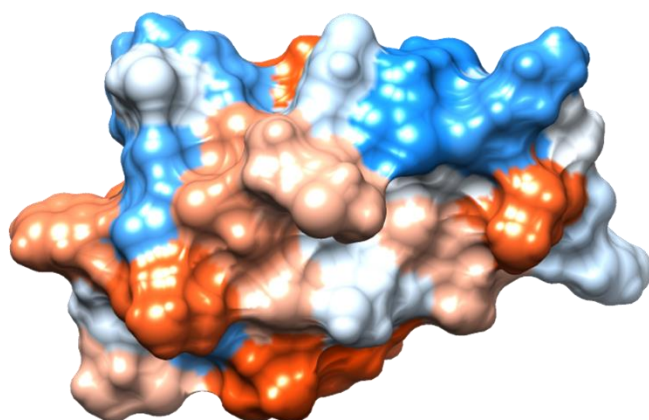


C7758

a

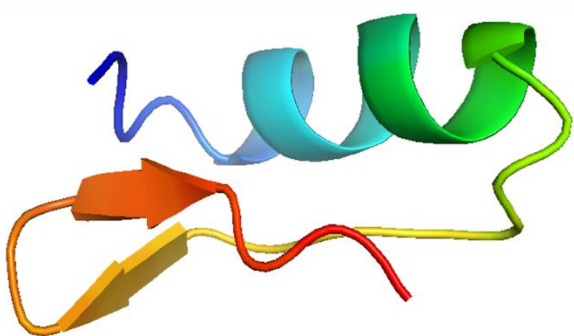


b

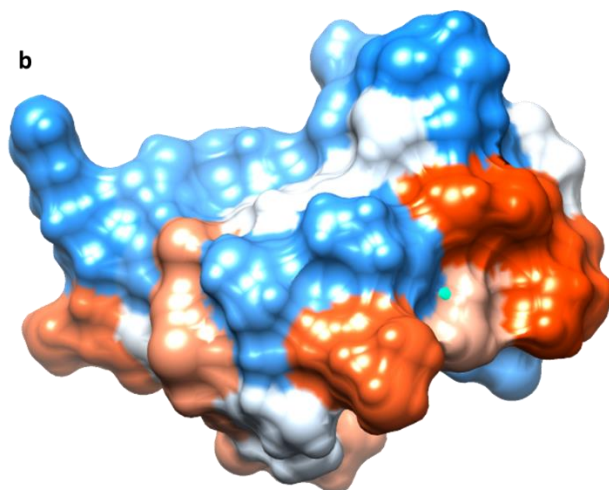


C7985

a

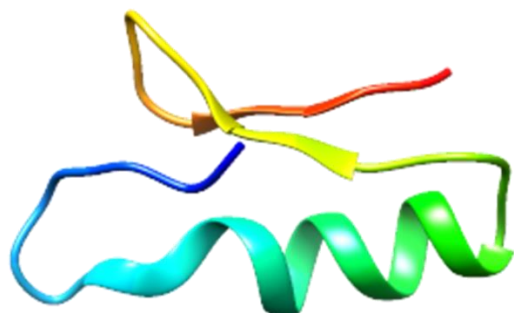


b

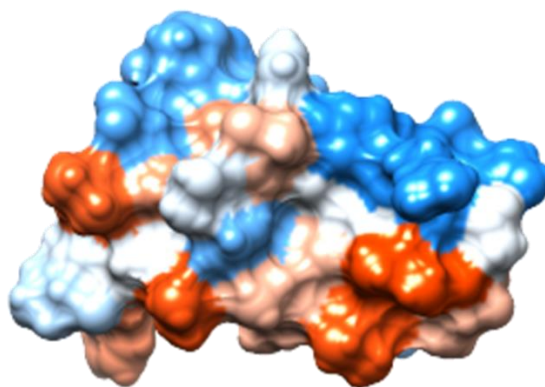


C8473

a

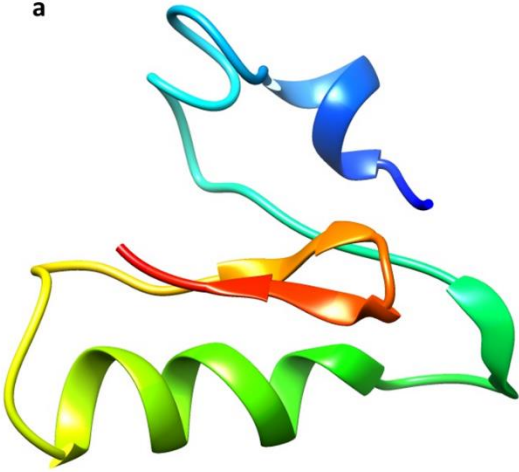


b

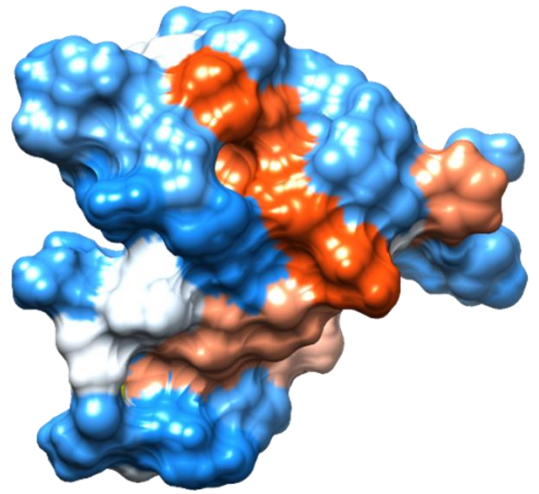


C10649

a

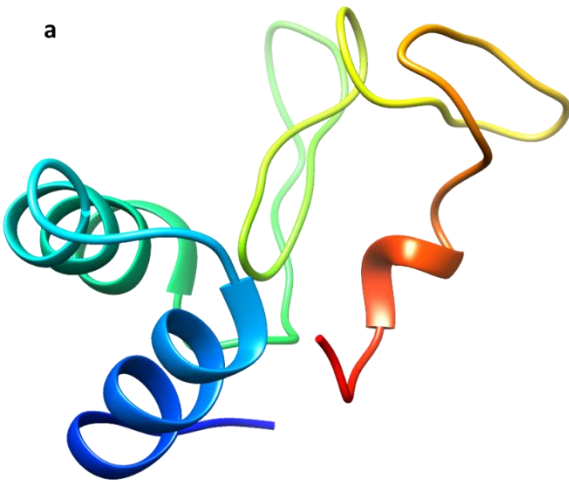


b

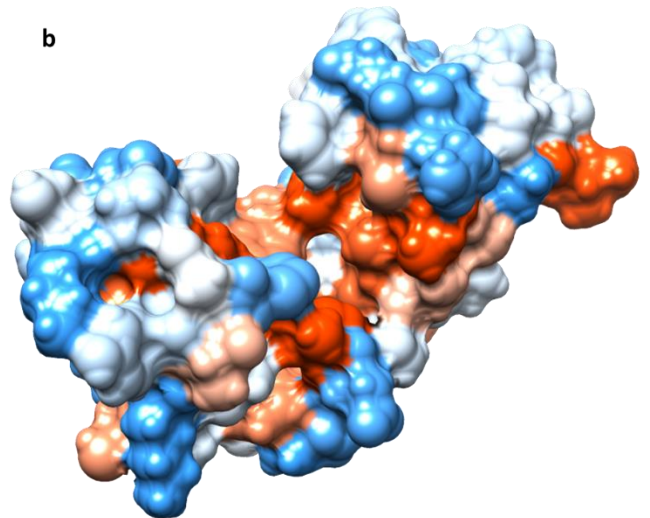


C12085

a

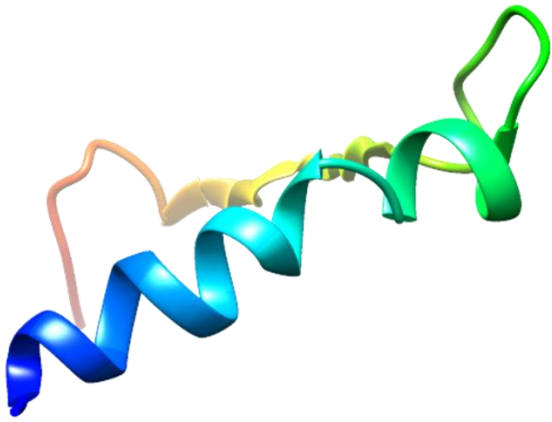


b

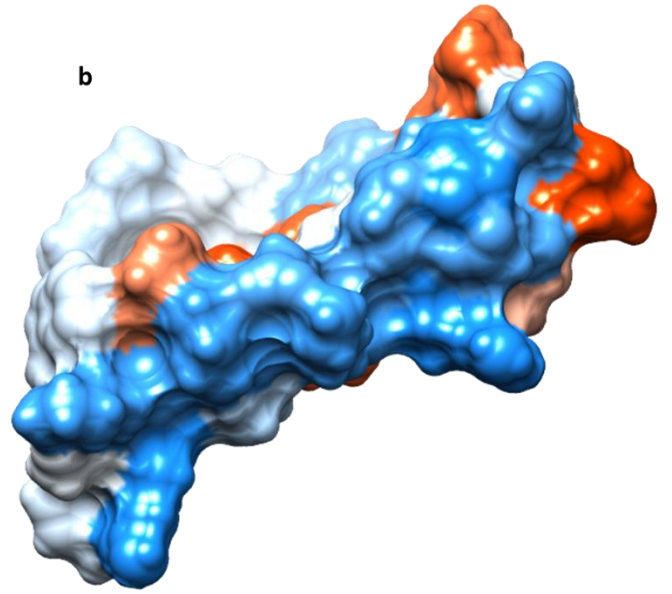


C12927

a

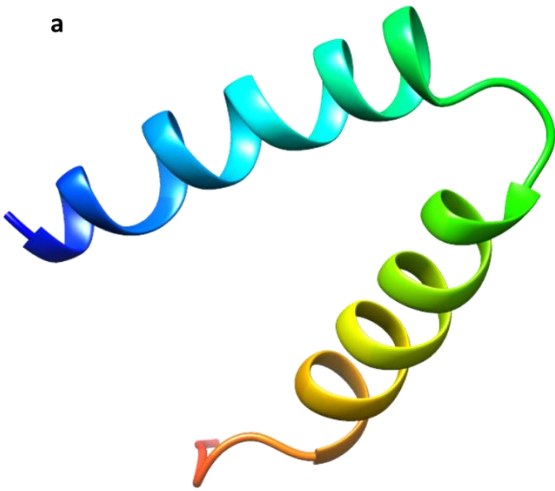


b

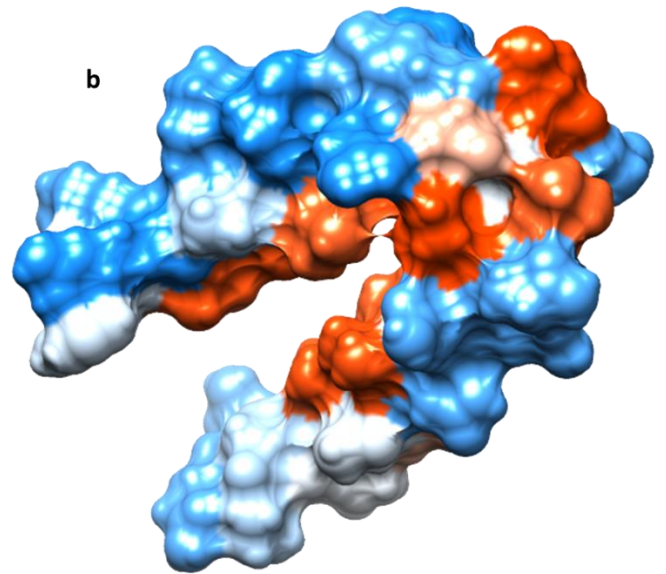


C12928

a

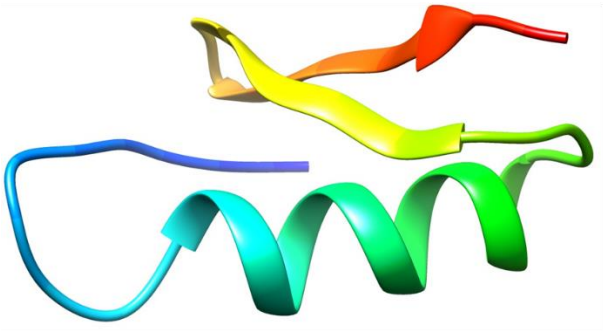


b

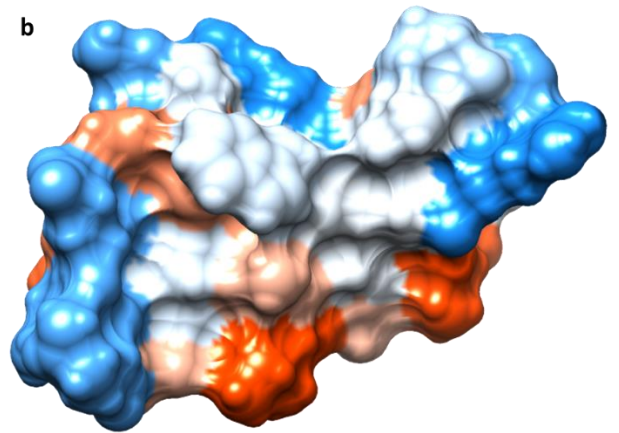


C13326

a

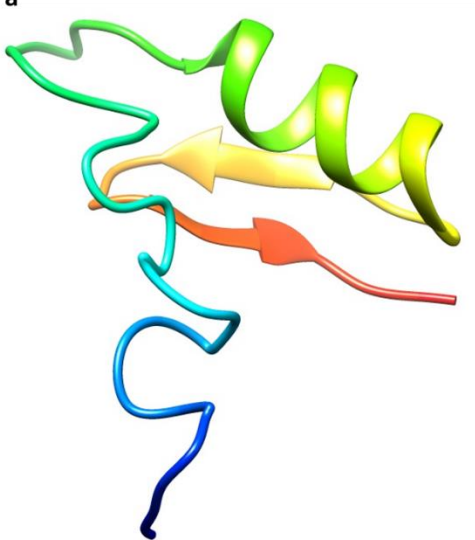


b

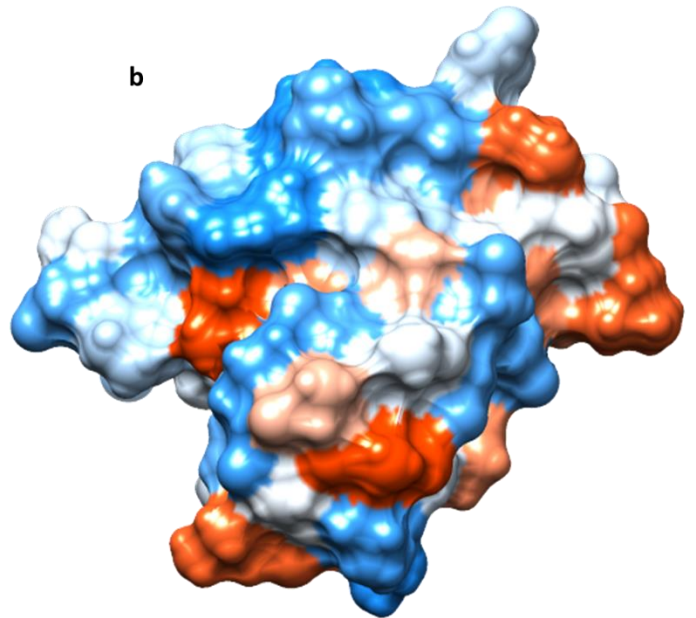


C13792

a

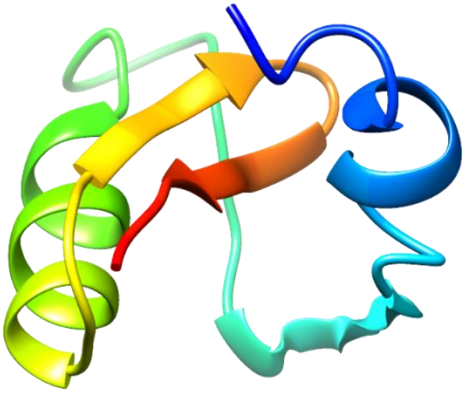


b

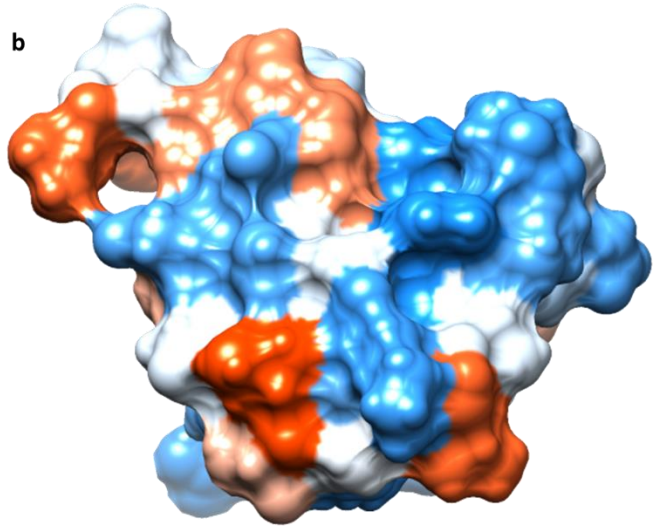


C13793

a

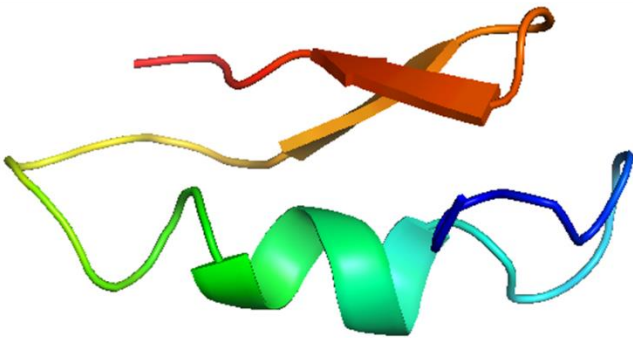


b

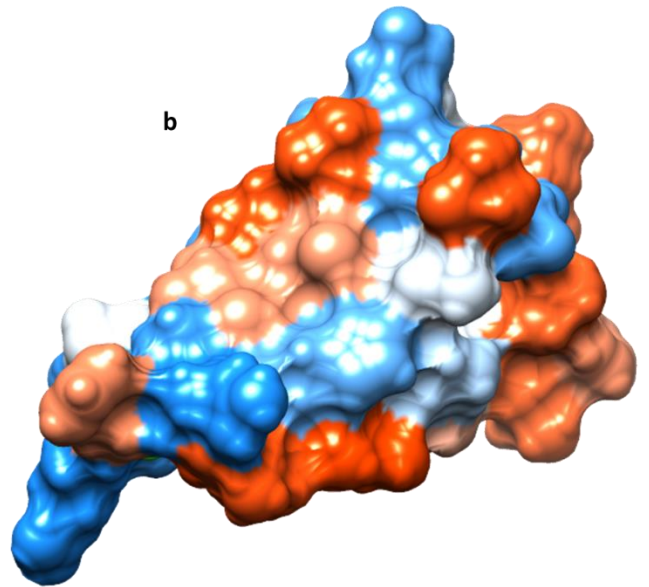


C14087

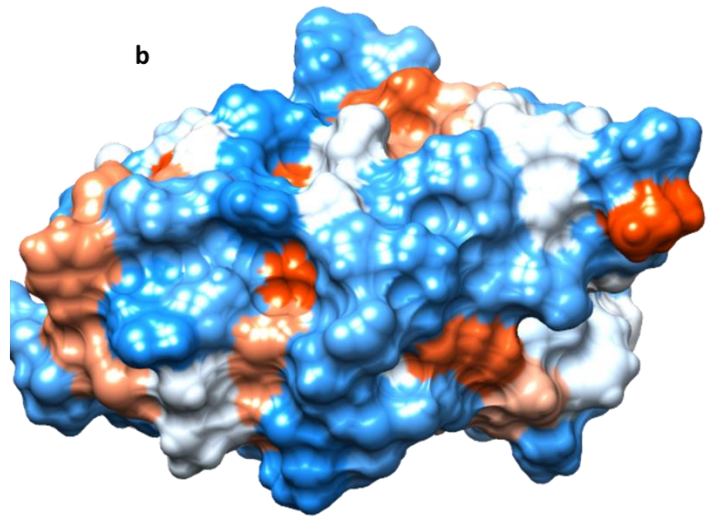
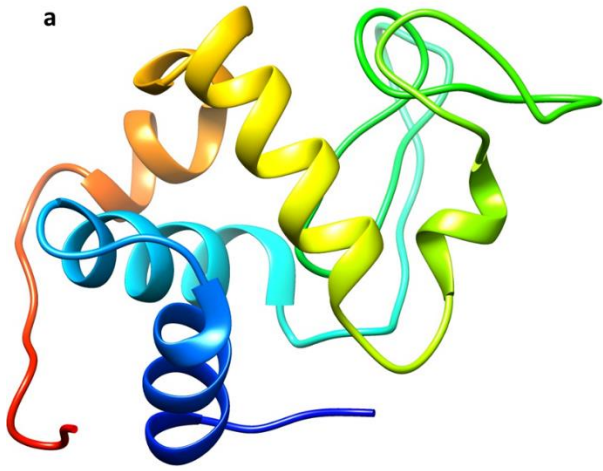
a



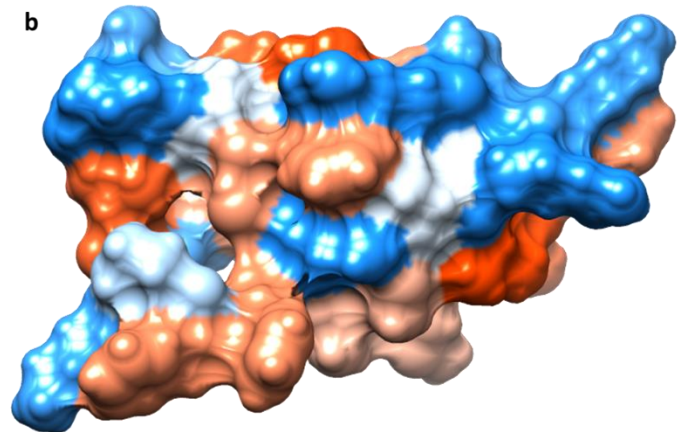
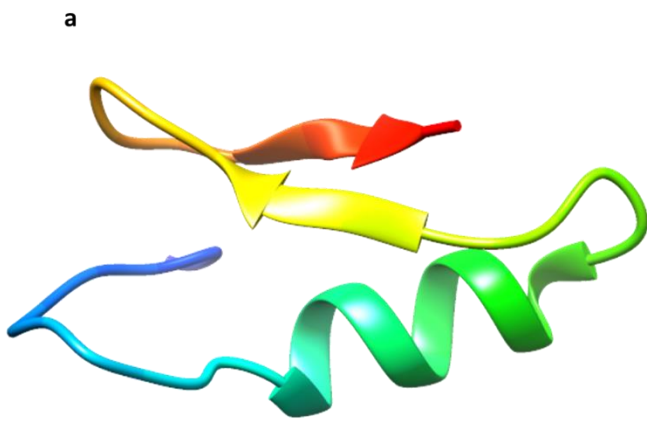
b



C14202



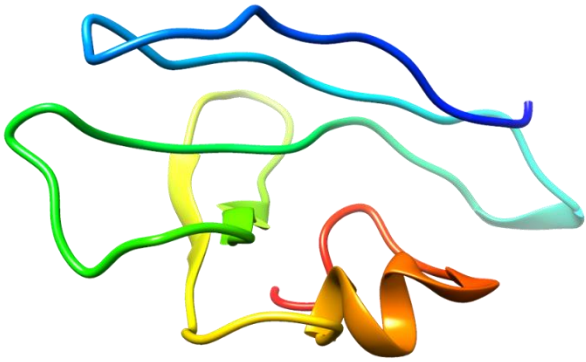
C15867



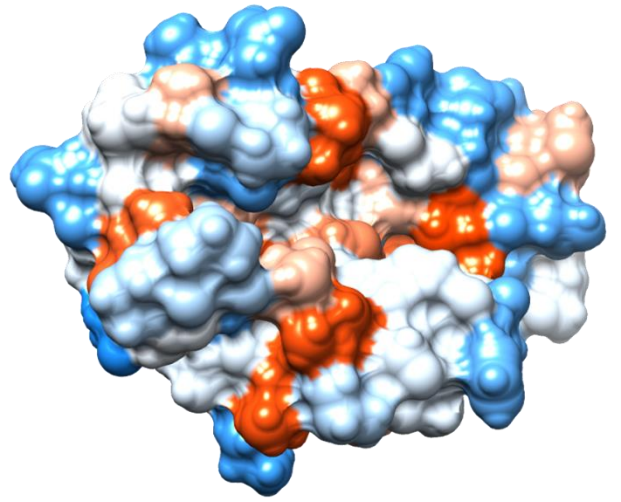


C16137

a

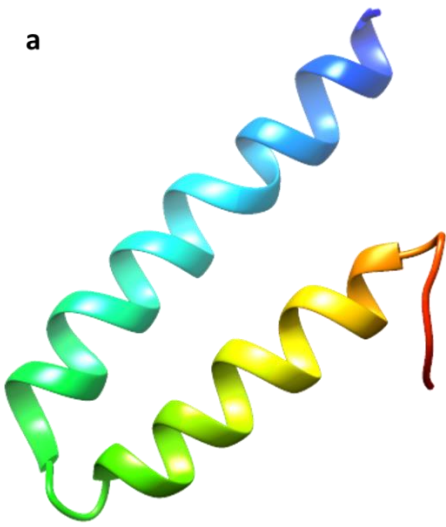


b

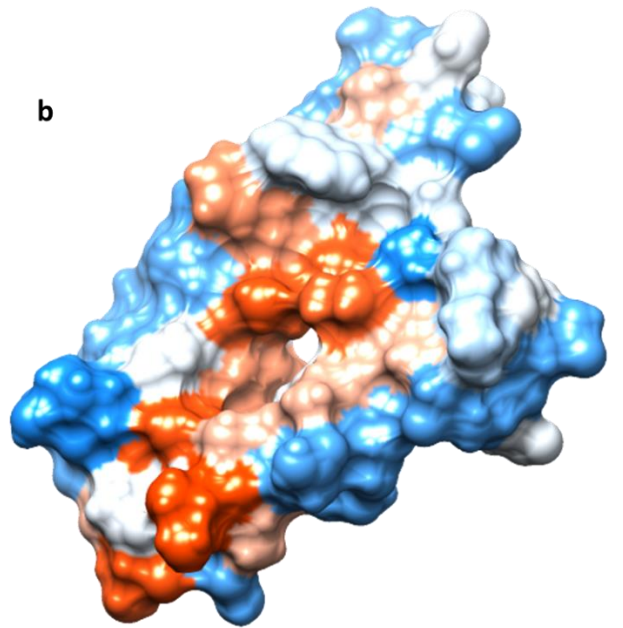


C16493

a

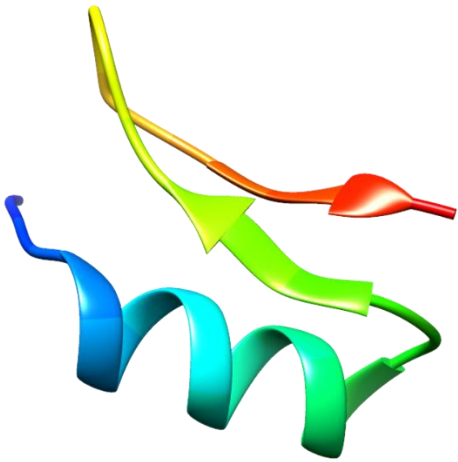


b

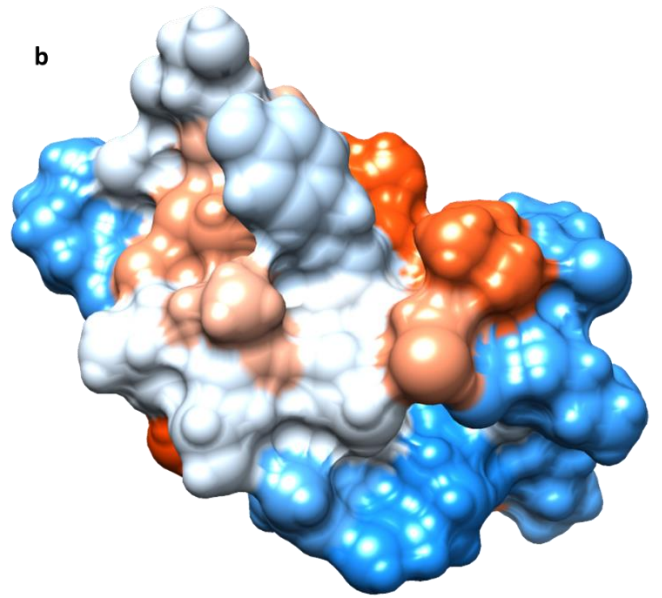


C16634

a

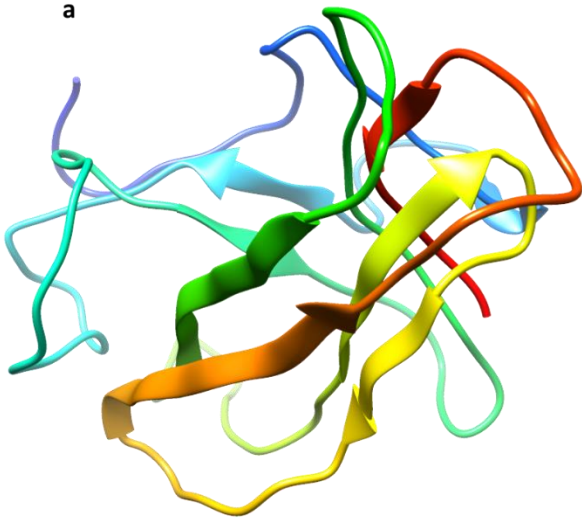


b

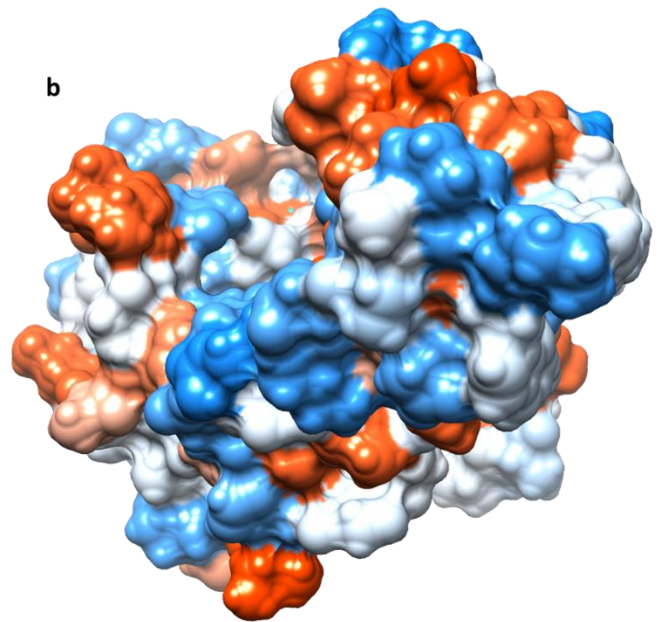


C16883

a

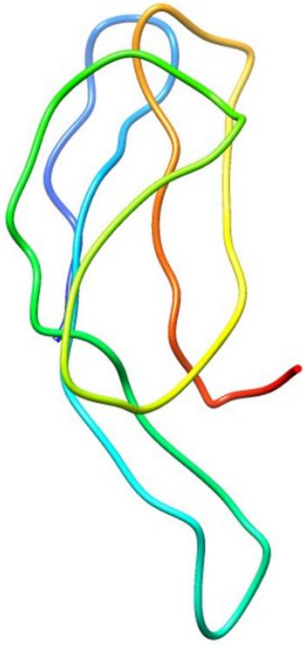


b

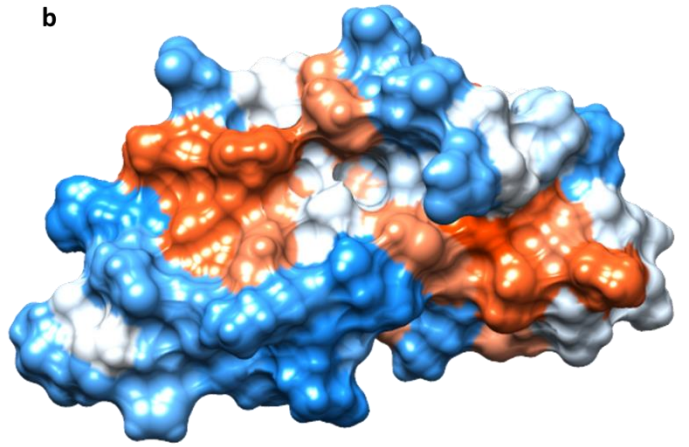


C21232

a

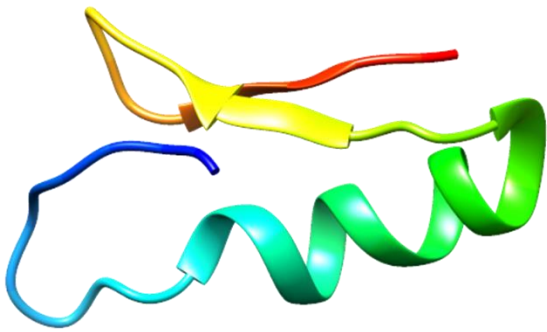


b

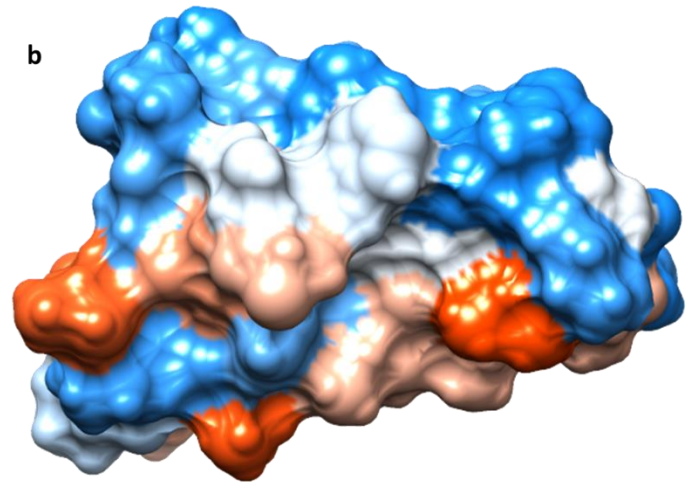


C29142

a

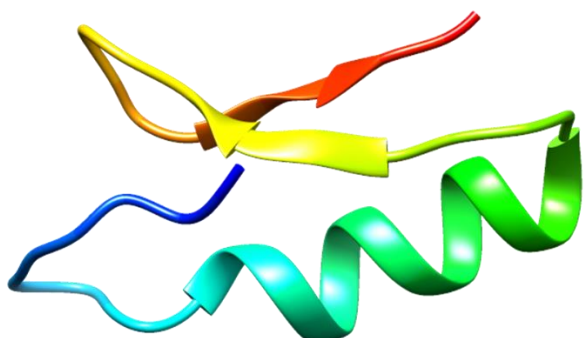


b

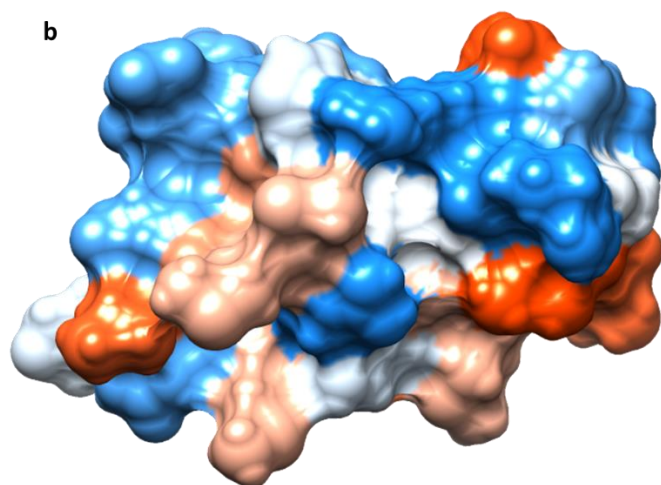


C34351

a

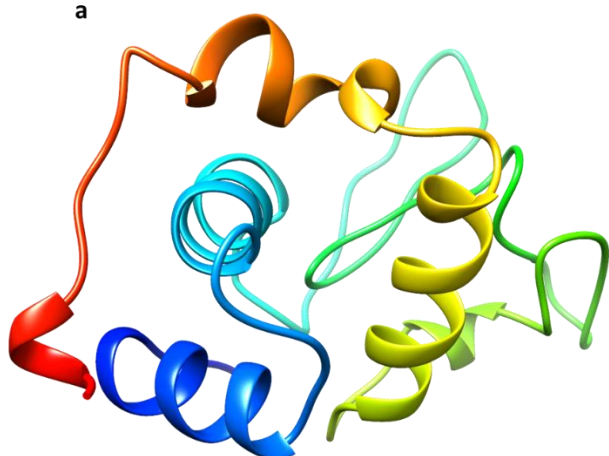


b

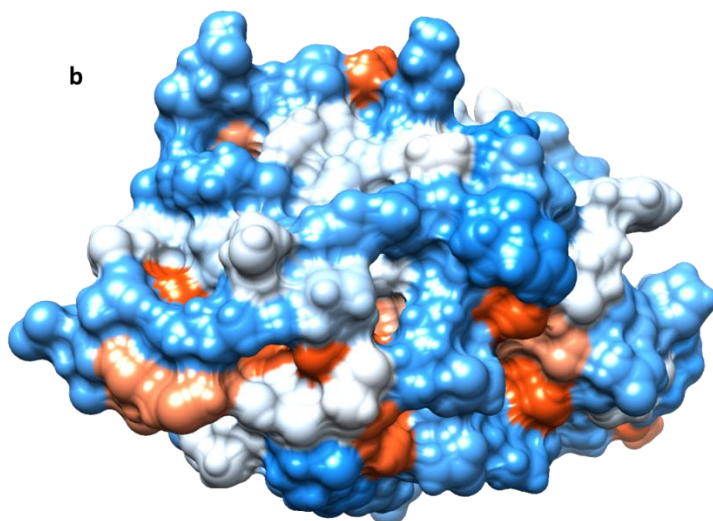


C36111

a

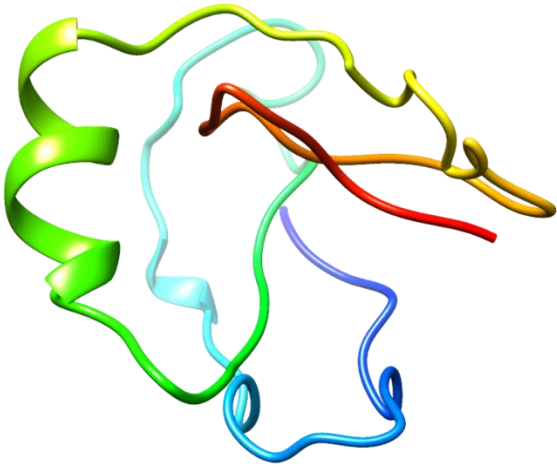


b

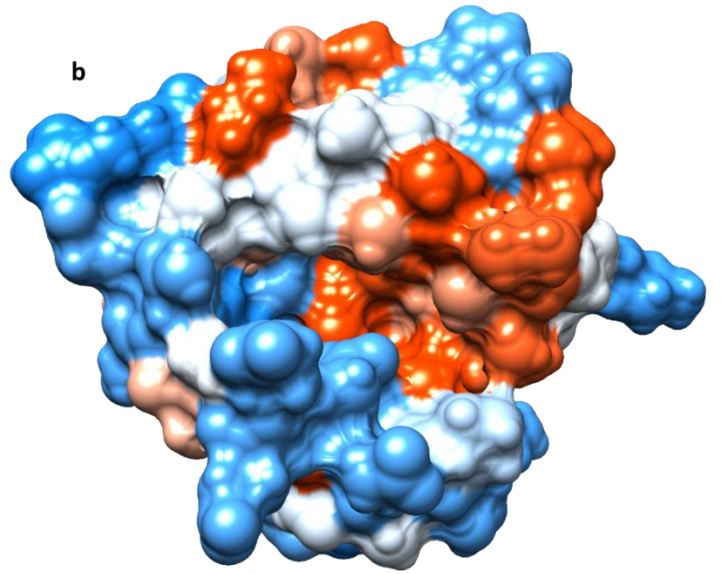


C37730

a

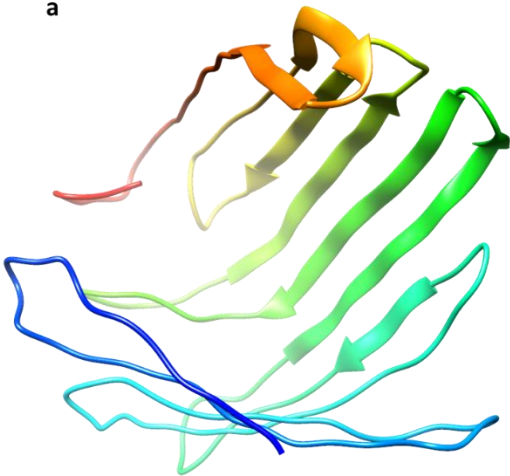


b

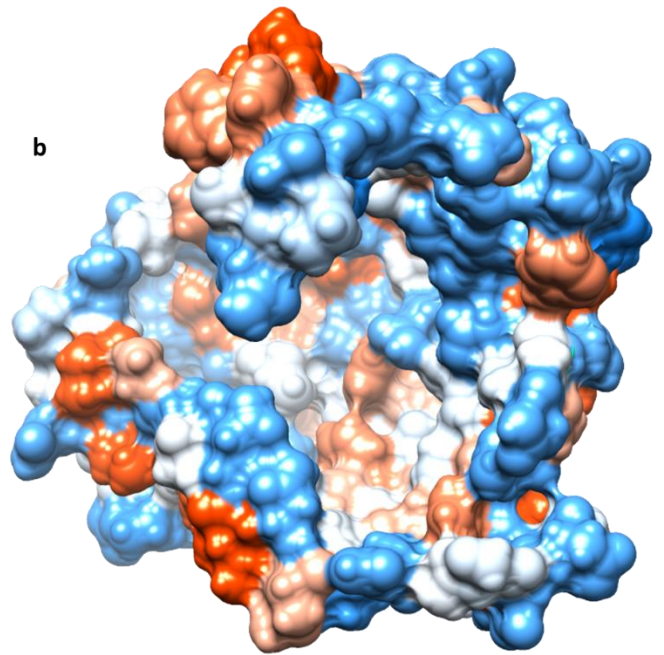


C40487

a

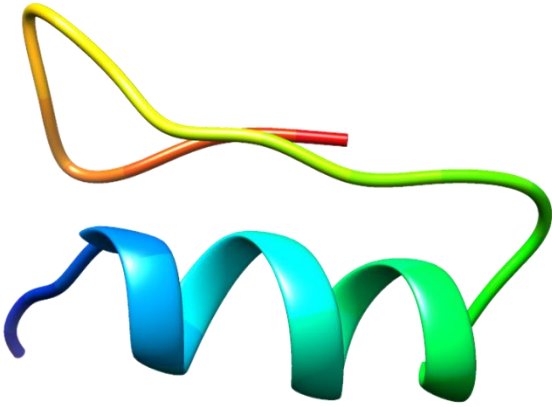


b

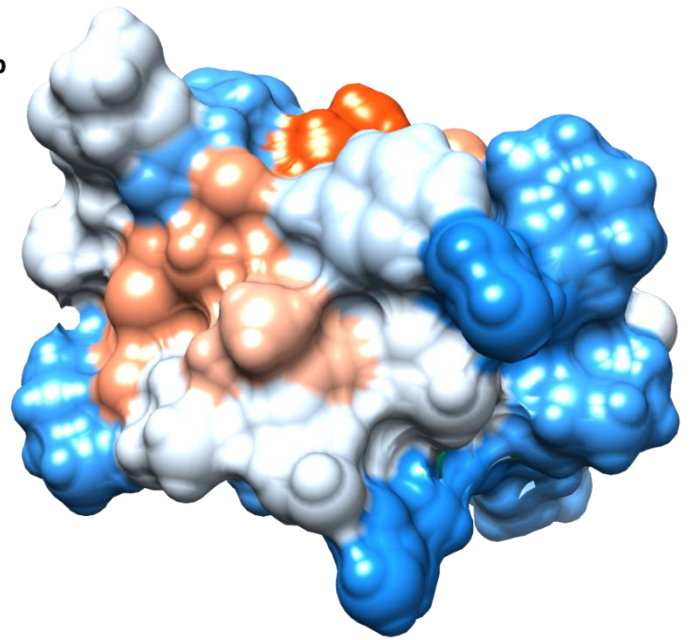


C46948

a



b

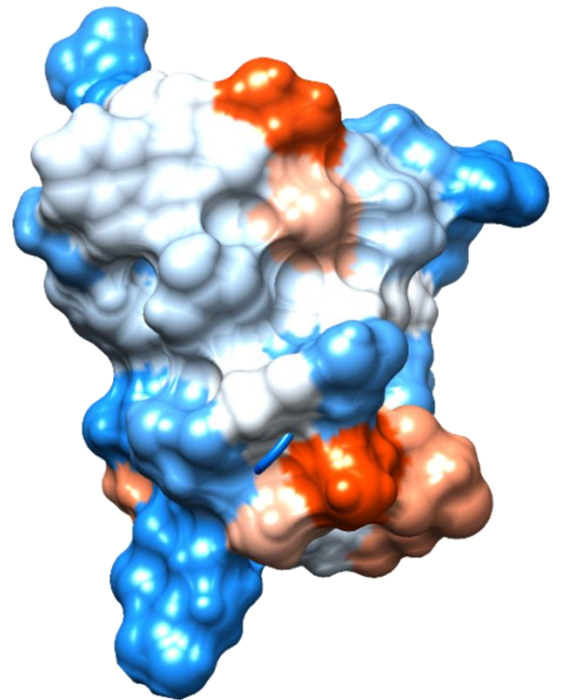


C49215

a

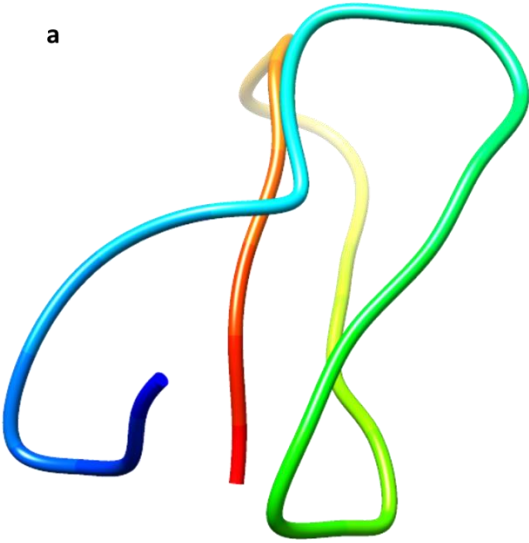


b

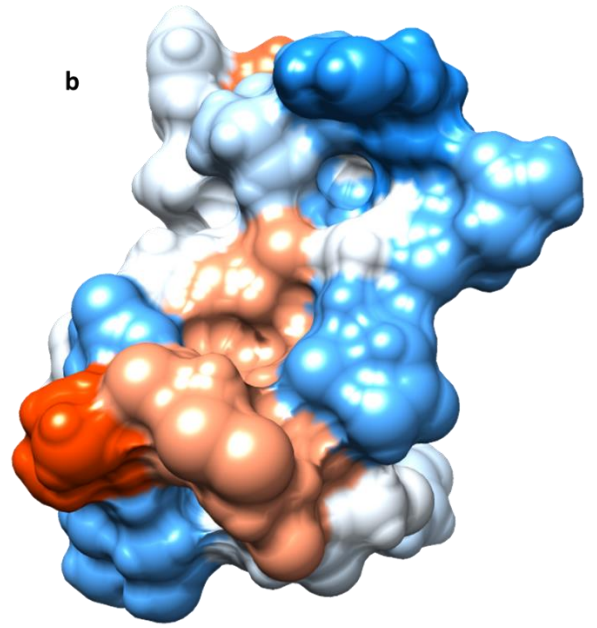


C53857

a

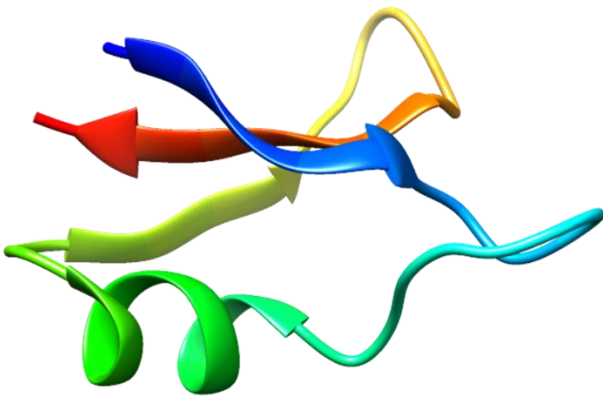


b

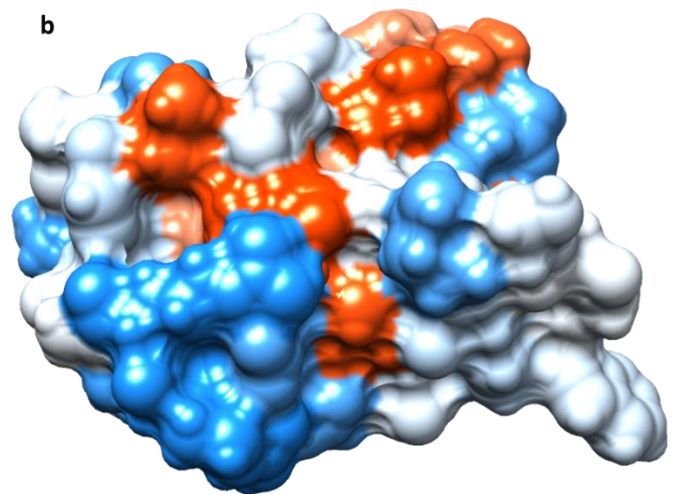


C69719

a



b



C73537

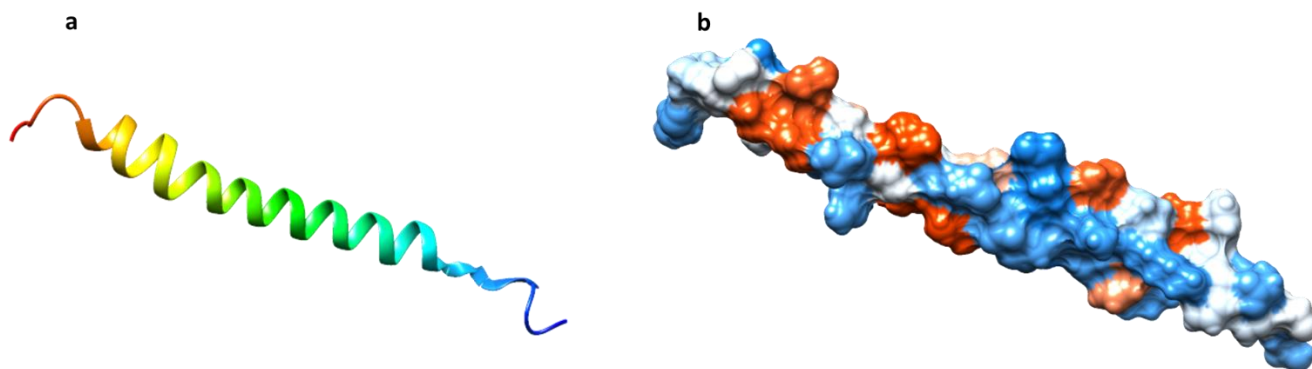
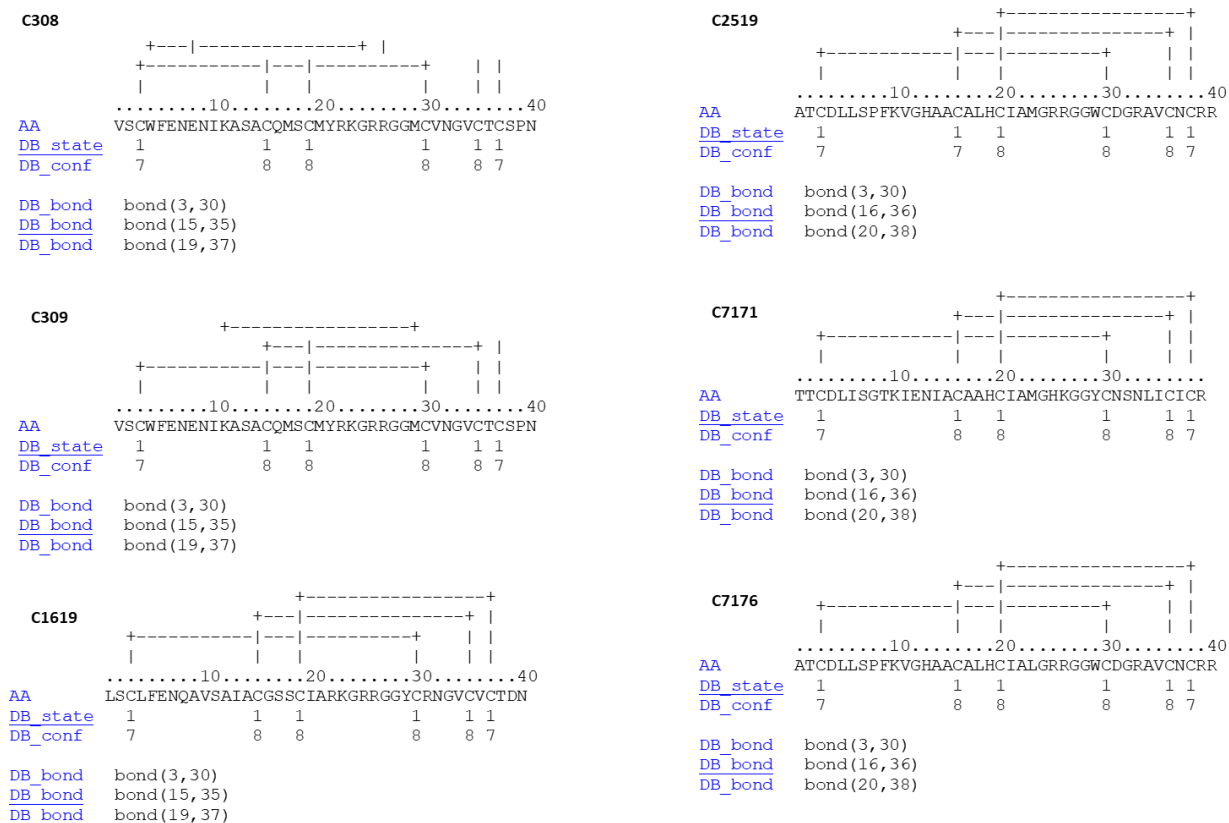


**Figure 15.** a) 3D model obtained for all the identified peptides by I-TASSER server; b) hydrophobicity surface obtained for all peptides where in orange-red are shown the most hydrophobic residues and in blue the most hydrophilic residues.

Through the DISULFIND server the disulfide bonds conformation was evaluated for the Cys-rich identified peptides (Figure 16).









#### 4.6. Molecular cloning in TOPO – VECTOR plasmid.

From the total RNA extracted from *H. illucens* larvae, infected with the *Micrococcus flavus* bacterium, cDNA was obtained by means of a retro-transcription reaction using the SuperScript™ III Reverse Transcriptase (Invitrogen) kit. The cDNA obtained was used to set up a PCR reaction, using the KOD DNA Polymerase kit (EMD Millipore Corp.) and using a pair of primers (forward and reverse) specific for the chosen AMPs (containing the restriction sites for BamHI and EcoRI).

- Primers for Hill\_COMB-BB\_C2519

FW: 5' – GGATCCGCAACCTGTGACCTCTTG – 3'

RV: 5' – GAATTCTTAGCGTCTGCAATTACAAAC – 3'

- Primers for Hill\_COMB-BB\_C15867

FW: 5' – GGATCCGTCACCTGTGATCTTCTAAA – 3'

RV: 5' – GAATTCTTATCTGCACACGCAAACG – 3'

- Primers for Hill\_COMB-BB\_C10649

FW: 5'- GGATCCCAGTTTGACAATCTAGAAGAT- 3'

RV: 5' – GAATTCTTAGGTGCATCTACAAACTC- 3'

- Primers for Hill\_COMB-BB\_C13792

FW: 5' – GGATCCAAGCAATCAAGTGATCCAGA – 3'

RV: 5' – GAATTCCTATAAGGTTCTGCAACGAC – 3'

The PCR products were subjected to agarose gel electrophoresis (1.2%) and the obtained inserts were recovered through band excision from the gel at the expected size: 135 bp for Hill\_COMB-BB\_C2519, 132 bp for Hill\_COMB-BB\_C15867, 183 bp for Hill\_COMB-BB\_C10649 and 198 bp Hill\_COMB-BB\_C13792 (including the 12 nucleotides of the restriction sites at the 3' and 5' ends) (Figure 17).

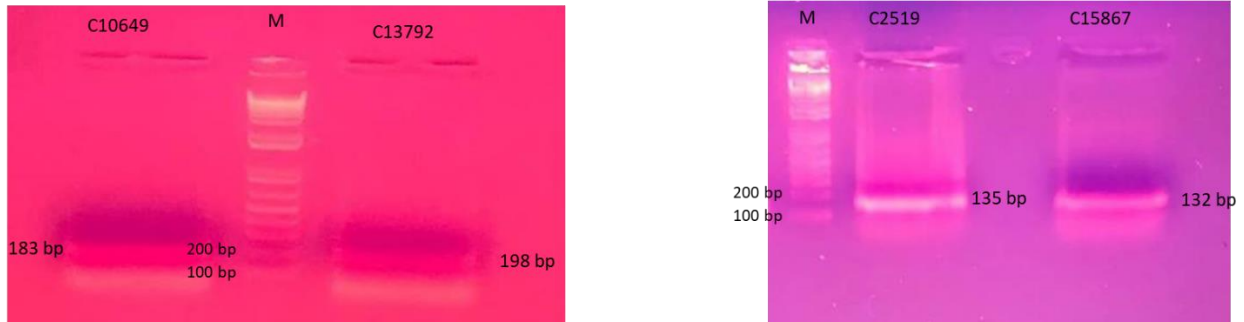


**Figure 17.** Agarose gel electrophoresis of the PCR products with the expected bands: 183 bp for C10649, 198 bp for C13792, 135 bp for C2519, and 132 bp for C15867.

The purified inserts were cloned using the pCR II - TOPO VECTOR cloning plasmid, the recombinant constructs were then transformed in chemically competent TOP-10 cells and the plasmids DNA were recovered by miniprep.

The obtained clones were subjected to sequencing analysis finding a 100% of identity (Figure 18, 19, 20, 21) with the sequences of the peptides identified in the transcriptome.

```

1      GGATCCGCAACCTGTGACCTCTTGAGTCCCTTCAAAGTGGGTCATGCTGCCTGCGCACTT      60
2      GGATCCGCAACCTGTGACCTCTTGAGTCCCTTCAAAGTGGGTCATGCTGCCTGCGCACTT      60
*****

1      CATTGTATTGCCATGGGACGACGAGGAGGCTGGTGCGATGGTCGAGCCGTTTGT AATTGC      120
2      CATTGTATTGCCATGGGACGACGAGGAGGCTGGTGCGATGGTCGAGCCGTTTGT AATTGC      120
*****

1      AGACGCTAAGAATTC      135
2      AGACGCTAAGAATTC      135
*****

```

**Figure 18.** C2519 alignment between the cloned sequence and the identified sequence in the transcriptome.

```

1      GGATCCGTCACCTGTGATCTTCTAAAACCTTTCTTTGGTCGCGCCCCCTTGCATGATGCAT      60
2      GGATCCGTCACCTGTGATCTTCTAAAACCTTTCTTTGGTCGCGCCCCCTTGCATGATGCAT      60
*****

1      TGTATTTTGCGGTTTAAAAAGCGTACTGGATTCTGTAGTAGACAAAACGTTTGCGTGTGC      120
2      TGTATTTTGCGGTTTAAAAAGCGTACTGGATTCTGTAGTAGACAAAACGTTTGCGTGTGC      120
*****

1      AGATAAGAATTC      132
2      AGATAAGAATTC      132
*****

```

**Figure 19.** C15867 alignment between the cloned sequence and the identified sequence in the transcriptome.

```

1      GGATCCCAGTTTGACAATCTAGAAGATACAGGAGTTGAGGAGAAAGTTCGT CATAAGCGC      60
2      GGATCCCAGTTTGACAATCTAGAAGATACAGGAGTTGAGGAGAAAGTTCGT CATAAGCGC      60
*****

1      CTAACCTGCCTATTCGACAATCGCCCCATCTCAGCATTGCGTGTGGTTCCAAC TGTGT      120
2      CTAACCTGCCTATTCGACAATCGCCCCATCTCAGCATTGCGTGTGGTTCCAAC TGTGT      120
*****

1      TCACGAAAAGGAAAACGTGGTGGATGGTGTGTCAATGGAGTTTGTAGATGCACCTAAGAA      180
2      TCACGAAAAGGAAAACGTGGTGGATGGTGTGTCAATGGAGTTTGTAGATGCACCTAAGAA      180
*****

1      TTC      183
2      TTC      183
***

```

**Figure 20.** C10649 alignment between the cloned sequence and the identified sequence in the transcriptome.

```

1      GGATCCAAGCAATCAAGTGATCCAGAGTCAGCGTTGTA CT CAGATATTCACCCAAGGTTT      60
2      GGATCCAAGCAATCAAGTGATCCAGAGTCAGCGTTGTA CT CAGATATTCACCCAAGGTTT      60
*****

1      AGGCGACAGCTTCCTTGCGATTATCTTAGCGGTTTGGGATT CGGCGAAGACGCCTGCAAC      120
2      AGGCGACAGCTTCCTTGCGATTATCTTAGCGGTTTGGGATT CGGCGAAGACGCCTGCAAC      120
*****

1      ACGGATTGTATTGCAAAAGGACATAAAAAGCGGTTTTTGC ACTGGACTCGTTTGTCGTTGC      180
2      ACGGATTGTATTGCAAAAGGACATAAAAAGCGGTTTTTGC ACTGGACTCGTTTGTCGTTGC      180
*****

1      AGAACCTTATAGGAATTC      198
2      AGAACCTTATAGGAATTC      198
*****

```

**Figure 21.** C13792 alignment between the cloned sequence and the identified sequence in the transcriptome.

The recombinant products were enzymatically hydrolyzed with the restriction enzymes BamHI and EcoRI in order to verify that the molecular cloning had taken place correctly (Figure 22).

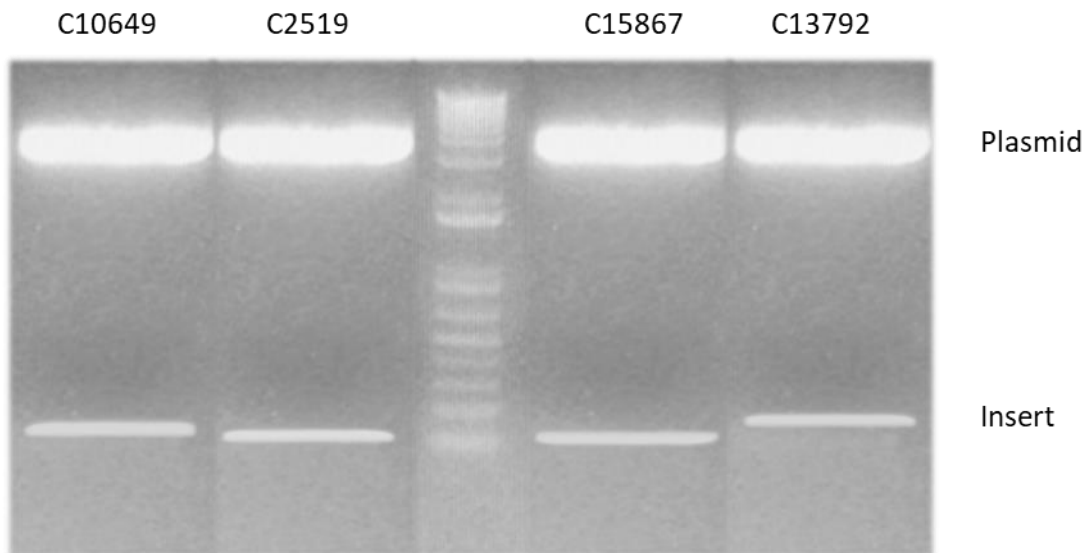


**Figure 22.** Enzymatic hydrolysis carried out with BamHI and EcoRI restriction enzymes of the obtained recombinant products.

#### 4.7. Molecular cloning in pGEX-4T1 expression plasmid.

The recombinant products obtained in TOPO vector have been enzymatically hydrolyzed with BamHI and EcoRI in order to recover only the genes of interest encoding for the AMPs and then cloned in the expression plasmid PGEX – 4T1. The recombinant constructs were then transformed in chemically competent DH5 $\alpha$  *E. coli* cells and the plasmid DNA were recovered by miniprep (Figure 23).

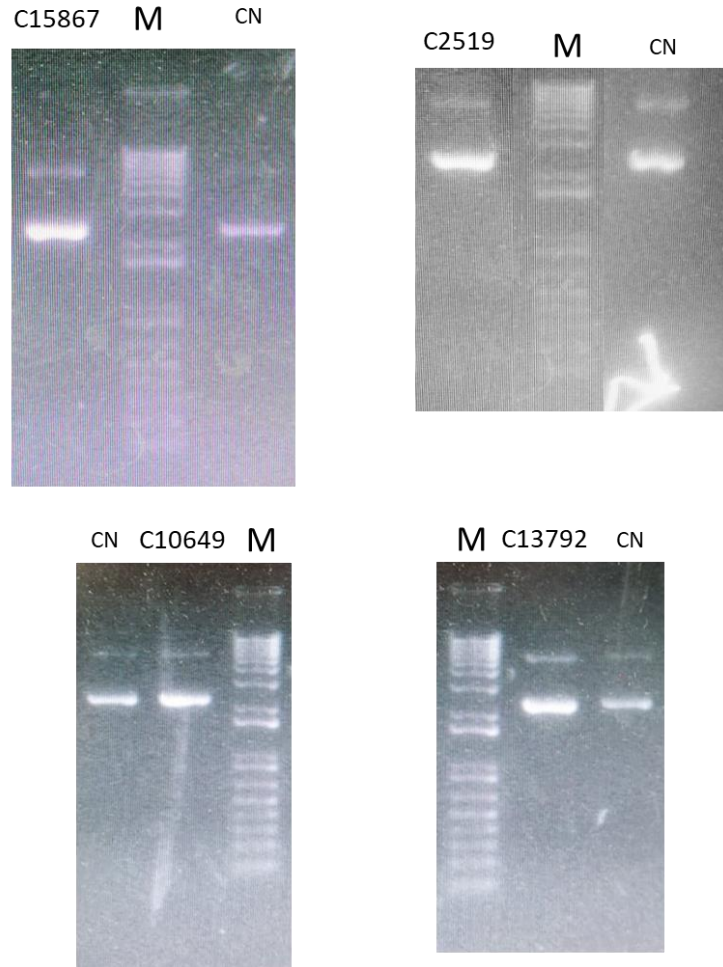


**Figure 23.** Miniprep of the recombinant products. CN is the negative control, which is only the plasmid without the insert.

The obtained fusion products (GST – Peptide) were subjected to sequencing analysis finding a 100% of identity (Figure 23, 24, 25, 26) with the sequences of the peptides identified in the transcriptome.

Score	Expect	Identities	Gaps	Strand
1491 bits(807)	0.0	807/807(100%)	0/807(0%)	Plus/Plus
Query 1	ATGTCCCCTATACTAGGTTATTGGAAAATTAAGGGCCTTGTGCAACCCACTCGACTTCTT	60		
Sbjct 1	ATGTCCCCTATACTAGGTTATTGGAAAATTAAGGGCCTTGTGCAACCCACTCGACTTCTT	60		
Query 61	TTGGAATATCTTGAAGAAAAATATGAAGAGCATTGTATGAGCGCGATGAAGGTGATAAA	120		
Sbjct 61	TTGGAATATCTTGAAGAAAAATATGAAGAGCATTGTATGAGCGCGATGAAGGTGATAAA	120		
Query 121	TGGCGAAACAAAAAGTTTGAATTGGGTTTGGAGTTTCCCAATCTTCCTTATTATATTGAT	180		
Sbjct 121	TGGCGAAACAAAAAGTTTGAATTGGGTTTGGAGTTTCCCAATCTTCCTTATTATATTGAT	180		
Query 181	GGTGATGTTAAATTAACACAGTCTATGGCCATCATACGTTATATAGCTGACAAGCACAAAC	240		
Sbjct 181	GGTGATGTTAAATTAACACAGTCTATGGCCATCATACGTTATATAGCTGACAAGCACAAAC	240		
Query 241	ATGTTGGGTGGTTGTCCAAAAGAGCGTGCAGAGATTTCAATGCTTGAAGGAGCGGTTTTG	300		
Sbjct 241	ATGTTGGGTGGTTGTCCAAAAGAGCGTGCAGAGATTTCAATGCTTGAAGGAGCGGTTTTG	300		
Query 301	GATATTAGATACGGTGTTTTCGAGAATTGCATATAGTAAAGACTTTGAAACTCTCAAAGTT	360		
Sbjct 301	GATATTAGATACGGTGTTTTCGAGAATTGCATATAGTAAAGACTTTGAAACTCTCAAAGTT	360		
Query 361	GATTTTCTTAGCAAGCTACCTGAAATGCTGAAAATGTTTGAAGATCGTTTATGTCATAAA	420		
Sbjct 361	GATTTTCTTAGCAAGCTACCTGAAATGCTGAAAATGTTTGAAGATCGTTTATGTCATAAA	420		
Query 421	ACATATTTAAATGGTGATCATGTAACCCATCCTGACTTCATGTTGTATGACGCTCTTGAT	480		
Sbjct 421	ACATATTTAAATGGTGATCATGTAACCCATCCTGACTTCATGTTGTATGACGCTCTTGAT	480		
Query 481	GTTGTTTTATACATGGACCCAATGTGCCGGATGCGTTCCCAAATAGTTTGTTTTAAA	540		
Sbjct 481	GTTGTTTTATACATGGACCCAATGTGCCGGATGCGTTCCCAAATAGTTTGTTTTAAA	540		
Query 541	AAACGTATTGAAGCTATCCACAAAATTGATAAGTACTTGAAATCCAGCAAGTATATAGCA	600		
Sbjct 541	AAACGTATTGAAGCTATCCACAAAATTGATAAGTACTTGAAATCCAGCAAGTATATAGCA	600		
Query 601	TGGCCTTTGCAGGGCTGGCAAGCCACGTTTGGTGGTGGCGACCATCCTCCAAAATCGGAT	660		
Sbjct 601	TGGCCTTTGCAGGGCTGGCAAGCCACGTTTGGTGGTGGCGACCATCCTCCAAAATCGGAT	660		
Query 661	CTGGTCCGCGTGGATCCGCAACCTGTGACCTCTTGAGTCCCTTCAAAGTGGGTGATGCT	720		
Sbjct 661	CTGGTCCGCGTGGATCCGCAACCTGTGACCTCTTGAGTCCCTTCAAAGTGGGTGATGCT	720		
Query 721	GCCTGCGCACTTCATTGTATTGCCATGGGACGACGAGGAGGCTGGTGCATGGTTCGAGCC	780		
Sbjct 721	GCCTGCGCACTTCATTGTATTGCCATGGGACGACGAGGAGGCTGGTGCATGGTTCGAGCC	780		
Query 781	GTTTGTAAATGCAGACGCTAAGAATTC 807			
Sbjct 781	GTTTGTAAATGCAGACGCTAAGAATTC 807			

**Figure 23.** C2519 alignment between the cloned sequence and the identified sequence in the transcriptome.



Score	Expect	Identities	Gaps	Strand
1485 bits(804)	0.0	804/804(100%)	0/804(0%)	Plus/Plus
Query 1	ATGTCCCCTATACTAGGTTATTGGAAAATTAAGGGCCTTGTGCAACCCACTCGACTTCTT	60		
Sbjct 1	ATGTCCCCTATACTAGGTTATTGGAAAATTAAGGGCCTTGTGCAACCCACTCGACTTCTT	60		
Query 61	TTGGAATATCTTGAAGAAAAATATGAAGAGCATTGTATGAGCGCGATGAAGGTGATAAA	120		
Sbjct 61	TTGGAATATCTTGAAGAAAAATATGAAGAGCATTGTATGAGCGCGATGAAGGTGATAAA	120		
Query 121	TGGCGAAACAAAAAGTTTGAATTGGGTTTGGAGTTTCCCAATCTTCCTTATTATATTGAT	180		
Sbjct 121	TGGCGAAACAAAAAGTTTGAATTGGGTTTGGAGTTTCCCAATCTTCCTTATTATATTGAT	180		
Query 181	GGTGATGTTAAATTAACACAGTCTATGGCCATCATACTGTTATATAGCTGACAAGCACAAAC	240		
Sbjct 181	GGTGATGTTAAATTAACACAGTCTATGGCCATCATACTGTTATATAGCTGACAAGCACAAAC	240		
Query 241	ATGTTGGGTGGTGTCCAAAAGAGCGTGCAGAGATTTCAATGCTTGAAGGAGCGGTTTTG	300		
Sbjct 241	ATGTTGGGTGGTGTCCAAAAGAGCGTGCAGAGATTTCAATGCTTGAAGGAGCGGTTTTG	300		
Query 301	GATATTAGATACGGTGTTCGAGAATTGCATATAGTAAAGACTTTGAAACTCTCAAAGTT	360		
Sbjct 301	GATATTAGATACGGTGTTCGAGAATTGCATATAGTAAAGACTTTGAAACTCTCAAAGTT	360		
Query 361	GATTTTCTTAGCAAGCTACCTGAAATGCTGAAAATGTTGAAAGATCGTTTATGTCATAAA	420		
Sbjct 361	GATTTTCTTAGCAAGCTACCTGAAATGCTGAAAATGTTGAAAGATCGTTTATGTCATAAA	420		
Query 421	ACATATTTAAATGGTGATCATGTAACCCATCCTGACTTCATGTTGTATGACGCTCTTGAT	480		
Sbjct 421	ACATATTTAAATGGTGATCATGTAACCCATCCTGACTTCATGTTGTATGACGCTCTTGAT	480		
Query 481	GTTGTTTTATACATGGACCCAATGTGCCTGGATGCGTCCCAAATAGTTTGTGTTTTAAA	540		
Sbjct 481	GTTGTTTTATACATGGACCCAATGTGCCTGGATGCGTCCCAAATAGTTTGTGTTTTAAA	540		
Query 541	AAACGTATTGAAGCTATCCACAAATTGATAAGTACTTGAAATCCAGCAAGTATATAGCA	600		
Sbjct 541	AAACGTATTGAAGCTATCCACAAATTGATAAGTACTTGAAATCCAGCAAGTATATAGCA	600		
Query 601	TGGCCTTTGCAGGGCTGGCAAGCCACGTTTGGTGGTGGCGACCATCCTCCAAAATCGGAT	660		
Sbjct 601	TGGCCTTTGCAGGGCTGGCAAGCCACGTTTGGTGGTGGCGACCATCCTCCAAAATCGGAT	660		
Query 661	CTGGTTCGCGTGGATCCGTCACCTGTGATCTTCTAAAACCTTCTTTGGTCGCGCCCT	720		
Sbjct 661	CTGGTTCGCGTGGATCCGTCACCTGTGATCTTCTAAAACCTTCTTTGGTCGCGCCCT	720		
Query 721	TGCATGATGCATTGTATTTTGCGGTTTAAAAAGCGTACTGGATTCTGTAGTAGACAAAAC	780		
Sbjct 721	TGCATGATGCATTGTATTTTGCGGTTTAAAAAGCGTACTGGATTCTGTAGTAGACAAAAC	780		
Query 781	GTTTGCCTGTGCAGATAAGAATTC	804		
Sbjct 781	GTTTGCCTGTGCAGATAAGAATTC	804		

**Figure 24.** C15867 alignment between the cloned sequence and the identified sequence in the transcriptome.

Score	Expect	Identities	Gaps	Strand
1580 bits(855)	0.0	855/855(100%)	0/855(0%)	Plus/Plus
Query 1	ATGTCCCCTATACTAGGTTATTGGAAAATTAAGGGCCTTGTGCAACCCACTCGACTTCTT			60
Sbjct 1	ATGTCCCCTATACTAGGTTATTGGAAAATTAAGGGCCTTGTGCAACCCACTCGACTTCTT			60
Query 61	TTGGAATATCTTGAAGAAAAATATGAAGAGCATTGTATGAGCGCGATGAAGGTGATAAA			120
Sbjct 61	TTGGAATATCTTGAAGAAAAATATGAAGAGCATTGTATGAGCGCGATGAAGGTGATAAA			120
Query 121	TGGCGAAACAAAAAGTTTGAATTGGGTTTGGAGTTTCCCAATCTTCTTATTATATTGAT			180
Sbjct 121	TGGCGAAACAAAAAGTTTGAATTGGGTTTGGAGTTTCCCAATCTTCTTATTATATTGAT			180
Query 181	GGTGATGTTAAATTAACACAGTCTATGGCCATCATACTGTTATATAGCTGACAAGCACAAC			240
Sbjct 181	GGTGATGTTAAATTAACACAGTCTATGGCCATCATACTGTTATATAGCTGACAAGCACAAC			240
Query 241	ATGTTGGGTGGTTGTCCAAAAGAGCGTGCAGAGATTTCAATGCTTGAAGGAGCGGTTTTG			300
Sbjct 241	ATGTTGGGTGGTTGTCCAAAAGAGCGTGCAGAGATTTCAATGCTTGAAGGAGCGGTTTTG			300
Query 301	GATATTAGATACGGTGTTCGAGAATTGCATATAGTAAAGACTTTGAAACTCTCAAAGTT			360
Sbjct 301	GATATTAGATACGGTGTTCGAGAATTGCATATAGTAAAGACTTTGAAACTCTCAAAGTT			360
Query 361	GATTTTCTTAGCAAGCTACCTGAAATGCTGAAAATGTTTGAAGATCGTTTATGTCATAAA			420
Sbjct 361	GATTTTCTTAGCAAGCTACCTGAAATGCTGAAAATGTTTGAAGATCGTTTATGTCATAAA			420
Query 421	ACATATTTAAATGGTGATCATGTAACCCATCCTGACTTCATGTTGTATGACGCTCTTGAT			480
Sbjct 421	ACATATTTAAATGGTGATCATGTAACCCATCCTGACTTCATGTTGTATGACGCTCTTGAT			480
Query 481	GTTGTTTTATACATGGACCCAATGTGCTGGATGCGTTCCTCCAAAATTAGTTTGTTTTAAA			540
Sbjct 481	GTTGTTTTATACATGGACCCAATGTGCTGGATGCGTTCCTCCAAAATTAGTTTGTTTTAAA			540
Query 541	AAACGTATTGAAGCTATCCACAAAATTGATAAGTACTTGAAATCCAGCAAGTATATAGCA			600
Sbjct 541	AAACGTATTGAAGCTATCCACAAAATTGATAAGTACTTGAAATCCAGCAAGTATATAGCA			600
Query 601	TGGCCTTTCAGGGCTGGCAAGCCACGTTTGGTGGTGGCGACCATCCTCCAAAATCGGAT			660
Sbjct 601	TGGCCTTTCAGGGCTGGCAAGCCACGTTTGGTGGTGGCGACCATCCTCCAAAATCGGAT			660
Query 661	CTGGTTCGCGTGGATCCCAGTTTGACAATCTAGAAGATACAGGAGTTGAGGAGAAAAGTT			720
Sbjct 661	CTGGTTCGCGTGGATCCCAGTTTGACAATCTAGAAGATACAGGAGTTGAGGAGAAAAGTT			720
Query 721	CGTCATAAGCGCCTAACCTGCCTATTCGACAATCGCCCCATCTCAGCATTTCGCGTGTGGT			780
Sbjct 721	CGTCATAAGCGCCTAACCTGCCTATTCGACAATCGCCCCATCTCAGCATTTCGCGTGTGGT			780
Query 781	TCCAACGTGTTTTACGAAAAGGAAAACGTGGTGGATGGTGTGCAATGGAGTTTGTAGA			840
Sbjct 781	TCCAACGTGTTTTACGAAAAGGAAAACGTGGTGGATGGTGTGCAATGGAGTTTGTAGA			840
Query 841	TGCACCTAAGAATTC			855
Sbjct 841	TGCACCTAAGAATTC			855

Figure 25. C10649 alignment between the cloned sequence and the identified sequence in the transcriptome.

Score	Expect	Identities	Gaps	Strand
1607 bits(870)	0.0	870/870(100%)	0/870(0%)	Plus/Plus
Query 1	ATGTCCCCTATACTAGGTTATTGGAAAAATTAAGGGCCTTGTGCAACCCACTCGACTTCTT	60		
Sbjct 1	ATGTCCCCTATACTAGGTTATTGGAAAAATTAAGGGCCTTGTGCAACCCACTCGACTTCTT	60		
Query 61	TTGGAATATCTTGAAGAAAAATATGAAGAGCATTGTATGAGCGCGATGAAGGTGATAAA	120		
Sbjct 61	TTGGAATATCTTGAAGAAAAATATGAAGAGCATTGTATGAGCGCGATGAAGGTGATAAA	120		
Query 121	TGGCGAAACAAAAAGTTTGAATTGGGTTTGGAGTTTCCCAATCTTCCTTATTATATTGAT	180		
Sbjct 121	TGGCGAAACAAAAAGTTTGAATTGGGTTTGGAGTTTCCCAATCTTCCTTATTATATTGAT	180		
Query 181	GGTGATGTTAAATTAACACAGTCTATGGCCATCATACGTTATATAGCTGACAAGCACAAC	240		
Sbjct 181	GGTGATGTTAAATTAACACAGTCTATGGCCATCATACGTTATATAGCTGACAAGCACAAC	240		
Query 241	ATGTTGGGTGGTTGTCCAAAAGAGCGTGCAGAGATTTCAATGCTTGAAGGAGCGGTTTTG	300		
Sbjct 241	ATGTTGGGTGGTTGTCCAAAAGAGCGTGCAGAGATTTCAATGCTTGAAGGAGCGGTTTTG	300		
Query 301	GATATTAGATACGGTGTTCGAGAATTGCATATAGTAAAGACTTTGAAACTCTCAAAGTT	360		
Sbjct 301	GATATTAGATACGGTGTTCGAGAATTGCATATAGTAAAGACTTTGAAACTCTCAAAGTT	360		
Query 361	GATTTTCTTAGCAAGCTACCTGAAATGCTGAAAATGTTTGAAGATCGTTTATGTCATAAA	420		
Sbjct 361	GATTTTCTTAGCAAGCTACCTGAAATGCTGAAAATGTTTGAAGATCGTTTATGTCATAAA	420		
Query 421	ACATATTTAAATGGTGATCATGTAACCCATCCTGACTTCATGTTGTATGACGCTCTTGAT	480		
Sbjct 421	ACATATTTAAATGGTGATCATGTAACCCATCCTGACTTCATGTTGTATGACGCTCTTGAT	480		
Query 481	GTTGTTTTATACATGGACCCAATGTGCCGGATGCGTTCCCAAATTAGTTTGTTTTAAA	540		
Sbjct 481	GTTGTTTTATACATGGACCCAATGTGCCGGATGCGTTCCCAAATTAGTTTGTTTTAAA	540		
Query 541	AAACGTATTGAAGCTATCCCACAAATTGATAAGTACTTGAATCCAGCAAGTATATAGCA	600		
Sbjct 541	AAACGTATTGAAGCTATCCCACAAATTGATAAGTACTTGAATCCAGCAAGTATATAGCA	600		
Query 601	TGGCCTTTCAGGGCTGGCAAGCCACGTTTGGTGGTGGCGACCATCCTCCAAAATCGGAT	660		
Sbjct 601	TGGCCTTTCAGGGCTGGCAAGCCACGTTTGGTGGTGGCGACCATCCTCCAAAATCGGAT	660		
Query 661	CTGGTCCGCGTGGATCCAAGCAATCAAGTGATCCAGAGTCAGCGTTGTAAGTACTCAGATATT	720		
Sbjct 661	CTGGTCCGCGTGGATCCAAGCAATCAAGTGATCCAGAGTCAGCGTTGTAAGTACTCAGATATT	720		
Query 721	CACCCAAGGTTTAGGCGACAGCTTCCTTGCGATTATCTTAGCGGTTTGGGATTCGGCGAA	780		
Sbjct 721	CACCCAAGGTTTAGGCGACAGCTTCCTTGCGATTATCTTAGCGGTTTGGGATTCGGCGAA	780		
Query 781	GACGCCTGCAACACGGATTGTATTGCAAAAGGACATAAAAGCGGTTTTTGCAGTGGACTC	840		
Sbjct 781	GACGCCTGCAACACGGATTGTATTGCAAAAGGACATAAAAGCGGTTTTTGCAGTGGACTC	840		
Query 841	GTTTGTGCTTGCAGAACCTTATAGGAATTC	870		
Sbjct 841	GTTTGTGCTTGCAGAACCTTATAGGAATTC	870		

**Figure 26.** C13792 alignment between the cloned sequence and the identified sequence in the transcriptome.

#### 4.8. Heterologous expression and purification of the C15867 and C2519 peptides.

Hill\_BB\_C15867 and Hill\_BB\_C2519 were expressed in *E. coli* BL21 (DE3) cells and the recombinant products recovered after cell lysis (Figure 28) were purified through affinity chromatography, exploiting the GST tag. In figure 29 and 30 are shown, respectively, the obtained chromatograms for C15867 and C2519 peptides.

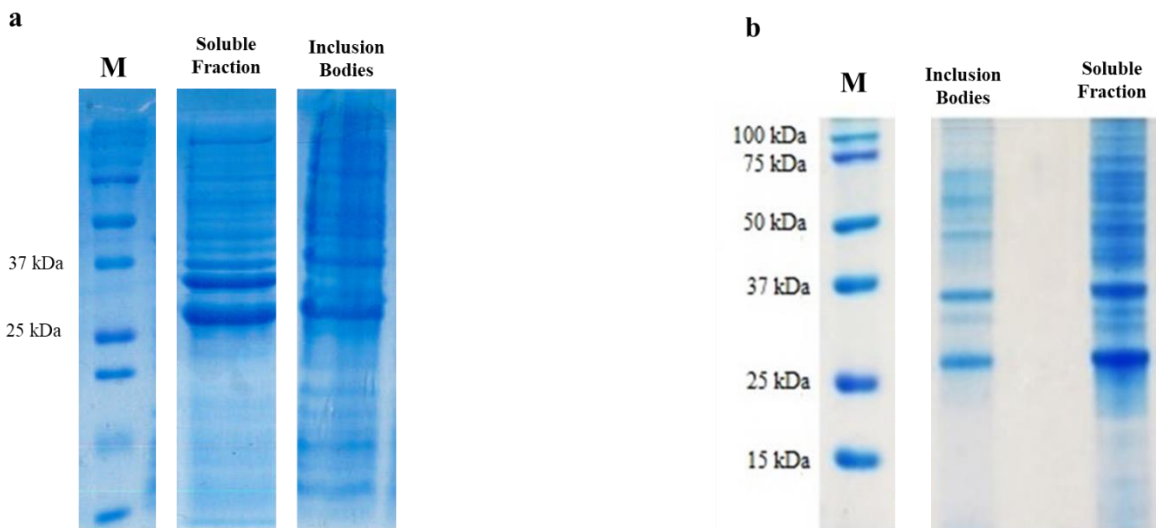


**Figure 28.** a) C15867 expression where are shown the soluble fraction and the inclusion bodies; b) C2519 expression where are shown the soluble fraction and the inclusion bodies.

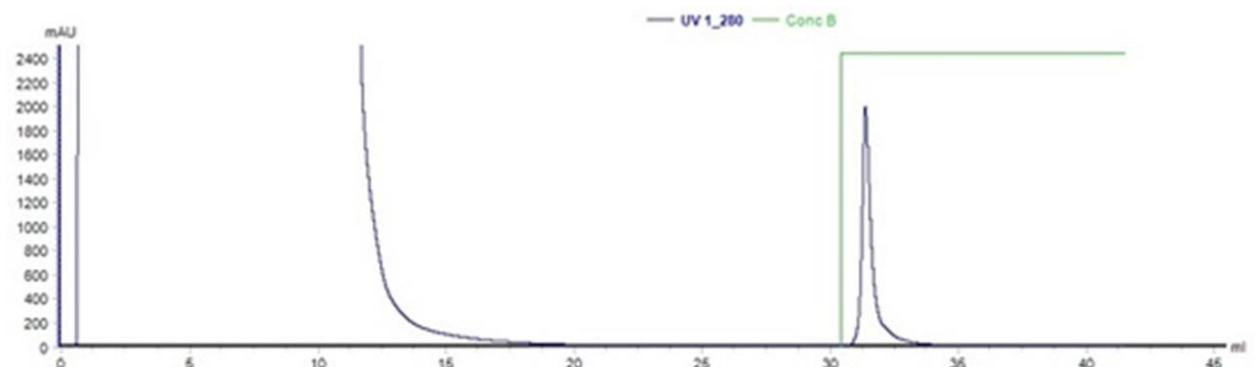


**Figure 29.** Chromatogram obtained for the C15867 peptide.

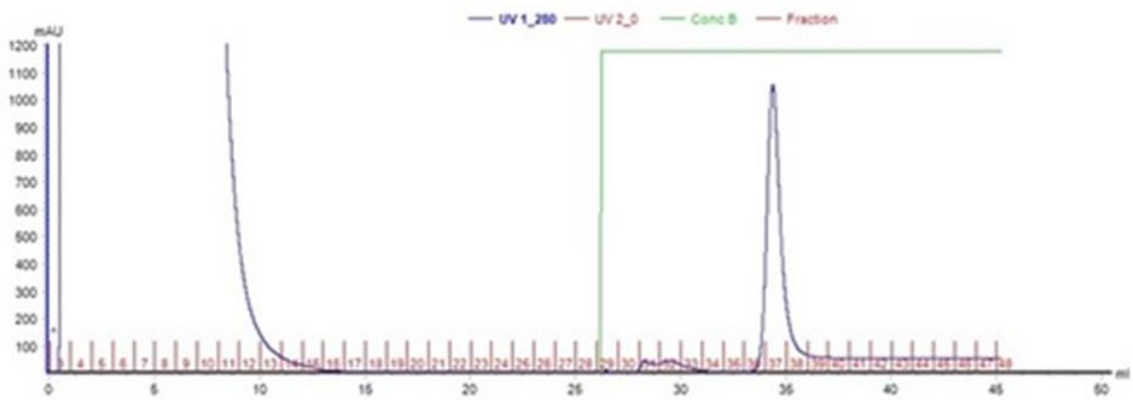


**Figure 30.** Chromatogram obtained for the C2519 peptide.

The recovered peak fraction for both C15867 and C2519 were analysed through SDS-PAGE and in Figure 31 and 32 are shown the obtained gels.

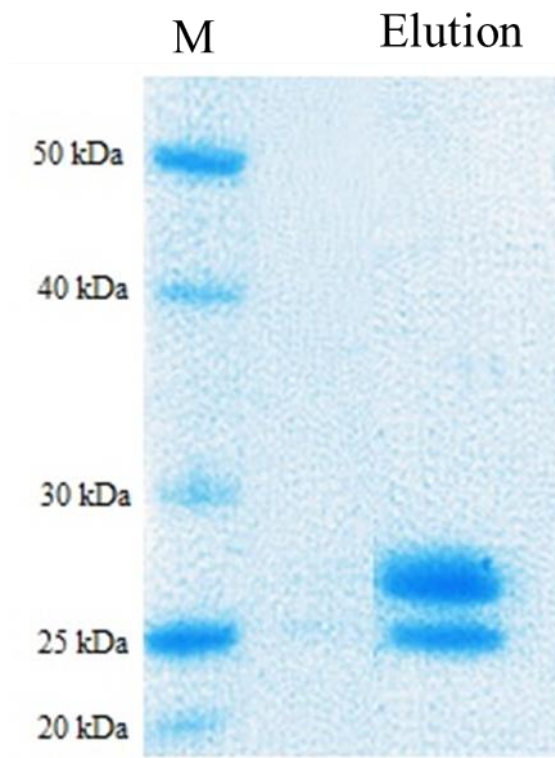


**Figure 31.** SDS-PAGE of the C2519 purification.

In the elution line in the gel (Figure 31) it is possible to see the presence of two bands: one corresponding to the GST tag alone (lower band) and a second one corresponding to the fusion protein GST-C2519 (upper band).

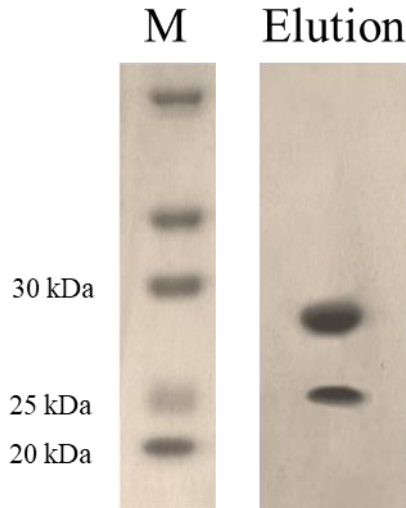


**Figure 32.** SDS-PAGE of the C15867 purification.

In the elution line in the gel (Figure 32) it is possible to see the presence of two bands: one corresponding to the GST tag alone (lower band) and a second one corresponding to the fusion protein GST-C15867 (upper band).

Both samples have been analysed through Mass spectrometry, in order to validate the primary structure, by performing a MALDI MAPPING and calculating the sequence coverage percentage.

In figure 33 and 34 are shown, respectively, the obtained results for the C15867 and C2519 peptides.

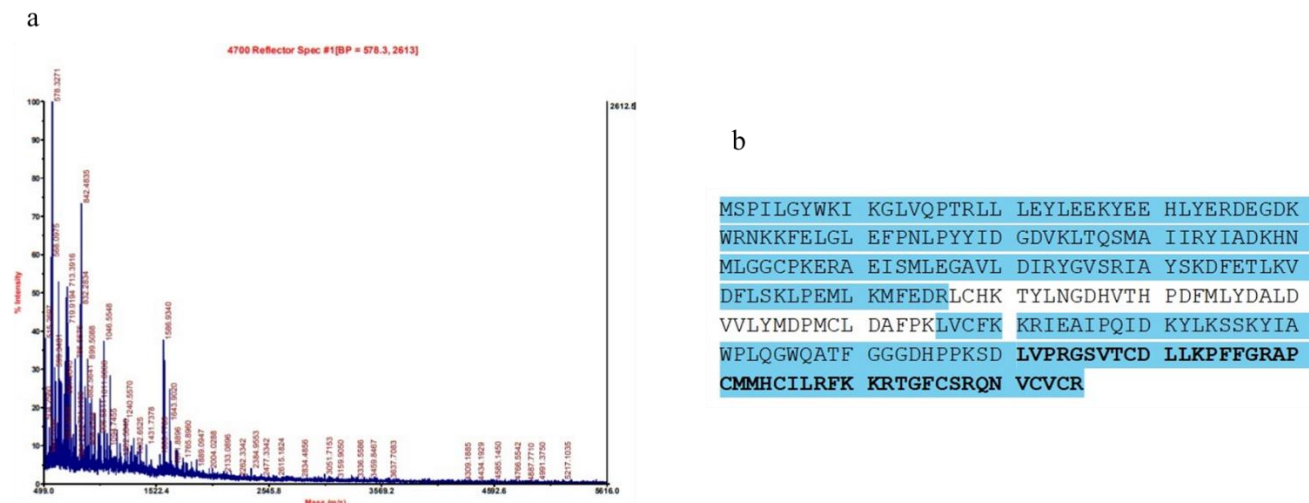


**Figure 33.** a) MALDI-TOF spectra of the GST-C15867 product; b) sequence coverage (in bold is shown the peptide sequence while the non-bolded sequence is the GST tag).

The MALDI MAPPING allowed to calculate the sequence coverage percentage:

$$\frac{N \text{ covered amino acids}}{N \text{ amino acids}} \times 100 \rightarrow \frac{230}{265} \times 100 = \mathbf{87\%}$$

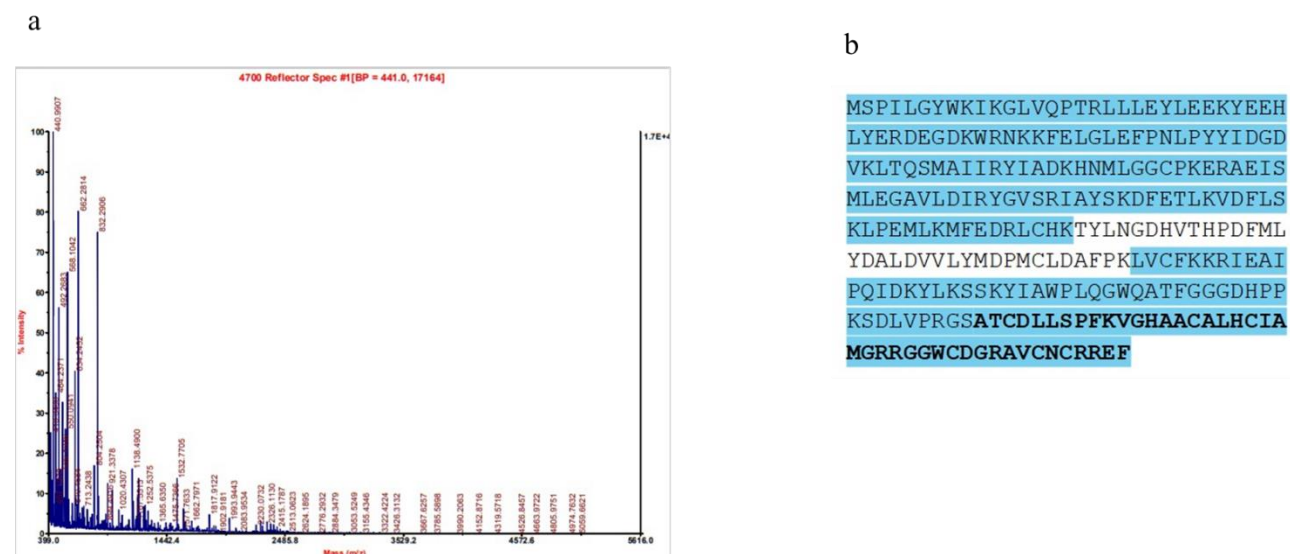


**Figure 34.** a) MALDI-TOF spectra of the GST-C2519 product; b) sequence coverage (in bold is shown the peptide sequence while the non-bolded sequence is the GST tag).

The MALDI MAPPING allowed to calculate the sequence coverage percentage:

$$\frac{N \text{ covered amino acids}}{N \text{ amino acids}} \times 100 \rightarrow \frac{233}{268} \times 100 = \mathbf{87\%}$$

For both GST-peptide products an 87% of sequence coverage has been calculated, where the non-covered sequence belongs to a short part of the GST protein while all the peptides sequences have been found, confirming the well occurred expression of both peptides.

Once the primary sequence of both products was confirmed by mass spectrometry, thrombin hydrolysis was performed in order to remove the GST tag and the samples have been then analysed through SDS-PAGE. In Figure 35 is shown the obtained gel for the C2519 and C15867 peptides, which confirms the well occurred thrombin hydrolysis.

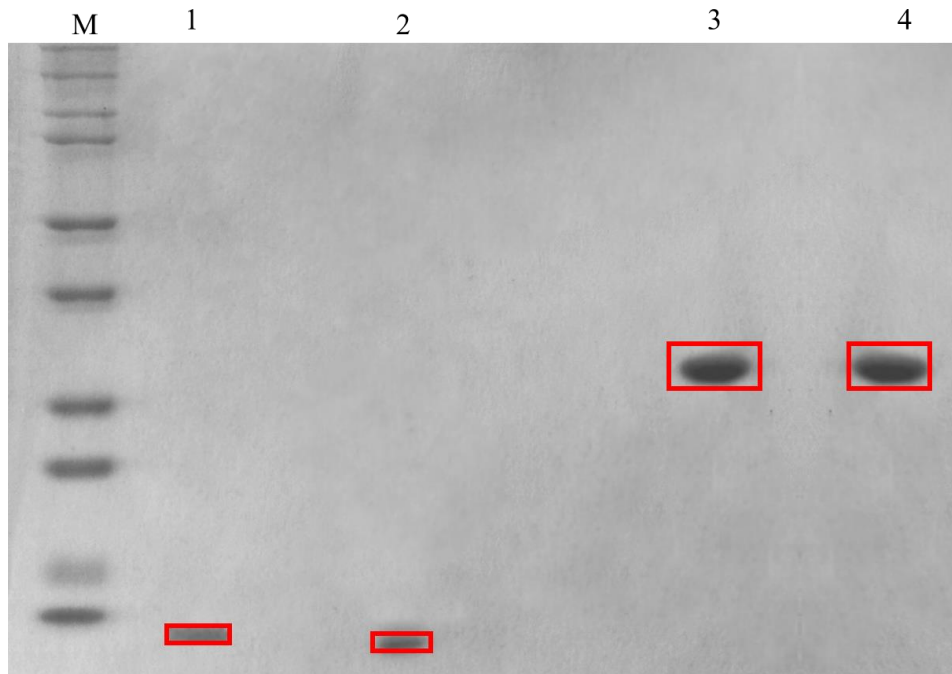


**Figure 35.** Thrombin hydrolysis. M: Marker; line 1: C15867 peptide recovered after the hydrolysis; line 2: C2519 peptide recovered after the hydrolysis; lines 3 and 4: GST tag alone after the thrombin hydrolysis.



#### 4.9. Minimum Inhibitory Concentration (MIC) of the C15867 peptide.

The C15867 peptide has been functionally characterized in order to evaluate its antibacterial activity against *E. coli* (BL21) by determining the Minimum Inhibitory Concentration (MIC). The obtained result is shown in Figure 36.

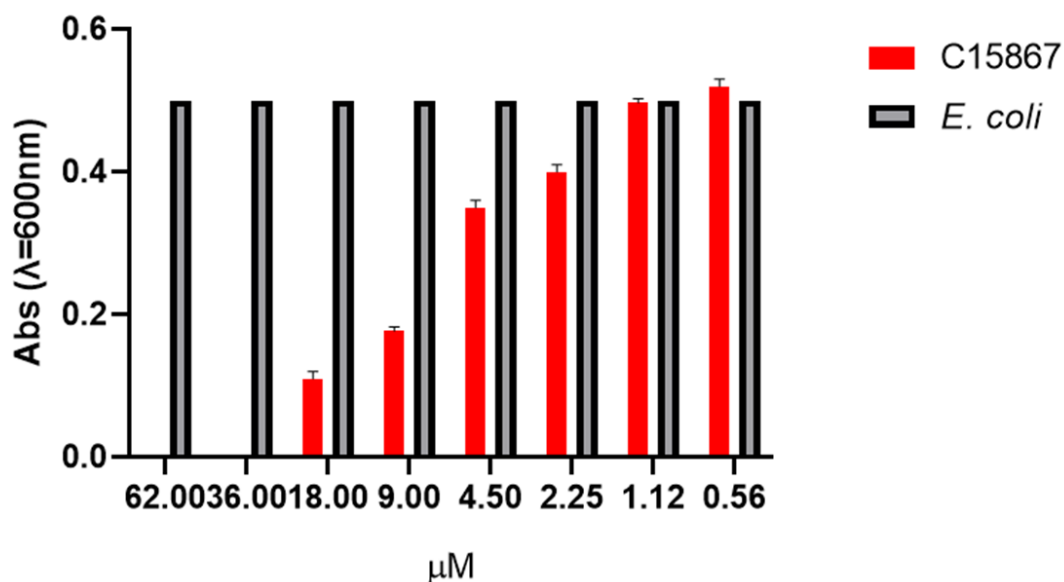


**Figure 36.** C15867 Minimum Inhibitory Concentration. *E. coli* (BL21) 0.5 OD/mL has been used as negative control.

The obtained result allowed to determine a value of 18 μM as C15867 MIC.

#### 4.10. Molecular Docking analysis for the *in silico* evaluation of the C15867 peptide interaction with the FtsZ protein and Lipopolysaccharide (LPS) targets.

The C15867 and FtsZ protein models were obtained through the I-TASSER Server and the putative structural basis of the protein-peptide complex model were obtained by molecular docking calculations performed with PatchDock Server and the structure has been refined through the FireDock Server. The obtained results revealed that a stable complex might be formed, with a Global Energy value of -46.80 Kcal/mol, Attractive Van der Waals Energy value of -24.27, Repulsive Van der Waals Energy value of 6.68 KJ/mol and the Atomic Contact Energy value of 5.17 KJ/mol. Through the PRODIGY Server the  $\Delta G$  and the  $K_d$  were calculated:  $\Delta G = -8.6$  Kcal/mol;  $K_d = 5.0 \times 10^{-7}$  M (25 C). A detailed analysis of the interactions at the peptide (Chain A) – protein (Chain B) interface suggested the involvement of (i) 102 non-bonded interactions; (ii) 2 salt bridges: Arg22

(Chain A) – Glu238 (Chain B) and Lys25 (Chain A) – Asp304 (Chain B); (iii) 5 hydrogen bonds: Asn34 (Chain A) – Asp187 (Chain B), Asn34 (Chain A) – Lys190 (Chain B), Cys38 (Chain A) – Ser231 (Chain B), Gln33 (Chain A) – Asp301 (Chain B), and Cys36 (Chain A) – Glu305 (Chain B), as shown in Figure 37.

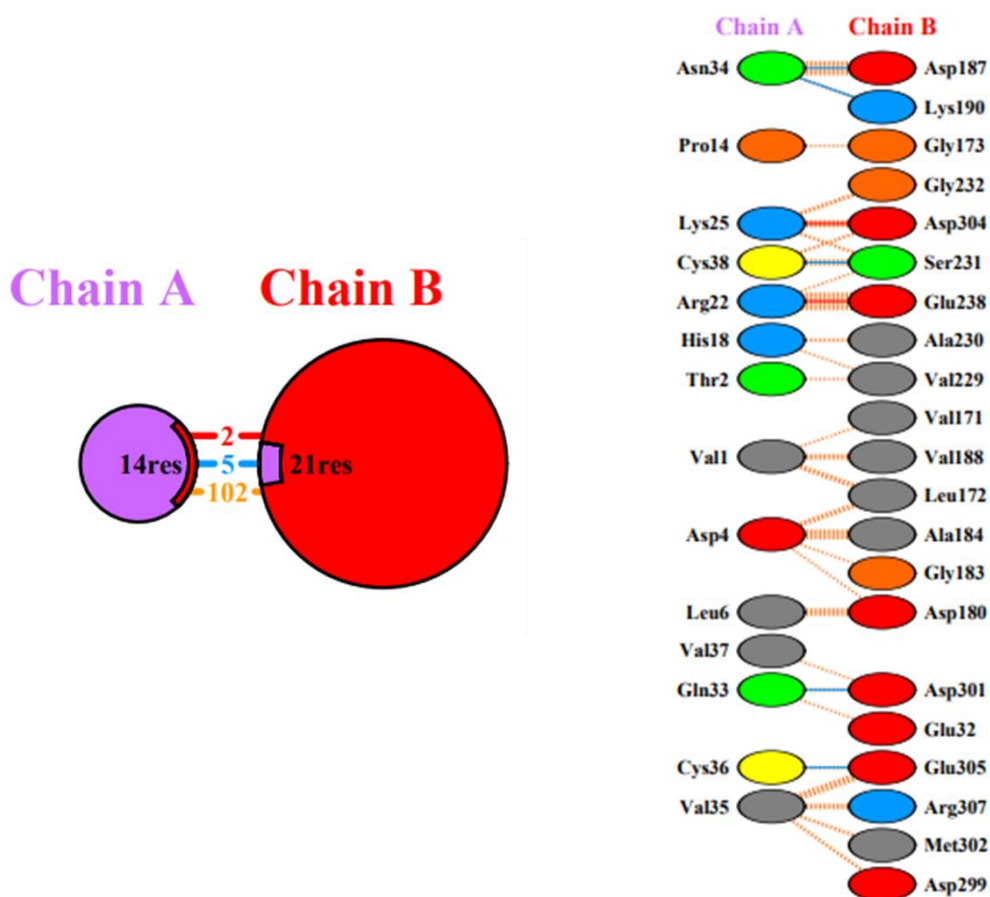


**Figure 37.** Schematic representation of the identified interactions occurring in the C15867-FtsZ complex. Chain A represents C15867 peptide while Chain B is FtsZ protein.

In Figure 38 the interactions occurring at the C15867-FtsZ interface are shown.

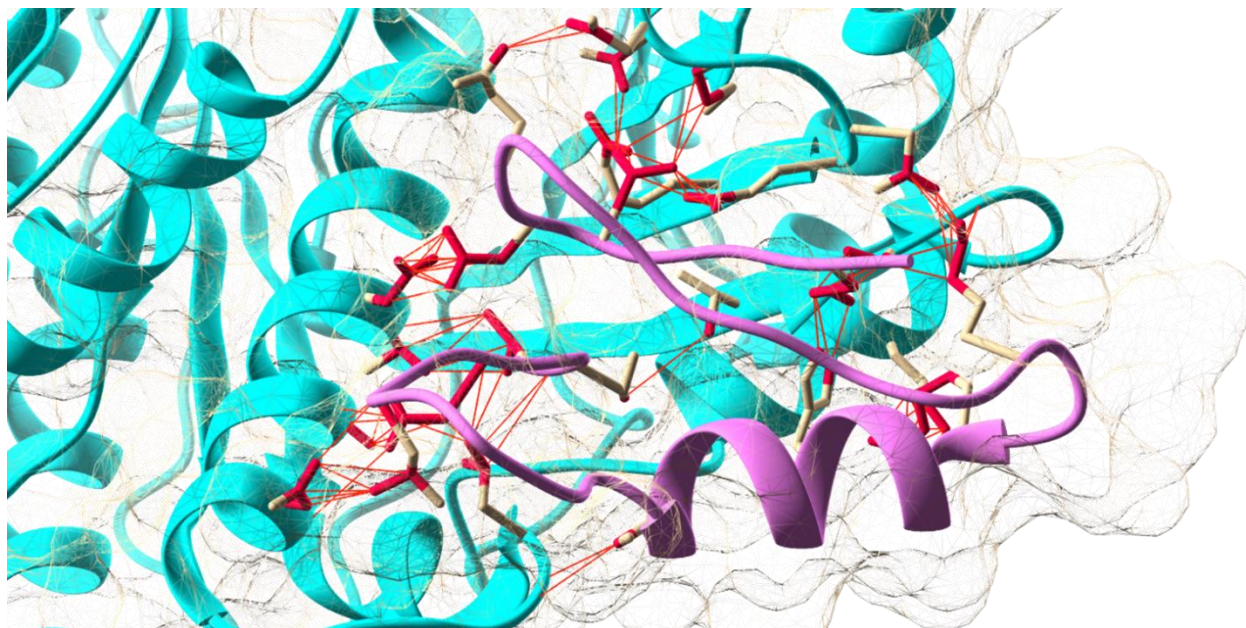


**Figure 38.** Interaction occurring at the C15867-FtsZ interface. The peptide is shown in light purple, the FtsZ protein in cyan, while in red are shown the amino acids of both protein and peptide involved in the interaction. Figure generated with UCSF CHIMERA software [51].

The obtained data have been compared to the molecular docking results obtained for the FtsZ-TL complex, revealing surprisingly the same values of  $\Delta G$  and  $K_d$ , as listed in Table 11, where also the occurring interactions are listed.

**Table 11.** Comparison of the molecular docking calculations obtained for the C15867-FtsZ and for the TemporinL-FtsZ complexes. In the table are compared the  $\Delta G$  and the  $K_d$  values, the number of non-bonded interactions, the hydrogen bonds and the salt bridges at the peptide-protein interface.

	<i>C15867 (Chain A)-FtsZ (chain B)</i>	<i>TemporinL Chain A)-FtsZ (Chain B)</i>
<i>ΔG</i>	- 8.6 Kcal/mol	- 8.7 Kcal/mol
<i>Kd</i>	5.0 E-07 M (25 C)	4.3 E-07 M (25 C)
<i>Non-boned interactions</i>	102	112
<i>Salt Bridges</i>	- Arg22 (Chain A)–Glu238 (Chain B) - Lys25 (Chain A)–Asp304 (Chain B)	/
<i>Hydrogen Bonds</i>	- Asn34 (Chain A)–Asp187 (Chain B) - Asn34 (Chain A)–Lys190 (Chain B) - Cys38 (Chain A)–Ser231 (Chain B) - Gln33 (Chain A)–Asp301 (Chain B) - Cys36 (Chain A)–Glu305 (Chain B)	- Leu13 (Chain A)–Gly106 (Chain B) - Leu13 (Chain A)–Thr110 (Chain B)

Moreover, the C15867-LPS molecular docking analysis has been performed. The obtained results revealed that a stable complex might be formed, with a Global Energy value of -26.59 Kcal/mol, Attractive Van der Waals Energy value of -26.62, Repulsive Van der Waals Energy value of 25.27 KJ/mol and the Atomic Contact Energy value of -10.73 KJ/mol. Through the Protein-Ligand Interaction Profiler (PLIP) Server, the occurring interactions at the peptide-ligand interface have been evaluated (Figure 39), highlighting the involvement of 3 hydrophobic interactions and 12 hydrogen bonds, as shown in Figure 40.

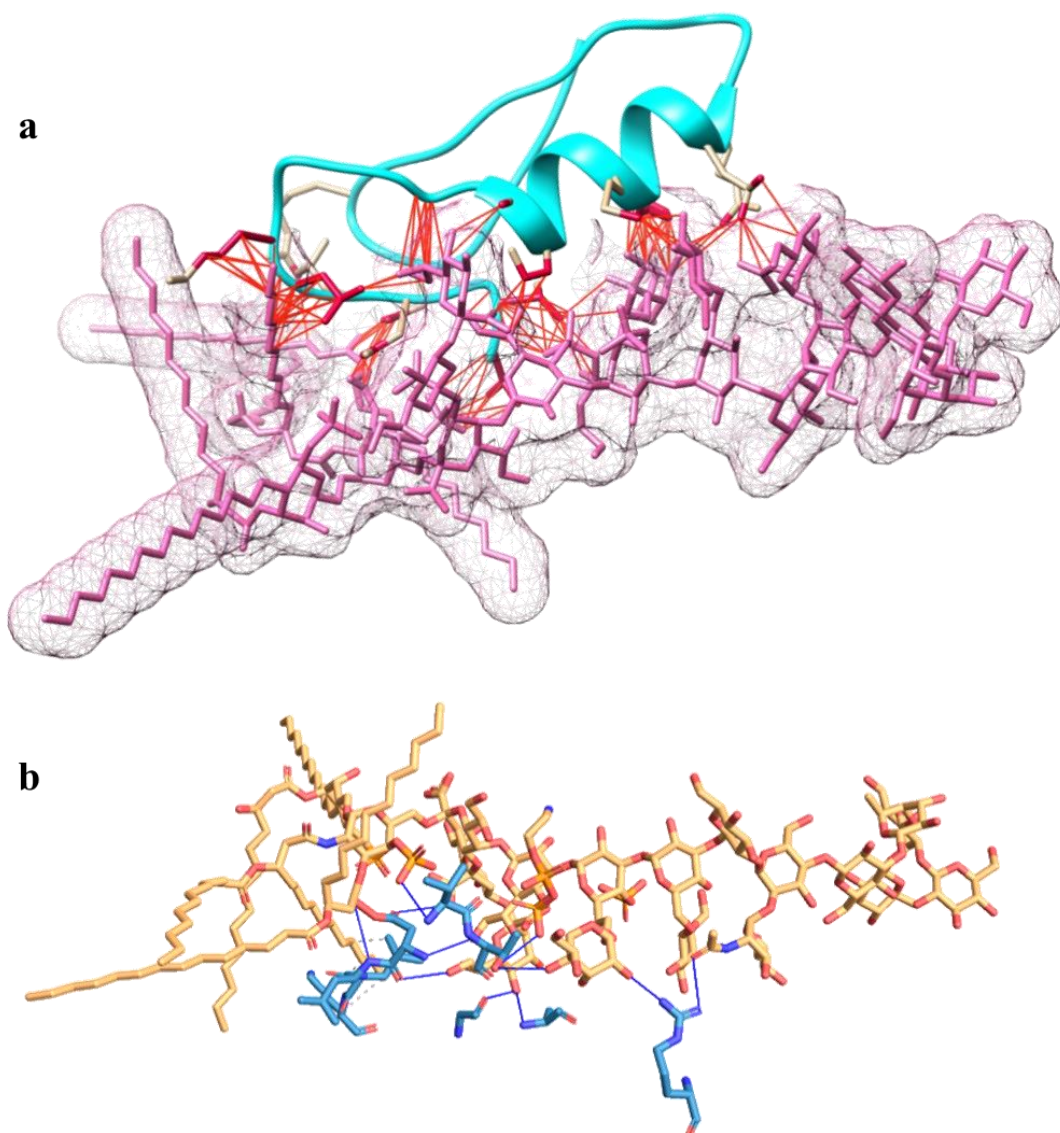


**Figure 40.** a) All the interactions occurring at the peptide-LPS interface. The peptide is shown in cyan color, while in light magenta the LPS molecule. Red lines represent the amino acids interactions. Figure generated with UCSF CHIMERA. b) Hydrogen bonds occurring at the C15867-LPS interface. Figure obtained from the PLIP Server.

▼ Hydrophobic Interactions ****					
Index	Residue	AA	Distance	Ligand Atom	Protein Atom
1	6A	LEU	2.93	294	374
2	7A	LYS	3.48	306	380
3	7A	LYS	3.74	319	379

▼ Hydrogen Bonds —									
Index	Residue	AA	Distance H-A	Distance D-A	Donor Angle	Protein donor?	Side chain	Donor Atom	Acceptor Atom
1	1A	VAL	3.18	3.52	100.94	✓	✗	331 [N3]	73 [O3]
2	2A	THR	2.87	3.78	156.60	✓	✓	343 [O3]	78 [O3]
3	2A	THR	3.47	3.78	100.93	✗	✓	78 [O3]	343 [O3]
4	2A	THR	3.15	3.85	130.65	✗	✓	57 [O3]	343 [O3]
5	4A	ASP	2.39	3.38	175.24	✓	✗	351 [Nam]	49 [O3]
6	4A	ASP	3.32	4.01	129.91	✗	✗	75 [O3]	354 [O2]
7	4A	ASP	2.83	3.70	153.88	✓	✓	357 [O3]	42 [O.co2]
8	5A	LEU	3.01	3.94	159.15	✓	✗	359 [Nam]	86 [O2]
9	11A	GLY	3.04	3.64	121.22	✗	✗	47 [O3]	416 [O2]
10	13A	ALA	3.24	4.00	134.35	✓	✗	428 [Nam]	47 [O3]
11	22A	ARG	2.59	2.97	102.90	✓	✓	504 [Ng+]	76 [O3]
12	22A	ARG	2.94	3.82	148.62	✓	✓	503 [Ng+]	113 [O2]

**Figure 41.** List of the hydrophobic interactions and hydrogen bonds identified by the PLIP Server.

The obtained results support the occurring interaction of the antimicrobial peptide with the bacterial membrane by contacting the LPS target, which is a usual target for antimicrobial peptides. Moreover, through the molecular docking analysis, the complex formation with a novel AMP's target, the FtsZ protein has been evaluated. The results encourage possible future studies, in order to evaluate and elucidate the mechanism of action of the C15867 peptide.

#### 4.11. Antibacterial activity of C6571, C46948, C16634 and C7985 peptides.

C6571, C46948, C16634 and C7985 peptides were purchased from Bio-Fab company. In collaboration with Prof. Piero Pucci, University of Naples, the antibacterial activity of C6571, C46948, C16634 and C7985 peptides has been evaluated. *Escherichia coli* (BL21) cells have been treated with two different concentrations of each peptide: 3  $\mu\text{M}$  and 12  $\mu\text{M}$ . Untreated bacterial cells represent the negative control of the experiment. The obtained results are shown in Figure 42 where it is possible to note the reduced cell viability after the treatment with the antimicrobial peptides. The data were published on *Scientific Reports*, Moretta et al., 2020 [199].

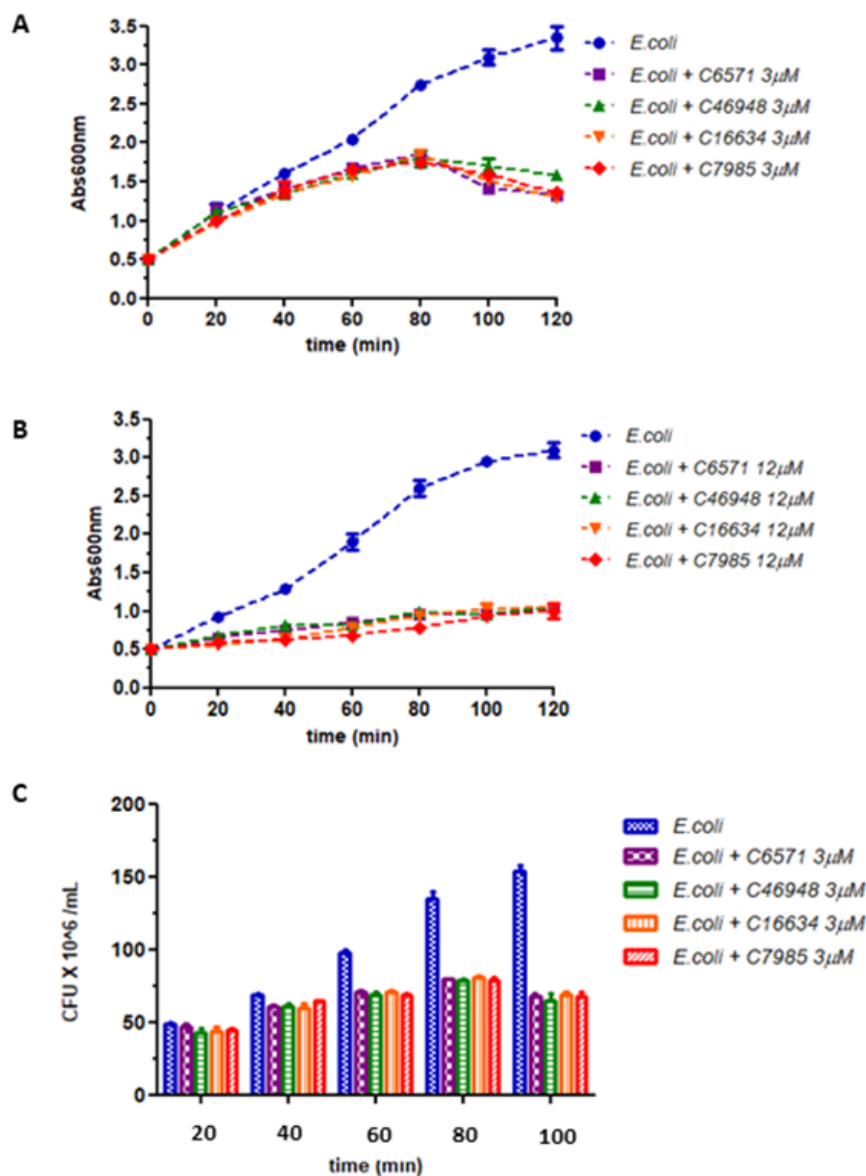


**Figure 42.** Bacterial growth profiles under treatment with two different concentrations, 3  $\mu\text{M}$  (A) and 12  $\mu\text{M}$  (B) of each antimicrobial peptide. (C) Cell viability after treatment with 3  $\mu\text{M}$  of each antimicrobial peptide.

#### 4.12. Chemical Synthesis on Solid Phase of the C12927, and C4669 peptides.

C12927 (4969.69 Da), and C4669 (4670.398 Da) peptides have been chemically synthesized at the Technische Hochschule Mittelhessen University of Applied Sciences, Gießen, Germany, exploiting the chemistry of the Fmoc protecting group. It was carried out using a Liberty Blue microwave synthesizer with an associated UV detector, which allows to follow the synthesis progress checking the coupling of each amino acid. 0.5 mg/mL of the obtained products have been then analysed through HPLC in order to check the presence of by-products. In Figure 43 and 44 are shown the obtained results.

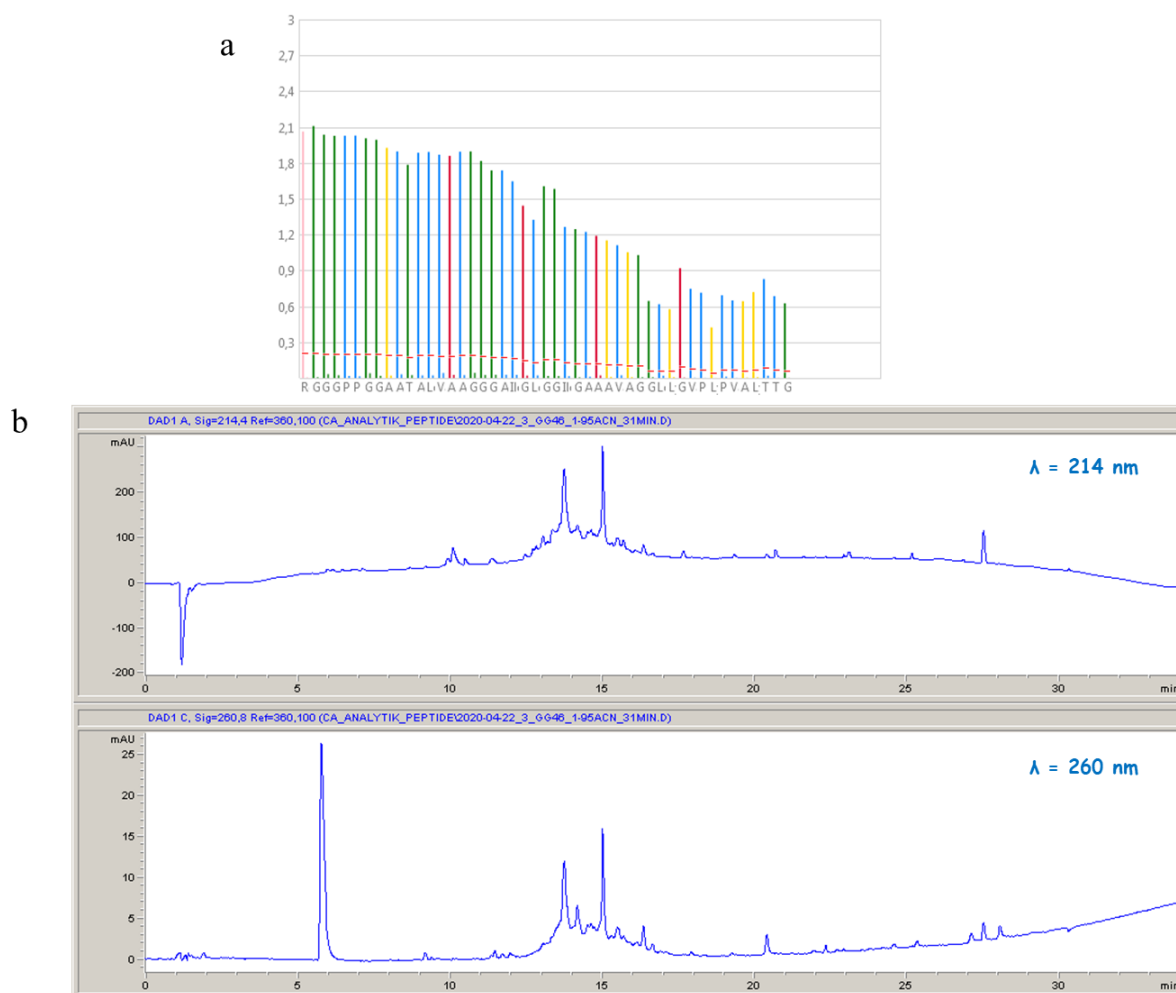


**Figure 43.** a) C12927 UV spectrum. b) chromatogram obtained for the C12927 peptide.



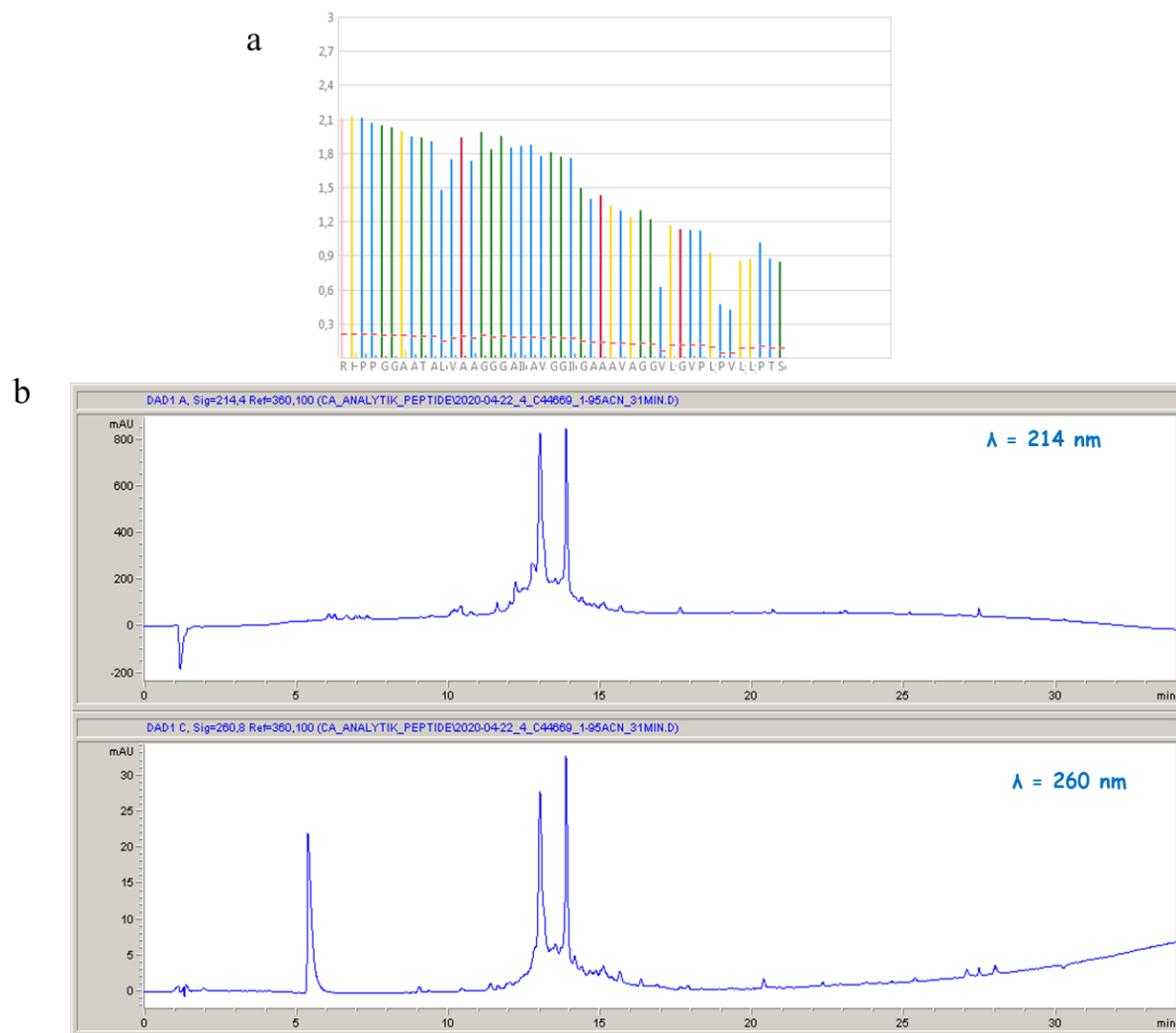


**Figure 44.** a) C4669 UV spectrum. b) chromatogram obtained for the C4669 peptide.

For both peptides the presence of by-products has been revealed by the HPLC analysis. Thus, in order to confirm that the chemical synthesis of the two peptides had taken place correctly, a MALDI-TOF analysis has been performed on both peptides. In figure 45 the MALDI-TOF spectra are shown.

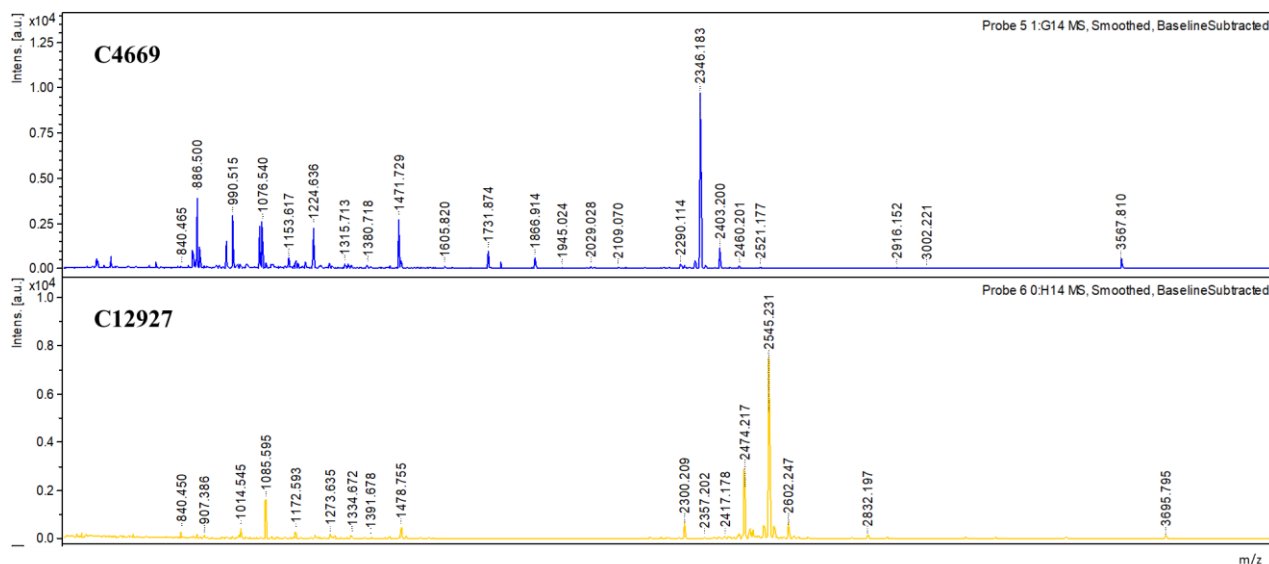


**Figure 45.** MALDI-TOF spectra obtained for the C4669 (in blue in the figure) and C12927 (in yellow in the figure) peptides.

The MALDI-TOF analysis revealed that the main peak for the C4669 is 2346.183 m/z (2346.183 Da since  $z = 1$ ) while the molecular weight of the peptide is 4670.398 Da. For the C12927 peptide, instead, the mass spectrometry analysis revealed the 2545.231 m/z as the main peak while the molecular weight of the peptide is 4969.69 Da. Thus, according to the mass spectrometry analysis, unfortunately, the chemical synthesis of the two peptides failed, which could be related to very high length of the two peptides.

#### 4.13. Isolation of putative antimicrobial peptides from *Hermetia illucens* larvae plasma.

*Hermetia illucens* larvae were infected with *E. Coli* (LGM2092), OD600 = 1, and *M. Flavus* (DSM1790), OD600 = 1 and incubated at 25 °C for 24 hours. Then, the hemolymph was extracted from larvae infected with *E. Coli* (LGM2092), larvae infected with *M. Flavus* (DSM 1790 strain) and from not-infected larvae, which represent the negative control. Through the centrifugation step the plasma was collected and the putative peptides were separated from high molecular weight proteins by treatment with Methanol/Acetic Acid/Water and subsequent centrifugation. The obtained supernatants were quantified through Bradford Assay: 0.16 mg/mL concentration was calculated for the supernatants deriving from not-infected larvae; 0.17 mg/mL concentration was calculated for the supernatants deriving from larvae infected with *E. Coli* (LGM2092); 0.24 mg/mL concentration was calculated for the supernatants deriving from larvae infected with *M. Flavus* (DSM1790). The samples were then qualitatively analysed through SDS-PAGE (Figure 46).

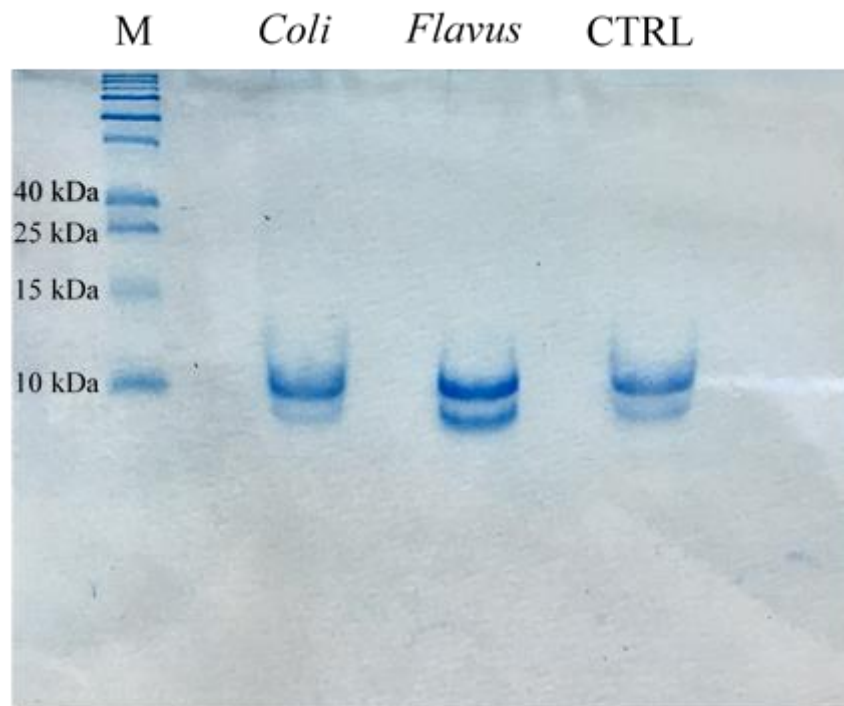


**Figure 46.** SDS-PAGE analysis of the supernatants obtained after precipitation with Methanol/Acetic Acid/Water. From left to right are shown: Marker; supernatant deriving from plasma extracted from larvae infected with *E. Coli* (LGM2092); supernatant deriving from plasma extracted from larvae infected with *M. Flavus* (DSM1790); supernatant deriving from plasma extracted from not-infected larvae.

4.14. Evaluation of the antibacterial activity of the plasma extracted from the infected and not infected larvae of *Hermetia illucens*.

For the evaluation of the antibacterial activity of the obtained samples, a *microdilution assay* has been performed against both *E. coli* (LGM2092) and *M. flavus* (DSM1790). Unlike the Minimum Inhibitory Concentration (MIC), different volumes of the samples and not concentrations were tested, since that in this case the samples in exam are not a single pure molecule but a pool of more molecules to which, at this point, is not possible to assign a concentration value. The assay has just the aim to evaluate an antibacterial activity of the samples. The graphs below show the tested volumes of each sample as a function of the optical density evaluated at the wavelength of 600 nm. The results are shown in Figure 47 and Figure 48.

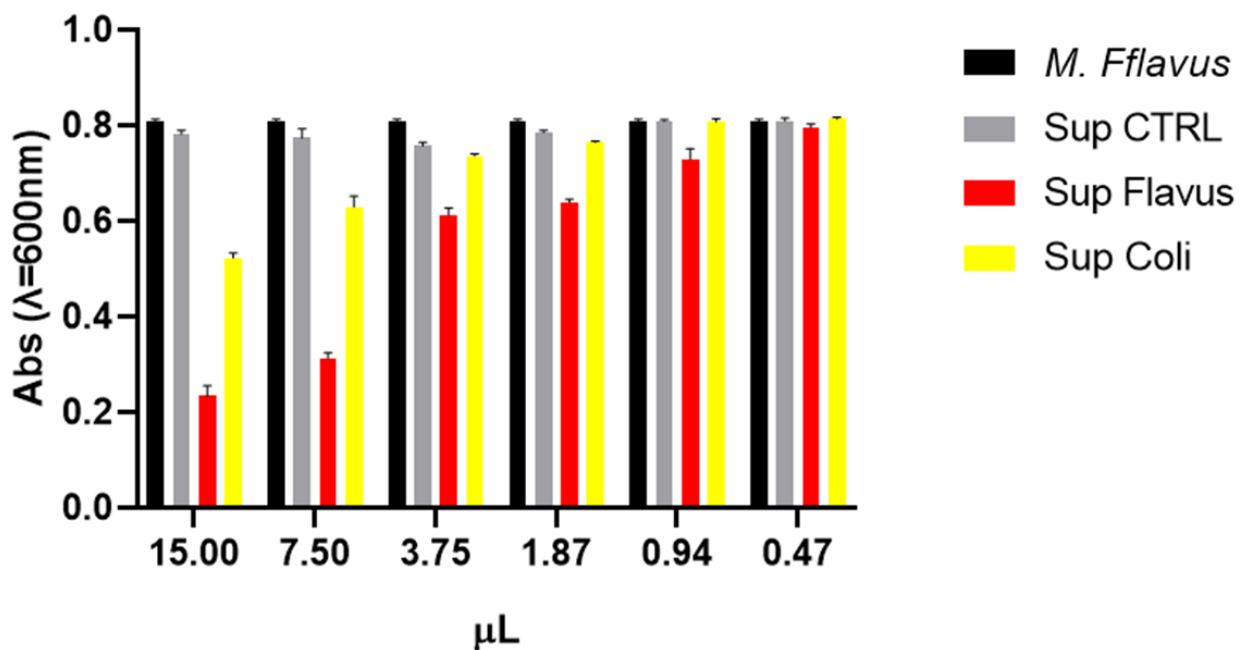


**Figure 47.** Microdilution assay performed against *M. flavus* (DSM1790).

The obtained data show that the supernatant obtained by precipitating the plasma extracted from larvae infected with *M. flavus* (DSM1790) lead to a reduction of 75% of *M. flavus* (DSM1790) growth, by using 15 μL of sample, and a reduction of 61% of *M. flavus* (DSM1790) growth by using 7.5 μL of sample. The supernatant obtained by precipitating the plasma extracted from larvae infected with *E. coli* (LGM2092) lead to a reduction of 38 % of cell growth by using 15 μL of sample.

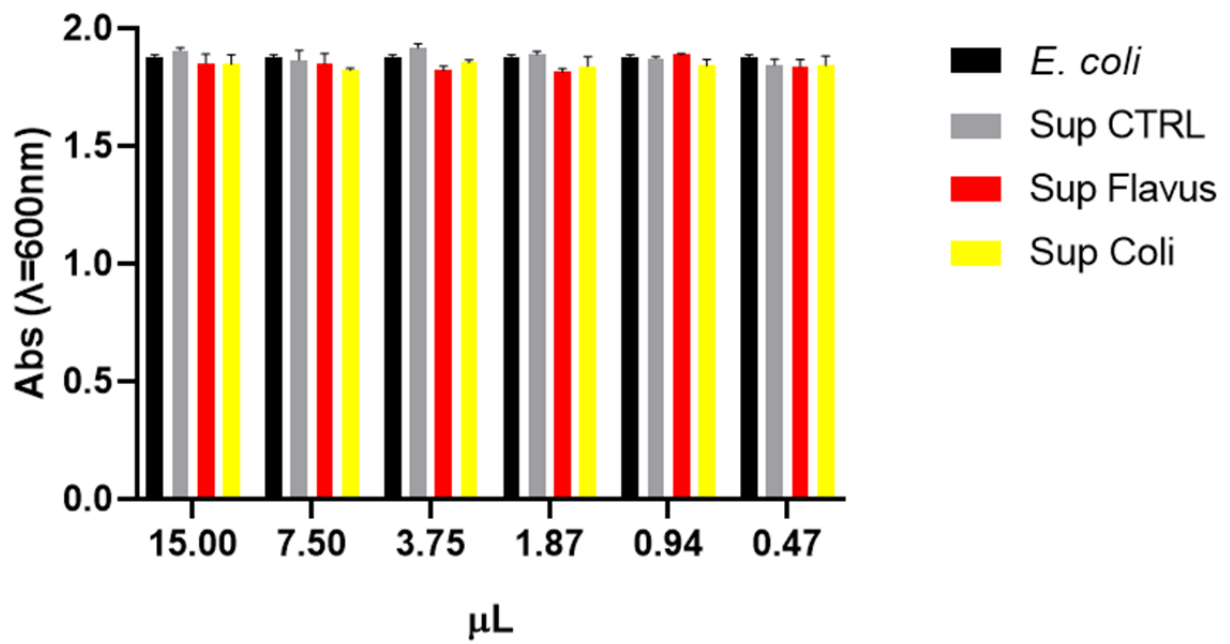


**Figure 48.** Microdilution assay performed against *E. coli* (LGM2092).

The obtained data show that no sample exerted an antibacterial effect against *E. coli* (LGM2092).

Bioautography (SDS-PAGE overlay method) was performed and the obtained result is shown in Figure 49.

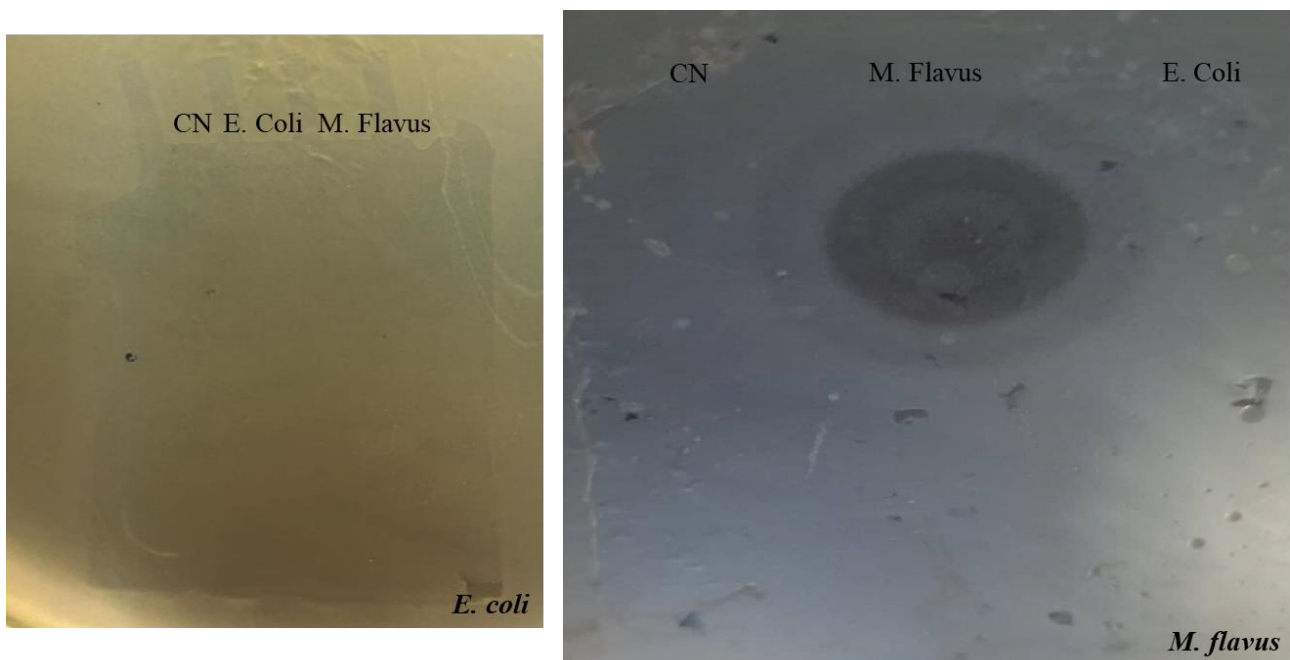


**Figure 49.** Bioautography assay performed against *E. coli* (LGM2092) (a) and *M. flavus* (DSM1790) (b).

The results show the formation of an inhibition zone on the plate with *M. flavus* (DSM1790), at the sample obtained by precipitation of the plasma extracted from larvae infected with *M. flavus* (DSM1790). No effect was detected against *E. coli* (LGM2092).

At the Eli Lilly S.P.A., Catania, Italy, a microdilution assay has been performed against both *E. coli* (strain isolated from pecorino cheese after 4 months of seasoning, at the University of Palermo, Italy) and *S. Aureus* (ATCC33826). The results obtained against *E. coli* (strain isolated from pecorino cheese after 4 months of seasoning, at the University of Palermo, Italy), show that the supernatant obtained by precipitating the plasma extracted from larvae infected with *M. flavus* (DSM1790) and *E. coli* (LGM2092) exerted an antibacterial activity. Particularly, the supernatant obtained by precipitating the plasma extracted from larvae infected with *M. flavus* (DSM1790), using 15  $\mu$ L showed a high reduction in cell growth (90%) while 15  $\mu$ L of the supernatant obtained by precipitating the plasma extracted from larvae infected with *E. coli* (LGM2092) lead to a reduction equal to 84% of the cell growth. At 7.5  $\mu$ L of used samples, the supernatant obtained by precipitating the plasma extracted from larvae infected with *M. flavus* (DSM1790) lead to a reduction of 48 % of the cell growth while the supernatant obtained by precipitating the plasma extracted from larvae infected with *E. coli* (LGM2092) lead to a reduction of 33% (Figure 50).

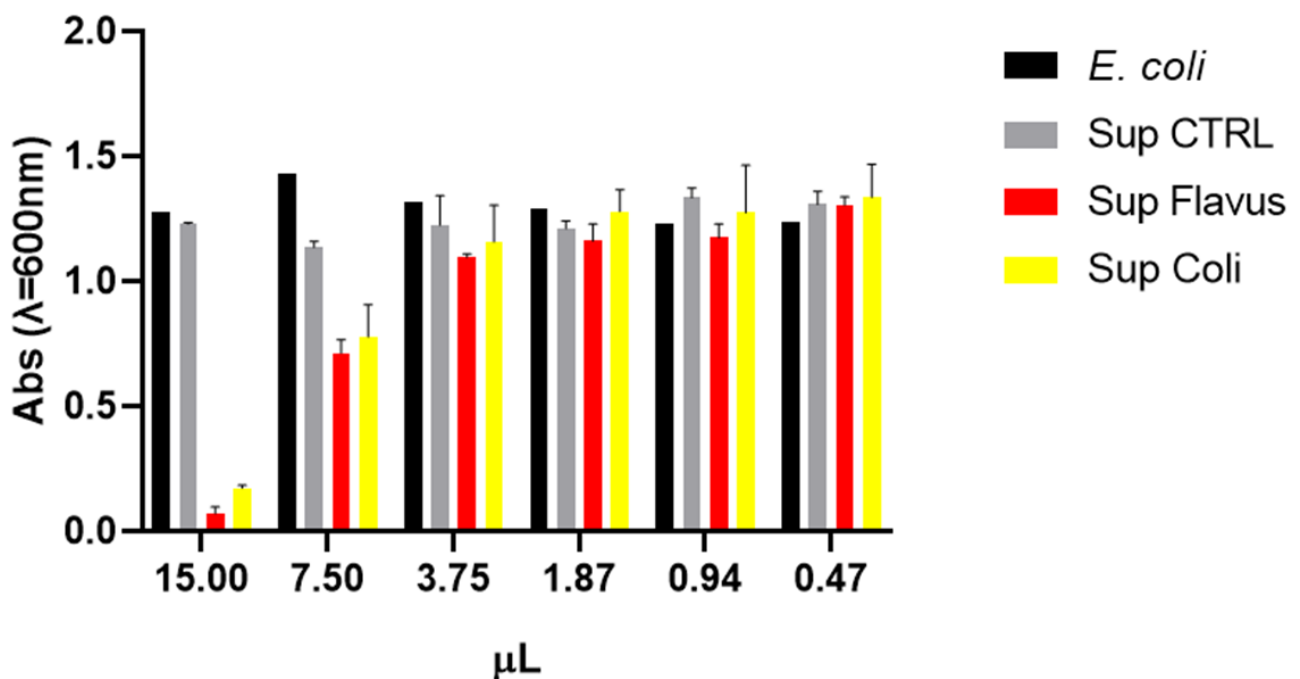


**Figure 50.** Microdilution assay performed against *E. coli* (strain isolated from pecorino cheese after 4 months of seasoning, at the University of Palermo, Italy).

The results obtained against *S. aureus* (ATCC33826), show that the supernatant obtained by precipitating the plasma extracted from larvae infected with *M. flavus* (DSM1790) and *E. coli* (LMG2092) exerted an antibacterial activity. Particularly, the supernatant obtained by precipitating the plasma extracted from larvae infected with *M. flavus* (DSM1790), using 15  $\mu$ L showed a high reduction in cell growth (88%) while 15  $\mu$ L of the the supernatant obtained by precipitating the plasma extracted from larvae infected with *E. coli* (LMG2092) lead to a reduction equal to 79% of the cell growth. At 7.5  $\mu$ L of used samples, the supernatant obtained by precipitating the plasma extracted from larvae infected with *M. flavus* (DSM1790) lead to a reduction of 78 % of the cell growth while the supernatant obtained by precipitating the plasma extracted from larvae infected with *E. coli* (LMG2092) lead to a reduction of 30% (Figure 51).

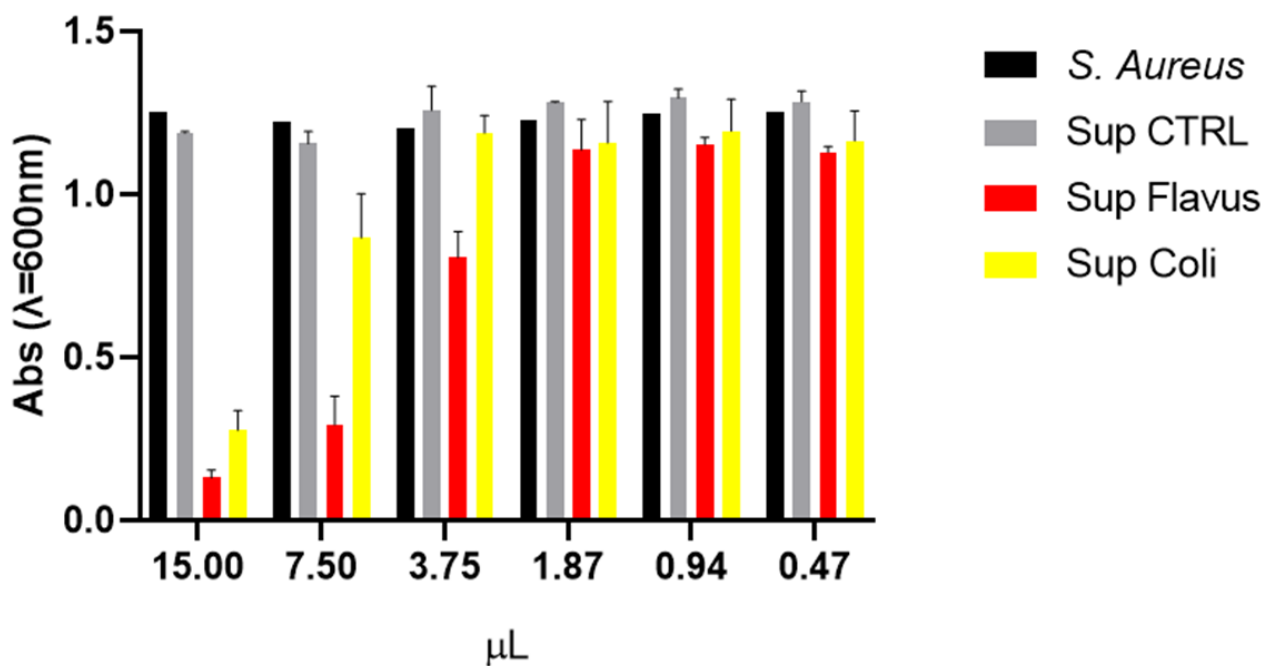


**Figure 51.** Microdilution assay performed against *S. aureus* (ATCC33826).

#### 4.15. Hemolymph analysis performed at the Technische Hochschule Mittelhessen University of Applied Sciences, Gießen, Germany

*Hermetia illucens* larvae, provided by Prof. Andreas Vilcinskis from the Justus-Liebig-Universität, Gießen, Germany, reared on two different diets (CF and CPC), were infected with *M. luteus*,  $OD_{\lambda=600} = 1$  and incubated at 25 °C for 24 hours. Then, the hemolymph was extracted from larvae infected with *M. luteus* and from not-infected larvae and through the centrifugation step the plasma was collected. 1:50 dilution of the plasma was analysed through HPLC in collaboration with Dr. Daniela Müller. In Figure 52 is shown the chromatogram obtained for the plasma extracted from not infected larvae reared on CF diet; in Figure 53 is shown the chromatogram obtained for the plasma extracted from larvae infected with *M. luteus*, reared on CF diet; in Figure 54 is shown an overlap of the two chromatograms.

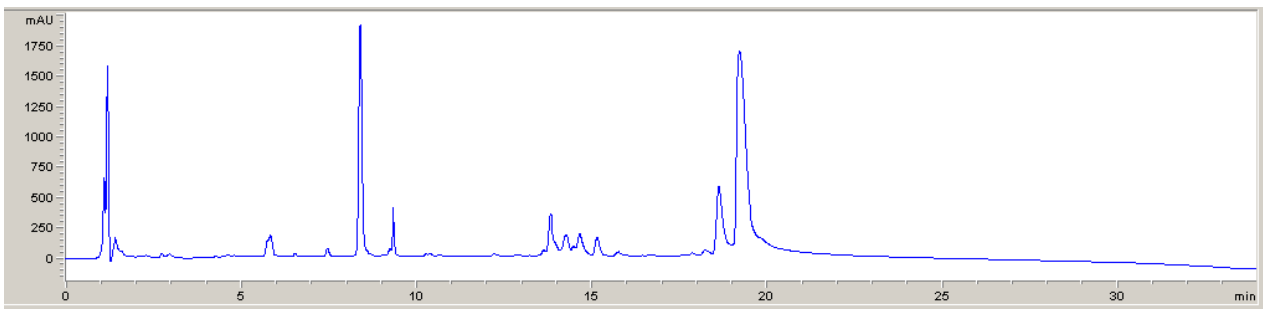


**Figure 52.** Chromatogram obtained for the plasma extracted from not infected larvae reared on CF diet.

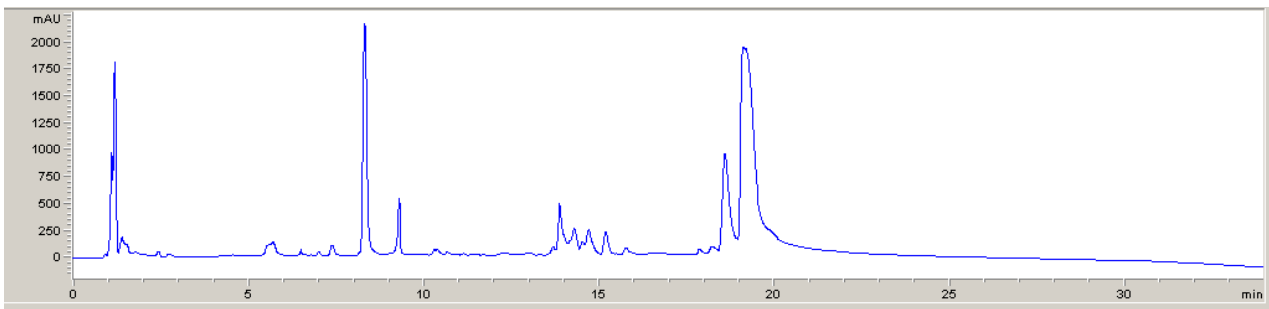


**Figure 53.** Chromatogram obtained for the plasma extracted from larvae infected with *M. luteus*, reared on CF diet.



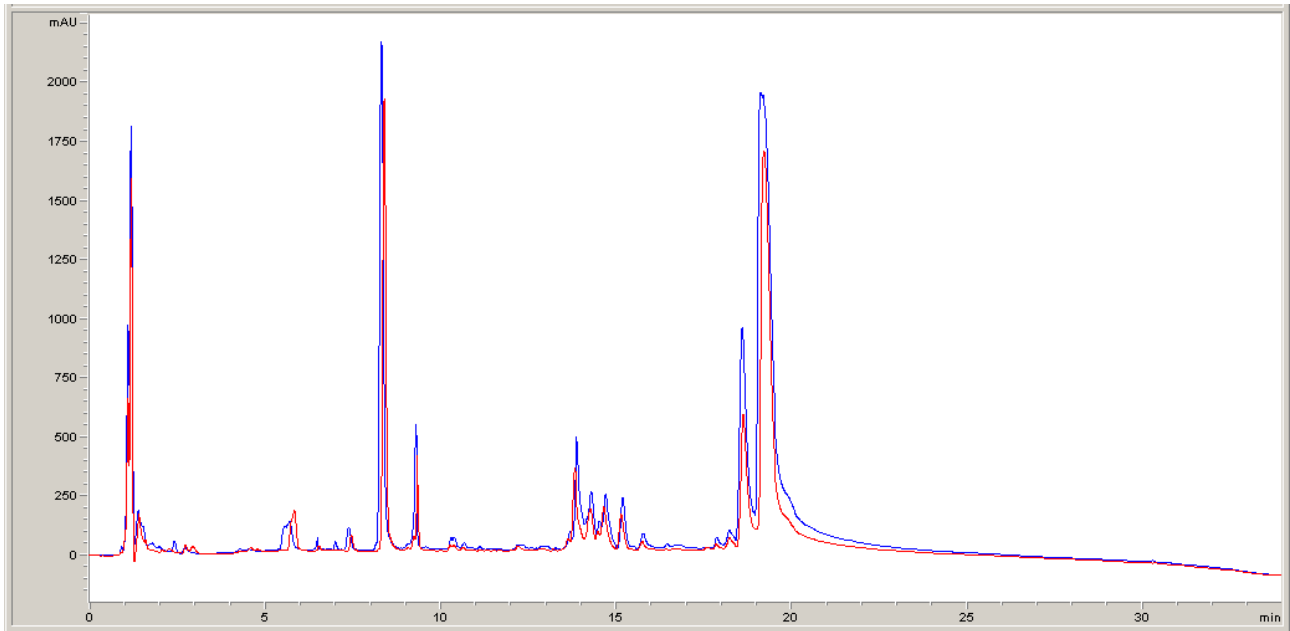


**Figure 54.** Overlap of the chromatogram obtained for the plasma extracted from not infected larvae (red peaks in the figure), reared on CF diet, and the chromatogram obtained for the plasma extracted from larvae infected with *M. luteus* (blue peaks in the figure), reared on CF diet.

In Figure 55 is shown the chromatogram obtained for the plasma extracted from not infected larvae reared on CPC diet; in Figure 56 is shown the chromatogram obtained for the plasma extracted from larvae infected with *M. luteus*, reared on CPC diet; in Figure 57 is shown an overlap of the two chromatograms.

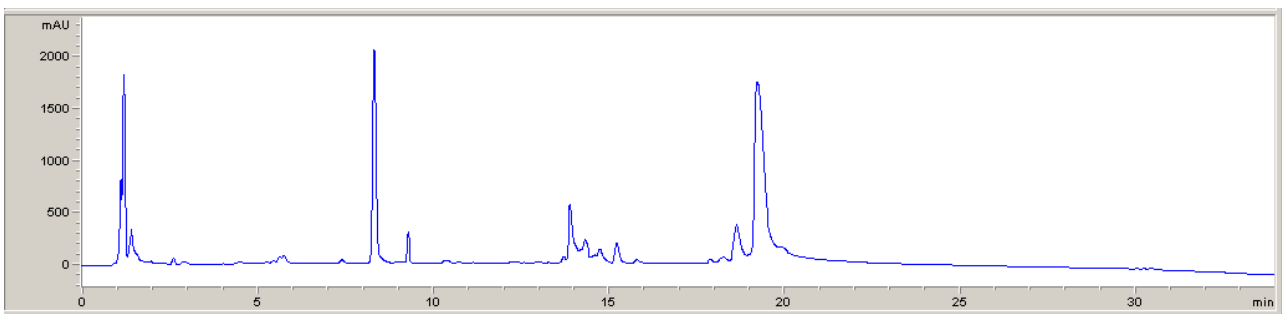


**Figure 55.** Chromatogram obtained for the plasma extracted from not infected larvae reared on CPC diet.

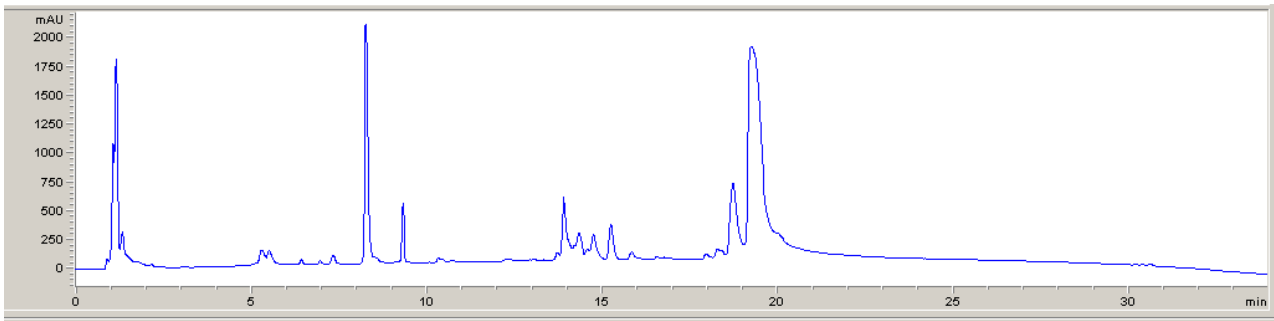


**Figure 56.** Chromatogram obtained for the plasma extracted from larvae infected with *M. luteus*, reared on CPC diet.

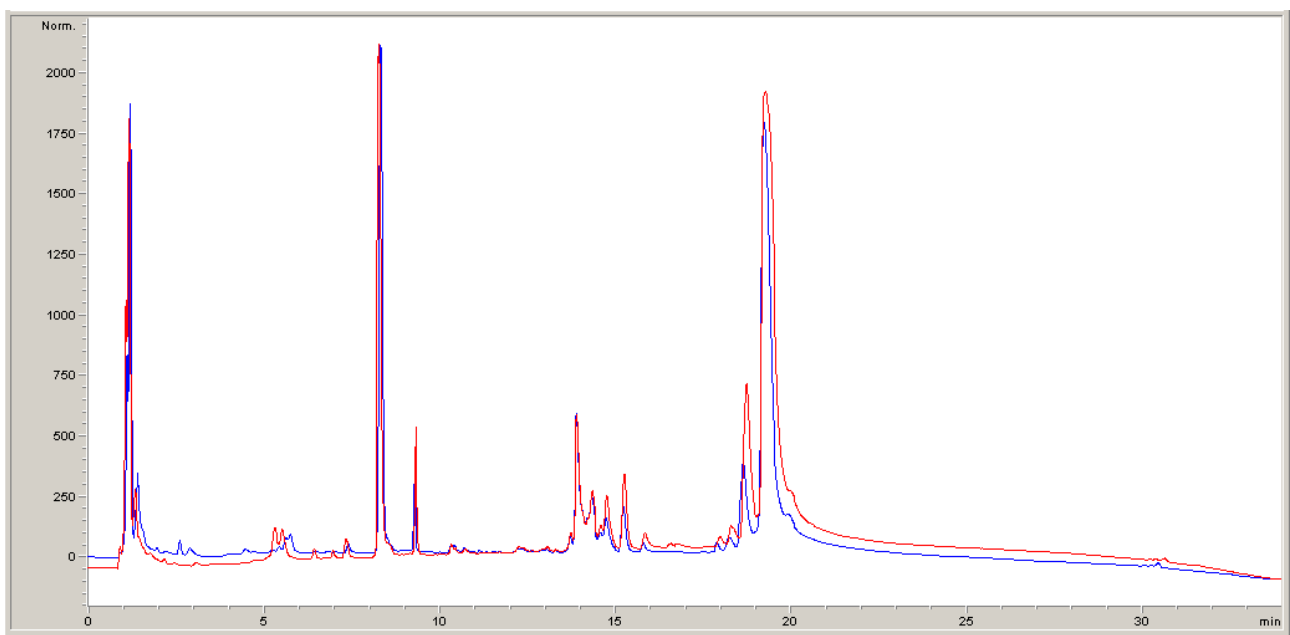


**Figure 57.** Overlap of the chromatogram obtained for the plasma extracted from not infected larvae (red peaks in the figure), reared on CPC diet, and the chromatogram obtained for the plasma extracted from larvae infected with *M. luteus* (blue peaks in the figure), reared on CPC diet.

Moreover, an overlap of the chromatogram obtained for the plasma extracted from not infected larvae reared on CF diet and the chromatogram obtained for the plasma extracted from not infected larvae reared on CPC diet, is shown below (Figure 58).

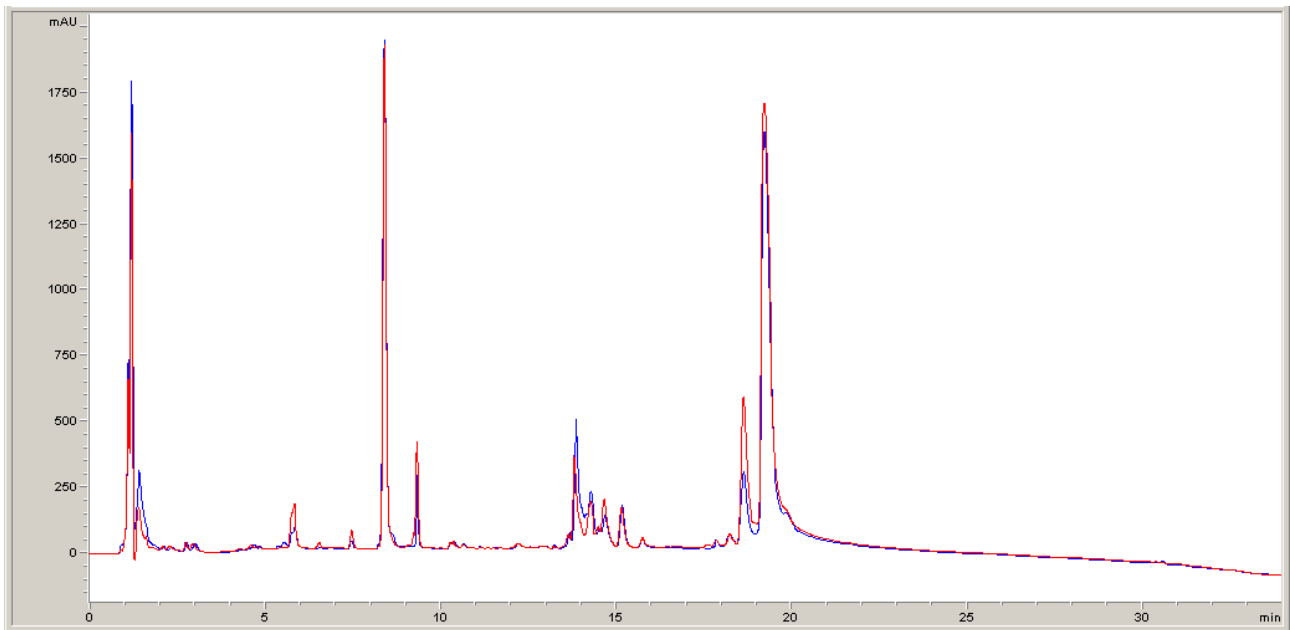


**Figure 58.** Overlap of the chromatogram obtained for the plasma extracted from not infected larvae reared on CF diet (red peaks in the figure) and the chromatogram obtained for the plasma extracted from not infected larvae reared on CPC diet (blue peaks in the figure).

A 1:50 dilution of the same sample has also been analysed through FLPC and the obtained chromatograms are shown below (Figure 59, 60, 61, 62).

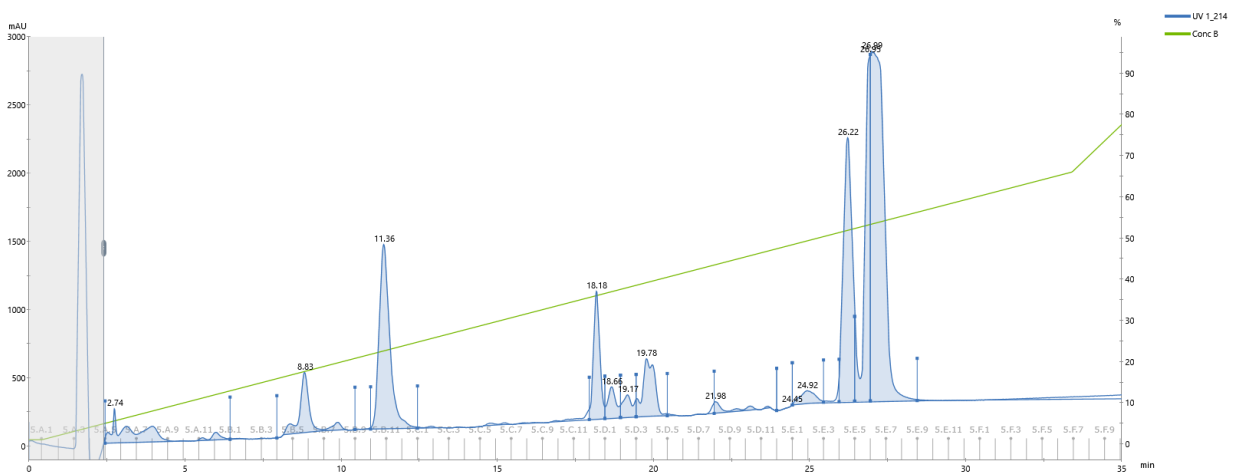


**Figure 59.** Chromatogram obtained for the plasma extracted from not infected larvae reared on CF diet.

In the following table (Table 12) is reported the peak list.

**Table 12.** From left to right are reported the Peak list, Retention Time (min), Peak Area (min\*mAU), Peak Area (%), Fractions and Peak Width (min). Data are related to the chromatogram shown in Figure 59.

Peak	Retention (min)	Area (min*mAU)	Area %	Fraction(s)	Width (min)
Peak A	2.737	184.6	4.75	5.A.5 - 5.A.12	4.002
Peak B	8.827	170.0	4.38	5.B.4 - 5.B.8	2.502
Peak C	11.362	533.9	13.75	5.B.10 - 5.B.12	1.500
Peak D	18.180	216.7	5.58	5.C.12	0.500
Peak E	18.663	70.54	1.82	5.D.1	0.500
Peak F	19.172	60.06	1.55	5.D.2	0.500
Peak G	19.780	191.7	4.93	5.D.3 - 5.D.4	1.000
Peak H	21.983	34.96	0.90	5.D.8 - 5.D.11	2.002
Peak I	24.447	0.02645	0.00	5.D.12	0.500
Peak J	24.922	53.47	1.38	5.E.1 - 5.E.2	1.000
Peak K	26.222	619.1	15.94	5.E.4	0.500
Peak L	26.947	477.5	12.30	5.E.5	0.500
Peak M	26.985	1271	32.74	5.E.6 - 5.E.8	1.502

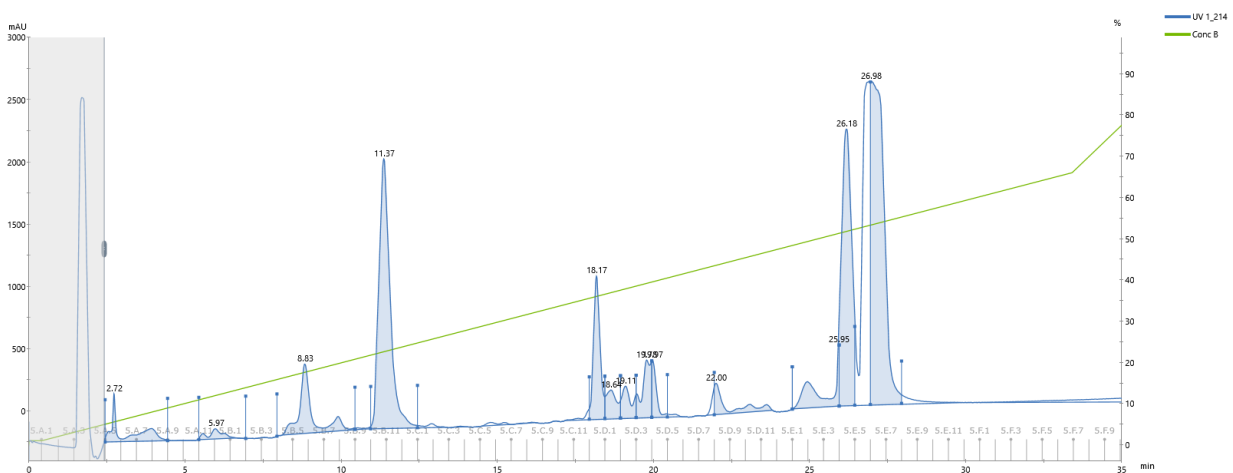


**Figure 60.** Chromatogram obtained for the plasma extracted from larvae infected with *M. luteus*, reared on CF diet.

In Table 13 is reported the obtained peak list.

**Table 13.** From left to right are reported the Peak list, Retention Time (min), Peak Area (min\*mAU), Peak Area (%), Fractions and Peak Width (min). Data are related to the chromatogram shown in Figure 60.

Peak	Retention (min)	Area (min*mAU)	Area %	Fraction(s)	Width (min)
Peak A	2.722	132.6	3.07	5.A.5 - 5.A.8	2.002
Peak B	5.968	42.31	0.98	5.A.11 - 5.B.1	1.502
Peak C	8.833	249.2	5.78	5.B.4 - 5.B.8	2.500
Peak D	11.365	872.9	20.24	5.B.10 - 5.B.12	1.500
Peak E	18.173	273.3	6.34	5.C.12	0.500
Peak F	18.640	88.93	2.06	5.D.1	0.500
Peak G	19.110	86.91	2.02	5.D.2	0.500
Peak H	19.782	149.2	3.46	5.D.3	0.500
Peak I	19.967	76.65	1.78	5.D.4	0.502
Peak J	22.002	106.3	2.46	5.D.8 - 5.D.12	2.500
Peak K	25.948	166.5	3.86	5.E.1 - 5.E.3	1.502
Peak L	26.183	791.5	18.35	5.E.4	0.500
Peak M	26.980	1276	29.60	5.E.6 - 5.E.7	1.000

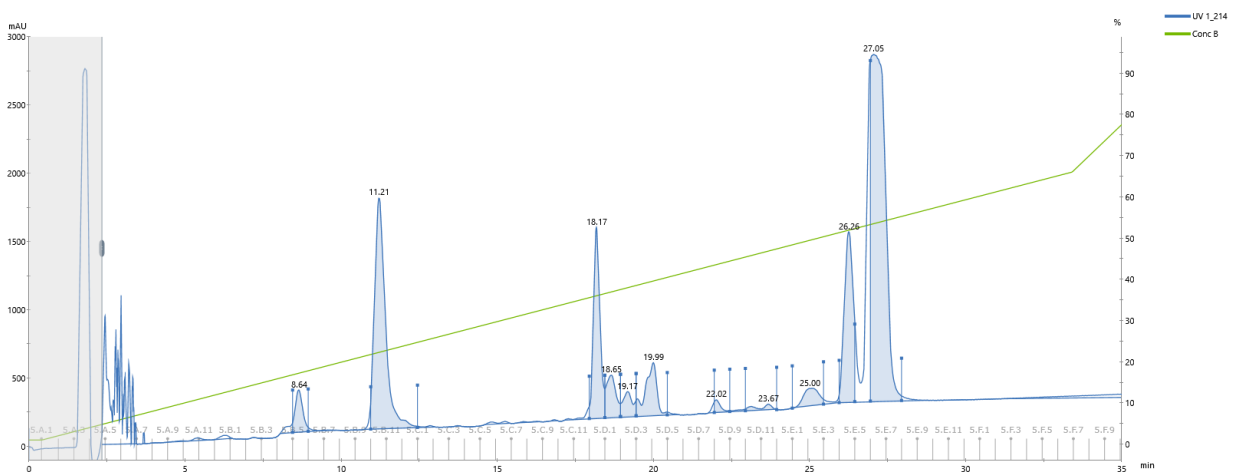


**Figure 61.** Chromatogram obtained for the plasma extracted from not infected larvae reared on CPC diet.

In Table 14 the obtained peak list is reported.

**Table 14.** From left to right are reported the Peak list, Retention Time (min), Peak Area (min\*mAU), Peak Area (%), Fractions and Peak Width (min). Data are related to the chromatogram shown in Figure 61.

Peak	Retention (min)	Area (min*mAU)	Area %	Fraction(s)	Width (min)
Peak A	8.638	85.05	2.59	5.B.5	0.500
Peak B	11.210	670.0	20.41	5.B.10 - 5.B.12	1.500
Peak C	18.173	330.9	10.08	5.C.12	0.500
Peak D	18.647	110.1	3.35	5.D.1	0.500
Peak E	19.168	64.30	1.96	5.D.2	0.500
Peak F	19.993	161.8	4.93	5.D.3 - 5.D.4	1.000
Peak G	22.015	19.81	0.60	5.D.8	0.500
Peak H	23.672	20.03	0.61	5.D.10 - 5.D.11	1.000
Peak I	24.997	71.65	2.18	5.E.1 - 5.E.2	1.000
Peak J	26.258	393.6	11.99	5.E.4	0.500
Peak K	27.052	1356	41.30	5.E.6 - 5.E.7	1.000

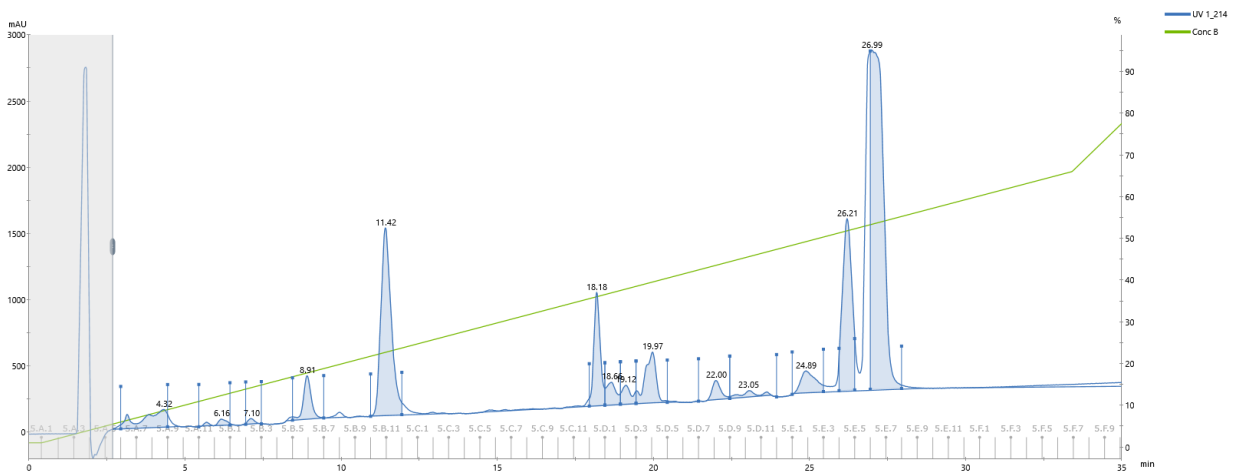


**Figure 62.** Chromatogram obtained for the plasma extracted from larvae infected with *M. luteus*, reared on CPC diet.

In the following table (Table 15) is reported the peak list.

**Table 15.** From left to right are reported the Peak list, Retention Time (min), Peak Area (min\*mAU), Peak Area (%), Fractions and Peak Width (min). Data are related to the chromatogram shown in Figure 62.

Peak	Retention (min)	Area (min*mAU)	Area %	Fraction(s)	Width (min)
Peak A	4.320	116.2	3.82	5.A.6 - 5.A.8	1.502
Peak B	6.157	19.07	0.63	5.A.11 - 5.A.12	1.000
Peak C	7.100	9.676	0.32	5.B.2	0.500
Peak D	8.908	93.73	3.08	5.B.5 - 5.B.6	1.000
Peak E	11.418	540.2	17.77	5.B.10 - 5.B.11	1.002
Peak F	18.183	201.5	6.63	5.C.12	0.500
Peak G	18.655	62.62	2.06	5.D.1	0.500
Peak H	19.115	48.63	1.60	5.D.2	0.500
Peak I	19.968	157.8	5.19	5.D.3 - 5.D.4	1.000
Peak J	21.998	45.77	1.51	5.D.7 - 5.D.8	1.000
Peak K	23.050	27.96	0.92	5.D.9 - 5.D.11	1.500
Peak L	24.887	90.16	2.97	5.E.1 - 5.E.2	1.000
Peak M	26.205	431.7	14.20	5.E.4	0.500
Peak N	26.990	1196	39.32	5.E.6 - 5.E.7	1.000

#### 4.16. Evaluation of the antibacterial activity of the collected fractions.

11 fractions have been collected from the CPC\_NI sample (Not Infected larvae and reared on CPC diet); 14 fractions from the CPC\_I sample (larvae reared on CPC diet and infected with *M. luteus*); 12 fractions from the CF\_NI sample (Not Infected larvae and reared on CF diet); 13 fractions from the CF\_I sample (larvae reared on CF diet and infected with *M. luteus*). All the fractions collected for the 4 samples were analysed through a microdilution assay in order to evaluate their antibacterial activity performed against both *E. coli* and *M. luteus*. The data have been analysed with Graphpad Prism 8.0.2.

In Figure 63 the microdilution assay performed against *M. luteus* of the 11 CPC\_NI fractions is shown.

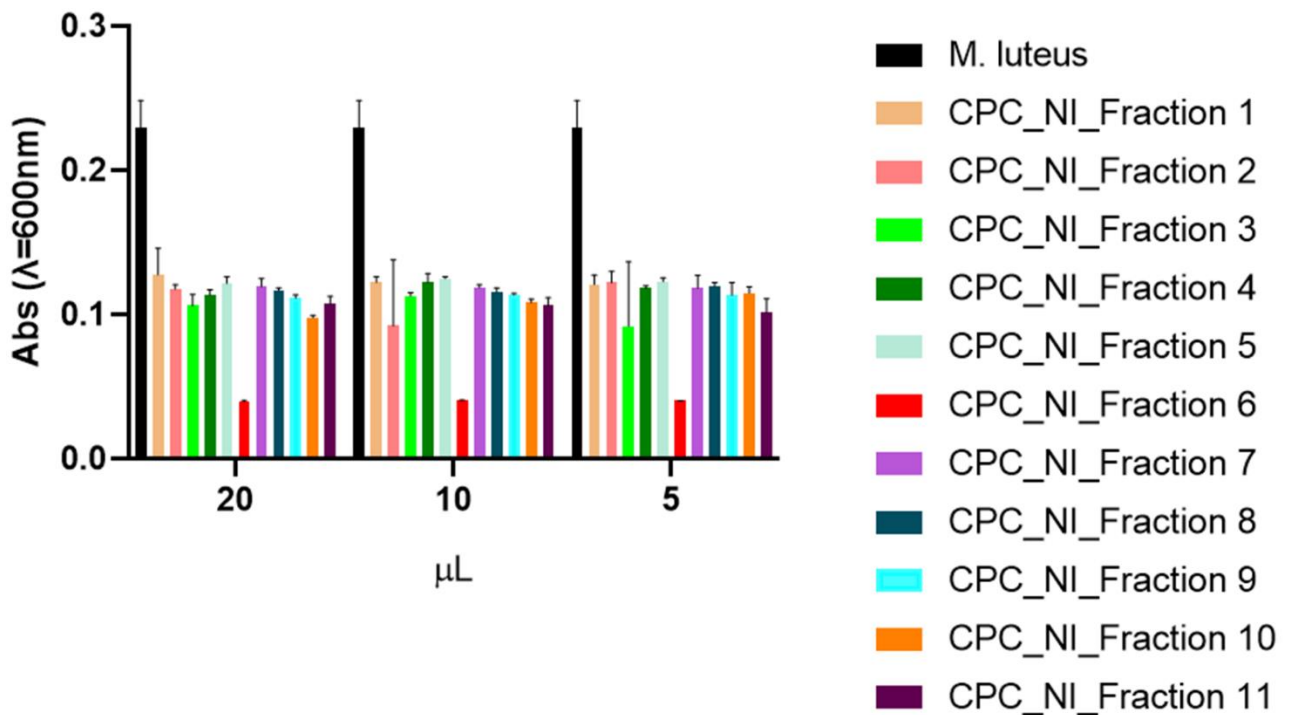


**Figure 63.** Microdilution assay of the 11 CPC\_NI fractions performed against *M. luteus*.

The obtained data show an interesting reduced of the cell growth caused by the Fraction number 6 by analyzing 20, 10 and 5 μL of the sample.

In Figure 64 the microdilution assay performed against *M. luteus* of the 14 CPC\_I fractions is shown.

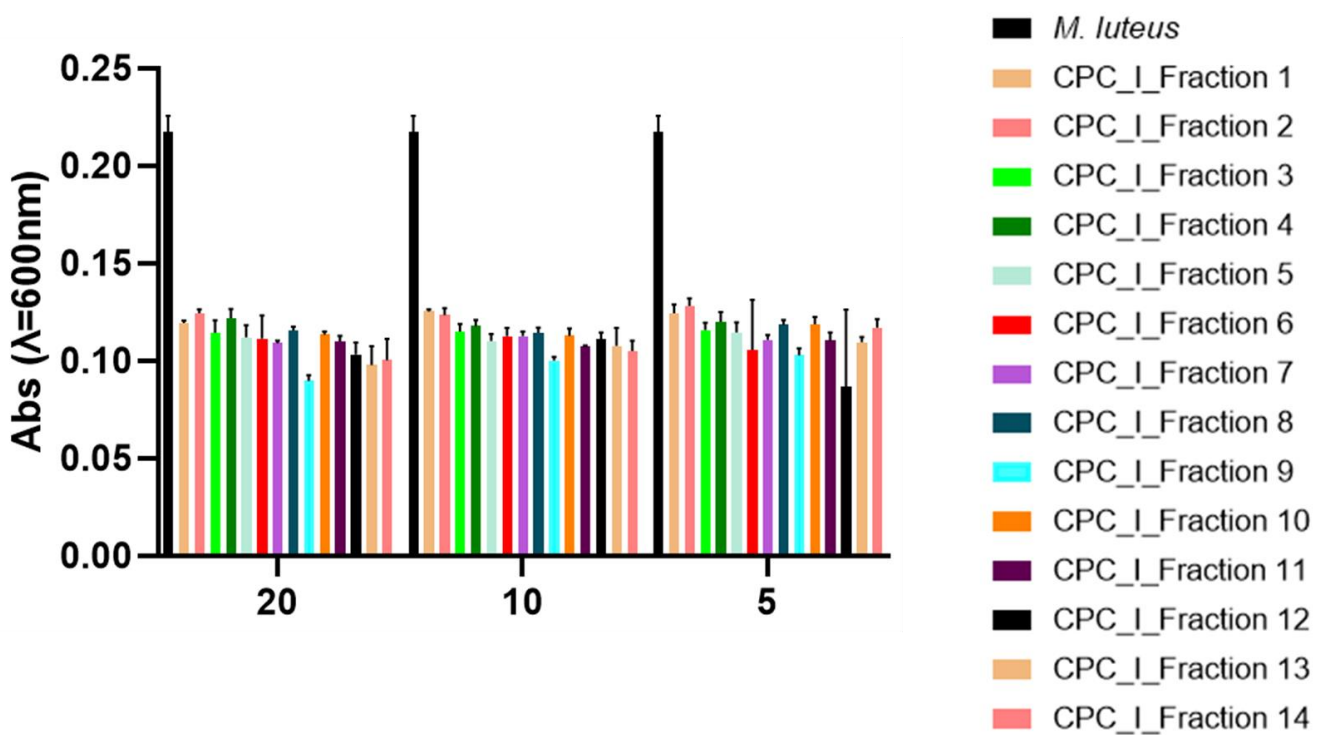




**Figure 64.** Microdilution assay of the 14 CPC\_I fractions performed against *M. luteus*.

The obtained results show no significant cell growth reduction by no sample.

In Figure 65 the microdilution assay performed against *M. luteus* of the 12 CF\_NI fractions is shown.

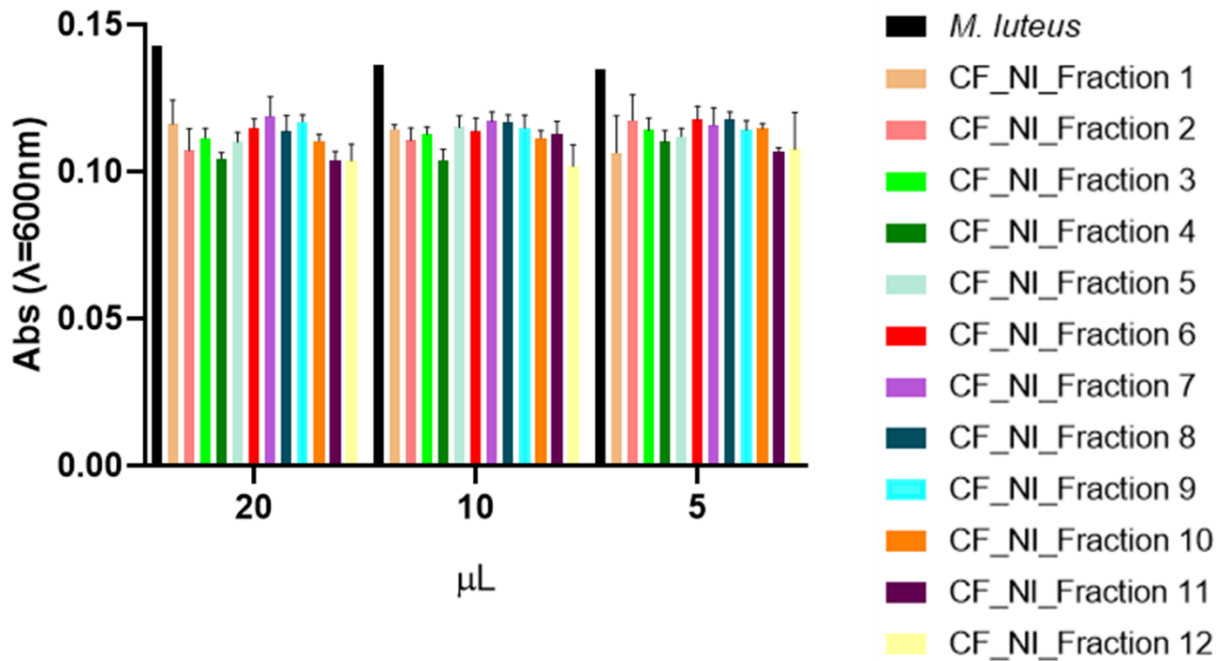


**Figure 65.** Microdilution assay of the 12 CF\_NI fractions performed against *M. luteus*.

The obtained data show no significant cell growth reduction by no sample.

In Figure 66 the microdilution assay performed against *M. luteus* of the 13 CF\_I fractions is shown.

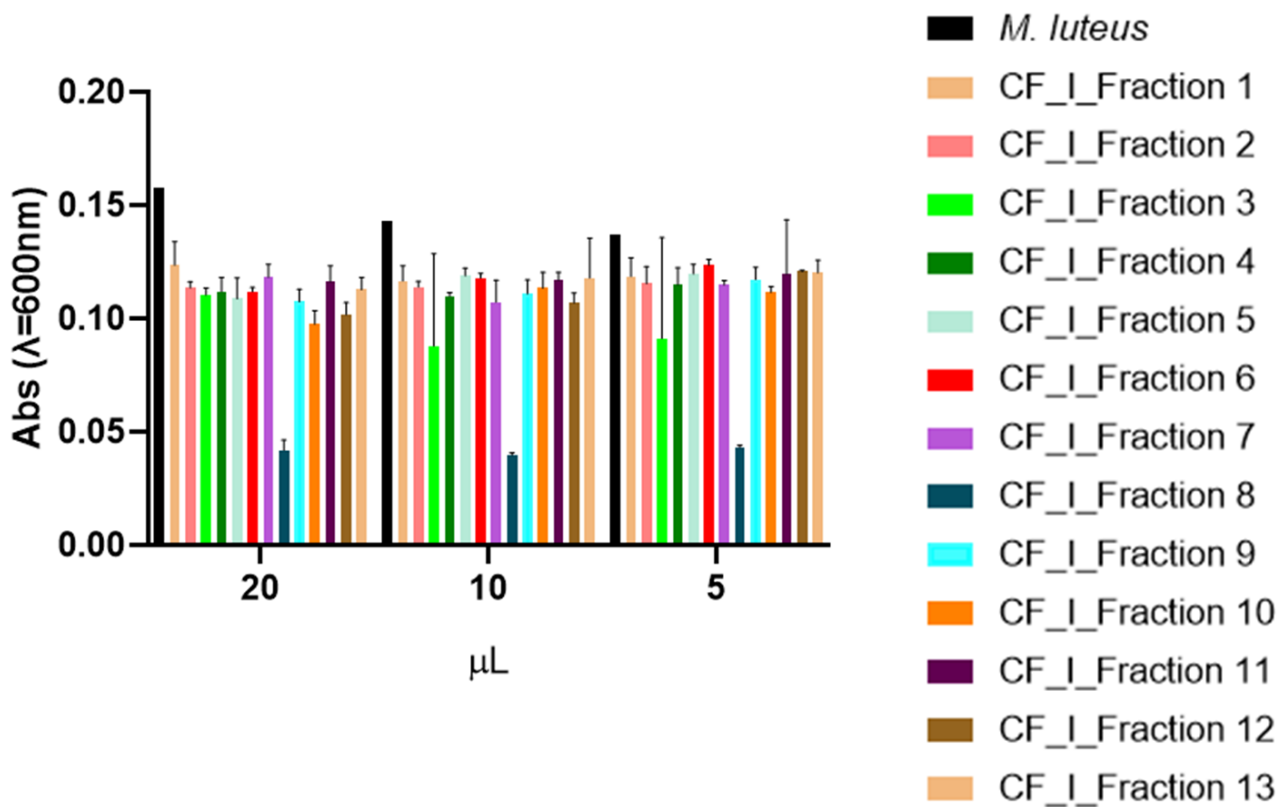


**Figure 66.** Microdilution assay of the 13 CF\_I fractions performed against *M. luteus*.

The obtained data show a growth reduction by Fraction number 8 by analyzing 20, 10 and 5 μL of the fraction.

In Figure 67 the microdilution assay performed against *E. coli* of the 11 CPC\_NI fractions is shown.

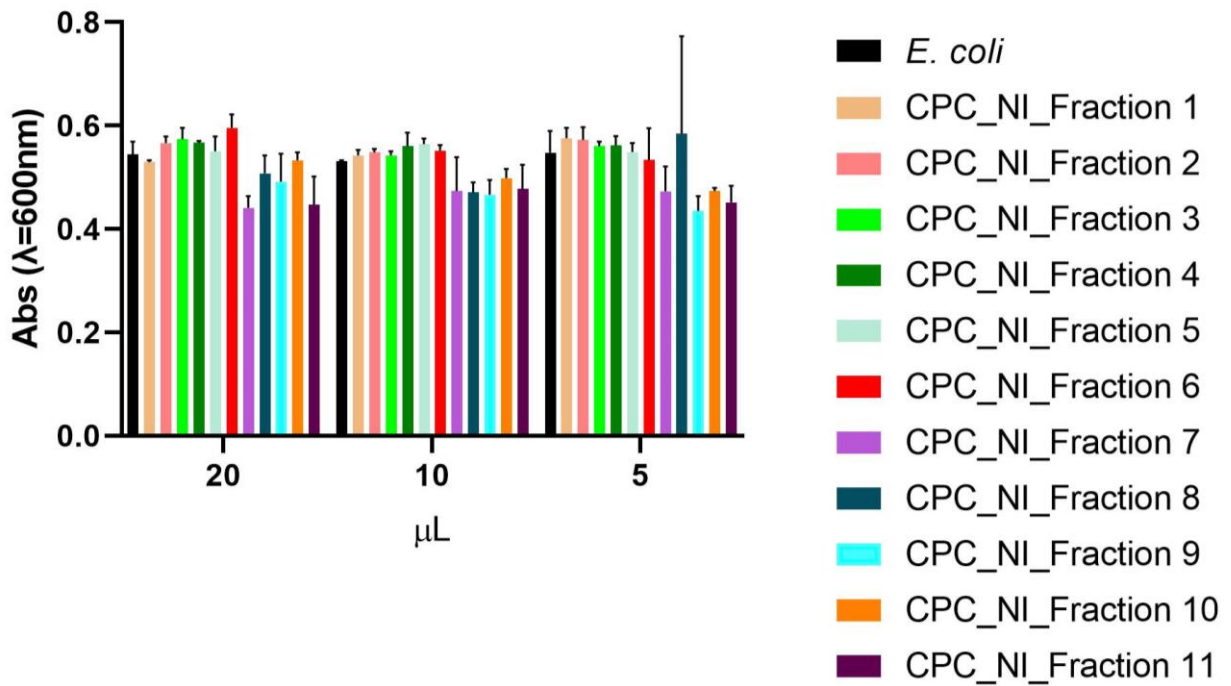


**Figure 67.** Microdilution assay of the 11 CPC\_NI fractions performed against *E. coli*.

The obtained results show no significant cell growth reduction after treating *E. coli* with the 11 fractions.

In Figure 68 the microdilution assay performed against *E. coli* of the 14 CPC\_I fractions is shown.

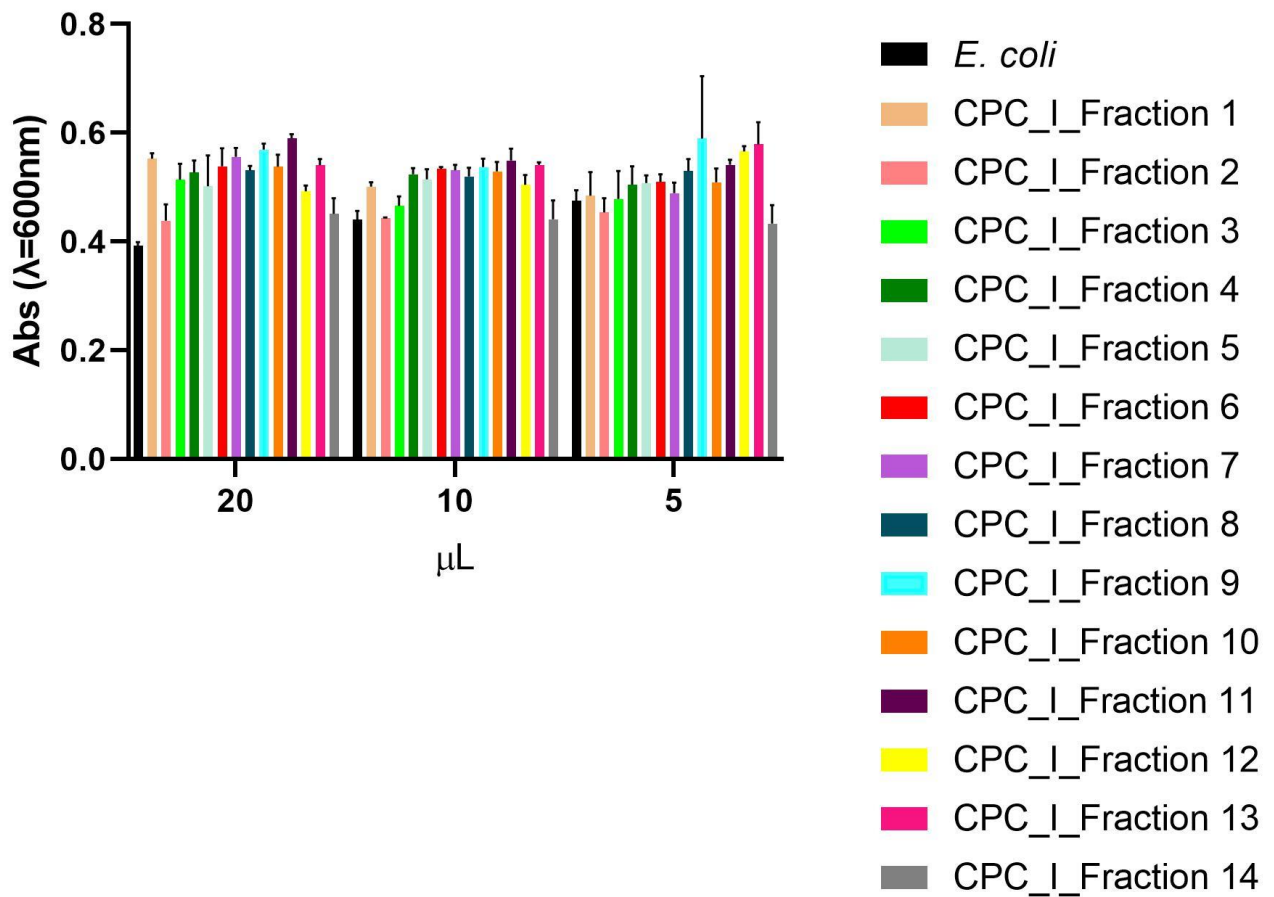


**Figure 68.** Microdilution assay of the 14 CPC\_I fractions performed against *E. coli*.

The obtained results show no significant cell growth reduction after treating *E. coli* with the 11 fractions.

In Figure 69 the microdilution assay performed against *E. coli* of the 12 CF\_NI fractions is shown.

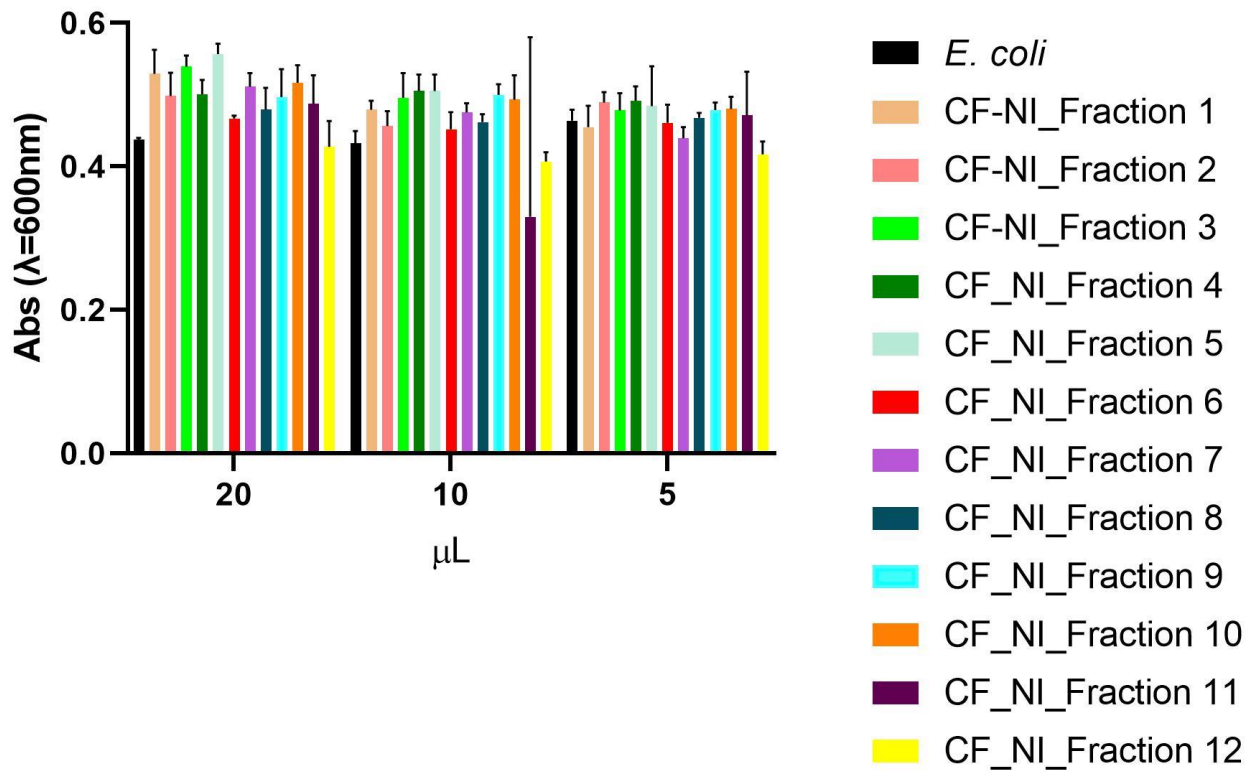


**Figure 69.** Microdilution assay of the 12 CF\_NI fractions performed against *E. coli*.

The obtained results show no significant cell growth reduction after treating *E. coli* with the 11 fractions.

In Figure 70 the microdilution assay performed against *E. coli* of the 13 CF\_I fractions is shown.

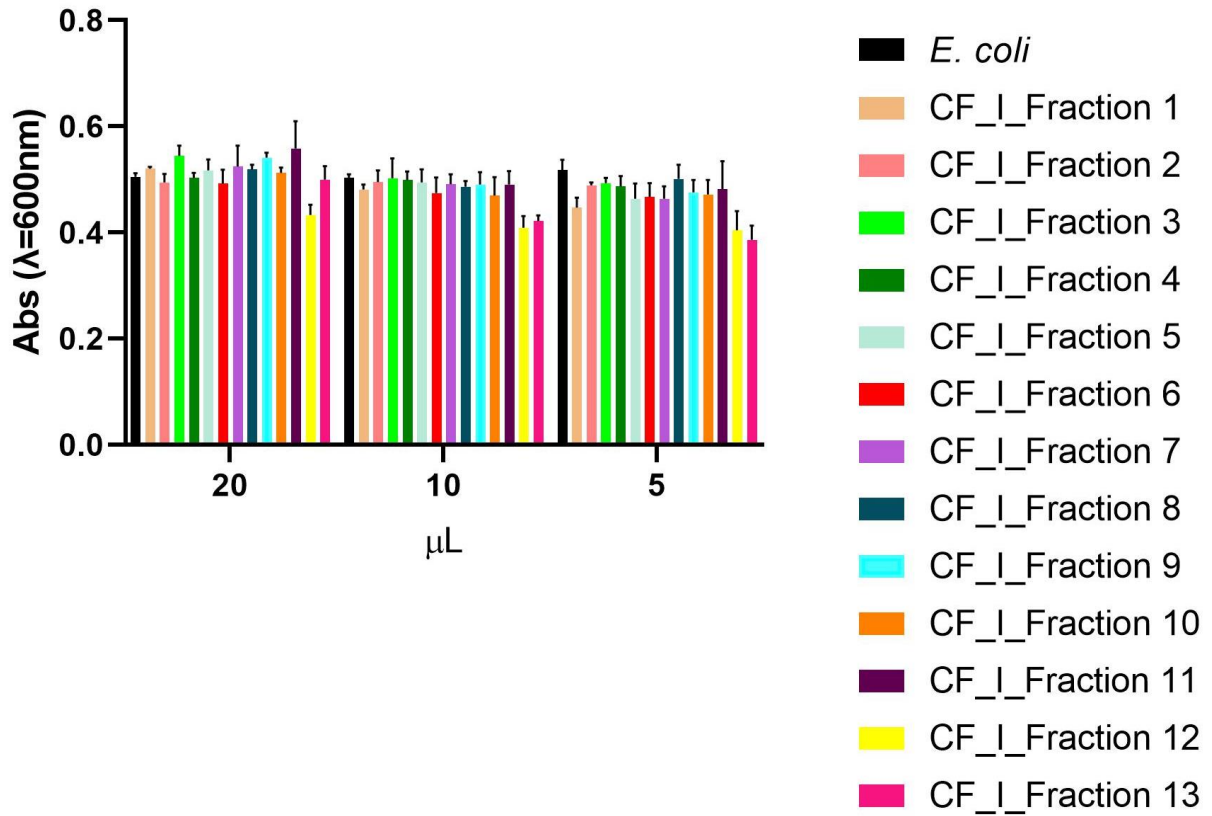


**Figure 70.** Microdilution assay of the 13 CF\_I fractions performed against *E. coli*.

The obtained results show no significant cell growth reduction after treating *E. coli* with the 11 fractions.

## 5. DISCUSSION

Antimicrobial peptides are great candidates as alternatives to conventional antibiotics, thanks to their low toxicity to eukaryotic cells and their broad spectrum of action against bacteria, fungi, viruses and cancer cells [41]. Antimicrobial peptides can kill bacteria through different mechanisms like membrane disruption or by targeting intracellular components or interfering with bacterial metabolism [42 - 44]. Most AMPs are cationic with the positive net charge promoting the electrostatic interaction with negatively charged bacterial membranes [45].

All living organisms produce antimicrobial peptides with insects being among the richest sources thanks to their high biodiversity and their extremely various living environment. The immune system of the insect *Hermetia illucens* is very developed since it feeds on decaying substrates and manure, and lives in environments extremely rich in pathogenic microorganisms. The production of antimicrobial peptides, synthesized by the fat body and haemocytes and then secreted into the hemolymph, is an essential part of the immune defence [46, 47]. In order to identify the AMPs produced by *Hermetia illucens*, the larvae and the combined males and females adults transcriptomes were assembled and all the obtained contigs were functionally annotated through the Blast2Go software leading to the identification of 68 putative peptides. These sequences were *in silico* analyzed through the CAMP database and the iACP online tool in order to evaluate their antimicrobial and anticancer activity. The AVPpred and the Antifp servers were used in order to predict, respectively, the antiviral and the antifungal activity of the identified peptides. The obtained results brought to the identification of 57 peptides, 13 of which were predicted as endowed with antimicrobial activity and 22 with both antimicrobial and anticancer activity, 8 with both antimicrobial and antiviral activity and 2 with both antimicrobial and antifungal activity, 7 with antimicrobial, anticancer and antiviral activity. Only one peptide was predicted as antimicrobial, antiviral and antifungal while 2 peptides with putative antimicrobial, anticancer and antifungal activity. Surprisingly, 2 peptides, corresponding to Hill\_LB\_C16634 and NHill\_AD\_C69719 contigs, resulted positive to all the activity predictions. The richest group of identified peptides belongs to defensins family, whose composition ranges from 34 to 51 amino acids [48, 49]. These peptides have a pattern of six cysteines, which are involved in the formation of three disulphide bonds: Cys1 – Cys4, Cys2 – Cys5 and Cys3 – Cys6, for insect defensins [50]. Thus, the identified defensins were *in silico* analysed through the DISULFIND web server confirming the right conformation of the disulphide bonds provided for insect defensins. Thus, the identified defensins have the common structure of insect defensins. Without prejudice to the variability of the sequences, and therefore the different amino acid composition that characterizes each peptide/protein, the identified defensins have the same secondary

structure characteristics identified for other insect-derived defensins, such as Defensin A from *Protophormia terraenovae* [268], Lucifensin from *Lucilia sericata* [269], Defensin A and Defensin B from *Anomala cuprea* [270], Royalisin from *Apis mellifera* [271] and Coprisinc from *Copris tripartitus* [272].

These peptides are active against Gram-negative bacteria such as *Escherichia coli* but mainly against Gram-positive bacteria, such as *Staphylococcus aureus*, *Micrococcus luteus*, *Bacillus subtilis*, *Bacillus thuringiensis*, *Aerococcus viridians* and *Bacillus megaterium*. Moreover, some insect defensins are also active against some fungi [51 - 54]. The second richest group of identified peptides is cecropins (Cecs). Cecs represent the most abundant family of linear  $\alpha$  helical antimicrobial peptides in insects, active against both Gram-negative and Gram-positive bacteria [57]. The bioinformatic approach represents a powerful means to predict the chemical-physical properties and the putative function of amino acid sequences and the obtained results allowed to select the most promising sequences. Following the *in silico* analysis, the prediction of the secondary and tertiary structure, and the AMPs length, were exploited to choose peptides to be produced by recombinant methodologies and by chemical synthesis on solid phase. The produced peptides have been then functionally analysed in order to evaluate their antibacterial activity against different bacteria.

**Hill\_BB\_C6571, Hill\_BB\_C46948, Hill\_BB\_C16634 and Hill\_BB\_C7985 peptides:** these peptides were purchased from Bio-Fab company and their antibacterial activity has been evaluated against *Escherichia coli* (BL21). The obtained results showed that already 3  $\mu$ M of each peptide was able to lead to a reduction of cell viability.

**Hill\_BB\_C2519, Hill\_BB\_C15867, Hill\_BB\_C10649 and Hill\_BB\_C13792 peptides:** these 4 antimicrobial peptides have been selected for the recombinant production. They all have been cloned in the cloning plasmid TOPO-VECTOR and then in the expression plasmid pGEX-4T1. The well occurred molecular cloning has been confirmed by sequencing analysis and enzymatic hydrolysis with BamHI and EcoRI restriction enzymes. Hill\_BB\_C15867 has also been successfully purified through chromatographic strategy and hydrolyzed with thrombin in order to remove the GST tag. The obtained peptide was functionally characterized and the obtained results revealed an antibacterial activity against *E. coli*. Thus, this peptide identified through transcriptomic and bioinformatic analysis, has been successfully produced in a recombinant way, purified through chromatography technique and revealed an antibacterial activity against *E. coli* (BL21) and 18  $\mu$ M has been calculated as MIC value. The obtained value falls perfectly within the range of MIC values calculated also for other antimicrobial peptides deriving from insect reported in the literature. Indeed, Peng et al., 2019 studied the antibacterial effect of some cecropins (Cec1, Cec2, Cec5, Cec7 and Cec9) deriving from



*Musca domestica* obtaining MIC values, performed against *Staphylococcus aureus* and *Candida albicans*, ranging from 8 to 32  $\mu\text{M}$  [273]. Moreover, the Ds-defensin peptide deriving from *Dermacentor silvarum* (Acari: Ixodidae), studied by Li et al., 2021, showed an antibacterial activity against Gram-positive and Gram-negative bacteria with MIC values of 25  $\mu\text{M}$  and 50  $\mu\text{M}$  [274], thus MIC values lower than the C15867 defensin identified in *H. illucens*.

Moreover, the Hill\_BB\_C2519 peptide has been purified and hydrolyzed with thrombin and the mass spectrometry analysis was performed. The antibacterial activity is ongoing, while the purification of the Hill\_BB\_C10649 and Hill\_BB\_C13792 is progress.

**Hill\_BB\_C4669 and Hill\_BB\_C12927 peptides:** the chemical synthesis on solid phase of Hill\_BB\_C4669 and Hill\_BB\_C12927 peptides has been performed exploiting the chemistry of the Fmoc protecting group. Unfortunately, after a lot of work, the mass spectrometry analysis revealed that the obtained products were not those desired, which could be probably related to the high length of the peptides.

Since the identified sequences all have an amino acid composition higher than 30 amino acids, the recombinant production remains the most suitable.

Furthermore, an *in vivo* approach has been performed to extract antimicrobial peptides from the *H. illucens* insect. The hemolymph was extracted from not-infected and larvae infected with *E. coli* (LMG2092) and *M. flavus* (DSM1790) and analysed through biological assays. The obtained results revealed an antibacterial activity of the plasma extracted from larvae infected with *M. flavus*. Moreover, at the Technische Hochschule Mittelhessen University of Applied Sciences, Gießen, Germany, the hemolymph extracted from not infected larvae and larvae infected with *M. luteus*, reared on two different diets, CPC (Cotton Pressed Cake) and CF (Chicken Food), was analysed through HPLC and FLPC techniques and the obtained fractions were analysed against *E. coli* and *M. luteus*. The results revealed an antibacterial activity against *M. luteus* by fraction 6 deriving from the hemolymph extracted from not infected larvae reared on CPC diet; fraction 8 deriving from the hemolymph extracted from infected larvae reared on CF diet.

Furthermore, at the Eli Lilly s.p.a. company, Catania, Sicily, the performed experiments shown that the peptide fraction, recovered from the plasma deriving from larvae infected with *M. flavus* (DSM1790), is active against a *E. coli* (strain isolated from pecorino cheese at the University of Palermo), and *S. aureus* (ATCC33826). The mass spectrometry analysis is ongoing in order to identify the active peptides extracted directly from the larvae plasma.

Thus, the obtained results, about the hemolymph analysis, show that the plasma extracted from the *H. illucens* larvae exert mostly an antibacterial activity against Gram-positive bacteria, suggesting the presence of AMPs belonging to the defensin class - since they are principally active against Gram-positive strains – and are among the most abundant in insects.

Despite the hard period caused by the SARS-CoV-2 pandemic, a lot of analysis has been performed during this Ph.D. and only a few experiments are still ongoing.

## 6. BIBLIOGRAPHY

1. Payne, D. J., Gwynn, M. N., Holmes, D. J., & Pompliano, D. L. (2007). Drugs for bad bugs: confronting the challenges of antibacterial discovery. *Nature reviews Drug discovery*, 6(1), 29-40.
2. Tommasi, R., Brown, D. G., Walkup, G. K., Manchester, J. I., & Miller, A. A. (2015). ESKAPEing the labyrinth of antibacterial discovery. *Nature reviews Drug discovery*, 14(8), 529-542.
3. Beceiro, A., Tomás, M., & Bou, G. (2013). Antimicrobial resistance and virulence: a successful or deleterious association in the bacterial world?. *Clinical microbiology reviews*, 26(2), 185-230.
4. Brown, E. D., & Wright, G. D. (2016). Antibacterial drug discovery in the resistance era. *Nature*, 529(7586), 336-343.
5. Falagas, M. E., Vouloumanou, E. K., Samonis, G., & Vardakas, K. Z. (2016). Fosfomycin. *Clinical Microbiology Reviews*, 29(2), 321-347.
6. Martens, E., & Demain, A. L. (2017). The antibiotic resistance crisis, with a focus on the United States. *The Journal of antibiotics*, 70(5), 520-526.
7. Neshani, A., Sedighian, H., Mirhosseini, S. A., Ghazvini, K., Zare, H., & Jahangiri, A. (2020). Antimicrobial peptides as a promising treatment option against *Acinetobacter baumannii* infections. *Microbial Pathogenesis*, 104238.
8. Gollan, B., Grabe, G., Michaux, C., & Helaine, S. (2019). Bacterial persisters and infection: past, present, and progressing. *Annual review of microbiology*, 73, 359-385.
9. Permana, A. D., Mir, M., Utomo, E., & Donnelly, R. F. (2020). Bacterially sensitive nanoparticle-based dissolving microneedles of doxycycline for enhanced treatment of bacterial biofilm skin infection: A proof of concept study. *International journal of pharmaceutics: X*, 2, 100047.
10. Vallet-Gely, I., Lemaitre, B., & Boccad, F. (2008). Bacterial strategies to overcome insect defences. *Nature Reviews Microbiology*, 6(4), 302-313.
11. Hillyer, J. F. (2016). Insect immunology and hematopoiesis. *Developmental & Comparative Immunology*, 58, 102-118.
12. Kanost, M. R., Jiang, H., & Yu, X. Q. (2004). Innate immune responses of a lepidopteran insect, *Manduca sexta*. *Immunological reviews*, 198(1), 97-105.

13. Lemaitre, B., & Hoffmann, J. (2007). The host defense of *Drosophila melanogaster*. *Annu. Rev. Immunol.*, 25, 697-743.
14. Marmaras, V. J., & Lampropoulou, M. (2009). Regulators and signalling in insect haemocyte immunity. *Cellular signalling*, 21(2), 186-195.
15. Tsakas, S., & Marmaras, V. J. (2010). Insect immunity and its signalling: an overview. *Invertebrate Survival Journal*, 7(2), 228-238.
16. Lavine, M. D., & Strand, M. R. (2002). Insect hemocytes and their role in immunity. *Insect biochemistry and molecular biology*, 32(10), 1295-1309.
17. Strand, M. R. (2008). The insect cellular immune response. *Insect science*, 15(1), 1-14.
18. Satyavathi, V. V., Minz, A., & Nagaraju, J. (2014). Nodulation: an unexplored cellular defense mechanism in insects. *Cellular signalling*, 26(8), 1753-1763.
19. Jiravanichpaisal, P., Lee, B. L., & Söderhäll, K. (2006). Cell-mediated immunity in arthropods: hematopoiesis, coagulation, melanization and opsonization. *Immunobiology*, 211(4), 213-236.
20. Janeway Jr, C. A., & Medzhitov, R. (2002). Innate immune recognition. *Annual review of immunology*, 20(1), 197-216.
21. Iwanaga, S., & Lee, B. L. (2005). Recent advances in the innate immunity of invertebrate animals. *BMB Reports*, 38(2), 128-150.
22. Nappi, A. J., & Christensen, B. M. (2005). Melanogenesis and associated cytotoxic reactions: applications to insect innate immunity. *Insect biochemistry and molecular biology*, 35(5), 443-459.
23. Fleming, A. (1929). On the antibacterial action of cultures of a penicillium, with special reference to their use in the isolation of *B. influenzae*. *British journal of experimental pathology*, 10(3), 226.
24. Zaffiri, L., Gardner, J., & Toledo-Pereyra, L. H. (2012). History of antibiotics. From salvarsan to cephalosporins. *Journal of Investigative Surgery*, 25(2), 67-77.
25. Bentley, R. (2009). Different roads to discovery; Prontosil (hence sulfa drugs) and penicillin (hence  $\beta$ -lactams). *Journal of industrial microbiology & biotechnology*, 36(6), 775-786.
26. Davies, J. (2006). Where have all the antibiotics gone?. *Canadian Journal of Infectious Diseases and Medical Microbiology*, 17.
27. Katz, M. L., Mueller, L. V., Polyakov, M., & Weinstock, S. F. (2006). Where have all the antibiotic patents gone?. *Nature biotechnology*, 24(12), 1529-1531.

28. Mahlapuu, M., Håkansson, J., Ringstad, L., & Björn, C. (2016). Antimicrobial peptides: an emerging category of therapeutic agents. *Frontiers in cellular and infection microbiology*, 6, 194.
29. Guaní-Guerra, E., Santos-Mendoza, T., Lugo-Reyes, S. O., & Terán, L. M. (2010). Antimicrobial peptides: general overview and clinical implications in human health and disease. *Clinical immunology*, 135(1), 1-11.
30. Zasloff, M. (1987). Magainins, a class of antimicrobial peptides from *Xenopus* skin: isolation, characterization of two active forms, and partial cDNA sequence of a precursor. *Proceedings of the National Academy of Sciences*, 84(15), 5449-5453.
31. Zasloff, M. (2002). Antimicrobial peptides of multicellular organisms. *nature*, 415(6870), 389-395.
32. Soravia, E., Martini, G., & Zasloff, M. (1988). Antimicrobial properties of peptides from *Xenopus* granular gland secretions. *FEBS letters*, 228(2), 337-340.
33. Steiner, H., Hultmark, D., Engström, Å., Bennich, H., & Boman, H. G. (1981). Sequence and specificity of two antibacterial proteins involved in insect immunity. *Nature*, 292(5820), 246-248.
34. Malik, E., Dennison, S. R., Harris, F., & Phoenix, D. A. (2016). pH dependent antimicrobial peptides and proteins, their mechanisms of action and potential as therapeutic agents. *Pharmaceuticals*, 9(4), 67.
35. Dossey, A. T. (2010). Insects and their chemical weaponry: new potential for drug discovery. *Natural product reports*, 27(12), 1737-1757.
36. Yi, H.Y.; Chowdhury, M.; Huang, Y.D.; Yu, X.Q. Insect antimicrobial peptides and their applications. *Appl. Microbiol. Biotechnol.* 2014, 98, 5807–5822.
37. Brogden, K. A. (2005). Antimicrobial peptides: pore formers or metabolic inhibitors in bacteria?. *Nature reviews microbiology*, 3(3), 238-250.
38. Steiner, H., Hultmark, D., Engström, Å., Bennich, H., & Boman, H. G. (1981). Sequence and specificity of two antibacterial proteins involved in insect immunity. *Nature*, 292(5820), 246-248.
39. Hultmark, D., Steiner, H., Rasmuson, T., & Boman, H. G. (1980). Insect immunity. Purification and properties of three inducible bactericidal proteins from hemolymph of immunized pupae of *Hyalophora cecropia*. *European Journal of Biochemistry*, 106(1), 7-16.
40. Tonk, M., Vilcinskas, A., & Rahnamaeian, M. (2016). Insect antimicrobial peptides: potential tools for the prevention of skin cancer. *Applied microbiology and biotechnology*, 100(17), 7397-7405.

41. Jin, G., & Weinberg, A. (2019, April). Human antimicrobial peptides and cancer. In *Seminars in cell & developmental biology* (Vol. 88, pp. 156-162). Academic Press.
42. Zasloff, M. "Antimicrobial peptides of multicellular organisms." *Nature* 415:6870 (2002): 389.
43. Vilcinskas A. 2013 Evolutionary plasticity of insect immunity. *J. Insect Physiol.* 59, 123–129. (doi: 10.1016/j.jinsphys.2012.08.018).
44. Makarova, O.; Johnston, P.; Rodriguez-Rojas, A.; El Shazely, B.; Morales, J.M.; Rolff, J. Genomics of experimental adaptation of *Staphylococcus aureus* to a natural combination of insect antimicrobial peptides. *Sci. Rep.* 2018, 8, 15359.
45. Bulet, P., & Stocklin, R. (2005). Insect antimicrobial peptides: structures, properties and gene regulation. *Protein and peptide letters*, 12(1), 3-11.
46. Ganz, T.; Lehrer, R.I. Defensins. *Pharmacol. Ther.* 1995, 66, 191–205.
47. Bulet P, Cociancich S, Reuland M, Sauber F, Bischoff R, Hegy G, Van Dorsselaer A, Hetru C, Hoffmann JA. A novel insect defensin mediates the inducible antibacterial activity in larvae of the dragonfly *Aeschna cyanea* (Paleoptera, Odonata). *Eur J Biochem.* 1992; 209:977–984.
48. Bonmatin JM, Bonnat JL, Gallet X, Vovelle F, Ptak M, Reichhart JM, Hoffmann JA, Keppi E, Legrain M, Achstetter T. Two-dimensional <sup>1</sup>H NMR study of recombinant insect defensin A in water: resonance assignments, secondary structure and global folding. *Journal of biomolecular NMR.* 1992; 2:235–256.
49. Cornet B, Bonmatin JM, Hetru C, Hoffmann JA, Ptak M, Vovelle F. Refined three-dimensional solution structure of insect defensin A. *Structure.* 1995; 3:435–448.
50. Berman, H. M., Bourne, P. E., Westbrook, J., & Zardecki, C. (2003). The protein data bank. In *Protein Structure* (pp. 394-410). CRC Press.
51. Pettersen, E. F., Goddard, T. D., Huang, C. C., Couch, G. S., Greenblatt, D. M., Meng, E. C., & Ferrin, T. E. (2004). UCSF Chimera—a visualization system for exploratory research and analysis. *Journal of computational chemistry*, 25(13), 1605-1612.
52. Bachère, E., Destoumieux, D., & Bulet, P. (2000). Penaeidins, antimicrobial peptides of shrimp: a comparison with other effectors of innate immunity. *Aquaculture*, 191(1-3), 71-88.
53. Lee YS, Yun EK, Jang WS, Kim I, Lee JH, Park SY, Ryu KS, Seo SJ, Kim CH, Lee IH. Purification, cDNA cloning and expression of an insect defensin from the great wax moth, *Galleria mellonella*. *Insect Mol Biol.* 2004; 13:65–72.
54. Lowenberger C, Bulet P, Charlet M, Hetru C, Hodgeman B, Christensen BM, Hoffmann JA. Insect immunity: isolation of three novel inducible antibacterial defensins from the vector mosquito, *Aedes aegypti*. *Insect Biochem Mol Biol.* 1995; 25:867–873.

55. Hultmark, D.; Engström, Å.; Bennich, H.; Kapur, R.; Boman, H.G. Insect immunity: Isolation and structure of cecropin D and four minor antibacterial components from *Cecropia* pupae. *Eur. J. Biochem.* 1982, 127, 207–217.
56. Moore, A.J.; Beazley, W.D.; Bibby, M.C.; Devine, D.A. Antimicrobial activity of cecropins. *J. Antimicrob. Chemother.* 1996, 37, 1077–1089.
57. Andrä, J.; Berninghausen, O.; Leippe, M. Cecropins, antibacterial peptides from insects and mammals, are potently fungicidal against *Candida albicans*. *Med. Microbiol. Immunol.* 2001, 189, 169–173.
58. Efimova, S.S.; Medvedev, R.Y.; Chulkov, E.G.; Schagina, L.V.; Ostroumova, O.S. Regulation of the Pore-Forming Activity of Cecropin A by Local Anesthetics. *Cell Tiss. Biol.* 2018, 12, 331–341.
59. Lee, E.; Kim, J.-K.; Jeon, D.; Jeong, K.-W.; Shin, A.; Kim, Y. Functional roles of aromatic residues and helices of papiliocin in its antimicrobial and anti-inflammatory activities. *Sci. Rep.* 2015, 5, 12048.
60. Fu, H.; Björstad, A.; Dahlgren, C.; Bylund, J. A bacterial cecropin-A peptide with a stabilized  $\alpha$ -helical structure possess an increased killing capacity but no proinflammatory activity. *Inflammation* 2004, 28, 337–343.
61. Yun, J.; Lee, D.G. Cecropin A-induced apoptosis is regulated by ion balance and glutathione antioxidant system in *Candida albicans*. *IUBMB Life* 2016, 68, 652–662.
62. Lu, D.; Geng, T.; Hou, C.; Huang, Y.; Qin, G.; Guo, X. *Bombyx mori* cecropin A has a high antifungal activity to entomopathogenic fungus *Beauveria bassiana*. *Gene* 2016, 583, 29–35.
63. Srisailam, S.; Arunkumar, A.I.; Wang, W.; Yu, C.; Chen, H.M. Conformational study of a custom antibacterial peptide cecropin B1: Implications of the lytic activity. *Biochim. Biophys. Acta* 2000, 1479, 275–285.
64. Giacometti, A.; Cirioni, O.; Ghiselli, R.; Viticchi, C.; Mocchegiani, F.; Riva, A.; Saba, V.; Scalise, G. Effect of mono-dose intraperitoneal cecropins in experimental septic shock. *Crit. Care Med.* 2001, 29, 1666–1669.
65. Lee, E.; Shin, A.; Kim, Y. Anti-inflammatory activities of cecropin a and its mechanism of action. *Arch. Insect Biochem. Physiol.* 2015, 88, 31–44.
66. Wang, J.; Ma, K.; Ruan, M.; Wang, Y.; Li, Y.; Fu, Y.V.; Song, Y.; Sun, H.; Wang, J. A novel cecropin B-derived peptide with antibacterial and potential anti-inflammatory properties. *PeerJ* 2018, 6, e5369.

67. Chen, L.; Deng, H.; Cui, H.; Fang, J.; Zuo, Z.; Deng, J.; Li, Y.; Wang, X.; Zhao, L. Inflammatory responses and inflammation-associated diseases in organs. *Oncotarget* 2017, 9, 7204–7218.
68. Hedengren M, Borge K, Hultmark D. Expression and evolution of the *Drosophila* attacin/diptericin gene family. *Biochem Biophys Res Commun.* 2000; 279:574–581.
69. Sun SC, Lindstrom I, Lee JY, Faye I. Structure and expression of the attacin genes in *Hyalophora cecropia*. *Eur J Biochem.* 1991; 196:247–254.
70. Ourth DD, Lockey TD, Renis HE. Induction of cecropin-like and attacin-like antibacterial but not antiviral activity in *Heliothis virescens* larvae. *Biochem Biophys Res Commun.* 1994; 200:35–44.
71. Dushay MS, Roethele JB, Chaverri JM, Dulek DE, Syed SK, Kitami T, Eldon ED. Two attacin antibacterial genes of *Drosophila melanogaster*. *Gene.* 2000; 246:49–57.
72. Carlsson, A.; Engström, P.; Palva, E.T.; Bennich, H. Attacin, an antibacterial protein from *Hyalophora cecropia*, inhibits synthesis of outer membrane proteins in *Escherichia coli* by interfering with *omp* gene transcription. *Infect. Immun.* 1991, 59, 3040–3045.
73. Bang K, Park S, Yoo JY, Cho S. Characterization and expression of attacin, an antibacterial protein encoding gene, from the beet armyworm, *Spodoptera exigua* (Hubner) (Insecta: Lepidoptera:Noctuidae). *Mol Biol Rep.* 2012; 39:5151–5159.
74. Hara S, Yamakawa M. A novel antibacterial peptide family isolated from the silkworm, *Bombyx mori*. *Biochem J.* 1995b; 310(Pt 2):651–656.
75. Bulet, P.; Dimarcq, J.L.; Hetru, C.; Lagueux, M.; Charlet, M.; Hegy, G.; Van Dorsselaer, A.; Hoffmann, J.A. A novel inducible antibacterial peptide of *Drosophila* carries an O-glycosylated substitution. *J. Biol. Chem.* 1993, 268, 14893–14897.
76. Gobbo, M.; Biondi, L.; Filira, F.; Gennaro, R.; Benincasa, M.; Scolaro, B.; Rocchi, R. Antimicrobial peptides: Synthesis and antibacterial activity of linear and cyclic drosocin and apidaecin 1b analogues. *J. Med. Chem.* 2002, 45, 4494–4504.
77. Levashina, E.A.; Ohresser, S.; Bulet, P.; Reichhart, J.M.; Hetru, C.; Hoffmann, J.A. Metchnikowin, a novel immune-inducible proline-rich peptide from *Drosophila* with antibacterial and antifungal properties. *Eur. J. Biochem.* 1995, 233, 694–700.
78. Moghaddam, M.R.B.; Gross, T.; Becker, A.; Vilcinskis, A.; Rahnamaeian, M. The selective antifungal activity of *Drosophila melanogaster* metchnikowin reflects the species dependent inhibition of succinate-coenzyme Q reductase. *Sci. Rep.* 2017, 7, 8192.
79. Xu XX, Zhong X, Yi HY, Yu XQ. *Manduca sexta* gloverin binds microbial components and is active against bacteria and fungi. *Dev Comp Immunol.* 2012; 38:275–284.



80. Axen A, Carlsson A, Engstrom A, Bennich H. Gloverin, an antibacterial protein from the immune hemolymph of *Hyalophora pupae*. *Eur J Biochem*. 1997; 247:614–619.
81. Mrinal N, Nagaraju J. Intron loss is associated with gain of function in the evolution of the gloverin family of antibacterial genes in *Bombyx mori*. *J Biol Chem*. 2008; 283:23376–23387.
82. Dimarcq, J.L.; Keppi, E.; Dunbar, B.; Lambert, J.; Reichhart, J.M.; Hoffmann, D.; Rankine, S.M.; Fothergill, J.E.; Hoffmann, J.A. Insect immunity. Purification and characterization of a family of novel inducible antibacterial proteins from immunized larvae of the dipteran *Phormia terranova* and complete amino-acid sequence of the predominant member, dipteracin A. *Eur. J. Biochem*. 1988, 171, 17–22.
83. Ishikawa, M.; Kubo, T.; Natori, S. Purification and characterization of a dipteracin homologue from *Sarcophaga peregrina* (flesh fly). *Biochem. J*. 1992, 287, 573–578.
84. Reichhart, J.M.; Meister, M.; Dimarcq, J.L.; Zachary, D.; Hoffmann, D.; Ruiz, C.; Richards, G.; Hoffmann, J.A. Insect immunity: Developmental and inducible activity of the *Drosophila* dipteracin promoter. *EMBO J*. 1992, 11, 1469–1477.
85. Ursic-Bedoya, R.; Buchhop, J.; Joy, J.B.; Durvasula, R.; Lowenberger, C. Prolixicin: A novel antimicrobial peptide isolated from *Rhodnius prolixus* with differential activity against bacteria and *Trypanosoma cruzi*. *Insect Mol. Biol*. 2011, 20, 775–786.
86. Wieprecht, T., Apostolov, O., & Seelig, J. (2000). Binding of the antibacterial peptide magainin 2 amide to small and large unilamellar vesicles. *Biophysical chemistry*, 85(2-3), 187-198.
87. Haney, E. F., Straus, S. K., & Hancock, R. E. (2019). Reassessing the host defense peptide landscape. *Frontiers in chemistry*, 7, 43.
88. Mankoci, S., Ewing, J., Dalai, P., Sahai, N., Barton, H. A., & Joy, A. (2019). Bacterial Membrane Selective Antimicrobial Peptide-Mimetic Polyurethanes: Structure–Property Correlations and Mechanisms of Action. *Biomacromolecules*, 20(11), 4096-4106.
89. Alghalayini, A., Garcia, A., Berry, T., & Cranfield, C. G. (2019). The use of tethered bilayer lipid membranes to identify the mechanisms of antimicrobial peptide interactions with lipid bilayers. *Antibiotics*, 8(1), 12.
90. Cassone, M., Frith, N., Vogiatzi, P., Wade, J. D., & Otvos, L. (2009). Induced resistance to the designer proline-rich antimicrobial peptide A3-APO does not involve changes in the intracellular target DnaK. *International Journal of Peptide Research and Therapeutics*, 15(2), 121-128.

91. Shah, P., Hsiao, F. S. H., Ho, Y. H., & Chen, C. S. (2016). The proteome targets of intracellular targeting antimicrobial peptides. *Proteomics*, 16(8), 1225-1237.
92. Graf, M., & Wilson, D. N. (2019). Intracellular antimicrobial peptides targeting the protein synthesis machinery. In *Antimicrobial Peptides* (pp. 73-89). Springer, Singapore.
93. Pasupuleti, M., Schmidtchen, A., & Malmsten, M. (2012). Antimicrobial peptides: key components of the innate immune system. *Critical reviews in biotechnology*, 32(2), 143-171.
94. Mardirossian, M., Sola, R., Degasperri, M., & Scocchi, M. (2019). Search for Shorter Portions of the Proline-Rich Antimicrobial Peptide Fragment Bac5 (1–25) That Retain Antimicrobial Activity by Blocking Protein Synthesis. *ChemMedChem*, 14(3), 343-348.
95. Baker, M. A., Maloy, W. L., Zasloff, M., & Jacob, L. S. (1993). Anticancer efficacy of Magainin2 and analogue peptides. *Cancer research*, 53(13), 3052-3057.
96. Schweizer, F. (2009). Cationic amphiphilic peptides with cancer-selective toxicity. *European journal of pharmacology*, 625(1-3), 190-194.
97. Papo, N., Shahar, M., Eisenbach, L., & Shai, Y. (2003). A novel lytic peptide composed of DL-amino acids selectively kills cancer cells in culture and in mice. *Journal of Biological Chemistry*, 278(23), 21018-21023.
98. Mai, J. C., Mi, Z., Kim, S. H., Ng, B., & Robbins, P. D. (2001). A proapoptotic peptide for the treatment of solid tumors. *Cancer research*, 61(21), 7709-7712.
99. Bulet, P., Hetru, C., Dimarcq, J. L., & Hoffmann, D. (1999). Antimicrobial peptides in insects; structure and function. *Developmental & Comparative Immunology*, 23(4-5), 329-344.
100. Harris, F., Dennison, S. R., Singh, J., & Phoenix, D. A. (2013). On the selectivity and efficacy of defense peptides with respect to cancer cells. *Medicinal research reviews*, 33(1), 190-234.
101. Hoskin, D. W., & Ramamoorthy, A. (2008). Studies on anticancer activities of antimicrobial peptides. *Biochimica et Biophysica Acta (BBA)-Biomembranes*, 1778(2), 357-375.
102. Henzler Wildman, K. A., Lee, D. K., & Ramamoorthy, A. (2003). Mechanism of lipid bilayer disruption by the human antimicrobial peptide, LL-37. *Biochemistry*, 42(21), 6545-6558.
103. Bevers, E. M., Comfurius, P., & Zwaal, R. F. A. (1996). Regulatory mechanisms in maintenance and modulation of transmembrane lipid asymmetry: pathophysiological implications. *Lupus*, 5(5), 480-487.

104. Utsugi, T., Schroit, A. J., Connor, J., Bucana, C. D., & Fidler, I. J. (1991). Elevated expression of phosphatidylserine in the outer membrane leaflet of human tumor cells and recognition by activated human blood monocytes. *Cancer research*, 51(11), 3062-3066.
105. Van Zoggel, H.; Hamma-Kourbali, Y.; Galanth, C.; Ladram, A.; Nicolas, P.; Courty, J.; Amiche, M.; Delbé, J. Antitumor and angiostatic peptides from frog skin secretions. *Amino Acids* 2012, 42, 385–395.
106. Lin, W. J., Chien, Y. L., Pan, C. Y., Lin, T. L., Chen, J. Y., Chiu, S. J., & Hui, C. F. (2009). Epinecidin-1, an antimicrobial peptide from fish (*Epinephelus coioides*) which has an antitumor effect like lytic peptides in human fibrosarcoma cells. *Peptides*, 30(2), 283-290.
107. Kołodziej, M., Joniec, J., Bartoszcze, M., Mirski, T., & Gryko, R. (2011). Peptides--a new strategy for combating viral infections. *Przegląd epidemiologiczny*, 65(3), 477-482.
108. Goodsell, D. S. (2015). Illustrations of the HIV life cycle. In *The Future of HIV-1 Therapeutics* (pp. 243-252). Springer, Cham.
109. Horne, W. S., Wiethoff, C. M., Cui, C., Wilcoxon, K. M., Amorin, M., Ghadiri, M. R., & Nemerow, G. R. (2005). Antiviral cyclic d, l- $\alpha$ -peptides: Targeting a general biochemical pathway in virus infections. *Bioorganic & medicinal chemistry*, 13(17), 5145-5153.
110. Mulder, K., Lima, L. A., Miranda, V., Dias, S. C., & Franco, O. L. (2013). Current scenario of peptide-based drugs: the key roles of cationic antitumor and antiviral peptides. *Frontiers in microbiology*, 4, 321.
111. Matanic, V. C. A., & Castilla, V. (2004). Antiviral activity of antimicrobial cationic peptides against Junin virus and herpes simplex virus. *International journal of antimicrobial agents*, 23(4), 382-389.
112. Andersen, J. H., Jenssen, H., Sandvik, K., & Gutteberg, T. J. (2004). Anti-HSV activity of lactoferrin and lactoferricin is dependent on the presence of heparan sulphate at the cell surface. *Journal of medical virology*, 74(2), 262-271.
113. Jenssen, H., Andersen, J. H., Uhlin-Hansen, L., Gutteberg, T. J., & Rekdal, Ø. (2004). Anti-HSV activity of lactoferricin analogues is only partly related to their affinity for heparan sulfate. *Antiviral research*, 61(2), 101-109.
114. Singh, K., & Rani, J. (2016). Sequential and structural aspects of antifungal peptides from animals, bacteria and fungi based on bioinformatics tools. *Probiotics and antimicrobial proteins*, 8(2), 85-101.
115. Aoki, W., & Ueda, M. (2013). Characterization of antimicrobial peptides toward the development of novel antibiotics. *Pharmaceuticals*, 6(8), 1055-1081.

116. Van der Weerden, N. L., Bleackley, M. R., & Anderson, M. A. (2013). Properties and mechanisms of action of naturally occurring antifungal peptides. *Cellular and molecular life sciences*, 70(19), 3545-3570.
117. Cruz, C. D., Shah, S., & Tammela, P. (2018). Defining conditions for biofilm inhibition and eradication assays for Gram-positive clinical reference strains. *BMC microbiology*, 18(1), 1-9.
118. Raheem, N., & Straus, S. K. (2019). Mechanisms of Action for Antimicrobial Peptides with Multiple Biological Functions. *Frontiers in microbiology*, 10, 2866.
119. Arslan, S. Y., Leung, K. P., & Wu, C. D. (2009). The effect of lactoferrin on oral bacterial attachment. *Oral microbiology and immunology*, 24(5), 411-416.
120. Overhage, J., Campisano, A., Bains, M., Torfs, E. C., Rehm, B. H., & Hancock, R. E. (2008). Human host defense peptide LL-37 prevents bacterial biofilm formation. *Infection and immunity*, 76(9), 4176-4182.
121. Brancatisano, F.L.; Maisetta, G.; Di Luca, M.; Esin, S.; Bottai, D.; Bizzarri, R.; Campa, M.; Batoni, G. Inhibitory effect of the human liver-derived antimicrobial peptide hepcidin 20 on biofilms of polysaccharide intercellular adhesin (PIA)-positive and PIA-negative strains of *Staphylococcus epidermidis*. *Biofouling* 2014, 30, 435–446.
122. Pletzer, D., Coleman, S. R., & Hancock, R. E. (2016). Anti-biofilm peptides as a new weapon in antimicrobial warfare. *Current opinion in microbiology*, 33, 35-40.
123. Pletzer, D., Coleman, S. R., & Hancock, R. E. (2016). Anti-biofilm peptides as a new weapon in antimicrobial warfare. *Current opinion in microbiology*, 33, 35-40.
124. Butts, A., & Krysan, D. J. (2012). Antifungal drug discovery: something old and something new. *PLoS Pathog*, 8(9), e1002870.
125. De Brucker, K.; Delattin, N.; Robijns, S.; Steenackers, H.; Verstraeten, N.; Landuyt, B.; Luyten, W.; Schoofs, L.; Dovgan, B.; Fröhlich, M.; et al. Derivatives of the mouse cathelicidin-related antimicrobial peptide (CRAMP) inhibit fungal and bacterial biofilm formation. *Antimicrob. Agents Chemother.* 2014, 58, 5395–5404.
126. Mansour, S.C.; De la Fuente-Núñez, C.; Hancock, R.E.W. Peptide IDR-1018: Modulating the immune system and targeting bacterial biofilms to treat antibiotic-resistant bacterial infections. *J. Pept. Sci.* 2015, 21, 323–329.
127. De La Fuente-Núñez, C.; Reffuveille, F.; Mansour, S.C.; Reckseidler-Zenteno, S.L.; Hernández, D.; Brackman, G.; Coenye, T.; Hancock, R.E. D-enantiomeric peptides that eradicate wild-type and multidrug-resistant biofilms and protect against lethal *Pseudomonas aeruginosa* infections. *Chem. Biol.* 2015, 22, 196–205.

128. Mataraci, E.; Dosler, S. In vitro activities of antibiotics and antimicrobial cationic peptides alone and in combination against methicillin-resistant *Staphylococcus aureus* biofilms. *Antimicrob. Agents Chemother.* 2012, 56, 6366–6371.
129. Valanne S, Wang JH, Rämet M: The *Drosophila* Toll signaling pathway. *J. Immunol.* 2011; 186:649–656.
130. Kleino A, Silverman N: The *Drosophila* IMD pathway in the activation of the humoral immune response. *Dev. Comp. Immunol.* 2014; 42:25–35.
131. Myllymäki H, Rämet M: JAK/STAT pathway in *Drosophila* immunity. *Scand. J. Immunol.* 2014; 79:377–385.
132. Ashok Y: *Drosophila* toll pathway: the new model. *Sci. Signal.* 2009; 2:jc1.
133. Shia AK, Glittenberg M, Thompson G, Weber AN, Reichhart JM, Ligoxygakis P: Toll-dependent antimicrobial responses in *Drosophila* larval fat body require Spätzle secreted by haemocytes. *J. Cell Sci.* 2009; 122:4505–4515.
134. Wang Y, Jiang H: Interaction of  $\beta$ -1,3-Glucan with Its recognition protein activates hemolymph proteinase 14, an initiation enzyme of the prophenoloxidase activation system in *Manduca sexta*. *J. Biol. Chem.* 2006; 281:9271–9278.
135. Mishima Y, Quintin J, Aimaniananda V, Kellenberger C, Coste F, Clavaud C, Hetru C, Hoffmann JA, Latgé JP, Ferrandon D et al.: The N-terminal domain of *Drosophila* Gram-negative binding protein 3 (GNBP3) defines a novel family of fungal pattern recognition receptors. *J. Biol. Chem.* 2009; 284:28687–28697.
136. Imler JL, Hoffmann JA: Toll receptors in *Drosophila*: a family of molecules regulating development and immunity. *Curr. Top. Microbiol. Immunol.* 2002; 270:63–79.
137. Kaneko T, N. S: Bacterial recognition and signalling by the *Drosophila* IMD pathway. *Cell. Microbiol.* 2005; 7:461–469.
138. Leulier F, Vidal S, Saigo K, Ueda R, Lemaitre B: Inducible expression of double-stranded RNA reveals a role for dFADD in the regulation of the antibacterial response in *Drosophila* adults. *Curr. Biol.* 2002; 12:996–1000.
139. Leulier F, Rodriguez A, Khush RS, Abrams JM, Lemaitre B: The *Drosophila* caspase Dredd is required to resist gram-negative bacterial infection. *EMBO Rep.* 2000; 1:353–358.
140. Ertürk-Hasdemir D, Broemer M, Leulier F, Lane WS, Paquette N, Hwang D, Kim CH, Stöven S, Meier P, Silverman N: Two roles for the *Drosophila* IKK complex in the activation of Relish and the induction of antimicrobial peptide genes. *Proc. Natl. Acad. Sci. U S A* 2009; 106:9779–9784.

141. O'Shea J, Plenge R: JAK and STAT signaling molecules in immunoregulation and immune mediated disease. *Immunity* 2012; 36:542–550.
142. Kiu H, Nicholson SE: Biology and significance of the JAK/STAT signalling pathways. *Growth Factors* 2012; 30:88–106.
143. Hara S, Yamakawa M. A novel antibacterial peptide family isolated from the silkworm, *Bombyx mori*. *Biochem J.* 1995b; 310(Pt 2):651–656.
144. Brown S, Hu N, Hombría JC: Identification of the first invertebrate interleukin JAK/STAT receptor, the *Drosophila* gene *domeless*. *Curr. Biol.* 2001; 11:1700–1705.
145. Binari R, Perrimon N: Stripe-specific regulation of pair-rule genes by hopscotch, a putative Jak family tyrosine kinase in *Drosophila*. *Genes Dev.* 1994; 8:300–312.
146. Yan R, Small S, Desplan C, Dearolf CR, Darnell JEJ: Identification of a Stat gene that functions in *Drosophila* development. *Cell* 1996; 84:421–430.
147. Brown KL, Hancock RE. 2006 Cationic host defense (antimicrobial) peptides. *Curr. Opin. Immunol.* 18, 24–30.
148. Andersson, D. I., Hughes, D., & Kubicek-Sutherland, J. Z. (2016). Mechanisms and consequences of bacterial resistance to antimicrobial peptides. *Drug Resistance Updates*, 26, 43-57.
149. Di Somma, A., Avitabile, C., Cirillo, A., Moretta, A., Merlino, A., Paduano, L., Duilio, A., & Romanelli, A. (2020). The antimicrobial peptide Temporin L impairs *E. coli* cell division by interacting with FtsZ and the divisome complex. *Biochimica et Biophysica Acta (BBA)-General Subjects*, 129606.
150. Rahnamaeian M et al. 2015 Insect antimicrobial peptides show potentiating functional interactions against Gram-negative bacteria. *Proc. R. Soc. B* 282, 20150293.
151. Cociancich S, Ghazi A, Hetru C, Hoffmann JA, Letellier L. Insect defensin, an inducible antibacterial peptide, forms voltage-dependent channels in *Micrococcus luteus*. *J Biol Chem.* 1993; 268:19239–19245.
152. Maget-Dana R, Ptak M. Penetration of the insect defensin A into phospholipid monolayers and formation of defensin A-lipid complexes. *Biophysical journal.* 1997; 73:2527–2533.
153. Vizioli J, Richman AM, Uttenweiler-Joseph S, Blass C, Bulet P. The defensin peptide of the malaria vector mosquito *Anopheles gambiae*: antimicrobial activities and expression in adult mosquitoes. *Insect Biochem Mol Biol.* 2001; 31:241–248.
154. Liu, X.; Guo, C.; Huang, Y.; Zhang, X.; Chen, Y. Inhibition of porcine reproductive and respiratory syndrome virus by Cecropin D in vitro. *Infect. Genet. Evol.* 2015, 34, 7–16.

155. Sato, H.; Feix, J.B. Peptide–membrane interactions and mechanisms of membrane destruction by amphipathic  $\alpha$ -helical antimicrobial peptides. *Biochim. Biophys. Acta.* 2006, 1758, 1245–1256.
156. Efimova, S.S.; Schagina, L.V.; Ostroumova, O.S. Channel-forming activity of cecropins in lipid bilayers: Effect of agents modifying the membrane dipole potential. *Langmuir* 2014, 30, 7884–7892.
157. Goyal, R. K., & Mattoo, A. K. (2016). Plant antimicrobial peptides. In *Host defense peptides and their potential as therapeutic agents* (pp. 111-136). Springer, Cham.
158. Travkova, O. G., Moehwald, H., & Brezesinski, G. (2017). The interaction of antimicrobial peptides with membranes. *Advances in colloid and interface science*, 247, 521-532.
159. Galdiero, E., Lombardi, L., Falanga, A., Libralato, G., Guida, M., & Carotenuto, R. (2019). Biofilms: novel strategies based on antimicrobial peptides. *Pharmaceutics*, 11(7), 322.
160. Lee, A. C. L., Harris, J. L., Khanna, K. K., & Hong, J. H. (2019). A comprehensive review on current advances in peptide drug development and design. *International journal of molecular sciences*, 20(10), 2383.
161. Jamasbi, E.; Lucky, S.S.; Li, W.; Hossain, M.A.; Gopalakrishnakone, P.; Separovic, F. Effect of dimerized melittin on gastric cancer cells and antibacterial activity. *Amino Acids* 2018.
162. Chen, J.; Guan, S.M.; Sun, W.; Fu, H. Melittin, the major pain-producing substance of bee venom. *Neurosci. Bull.* 2016, 32, 265–272.
163. Rady, I.; Siddiqui, I.A.; Rady, M.; Mukhtar, H. Melittin, a major peptide component of bee venom, and its conjugates in cancer therapy. *Cancer Lett.* 2017, 402, 16–31.
164. Borah A, Deb B, Chakraborty S (2020) A crosstalk on antimicrobial peptides. *Int J Pept Res Ther.* doi:10.1007/s10989-020-10075-x.
165. Jenssen H, Hamill P, Hancock RE (2006) Peptide antimicrobial agents. *Clin Microbiol Rev* 19(3):491-511
166. Huan Y, Kong Q, Mou H, Yi H (2020) Antimicrobial peptides: Classification, design, application and research progress in multiple fields. *Front Microbiol* 11:582779
167. Soltani S, Hammami R, Cotter PD, Rebuffat S, Said LB, Gaudreau H, Bédard F, Biron E, Drider D, Fliss I (2021) Bacteriocins as a new generation of antimicrobials: toxicity aspects and regulations. *FEMS Microbiol Rev* 45(1): fuaa039
168. Boparai JK, Sharma PK (2020) Mini review on antimicrobial peptide, sources, mechanism and recent applications. *Protein Pept Lett.*27(1):4-16

169. Magana M, Pushpanathan M, Santos AL, Leanse L, Fernandez M, Ioannidis A, Giulianotti MA, Apidianakis Y, Bradfute S, Ferguson AL, Cherkasov A, Seleem MN, Pinilla C, de la Fuente-Nunez C, Lazaridis T, Dai T, Houghten RA, Hancock REW, Tegos GP (2020) The value of antimicrobial peptides in the age of resistance. *Lancet Infect Dis* 20(9):e216-e230
170. Montesinos E (2007) Antimicrobial peptides and plant disease control. *FEMS Microbiol Lett.* 270(1):1-11.
171. Hegedüs N, Marx F (2013) Antifungal proteins: More than antimicrobials? *Fungal Biol Rev* 26(4):132-145.
172. Salas CE, Badillo-Corona JA, Ramírez-Sotelo G, Oliver-Salvador C (2015) Biologically active and antimicrobial peptides from plants. *Biomed Res Int* 2015:102129
173. López-Meza JE, Ochoa-Zarzosa A, Aguilar JA, Loeza-Lara PD (2011) Antimicrobial peptides: diversity and perspectives for their biomedical application. In book: *Biomedical Engineering, Trends, Research and Technologies*. doi: 10.5772/13058.
174. Meneguetti BT, Machado LD, Oshiro KG, Nogueira ML, Carvalho CM, Franco OL (2017) Antimicrobial peptides from fruits and their potential use as biotechnological tools-a review and outlook. *Front Microbiol* 7:2136
175. Li Y, Xiang Q, Zhang Q, Huang Y, Su Z (2012) Overview on the recent study of antimicrobial peptides: origins, functions, relative mechanisms and application. *Peptides* 37(2):207-215
176. Moretta A, Salvia R, Scieuzo C, Di Somma A, Vogel H, Pucci P, Sgambato A, Wolff M, Falabella P (2020) A bioinformatic study of antimicrobial peptides identified in the Black Soldier Fly (BSF) *Hermetia illucens* (Diptera: Stratiomyidae). *Sci Rep* 10:16875. doi.org/10.1038/s41598-020-74017-9
177. Wu Q, Patočka J, Kuča K (2018) Insect antimicrobial peptides, a mini review. *Toxins* 10(11):461
178. Carlsson A, Engström P, Palva ET, Bennich H (1991) Attacin, an antibacterial protein from *Hyalophora cecropia*, inhibits synthesis of outer membrane proteins in *Escherichia coli* by interfering with *omp* gene transcription. *Infect Immun* 59:3040–3045
179. Patočka J, Nepovimovab E, Klimovac B, Wud Q, Kucab K (2018) Antimicrobial Peptides: Amphibian Host Defense Peptides. *Curr Med Chem* 25:1-21
180. Yang D, Chertov O, Oppenheim JJ (2001) The role of mammalian antimicrobial peptides and proteins in awakening of innate host defenses and adaptive immunity. *Cell Mol Life Sci* 58:978–989



181. Aminov RI (2010) A brief history of the antibiotic era: lessons learned and challenges for the future. *Front Microbiol* 1:134
182. Parisien A, Allain B, Zhang J, Mandeville R, Lan CQ (2008). Novel alternatives to antibiotics: bacteriophages, bacterial cell wall hydrolases, and antimicrobial peptides. *J Appl Microbiol* 104(1):1-13
183. Lei J, Sun L, Huang S, Zhu C, Li P, He J, Mackey V, Coy DH, He Q (2019) The antimicrobial peptides and their potential clinical applications. *Am J Transl Res* 11(7):3919-3931
184. Schweizer F (2009). Cationic amphiphilic peptides with cancer-selective toxicity. *Eur J Pharmacol* 625(1-3):190-194
185. Scholl D, Martin DW (2008) Antibacterial efficacy of R-type pyocins towards *Pseudomonas aeruginosa* in a murine peritonitis model. *Antimicrobial agents and chemotherapy*, 52(5):1647-1652
186. Waite RD, Curtis MA (2009). *Pseudomonas aeruginosa* PAO1 pyocin production affects population dynamics within mixed-culture biofilms. *J Bacteriol* 191(4):1349-1354
187. Hancock RE, Sahl HG (2006). Antimicrobial and host-defense peptides as new anti-infective therapeutic strategies. *Nat. Biotechnol* 24(12):1551-1557
188. Guaní-Guerra E, Santos-Mendoza T, Lugo-Reyes SO, Terán LM (2010) Antimicrobial peptides: general overview and clinical implications in human health and disease. *Clin Immunol* 135(1):1-11
189. Andersson, D. I., Balaban, N. Q., Baquero, F., Courvalin, P., Glaser, P., Gophna, U., Kishony, R., Molin, S., & Tønjum, T. (2020). Antibiotic resistance: turning evolutionary principles into clinical reality. *FEMS microbiology reviews*, 44(2), 171-188.
190. Majewski K, Kozłowska E, Żelechowska P, Brzezińska-Błaszczyk E (2018) Serum concentrations of antimicrobial peptide cathelicidin LL-37 in patients with bacterial lung infections. *Cent Eur J Immunol* 43(4):453
191. Hiemstra PS, Amatngalim GD, van der Does AM, Taube C (2016) Antimicrobial peptides and innate lung defenses: role in infectious and noninfectious lung diseases and therapeutic applications. *Chest* 149(2):545-551
192. Lai Y, Gallo RL (2009) AMPed up immunity: how antimicrobial peptides have multiple roles in immune defense. *Trends Immunol* 30(3):131-141
193. Rahnamaeian M (2011) Antimicrobial peptides: modes of mechanism, modulation of defense responses. *Plant Signal Behav* 6(9):1325-1332

194. Balestrieri B, Maekawa A, Xing W, Gelb M H, Katz HR, Arm JP (2009) Group V secretory phospholipase A2 modulates phagosome maturation and regulates the innate immune response against *Candida albicans*. *J Immunol* 182(8):4891-4898
195. Sunderkötter C, Becker K (2015) Frequent bacterial skin and soft tissue infections: diagnostic signs and treatment. *J Dtsch Dermatol Ges* 13(6):501-526
196. Ramos R, Silva JP, Rodrigues AC, Costa R, Guardão L, Schmitt F, Soares R, Vilanova M, Domingues L, Gama M (2011) Wound healing activity of the human antimicrobial peptide LL37. *Peptides* 32(7):1469-1476
197. Hancock, R.E.W., Sahl, H.G., 2006. Antimicrobial and host-defense peptides as new anti-infective therapeutic strategies. *Nat. Biotechnol.* doi:10.1038/nbt1267.
198. Lakshmaiah Narayana, J., Chen, J.-Y., 2015. Antimicrobial peptides: Possible anti-infective agents. *Peptides* 72, 88–94. doi:https://doi.org/10.1016/j.peptides.2015.05.012.
199. Yi, H.-Y., Chowdhury, M., Huang, Y.-D., Yu, X.-Q., 2014. Insect antimicrobial peptides and their applications. *Appl. Microbiol. Biotechnol.* 98, 5807–5822.
200. Semple F, MacPherson H, Webb S, Cox SL, Mallin LJ, Tyrrell CGR, Semple CA, Nix MA, Millhauser GL, Dorin JR (2011) Human  $\beta$ -defensin 3 affects the activity of pro-inflammatory pathways associated with MyD88 and TRIF. *Eur. J. Immunol* 41(11):3291-3300
201. Heilborn JD, Nilsson MF, Sørensen O, Ståhle-Bäckdahl M, Kratz G, Weber G, Borregaard N (2003) The cathelicidin anti-microbial peptide LL-37 is involved in re-epithelialization of human skin wounds and is lacking in chronic ulcer epithelium. *J Invest Dermatol* 120(3):379-389
202. Koczulla R, Von Degenfeld G, Kupatt C, Krötz F, Zahler S, Gloe T, Issbrücker K, Unterberger P, Zaiou M, Lebherz C, Karl A, Raake P, Pfosser A, Boekstegers P, Welsch U, Hiemstra PS, Vogelmeier C, Gallo RL, Clauss R, Bals R (2003) An angiogenic role for the human peptide antibiotic LL-37/hCAP-18. *J Clin Invest* 111(11):1665-1672
203. Davidovici BB, Sattar N, Jörg PC, Puig L, Emery P, Barker JN, van de Kerkhof P, Ståhle M, Nestle FO, Girolomoni G, Krueger JG (2010) Psoriasis and systemic inflammatory diseases: potential mechanistic links between skin disease and co-morbid conditions. *J Invest Dermatol* 130(7):1785-1796
204. Wrone-Smith T, Nickoloff BJ (1996) Dermal injection of immunocytes induces psoriasis. *J Clin Invest* 98(8):1878-1887

205. Ellis CN, Gorsulowsky DC, Hamilton TA, Billings JK, Brown MD, Headington JT, Cooper KD, Baadsgaard O, Duell EA, Annesley TM, Voorhees JJ (1986) Cyclosporine improves psoriasis in a double-blind study. *Jama*, 256(22):3110-3116
206. Harder J, Schröder JM (2005) Psoriatic scales: a promising source for the isolation of human skin-derived antimicrobial proteins. *J Leukocyte Biol* 77(4):476-486
207. Harder J, Bartels J, Christophers E, Schröder JM (2001) Isolation and Characterization of Human  $\mu$ -Defensin-3, a Novel Human Inducible Peptide Antibiotic. *J Biol Chem* 276(8):5707-5713
208. Braff MH, Mi'ci AH, Di Nardo A, Lopez-Garcia B, Howell MD, Wong C, Gallo RL (2005) Structure-function relationships among human cathelicidin peptides: dissociation of antimicrobial properties from host immunostimulatory activities. *J Immunol* 174(7):4271-4278
209. Mookherjee N, Brown KL, Bowdish DM, Doria S, Falsafi R, Hokamp K, Roche FN, Mu R, Doho GH, Pistolic J, Powers JP, Bryan J, Brinkman FSL, Hancock REW (2006) Modulation of the TLR-mediated inflammatory response by the endogenous human host defense peptide LL-37. *J Immunol* 176(4):2455-2464
210. Yang D, Chen Q, Schmidt AP, Anderson GM, Wang JM, Wooters J, Oppenheim JJ, Chertov O (2000) LL-37, the neutrophil granule- and epithelial cell-derived cathelicidin, utilizes formyl peptide receptor-like 1 (FPR1) as a receptor to chemoattract human peripheral blood neutrophils, monocytes, and T cells. *J Exp Med* 192(7):1069-1074
211. Tomberlin JK, Sheppard DC. 2002. Factors influencing mating and oviposition of black soldier flies (Diptera: Stratiomyidae) in a colony. *J Entomol Sci* 37(4):345-352.
212. Rozkosný, R. (1983). *A Biosystematic Study of the European Stratiomyidae (Diptera): Volume 2-Clitelliinae, Hermediinae, Pachygasterinae and Bibliography (Vol. 25)*. Springer Science & Business Media.
213. Gobbi, P., Martinez-Sanchez, A., & Rojo, S. (2013). The effects of larval diet on adult life-history traits of the black soldier fly, *Hermetia illucens* (Diptera: Stratiomyidae). *European Journal of Entomology*, 110(3), 461.
214. Newton, L. A. R. R. Y., Sheppard, C. R. A. I. G., Watson, D. W., Burtle, G. A. R. Y., & Dove, R. O. B. E. R. T. (2005). Using the black soldier fly, *Hermetia illucens*, as a value-added tool for the management of swine manure. *Animal and Poultry Waste Management Center*, North Carolina State University, Raleigh, NC, 17.

215. Sheppard, D. C., Tomberlin, J. K., Joyce, J. A., Kiser, B. C., & Sumner, S. M. (2002). Rearing methods for the black soldier fly (Diptera: Stratiomyidae). *Journal of medical entomology*, 39(4), 695-698.
216. Tomberlin, J. K., & Sheppard, D. C. (2001). Lekking behavior of the black soldier fly (Diptera: Stratiomyidae). *Florida Entomologist*, 729-729.
217. Diener S, Zurbrugg C, Tockner K. 2009. Conversion of organic material by black soldier fly larvae—establishing optimal feeding rates. *Waste Manag Res* 27:603–610.
218. Zhang, J., Huang, L., He, J., Tomberlin, J. K., Li, J., Lei, C., ... & Yu, Z. (2010). An artificial light source influences mating and oviposition of black soldier flies, *Hermetia illucens*. *Journal of insect science*, 10(1).
219. Furman, D. P., Young, R. D., & Catts, P. E. (1959). *Hermetia illucens* (Linnaeus) as a factor in the natural control of *Musca domestica* Linnaeus. *Journal of Economic Entomology*, 52(5), 917-921.
220. Peterson, B. V., & Davies, D. M. (1960). Observations on some insect predators of black flies (Diptera: Simuliidae) of Algonquin Park, Ontario. *Canadian Journal of Zoology*, 38(1), 9-18.
221. Feener Jr, D. H., & Brown, B. V. (1997). Diptera as parasitoids. *Annual review of entomology*, 42(1), 73-97.
222. Vogel, H., Müller, A., Heckel, D. G., Gutzeit, H., & Vilcinskas, A. (2018). Nutritional immunology: diversification and diet-dependent expression of antimicrobial peptides in the black soldier fly *Hermetia illucens*. *Developmental & Comparative Immunology*, 78, 141-148.
223. Altschul, S. F., Gish, W., Miller, W., Myers, E. W., & Lipman, D. J. (1990). Basic local alignment search tool. *Journal of molecular biology*, 215(3), 403-410.
224. Gish, W., & States, D. J. (1993). Identification of protein coding regions by database similarity search. *Nature genetics*, 3(3), 266-272.
225. Madden, T. L., Tatusov, R. L., & Zhang, J. (1996). [9] Applications of network BLAST server. *Methods in enzymology*, 266, 131-141.
226. Zhang, Z., Schwartz, S., Wagner, L., & Miller, W. (2000). A greedy algorithm for aligning DNA sequences. *Journal of Computational biology*, 7(1-2), 203-214.
227. Zhang, Z., Schwartz, S., Wagner, L., & Miller, W. (2000). A greedy algorithm for aligning DNA sequences. *Journal of Computational biology*, 7(1-2), 203-214.

228. Johnson, M., Zaretskaya, I., Raytselis, Y., Merezhuk, Y., McGinnis, S., & Madden, T. L. (2008). NCBI BLAST: a better web interface. *Nucleic acids research*, 36(suppl\_2), W5-W9.
229. Altschul, S. F., Boguski, M. S., Gish, W., & Wootton, J. C. (1994). Issues in searching molecular sequence databases. *Nature genetics*, 6(2), 119-129.
230. Götz S., Garcia-Gomez JM., Terol J., Williams TD., Nagaraj SH., Nueda MJ., Robles M., Talon M., Dopazo J. and Conesa A. (2008). High-throughput functional annotation and data mining with the Blast2GO suite. *Nucleic acids research*, 36(10), 3420-35.
231. Mortazavi, A., Williams, B. A., McCue, K., Schaeffer, L., & Wold, B. (2008). Mapping and quantifying mammalian transcriptomes by RNA-Seq. *Nature methods*, 5(7), 621-628.
232. Duckert, P., Brunak, S., & Blom, N. (2004). Prediction of proprotein convertase cleavage sites. *Protein Engineering Design and Selection*, 17(1), 107-112.
233. Artimo, P., Jonnalagedda, M., Arnold, K., Baratin, D., Csardi, G., De Castro, E., ... & Grosdidier, A. (2012). ExPASy: SIB bioinformatics resource portal. *Nucleic acids research*, 40(W1), W597-W603.
234. Waghu, F. H., Barai, R. S., Gurung, P., & Idicula-Thomas, S. (2016). CAMPR3: a database on sequences, structures and signatures of antimicrobial peptides. *Nucleic acids research*, 44(D1), D1094-D1097.
235. Waghu, F. H., & Idicula-Thomas, S. (2020). Collection of antimicrobial peptides database and its derivatives: Applications and beyond. *Protein Science*, 29(1), 36-42.
236. Chen, W., Ding, H., Feng, P., Lin, H., & Chou, K. C. (2016). iACP: a sequence-based tool for identifying anticancer peptides. *Oncotarget*, 7(13), 16895.
237. Feng, P. M., Chen, W., Lin, H., & Chou, K. C. (2013). iHSP-PseRAAAC: Identifying the heat shock protein families using pseudo reduced amino acid alphabet composition. *Analytical Biochemistry*, 442(1), 118-125.
238. Ding, H., Deng, E. Z., Yuan, L. F., Liu, L., Lin, H., Chen, W., & Chou, K. C. (2014). iCTX-type: a sequence-based predictor for identifying the types of conotoxins in targeting ion channels. *BioMed research international*, 2014.
239. Chou, K. C. (2011). Some remarks on protein attribute prediction and pseudo amino acid composition. *Journal of theoretical biology*, 273(1), 236-247.
240. Chou, K. C. (2001). Prediction of protein cellular attributes using pseudo-amino acid composition. *Proteins: Structure, Function, and Bioinformatics*, 43(3), 246-255.

241. Thakur, N., Qureshi, A., & Kumar, M. (2012). AVPPred: collection and prediction of highly effective antiviral peptides. *Nucleic acids research*, 40(W1), W199-W204.
242. Agrawal, P., Bhalla, S., Chaudhary, K., Kumar, R., Sharma, M., & Raghava, G. P. (2018). In silico approach for prediction of antifungal peptides. *Frontiers in microbiology*, 9, 323.
243. Wang, G., Li, X., & Wang, Z. (2016). APD3: the antimicrobial peptide database as a tool for research and education. *Nucleic acids research*, 44(D1), D1087-D1093.
244. Wang, G., Li, X., & Wang, Z. (2009). APD2: the updated antimicrobial peptide database and its application in peptide design. *Nucleic acids research*, 37(suppl\_1), D933-D937.
245. Wang, Z., & Wang, G. (2004). APD: the antimicrobial peptide database. *Nucleic acids research*, 32(suppl\_1), D590-D592.
246. Bjellqvist, B., Hughes, G. J., Pasquali, C., Paquet, N., Ravier, F., Sanchez, J. C., ... & Hochstrasser, D. (1993). The focusing positions of polypeptides in immobilized pH gradients can be predicted from their amino acid sequences. *Electrophoresis*, 14(1), 1023-1031.
247. Bjellqvist, B., Basse, B., Olsen, E., & Celis, J. E. (1994). Reference points for comparisons of two-dimensional maps of proteins from different human cell types defined in a pH scale where isoelectric points correlate with polypeptide compositions. *Electrophoresis*, 15(1), 529-539.
248. Roy, A Kucukural, Y Zhang. I-TASSER: a unified platform for automated protein structure and function prediction. *Nature Protocols*, 5: 725-738 (2010)
249. Yang, J., Yan, R., Roy, A., Xu, D., Poisson, J., & Zhang, Y. (2015). The I-TASSER Suite: protein structure and function prediction. *Nature methods*, 12(1), 7-8.
250. Yang, J., & Zhang, Y. (2015). I-TASSER server: new development for protein structure and function predictions. *Nucleic acids research*, 43(W1), W174-W181.
251. Zheng, W., Zhang, C., Wuyun, Q., Pearce, R., Li, Y., & Zhang, Y. (2019). LOMETS2: improved meta-threading server for fold-recognition and structure-based function annotation for distant-homology proteins. *Nucleic acids research*, 47(W1), W429-W436.
252. Wu, S., & Zhang, Y. (2007). LOMETS: a local meta-threading-server for protein structure prediction. *Nucleic acids research*, 35(10), 3375-3382.
253. Zhang, Y., & Skolnick, J. (2004). SPICKER: a clustering approach to identify near-native protein folds. *Journal of computational chemistry*, 25(6), 865-871.

254. Ceroni, A., Passerini, A., Vullo, A., & Frasconi, P. (2006). DISULFIND: a disulfide bonding state and cysteine connectivity prediction server. *Nucleic acids research*, 34(suppl\_2), W177-W181.
255. Vullo, A., & Frasconi, P. (2004). Disulfide connectivity prediction using recursive neural networks and evolutionary information. *Bioinformatics*, 20(5), 653-659.
256. Frasconi, P., Passerini, A., & Vullo, A. (2002, September). A two-stage SVM architecture for predicting the disulfide bonding state of cysteines. In *Proceedings of the 12th IEEE Workshop on Neural Networks for Signal Processing* (pp. 25-34). IEEE.
257. Ceroni, A., Frasconi, P., Passerini, A., & Vullo, A. (2003). Predicting the disulfide bonding state of cysteines with combinations of kernel machines. *Journal of VLSI signal processing systems for signal, image and video technology*, 35(3), 287-295.
258. Schneidman-Duhovny, D.; Inbar, Y.; Nussinov, R.; Wolfson, H.J. PatchDock and SymmDock: Servers for rigid and symmetric docking. *Nucleic Acids Res.* 2005, 33, W363–W367.
259. Mashiach, E.; Schneidman-Duhovny, D.; Andrusier, N.; Nussinov, R.; Wolfson, H.J. FireDock: A web server for fast interaction refinement in molecular docking. *Nucleic Acids Res.* 2008, 36, W229–W232.
260. Laskowski, R.A. PDBsum new things. *Nucleic Acids Res.* 2008, 37 (Suppl. 1), D355–D359.
261. De Beer, T.A.; Berka, K.; Thornton, J.M.; Laskowski, R.A. PDBsum additions. *Nucleic Acids Res.* 2013, 42, D292–D296.
262. Laskowski, R.A. PDBsum: Summaries and analyses of PDB structures. *Nucleic Acids Res.* 2001, 29, 221–222.
263. Xue, L.C.; Rodrigues, J.P.; Kastritis, P.L.; Bonvin, A.M.; Vangone, A. PRODIGY: A web server for predicting the binding affinity of protein–protein complexes. *Bioinformatics* 2016, 32, 3676–3678.
264. Vangone, A.; Bonvin, A.M. Contacts-based prediction of binding affinity in protein–protein complexes. *Elife* 2015, 4, e07454.
265. Kim, S., Thiessen, P. A., Bolton, E. E., Chen, J., Fu, G., Gindulyte, A., Han, L., He, J., He, S., Shoemaker, B., A., & Bryant, S. H. (2016). PubChem substance and compound databases. *Nucleic acids research*, 44(D1), D1202-D1213.
266. Adasme, M. F., Linnemann, K. L., Bolz, S. N., Kaiser, F., Salentin, S., Haupt, V. J., & Schroeder, M. (2021). PLIP 2021: expanding the scope of the protein–ligand interaction profiler to DNA and RNA. *Nucleic Acids Research*.

267. Zdybicka-Barabas, A., Bulak, P., Polakowski, C., Bieganski, A., Waśko, A., & Cytryńska, M. (2017). Immune response in the larvae of the black soldier fly *Hermetia illucens*. *Invertebrate Survival Journal*, 14(1), 9-17.
268. Cornet, B., Bonmatin, J. M., Hetru, C., Hoffmann, J. A., Ptak, M., & Vovelle, F. (1995). Refined three-dimensional solution structure of insect defensin A. *Structure*, 3(5), 435-448.
269. Nygaard, M. K. E., Andersen, A. S., Kristensen, H. H., Krogfelt, K. A., Fojan, P., & Wimmer, R. (2012). The insect defensin lucifensin from *Lucilia sericata*. *Journal of biomolecular NMR*, 52(3), 277-282.
270. Yamauchi, H., 2001. Two novel insect defensins from larvae of the cupreous chafer, *Anomala cuprea*: purification, amino acid sequences and antibacterial activity. *Insect Biochem. Mol. Biol.* 32, 75–84. doi:[https://doi.org/10.1016/S0965-1748\(01\)00082-0](https://doi.org/10.1016/S0965-1748(01)00082-0).
271. Fujiwara, S., Imai, J., Fujiwara, M., Yaeshima, T., Kawashima, T., Kobayashi, K., 1990. A potent antibacterial protein in royal jelly. Purification and determination of the primary structure of royalisin. *J. Biol. Chem.* 265, 11333–11337.
272. Hwang, J.-S., Lee, J., Kim, Y.-J., Bang, H.-S., Yun, E.-Y., Kim, S.-R., Suh, H.-J., Kang, B.-R., Nam, S.-H., Jeon, J.-P., Kim, I., Lee, D.G., 2009. Isolation and Characterization of a Defensin-Like Peptide (Coprison) from the Dung Beetle, *Copris tripartitus*. *Int. J. Pept.* 2009, 136284. doi:10.1155/2009/136284.
273. Peng, J., Wu, Z., Liu, W., Long, H., Zhu, G., Guo, G., & Wu, J. (2019). Antimicrobial functional divergence of the cecropin antibacterial peptide gene family in *Musca domestica*. *Parasites & vectors*, 12(1), 1-10.
274. Li, F., Gao, Z., Wang, K. et al. A novel defensin-like peptide contributing to antimicrobial and antioxidant capacity of the tick *Dermacentor silvarum* (Acari: Ixodidae). *Exp Appl Acarol* 83, 271–283 (2021). <https://doi.org/10.1007/s10493-020-00584-1>.



## **7. APPENDIX**

### **A1. Agarose gel electrophoresis (1.2% w/v)**

1.2 g Agarose (Euroclone, EMR911100)

100 mL TAE (Tris Acetate-EDTA) 1X

5  $\mu$ L Ethidium bromide (Invitrogen, 15585-011) before pouring gel.

### **A2. TAE (Tris Acetate-EDTA) buffer 50X**

242 g Trizma base (Sigma Aldrich, #T1503)

20.81 g EDTA (Sigma Aldrich, #E4884)

57.1 mL Glacial acetic acid (Sigma Aldrich, #33209)

Final volume: 1 L distilled water

### **A3. DNA Extraction from Agarose Gel**

Purification of double-stranded DNA from TAE agarose gel was conducted using Quantum Prep™ Freeze 'N Squeeze DNA gel Extraction Spin column.

1. Excise the band of interest using a clean razor blade and trim excess of agarose from all sides.
2. Chop the trimmed gel slice and place it into the filter cup.
3. Freeze 5 minutes at -20°C.
4. Centrifuge the sample at 13000 x g for 3 minutes at room temperature.
5. Collect the purified DNA.

Ethanol precipitation of the purified DNA was performed to further purify the sample.

### **A4. LB Agar (1.5%) plates**

1.5 g Agar bacteriological (OXOID, LP0011)

100 mL Luria Bertani (LB) broth

Autoclave (Compact 40 Benchtop Priorclave): 121°C 15 min.

#### **A5. X-Gal (5-Bromo-4-chloro-3-indolyl-b-D-galactopyranoside) (40 µg/µL)**

40 mg X-Gal (Sigma Aldrich, B4252)

1 mL DMSO (Dimethyl sulfoxide) (Sigma Aldrich, 67-68-5 )

Wrap in foil to protect from the light

Sterilize by filtration (0.22 µm PES, sterile syringe filter) and store at -20°C.

#### **A6. Liquid bacterial culture: LB (Luria – Bertani) Broth**

10 g Tryptone enzymatic digest from Casein (Fluka Analytical, #95039)

5 g Selected yeast extract (Sigma Aldrich, #Y0875)

10 g Sodium chloride (Sigma Aldrich, #31434)

Final volume: 1 L distilled water

Autoclave (Compact 40 Benchtop Priorclave): 121°C 15 min.

#### **A7. Ca<sup>2+</sup> competent cells transformation**

Transformation is a key process in molecular cloning, by which multiple copies of recombinant DNA molecules are produced. The ability to take up free, extracellular genetic material is the prerequisite for bacterial competent cells to undergo transformation. The objective is to obtain the replication of sequence of interest of a recombinant plasmid.

It consists on the following steps:

1. Thaw cells in ice.
2. Pipet max 30 ng of DNA into cells.
3. Mix gently.

4. Ice for 30 minutes.
5. Incubate at 42°C for 45 seconds.
6. Ice for 15 minutes.
7. Add SOC (Super Optimal broth with Catabolite repression) up to 1 mL.
8. Incubate 1 hour at 37°C.
9. Plate on LB agar medium containing appropriate antibiotic

### **A8. Mini-prep procedure**

Mini-preparation of plasmid DNA is a rapid, small-scale isolation of plasmid DNA from bacteria. Mini-preps are used in the process of molecular cloning to analyse bacterial clones.

The kit used for mini-prep was Fast Plasmid Mini Kit and it consist on:

1. Pellet 1.5 ml of fresh bacterial culture at maximum speed for 1 minute in the provided 2 ml Culture Tube.
2. Remove medium by decanting, taking care not to disturb bacterial pellet.
3. Add 400 µL of ICE-COLD Complete Lysis Solution.
4. Mix thoroughly by constant vortexing at the highest setting for a full 30 seconds. This step is critical for obtaining maximum yield.
5. Incubate the lysate at room temperature for 3 minutes.
6. Transfer the lysate to a Spin Column Assembly by decanting or pipetting.
7. Centrifuge the Spin Column Assembly for 60 seconds at maximum speed.
8. Add 400 µL of DILUTED Wash Buffer to the Spin Column Assembly.
9. Centrifuge the Spin Column Assembly for 60 seconds at maximum speed.
10. Remove the Spin Column from the centrifuge and decant the filtrate from the Spin Column Assembly Waste Tube. Place the Spin Column back into the Waste Tube and return it to the centrifuge.
11. Centrifuge at maximum speed for 1 minute to dry the Spin Column.

12. Transfer the Spin Column into a Collection Tube.
13. Add 50  $\mu$ L of Elution Buffer directly to the centre of the Spin Column membrane and cap the Collection Tube over the Spin Column.
14. Centrifuge at maximum speed for 60 seconds.
15. Remove and discard the Spin Column.
16. The eluted DNA can be used immediately for downstream applications or stored at  $-20^{\circ}\text{C}$

### **A9. Midi-prep procedure**

Midi-preparation of plasmid DNA is a plasmid DNA isolation technique from bacteria. It differ from mini-prep because of the initial bacteria culture used. It leads to get more plasmid DNA. The kit used for midi-prep was the HiPure PureLink™ Plasmid Midiprep and it consist on:

1. Harvest 50 mL bacterial culture by centrifuging the overnight LB culture at  $4000 \times g$  for 10 minutes. Remove all medium.
2. Add 4 mL Resuspension Buffer (R3) with RNase A to the cell pellet and resuspend the cells until homogeneous.
3. Add 4 mL Lysis Buffer (L7). Mix gently by inverting the capped tube until the lysate mixture is thoroughly homogenous.
4. Incubate at room temperature for 5 minutes.
5. Add 4 mL Precipitation Buffer (N3) and mix immediately by inverting the capped tube until the mixture is thoroughly homogeneous.
6. Centrifuge the mixture at  $>12000 \times g$  for 10 minutes at room temperature.
7. Load the supernatant onto the equilibrated (EQ Buffer) column. Allow the solution in the column to drain by gravity flow.
8. Wash the column twice with 10 mL Wash Buffer (W8). Allow the solution in the column to drain by gravity flow after each wash. Discard the flow-through.
9. Proceed to Elute and precipitate DNA using 5 mL Elution Buffer (E4) to the column and allow the solution to drain by gravity flow.
10. The elution tube contains the purified DNA.

11. Discard the column and add 3.5 mL isopropanol to the elution tube. Mix well.
12. Centrifuge the tube at  $>12000 \times g$  for 30 minutes at 4°C.
13. Carefully remove and discard the supernatant and resuspend the pellet in 3 mL 70% ethanol.
14. Centrifuge the tube at  $>12000 \times g$  for 5 minutes at 4°C.
15. Carefully remove and discard the supernatant and air-dry the pellet for 10 minutes.
16. Resuspend the DNA pellet in TE Buffer (TE).

#### **A10. IPTG (isopropyl b-D-1-thiogalactopyranoside) (1M)**

5.96 g of IPTG (Sigma Aldrich, # 367-93-1)

Final volume: 25 mL distilled water

Filter through 0.22  $\mu\text{m}$  PES, sterile syringe filter

Make 1 mL aliquots, store at -20°C

#### **A11. SDS-PAGE solutions**

##### **➤ Running buffer (10X)**

60 g Trizma base (248 mM) (Sigma Aldrich, #T1503)

288 g Glycine (1.92 M) (Sigma Aldrich, #50046)

20 g Sodium Dodecyl Sulfate (1 % w/v) (Bio-Rad #1610302)

Final volume: 2 L distilled water

##### **➤ Laemli 4X**

25% v/v Glycerol (Sigma Aldrich, #56-81-5)

5%  $\beta$ -mercaptoethanol (Sigma Aldrich, #60-24-2)

2% w/v Sodium Dodecyl Sulfate (1 % w/v) (Bio-Rad #1610302)

0.01% w/v bromophenol blue (Bio-Rad #1610404)

65 mM TrisHCl, pH 6.8

##### **➤ Coomassie solution**

1.25 g Coomassie blue brilliant R-250 (Bio-Rad, # 1610400)

225 mL Methanol (Sigma Aldrich, #322415)

50 mL Glacial acetic acid (Sigma Aldrich, #33209)

225 mL distilled water

➤ **Destaining solution**

300 mL Methanol (30%) (Sigma Aldrich, #322415) or alternatively Ethanol (30%) (Sigma Aldrich, #16368)

100 mL Glacial acetic acid (10%) (Sigma Aldrich, #33209)

600 mL distilled water

## **8. PUBLICATIONS**



OPEN

# A bioinformatic study of antimicrobial peptides identified in the Black Soldier Fly (BSF) *Hermetia illucens* (Diptera: Stratiomyidae)

Antonio Moretta<sup>1</sup>, Rosanna Salvia<sup>1</sup>, Carmen Scieuzo<sup>1</sup>, Angela Di Somma<sup>2</sup>, Heiko Vogel<sup>3</sup>, Pietro Pucci<sup>4</sup>, Alessandro Sgambato<sup>5,6</sup>, Michael Wolff<sup>7</sup> & Patrizia Falabella<sup>1</sup>✉

Antimicrobial peptides (AMPs) play a key role in the innate immunity, the first line of defense against bacteria, fungi, and viruses. AMPs are small molecules, ranging from 10 to 100 amino acid residues produced by all living organisms. Because of their wide biodiversity, insects are among the richest and most innovative sources for AMPs. In particular, the insect *Hermetia illucens* (Diptera: Stratiomyidae) shows an extraordinary ability to live in hostile environments, as it feeds on decaying substrates, which are rich in microbial colonies, and is one of the most promising sources for AMPs. The larvae and the combined adult male and female *H. illucens* transcriptomes were examined, and all the sequences, putatively encoding AMPs, were analysed with different machine learning-algorithms, such as the Support Vector Machine, the Discriminant Analysis, the Artificial Neural Network, and the Random Forest available on the CAMP database, in order to predict their antimicrobial activity. Moreover, the iACP tool, the AVPpred, and the Antifp servers were used to predict the anticancer, the antiviral, and the antifungal activities, respectively. The related physicochemical properties were evaluated with the Antimicrobial Peptide Database Calculator and Predictor. These analyses allowed to identify 57 putatively active peptides suitable for subsequent experimental validation studies.

With over one million described species, insects represent the most diverse as well as the largest class of organisms in the world, due to their ability to adapt to recurrent changes and to their resistance against a wide spectrum of pathogens<sup>1</sup>. Their immune system, exclusively based on the innate, well-developed immune response, allows a general and rapid response to various invading organisms<sup>2,3</sup>. The humoral immune response includes the enzymatic cascade that regulates the activation of coagulation and melanization of the hemolymph, the production of reactive oxygen (ROS) and nitrogen (RNS) species, and the production of antimicrobial peptides (AMPs)<sup>4</sup>.

Today, the problem of antibiotic resistance represents one of the greatest threats in the medical field<sup>4</sup>. The constant need to find alternative solutions has increased the interest in AMPs over time. AMPs are small molecules, consisting of 10–100 amino acids, that have been identified in many organisms such as bacteria, fungi, plants, vertebrates and invertebrates, including insects<sup>5</sup>. They are cationic molecules that exhibit activities against bacteria, fungi, viruses, and parasites<sup>5</sup>. In addition to these known activities, many peptides also exert a cytotoxic effect against cancer cells<sup>6</sup>.

<sup>1</sup>Department of Sciences, University of Basilicata, Via dell'Ateneo Lucano 10, 85100 Potenza, Italy. <sup>2</sup>Department of Chemical Sciences, University Federico II of Napoli, Via Cinthia 6, 80126 Napoli, Italy. <sup>3</sup>Department of Entomology, Max Planck Institute for Chemical Ecology, Hans-Knöll-Straße 8, 07745 Jena, Germany. <sup>4</sup>CEINGE Advanced Biotechnology, Via Gaetano Salvatore 486, Naples, Italy. <sup>5</sup>Centro di Riferimento Oncologico della Basilicata (IRCCS-CROB), Rionero in Vulture, PZ, Italy. <sup>6</sup>Department of Translational Medicine and Surgery, Università Cattolica del Sacro Cuore, Rome, Italy. <sup>7</sup>Institute of Bioprocess Engineering and Pharmaceutical Technology, Technische Hochschule Mittelhessen, Wiesenstrasse 14, 35390 Giessen, Germany. ✉email: patrizia.falabella@unibas.it



The discovery of the first AMP derived from insects, dates back to 1980s, when Boman et al.<sup>7</sup> identified and isolated the first cecropin from the lepidopteran *Hyalophora cecropia*. Since then, many other AMPs have been discovered. Due to their high biodiversity, insects are considered to be among the richest and most innovative sources for these molecules. Insect AMPs can be classified into four families:  $\alpha$ -helical peptides (e.g. cecropins), cysteine-rich peptides (e.g. defensins), proline-rich peptides, and glycine-rich peptides<sup>8</sup>. Despite their diversity, AMPs share two common features: the tendency to adopt an amphipathic conformation and the presence of a large number of basic residues, which determine the net positive charge at a neutral pH<sup>9</sup>. The established electrostatic forces between the positive amino acid residues of a peptide and the negative charges exposed on microorganism cell surfaces allow their interaction with bacterial membranes. Moreover, the cationic nature of these peptides allows the interaction with the negatively charged molecules exposed on cancer cell surfaces, such as phospholipid phosphatidylserine (PS), O-glycosylated mucins, sialylated gangliosides, and heparin sulfate, in contrast to the typical zwitterionic nature of the normal mammalian membranes<sup>6,10,11</sup>. According to their mechanism of action, AMPs can be grouped in two categories<sup>12</sup>, (1) the membranolytic mechanism, described by three different putative models: “carpet”, “toroidal” and “barrel-stave” model<sup>13</sup>, and (2) the non-membranolytic one, characterised by their direct interaction with intracellular targets such as DNA, RNA and proteins<sup>14–16</sup>.

To date, more than 3000 AMPs have been discovered and reported to the Antimicrobial Peptide Database (APD, <https://aps.unmc.edu/AP/>), which contains exactly 3104 AMPs from six kingdoms: 343 from bacteria, 5 from archaea, 8 from protists, 20 from fungi, 349 from plants, and 2301 from animals. The amount of AMPs in insects varies according to the species, i.e. more than 50 AMPs have been found in the invasive ladybird *Harmoinia axyridis*<sup>17</sup>, whereas none was identified in the pea aphid *Acyrtosiphon pisum*<sup>18</sup>. The non-pest insect *Hermetia illucens* (Diptera: Stratiomyidae), also known as the Black Soldier Fly (BSF), is among the most promising sources for AMPs being able to live in hostile environments rich in microbial colonies<sup>19</sup>. In this study, we have analysed the larvae and the combined adult male and female *H. illucens* transcriptomes in order to identify AMPs, which were then analysed with the CAMP (Collection of Antimicrobial Peptides) database (<https://www.camp.bicni.rh.res.in/>)<sup>20–23</sup>. Moreover, the iACP online tool (<https://lin.uestc.edu.cn/server/iACP>) was used to predict the anticancer activity of the identified peptides while the AVPPred (<https://crdd.osdd.net/servers/avppred>) server was used to predict the antiviral activity of the identified peptides while the Antifp server (<https://webs.iiitd.edu.in/raghava/antifp>) was used to predict their antifungal activity, and their physicochemical properties were evaluated with the Antimicrobial Peptide Database Calculator and Predictor (APD3).

## Results

**De novo transcriptome assembly and gene identification.** A Next-Generation sequencing (RNAseq) of the RNA isolated from larvae and combined adult male and female *H. illucens* transcriptomes was performed for an unambiguous identification of the peptide candidates. Sequencing and de novo assembly of the transcriptomes led to the identification of 25,197 unique nucleotide sequences (contigs) in the larvae transcriptome, and 78,763 contigs in the combined adults. These contigs were functionally annotated using Blast2GO software (<https://www.blast2go.org>). A total of 68 genes, encoding putative AMPs in the *H. illucens* transcriptomes, were finally identified.

**Antimicrobial, anticancer, antiviral and antifungal activity prediction.** All identified 68 sequences, encoding putative AMPs, were analysed in silico by the four machine-learning algorithms, such as Support Vector Machine (SVM), Discriminant Analysis (DA), Artificial Neural Network (ANN), and Random Forest (RF), available on the free online CAMP database, in order to predict their antimicrobial activity. The results are shown in Table 1. Table 2 reports the anticancer and non-anticancer scores obtained using the iACP tool. Table 3 shows the results obtained with the AVPPred server to predict the antiviral activity and with the Antifp server used to predict the antifungal activity. These analyses allowed the identification of 57 putatively active peptides: 13 sequences were predicted to be only antimicrobial while the others showed different combinations of antimicrobial, antiviral, anticancer or antifungal activity. In particular, 22 were both putative antimicrobial and anticancer; eight were both putative antimicrobial and antiviral; two were both putative antimicrobial and antifungal; seven were putative antimicrobial, anticancer and antiviral; one was putative antimicrobial antifungal and antiviral; two were putative antimicrobial, anticancer and antifungal while two potentially cover the complete range of analyzed biological activities (antimicrobial, anticancer, antifungal and antiviral). The remaining 11 did not show any activity according to the in silico investigation. In Supplementary Table S1 all the predicted activities are listed.

**Physicochemical properties of the identified peptides.** The 57 identified, putatively active, peptides belong to different classes of AMPs including defensins, cecropins, attacins and lysozyme (Fig. 1). Although attacins and lysozyme are proteins due to their high molecular weight, they belong to AMPs' classes because of their antibacterial activity. The physicochemical properties of these peptides were evaluated with the Antimicrobial Peptide Database Calculator and Predictor APD3 (Table 4). Figure 2 shows the graphical representation of the calculated physicochemical properties of the 57 identified peptides, whereas Table 5 reports their amino acid composition and the amino acid frequency, compared to the amino acid composition of the patent AMPs available in the APD database. The highest amino acid content in all the analysed AMPs was found for Gly, Ala, Arg, Asn, Cys, Leu, Ser residues, whereas the lowest content was found for His, Met, Trp, Tyr residues (Table 5). A graphical representation of the amino acid composition of each identified peptide is shown in Supplementary Fig. 1. The molecular mass of the identified peptides ranges from 3000 Da for the smallest peptide Hill\_BB\_C7985 to 19,000 Da for the largest peptide Hill\_BB\_C9237, with an average of approximately 7000 Da. The amino acid sequences varied from a minimum value of 31 residues to a maximum of 186 residues, and an

Peptide	Sequence	SVM	RF	ANN	DA
Hill_BB_C14202	KRFTKCTLARELFQRGIPKSELPDWVCLVRWESNYQTAMNKNRDRGSDWYGLFQINDKWWCKGHIK-SHNACGLSCNELLKDDISKAVTCARLIKRRQQGFRAWYGLWNHCTKVKPSIHECF	1.000	0.800	AMP	1.000
Hill_BB_C3566	AKMSRCGVANMLLKYGFPRKDLADWVCLIEHESSFRNTVVGPPNTDGRSDYGLFQINSRYWCSGDGSPSHNM-CRIPCRMLLSNDMTHSIRCAVTVFRKQGLSAWYGSWGHCQGNAPSVCNFRSYNNLYYK	1.000	0.916	AMP	1.000
Hill_BB_C1152	RYGFPRNQLADWICLVEWESSFRTDVAGPPNGDGRSDWGLFQINDRYWCQSANYGNSHNICGVSCERLLSDDIT-TAVNCVRKIYAAHGFSGWNAWTQHCHSPSSVEHCFVESDCLPGGVSFDKHWL	1.000	0.8045	AMP	1.000
Hill_BB_C1153	ASGRQFERCELARILHNRYGFPRNQLADWICLVEWESSFRNAVGPNSDGRSDWGLFQINDRYWCKSSNYRNSH-NMCGVSCHELLSDDITAVNCVRKIYAAHGFSGWNAWTQH	1.000	0.918	AMP	1.000
Hill_BB_C2676	TVYSRCGFAQTLYDYGVTDMLANWVCLVQYESSFNDQAVGAINYNGTQDFGLFQINNKYWCQGAVSSSD-SCGIACSTLLGNLSASWSCAQLVYQQGFSAWYGLWLNCCNGTAPSVADCF	1.000	0.611	AMP	1.000
Hill_BB_C269	KVFTRCQLAKELIRYDFPRTFLSNWVCLIESESGRSTSKTLQLPNTSANYGIFQINSKTWCRKGRKGLCEMKCED-FLNDDISDDARCAKQIYNRHGFQGWPGWVVKCRGRALPDVLKC	1.000	0.8725	AMP	1.000
Hill_BB_C1169	SNGPRDYGLFQINNQYWCQGNVKSANECHIACTSLLSDDITHALNCAKKIKAQQGFKAWYGLWNYCQKSKPS-VKECF	0.937	0.8045	AMP	0.993
Hill_BB_C779	KVYTRCEMARILYHDHGVKNLTLANWVCLIEHESGFNDEAVGALNSNGTRDYGLFQINNKYWCKGNVASSD-SCKIACSTALLGNVDASWKAQLVYKEQGFKAUYGW	1.000	0.7555	AMP	1.000
Hill_LB_C36111	KQFNKCSLATELSRLGPKSELPDWVCLVQYHESNFKTWINKKNSSNGSWDFGLFQINDKWWCEGHIRSHNTCN-VKCEELVTEIEKALECAKVIKRERGYKAWYGLWLNCCNQKPKSVDCECF	1.000	0.8235	AMP	1.000
Hill_LB_C12085	KTFTKCSLAKTLYAHGIPKSELPDWVCLVQYHESGFRTDVGALNSNGTRDYGLFQINNKYWCKGNISSYNECNI-ACSAALLSDDI	0.890	0.871	AMP	0.987
Hill_BB_C1290	QLNIQGGGAKSPLSDFDLNVQGGARKYYNNGHKPLHGTEDYNQHLGGPYGYSRPNFSGGLLFTHRFKLCSLSKL-LIVC	0.581	0.5055	AMP	0.554
Hill_BB_C7347	QLNIQGGGSPHSGFNLSIQGQKKLWESNNKRNTLHGTGQYSQHF	0.307	0.374	NAMP	0.031
Hill_BB_C9109	QIFAQGGGSPGKGYDIYAQGRAKLWESQNRNSLHGTASYSQHLGGPYGNSRPNVGGGLIFTHRF	0.351	0.6175	AMP	0.270
Hill_BB_C11804	QLNIQGGGSPHSGFNLSIQGQKKLWESNNKRNTLHGTGQYSQHF	0.307	0.374	NAMP	0.031
Hill_BB_C309	VSCWFENENIKASACQMSCMYRKRGRRGGMCVNGVCTCSPN	0.827	0.6825	AMP	0.908
Hill_BB_C1827	TTCTHLNCKLHCVLYRKRGRCDRFRNICKCI	0.898	0.8805	AMP	0.995
Hill_BB_C5878	LSCLFENQAISAACGASCITRKRGRRGWCSNGVCRCTPN	0.971	0.941	AMP	0.994
Hill_BB_C8756	QPYQLQYEEEDGPEYARELPIEEEELPSQVVEQHQAQRATCDLLSPFKVGHAAACVLDGFAMGRRGGWC	0.266	0.0085	NAMP	0.037
Hill_BB_C13793	KESSDPDSALYSDIHFRFRQLPCDYLSGLGFGEACNTDCIAKGKSGFCTGLVCRCRTL	0.503	0.5453	AMP	0.645
NHill_AD_C73537	GQSEASWKKVFKPVEKLGQRVRDATIQGIGIAQQGANVLATVRGGPPQ	0.633	0.870	AMP	0.904
NHill_AD_C16493	GQSEAGWKRVPVEKFGQRVRDAGVQGIAIAQQGANVLATARGGPPQQG	0.633	0.842	AMP	0.885
NHill_AD_C12927	GWWKRVFKPVEKLGQRVRDAGIQGLEIAQQGANVLATARGGPPQQG	0.672	0.9075	AMP	0.955
NHill_AD_C12928	GWWKRVFKPVERLQQRVRDAGIQGLEIAQQGANVLATVRGGPPQQG	0.773	0.911	AMP	0.969
NHill_AD_C4669	SWFKVFKPVEKVGQRVRDAGIQGVAIAQQGANVLATARGGPPH	0.574	0.745	AMP	0.899
Hill_BB_C3195	GWWKRVFKPVEKLGQRVRDAGIQGIAIAQQGANVLATVRGGPPQ	0.868	0.9945	AMP	0.988
Hill_SB_C698	GQSEAGWKRVPVEKFGQRVRDAGIQGIEIAQQGANVLATARGGPPQQG	0.558	0.718	AMP	0.770
Hill_SB_C2730	GWWKRVFKPVEKLGQRVRDAGIQGLEIAQQGANVLATVRGGPPQQG	0.700	0.9095	AMP	0.959
Hill_SB_C1875	GQGESRSLWKKIFKVPVEKLGQRVRDAGIQGIAIAQQGANVLATVRGGPPQ	0.714	0.9115	AMP	0.949
Hill_BB_C5151	GQSESRLWKKLFPVERAGQRIRDATIKGIVIAQQGANVLATIRGGPAIPPGQG	0.641	0.944	AMP	0.935
Hill_BB_C390	FNNLPICVEGLAGDIGSILLGVESDIGALAGAIANLALIGECAAQGEAGAAICA	0.946	0.685	AMP	0.822
NHill_AD_C53857	CINNGDGCQPDGRQGNCCSGYCHKEPGWVTGYCR	0.811	0.742	AMP	0.973
NHill_AD_C49215	CIANGNGCQPDGRQGNCCSGFCYKQRGWVAGYCRRR	0.961	0.8735	AMP	0.999
Hill_BB_C2323	QLNIQGGGSPHSGFDLSVQGRAKIWESDNGRNTLYGTGQYQHLGGPYGNSRPNFSGGLMFSHRF	0.163	0.048	NAMP	0.007
Hill_BB_C7345	SIDDLTISEDGEDHVEIITDDEVQRAKR	0.456	0.1395	NAMP	0.024
Hill_BB_C7346	QLNIQGGGSPHSGFDLNVQGRAKIWESNNGRNTLHGTGEYSQHLGGPYGNSRPNFSGGLLFTHRF	0.223	0.1105	NAMP	0.019
Hill_BB_C11803	QLNIQGGGSPHSGFNLSIQGQKKLWESNNKRNTLHGTGQYSQHFQGGPYGNSRPNFSGGLVFTHRF	0.278	0.3295	AMP	0.030
Hill_BB_C21232	QLNIQGGGSKSTFLILISMVRESNNGHETLHGTGDYDYNQHLGGPYGNSRPNFSGGLLFTHRFKLCSLSKLLIVCVF-SKCRK	0.749	0.8505	AMP	0.865
NHill_AD_C17624	QIFAQGGGSPGKGYDIYAQGRAKLWESQNRNSLHGTASYSQHLGGPYGNSRPNVGGGLIFTHRF	0.284	0.515	NAMP	0.170
Hill_LB_C16634	IKCTASICTQICRILKYKCYCASASRCVCLK	0.992	0.913	AMP	0.999
Hill_LB_C37730	AFAFDVTRKINPETSASVERPEVSEYPEIPKGTKLQEFVMMDIEIEEGADNRAETIQRICKVPSQCNCQICRVLGKCK-GYCKNASTCVCLG	0.988	0.9565	AMP	0.984
Hill_BB_C46948	RKCTASQCTRVCKKLYKRGYQSSTKVC	0.968	0.9375	AMP	0.999
Hill_BB_C16137	MNIQGNVSNPAGGQDVTVTAGKQFGSDNANITAGGFAGNTLRGPPNAGVFASANANGHLSVSKTVVPGIS-STTSHGASANLFR	0.886	0.8225	AMP	0.758
Hill_BB_C16883	QLSGSITPDMAGNNVIMASKFLGNPNHNIGGVFASGNTSRNTPSLGAFGTLNLKDHSLGVSKTITPGVSDTF-SQNARLIILKTPDHRVDANVFNHSHRLNNGAFDKRGGSLDYTHRAGHSLSLGASHIPKFGTTAELTGKANLW-KSPSGLSTFDLTGSAS	1.000	0.9275	AMP	1.000
Hill_BB_C10074	SPQDGRRRGSASVTVNNESRRGTVDRAADLNARLWEGNRRSSLDANAYYQRHFGGPMGTGRPDAGVGLNFRHRF	0.400	0.4375	NAMP	0.566
Hill_BB_C9237	MNIQGNVSNPAGGQDVTVTAGKQFGSDNTNITAGAFAGNTLRGPPNAGVFASANANSHLSVSKTVVPGV-SATTSHAASANLFRNDQHSVNAQAFSSATKLNDFGQFKHGAGLNYNNANGHGASIGVKNIPFGSSMDVGA-RANIFQNPNTSFDVMANSRTHLSGPFQKTNFVGSAGITRRF	1.000	0.9505	AMP	1.000

Continued

Peptide	Sequence	SVM	RF	ANN	DA
NHill_AD_C40487	MNIQGNVSNPAGGQDVTVTAGKQFGSDNTNITAGAFAGNTLRGPPNAGVFASANANGHLSVSKTVVPGVS-STTSHAASANLFRNDQHNVNAQAFSSATKLNDFQFKQHAGLNNYNNANGHGASIGVKNKIPGFGSSMDVGA-RANIFQNPNTSFDVMANSRTHLSGPFQGKTNF	1.000	0.9745	AMP	1.000
Hill_BB_C7758	AACDLFSALNVASSICAAHCLYLGYKGGYCDSKLVCVCR	0.985	0.819	AMP	0.988
Hill_BB_C14087	VTCDLLEPFLGPAPCMIHICIVFRKRTGYCNSQNVCVCRG	0.712	0.6305	AMP	0.709
Hill_LB_C29142	ATCDLLSPFKVGHAAACAAHCIARGKRRGGWCDKRAVCNCRK	0.956	0.9455	AMP	0.999
Hill_BB_C308	VSCWFENENIKASACQMSCMYRKRGRGGMCVNGVCTCSPN	0.827	0.6825	AMP	0.908
Hill_BB_C1619	LSCLFENQAVSAIACGSSCIARKGRRGGYCRNGVGVCTDN	0.972	0.900	AMP	0.972
Hill_BB_C1826	TTCTHLNCKLHCLLQKRKRSRGRCDRFNICKCIS	0.878	0.9105	AMP	0.995
Hill_BB_C6571	ATCTNWNCRITQCIARGKRRGGYCVERNICKCTS	0.950	0.9815	AMP	0.992
Hill_BB_C7081	ATCDLISGTKIENVACAAHCIAMGHKGGYCNSNLICICR	0.987	0.907	AMP	0.979
Hill_BB_C7985	FTCSNLGCKAQCIIILGNRSGGCNRLGVCQCN	0.991	0.9175	AMP	0.999
Hill_BB_C7176	ATCDLLSPFKVGHAAACALHICIALGRRGGWCDGRAVCNCR	0.933	0.938	AMP	0.996
Hill_BB_C2519	ATCDLLSPFKVGHAAACALHICIALGRRGGWCDGRAVCNCR	0.895	0.8835	AMP	0.987
Hill_BB_C8473	ATCDLLSPFGVGHAAACAVHICIALGRRGGWCDGRAVCNCR	0.855	0.8145	AMP	0.977
Hill_BB_C34351	AMCDLLSGLNMGRSVCAMRILKGRGGWCDQGVNCRV	0.816	0.6875	AMP	0.971
Hill_BB_C4683	RPDNIYLEDSSQVAELVRHKRLSCLFENEAISALACGASCITRKGRRGGWCSNGVCHCTPN	0.734	0.5745	AMP	0.645
Hill_BB_C4977	LSCWFENEDIKATACAMSCIYRKRKGRGRCENGICRCTPN	0.828	0.7115	AMP	0.913
Hill_BB_C13326	LSCLFENQAVSAIACGASCITRKGRRGGWCSNGVCRCTPN	0.975	0.9475	AMP	0.991
Hill_BB_C7171	TTCDLISGTKIENIACAAHCIAMGHKGGYCNSNLICICR	0.981	0.8805	AMP	0.984
Hill_BB_C10649	QFDNLEDTGVEEKVRHKRLTCLFDNRPISAFACGSCNCSRKGRGGWCVNGVCRCT	0.860	0.595	AMP	0.983
Hill_BB_C13792	KQSSDPESALYSDIHPRFRQLPCDYLSGLFGFEDACNTDIAKHGKSGFCTGLVCRCTRL	0.995	0.9725	AMP	0.965
Hill_BB_C15867	VTCDLLKPFGRAPCMHHCILRFKRTGFCSRQNVCVCR	0.826	0.5095	AMP	0.885
NHill_AD_C69719	DVSIQSCVWGGSNVSDCNCECKRRGYKGGHCGSFLNNICWCET	0.984	0.913	AMP	0.993
Hill_BB_C49430	APQFGGQIGFGGGGFGGGGFGPGGFRPGGVAEFQESSSVNVERETFDQGGFEISDSSVTSSVSSEFRD	0.012	0.2715	NAMP	0.031

**Table 1.** Prediction of the antimicrobial activity through the CAMP database. From left to right are shown in order: peptide contig, peptide sequence, Support Vector Machine (SVM) score, Random Forest (RF) score, Artificial Neural Network (ANN) result and the Discriminant Analysis (DA) score.

average of approximately 66 residues. The total hydrophobic ratio showed the lowest value of 26 for the peptide NHill\_AD\_C53857 and the highest of 60 for the peptide Hill\_BB\_C390, and an average value of approximately 40. The total net charge of the identified peptides ranged from  $-6$ , for the Hill\_BB\_C390 peptide to  $+9$  for the Hill\_BB\_C14202 peptide, with an average value of  $+3$ , while the Isoelectric Point (pI) varied from 3.34 for the Hill\_BB\_C390 peptide to 11.83 for the NHill\_AD\_C12928 peptide, with an average value of 8.79.

**Bacterial cell growth and viability.** Four putative antimicrobial peptides, namely Hill\_BB\_C6571, Hill\_BB\_C16634, Hill\_BB\_C46948 and Hill\_BB\_C7985, that showed high antimicrobial score values with all prediction softwares were selected and chemically synthesised. The antimicrobial activity of these peptides was verified by monitoring *E. coli* cells growth in the presence of different concentrations of each peptide in comparison with untreated cells. Supplementary Fig. 2 shows the growth curves of *E. coli* cells in the presence of  $3 \mu\text{M}$  (A) or  $12 \mu\text{M}$  (B) concentrations of each peptide. A clear decrease in the growth curves was observed at both concentrations compared to untreated cells (blue line) with bacteria impaired to achieve the exponential phase at  $12 \mu\text{M}$  due to rapid death. The reduction in cell viability was observed with increasing concentration of each peptide in comparison with untreated cells.

Next, cell viability of *E. coli* was also evaluated by treatment with  $3 \mu\text{M}$  of each peptide (Supplementary Fig. 2C) confirming a decrease of about 50% in cell viability after 100 min treatment with all four peptides analysed.

## Discussion

AMPs are promising candidates as alternatives to conventional antibiotics, thanks to their low toxicity to eukaryotic cells and their broad spectrum of action against bacteria, mycobacteria, fungi, viruses and cancer cells<sup>24</sup>. AMPs can kill bacteria through different mechanisms including membrane disruption, targeting intracellular components, or interfering with the bacterial metabolism<sup>25–27</sup>. Furthermore, most AMPs are cationic, with the positive net charge promoting the electrostatic interaction with negatively charged bacterial membranes<sup>28</sup>.

All living organisms produce AMPs with insects being among the richest sources due to their high biodiversity and their extremely varied living environments. The immune system of the insect *H. illucens* is very developed, as this species feeds on decaying substrates and manure, which are extremely rich in pathogenic microorganisms, as it is possible to observe also in other species, such as in *Eristalis tenax*. Twenty-two AMPs were indeed identified in the Diptera *E. tenax*, that has been able to adapt to different aquatic habitats (sewage tanks and manure pits) with heavy microbial load<sup>29</sup>. AMPs, which are synthesized by the fat body and hemocytes and then secreted into

Peptide	Sequence	Anticancer score	Non-anticancer score
Hill_BB_C14202	KRFTKCTLARELFQRGIPKSELPDWWVCLVRWESNYQTAMNKNRRDGSWDYGLFQINDKWWCKGHK-SHNACGLSCNELLKDDISKAVTCARLIKRQQGFRAWYGLWLNHCTKVKPSIHECF	0.452542	0.547458
Hill_BB_C3566	AKMSRCGVANMLLKYGFPRKDLADWVCLIEHESSFRNTNVGPPNTDGSRDYGLFQINSRYWCSGDGSPH-NMCRIPCRMLNSNDMTHSIRCAVTVFRKQGLSAWYGSWGHCCQGNAPSVENCFRSYNNLYYGK	0.603649	0.396351
Hill_BB_C1152	RYGFPRNQLADWICLVWESSFRTDVAGPPNGDGSRDWGLFQINDRYWCQSANYGNSHNICGVSCER-LLSDDITAVNCVRKIYAAHGFSGWNAWTQHCHSPSSVEHCFVESDCLPGGVSFDKHWL	0.744031	0.255969
Hill_BB_C1153	ASGRQFRCELARILHNRYGPPRNQLADWICLVWESSFRNAVGPNSDGSRDWGLFQINDRYWCKSS-NYRNSHNMGCVSCEHLLSDDITAVNCVRKIYAAHGFSGWNAWTQH	0.322215	0.677785
Hill_BB_C2676	TVYSRCGFAQTLYDYGVTDMMNTLANVWVCLVQYESSFNDAVGAINGTQDFGLFQINNKYWCQ-GAVSSSDSCGIACSTLLGNLSASWSCAQLVYQQGFSAWYGLWLNCCNGTAPSVADCF	0.508041	0.491959
Hill_BB_C269	KVFTRCQLAKELIRYDFPRTFLSNVWVCLIESESGRSTKTLQLPNTSANYGIFQINSKTWCRKGRKGG-LCEMKCEDFLNDDISDDARCAKQIYNRHGFQGWPGVWVKCRGRALPDVLC	0.353721	0.646279
Hill_BB_C1169	SNGPRDYGLFQINNQYWCQGNVKSANECHIACTSLLSDDITHALNCAKKIKAQQGFKAWYGLWNYC-QKSKPSVKECF	0.995537	0.004463
Hill_BB_C779	KVYTRCEMARILYHDHGVKNLTLANVWVCLIEHESGFNDEAVGALNSNGTRDYGLFQINNKYWCKGN-VASSDSCKIACALLGNVDASWKAQLVYKEQGFKAUYGW	0.717440	0.282560
Hill_LB_C36111	KQFNKCSLATELSRLGPKSELPDWWVCLVQYHESNFKTWINKKNSNGSWDFGLFQINDKWWCEGHIR-SHNTCNVKEELVTEDEKALECAKVKRERGKAWYGLWLNCCNQKPKPSVDEC	0.644890	0.355110
Hill_LB_C12085	KTFTKCSLAKTYAHGIPKSELPDWWVCLVQYHESGFRTDAVGAALNSNGTRDYGLFQINNKYWCKGNISYN-ECNIACALLSDDI	0.500000	0.500000
Hill_BB_C1290	QLNIQGGAKSPLSDFDLNVQGGARKYYNNGHKPLHGTEDYNQHLGGPYGYSRPNFGGGLLFTHR-FKLCSLKLLIVC	0.878792	0.121208
Hill_BB_C7347	QLNIQGGGSPHSGFNLSIQGQKKLWESNNKRNTLHGTGQYSQHF	0.005102	0.994898
Hill_BB_C9109	QIFAQGGGSPGKGYDIYAQGRAKLWESQNRNSLHGTASYSQHLGGPYGNSRPNVGGGLIFTHRF	0.115082	0.884918
Hill_BB_C11804	QLNIQGGGSPHSGFNLSIQGQKKLWESNNKRNTLHGTGQYSQHF	0.005102	0.994898
Hill_BB_C309	VSCWFENENIKASACQMSCMYRKRGRGGMVCVNGVCTCSPN	0.444002	0.555998
Hill_BB_C1827	TTCTHLNCKLHCVLYRKRGRCDRFRNICKCI	0.215222	0.784778
Hill_BB_C5878	LSCLFENQAISAACGASCITRKRGRGGWCSNGVCRCTPN	0.724609	0.275391
Hill_BB_C8756	QPYQLQYEEEDGPEYARELPIEEEELPSQVVEQHQAQRATCDLLSPFKVGHAAACVLDGFAMGRRGGWC	0.000000	1.000000
Hill_BB_C13793	KESSDPDSALYSDIHFRFRQLPCDYLSGLGFGEACNTDCIAKGKSGFCTGLVCRCRTL	0.051485	0.948515
NHill_AD_C73537	GQSEASWKKVFKPVEKLGQRVRDATIQGIGIAQQGANVLATVRGGPPQ	0.508308	0.491692
NHill_AD_C16493	GQSEAGWKRVPVEKFGQRVRDAGVQGIAIAQQGANVLATARGGPPQQG	0.520865	0.479135
NHill_AD_C12927	GWWKRVFKPVEKLGQRVRDAGIQGLEIAQQGANVLATARGGPPQQG	0.389374	0.610626
NHill_AD_C12928	GWWKRVFKPVERLQQRVRDAGIQGLEIAQQGANVLATVRGGPPQQG	0.492318	0.507682
NHill_AD_C4669	SWFKVFKPVEKVGQRVRDAGIQGVAIAQQGANVLATARGGPPH	0.901851	0.098149
Hill_BB_C3195	GWWKRVFKPVEKLGQRVRDAGIQGIAIAQQGANVLATVRGGPPQ	0.839903	0.160097
Hill_SB_C698	GQSEAGWKRVPVEKFGQRVRDAGIQGLEIAQQGANVLATARGGPPQQG	0.519633	0.480367
Hill_SB_C2730	GWWKRVFKPVEKLGQRVRDAGIQGLEIAQQGANVLATVRGGPPQQG	0.481171	0.518829
Hill_SB_C1875	GQGESRSLWKKIFKVEKLGQRVRDAGIQGIAIAQQGANVLATVRGGPPQ	0.702695	0.297305
Hill_BB_C5151	GQSESRLWKKLFPVERAGQRIRDATIKGIVIAQQGANVLATIRGGPAIPPGQG	0.870751	0.129249
Hill_BB_C390	FNNLPICVEGLAGDIGSILLGVESDIGALAGAIANLALIGECAAQGEAGAAICA	0.908553	0.091447
NHill_AD_C53857	CINNGDGCQPDGRQGNCCSGYCHKEPGWVTGYCR	0.991593	0.008407
NHill_AD_C49215	CIANGNGCQPDGRQGNCCSGFCYKQRGWVAGYCRRR	0.994731	0.005269
Hill_BB_C2323	QLNIQGGGSPHSGFDLSVQGRAKIWESDNGRNTLYGTGQYQHLGGPYGNSEPSFGGGLMFSHRF	0.071113	0.928887
Hill_BB_C7345	SIDDLTLESDGEDHVEIITDDEVQRAKR	0.014171	0.985829
Hill_BB_C7346	QLNIQGGGSPHSGFDLNVQGRAKIWESNNGRNTLHGTGEYSQHLGGPYGNSRPNFGGGLLFTHRF	0.035845	0.964155
Hill_BB_C11803	QLNIQGGGSPHSGFNLSIQGQKKLWESNNKRNTLHGTGQYSQHFQGGPYGNSRPNFGGGLVFTHRF	0.066283	0.933717
Hill_BB_C21232	QLNIQGGSKSTFLILISMVRESNNGHETLHGTGDYDYNQHLGGPYGNSRPNFGGGLLFTHRFKLCSLK-LIVCVFSKCRK	0.945162	0.054838
NHill_AD_C17624	QIFAQGGGSPGKGYDIYAQGRAKLWESQNRNSLHGTASYSQHLGGPYGNSRPNVGGGLIFTHRF	0.075412	0.924588
Hill_LB_C16634	IKTASICTQICRILKYKCYCASASRCVCLK	0.960433	0.039567
Hill_LB_C37730	AFAFDVTRKINPETSAYERPEVSEYPEIPKGTKLQEFVMMDIEIEEGADNRAETIQRKCVPSQCNCQICRV-LGKCKGYCKNASTCVCLG	0.006798	0.993202
Hill_BB_C46948	RKCTASQCTRVCKKLGKRYGQSSKTCVC	0.782932	0.217068
Hill_BB_C16137	MNIQGNVSNPAGGQDVTVTAGKQFGSDNANITAGGFAGNTLRGPPNAGVFASANANGHLSVSKTV-VPGISSTTSHGASANLFR	0.574294	0.425706
Hill_BB_C16883	QLSGSITPDMAGGNVIMASKFLGNPNHNIGGVFASGNTSRNTPSLGAFGLTLNLKDHSLGVSKTIT-PGVSDTFSQARLILKTPDHRVDANVFNHSHTRLNNGFAFDKRGSLDYTHRAGHSLGASHIPKFGT-TAELTGKANLWKSPLSTFDLTGSAS	0.883543	0.116457
Hill_BB_C10074	SPQDGRRRGSASVTVNNESRRGTVDRAADLNARLWEGNRRSSLDANAYQRHFGGPMGTGRPDAGVGL-NFRHRF	0.000017	0.999983
Continued			

Peptide	Sequence	Anticancer score	Non-anticancer score
Hill_BB_C9237	MNIQGNVAVSNPAGGQDVTVTAGKQFGSDNTNITAGAFAGGNTLRGPPNAGVFASANANSHLSVSKTV-VPGVSAATTSAAASANLFRNDQHSVNAQAFSSATKLNDFGQFKQHAGLNYYNANGHGASIGVKNKIPGF-GSSMDVGARANIFQNPNTSFDVMANSRTHLSGPFQGKTNFVGSAGITRRF	0.434155	0.565845
NHill_AD_C40487	MNIQGNVAVSNPAGGQDVTVTAGKQFGSDNTNITAGAFAGGNTLRGPPNAGVFASANANGHLSVSKTV-VPGVSSSTTSHAASANLFRNDQHNVNAQAFSSATKLNDFGQFKQHAGLNYYNANGHGASIGVKNKIPGF-GSSMDVGARANIFQNPNTSFDVMANSRTHLSGPFQGKTNF	0.443017	0.556983
Hill_BB_C7758	AACDLFSAALNVASSICAAHCLYLGYKGGYCDSKLVCVCR	0.791573	0.208427
Hill_BB_C14087	VTCDLLEPFLGPAPCMIHCIIVFRKRRTGYCNSQNVCVCRG	0.391809	0.608191
Hill_LB_C29142	ATCDLLSPFKVGHAAACAAHCIARGKRGGWCDKRAVCNCRK	0.450101	0.549899
Hill_BB_C308	VSCWFENENIKASACQMSCMYRKRRGGMCVNGVCTCSPN	0.444002	0.555998
Hill_BB_C1619	LSCLFENQAVSAIACGSSCIARKGRRGGYCRNGVVCVTDN	0.954283	0.045717
Hill_BB_C1826	TTCTHLNCKLHCLLQRKRSGRCDRFRNICKCIS	0.068550	0.931450
Hill_BB_C6571	ATCTNWNCRQTQCIARGKRGGYCVERNICKCTS	0.842113	0.157887
Hill_BB_C7081	ATCDLISGTKIENVACAACIAMGHKGGYCNLSLICIR	0.945143	0.054857
Hill_BB_C7985	FTCSNLGCKAQCIILGNRSGGCNRLGVQCQN	0.822369	0.177631
Hill_BB_C7176	ATCDLLSPFKVGHAAACALHICALGRRGGWCDGRAVCNCR	0.011073	0.988927
Hill_BB_C2519	ATCDLLSPFKVGHAAACALHICALGRRGGWCDGRAVCNCR	0.020927	0.979073
Hill_BB_C8473	ATCDLLSPFKVGHAAACAVHICALGRRGGWCDGRAVCNCR	0.165217	0.834783
Hill_BB_C34351	AMCDLLSGLNMGSRVCMRCLKGRGGWCDQGVNCRV	0.029224	0.970776
Hill_BB_C4683	RPDNIEYLEDQVAELVRHKRLSCLFENEAIASALACGASCITRKRGGWCSNGVCHCTPN	0.224878	0.775122
Hill_BB_C4977	LSCWFENEDIKATACAMSCIYRKRGGRCENGICRTPN	0.106600	0.893400
Hill_BB_C13326	LSCLFENQAVSAIACGASCITRKRGGWCSNGVCRCTPN	0.701191	0.298809
Hill_BB_C7171	TTCDLISGTKIENIACAACIAMGHKGGYCNLSLICIR	0.952388	0.047612
Hill_BB_C10649	QFDNLEDTGVEEKVRHKRLTCLFDNRPIAFACGSNCVSRKGRGGWCVNGVCRCT	0.974103	0.025897
Hill_BB_C13792	KQSSDPESALYSIDHPRFRRLPCDYLSGLGFGEADACNTDCIAKGHKGSGFCTGLVCRCTRL	0.295265	0.704735
Hill_BB_C15867	VTCDLLKPFGRAPCMMHCIILRFRKRRTGFCRQNVVCR	0.182360	0.817640
NHill_AD_C69719	DVSIQSCVWGGSNVSDCNCECKRRYKGGHCGSFLNNICWCET	0.924393	0.075607
Hill_BB_C49430	APQFGGQIGGFGGGGGGGGGFPGGGFRPGGVAEFQESSSVNVERETFDQGGFEISDSSVTSVSSVESFRD	0.330011	0.669989

**Table 2.** Prediction of the anticancer activity through the iACP tool. From left to right are shown in order: peptide contig, peptide sequence, the anticancer and non-anticancer scores related to each sequence.

the hemolymph, are an essential part of the immune defense<sup>30,31</sup>. In this study, we focused on the gene level in order to identify all putative genes encoding AMPs (Fig. 3).

The transcriptomes of *H. illucens* larvae as well as the combined male and female adults were assembled, and all the obtained contigs were functionally annotated through the Blast2Go software resulting in the identification of 68 putative peptides of interest. These sequences were analyzed in silico through the CAMP database and the iACP online tool in order to evaluate their antimicrobial and anticancer activity, respectively. Additionally, the AVPPred and the Antifp servers were used to predict the antiviral and the antifungal activity, respectively, of the identified peptides. Our results led to the identification of 57 peptides, 13 of which were predicted as endowed with an antimicrobial activity, 22 with an antimicrobial and anticancer activity, eight with an antimicrobial and antiviral activity, two with an antimicrobial and antifungal activity, seven with an antimicrobial, anticancer and antiviral activity (Supplementary Table S1). Only one peptide was predicted as antimicrobial, antiviral and antifungal activity, whereas two peptides were predicted to have a putative antimicrobial, anticancer and antifungal activity (Supplementary Table S1). Surprisingly, two peptides, corresponding to Hill\_LB\_C16634 and NHill\_AD\_C69719 contigs, resulted positive to all activity predictions (Supplementary Table S1). Most of the identified peptides belong to defensins and cecropins families, whose composition ranges from 34 to 51 amino acids<sup>32,33</sup>. These peptides have a pattern of six cysteines, which are involved in the formation of three disulphide bonds, Cys1–Cys4, Cys2–Cys5 and Cys3–Cys6, for insect defensins<sup>34</sup>. Insect defensins are active against Gram-negative bacteria such as *Escherichia coli*, but mainly against Gram-positive bacteria, such as *Staphylococcus aureus*, *Micrococcus luteus*, *Bacillus subtilis*, *Bacillus thuringiensis*, *Aerococcus viridians* and *Bacillus megaterium*. Moreover, some insect defensins are also active against fungi<sup>35–39</sup>. For example, the royalisin peptide, isolated from the royal jelly of *Apis mellifera*, consists of 51 amino acids, and the six cysteine residues are involved in the formation of three disulphide bonds and are active against Gram-positive bacteria and fungi<sup>40</sup>. Defensin targets have not been identified yet, and studies of the structure–activity relationship could be useful to understand the molecular mechanism underlying their bioactivity<sup>41</sup>.

Cecropins were first purified from the moth *H. cecropia* and represent the most abundant family of linear  $\alpha$ -helical AMPs in insects, active against both Gram-negative and Gram-positive bacteria<sup>42</sup>. Insect cecropins, mainly derived from lepidopteran and dipteran species, are the cecropins A, B and D. These consist of 35–37 amino acids with no cysteine residues and are able to lyse the bacterial membrane and to reduce the proline uptake. For example, cecropin B, a linear cationic peptide consisting of 35 amino acids, reduces the lethality of *E. coli* load and plasma endotoxin levels, and also shows an antifungal activity against *Candida albicans*<sup>42,43</sup>. Moreover, a cecropin-like peptide was isolated from the salivary glands of the female mosquito *Aedes aegypti*,

Peptide	AVPpred: antiviral activity prediction					Antifp: antifungal activity prediction	
	AVP motif (model)	Alignment model	Composition model	Physio-chemical model	Overall prediction	Score	Prediction
Hill_BB_C14202	-	Non-AVP	53.26	64.08	Yes	0.20892203	Non-antifungal
Hill_BB_C3566	-	Non-AVP	42.65	64.08	No	0.26737087	Non-antifungal
Hill_BB_C1152	-	Non-AVP	31.33	64.08	No	-0.21250625	Non-antifungal
Hill_BB_C1153	-	Non-AVP	38.83	64.08	No	-0.37506205	Non-ANTIFUNGAL
Hill_BB_C2676	-	Non-AVP	46.61	64.08	No	-0.17216018	Non-antifungal
Hill_BB_C269	-	Non-AVP	52.07	64.08	Yes	-0.025392142	Non-antifungal
Hill_BB_C1169	-	Non-AVP	44.47	64.08	No	0.072220496	Non-antifungal
Hill_BB_C779	-	Non-AVP	41.2	64.08	No	-0.33302841	Non-antifungal
Hill_LB_C36111	-	Non-AVP	40.25	64.08	No	-0.21911853	Non-antifungal
Hill_LB_C12085	-	Non-AVP	42.31	64.08	No	0.139426	Non-antifungal
Hill_BB_C1290	-	Non-AVP	31.53	64.08	No	0.11095482	Non-antifungal
Hill_BB_C7347	-	Non-AVP	39.24	64.12	No	-0.040857298	Non-antifungal
Hill_BB_C9109	-	Non-AVP	23.7	64.08	No	-0.068718526	Non-antifungal
Hill_BB_C11804	-	Non-AVP	39.24	64.12	No	-0.040857298	Non-antifungal
Hill_BB_C309	-	Non-AVP	48.85	64.73	No	0.065455296	Non-antifungal
Hill_BB_C1827	-	Non-AVP	46.85	49.78	No	0.73998352	Antifungal
Hill_BB_C5878	Yes	Non-AVP	50.55	67.39	Yes	-0.16644401	Non-antifungal
Hill_BB_C8756	-	Non-AVP	26.31	64.08	No	-0.34776804	Non-antifungal
Hill_BB_C13793	-	Non-AVP	42.66	64.09	No	0.25709331	Non-antifungal
NHill_AD_C73537	-	Non-AVP	33.7	63.94	No	-0.36753515	Non-antifungal
NHill_AD_C16493	-	Non-AVP	34.66	64.07	No	-0.43908213	Non-antifungal
NHill_AD_C12927	-	Non-AVP	39.89	64.07	No	-0.47185039	Non-antifungal
NHill_AD_C12928	-	Non-AVP	40.33	64.09	No	-0.40020762	Non-antifungal
NHill_AD_C4669	-	Non-AVP	36.71	63.87	No	-0.031971647	Non-antifungal
Hill_BB_C3195	-	Non-AVP	37.43	64.08	No	-0.24406508	Non-antifungal
Hill_SB_C698	-	Non-AVP	33.23	64.07	No	-0.43908213	Non-antifungal
Hill_SB_C2730	-	Non-AVP	39.88	64.09	No	-0.38062322	Non-antifungal
Hill_SB_C1875	-	Non-AVP	34.95	63.96	No	-0.22572859	Non-antifungal
Hill_BB_C5151	-	Non-AVP	31.71	64.03	No	-0.34876968	Non-antifungal
Hill_BB_C390	-	Non-AVP	52.45	64.08	Yes	-0.67921544	Non-antifungal
NHill_AD_C53857	-	Non-AVP	51.96	65.69	Yes	0.12385895	Non-antifungal
NHill_AD_C49215	-	Non-AVP	46.35	65.52	No	0.2406468	Non-antifungal
Hill_BB_C2323	-	Non-AVP	19.92	64.08	No	-0.10977439	Non-antifungal
Hill_BB_C7345	-	Non-AVP	26.56	47.85	No	-0.87408278	Non-antifungal
Hill_BB_C7346	-	Non-AVP	23.75	64.08	No	-0.059453989	Non-antifungal
Hill_BB_C11803	-	Non-AVP	28.99	64.08	No	-0.052337869	Non-antifungal
Hill_BB_C21232	-	Non-AVP	44.14	64.08	No	-0.070217673	Non-antifungal
NHill_AD_C17624	-	Non-AVP	23.01	64.08	No	-0.15660532	Non-antifungal
Hill_LB_C16634	-	Non-AVP	53.29	64.88	Yes	0.7067461	Antifungal
Hill_LB_C37730	-	Non-AVP	34.85	64.08	No	0.38202837	Non-antifungal
Hill_BB_C46948	-	Non-AVP	48.59	64.22	No	0.71418843	antifungal
Hill_BB_C16137	-	Non-AVP	28.08	64.08	No	0.010457995	Non-antifungal
Hill_BB_C16883	-	Non-AVP	25.14	64.08	No	-0.52680116	Non-antifungal
Hill_BB_C10074	-	Non-AVP	12.45	64.08	No	-0.19881079	Non-antifungal
Hill_BB_C9237	-	Non-AVP	28.71	64.08	No	0.32515345	Non-antifungal
NHill_AD_C40487	-	Non-AVP	28.54	64.08	No	0.37181457	Non-antifungal
Hill_BB_C7758	-	Non-AVP	61.82	64.18	Yes	0.18741319	Non-antifungal
Hill_BB_C14087	Yes	Non-AVP	63.07	66.59	Yes	0.10302883	Non-antifungal
Hill_LB_C29142	-	Non-AVP	52.07	64.12	Yes	0.33363813	Non-antifungal
Hill_BB_C308	-	Non-AVP	48.85	64.73	No	0.065455296	Non-antifungal
Hill_BB_C1619	Yes	Non-AVP	52.47	68.2	Yes	-0.12761437	Non-antifungal
Hill_BB_C1826	-	Non-AVP	46.42	49.91	No	0.2129187	Non-antifungal
Hill_BB_C6571	-	Non-AVP	49.54	67	No	0.5009657	Antifungal
Hill_BB_C7081	-	Non-AVP	51.03	64.65	Yes	0.35232096	Non-antifungal
Hill_BB_C7985	-	Non-AVP	48.06	65.99	No	0.44711187	Non-antifungal

Continued

Peptide	AVPpred: antiviral activity prediction					Antifp: antifungal activity prediction	
	AVP motif (model)	Alignment model	Composition model	Physio-chemical model	Overall prediction	Score	Prediction
Hill_BB_C7176	-	Non-AVP	55.82	64.95	Yes	0.27115344	Non-antifungal
Hill_BB_C2519	-	Non-AVP	53.4	64.85	Yes	0.27115344	Non-antifungal
Hill_BB_C8473	-	Non-AVP	47.7	64.69	No	0.21172458	Non-antifungal
Hill_BB_C34351	-	Non-AVP	50.25	64.13	Yes	0.10334371	Non-antifungal
Hill_BB_C4683	-	Non-AVP	39.94	64.09	No	-0.25553273	Non-antifungal
Hill_BB_C4977	-	Non-AVP	52.52	65.92	Yes	0.0078493215	Non-antifungal
Hill_BB_C13326	Yes	Non-AVP	56.26	68.51	Yes	-0.21725812	Non-antifungal
Hill_BB_C7171	-	Non-AVP	44.07	64.19	No	0.21225639	Non-antifungal
Hill_BB_C10649	-	Non-AVP	45.72	64.11	No	-0.13179766	Non-antifungal
Hill_BB_C13792	-	Non-AVP	47.38	64.08	No	1.0166485	Antifungal
Hill_BB_C15867	-	Non-AVP	66.1	63.61	Yes	0.70687492	Antifungal
NHill_AD_C69719	Yes	Non-AVP	47.27	64.08	Yes	0.91354184	Antifungal
Hill_BB_C49430	-	Non-AVP	33.03	64.08	No	-0.36274044	Non-antifungal

**Table 3.** Results obtained with the AVPpred server for the antiviral activity prediction and with Antifp server for the antifungal activity prediction. From left to right are shown in order: peptide contig, AVP motif model results, alignment model results, composition model results, the physio-chemical model results, the overall results for the antiviral prediction, antifungal score and prediction result for the antifungal activity.

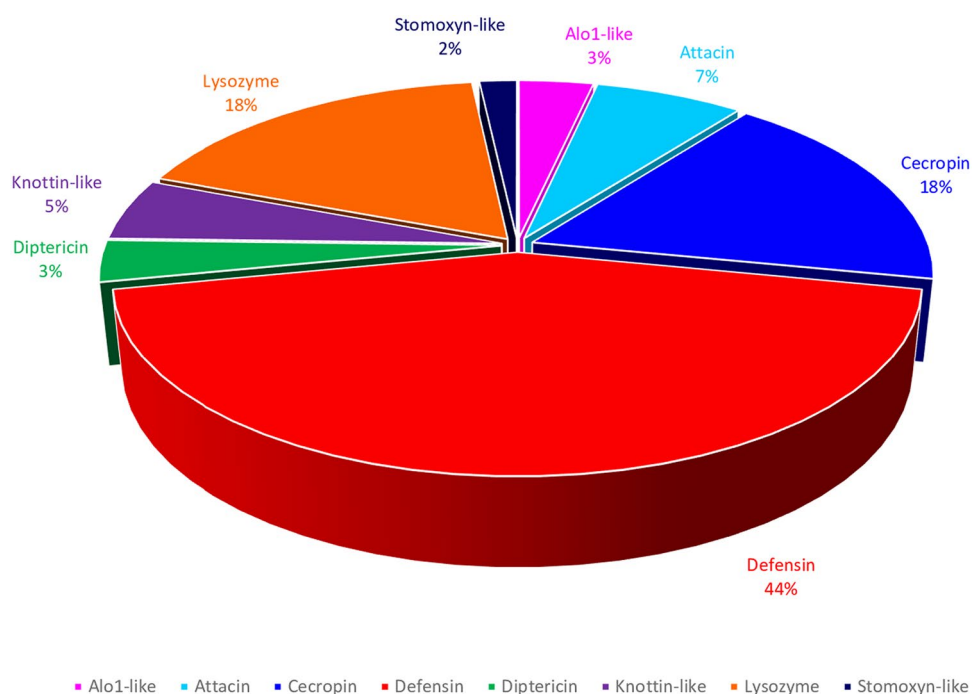


**Figure 1.** Graphic representation of the identified AMP classes from larvae and adult transcriptomes. The pie chart shows that the largest number of identified peptides belongs to the class of defensins.

showing antiviral activity against the Dengue virus. Glycine residue is the most spread among the peptides that we identified and is particularly related to Attacin proteins<sup>44,45</sup>. Although the mechanism of action of the different AMPs has not yet been fully elucidated, it appears that AMPs, unlike antibiotics, have more difficulty in causing a microbial resistance, and most of them do not destroy normal cells of higher animals<sup>46</sup>. Recently, it has been demonstrated that the clavaspirin peptide from tunicate *Styela clava* exhibits the ability to kill drug-resistant pathogens, such as *S. aureus*, without a detectable resistance<sup>47</sup>. Moreover, it was demonstrated that two proline rich peptides (Lser-PRP2 and Lser-PRP3) do not interfere with protein synthesis but both were able to bind the bacterial chaperone DnaK and are therefore able to inhibit protein folding<sup>48</sup>. The characteristics of AMPs make them excellent candidates for the development of new drugs.

The bioinformatic approach represents a powerful tool to predict the physicochemical properties and the putative function of amino acid sequences. However, we aimed to go beyond the simple functional annotation which typically exclusively relies on sequence similarities to peptides deposited in public databases. Indeed,

Peptide	Lenght (aa)	Molecular weight (g/mol)	Total hydrophobic Ratio (%)	Total net charge	pI	Boman Index (kcal/mol)
Hill_BB_C14202	121	14,282.443	38	+9	9.32	2.14
Hill_BB_C3566	131	14,871.993	36	+6	8.99	1.87
Hill_BB_C1152	126	14,259.799	38	-5	5.55	1.8
Hill_BB_C1153	112	13,084.607	37	+1	7.84	2.37
Hill_BB_C2676	122	13,394.838	41	-5	3.80	0.88
Hill_BB_C269	119	13,730.8	36	+8	9.24	2.26
Hill_BB_C1169	77	8763.954	37	+4	8.80	1.59
Hill_BB_C779	107	12,074.699	42	+1	7.76	1.32
Hill_LB_C36111	121	14,214.145	37	+2	8.15	2.13
Hill_LB_C12085	84	9307.51	38	0	6.88	1.45
Hill_BB_C1290	77	8480.598	29	+4	9.30	1.39
Hill_BB_C309	40	4422.19	42	+3	8.67	1.83
Hill_BB_C1827	31	3686.457	41	+6	9.38	2.53
Hill_BB_C5878	40	4204.904	45	+4	8.98	1.56
Hill_BB_C13793	61	6712.597	34	0	6.88	2.22
NHill_AD_C73537	49	5259.014	36	+4	10.43	1.49
NHill_AD_C16493	51	5404.099	37	+4	10.93	1.63
NHill_AD_C12927	46	4969.69	36	+4	10.93	1.65
NHill_AD_C12928	46	5024.777	36	+5	11.83	1.78
NHill_AD_C4669	44	4670.398	40	+5	11.07	1.32
Hill_BB_C3195	44	4726.506	40	+5	11.07	1.16
Hill_SB_C698	51	5476.163	35	+3	10.26	1.78
Hill_SB_C2730	46	4997.744	36	+4	10.93	1.60
Hill_SB_C1875	50	5312.123	36	+5	11.00	1.61
Hill_BB_C5151	55	5823.746	36	+6	11.47	1.61
NHill_AD_C53857	34	3679.079	26	0	6.70	2.23
NHill_AD_C49215	36	3985.541	33	+5	9.18	2.69
Hill_BB_C21232	82	9053.427	34	+5	9.46	1.32
Hill_LB_C16634	32	3531.395	53	+6	9.18	0.75
Hill_LB_C37730	90	10,059.611	38	-2	5.17	1.93
Hill_BB_C46948	30	3390.071	33	+8	9.64	2.58
Hill_BB_C16137	86	8328.081	34	+2	9.98	1.11
Hill_BB_C16883	164	17,080.992	32	+5	9.89	1.51
Hill_BB_C9237	186	18,942.725	34	+6	10.36	1.52
NHill_AD_C40487	176	17,910.512	34	+4	9.87	1.52
Hill_BB_C7758	39	4089.842	56	+1	7.81	0.07
Hill_BB_C14087	40	4501.427	47	+3	8.69	1.28
Hill_LB_C29142	40	4275.055	50	+6	9.38	1.72
Hill_BB_C308	40	4422.19	42	+3	8.67	1.83
Hill_BB_C1619	40	4183.84	45	+3	8.69	1.7
Hill_BB_C1826	32	3752.517	40	+6	9.43	2.7
Hill_BB_C6571	32	3597.19	37	+5	9.18	2.7
Hill_BB_C7081	39	4055.809	51	+1	7.83	0.55
Hill_BB_C7985	31	3233.819	45	+3	8.70	1.18
Hill_BB_C7176	40	4259.049	52	+4	8.98	1.45
Hill_BB_C2519	40	4277.088	52	+4	8.98	1.52
Hill_BB_C8473	40	4249.98	52	+2	8.37	1.62
Hill_BB_C34351	40	4330.189	50	+2	8.36	1.46
Hill_BB_C4683	61	6736.674	39	+1	7.79	2.25
Hill_BB_C4977	40	4486.229	40	+3	8.66	2.33
Hill_BB_C13326	40	4162.859	45	+4	8.96	1.35
Hill_BB_C7171	39	4099.862	48	+1	7.54	0.64
Hill_BB_C10649	56	6263.181	37	+4	7.54	2.58
Hill_BB_C13792	61	6725.639	34	+1	7.78	2.17
Hill_BB_C15867	39	4566.65	51	+7	9.69	1.68
NHill_AD_C69719	44	4763.313	34	+1	6.71	1.66
Hill_BB_C390	55	5182.986	60	-6	4.06	-



**Table 4.** Prediction of physicochemical properties using the Antimicrobial Peptide Database Calculator and Predictor (APD3) and the Compute pI/Mw tool—Expasy. From left to right are shown in order: peptide contig, the peptide length, the molecular weight, the total hydrophobic ratio, the total net charge, the isoelectric point (pI) and the Boman index.

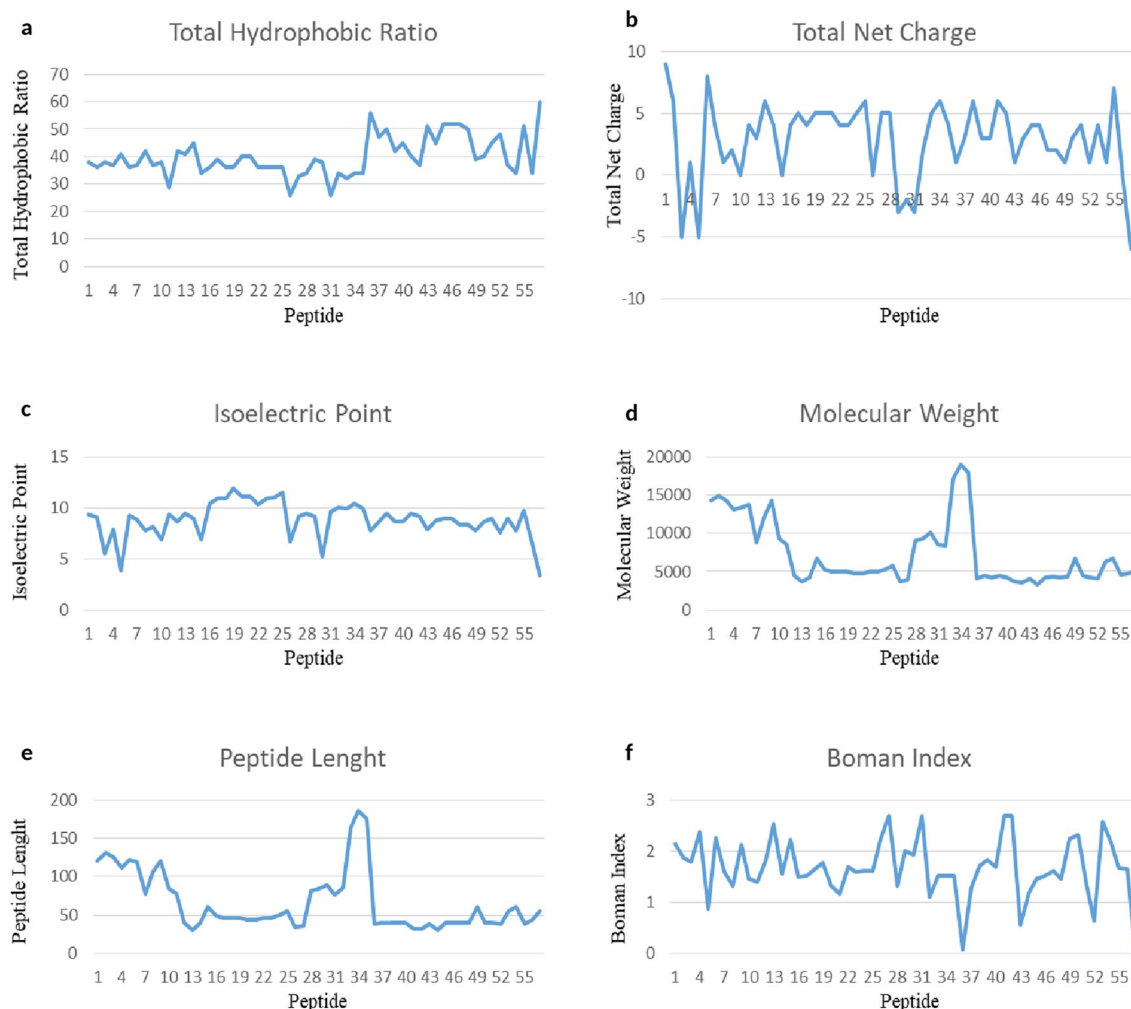


**Figure 2.** Graphical representation of the physicochemical properties of the 57 peptides with putative activity: (a) total hydrophobic ratio; (b) total net charge; (c) isoelectric point; (d) molecular weight; (e) peptide length; (f) Boman Index.

the approach we reported is based on the use of several softwares, previously employed to perform similar analyses<sup>49–51</sup>, that exploit different algorithms for the determination of a score that predicts the biological activity of unknown peptides. We demonstrated that a similar approach can provide reliable indications about the potential biological activities of candidate AMPs, as confirmed by our preliminary tests on the antimicrobial activity of four identified AMPs (Supplementary Fig. 2). However, validation studies were out of the scope of this study which was essentially aimed to identify a set of candidate peptides which could serve as a starting point for subsequent functional characterization of *H. illucens* AMPs by our group, as well as by other researchers in the field. Indeed, following the *in silico* analysis, the largest peptides could be produced by recombinant methodologies while chemical synthesis could be used for smaller ones. Structural analysis could be performed through mass spectrometry and circular dichroism (CD) and the biological activity could be evaluated by *in vitro* tests. The produced peptides, in fact, could be tested *in vitro* to validate their activity against different bacterial strains, both Gram-negative and Gram-positive bacteria, cancer cell lines, and fungi. Moreover, the peptides showing interesting biological activities, could be produced in fusion with suitable tags to investigate their mechanism of action through functional proteomics experiments and advanced mass spectrometry methodologies, in order to characterise their interaction(s) with target protein (mainly components of the biological membranes), thus identifying the possible protein targets.

Amino acid composition of peptides identified in <i>Hermetia illucens</i>			Amino acid composition of patent AMPs in the APD database
Amino acid three letter code	Amino acid frequency	Amino acid composition (%)	Amino acid composition (%)
Ala	297	7.98816	7.61
Arg	230	6.18612	5.81
Asn	258	6.93921	3.85
Asp	142	3.81926	2.65
Cys	262	7.04679	6.86
Glu	113	3.03927	2.69
Gln	166	4.46477	2.57
Gly	406	10.91985	11.56
His	89	2.39376	2.16
Ile	175	4.70683	5.93
Leu	242	6.50888	8.34
Lys	205	5.51372	9.55
Met	42	1.12964	1.25
Phe	143	3.84615	4.08
Pro	124	3.33513	4.69
Ser	270	7.26197	6.07
Thr	168	4.51856	4.51
Trp	85	2.28617	1.64
Tyr	85	2.28617	2.48
Val	216	5.80957	5.7
Total	3718	100	100

**Table 5.** Amino acid frequency and amino acid composition of the identified peptides. As it is shown, the Gly, Ala, Arg, Asn, Cys, Leu, Ser residues are the most abundant, whereas the lowest content is associated with the His, Met, Trp, Tyr residues.

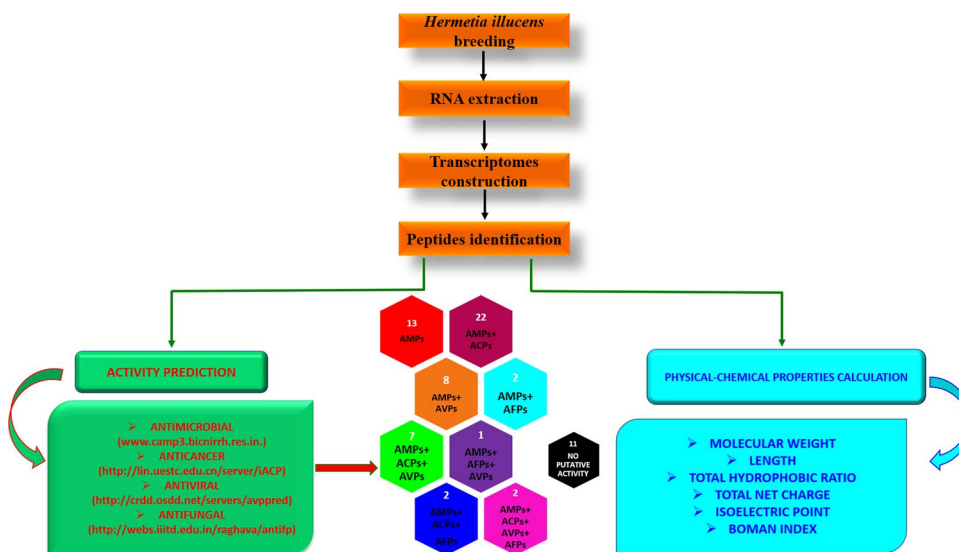


**Figure 3.** Strategies carried out in order to identify peptides from *Hermetia illucens* insect.

## Materials and methods

**Rearing of *Hermetia illucens* and RNA isolation.** *Hermetia illucens* larvae were reared on different diets in order to minimize the possible effect of a specific substrate on the expression of peptides, according to the protocol adopted by Vogel et al.<sup>52</sup> The adults were reared in an environmental chamber under controlled conditions: temperature  $27 \pm 1.0$  °C, humidity  $70\% \pm 5\%$ , and a photoperiod of 12:12 h [L:D]. Since it is not clear whether all AMPs are expressed in a similar fashion across different larval instars, RNA was obtained from two different instars, in order to identify the maximum number of expressed AMPs. Thus, using the TRI Reagent following the manufacturer's instructions (Sigma, St. Louis, Missouri, USA), RNA was extracted from adults

total body and from two larval stages: 2<sup>nd</sup> and 5<sup>th</sup> instar larvae whose isolated RNA was subsequently pooled in a 1:1 ratio for RNAseq. A DNase (Turbo DNase, Ambion Austin, Texas, USA) treatment was carried out to eliminate any contaminating DNA. After the DNase enzyme removal, the RNA was further purified using the RNeasy MinElute Clean up Kit (Qiagen, Venlo, Netherlands) following the manufacturer's protocol, and eluted in 20  $\mu$ L of RNA Storage Solution (Ambion Austin, Texas, USA). The RNA integrity was verified on an Agilent 2100 Bioanalyzer using the RNA Nano chips (Agilent Technologies, Palo Alto, CA), and the RNA quantity was determined by a Nanodrop ND1000 spectrophotometer.

**RNA-Seq, de novo larvae and combined adult male and female transcriptomes assembly and gene identification.** The transcriptome sequencing of all RNA samples was performed with a poly(A)<sup>+</sup> enriched mRNA fragmented to an average of 150 nucleotides. The sequencing was carried out by the Max Planck Genome Center (<https://mpgc.mpiiz.mpg.de/home/>) using standard TruSeq procedures on an Illumina HiSeq2500 sequencer. The de novo transcriptome assembly was carried out using a CLC Genomics Workbench v7.1 (<https://www.clcbio.com>) which is designed to assemble large transcriptomes using sequences from short-read sequencing platforms. All obtained sequences (contigs) were used as queries for a BLASTX search<sup>53</sup> in the 'National Center for Biotechnology Information' (NCBI) non-redundant (nr) database, considering all hits with an E-value cut-off of  $10^{-5}$ . The transcriptomes were annotated using BLAST, Gene Ontology, and InterProScan searches using Blast2GO PRO v2.6.1 (<https://www.blast2go.de>)<sup>54</sup>. To optimize the annotation of the obtained data, GO slim was used, a subset of GO terms that provides a higher level of annotations and allows a more global view of the result. Candidate AMP genes were identified through an established reference set of insect-derived AMPs and lysozymes, and additional filtering steps to avoid interpreting incomplete genes or allelic variants as further AMP genes<sup>52</sup>.

**In silico analysis for the antimicrobial, anticancer, antiviral and antifungal activity prediction.** The sequences, functionally annotated as antimicrobial peptides by the Blast2Go software, were analysed with Prop 1.0<sup>55</sup> and Signal P 4.0<sup>56</sup> Servers in order to identify the signal peptide and the pro-peptide region. The mature and active peptide regions were analysed in silico by four machine-learning algorithms, available on the CAMP database<sup>57</sup>: Support Vector Machine (SVM), Discriminant Analysis (DA), Artificial Neural Network (ANN), and Random Forest (RF), in order to predict their antimicrobial activity. The minimum calculated threshold for a sequence in order to be considered antimicrobial is 0.5<sup>67–69</sup>. When all the sequences were analyzed with the algorithms, the ones with a score higher than 0.5 were automatically considered putative antimicrobials by the software. We would like to point out that the threshold is intrinsically set by the software, and can't be modified by the user. This is true for the SVM, RF and DA algorithms that report the result in a numerical form (score) while the ANN algorithm provides the results as categories, namely either AMP (antimicrobial) or NAMP (not-antimicrobial). All sequences that showed a positive result with all four statistical methods, were considered as antimicrobial. The iACP tool<sup>58–62</sup> was used to predict the anticancer activity of the same sequences, providing the results in a numerical form. The prediction of the antiviral activity was performed in silico with the online server AVPPred. It exploits four different models: (1) the AVP motif, which returns the result as YES or NO; (2) the Alignment model, which gives the result in the form AVP or Non-AVP; (3) the Composition model and the (4) the Physico-chemical model, which return their results in a numerical form (percentage). The overall result is expressed with a YES, if the peptide results have a putative antiviral activity, and with a NO, if otherwise<sup>63</sup>. The Antifp server was used to predict the antifungal activity, and provides the result as a numerical score<sup>64</sup>. For this analysis, a threshold of 0.5 was used.

**Evaluation of the physicochemical properties.** The corresponding physicochemical properties of identified putative active peptides following an in silico analysis, such as peptide length, molecular weight, total hydrophobic ratio, total net charge, isoelectric point, and the Boman Index, were determined by the Antimicrobial Peptide Database Calculator and Predictor (APD3)<sup>65–67</sup> and the Compute pI/Mw tool—Expasy<sup>68, 69</sup>.

**Bacterial cell growth and viability.** Four putative antimicrobial peptides, namely Hill\_BB\_C6571, Hill\_BB\_C16634, Hill\_BB\_C46948 and Hill\_BB\_C7985, that showed high antimicrobial score values with all prediction softwares were selected and chemically synthesised (Bio-Fab Research, Rome, Italy). *E. coli* cells were incubated overnight in LB medium at 37 °C. The culture was then diluted to a concentration of 0.08 OD<sub>600</sub>/mL in fresh medium and grown at 37 °C for 90 min. At an OD/mL value of 0.5, the antimicrobial peptides were added to the culture at a final concentration of 3 or 12  $\mu$ M. Growth of the culture was evaluated every 20 min for a total of 120 min by assessing absorbance at 600 nm.

Cell viability was evaluated by enumerating Colony Forming Units (CFU) after 16 h of incubation with 3  $\mu$ M of each peptide. Serial dilutions of bacterial cultures up to a concentration of  $10^{-6}$  cells both for treated and untreated samples were prepared. Finally, 100  $\mu$ L of each sample was plated on LB agar every 20 min for a total of 100 min. Plates were incubated for 16 h at 37 °C and the CFUs occurring on each plate were then counted. Experiments were performed in triplicate.

Received: 13 May 2020; Accepted: 21 September 2020

Published online: 09 October 2020

## References

- Hillyer, J. F. Insect immunology and hematopoiesis. *Dev. Comp. Immunol.* **58**, 102–118 (2016).

2. Tsakas, S. & Marmaras, V. J. Insect immunity and its signalling: An overview. *Invert. Surviv. J.* **7**, 228–238 (2010).
3. Marmaras, V. J. & Lampropoulou, M. Regulators and signalling in insect haemocyte immunity. *Cell Signal.* **21**, 186–195 (2009).
4. Brandenburg, L. O., Merres, J., Albrecht, L. J., Varoga, D. & Pufe, T. Antimicrobial peptides: Multifunctional drugs for different applications. *Polymers.* **4**, 539–560 (2012).
5. Lavine, M. D. & Strand, M. R. Insect hemocytes and their role in immunity. *Insect. Biochem. Mol. Biol.* **32**, 1295–1309 (2002).
6. Hoskin, D. W. & Ramamoorthy, A. Studies on anticancer activities of antimicrobial peptides. *BBA Biomembr.* **1778**, 357–375 (2008).
7. Steiner, H., Hultmark, D., Engström, Å., Bennich, H. & Boman, H. G. Sequence and specificity of two antibacterial proteins involved in insect immunity. *Nature* **292**, 246–248 (1981).
8. Otvos, L. Jr. Antibacterial peptides isolated from insects. *J. Pep. Sci.* **6**, 497–511 (2000).
9. Wimley, W. C. & Hristova, K. Antimicrobial peptides: Successes, challenges and unanswered questions. *J. Memb. Biol.* **239**, 27–34 (2011).
10. Gaspar, D., Veiga, A. S. & Castanho, M. A. From antimicrobial to anticancer peptides. A review. *Front. Microbiol.* **4**, 294 (2013).
11. Schweizer, F. Cationic amphiphilic peptides with cancer-selective toxicity. *Eur. J. Pharmacol.* **625**, 190–194 (2009).
12. Epanand, R. M. & Vogel, H. J. Diversity of antimicrobial peptides and their mechanisms of action. *BBA Biomembr.* **1462**, 11–28 (1999).
13. Guilhelmelli, F. *et al.* Antibiotic development challenges: The various mechanisms of action of antimicrobial peptides and of bacterial resistance. *Front. Microbiol.* **4**, 353 (2013).
14. Le, C. F., Fang, C. M. & Sekaran, S. D. Intracellular targeting mechanisms by antimicrobial peptides. *Antimicrob. Agents Chemother.* **61**, e02340-e2416 (2017).
15. Vilcinskis, A., Krishnendu, M. & Vogel, H. Expansion of the antimicrobial peptide repertoire in the invasive ladybird *Harmonia axyridis*. *P. Roy. Soc. B.* **280**, 20122113 (2013).
16. Di Somma, A. *et al.* The antimicrobial peptide Temporin L impairs *E. coli* cell division by interacting with FtsZ and the divisome complex. *Biochim. Biophys. Acta Gen. Subj.* **1864**, 129606 (2020).
17. Gerardo, N. M. *et al.* Immunity and other defenses in pea aphids, *Acyrtosiphon pisum*. *Genome Biol.* **11**, R21 (2010).
18. Makkar, H. P., Tran, G., Heuzé, V. & Ankers, P. State-of-the-art on use of insects as animal feed. *Anim. Feed. Sci. Tech.* **197**, 1–33 (2014).
19. Thomas, S., Karnik, S., Barai, R. S., Jayaraman, V. K. & Idicula-Thomas, S. CAMP: A useful resource for research on antimicrobial peptides. *Nucleic Acids Res.* **38**, D774–D780 (2009).
20. Liaw, A. & Wiener, M. Classification and regression by RandomForest. *R News.* **2**, 18–22 (2002).
21. Müller, K. R., Mika, S., Ratsch, G., Tsuda, K. & Schölkopf, B. An introduction to kernel-based learning algorithms. *IEEE T. Neural Netw.* **12**, 181–201 (2001).
22. Kulkarni, A., Jayaraman, V. K. & Kulkarni, B. D. Support vector classification with parameter tuning assisted by agent-based technique. *Comput. Chem. Eng.* **28**, 311–318 (2004).
23. Vogel, H., Müller, A., Heckel, D. G., Gutzzeit, H. & Vilcinskis, A. Nutritional immunology: diversification and diet-dependent expression of antimicrobial peptides in the black soldier fly *Hermetia illucens*. *Dev. Comp. Immunol.* **78**, 141–148 (2018).
24. Hu, H. *et al.* Broad activity against porcine bacterial pathogens displayed by two insect antimicrobial peptides moricin and cecropin B. *Mol. Cells.* **35**, 106–114 (2013).
25. Jozefiak, A. & Engberg, R. M. Insect proteins as a potential source of antimicrobial peptides in livestock production. A review. *J. Anim. Feed Sci.* **26**, 87–99 (2017).
26. Bechinger, B. & Gorr, S. U. Antimicrobial peptides: Mechanisms of action and resistance. *J. Dent. Res.* **96**, 254–260 (2017).
27. Oñate-Garzón, J. *et al.* Antimicrobial activity and interactions of cationic peptides derived from *Galleria mellonella* cecropin D-like peptide with model membranes. *J. Antibiot.* **70**, 238–245 (2017).
28. Yeaman, M. R. & Yount, N. Y. Mechanisms of antimicrobial peptide action and resistance. *Pharmacol. Rev.* **55**, 27–55 (2003).
29. Hirsch, R. *et al.* Antimicrobial peptides from rat-tailed maggots of the drone fly *Eristalis tenax* show potent activity against multidrug-resistant gram-negative bacteria. *Microorganisms.* **8**, E626 (2020).
30. Bulet, P. & Hetru, C. Antimicrobial peptides in insects: Structure and function. *Dev. Comp. Immunol.* **23**, 329–344 (1999).
31. Hoffmann, J. A. & Reichhart, J. M. *Drosophila* innate immunity: An evolutionary perspective. *Nat. Immunol.* **3**, 121–126 (2002).
32. Yi, H. Y., Chowdhury, M., Huang, Y. D. & Yu, X. Q. Insect antimicrobial peptides and their applications. *Appl. Microbiol. Biotechnol.* **98**, 5807–5822 (2014).
33. Yamada, K. & Natori, S. Purification, sequence and antibacterial activity of two novel sapecin homologues from *Sarcophaga embryonic* cells: Similarity of sapecin B to charybdotoxin. *Biochem. J.* **291**, 275–279 (1993).
34. Bachère, E., Destoumieux, D. & Bulet, P. Penaeidins, antimicrobial peptides of shrimp: A comparison with other effectors of innate immunity. *Aquaculture* **191**, 71–88 (2000).
35. Hirsch, R. *et al.* Profiling antimicrobial peptides from the medical maggot *Lucilia sericata* as potential antibiotics for MDR Gram-negative bacteria. *J. Antimicrob. Chemother.* **74**, 96–107 (2019).
36. Hetru, C., Troxler, L. & Hoffmann, J. A. *Drosophila melanogaster* antimicrobial defense. *J. infect. Dis.* **187**, S327–S334 (2003).
37. Lehane, M. J., Wu, D. & Lehane, S. M. Midgut-specific immune molecules are produced by the blood-sucking insect *Stomoxys calcitrans*. *Proc. Nat. Acad. Sci.* **94**, 11502–11507 (1997).
38. Ueda, K., Imamura, M., Saito, A. & Sato, R. Purification and cDNA cloning of an insect defensin from larvae of the longicorn beetle, *Acalolepta luxuriosa*. *Appl. Entomol. Zool.* **40**, 335–345 (2005).
39. Thevissen, K., Kristensen, H. H., Thomma, B. P., Cammue, B. P. & Francois, I. E. Therapeutic potential of antifungal plant and insect defensins. *Drug Discov Today.* **12**, 966–971 (2007).
40. Fujiwara, S. *et al.* A potent antibacterial protein in royal jelly. Purification and determination of the primary structure of royalisin. *J. Biol. Chem.* **265**, 11333–11337 (1990).
41. Wu, Q., Patočka, J. & Kuča, K. Insect antimicrobial peptides, a mini review. *Toxins.* **10**, 461 (2018).
42. Andrä, J., Berninghausen, O. & Leippe, M. Cecropins, antibacterial peptides from insects and mammals, are potently fungicidal against *Candida albicans*. *Med. Microbiol. Immunol.* **189**, 169–173 (2001).
43. Srisailam, S., Arunkumar, A. I., Wang, W., Yu, C. & Chen, H. M. Conformational study of a custom antibacterial peptide cecropin B1: Implications of the lytic activity. *BBA-Protein Struct. Mol. Enzym.* **1479**, 275–285 (2000).
44. Hedengren, M., Borge, K. & Hultmark, D. Expression and evolution of the *Drosophila* attacin/diptericin gene family. *Biochem. Biophys. Res. Co.* **279**, 574–581 (2000).
45. Sun, S. C., Asling, B. & Faye, I. Organization and expression of the immunoresponsive lysozyme gene in the giant silk moth, *Hyalophora cecropia*. *J. Biol. Chem.* **266**, 6644–6649 (1991).
46. Luplertlop, N. *et al.* Induction of a peptide with activity against a broad spectrum of pathogens in the *Aedes aegypti* salivary gland, following infection with dengue virus. *PLoS Pathog.* **7**, e1001252 (2011).
47. Akbari, R. *et al.* Highly synergistic effects of melittin with conventional antibiotics against multidrug-resistant isolates of *acinetobacter baumannii* and *pseudomonas aeruginosa*. *Microb. Drug Resist.* **25**, 193–202 (2019).
48. Cytryńska, M. *et al.* Proline-rich antimicrobial peptides in medicinal maggots of *Lucilia sericata* interact with bacterial DnaK but do not inhibit protein synthesis. *Front. Pharmacol.* **11**, 532 (2020).
49. Grafskaia, E. N. *et al.* Discovery of novel antimicrobial peptides: A transcriptomic study of the sea anemone *Cnidopus japonicus*. *J. Bioinform. Comput. Biol.* **16**, 1840006 (2018).
50. Pavlova, A. S. *et al.* Identification of antimicrobial peptides from novel *Lactobacillus fermentum* strain. *Protein J.* **39**, 73–84 (2020).

51. Waghu, F. H. & Idicula-Thomas, S. Collection of antimicrobial peptides database and its derivatives: Applications and beyond. *Protein Sci.* **29**, 36–42 (2020).
52. Altschul, S. F. *et al.* Gapped BLAST and PSI-BLAST: A new generation of protein database search programs. *Nucleic Acids Res.* **25**, 3389–3402 (1997).
53. Götz, S. *et al.* High-throughput functional annotation and data mining with the Blast2GO suite. *Nucleic Acids Res.* **36**, 3420–3435 (2008).
54. Vogel, H., Badapanda, C., Knorr, E. & Vilcinskas, A. RNA-sequencing analysis reveals abundant developmental stage-specific and immunity-related genes in the pollen beetle *M. elygethes aeneus*. *Insect Mol. Biol.* **23**, 98–112 (2014).
55. Duckert, P., Brunak, S. & Blom, N. Prediction of proprotein convertase cleavage sites. *Protein Eng. Des. Sel.* **17**, 107–112 (2004).
56. Petersen, T. N., Brunak, S., Von Heijne, G. & Nielsen, H. SignalP 4.0: Discriminating signal peptides from transmembrane regions. *Nat. Methods.* **8**, 785 (2011).
57. Waghu, F. H., Barai, R. S., Gurung, P. & Idicula-Thomas, S. CAMPR3: A database on sequences, structures and signatures of antimicrobial peptides. *Nucleic Acids Res.* **44**, D1094–D1097 (2016).
58. Chen, W., Ding, H., Feng, P., Lin, H. & Chou, K. C. iACP: A sequence-based tool for identifying anticancer peptides. *Oncotarget.* **7**, 16895–16909 (2016).
59. Feng, P. M., Chen, W., Lin, H. & Chou, K. C. iHSP-PseRAAAC: Identifying the heat shock protein families using pseudo reduced amino acid alphabet composition. *Anal. Biochem.* **442**, 118–125 (2013).
60. Ding, H. *et al.* iCTX-type: A sequence-based predictor for identifying the types of conotoxins in targeting ion channels. *BioMed Res. Int.* **2014**, 286419 (2014).
61. Chou, K. C. Some remarks on protein attribute prediction and pseudo amino acid composition. *J. Theor. Biol.* **273**, 236–247 (2011).
62. Chou, K. C. Prediction of protein cellular attributes using pseudo-amino acid composition. *PROTEINS.* **43**, 246–255 (2001).
63. Thakur, N., Qureshi, A. & Kumar, M. AVPPred: Collection and prediction of highly effective antiviral peptides. *Nucleic Acids Res.* **40**, W199–W204 (2012).
64. Agrawal, P. *et al.* In silico approach for prediction of antifungal peptides. *Front. Microbiol.* **9**, 323 (2018).
65. Wang, G., Li, X. & Wang, Z. APD3: The antimicrobial peptide database as a tool for research and education. *Nucleic Acids Res.* **44**, D1087–D1093 (2016).
66. Wang, G., Li, X. & Wang, Z. APD2: The updated antimicrobial peptide database and its application in peptide design. *Nucleic Acids Res.* **37**, D933–D937 (2009).
67. Wang, Z. & Wang, G. APD: The antimicrobial peptide database. *Nucleic Acids Res.* **32**, D590–D592 (2004).
68. Bjellqvist, B. *et al.* The focusing positions of polypeptides in immobilized pH gradients can be predicted from their amino acid sequences. *Electrophoresis* **14**, 1023–1031 (1993).
69. Bjellqvist, B., Basse, B., Olsen, E. & Celis, J. E. Reference points for comparisons of two-dimensional maps of proteins from different human cell types defined in a pH scale where isoelectric points correlate with polypeptide compositions. *Electrophoresis* **15**, 529–539 (1994).

## Author contributions

Conceptualization, F.P.; data curation, A.M., R.S. and C.S.; formal analysis, A.M and H.V.; methodology, A.M, R.S., C.S., H.V., A.D.S. and F.P. ; project administration, F.P.; supervision, F.P.; validation, H.V., P.P., A.S., M.W. and F.P.; writing—original draft, F.P.; writing—review and editing, A.M., R.S., C.S., H.V., P.P., A.S. and M.W.

## Funding

This research was supported by the Italian Ministry of Instruction, University and Research (MIUR) within the frameworks of two projects (PON R&I 2014–2020, protocol ARS01\_00597 and PRIN 2017, protocol Prot. 2017AHTCK7).

## Competing interests

The authors declare no competing interests.

## Additional information

**Supplementary information** is available for this paper at <https://doi.org/10.1038/s41598-020-74017-9>.

**Correspondence** and requests for materials should be addressed to P.F.

**Reprints and permissions information** is available at [www.nature.com/reprints](http://www.nature.com/reprints).

**Publisher's note** Springer Nature remains neutral with regard to jurisdictional claims in published maps and institutional affiliations.



**Open Access** This article is licensed under a Creative Commons Attribution 4.0 International License, which permits use, sharing, adaptation, distribution and reproduction in any medium or format, as long as you give appropriate credit to the original author(s) and the source, provide a link to the Creative Commons licence, and indicate if changes were made. The images or other third party material in this article are included in the article's Creative Commons licence, unless indicated otherwise in a credit line to the material. If material is not included in the article's Creative Commons licence and your intended use is not permitted by statutory regulation or exceeds the permitted use, you will need to obtain permission directly from the copyright holder. To view a copy of this licence, visit <http://creativecommons.org/licenses/by/4.0/>.

© The Author(s) 2020

# A Bioinformatic Study of Antimicrobial Peptides Identified in the Black Soldier Fly (BSF) *Hermetia illucens* (Diptera: Stratiomyidae)

Antonio Moretta<sup>1</sup>, Rosanna Salvia<sup>1</sup>, Carmen Scieuzo<sup>1</sup>, Angela Di Somma<sup>2</sup>, Heiko Vogel<sup>3</sup>, Pietro Pucci<sup>4</sup>, Alessandro Sgambato<sup>5,6</sup>, Michael Wolff<sup>7</sup>, Patrizia Falabella\*<sup>1</sup>

1 Department of Sciences, University of Basilicata, Via dell'Ateneo Lucano 10, 85100, Potenza, Italy.

2 Department of Chemical Sciences, University Federico II of Napoli, Via Cinthia 6, 80126 Napoli. Italy

3 Department of Entomology, Max Planck Institute for Chemical Ecology, Hans-Knöll-Straße 8, D-07745, Jena, Germany.

4 CEINGE Advanced Biotechnology, Via Gaetano Salvatore 486, Naples, Italy.

5 Centro di Riferimento Oncologico della Basilicata (IRCCS-CROB), Rionero in Vulture (PZ), Italy;

6 Department of Translational Medicine and Surgery, Università Cattolica del Sacro Cuore, Rome, Italy.

7 Institute of Bioprocess Engineering and Pharmaceutical Technology, Technische Hochschule Mittelhessen, Wiesenstrasse 14, 35390 Giessen, Germany.

\* Corresponding author: patrizia.falabell@unibas.it

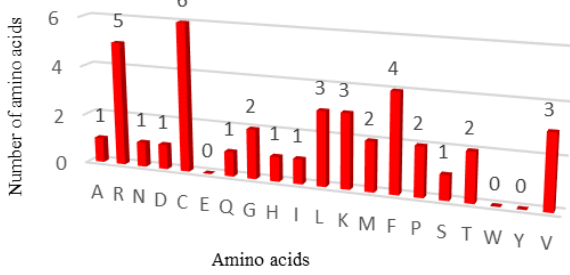
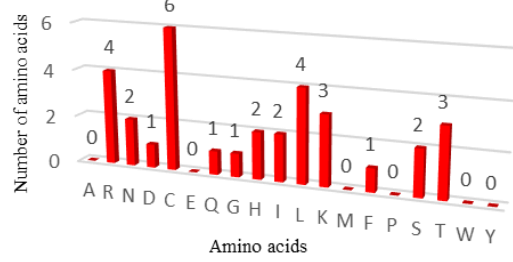
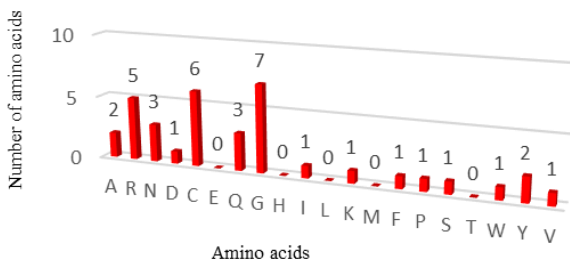
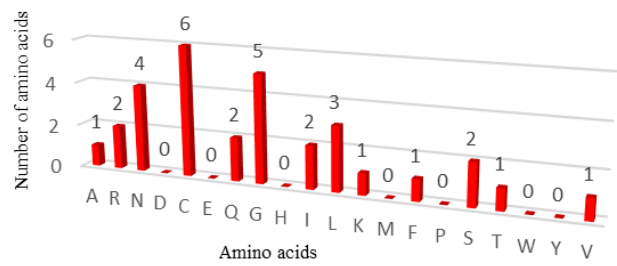
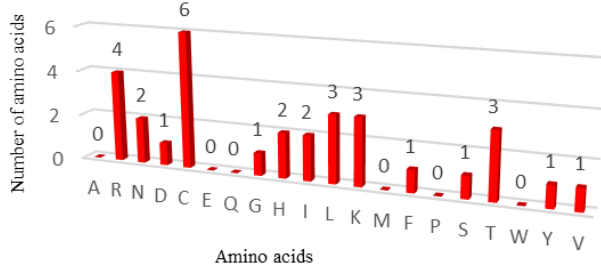
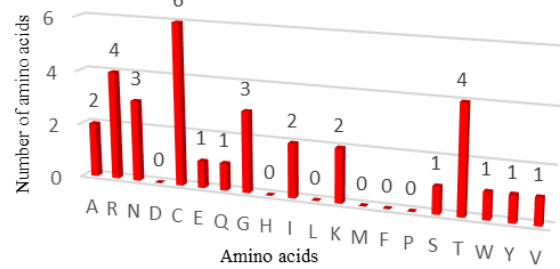
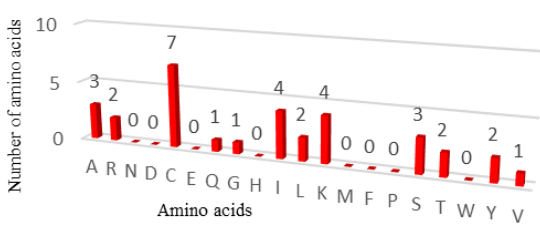
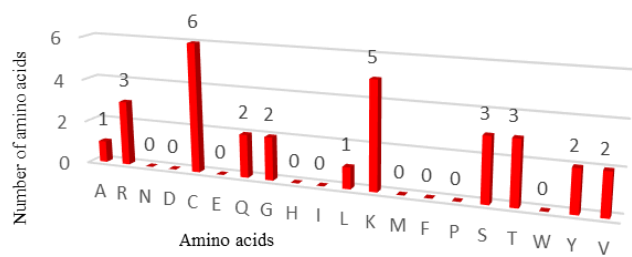
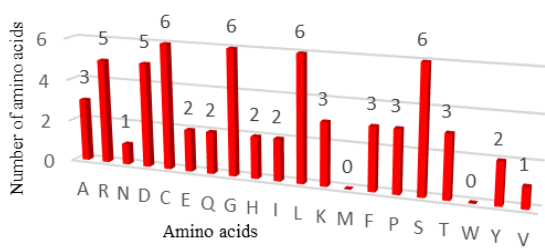
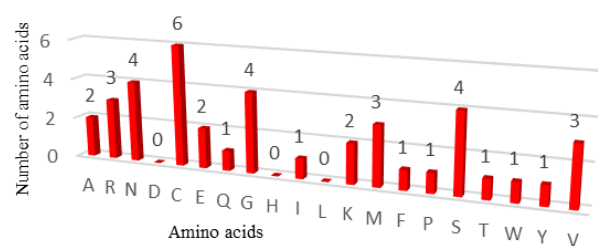
PREDICTED ACTIVITY	PEPTIDE
AMPs	Hill_BB_C1153
	Hill_BB_C309
	Hill_BB_C13793
	NHill_AD_C12927
	NHill_AD_C12928
	Hill_SB_C2730
	Hill_LB_C37730
	Hill_BB_C9237
	NHill_AD_C40487
	Hill_BB_C308
	Hill_BB_C1826
	Hill_BB_C8473
	Hill_BB_C4683

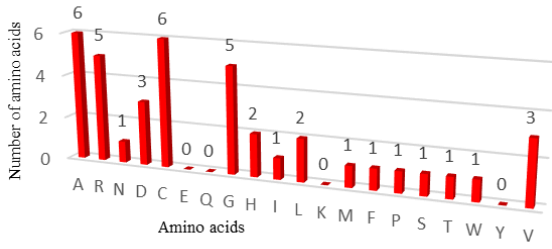
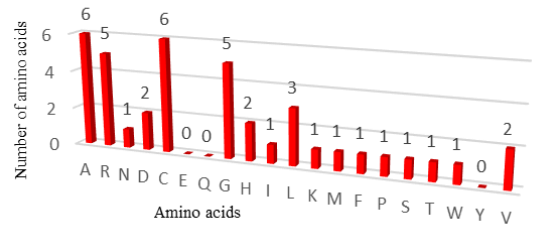
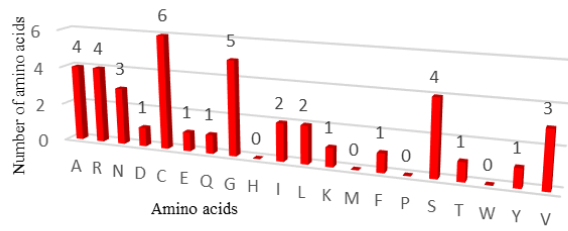
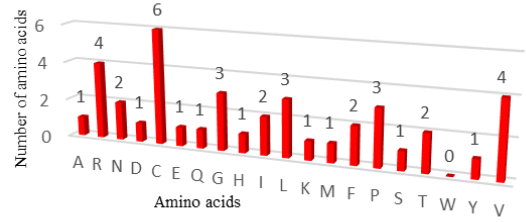
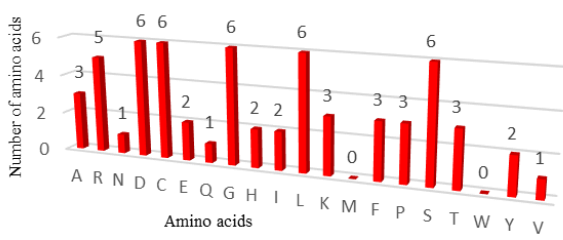
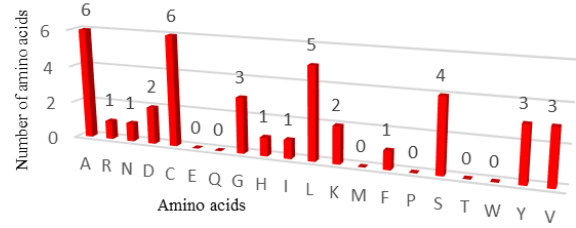
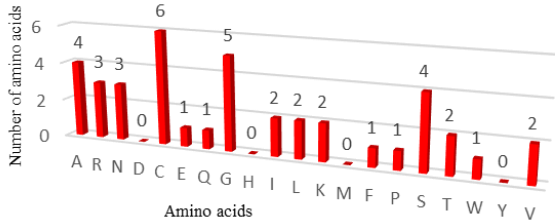
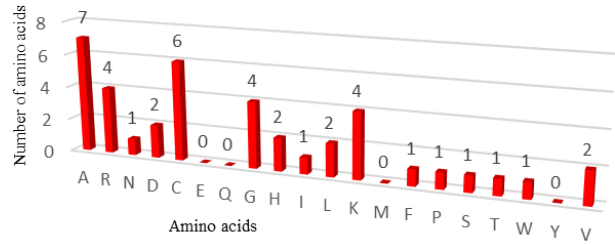
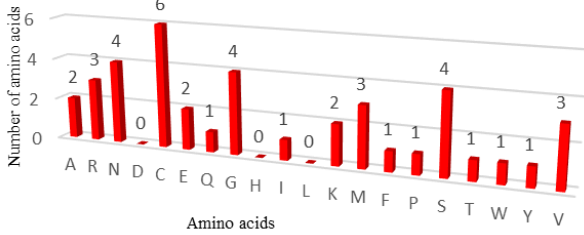
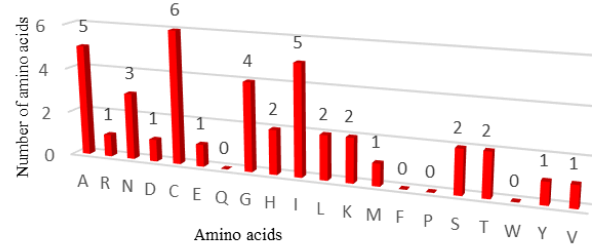
AMPs + ACPs	<p>Hill_BB_C3566</p> <p>Hill_BB_C1152</p> <p>Hill_BB_C2676</p> <p>Hill_BB_C1169</p> <p>Hill_BB_C779</p> <p>Hill_LB_C36111</p> <p>Hill_LB_C12085</p> <p>Hill_BB_C1290</p> <p>NHill_AD_C73537</p> <p>NHill_AD_C16493</p> <p>NHill_AD_C4669</p> <p>Hill_BB_C16137</p> <p>Hill_BB_C3195</p> <p>Hill_SB_C698</p> <p>Hill_SB_C1875</p> <p>Hill_BB_C5151</p> <p>NHill_AD_C49215</p> <p>Hill_BB_C21232</p> <p>Hill_BB_C16883</p> <p>Hill_BB_C7985</p> <p>Hill_BB_C7171</p> <p>Hill_BB_C10649</p>
AMPs + AVPs	<p>Hill_BB_C14202</p> <p>Hill_BB_C269</p> <p>Hill_BB_C14087</p> <p>Hill_LB_C29142</p> <p>Hill_BB_C7176</p> <p>Hill_BB_C2519</p> <p>Hill_BB_C34351</p> <p>Hill_BB_C4977</p>
AMPs + AFPs	<p>Hill_BB_C1827</p> <p>Hill_BB_C13792</p>

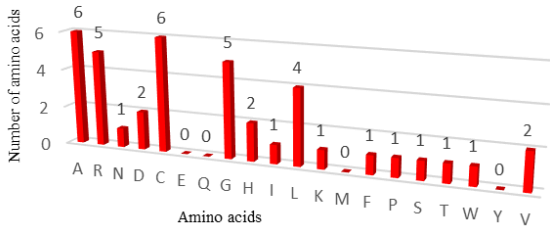
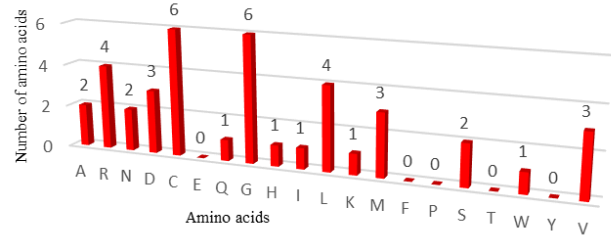
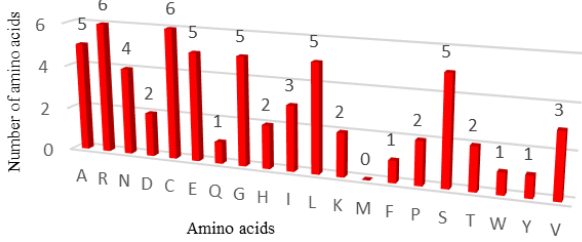
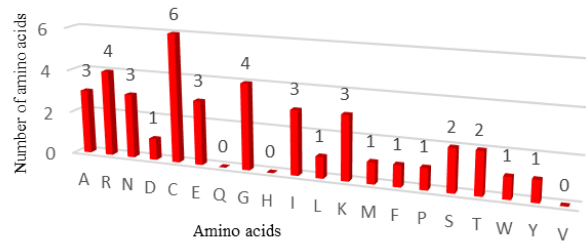
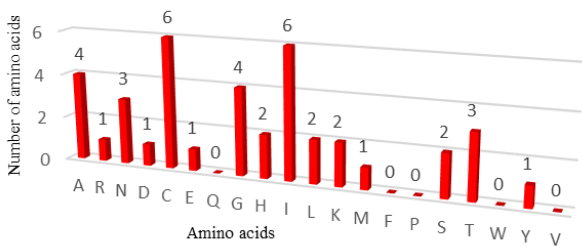
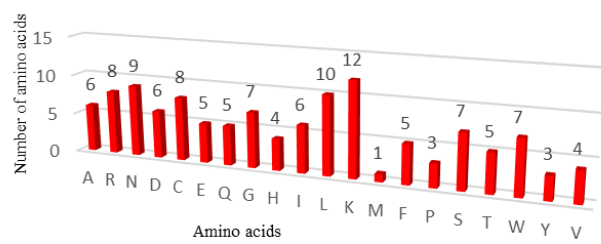
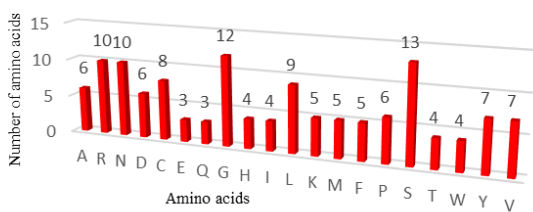
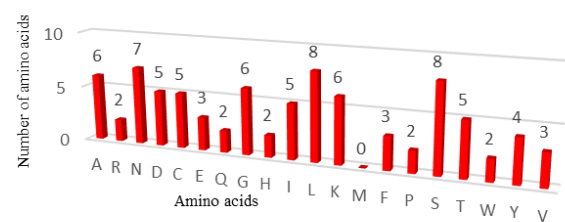
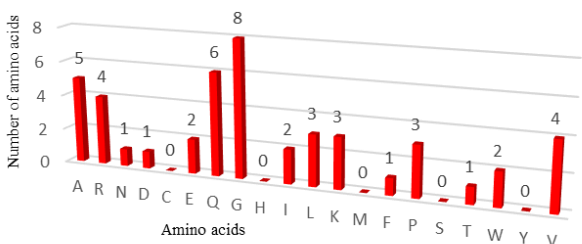
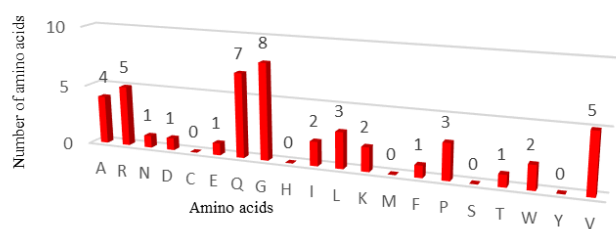
AMPs + ACPs + AVPs	Hill_BB_C5878 Hill_BB_C390 NHill_AD_C53857 Hill_BB_C7758 Hill_BB_C1619 Hill_BB_C7081 Hill_BB_C13326
AMPs + AFPs + AVPs	Hill_BB_C15867
AMPs + ACPs + AFPs	Hill_BB_C46948 Hill_BB_C6571
AMPs + ACPs + AVPs + AFPs	Hill_LB_C16634 NHill_AD_C69719

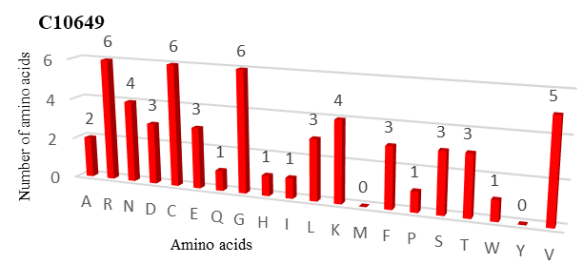
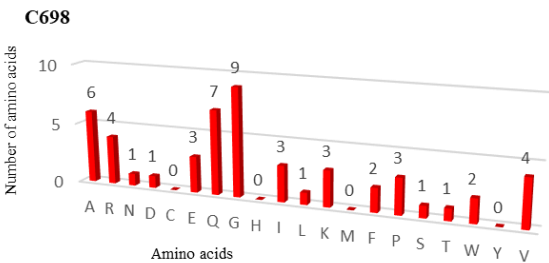
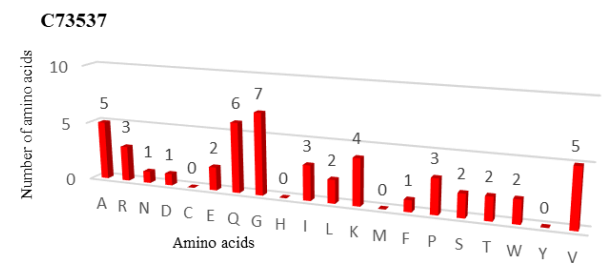
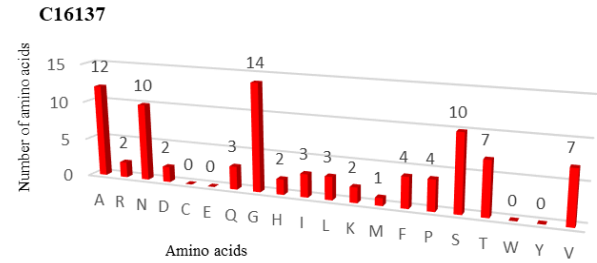
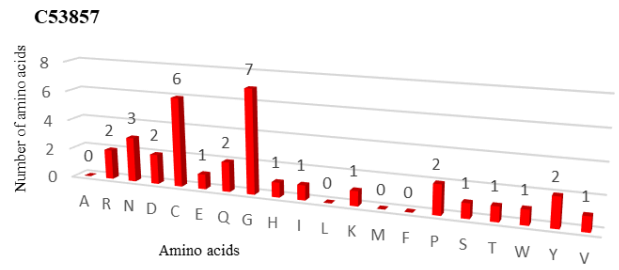
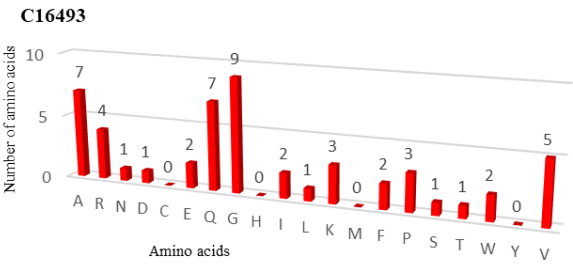
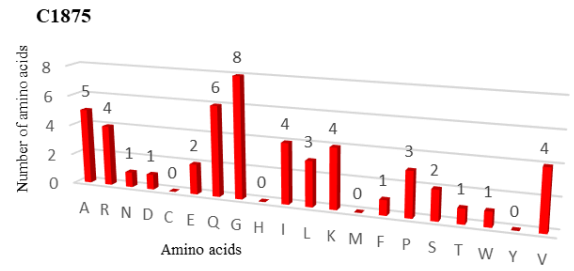
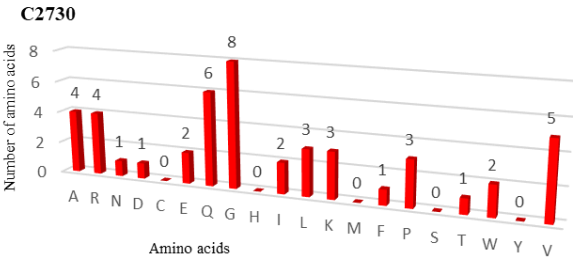
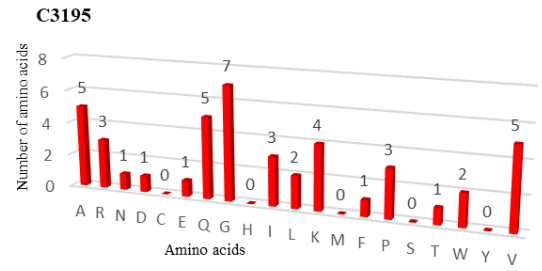
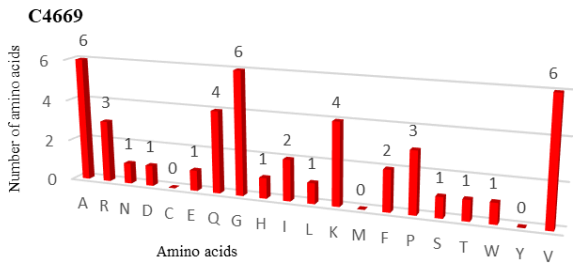
**Supplementary Table S1. Summary of all activities predicted for the identified peptides.** The acronyms AMPs, ACPs, AVPs and AFPs represent antimicrobial, anticancer, antiviral, and antifungal, respectively.

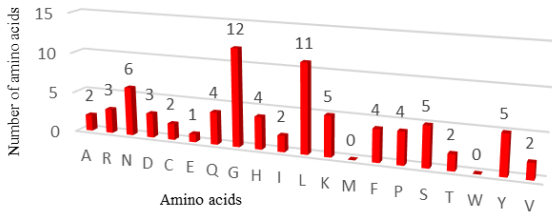
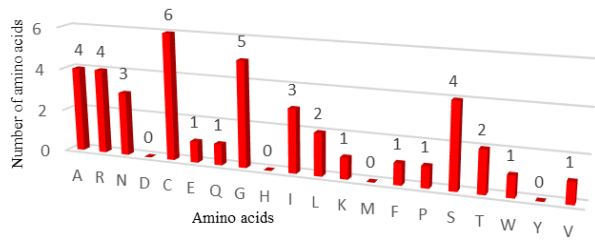
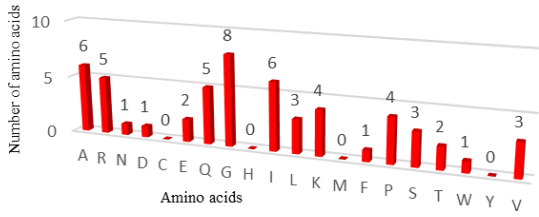
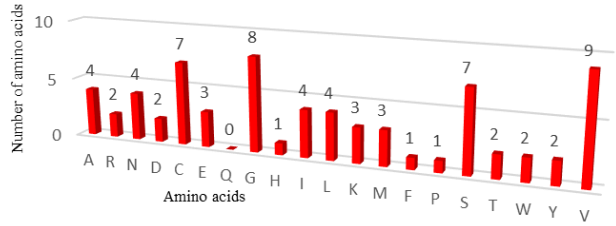
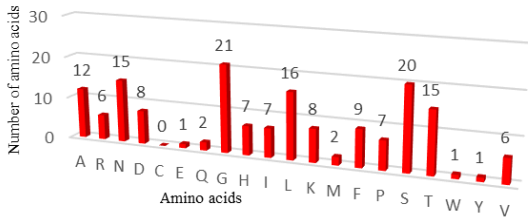
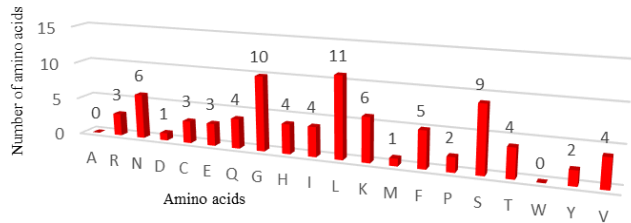
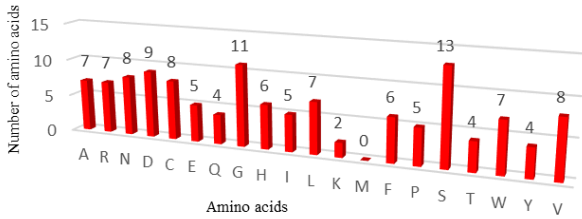
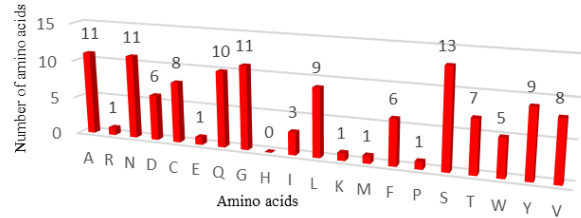
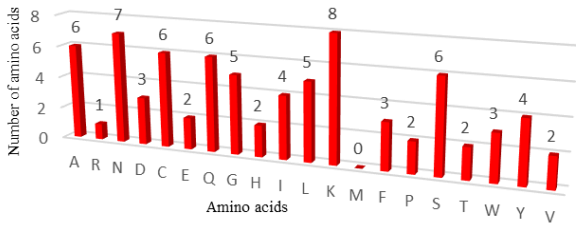
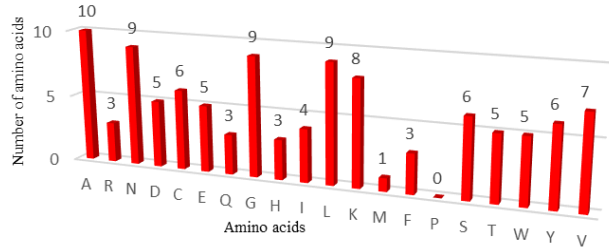


**C15867****C1826****C49215****C7985****C1827****C6571****C16643****C46948****C13792****C309**

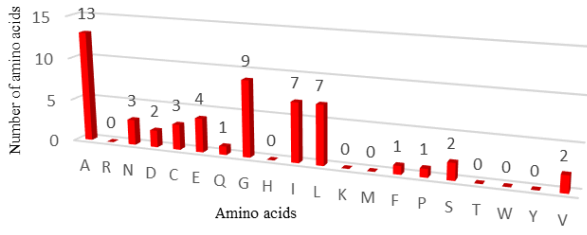
**C8473****C2519****C1619****C14087****C13793****C7758****C13326****C29142****C308****C7081**

**C7176****C34351****C4683****C4977****C7171****C14202****C3566****C12085****C12927****C12928**

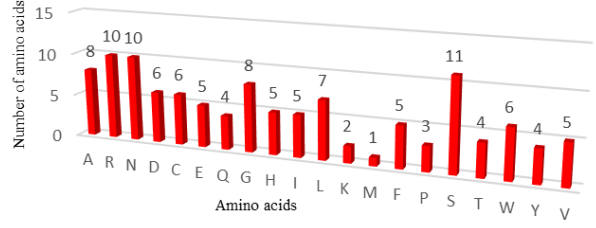


**C1290****C5878****C5151****C69719****C16883****C21232****C1152****C2676****C1169****C779**

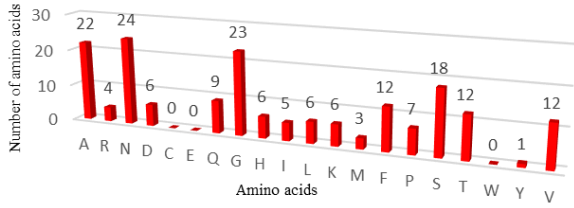
**C390**



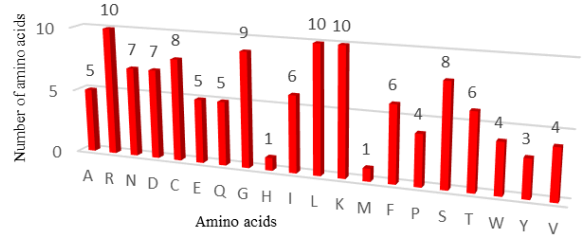
**C1153**



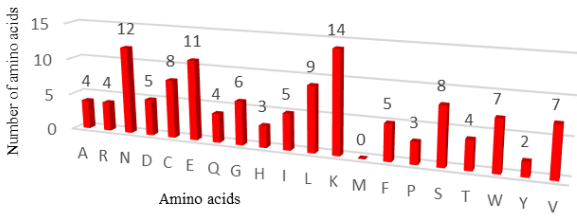
**C40487**



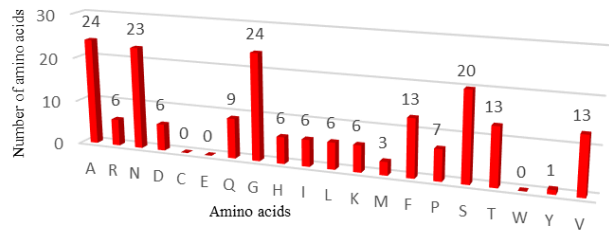
**C269**



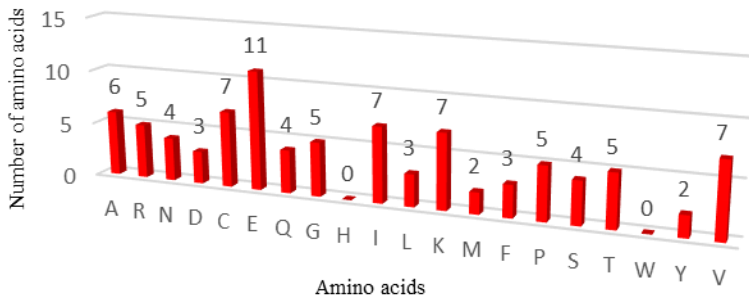
**C36111**



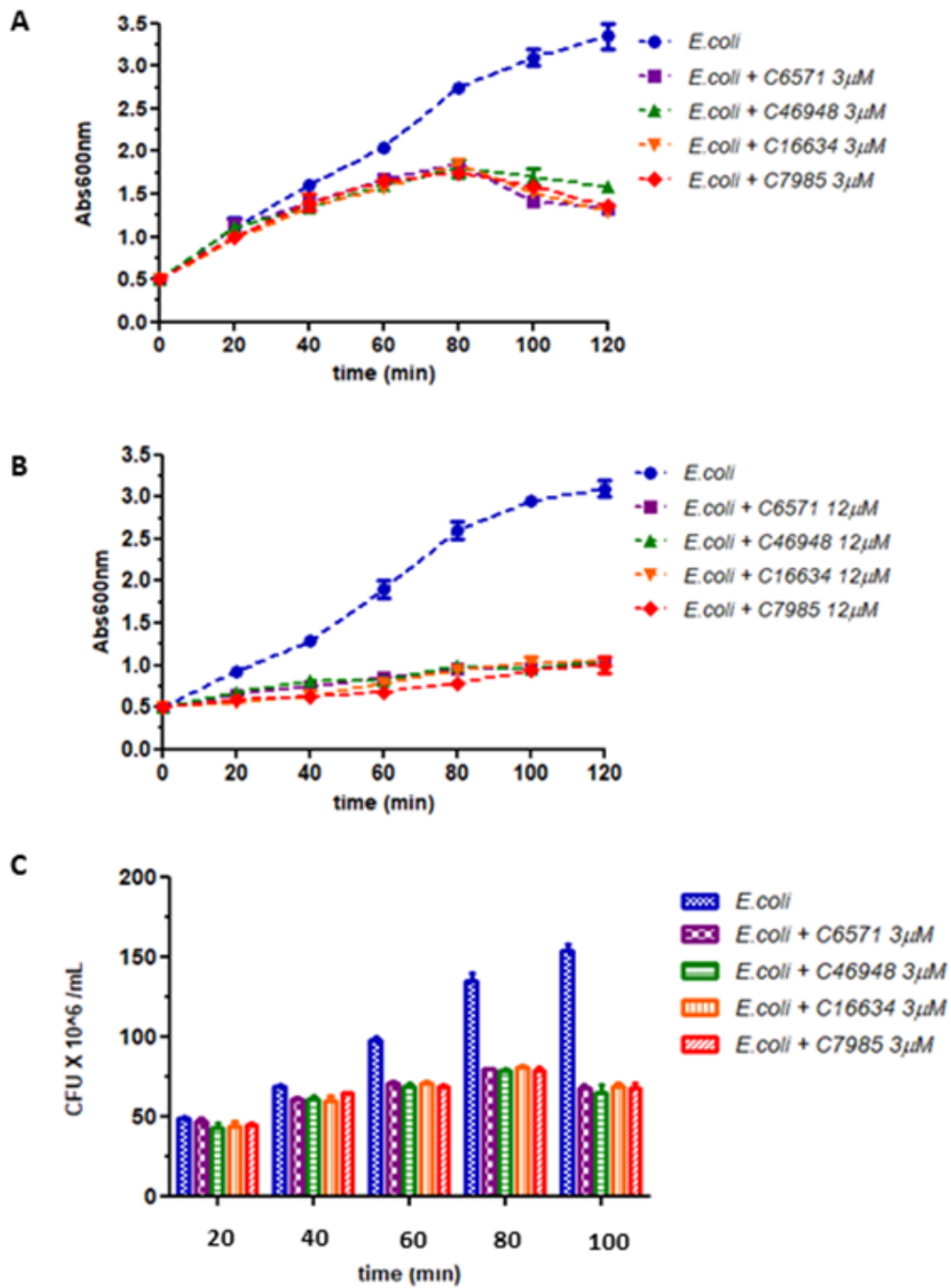
**C9237**



**C37730**



**Supplementary Figure 1. Graphical representation of the 57 identified peptides' amino acid composition. Bar represents the number of each amino acid for each peptide.**



**Supplementary Figure 2.** Bacterial growth profiles under treatment with two different concentrations, 3  $\mu$ M (A) and 12  $\mu$ M (B) of each antimicrobial peptide. (C) Cell viability after treatment with 3  $\mu$ M of each antimicrobial peptide.



# Insect antimicrobial peptides: potential weapons to counteract the antibiotic resistance

M. D. Manniello<sup>1</sup> · A. Moretta<sup>1</sup> · R. Salvia<sup>1,2</sup> · C. Scieuzo<sup>1,2</sup> · D. Lucchetti<sup>3</sup> · H. Vogel<sup>4</sup> · A. Sgambato<sup>3,5</sup> · P. Falabella<sup>1,2</sup>

Received: 23 November 2020 / Revised: 19 January 2021 / Accepted: 29 January 2021  
© The Author(s) 2021

## Abstract

Misuse and overuse of antibiotics have contributed in the last decades to a phenomenon known as antibiotic resistance which is currently considered one of the principal threats to global public health by the World Health Organization. The aim to find alternative drugs has been demonstrated as a real challenge. Thanks to their biodiversity, insects represent the largest class of organisms in the animal kingdom. The humoral immune response includes the production of antimicrobial peptides (AMPs) that are released into the insect hemolymph after microbial infection. In this review, we have focused on insect immune responses, particularly on AMP characteristics, their mechanism of action and applications, especially in the biomedical field. Furthermore, we discuss the Toll, Imd, and JAK-STAT pathways that activate genes encoding for the expression of AMPs. Moreover, we focused on strategies to improve insect peptides stability against proteolytic susceptibility such as D-amino acid substitutions, N-terminus modification, cyclization and dimerization.

**Keywords** Immune system · Antibacterial peptides · Resistant bacteria · Mechanism of action · Signaling pathways

## Introduction

### The antibiotic resistance as a global concern

Today, the identification of novel antibacterial therapeutics represents an auspicious perspective [1]. In fact, the inappropriate consumption and overuse of the first-line maintenance

therapies have favored, in the last decades, an increasing selection of antibiotic-resistant pathogens. This phenomenon, together with the lack of availability of new molecules, represents real issues in health care [2, 3]. The multi-drug-resistant pathogens, such as ESKAPE (i.e. *Enterococcus faecium*, *Staphylococcus aureus*, *Klebsiella pneumoniae*, *Acinetobacter baumannii*, *Pseudomonas aeruginosa*, and *Enterobacter*) species, are considered practically resistant to most of the available antibiotics and have played a critical role in the growth of nosocomial infections [4, 5]. Moreover, the World Health Organization (WHO) has recently updated the priority list constituted of 12 bacterial pathogens against which there is a need to develop new antibiotics. The WHO list is divided into three categories according to the urgency of need for new antibiotics: critical, high, and medium priority. The category with a critical priority comprises the Gram-negative species *P. aeruginosa*, and *A. baumannii*, both carbapenem-resistant bacteria frequently associated with severe and often lethal diseases such as bloodstream infections and pneumonia. Several Gram-positive species constitute the high priority list, among which *S. aureus* methicillin-resistant (MRSA), and vancomycin-intermediate and resistant [6].

---

M. D. Manniello, A. Moretta, R. Salvia and C. Scieuzo contributed equally to this work.

---

✉ P. Falabella  
patrizia.falabella@unibas.it

<sup>1</sup> Department of Sciences, University of Basilicata, Via dell'Ateneo Lucano 10, 85100 Potenza, Italy

<sup>2</sup> Spinoff XFlies S.R.L, University of Basilicata, Via dell'Ateneo Lucano 10, 85100 Potenza, Italy

<sup>3</sup> Department of Translational Medicine and Surgery, Università Cattolica del Sacro Cuore, Rome, Italy

<sup>4</sup> Department of Entomology, Max Planck Institute for Chemical Ecology, Hans-Knöll-Straße 8, 07745 Jena, Germany

<sup>5</sup> Centro di Riferimento Oncologico Della Basilicata (IRCCS-CROB), Rionero in Vulture (PZ), Italy



The increasing rate of antibiotic resistance represents a particularly challenging issue in the treatment of topical infections. Several complications such as chronic skin and soft tissue infections which can complicate the clinical course of ulcers, diabetic foot infections, post-surgical infections, and burn wounds are characterized by a progressive worsening of their clinical outcome, when antibiotic-resistant pathogens are involved. Likewise, the Gram-negative bacterium *A. baumannii* has been reported as responsible for a variety of antibiotic-resistant infections such as wound, skin, and urinary tract infections, but also pneumonia and bacteremia [7].

Bacterial infections of the lower respiratory tract, often related to bronchiectasis, represent an increasing and common chronic respiratory disease, associated not only with cystic fibrosis (CF) lung disease but also to chronic obstructive pulmonary disease. The clinical course of an antibiotic-resistant bronchiectasis can face, therefore, a progression of the health-condition worsening, due to the establishment of an infection-inflammation cycle uncontrollable by available drugs [8–10]. Lung infections associated with bronchiectasis may evolve to respiratory failure and death. Moreover, reduced quality of life and an increase in healthcare costs can worsen the patient compliance [11].

It is noteworthy that the successful management of bacterial infections is the product of combined actions of the host immune response and the administration of antibiotics. Hence, deficiencies of the host immune system and/or reduced efficacy of antibiotics due to the presence of resistant pathogens might, unfortunately, contribute to switching towards a persistent infection. Chronic bacterial infections are associated with increased morbidity and mortality from the infection itself as well as an increased risk of dissemination of disease which is a life-threatening condition difficult to treat, especially in the presence of antibiotic-resistant pathogens.

Therefore, along with the irresponsible use of antibiotics, the related resistance issue towards the most commonly used molecules represents a global concern [12]. The aim to find alternative drugs has demonstrated to be a real challenge, as well [13, 14].

### The biofilm issue

Bacterial pathogens have established various ways to defeat the host's immune response so that bacterial virulence has been analyzed for decades. In nature, bacteria are physically grouped in clusters and embedded by extracellular polymeric substances [15]. In clinical settings, pathogen bacteria can effortlessly survive when colonizing surfaces (e.g. on wounds, scar tissue, medical implants), since sessile cells are less prone than planktonic to interact with the ordinarily used antimicrobials. Biofilms are bacterial communities

embedded within an extracellular matrix and adherent to a surface. Biofilm formation is one of the main mechanisms of surviving, and it regards a wide range of microbes that commonly cause chronic infections [16]. One essential feature of biofilms is the intrinsic resistance of the bacterial community to the host immune system by decreasing efficacy of antibodies and antimicrobial peptides (AMPs) as well as phagocytic uptake within it thus hampering leukocyte-mediated killing. Moreover, the biofilm extracellular matrix component can partly limit the diffusion of antibiotics, thus, reducing their antimicrobial efficacy. The most relevant clinical biofilm-forming bacteria comprise the Gram-negative *A. baumannii*, *Escherichia coli*, *K. pneumoniae*, and *P. aeruginosa*, along with Gram-positive *S. aureus* and the less virulent *Staphylococcus epidermidis*.

Over 80% of chronic wounds are related to bacterial biofilms, in which the most commonly isolated pathogens are *S. aureus* and *P. aeruginosa* [17–23]. Humans are transporters of *S. aureus* infections; a range of 20–75% of humans demonstrated to be intermediate carriers. Several human body sites, such as nasal cavities, pharynx, perineum, and skin represent the primary sites for colonization. Commonly, the colonization by *S. aureus* causes no serious health problems in healthy individuals. However, the risk of developing *S. aureus* infection increases in the case of hospitalized patients with wounds, burns, and chronic ulcers [14]. *P. aeruginosa* is a ubiquitous bacterium that colonizes the natural environment near humans. Nevertheless, it represents a crucial but also one of the most resistant pathogens in CF lung disease [24]. Both representative species have been often associated with a biofilm mode of growth when isolated in the lower airways and portrayed as highly recalcitrant to the antibiotic treatments [25–27].

### Failure of the common pharmacological approaches

Multiple reasons for clinical failure can be mentioned when referring to antibiotic resistance. Poor pharmacokinetics of drugs in infection sites, or the bacterial phenotype of persistence, associated with the ability to survive in protected niches such as biofilms, foster the clinical failure. As mentioned above, specific bacteria may persist during the antibiotic treatment when drugs are administered at concentrations that should be lethal. Hence, this behavior may cause prolonged and recurrent infections [11]. Thus, antibiotic resistance is associated with higher medical costs, longer hospitalization, and increased mortality. To fight antibiotic resistance, a great effort has been devoted in the last decades to the development of new molecules, acting as antibiotics. Nevertheless, only a few new classes of antibiotics reached market availability in the last 3 decades, and others are still in human clinical trial. The clinical outcomes of resistant infections are also related to the host response to infection

and to pathogen-derived toxic compounds. *S. aureus*, for example, can produce molecules able to counteract neutrophil's action, i.e. preventing the adhesion to the blood vessels and their transmigration into the site of infection or eliciting cell death [28].

Regarding the skin infection management, the increasing issue related to resistance to the commonly used antibiotics mainly concerns the involvement of the deeper tissues which can cause the clinical worsening of wounds with clearly systemic infection risk. *S. aureus* is also associated with catheter-related bacteremia and intubation-related infections, such as pneumonia and bloodstream infections. Since the increasing resistance of bacterial pathogens often needs the use of more toxic agents to be counteracted, the antimicrobial therapy by topical application involves the use of not only suitable (e.g. considering toxic antibiotics) but also higher dosing as well [13, 29–31].

## Natural sources of antimicrobials

Screening of natural products has allowed the identification of some of the most active drugs. Biologically, active natural peptides can represent useful alternatives being characterized by high therapeutic efficacy, a low probability of resistance emerging in target cells, and limited side effects. To this aim, the exploitation of new compounds and the identification of their mechanisms of action is essential for further development. Antimicrobial peptides (AMPs), small molecules composed of 10–100 amino acid residues produced by all organisms, are attractive candidates for the design of new antibiotics because of their natural antimicrobial properties and a low propensity for the development of resistance [32]. Indeed, these natural peptides have retained their activity over the course of the evolution, triggering little or no resistance, and might represent a valuable alternative to classical drugs. Moreover, several evidence suggest that they can display anticancer activities characterized by a strong selectivity and efficacy on cancer cells so that many of them are also indicated as anticancer peptides (ACPs) [33–35]. Therefore, AMPs and ACPs are the focus of a large number of studies aimed at developing new antibiotics against multi-resistant bacteria (MDR) and new anticancer drugs AMPs are usually cationic and amphipathic and their structure includes both hydrophobic and hydrophilic moieties with a highly positive net charge (ranging from +2 to +9). They can be effective on a wide spectrum of microorganisms and can display powerful antimicrobial activities against antibiotic-resistant bacteria. Insects are an almost inexhaustible source of biologically active compounds. Natural products deriving from insects have been used for centuries in traditional medicine and still represent an essential source of healing substances in developing countries.

## Insects as natural sources of antimicrobials

### Overview

Considering over one million described species, insects represent the largest class of organisms, due to their ability to adapt to recurrent changes and their resistance to a broad spectrum of pathogens [36, 37]. This resistance skill is related to their immune system, based exclusively on the innate immune response, which allows a broad and fast response to invading organisms [1, 38–40]. With the aim to prevent the entrance of pathogens within the hemocoel cavity, the first protection is represented by physical barriers such as the cuticle, the intestinal wall, and the tracheas (Fig. 1) [40, 41].

In recent years, an increasing number of insect AMPs have been proving useful in several applications concerning the pharmaceutical as well as the agricultural fields. Moreover, insect AMPs aroused great interest for their biomedical application thanks to the growing number of identified peptides that can inhibit human pathogens. AMPs susceptible pathogen bacteria include multidrug-resistant *E. coli*, *K. pneumoniae*, *Bacillus coagulans*, *Citrobacter freundii*, *Francisella tularensis*, *Streptococcus sanguinis*, and *S. aureus* [41–45]. Besides, some insect AMPs can also inhibit virus replication such as the two alloferons from the blowfly *Calliphora vicina*. These compounds have been demonstrated to be active against both human influenza viruses A and B [46]. Furthermore, melittin, peptide derivative from *Apis mellifera*, shows antiviral activity against herpes simplex virus 1 (HSV-1) [47]. Several fungi are also susceptible to insect AMPs including *Pichia pastoris*, *Aspergillus fumigatus*, *Cryptococcus neoformans*, *Botrytis cinerea*, *Fusarium* spp., *Neurospora crassa*, and *Trichoderma viride* [48–50]. Given the increasing bacterial resistance to antibiotics, there is a great interest in verifying the AMPs suitability for the treatment of recalcitrant bacterial infections and killing of resistant bacteria. Several reports have highlighted that insect-derived AMPs can represent good candidates as alternatives to conventional antibiotics [51–53]. However, the treatments to inhibit pathogenic infections using cecropins, positively charged AMPs originally isolated from insects, for example, have suffered from some limitations. Indeed, they represent a target of human elastase produced by neutrophils, which are recruited during infections, or can be subjected to protease degradation [54, 55].

Insect AMPs represent a highly promising alternative to overcome medical problems associated with antibiotic resistance. Several studies have been performed using insect cecropins in the functionalization of biomaterials used in biomedicine, such as hydrogels and polyurethane

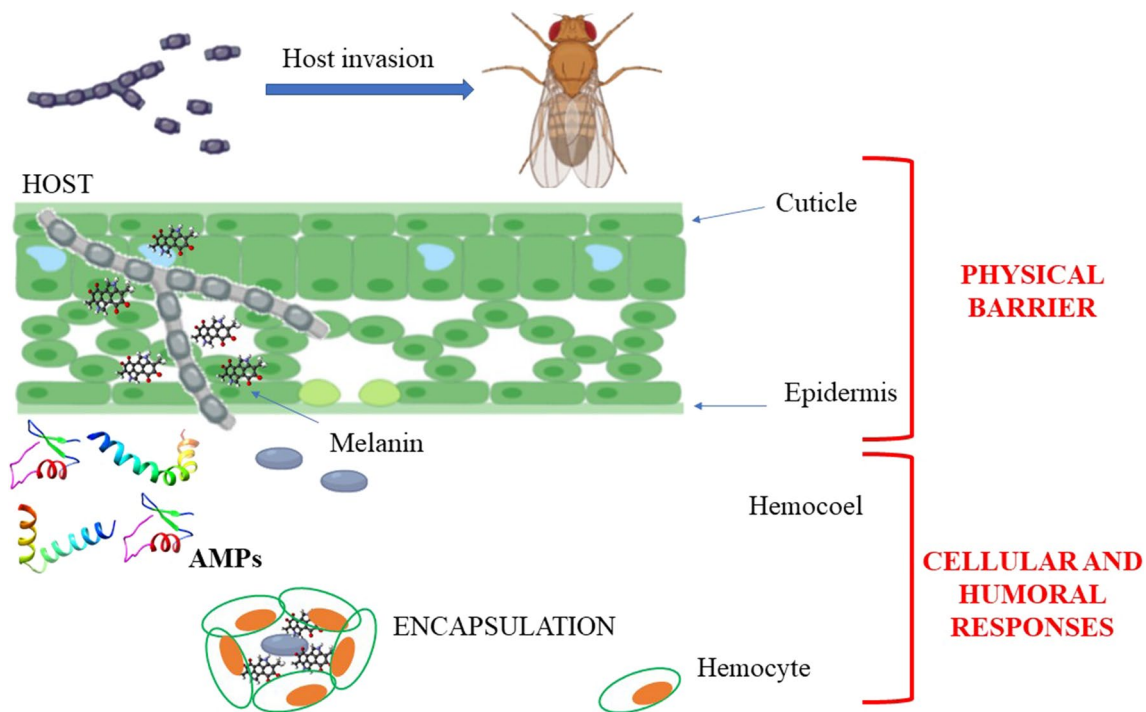


**Fig. 1** Schematic representation of insect immunity system. The first protections against the host invasion are physical barriers, including cuticle and epidermis. When pathogens succeed in overcoming these barriers, cellular and humoral immune responses are triggered,

involving melanization, AMP production, and/or reaction mediated by hemocytes. Adapted from Lu and St. Leger, 2016, created with BioRender.com

surfaces [56, 57]. Moreover, cecropin expression in transgenic plants can confer resistance to bacterial and fungal pathogens [58, 59]. Transgenic expression of an insect cecropin (sarcotoxin-IA) and defensin (*Galleria mellonella* named gallerimycin) in tobacco also confers resistance to fungi [60].

### Organization of insect immunity system

All invertebrates including insects have a defense mechanism exclusively based on a powerful innate immune system, which allows a general and rapid response to different invading organisms [61]. The first protection against pathogens is represented by physical barriers such as the cuticle, the intestinal wall including the peritrophic membrane, and the tracheas [62]. If the foreign organisms pass through these defensive barriers, penetrating the hemocoel, the immune response is triggered. The innate immune system is conserved across all organisms comprising cellular responses and humoral responses. In insects, cellular immune responses are mediated by hemocytes, the cellular component of hemolymph responsible for nodulation, encapsulation and phagocytosis of invading pathogens. On the other hand, the haemocytes together with the fat body cells are also involved in the mechanisms of the humoral response

that includes AMP synthesis, the enzymatic cascade that regulates the activation of hemolymph coagulation and melanization, and the production of reactive oxygen (ROS) and nitrogen (RNS) species [63].

The clear separation between humoral and cellular response is more conventional than functional; some of the humoral factors regulate the activity of haemocytes and, at the same time, haemocytes are the source of several molecules involved in the humoral response. Furthermore, they often share the same signal transduction pathways, even if activated by different stimuli [38, 64].

Among the humoral immune response in insects the production of melanin, a highly toxic phenolic biopolymer is involved both in the defense against pathogens and in the repair of cuticular wounds to prevent the loss of hemolymph [65]. Melanogenesis is regulated by the pro-phenoloxidase (proPO) system, a cascade of serine proteases and inhibitors of serine proteases that finely control the activation of proPO, the precursor of phenoloxidase (PO), after the recognition of an external elicitor [66]. Many data have shown that proPO is synthesized and accumulated in haemocytes and, when necessary, released by a lytic process which does not necessarily lead the cell to death [67]. Other studies have shown that proPO is localized on the surface of hemocytes. This localization could facilitate the deposition of melanin

directly on the foreign agent [68, 69]. Melanin is a very toxic compound and its systemic diffusion would be extremely harmful for the insect: the localization of its synthesis is essential to ensure the survival of the insect during the activation of melanogenesis [70]. Melanogenesis also generates cytotoxic intermediates, such as quinones and semiquinones, which favor the synthesis ROS and RNS. Moreover, these intermediates, alone or in combination with ROS and RNS, are cytotoxic molecules that participate in the elimination of the pathogen [71].

Cellular immune response is mediated by hemocytes. In most species of different orders, such as *Lepidoptera*, *Diptera* (except *Drosophila*), *Orthoptera*, *Blattoidei*, *Coleoptera*, *Hymenoptera*, *Hemiptera*, and *Collemboli*, the hemocytes are differentiated into granulocytes, plasmatocytes, spherulocytes, and oenocytoids [64, 72]. In *Lepidoptera*, granulocytes and plasmatocytes, which represent more than 50% of the circulating hemocytes, show adhesive ability. Plasmatocytes are also involved in the production of AMPs as well as in the release of extracellular matrix components [39]. The other two components of hemocytes, the spherulocytes, which carry cuticle components, and the oenocytoids, containing precursors of the activation cascade of the PO, have not any adhesive ability [39].

Phagocytosis, mediated by hemocytes, includes the recognition and encapsulation of foreign agents through

modifications of the hemocyte cytoskeleton and ends with the transport of the phagocyte material into the phagosomes where it is completely degraded thanks to the action of hydrolase, ROS and nitric oxide [72] (Fig. 2). In most insect orders, both granulocytes and plasmatocytes are responsible for phagocytosis while in *Drosophila melanogaster* this role is played by plasmatocytes alone [64, 72]. During the immune response, the nodulation process is activated when a large number of bacteria cannot be phagocytized by a single hemocyte. In this process, several kinds of hemocytes recognize and surround microorganisms, thus forming complexes that may or may not undergo melanization [73] (Fig. 2). In the encapsulation process, hemocytes adhere to surfaces of invading agents that are too big to be phagocytized, such as parasites, protozoa or nematodes consequently forming a capsule, made up of several cell layers, that undergoes melanization. Inside the capsule, the pathogenic organism is killed by asphyxiation or by the production of cytotoxic free radicals [72]. Granulocytes and plasmatocytes are involved in capsule formation in *Lepidoptera* [64, 72] while this role is played by plasmatocytes and lamellocytes in *D. melanogaster* [74] (Fig. 2).

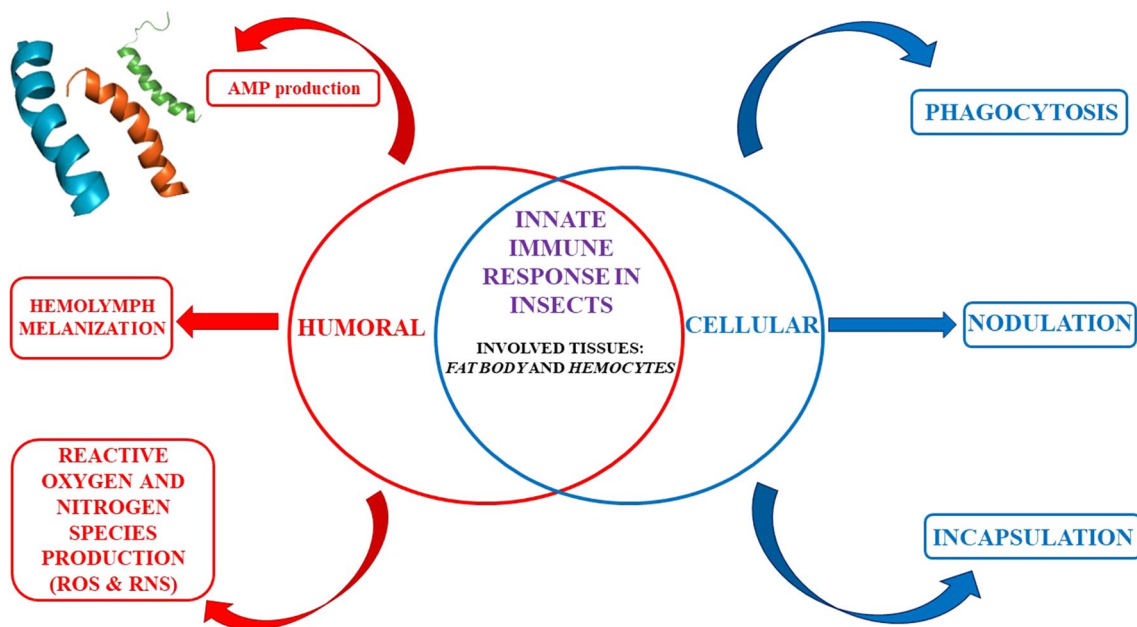


**Fig. 2** Insects innate immune response can be humoral or cellular. Humoral immunity consists of AMPs production by the fat body and/or hemocytes; hemolymph melanization and production of the reactive oxygen and nitrogen species. Cellular immunity consists of phagocytosis, nodulation and encapsulation processes. Phagocytosis determines the internalization of foreign agents by the hemocytes and the transport of the phagocyte material into the phagosomes

where it is degraded. Nodulation occurs when bacteria are too much to be incorporated by a single hemocyte. Indeed, several hemocytes together recognize and surround foreign agents. In the encapsulation process, hemocytes create a capsule made up of several cell layers that undergoes melanization. Inside the capsule, the pathogenic organism is killed by asphyxiation and/or production of cytotoxic free radicals [64, 72]

## Activation of the insect immune response

The triggering of the insect immune response is generated only when the exogenous agent is recognized, identifying specific and preserved molecules located on the pathogen surface the defined as pathogen-associated molecular patterns (PAMPs) [75]. PAMPs are molecular components potentially present in all microorganisms but absent in higher organisms. Examples of PAMPs comprise Gram-positive lipoteichoic acid and peptidoglycan, Gram-negative bacteria lipopolysaccharide (LPS), and fungi  $\beta$ -1,3-glucan [76]. These non-self-molecules are recognized by specific receptors (named pattern-recognition proteins, PRPs), which can be both humoral and cellular. Immunolectins, peptidoglycan recognition proteins (PGRPs), and Gram-negative binding proteins (GNBPs) are proteins circulating in the hemolymph and capable of recognizing specific antigens [40]. Peptidoglycan-recognition protein LC (PGRP-LC) and integrins, on the other hand, are receptors found on the surface of immune cells, which, respectively, recognize surface components of Gram-negative bacteria and the RGD motif (Arg-Gly-Asp) [36, 40]. The latter is found in the proteins of the extracellular matrix and in some soluble proteins such as collagen, fibronectin, and laminin. The binding of integrins to the RGD motif, for example, represents the first step for the recognition of exogenous agents. Furthermore, it is involved in bacterial phagocytosis or in the encapsulation process [40]. When the receptors, both humoral and cellular, bind to pathogen-associated molecules, specific immune responses are triggered based on the type of invader [1, 39, 40]. The humoral immune response includes the production of AMPs, the enzymatic cascade that regulates the activation of hemolymph coagulation, melanization, and the production of reactive oxygen as well as nitrogen species (often indicated as ROS and RNS, respectively) [71] (Fig. 2).

Due to the relevance of AMP function in insects, in the following section, we focused on insect AMPs with a special emphasis on their classification, overviewing their structural and functional characteristics, along with reviewing the signaling pathways which activate the encoding AMP genes and their mechanism of action.

## Overview of insect antimicrobial peptides

Insects can interact with the ecosystem using chemical substances. Besides, a variety of species can contribute to investigate the potential of new molecules [77]. Although it is possible to find smaller or larger peptides in nature, AMPs comprise small molecules whose amino acid composition ranges from 12 to 50 amino acids [53].

AMPs are involved in several defence-related processes such as the binding and the neutralization of endotoxins, the

modulation of the immune responses to infection, and the pathogens killing [78]. The first insect AMP, the cecropin, was identified in the 1980 from the pupae of *Hyalophora cecropia* [42, 79]. AMPs show a wide range of antibacterial, antiviral, anticancer, and antifungal activity [80–82]. In the last few years, the number of identified insect peptides has considerably increased, thanks to the published insect genome, transcriptome, and proteomic datasets (OMIC analysis). Mass spectrometry methodologies are adopted for the analysis of insect hemolymph, extracted from bacteria-induced larvae [83]. Both peptides and proteins have been considered as a promising choice to treat various diseases. It is now known that the adoption of AMPs is a promising alternative to substitute or support the current antimicrobial approach. Moreover, 3180 AMPs have been identified from different kingdoms, among which bacteria (i.e. 355 bacteriocins), fungi (20 AMPs), plants (352 AMPs), and animal sources (2356 AMPs) [84] (<http://aps.unmc.edu/AP/>). So far, the Antimicrobial Peptide Database is currently reporting 311 out of the 3180 insect-derived AMPs [84]. Surely, theOMIC analysis can also contribute to increasing the number of peptides or proteins isolated by insects that could have antimicrobial activity and become new potential AMPs [85].

Most insect AMPs are cationic molecules due to the presence of basic residues with activities against bacteria. According to their amino acid sequences and structures, AMPs can be classified in four different groups: cysteine-rich peptides (e.g. defensins), the  $\alpha$ -helical peptides (e.g. cecropins), glycine (Gly) -rich proteins (e.g. attacins), and proline-rich peptides (e.g. drosocins) [86, 87]. Number of AMPs in insects can widely vary among species: for example, 57 putatively active peptides were identified in *Hermetia illucens*, while very few peptides were identified in aphids [88, 89]. *H. illucens* is one of the most promising sources for AMPs, as the larval instar feed on vegetal and animal decaying organic substrates. Larvae are capable of producing several AMPs, which protect the insect from the pathogens in the substrate and are able to restore substrate health conditions, reducing the bacterial load of pathogenic species such as *E. coli* and *Salmonella enterica* [90, 91]. Recently a stomoxynZH1 from *H. illucens* was cloned and expressed in bacterial cells and tested against different bacterial and fungal strains, resulting in inhibition of *S. aureus* and *E. coli* (growing bacteria), as well as *Rhizoctonia solani* and *Sclerotinia sclerotiorum* (Lib.) de Bary (fungi) [92].

## Defensins (cysteine-rich AMPs)

Defensins are small cationic peptides due to the presence of basic amino acids, particularly arginine [93]. They consist of about 34–51 residues and contain six conserved cysteines (Cys) which form three intramolecular disulfide bridges. Insect defensins have been identified in several insect orders

such as Hemiptera, Coleoptera, Diptera, Hymenoptera, and Lepidoptera, but also in the ancient order of Odonata, suggesting that they might derive from a common ancestor gene [94].

From a structural point of view, defensins show an N-terminal loop, an  $\alpha$ -helix, followed by an antiparallel  $\beta$ -sheet, as shown in Fig. 3 for the defensin lucifensin (2LLD, PDB code) from *Lucilia sericata* (ATCDLLSGTGVKH-SACAAHCLLRGNRGGYCNGRAICVCRN) [95–98].

Two intramolecular disulfide bonds connect the  $\beta$ -sheet and the  $\alpha$ -helix, forming a Cys-stabilized alpha beta (CS $\alpha\beta$ ) structure [97]. Considering the insect defensins, the Cys are linked as Cys1—Cys4, Cys2—Cys5, and Cys3—Cys6 [99]. For example, Defensin A sequence from *Protophormia terraenovae* is shown in Fig. 4, and Fig. 5.

Insect defensins are particularly active against Gram-positive bacteria such as *S. aureus*, *Bacillus subtilis*, *Micrococcus luteus*, and *Bacillus megaterium*. Nevertheless, some of them have also shown antimicrobial activity against Gram-negative bacteria such as *E. coli* [100, 101]. In Table 1, the major insect defensins with reported antimicrobial activity are listed.

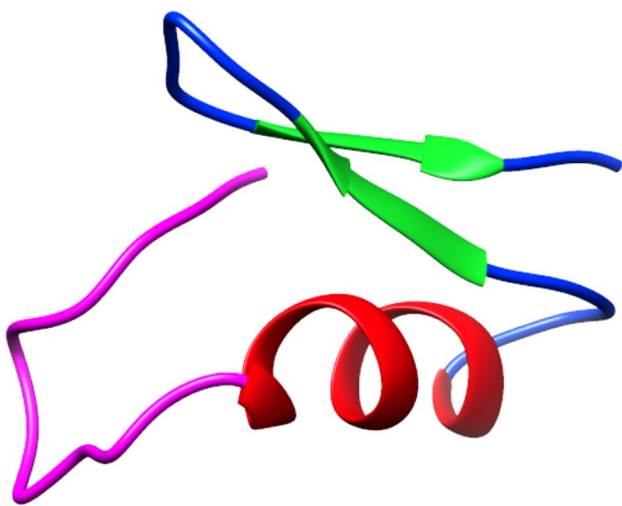
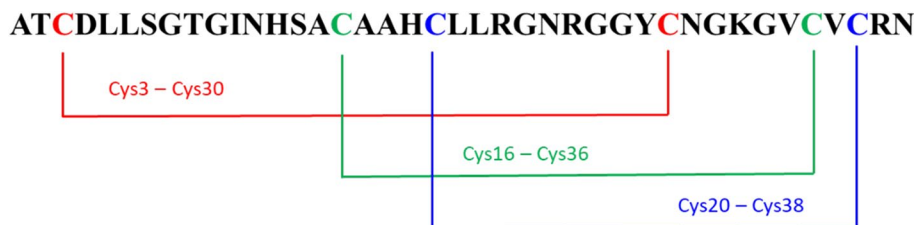


**Fig. 3** Structural representation of lucifensin, a defensin antimicrobial peptide identified in *Lucilia sericata*, obtained from the Protein Data Bank [95]. The N-terminal loop is shown magenta; the  $\alpha$ -helix region in red and the antiparallel  $\beta$ -sheet in green. The image has been generated with UCSF CHIMERA software [98]

**Fig. 4** Disulfide bonds amongst Cys of insect Defensins A from *Protophormia terraenovae*



## Cecropins ( $\alpha$ -helical AMPs)

AMPs belonging to the cecropin family represent the most abundant linear  $\alpha$ -helical AMPs in insects [38]. They were isolated for the first time from hemolymph of the lepidopteran *Hyalophora cecropia*. Before maturation, insect cecropins are composed by a range between 58 and 79 amino acids. The active forms contain between 34 and 55 residues and are mainly active against Gram-negative bacteria, and, to a lesser extent, against Gram-positive bacteria [112, 113]. It has been also demonstrated that some cecropins can exhibit (i) antifungal activity, (ii) a low toxicity against normal mammalian cells, and (iii) a weak, or absent in some cases, hemolytic effect against mammalian erythrocytes [114]. Moreover, most cecropins are subjected to amidation of the C-terminus, a post-translational modification that increases their antimicrobial activity [81]. Circular dichroism analyses demonstrated that in aqueous solution, cecropins assume a random coiled structure. However, upon the interaction with microbial membranes, cecropins adopt a  $\alpha$ -helical conformation [115, 116]. In Fig. 6a, b, the structures of papiliocin (2LA2, PDB code) from *Papilio xuthus*, and GK cecropin-like peptide (2MMM, PDB code) from *Aedes aegypti*, respectively, are shown.

Several insect cecropins have been studied so far from both a structural and a biological point of view, evaluating their in vitro activity. For example, cecropin A has a stabilized  $\alpha$ -helical structure and has been shown to reduce both NADP<sup>+</sup> and glutathione levels, inducing oxidative stress by forming ROS, but its mechanism of action is still unknown [117, 118].

Cecropin A shows activity against the fungus *Beauveria bassiana* in silkworm larvae [119] but cecropin B, a linear cationic peptide, shows the highest and wide antibacterial activity among the cecropins family [120]. It has been reported that cecropin B decreases the bacterial load of *E. coli* and the concentration of plasma endotoxin it has exhibited antifungal activity against *Candida albicans* [115, 121]. Some cecropins also show anti-inflammatory activity [122, 123]. Inflammation is a protective response of a tissue triggered by pathogen infection and involved in the reparative processes [124]. In Table 2, the major insect cecropins with reported antimicrobial activity are listed.

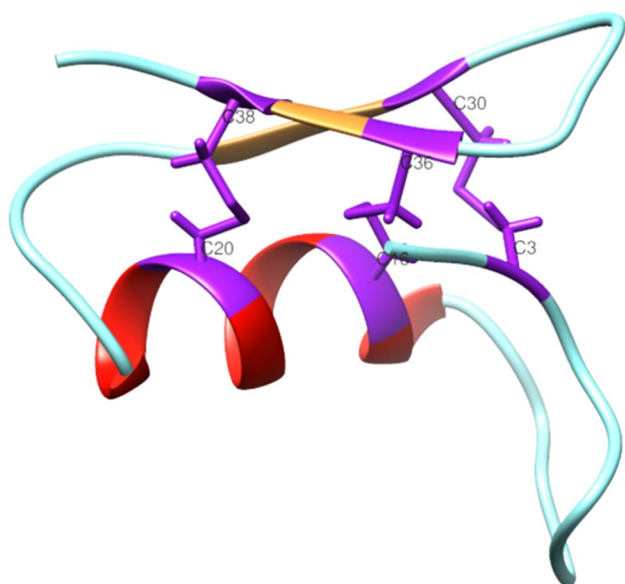


**Fig. 5** Structural representation of disulfide bonds in lucifensin. The loop is shown in cyan, the  $\alpha$ -helix region in red, and the antiparallel  $\beta$ -sheet in orange while the cysteine residues, and the disulfide bonds are in purple. The image has been generated using UCSF CHIMERA software [98]

## Attacins

Attacins are Gly-rich proteins, first purified from the hemolymph of *H. cecropia* bacteria-immunized pupae. Attacins are produced as pre-pro-proteins with a signal peptide, a pro-peptide, an N-terminal attacin domain and two Gly-rich domains, called G1 and G2 domains [130].

They can be divided in two groups: the acidic (i.e. attacin E, and F), and basic (i.e. attacins A–D) attacins [131]. Even though attacins are encoded by two different genes [132] and they have been identified in lepidopteran and dipteran species [133–137], they show high similarity in the amino acid sequences.

They are mostly active against Gram-negative bacteria, particularly *E. coli* and some Gram-positive bacteria. For example the attacin peptide from *Spodoptera exigua*, is active against *E. coli* and *Pseudomonas cichorii* but also against Gram-positive *Bacillus subtilis* and *Listeria monocytogenes* [138, 139].

## Glycine-rich AMPs

Gloverins are Gly-rich peptides identified in the *Lepidoptera*

**Table 1** Examples of insect defensins with reported antimicrobial activity

Peptide (species)	SwissProt accession number	Antimicrobial activity	Reference
Defensin ( <i>Phlebotomus duboscqi</i> )	P83404	Gram-positive bacteria	[102]
Tenecin 1 ( <i>Tenebrio molitor</i> )	Q27023		[103]
Defensin ( <i>Bombus pascuorum</i> )	P81462	Gram-positive and Gram-negative bacteria	[104]
Coprisinc ( <i>Copris tripartitus</i> )	A9XFZ7		[105]
Defensin 1 ( <i>Acalolepta luxuriosa</i> )	Q9BK52		[106]
Defensin A ( <i>Anomala cuprea</i> )	P83669	Gram-positive bacteria	[107]
Defensin B ( <i>Anomala cuprea</i> )	P83668	Gram-positive and Gram-negative bacteria	
Defensin ( <i>Calliphora vicina</i> )	C0HJX7	Gram-positive bacteria	[108]
Royalisin ( <i>Apis mellifera</i> )	P17722		[109]
Defensin ( <i>Pyrrhocoris apterus</i> )	P37364	Gram-positive and Gram-negative bacteria	[110]
Defensin ( <i>Oryctes rhinoceros</i> )	O96049	Gram-positive bacteria	[111]

insect order and synthesized as pre-pro-proteins [140]. They

**Fig. 6** Structural representation of (a) papiliocin, identified in *Papilio xuthus* insect and (b) GK cecropin-like peptide from *Aedes aegypti*, obtained from the Protein Data Bank [95]. Images have been generated with UCSF CHIMERA software [98]

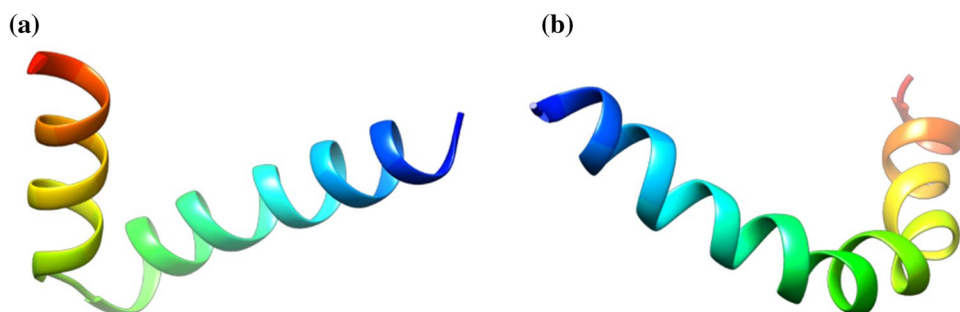


**Table 2** Examples of insect cecropins with reported antimicrobial activity. All the listed cecropins are active against both Gram-positive and Gram-negative bacteria

Peptide (species)	SwissProt accession number	Antimicrobial activity	Reference
Cecropin A ( <i>Spodoptera litura</i> )	Q9XZG9	Gram-positive and Gram-negative bacteria	[125]
Cecropin B ( <i>Spodoptera litura</i> )	Q9XZH0		
Stomoxyn ( <i>Stomoxys calcitrans</i> )	Q8T9R8		[126]
Cecropin A ( <i>Hyalophora cecropia</i> )	P01507		[38]
Cecropin B ( <i>Hyalophora cecropia</i> )	P01508		[113]
Cecropin D ( <i>Hyalophora cecropia</i> )	P01510		[127]
Cecropin A ( <i>Bombyx mori</i> )	Q27239		[113]
Cecropin B ( <i>Bombyx mori</i> )	P04142		
Cecropin D ( <i>Bombyx mori</i> )	O76146		
Papiliocin ( <i>Papilio xuthus</i> )	D8L127		[128]
Cecropin B ( <i>Antheraea pernyi</i> )	P01509		[129]
Cecropin B ( <i>Antheraea pernyi</i> )	P01511		

Diptericin (*Phormia terraenovae*)

**DLHIPPPDNKINWPQLSGGGGSPKTGYDININAQKQK**

**Fig. 7** Sequence of a glycine-rich peptide, Diptericin from *Phormia terraenovae*. Highlighted in red the glycine residues

are basic molecules, and, in aqueous solution, they take a random coil structure, assuming an  $\alpha$ -helical structure in a hydrophobic environment [141]. The first gloverin peptide was purified from the hemolymph of *Hyalophora gloveri* pupae [141]. Gloverin peptides are mostly active against Gram-negative bacteria, particularly *E. coli*, but some of them exhibit antimicrobial activity against Gram-positive bacteria, fungi, and viruses [140, 142]. Gloverin peptide identified in *Manduca sexta*, although exhibiting activity against the Gram-positive bacteria *Bacillus cereus*, *Saccharomyces cerevisiae*, and *C. neoformans*, show no activity against *E. coli* [140].

Diptericins are another class of Gly-rich peptides. Diptericins A–C have been isolated from immunized larvae of *Phormia terraenovae* (Fig. 7), in *Sarcophaga peregrina* and in *D. melanogaster* [143–145]. Prolixicin, a 21 amino acid peptide, has been isolated from *Rhodnius prolixus* and it is released by midgut tissues after the hemolymph bacterial infection [39].

### Proline-rich AMPs

Proline-rich AMPs have a high content of Pro residues. Among them, Lebocins are proline-rich peptides first isolated from the hemolymph of *Bombyx mori* immunized with *E. coli* [146]. Lebocins show antimicrobial action against Gram-positive and Gram-negative bacteria, as well as against some fungi. They were identified in *B. mori*, and require the O-glycosylation for their full activity mainly against *Acinetobacter sp.* and *E. coli*

Drosocin (*Drosophila melanogaster*)

**GKPRPYSRPTSHRPIRV**

**Fig. 8** Sequence of a proline-rich peptide, Drosocin from *Drosophila melanogaster*. Highlighted in red the proline residues

[146]. Other proline-rich AMPs have been identified, such as drosocin, produced by *D. melanogaster* (Fig. 8). Drosocin is an O-glycosylated 19 amino acid peptide and shows a significant sequence homology with Apidaecin IB peptide, isolated from *A. mellifera* [147, 148]. Apidaecins are involved in the honeybee humoral defense against microbial invasion [148].

Moreover, a 26-residue proline-rich immune-inducible linear peptide called Metchnikowin, has been identified in *D. melanogaster*, by Levashina et al. [149]. However, this peptide is not active against Gram-negative bacteria, whereas it exhibits antimicrobial activity against Gram-positive bacteria and fungi. Concerning the antifungal activity, Metchnikowin targets the iron-sulfur subunit (SdhB) of succinate-coenzyme Q reductase [150] and it interacts with the fungal enzyme (1,3)-glucanoyltransferase Gel1 (FgBGT) which is involved in fungal cell wall synthesis [150].



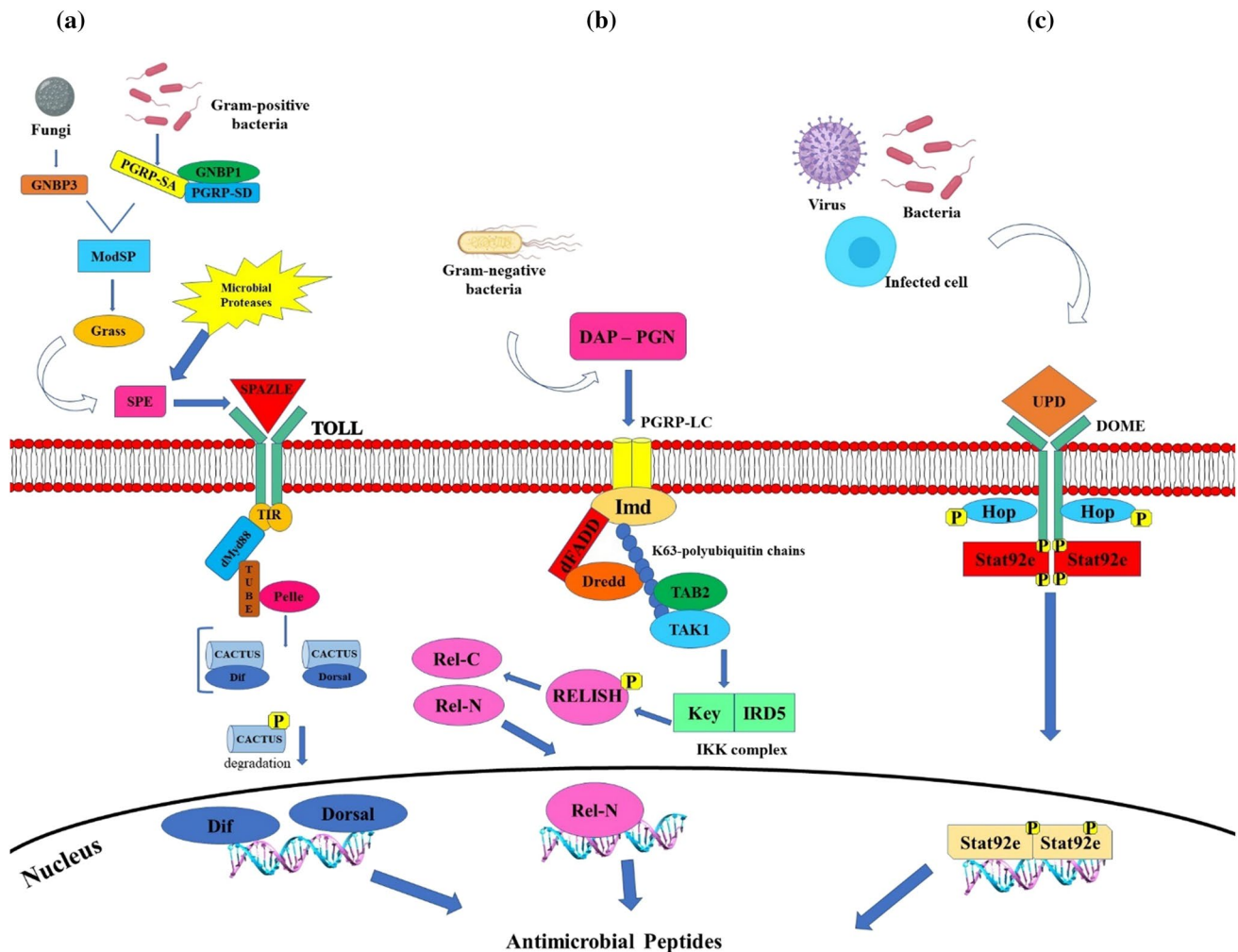


**Fig. 9** Schematic representation of Toll (a), Imd (b), and JAK-STAT (c) signaling pathways. In insects, the Toll pathway is mainly involved in fungi and Gram-positive bacteria detection. Pathogen recognition peptidoglycan recognition proteins (PGRP) activate a serine proteases cascade, involving ModSP and Grass proteins, which in turn, cleaving the inactive form of Spätzle protein, switch on the molecule. These interactions initiate protease cascades. Spätzle activates the dimer Toll receptor, which, in turn recruits cytoplasmic proteins (dMyD88, Tube, and Pelle) involved in the activation of Cactus signaling. In normal cellular condition, Cactus protein is coupled with the Nuclear Factor kappa B (NF- $\kappa$ B) transcription factors Dorsal-related immunity factor (DIF) and Dorsal, but following the Toll pathway activation, it is phosphorylated, detached from DIF and Dorsal and degraded. Then, both DIF and Dorsal can translocate in the nucleus and induce the transcriptional regulation of specific AMP genes (A) [160]. The insect Imd signaling pathway is activated following the binding between PGRP-LC and meso-diaminopimelic acid (DAP)-type peptidoglycan of Gram-negative and some Gram-positive bacteria. The Imd protein is activated following the cleavage by the Fas-associated death domain (FADD) and the death related ced-3/

Nedd2-like caspase (DREDD). The K63-polyubiquitin chains help to link this complex with TAK1 and TAB2 proteins that, in turn, act on the IKK complex, which phosphorylates the NF- $\kappa$ B-like nuclear factor Relish. Consequently, TAK1 and TAB2 proteins are activated, that in turn, act on the IKK complex, composed of Immune Response Deficient 5 (IRD5) and Kenny (Key). This activated complex cleaves Relish. In this way, the Rel DNA-binding domain is released from the C-terminal ankyrin-repeat/I $\kappa$ B-like domain, and translocates to the nucleus inducing specific AMP genes transcription (B) [160]. In insect, JAK/STAT pathway is activated when the cytokine receptor, Domeless (Dome), binds the Unpaired (Upd) cytokines which induces the JAK tyrosine kinase Hopscotch (Hop) to phosphorylate itself and the Dome cytoplasmic component. Simultaneously, the signal transducer and activator of transcription at 92E (Stat92e) bind to the phospho tyrosines on Dome, and they are phosphorylated by Hop. Phosphorylated Stat92e separates itself from the receptor, dimerize and relocate into the nucleus, where it induces the transcription of Thioester-containing protein genes (Teps) and Turandot (Tot) genes. Proteins derived from the transcription of these genes are involved in phagocytosis and melanization processes [160, 161]

## Signaling pathways and mechanisms of action

### AMP gene activation—Toll, Imd, and JAK-STAT pathways

Several signaling molecules are activated after detection of foreign microorganisms by pattern-recognition receptors. Among these, the main pathways are the Immune Deficiency (Imd), the JAK-STAT, and the Toll pathways, which have been well described in *D. melanogaster* (Fig. 6) [151–153]. Antigens of both Gram-positive bacteria and fungi can induce the Toll pathway by activating cellular immunity (Fig. 9a) [153]. Afterward, the signaling pathways involved in humoral immune responses are activated, leading to the release of AMPs, such as drosomycin, by the fat body [39]. The Toll pathway activates the nuclear factor  $\kappa$ B (nuclear factor kappa-light-chain enhancer of activated B cells—NF- $\kappa$ B) reacting in response to stress stimuli, such as in the presence of bacterial or viral antigens [153, 154]. The transmembrane receptor Toll is activated by the extracellular cytokine-like polypeptide, called Spätzle, previously cleaved by serine protease cascades that, in turn, is triggered by the recognition of foreign agents [155]. Specifically, the Toll activation is mediated by peptidoglycan recognition proteins (PGRPs), Gram-negative binding protein (GNBP) 1 in the case of Gram-positive bacterial infection, whereas Toll activation is mediated by GNBP 3 in the case of fungal infections [156, 157]. Toll signaling is activated when Spätzle binds the Toll receptor (Fig. 9a) [158]. The dimerization of the intracytoplasmic TIR (toll-interleukin receptor) domains consequently starts, leading then to the binding of the adaptor protein Myeloid differentiation primary response 88 (MyD88) [153]. This protein binds the adaptor protein, Tube, which recruits the protein kinase Pelle for its autophosphorylation and phosphorylation and degradation of an I $\kappa$ B inhibitor, Cactus. The NF- $\kappa$ B transcription factors Dorsal or Dif are then translocated into the nucleus where they activate the transcription of AMPs [159].

Concerning the infection signaling by Gram-negative bacteria, the Imd signaling pathway is activated when the PGRP-LC receptors bind meso-diaminopimelic acid (DAP)-type peptidoglycan 2 (Fig. 9b). Imd binds to the Fas-associated protein with death domain (FADD), while the caspase called DREDD (FADD-death-related ced-3/Nedd2-like protein) is recruited to cleave the Imd protein, which is then activated by K63-ubiquitination [163, 164]. The K63-polyubiquitin chains recruit TAK1 (transforming growth factor beta (TGF- $\beta$ )-activated kinase 1), which activates the IKK complex involved in the phosphorylation of the NF- $\kappa$ B-like nuclear factor Relish. After Relish cleavage and

phosphorylation, it reaches the nucleus where it activates transcription of specific AMPs, such as diptericin (Fig. 9b) [165].

In the Janus kinase-signal transducer and activator of transcription (JAK-STAT), JAKs are activated after the binding of a cytokine to its receptors and phosphorylate-specific tyrosine residues on the cytoplasmic part of the receptor and these residues then bind to STAT molecules [160, 166] (Fig. 9c). The STAT tyrosine residues are then phosphorylated by JAKs, leading to dimers formation and to the translocation into the nucleus, where they bind the promoters of their target genes [167]. In *D. melanogaster*, the JAK-STAT pathway ligands consist of three cytokine-like proteins called unpaired (upd), upd2 and upd3 [146]. The Dome receptor [168] binds to a single JAK molecule, hopscotch (hop) [169], and one STAT transcription factor, Stat92E for the induction of immune response genes [170].

However, the humoral immune response in *D. melanogaster* is principally controlled by the Toll and Imd pathways leading to the production of AMPs [153].

### Insect AMP mechanism of action

Most insect AMPs show a positive net charge which allows the interaction with the negatively charged molecules exposed on the bacterial cell surfaces, i.e. LPS of Gram-negative and teichoic acids of Gram-positive bacteria, respectively. Then, the electrostatic attraction is the first interaction that occurs between peptides and cell membranes [86, 171]. Hence, AMPs can generate an unbalancing of ion flows across the membrane (i.e. depolarization). This process consequently produces permeabilization of the bacterial membrane [172]. After reaching the onset concentrations, the formation of pores and the subsequent cell death can be induced (Fig. 10). As demonstrated for other peptides deriving from different organisms, insect AMPs can also act through a non-membranolytic mechanism (Fig. 11) [78]. In this case, AMPs lead to bacterial death by interacting with intracellular targets, as observed, for example, for the Temporin L peptide derived from *Rana temporaria*. It inhibits cell division by binding the FtsZ protein that is the key factor of the divisome complex and is essential in Z-ring formation in *E. coli* [173]. Insect proline-rich peptides are also able to bind other intracellular targets such as the chaperone DnaK or the protein synthesis apparatus [174] (Fig. 11).

We focused our main attention on the mechanism of action of defensins, cecropins and attacins AMPs. Insect defensins may lead to bacterial death through the membranolytic mechanism leading to pore formation on the bacterial membranes or can interact with phospholipids to induce microheterogeneity in the lipid membrane [175, 176] (Fig. 10a). LPS could represent a barrier for the antibacterial activity of insect defensins. Indeed, it has been demonstrated

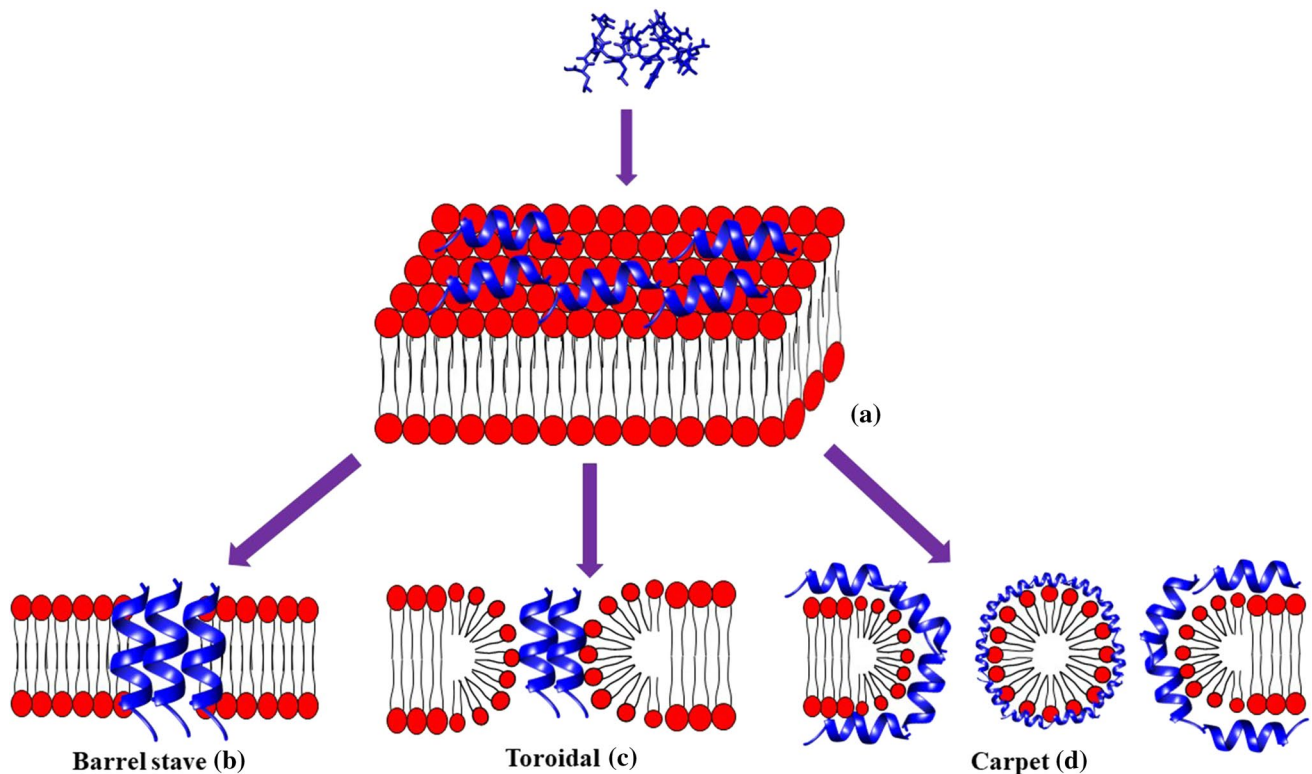


**Fig. 10** Schematic representation of AMP interaction with the bacterial membrane. Membranolytic mechanisms begin with adsorption of AMP on target cell membrane (a). In the barrel-stave model peptides permeate through the bilayer (b); in the toroidal pore mechanism, peptides interact with the head groups of the lipids, induce the bilayer

curvature and perpendicularly insert into the membrane bilayer (c); in the carpet model, peptides cover all the membrane the membrane, the peptide non-polar side chains bind the membrane hydrophobic core while the polar residues with the lipid phosphates, forming micelles with the fragmented membrane (d)

that *E. coli* strains with mutants of LPS are more sensitive to insect defensins [177].

Several studies have been performed to understand cecropin mechanism of action and to identify the functions of specific residues. Most mature cecropins have a tryptophan (Trp) residue in the first or second positions, which confers antimicrobial activity to the peptide [1, 72, 171, 176]. It has been demonstrated that the Trp2 and Phe5 residues in papiliocin peptide, identified in *Papilio xuthus*, are essential for the peptide interaction with LPS in the outer membrane and then for the permeabilization of the inner membrane of Gram-negative bacteria [175].

Although cecropins do not interact with specific receptors, several mechanisms have been proposed to explain the pore formation (Fig. 10). Among these, the carpet model, characterized by high peptide concentration, that leads to the membrane disruption by micelles formation (membranolytic mechanism) (Fig. 10d), is the most accredited. In particular, the interaction via the carpet mechanism assumes that peptides cover the membrane and interact only with the lipid head groups. They associate with the bacterial membrane and then the peptide non-polar side chains fit in the membrane hydrophobic

core while the polar residues interact with the lipid phosphates, forming micelles with the fragmented membrane [178, 179]. At low peptide concentrations, cecropins can form channels or pores in specific sections of the membrane [115, 178, 180].

The toroidal pore mechanism, considered as a part of the membranolytic mechanism, consists of peptides insertion, perpendicularly into the bacterial membrane bilayer, a subsequent interaction with the head groups of the lipids to finally induce the bilayer curvature (Fig. 10c). Instead, the barrel-stave pore formation model suggests that the peptides permeate through the bilayer [181] (Fig. 10b). It has been observed that cecropins identified in *H. cecropia* form a barrel (barrel-stave model), which penetrate the bacterial membrane. Concerning peptides shorter than 22 residues they, however, act through a toroidal pore model, in which the pore is composed by both lipids and peptides [178].

Furthermore, several studies described the ability of AMPs to overpass the membrane using a specific interaction with bacterial phosphatidylethanolamine present at higher concentration onto the bacterial membranes [172]. Nonetheless, it is widely accepted that AMPs can target

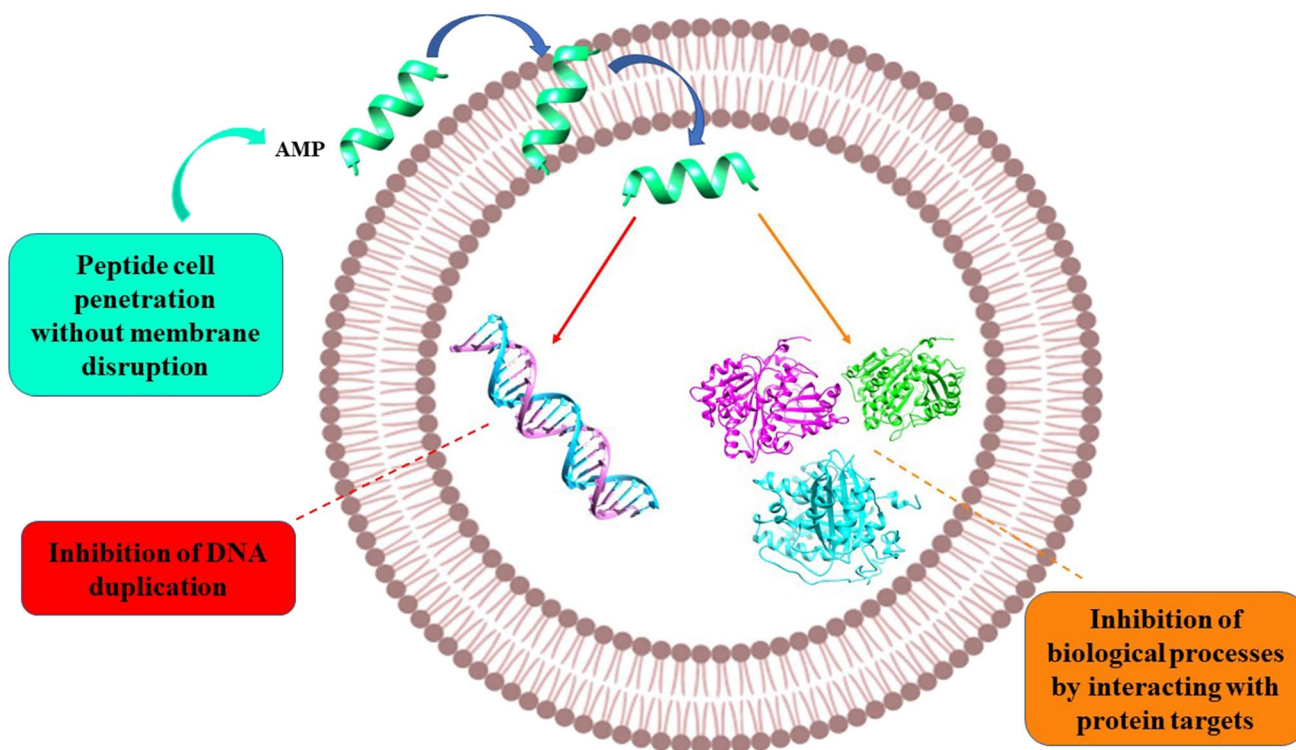


**Fig. 11** Schematic representation of AMP non-membranolytic mechanism. In this case, AMPs can penetrate into the bacterial cell without membrane break, causing bacterial death by interacting with intracel-

lular targets, including DNA and proteins involved in cellular division or protein synthesis

several functions of the bacterial cytoplasm, including the synthesis of nucleic acids, proteins, enzymes, and cell walls. The ability to interfere with several bacterial biosynthetic pathways explain the difficulty in developing resistance towards AMPs [182–184].

Regarding attacin peptides, they can inhibit *E. coli* cells growth by preventing the synthesis of several bacterial porins, which are outer membrane proteins, such as OmpA, OmpC, and OmpF by binding to LPS without penetrating the inner membrane or cytoplasm [139]. Moreover, a well-known peptide, called melittin, is a 26 residues peptide toxin identified in *A. mellifera* venom and is effective against bacteria [185, 186]. It has a strong antibacterial activity against several bacteria and it binds to membrane surfaces leading to pore formation and then to cell lysis [187].

### Stability improvements of peptides against proteolytic susceptibility

#### Overview

The main disadvantage of peptide structure is the susceptibility toward both host and microbial proteolytic

degradation, that may occur before the AMPs can exhibit the pharmacological effect [188]. Therefore, different strategies have been exploited so far.

Peptide drug candidates must deal with bioavailability and biodistribution issues. In reaching the biophase, AMPs have shown low stability in plasma, low oral bioavailability due to protease susceptibility, and rapid hepatic as well as renal clearances. Biopharmaceutical issues, such as high hydrophilicity and a poor ability to cross physiological barriers, must also be considered. Medicinal chemistry can also help with modifications of the wild-type sequence to improve the poor molecular stability or to modulate the conformational flexibility [189, 190]. For instance, the first studies about drosocin, an O-glycosylated AMP from the fruit fly (i.e. *D. melanogaster*), demonstrated inactivity when injected into *E. coli*-infected mice. Drosocin demonstrated a loss of stability and consequently a loss of antibacterial activity [15, 147]. A series of subsequent studies showed that serum stability of the molecule was improved by considering the non-glycosylated drosocin analogs, which reported an extended half-life in mouse serum and improved activity against Gram-negative pathogens *E. coli* and *K. pneumoniae*. Therefore, drosocin analogs with trans-4-hydroxy-L-proline positions were found

to be four- to eight-time more stable in mouse serum than the unmodified analogs [191].

Furthermore, not only the linear and free chain terminations but also the presence of multiple cleavage sites can be readily recognized by the host and bacterial proteases, which can promptly degrade AMPs into inactive fragments. However, after chemical modifications integrated to improve molecular strength against hydrolysis a new structure of AMP is achieved, so it is fundamental to analyze the new AMP characteristics, to avoid, among other issues, bioaccumulation and toxicity [192]. Likewise, the eventual risk of immunogenic effects must be considered [189, 190].

Hence, researchers have to consider structural and functional information such as the study of secondary structure, amino acid composition, length, cationicity, hydrophobicity, and amphipathicity to better obtain a suitable drug candidate with improved stability in vivo.

The chemical modifications play thus a crucial role in the improvement of both the pharmacological activity and biocompatibility, as well as contributing to the chemical stability of the AMP molecules [193–196]. Practically, the main chemical modifications can be included directly during the solid-phase peptide synthesis technique, by which the linear peptide precursor can be assembled from the C-terminal residue, which is linked to the solid resin support. To prevent unwanted couplings during synthesis, a well-known approach considers the use of 9-fluorenylmethyloxycarbonyl (Fmoc) protecting groups. After purification, the obtained linear peptide is let to fold and to cyclize in an appropriate alkaline buffer [197]. Hence, an extra rigidity of the peptide structure may contribute to protract the elimination half-life [198–200].

Including also a broader consideration of the sources, a summary of the most frequent AMP modifications is reported below.

### D-Amino acid substitutions

AMPs can be modified mainly by introducing D-amino acids (DAA) not only in specific regions but also involving all the wild-type sequences. DAA contributes to the partial or the total reversion of the stereochemistry, contributing to enhancing the stability of the peptide against stereospecific proteases [195].

Several studies explored the effect of amino acid substitutions with specific D-amino acids on AMPs activity. To improve the proteolytic resistance, two peptides isolated from the venom of the social wasp *Polybia paulista*, i.e. polybia-MPI and polybia-CP [201], were both partially and totally substituted with DAA. As reported by Zhao and co-workers, the selected AMP was specifically modified with two strategies: (i) by realizing an MPI-analog with D-lysine

(D-Lys-MPI); by obtaining (ii) the D-enantiomer of polybia-MPI (D-MPI). Subsequently, the properties of both D-MPI and D-Lys-MPI were compared [202]. Hence, the authors found that the D-Lys-MPI gained extra stability, together with a loss of the antimicrobial activity due to the impairment of the  $\alpha$ -helix. On the contrary, to retain the antimicrobial effect as well as to improve molecular stability, the D-MPI demonstrated stable when tested with trypsin and chymotrypsin, and its antimicrobial activity revealed like the wild-type compound (i.e. L-MPI). Against all tested bacteria, the minimal inhibitory concentrations (MIC) of the D-MPI demonstrated greater than the D-Lys-MPI, with an auspicious antimicrobial effect towards both *P. aeruginosa* (MIC 64  $\mu$ M), and *S. aureus* (MIC 16  $\mu$ M). Instead, the minimal bactericidal concentration (MBC) was found twofold and fourfold higher, respectively, than MIC values. Taken together, these results have contributed to confirming that the effect of polybia-MPI did not require stereospecific interactions. Therefore, the D-substitution may offer a chemical strategy to improve the stability of the selected APM against protease degradation [202].

The partial and total substitution of DAA in the wild-type sequence was also reported by Jia and co-workers using the polybia-CP compound. Their results demonstrated that both the polybia-CP D-analog, as well as the D-Lys analog, indicated comparable antibacterial activity than the polybia-CP wild-type compound. Furthermore, both MIC and MBC values were not disturbed by each substitution strategy, even though a molecular stability improvement against the enzymatic degradation was observed. Moreover, the D-analog of polybia-CP (D-CP) demonstrated stability to both trypsin and chymotrypsin proteolytic effect, whereas D-Lys analog revealed resistance to trypsin only [203].

However, although preventing protease degradation, partial or total substitution with D-amino amino acids has been demonstrated to be very costly [204].

### N-terminal modifications

The half-life in plasma of a peptide seems related to the typology of the N-terminus residue. N-terminal residues such as Alanine (Ala), Gly, Methionine (Met), Serine (Ser), Threonine (Thr), or Valine (Val) confer to peptides longer half-life. On the contrary, peptides with shorter half-life have been characterized by Arginine (Arg), Aspartate (Asp), Leucine (Leu), Lysine (Lys), or Phenylalanine (Phe) linked at the N-terminus. Likewise, if peptide domains report an enrichment in residues such as Glutamine (Gln), Proline (Pro), Ser, and Thr they are more susceptible to enzymatic degradation [188]. Hence, to block the aminopeptidase action as well as to increase the proteolytic degradation stability of peptides intended for therapeutic use, a common

strategy to overpass enzymatic degradation is the acetylation of the N-terminus [195].

Bacteria and eukaryotes can exhibit the N-alkylation of amino acids. For instance, peptides with N-methyl amino acid display an improved resistance against proteolytic degradation, but also a better ability to permeate membranes than their original peptides. N-methyl-amino acids also characterize drugs like cyclosporin A [205]. This cyclic peptide has seven N-methyl-amino acids, and it displays potent bioactivity, and good oral bioavailability [206]. Concerning N-alkylation, Liu and co-workers modified the wild-type sequence of the peptide anoplin in two main ways. They chemically modified the anoplin, the smallest linear  $\alpha$ -helical AMP isolated from the venom sac of solitary spider wasps *Anoplius samariensis*, with N-methyl amino acids selecting specific positions, as well as introducing fatty acids with various chain lengths. Initially, the authors underwent anoplin with single and multiple N-methyl amino acid substitutions to determine the cleave sites which are recognized by trypsin and chymotrypsin and, therefore, to confer resistance against peptide degradation. Hence, N-methyl amino acids replaced specific residues of Leu, Ile, Lys, and Arg, identified to be sensitive to enzymatic cleavage. The authors found that the steric burden of the N-methyl amino group influenced the molecule conformation and, consequently, the interaction with peptidases. Further evaluations were also conducted to explain whether the antimicrobial activity was affected, as well. For instance, analogs with single and multiple N-methyl amino acid substitutions demonstrated lacking antimicrobial effect against American Type Culture Collection (ATCC) strains of *E. coli*, *S. aureus*, *B. subtilis*, *P. aeruginosa*, and *K. pneumoniae*. The depletion of antimicrobial activity was influenced by the positions or by the number of amino acids replaced with N-methylation. In addition, further explanations were connected to the decrease of the conformational flexibility and to the removal of potential hydrogen bonding that can occur at specific positions. Nonetheless, a slight increase of MIC values when the N-methyl amino acid replacements pertained to the proximity of the C- or N-terminals was also observed [206]. Subsequently, to enhance the antimicrobial activity, the analogs that showed the high proteolytic stability were chosen for the second chemical adjustment. Hence, the N-terminal was modified by introducing fatty acids with chain lengths ranging from C8 to C14. The antimicrobial activity of the N-methylated lipopeptides with C12/C14 exhibited greater antimicrobial effects against both Gram-negative and Gram-positive bacteria, selecting the C12 compound as the most promising analog. However, the cytotoxicity of N-methylated and C12-analog was also observed, due to the non-selectivity membrane affinity of lipid, inducing hemolytic activity [206].

Zhong and colleagues reported a series of new monomer and dimer peptides that they synthesized by conjugating

fatty acids at the N-terminus. The selected AMP was a partial DAA substituted analogue of anoplin. Along with the dimerization of the AMP, the authors showed an alternative method to improve both the anoplin antimicrobial activity and the stability. Moreover, the authors found the lowest MIC when the chain length ranged between C8 and C12. Specifically, a fatty acid chain of C10 showed the lowest MIC towards *P. aeruginosa* ATCC 27853. Against both *S. aureus* species, i.e. ATCC 25923 and MRSA 936, they found a MIC of 8  $\mu$ M. The dimerization of the helix brought greater MICs for almost all tested species of Gram-negative bacteria. Focusing also on *S. aureus* biofilm inhibition percentage, the authors reported a high rate using a concentration of 2xMIC of peptides characterized by chain lengths of C8, C10, and C12. The biofilm inhibition was then found comparable to unmodified anoplin and polymyxin taken as controls. Considering *P. aeruginosa* species, the authors also found a better rate percentage of inhibition using peptides with the fatty acids chain lengths of C10, and C12, both taken at 2xMIC concentration, whereas using dimers, the effect of inhibition was not significant. The authors also suggested that, in combination with conventional antibiotics, the modified AMPs with a fatty acid chain, along with dimer constitution from modified peptides, may open the way to synergism towards the inhibition of the biofilm formation [207].

## Cyclization and dimerization

Molecular stability represents a crucial requirement for AMPs to be used as new active pharmaceutical ingredients. Several disulfide-rich peptide families, such as plant cycloptides [208] or primate-related  $\theta$ -defensin [209] display Cys-stabilized structures with a well-defined three-dimensional motif. Focusing on AMP modifications, it is possible to realize the cyclization by three main post-translational methods, i.e. by peptide, lactam, or disulfide bonds. Therefore, by chemical or biological approaches, it is possible to restrict the conformational bend of the peptide structure by introducing some conformational constraints. The modification of the wild-type sequence by cyclization confers rigidity to peptide chains, so the new structural achievement exhibits a minor attitude to be hydrolyzed by proteases [195, 196, 210]. Nonetheless, chemical modifications might also affect the pharmacological effect.

The bioactive conformation of drosocin, a 19-residue proline-rich inducible antibacterial peptide from *D. melanogaster* [147, 211], and apidaecin, a 17-residue from *Apis mellifera* [104] were studied by Gobbo and co-workers. They showed that only the large cyclic dimer of apidaecin moderately retained the antimicrobial activity and the obtained bending of the peptide chain was then not a structural

element characteristic of the bioactive conformation of drosocin and apidaecin [148].

To be provided with more information about cyclic and circular peptides, it is possible to consult an open-access database <http://www.cybase.org.au/> [212]. Furthermore, most of the approved antimicrobial peptides by the FDA are cyclic structures (e.g. vancomycin, oritavancin, dalbavancin, and telavancin). Due to their higher stability in vivo than that of their linear equivalents, molecular stability represents, therefore, a key factor in reaching the approval [213].

### Insect AMPs to counteract the bacterial biofilm issue

The AMPs used against biofilm act in different way such as (i) the inhibition of planktonic bacteria to adhere to the substrate and the increase the expression regarding motility genes check, (ii) the downregulation of the extracellular matrix synthesis, and (iii) direct bacterial killing. However, most AMP databases consider the AMP antibacterial activity against planktonic bacteria. To fill this gap, Di Luca and co-workers created a database (<http://baamps.it/>) to address the organization of the AMP antibiofilm activity and to support the antibiofilm study. The antibiofilm field can be considered an emerging research area as reported by Home and Di Luca [214, 215].

Several AMPs, particularly insect cecropins, show the ability to counteract biofilm formation. As reported above, biofilms are a group of microbial cells irreversibly associated to a surface and enclosed in a self-produced matrix, which consists of DNA, polysaccharides, and proteins. It constitutes a barrier that protects bacteria from a variety of chemical, physical, and biological stresses [216]. Biofilms can grow on several surfaces including human skin, teeth, as well as bone and urinary tracts implants, valves, and other artificial implants. When bacteria switch to the biofilm mode of growth, the biomaterial-associated infections are difficult to treat with conventional antibiotic therapies [217]. A crucial problem connected to infections causing respiratory illness is also represented by biofilm development within the lung.

Several studies are reported on insect AMP with antibiofilm effect. Hwang and co-workers focused on a defensin-like peptide derived from the dung beetle *Copris tripartitus*. The authors investigated the antimicrobial and antibiofilm activities of a *C. tripartitus*-derived APM, the coprisin, alone, or in combination with conventional antibiotics. The antibacterial susceptibility testing was conducted against Gram-positive and Gram-negative bacterial strains including *E. faecium* ATCC 19434, *S. aureus* ATCC 25923, *S. mutans* KCTC 3065 from the Korean Collection for Type Cultures (KCTC), two *E. coli* strains, i.e. O-157 ATCC 25922, and ATCC 43895 respectively, and *P. aeruginosa* ATCC 27853. Using the Tissue Culture

Plate Method, the antibiofilm activity with a pre-formed biofilm method was tested. A high percentage of biofilm inhibition reported as mean  $\pm$  SD was found when coprisin was tested against Gram-negative species, ranging between  $80.4 \pm 4.4\%$  and  $86.2 \pm 3.3\%$ . The combination of coprisin and ampicillin reporting the highest percentage of biofilm inhibition against *E. coli* O-157 and *P. aeruginosa*, i.e.  $90.1 \pm 2.9\%$  and  $91.7 \pm 2.5\%$ , respectively [218].

Chemical synthesized Pro9-3 and Pro9-3D defensins, originated from beetle *Protaetia brevitarsis*, inhibited biofilm formation in *E. coli* and *A. baumannii* in a concentration-dependent manner. Pro9-3 peptide was also modified to increase cationicity and resistance to protease activity, adding Arg to the N-terminus: this modification highly increases the ability to inhibit biofilm formation and to disrupt the mature biofilms, also of MDR strains (MDREC 1229 and MDRAB 12010) [219].

Uropathogenic *E. coli* biofilms are a typical complication of urinary tract infections that contribute to chronicize the disease. Insect AMP cecropin A from *G. mellonella* is able to disrupt planktonic and sessile biofilm cells, alone or combined with the antibiotic nalidixic acid. This finding clearly highlights the high potential of synergistic action between AMPs and classical antibiotics to treat in vivo infection [220].

Very interesting studies showed the antibiofilm performances of a complex mixture of defensin, cecropin, diphtericin, proline-rich, and domesticin-like peptides, induced by *C. vicina* immune response after *E. coli* M17 strain infection. In nature, *C. vicina* lives in extremely contaminated areas, rich in bacteria, so this insect innately produces a lot of AMPs simultaneously. The AMP complex displays strong biofilm-breaking activity against human antibiotic-resistant pathogens, such as different strains of *E. coli*, *S. aureus*, *P. aeruginosa*, *K. pneumoniae*, and *A. baumannii*. The inhibition degree is strictly related to specific bacterial strains. The possible synergy between AMP mixture and many common antibiotics (meropenem, amikacin, kanamycin, ampicillin, vancomycin, cefotaxime, clindamycin, erythromycin, chloramphenicol, oxacillin, tetracycline, ciprofloxacin, gentamicin, and polymyxin B) was also evaluated, demonstrating different positive level of interaction in all bacteria, except polymyxin B in *E. coli*. Moreover, this AMP cocktail does not have toxicity to human cells [221, 222].

### AMPs in ongoing clinical trials

Currently, there are still no insect-derived AMP products derived from insects on the biopharmaceutical market [223]. Surely, the insect AMPs may be exploited as an

alternative to conventional antibiotics, or a support to synergize their activity.

Although many insect AMPs are synthesized and tested against bacterial strains, few clinical studies are achieved, especially concerning anticancer activity. For example, two peptides from *Oryctes rhinoceros*, the rhinoceros beetle, were successfully tested: the defensin ALYLAI $\text{RRR-NH}_2$  strongly inhibited MRSA in vivo and in vitro; the D-peptide B, an anticancer peptide, disrupted mouse myeloma cells in vitro with no effects on normal leukocytes [224, 225]. Another AMP molecule, Pierisin-1, AMP from *Pieris rapae*, shows anticancer activity, inducing apoptosis and cytotoxicity in some mammalian cancer cell lines (lung, renal, colorectal, bladder, cervical, and liver) by mono-ADP-ribosylation of DNA [226, 227].

Currently, the clinical use of insect AMPs is really limited because of lacking information concerning bioavailability, instability to proteases, toxicity and side effects [228].

## Conclusions

Insects lack adaptive immunity and base their survival on the production of broad-spectrum AMPs which allow them to create powerful defense mechanisms to counteract infections. In fact, due to the variety of substrates they eat and to the environments in which they live, insects have developed a great variety of responses within the innate immunity. For this reason, with over 1 million described species, they constitute an almost inexhaustible source of biologically active compounds. Several bacteria developed multidrug resistance to modern antibiotics, thus there is a great interest in finding and developing new antimicrobial drugs. Most insect AMPs are cationic due to the presence of basic residues in their amino acid sequences. Thus, they are positively charged at physiological pH, and the positive net charge facilitates their binding to negatively charged microbial surfaces through electrostatic interactions. Thanks to their antibacterial activity and to their ability to be active against fungi, viruses and some cancer cell lines, insect AMPs attract great attention in the biomedical field. In addition, it has been demonstrated that some peptides exhibit an antibiofilm activity and this characteristic makes them good candidates for the use on medical devices to drastically reduce the formation of microbial colonies and biofilm development. The balance of several advantageous parameters from innovative drug delivery systems, along with further chemical stability may confer to AMP-based therapies a suitable potency and biocompatibility. Therefore, considering their broad-spectrum antimicrobial activity, AMPs represent interesting candidates

for therapeutic use and will certainly be the object of further research in the future. Moreover, the possibility to use the arsenal of insect AMPs will constitute a great advantage as the management of insects in the laboratory and at higher levels has many advantages: low environmental impact, significantly reduced research cost and time, thanks to the simplicity in breeding them and the high rate of reproduction. In addition, insects breeding overcome ethical problems.

**Author contributions** Conceptualization: PF; writing—original draft preparation: PF, MDM, AM, RS, and CS; writing—review and editing: MDM, AM, RS, CS, AS, DL, HV, and PF; supervision: PF.

**Funding** Open access funding provided by Università degli Studi della Basilicata within the CRUI-CARE Agreement. This research was supported by the Italian Ministry of Instruction, University and Research (MIUR) within the frameworks of the project PRIN 2017 (protocol Prot. 2017AHTCK7).

## Compliance with ethical standards

**Conflicts of interest** The authors declare that they have no conflict of interest.

**Open Access** This article is licensed under a Creative Commons Attribution 4.0 International License, which permits use, sharing, adaptation, distribution and reproduction in any medium or format, as long as you give appropriate credit to the original author(s) and the source, provide a link to the Creative Commons licence, and indicate if changes were made. The images or other third party material in this article are included in the article's Creative Commons licence, unless indicated otherwise in a credit line to the material. If material is not included in the article's Creative Commons licence and your intended use is not permitted by statutory regulation or exceeds the permitted use, you will need to obtain permission directly from the copyright holder. To view a copy of this licence, visit <http://creativecommons.org/licenses/by/4.0/>.

## References

1. Martens E, Demain AL (2017) The antibiotic resistance crisis, with a focus on the United States. *J Antibiot*. <https://doi.org/10.1038/ja.2017.30> ((Tokyo))
2. Payne DJ, Gwynn MN, Holmes DJ, Pompliano DL (2007) Drugs for bad bugs: confronting the challenges of antibacterial discovery. *Nat Rev Drug Discov* 6:29–40
3. Tommasi R, Brown DG, Walkup GK, Manchester JI, Miller AA (2015) ESKAPEing the labyrinth of antibacterial discovery. *Nat Rev Drug Discov* 14:529–542
4. Beceiro A, Tomás M, Bou G (2013) Antimicrobial resistance and virulence: a successful or deleterious association in the bacterial world? *Clin Microbiol Rev*. <https://doi.org/10.1128/CMR.00059-12>
5. Ghosh A, Saran N, Saha S (2020) Survey of drug resistance associated gene mutations in *Mycobacterium tuberculosis*, ESKAPE and other bacterial species. *Sci Rep* 10:1–11. <https://doi.org/10.1038/s41598-020-65766-8>



6. WHO (2017) Global priority list of antibiotic-resistant bacteria to guide research, discovery, and development of new antibiotics. <https://www.who.int/medicines/publications/global-priority-list-antibiotic-resistant-bacteria/en/>. Accessed 13 Feb 2021
7. Neshani A, Sedighian H, Mirhosseini SA, Ghazvini K, Zare H, Jahangiri A (2020) Antimicrobial peptides as a promising treatment option against *Acinetobacter baumannii* infections. *Microb Pathog*. <https://doi.org/10.1016/j.micpath.2020.104238>
8. De Soyza A, Aksamit T (2016) Ciprofloxacin dry powder for inhalation in non-cystic fibrosis bronchiectasis. *Expert Opin Orphan Drugs* 4:875–884
9. McShane PJ, Weers JG, Tarara TE, Haynes A, Durbha P, Miller DP, Mundry T, Operschall E, Elborn JS (2018) Ciprofloxacin dry powder for inhalation (ciprofloxacin DPI): technical design and features of an efficient drug–device combination. *Pulm Pharmacol Ther* 50:72–79
10. Varga JJ, Barbier M, Mulet X, Bielecki P, Bartell JA, Owings JP, Martinez-Ramos I, Hittle LE, Davis MR, Damron FH (2015) Genotypic and phenotypic analyses of a *Pseudomonas aeruginosa* chronic bronchiectasis isolate reveal differences from cystic fibrosis and laboratory strains. *BMC Genom* 16:883
11. Gollan B, Grabe G, Michaux C, Helaine S (2019) Bacterial persists and infection: past, present, and progressing. *Annu Rev Microbiol* 73:359–385. <https://doi.org/10.1146/annurev-micro-020518-115650>
12. Bush K, Page MGP (2017) What we may expect from novel antibacterial agents in the pipeline with respect to resistance and pharmacodynamic principles. *J Pharmacokinet Pharmacodyn* 44:113–132. <https://doi.org/10.1007/s10928-017-9506-4>
13. Dian Permana A, Mir M, Utomo E, Donnelly RF (2020) Bacterially sensitive nanoparticle-based dissolving microneedles of doxycycline for enhanced treatment of bacterial biofilm skin infection: a proof of concept study. *Int J Pharm*. <https://doi.org/10.1016/j.ijpharm.2020.119220>
14. Haisma EM, Göblyös A, Ravensbergen B, Adriaans AE, Cordfunke RA, Schrupf J, Limpens RWAL, Schimmel KJM, Den Hartigh J, Hiemstra PS, Drijfhout JW, El Ghalbzouri A, Nibbering PH (2016) Antimicrobial peptide P60.4Ac-containing creams and gel for eradication of methicillin-resistant *Staphylococcus aureus* from cultured skin and airway epithelial surfaces. *Antimicrob Agent Chemother* 60:4063–4072. <https://doi.org/10.1128/AAC.03001-15>
15. Martínez LC, Vadyvaloo V (2014) Mechanisms of post-transcriptional gene regulation in bacterial biofilms. *Front Cell Infect Microbiol* 4:38. <https://doi.org/10.3389/fcimb.2014.00038>
16. Sharma D, Choudhary M, Vashist J, Shrivastava R, Bisht GS (2019) Cationic antimicrobial peptide and its poly-N-substituted glycine congener: antibacterial and antibiofilm potential against *A. baumannii*. *Biochem Biophys Res Commun* 518:472–478. <https://doi.org/10.1016/j.bbrc.2019.08.062>
17. Bjarnsholt T, Alhede M, Alhede M, Eickhardt-Sørensen SR, Moser C, Köhl M, Jensen PØ, Høiby N (2013) The in vivo biofilm. *Trends Microbiol* 21:466–474. <https://doi.org/10.1016/j.tim.2013.06.002>
18. Bjarnsholt T, Ciofu O, Molin S, Givskov M, Høiby N (2013) Applying insights from biofilm biology to drug development—can a new approach be developed? *Nat Rev Drug Discov* 12:791–808. <https://doi.org/10.1038/nrd4000>
19. Lindsay D, Von Holy A (2006) Bacterial biofilms within the clinical setting: what healthcare professionals should know. *J Hosp Infect* 64:313–325
20. Moskowitz SM, Foster JM, Emerson J, Burns JL (2004) Clinically feasible biofilm susceptibility assay for isolates of *Pseudomonas aeruginosa* from patients with cystic fibrosis. *J Clin Microbiol* 42:1915–1922. <https://doi.org/10.1128/JCM.42.5.1915-1922.2004>
21. Visaggio D, Pasqua M, Bonchi C, Kaever V, Visca P, Imperi F (2015) Cell aggregation promotes pyoverdine-dependent iron uptake and virulence in *Pseudomonas aeruginosa*. *Front Microbiol* 6:902. <https://doi.org/10.3389/fmicb.2015.00902>
22. Webb JS, Givskov M, Kjelleberg S (2003) Bacterial biofilms: prokaryotic adventures in multicellularity. *Curr Opin Microbiol* 6:578–585
23. Wei Q, Ma LZ (2013) Biofilm matrix and its regulation in *Pseudomonas aeruginosa*. *Int J Mol Sci* 14:20983–21005
24. Jimenez PN, Koch G, Thompson JA, Xavier KB, Cool RH, Quax WJ (2012) The multiple signaling systems regulating virulence in *Pseudomonas aeruginosa*. *Microbiol Mol Biol Rev* 76:46–65
25. Aslam S, Darouiche RO (2011) Role of antibiofilm-antimicrobial agents in controlling device-related infections. *Int J Artif Organs* 34:752–758. <https://doi.org/10.5301/ijao.5000024>
26. Flume PA, VanDevanter DR (2015) Clinical applications of pulmonary delivery of antibiotics. *Adv Drug Deliv Rev* 85:1–6
27. Majik MS, Parvatkar PT (2014) Next generation biofilm inhibitors for *Pseudomonas aeruginosa*: synthesis and rational design approaches. *Curr Top Med Chem* 14:81–109
28. Valedo A, Cabanes D, Sousa S (2016) Bacterial toxins as pathogen weapons against phagocytes. *Front Microbiol*. <https://doi.org/10.3389/fmicb.2016.00042>
29. Lam PL, Lee KKH, Wong RSM, Cheng GYM, Bian ZX, Chui CH, Gambari R (2018) Recent advances on topical antimicrobials for skin and soft tissue infections and their safety concerns. *Crit Rev Microbiol* 44:40–78. <https://doi.org/10.1080/1040841X.2017.1313811>
30. Moir DT, Opperman TJ, Butler MM, Bowlin TL (2012) New classes of antibiotics. *Curr Opin Pharmacol* 12:535–544
31. Wright GD (2017) Antibiotic adjuvants: rescuing antibiotics from resistance. *Trends Microbiol* 24:862–871. <https://doi.org/10.1016/j.tim.2016.06.009>
32. Bradshaw JP (2003) Cationic antimicrobial peptides. *BioDrugs* 17(4):233–240
33. Hoskin DW, Ramamoorthy A (2008) Studies on anticancer activities of antimicrobial peptides. *Biochimica et Biophysica Acta (BBA)—Biomembranes*. 1778(2):357–375
34. Schweizer F (2009) Cationic amphiphilic peptides with cancer-selective toxicity. *Eur J Pharmacol* 625(1–3):190–194
35. Guzmán-Rodríguez JJ, Ochoa-Zarzosa A, López-Gómez R, & López-Meza JE (2015) Plant antimicrobial peptides as potential anticancer agents. *BioMed research international*, 2015.
36. Hillyer JF (2016) Insect immunology and hematopoiesis. *Dev Comp Immunol* 58:102–118
37. Vallet-Gely I, Lemaitre B, Bocard F (2008) Bacterial strategies to overcome insect defences. *Nat Rev Microbiol*. <https://doi.org/10.1038/nrmicro1870>
38. Kanost MR, Jiang H, Yu XQ (2004) Innate immune responses of a lepidopteran insect, *Manduca sexta*. *Immunol Rev*. <https://doi.org/10.1111/j.0105-2896.2004.0121>
39. Lemaitre B, Hoffmann J (2007) The Host Defense of *Drosophila melanogaster*. *Annu Rev Immunol* 25:697–743. <https://doi.org/10.1146/annurev.immunol.25.022106.141615>
40. Tsakas S, Marmaras VJ (2010) Insect immunity and its signaling: an overview. *Invertebr Surviv J* 7:228–238
41. Lu HL, Leger RS (2016) Insect immunity to *Entomopathogenic fungi*. *Adv Genet* 94:251–285
42. Hultmark D, Steiner H, Rasmuson T, Boman HG (1980) Insect immunity. Purification and properties of three inducible bactericidal proteins from hemolymph of immunized pupae of *Hyalophora cecropia*. *Eur J Biochem* 106:7–16. <https://doi.org/10.1111/j.1432-1033.1980.tb05991>

43. Ursic-Bedoya R, Buchhop J, Joy JB, Durvasula R, Lowenberger C (2011) Prolixicin: a novel antimicrobial peptide isolated from *Rhodnius prolixus* with differential activity against bacteria and *Trypanosoma cruzi*. *Insect Mol Biol* 20:775–786. <https://doi.org/10.1111/j.1365-2583.2011.01107>
44. Vilcinskas A (2011) Anti-infective therapeutics from the Lepidopteran model host *Galleria mellonella*. *Curr Pharm Des* 17:1240–1245
45. Vonkavaara M, Pavel STI, Hölzl K, Nordfelth R, Sjöstedt A, Stöven S (2013) Francisella is sensitive to insect antimicrobial peptides. *J Innate Immun* 5:50–59. <https://doi.org/10.1159/000342468>
46. Kruse T, Kristensen HH (2008) Using antimicrobial host defense peptides as anti-infective and immunomodulatory agents. *Expert Rev Anti Infect Ther*. <https://doi.org/10.1586/14787210.6.6.887>
47. Chernysh S, Kim SI, Bekker G, Pleskach VA, Filatova NA, Anikin VB, Platonov VG, Bulet P (2002) Antiviral and antitumor peptides from insects. *Proc Natl Acad Sci U S A* 99:12628–12632. <https://doi.org/10.1073/pnas.192301899>
48. Imamura M, Wada S, Ueda K, Saito A, Koizumi N, Iwahana H, Sato R (2009) Multipetide precursor structure of acaloleptin A isoforms, antibacterial peptides from the Udo longicorn beetle, *Acalolepta luxuriosa*. *Dev Comp Immunol* 33:1120–1127. <https://doi.org/10.1016/j.dci.2009.06.004>
49. Langen G, Imani J, Altincicek B, Kieseritzky G, Kogel KH, Vilcinskas A (2006) Transgenic expression of gallerimycin, a novel antifungal insect defensin from the greater wax moth *Galleria mellonella*, confers resistance to pathogenic fungi in tobacco. *Biol Chem* 387:549–557. <https://doi.org/10.1515/BC.2006.071>
50. Pöppel AK, Koch A, Kogel KH, Vogel H, Kollwe C, Wiesner J, Vilcinskas A (2014) Lucimycin, an antifungal peptide from the therapeutic maggot of the common green bottle fly *Lucilia sericata*. *Biol Chem* 395:649–656. <https://doi.org/10.1515/hsz-2013-0263>
51. Hancock REW, Sahl HG (2006) Antimicrobial and host-defense peptides as new anti-infective therapeutic strategies. *Nat Biotechnol*. <https://doi.org/10.1038/nbt1267>
52. Lakshmaiah Narayana J, Chen J-Y (2015) Antimicrobial peptides: possible anti-infective agents. *Peptides* 72:88–94. <https://doi.org/10.1016/j.peptides.2015.05.012>
53. Yi H-Y, Chowdhury M, Huang Y-D, Yu X-Q (2014) Insect antimicrobial peptides and their applications. *Appl Microbiol Biotechnol* 98:5807–5822
54. Liu D, Liu J, Li J, Xia L, Yang J, Sun S, Ma J, Zhang F (2017) A potential food biopreservative, CecXJ-37N, non-covalently intercalates into the nucleotides of bacterial genomic DNA beyond membrane attack. *Food Chem* 217:576–584. <https://doi.org/10.1016/j.foodchem.2016.09.033>
55. Romoli O, Mukherjee S, Mohid SA, Dutta A, Montali A, Franzolin E, Brady D, Zito F, Bergantino E, Rampazzo C, Tettamanti G, Bhunia A, Sandrelli F (2019) Enhanced silkworm Cecropin B antimicrobial activity against *Pseudomonas aeruginosa* from single amino acid variation. *ACS Infect Dis* 5:1200–1213. <https://doi.org/10.1021/acsinfecdis.9b00042>
56. Cole MA, Scott TF, Mello CM (2016) Bactericidal hydrogels via surface functionalization with Cecropin A. *ACS Biomater Sci Eng* 2:1894–1904. <https://doi.org/10.1021/acsbiomaterials.6b00266>
57. Querido MM, Felgueiras HP, Rai A, Costa F, Monteiro C, Borges I, Oliveira D, Ferreira L, Martins MCL (2018) Cecropin-melittin functionalized polyurethane surfaces prevent *Staphylococcus epidermidis* adhesion without inducing platelet adhesion and activation. *Adv Mater Interfaces* 5:1801390. <https://doi.org/10.1002/admi.201801390>
58. Coca M, Peñas G, Gómez J, Campo S, Bortolotti C, Messeguer J, Segundo BS (2006) Enhanced resistance to the rice blast fungus *Magnaporthe grisea* conferred by expression of a cecropin A gene in transgenic rice. *Planta* 223:392–406. <https://doi.org/10.1007/s00425-005-0069-z>
59. Jan PS, Huang HY, Chen HM (2010) Expression of a synthesized gene encoding cationic peptide cecropin B in transgenic tomato plants protects against bacterial diseases. *Appl Environ Microbiol* 76:769–775. <https://doi.org/10.1128/AEM.00698-09>
60. Mitsuhashi I, Matsufuru H, Ohshima M, Kaku H, Nakajima Y, Murai N, Natori S, Ohashi Y (2000) Induced expression of sarcotoxin IA enhanced host resistance against both bacterial and fungal pathogens in transgenic tobacco. *Mol Plant-Microbe Interact* 13:860–868. <https://doi.org/10.1094/MPMI.2000.13.8.860>
61. Cooper D, Eleftherianos I (2017) Memory and specificity in the insect immune system: current perspectives and future challenges. *Front Immunol* 8:539. <https://doi.org/10.3389/fimmu.2017.00539>
62. Pesch Y, Riedel D, Patil K, Loch G, Behr M (2016) Chitinases and imaginal disc growth factors organize the extracellular matrix formation at barrier tissues in insects. *Sci Rep* 6:18340. <https://doi.org/10.1038/srep18340>
63. Sheehan G, Farrell G, Kavanagh K (2020) Immune priming: the secret weapon of the insect world. *Virulence* 11:238–246. <https://doi.org/10.1080/21505594.2020.1731137>
64. Strand MR (2008) The insect cellular immune response. *Insect Sci*. <https://doi.org/10.1111/j.1744-7917.2008.00183>
65. Tang H (2009) Regulation and function of the melanization reaction in *Drosophila*. *Fly* 3:105–111
66. Nakhleh J, Moussawi LE, Osta MA (2017) Chapter three—the melanization response in Insect Immunity. *Advances in Insect Physiology* 52:83–109
67. Cerenius L, Lee BL, Söderhäll K (2008) The proPo-system: pros and cons for its role in invertebrate immunity. *Trends Immunol* 29:263–271
68. Ling E, Yu XQ (2005) Prophenoloxidase binds to the surface of hemocytes and is involved in hemocyte melanization in *Manduca sexta*. *Insect Biochem Mol Biol* 35:1356–1366
69. Pascale M, Laurino S, Vogel H, Grimaldi A, Monné M, Riviello L, Tettamanti G, Falabella P (2014) The Lepidopteran endoribonuclease-U domain protein P102 displays dramatically reduced enzymatic activity and forms functional amyloids. *Dev Comp Immunol* 47(1):129–139
70. Falabella P, Riviello L, Pascale M, Lelio ID, Tettamanti G, Grimaldi A, Iannone C, Monti M, Pucci P, Tamburro AM, Deeguileor M, Gigliotti S, Pennacchio F (2012) Functional amyloids in insect immune response. *Insect Biochem Mol Biol* 42:203–211. <https://doi.org/10.1016/j.ibmb.2011.11.011>
71. Nappi AJ, Christensen BM (2005) Melanogenesis and associated cytotoxic reactions: applications to insect innate immunity. *Insect Biochem Mol Biol* 35:443–459. <https://doi.org/10.1016/j.ibmb.2005.01.014>
72. Lavine MD, Strand MR (2002) Insect hemocytes and their role in immunity. *Insect Biochem Mol Biol* 32:1295–1309. [https://doi.org/10.1016/S0965-1748\(02\)00092-9](https://doi.org/10.1016/S0965-1748(02)00092-9)
73. Satyavathi VV, Minz A, Nagaraju J (2014) Nodulation: an unexplored cellular defense mechanism in insects. *Cell Signal* 26:1753–1763. <https://doi.org/10.1016/j.cellsig.2014.02.024>
74. Williams MJ (2007) *Drosophila hemopoiesis* and cellular immunity. *J Immunol* 178:4711–4716
75. Janeway CA Jr, Medzhitov R (2002) Innate immune recognition. *Annu Rev Immunol* 20:197–216
76. Iwanaga S, Lee BL (2005) Recent advances in the innate immunity of invertebrate animals. *J Biochem Mol Biol* 38:128
77. Dossey AT (2010) Insects and their chemical weaponry: new potential for drug discovery. *Nat Prod Rep* 27:1737–1757
78. Brogden KA (2005) Antimicrobial peptides: pore formers or metabolic inhibitors in bacteria? *Nat Rev Microbiol* 3:238–250

79. Steiner H, Hultmark D, Engström Å, Bennich H, Boman HG (1981) Sequence and specificity of two antibacterial proteins involved in insect immunity. *Nature* 292:246–248. <https://doi.org/10.1038/292246a0>
80. Jin G, Weinberg A (2019) Human antimicrobial peptides and cancer. *Semin Cell Dev Biol* 88:156–162. <https://doi.org/10.1016/j.semcdb.2018.04.006>
81. Tonk M, Vilcinskas A, Rahnamaeian M (2016) Insect antimicrobial peptides: potential tools for the prevention of skin cancer. *Appl Microbiol Biotechnol* 100:7397–7405
82. Zasloff M (2002) Antimicrobial peptides of multicellular organisms. *Nature* 415:389–395
83. Vilcinskas A (2013) Evolutionary plasticity of insect immunity. *J Insect Physiol* 59:123–129. <https://doi.org/10.1016/j.jinsphys.2012.08.018>
84. Welcome to the APD3 [WWW Document], n.d. URL <http://aps.unmc.edu/AP/>. Accessed 4 feb 2020
85. Brady D, Grapputo A, Romoli O, Sandrelli F (2019) Insect cecropins, antimicrobial peptides with potential therapeutic applications. *Int J Mol Sci* 20:5862. <https://doi.org/10.3390/ijms20235862>
86. Bulet P, Stocklin R (2005) Insect antimicrobial peptides: structures, properties and gene regulation. *Protein Pept Lett* 12:3–11. <https://doi.org/10.2174/0929866053406011>
87. Makarova O, Johnston P, Rodriguez-Rojas A, El Shazely B, Morales JM, Rolff J (2018) Genomics of experimental adaptation of *Staphylococcus aureus* to a natural combination of insect antimicrobial peptides. *Sci Rep* 8:15359. <https://doi.org/10.1038/s41598-018-33593-7>
88. Gerardo NM, Altincicek B, Anselme C et al (2010) Immunity and other defenses in pea aphids. *Acyrtosiphon pisum* Genome Biol 11:R21. <https://doi.org/10.1186/gb-2010-11-2-r21>
89. Moretta A, Salvia R, Scieuzo C, Di Somma A, Vogel H, Pucci P, Sgambato A, Wolff M, Falabella P (2020) A bioinformatic study of antimicrobial peptides identified in the black soldier fly (BSF) *Hermetia illucens* (Diptera: Stratiomyidae). *Sci Rep* 10:16875. <https://doi.org/10.1038/s41598-020-74017-9>
90. Erickson MC, Islam M, Sheppard C, Liao J, Doyle MP (2004) Reduction of *Escherichia coli* O157:H7 and *Salmonella enterica* serovar Enteritidis in chicken manure by larvae of the black soldier fly. *J Food Prot* 67:685–690. <https://doi.org/10.4315/0362-028x-67.4.685>
91. Liu Q, Tomberlin JK, Brady JA, Sanford MR, Yu Z (2008) Black soldier fly (Diptera: Stratiomyidae) larvae reduce *Escherichia coli* in dairy manure. *Environ Entomol* 37:1525–1530. <https://doi.org/10.1603/0046-225x-37.6.1525> (PMID: 19161696)
92. Elhag O, Zhou D, Song Q, Soomro AA, Cai M, Zheng L, Yu Z, Zhang J (2017) Screening, expression, purification and functional characterization of novel antimicrobial peptide genes from *Hermetia ILLUCENS* (L.). *PLoS ONE* 12:e0169582–e0169582. <https://doi.org/10.1371/journal.pone.0169582>
93. Ganz T, Lehrer RI (1995) Defensins. *Pharmacol Ther* 66:191–205. [https://doi.org/10.1016/0163-7258\(94\)00076-F](https://doi.org/10.1016/0163-7258(94)00076-F)
94. Bulet P, Cociancich S, Reuland M, Sauber F, Bischoff R, Hegy G, Van Dorsseleer A, Hetru C, Hoffmann JA (1992) A novel insect defensin mediates the inducible antibacterial activity in larvae of the dragonfly *Aeshna cyanea* (Paleoptera, Odonata). *Eur J Biochem* 209:977–984. <https://doi.org/10.1111/j.1432-1033.1992.tb17371.x>
95. Berman HM, Westbrook J, Zardocki C, Bourne PE (2003) The protein data bank. CRC Press, Protein Struct Determ Anal Appl Drug Discov, p 389
96. Bonmatin J-M, Bonnat J-L, Gallet X, Vovelle F, Ptak M, Reichhart J-M, Hoffmann JA, Keppe E, Legrain M, Achstetter T (1992) Two-dimensional <sup>1</sup>H NMR study of recombinant insect defensin A in water: resonance assignments, secondary structure and global folding. *J Biomol NMR* 2:235–256
97. Cornet B, Bonmatin J-M, Hetru C, Hoffmann JA, Ptak M, Vovelle F (1995) Refined three-dimensional solution structure of insect defensin A. *Structure* 3:435–448. [https://doi.org/10.1016/S0969-2126\(01\)00177-0](https://doi.org/10.1016/S0969-2126(01)00177-0)
98. Pettersen EF, Goddard TD, Huang CC, Couch GS, Greenblatt DM, Meng EC, Ferrin TE (2004) UCSF Chimera: a visualization system for exploratory research and analysis. *J Comput Chem* 25:1605–1612. <https://doi.org/10.1002/jcc.20084>
99. Bachère E, Destoumieux D, Bulet P (2000) Penaeidins, antimicrobial peptides of shrimp: a comparison with other effectors of innate immunity. *Aquaculture* 191:71–88. [https://doi.org/10.1016/S0044-8486\(00\)00419-1](https://doi.org/10.1016/S0044-8486(00)00419-1)
100. Lee YS, Yun EK, Jang WS, Kim I, Lee JH, Park SY, Ryu KS, Seo SJ, Kim CH, Lee IH (2004) Purification, cDNA cloning and expression of an insect defensin from the great wax moth, *Galleria mellonella*. *Insect Mol. Biol.* 13:65–72. <https://doi.org/10.1111/j.1365-2583.2004.00462.x>
101. Lowenberger C, Bulet P, Charlet M, Hetru C, Hodgeman B, Christensen BM, Hoffmann JA (1995) Insect immunity: isolation of three novel inducible antibacterial defensins from the vector mosquito, *Aedes aegypti*. *Insect Biochem. Mol. Biol.* 25:867–873. [https://doi.org/10.1016/0965-1748\(95\)00043-U](https://doi.org/10.1016/0965-1748(95)00043-U)
102. Boulanger N, Lowenberger C, Volf P, Ursic R, Sigutova L, Sabatier L, Svobodova M, Beverley SM, Späth G, Brun R, Pesson B, Bulet P (2004) Characterization of a defensin from the sand fly *Phlebotomus duboscqi* induced by challenge with bacteria or the protozoan parasite *Leishmania major*. *Infect Immun* 72:7140–7146. <https://doi.org/10.1128/IAI.72.12.7140-7146.2004>
103. Moon HJ, Lee SY, Kurata S, Natori S, Lee BL (1994) Purification and molecular cloning of cDNA for an inducible antibacterial protein from larvae of the coleopteran, *Tenebrio molitor*. *J Biochem* 116:53–58. <https://doi.org/10.1093/oxfordjournals.jbchem.a124502>
104. Rees JA, Moniatte M, Bulet P (1997) Novel antibacterial peptides isolated from a European bumblebee, *Bombus pascuorum* (Hymenoptera, apoidea). *Insect Biochem Mol Biol* 27:413–422. [https://doi.org/10.1016/S0965-1748\(97\)00013-1](https://doi.org/10.1016/S0965-1748(97)00013-1)
105. Hwang J-S, Lee J, Kim Y-J, Bang H-S, Yun E-Y, Kim S-R, Suh H-J, Kang B-R, Nam S-H, Jeon J-P, Kim I, Lee DG (2009) Isolation and characterization of a defensin-like peptide (coprisin) from the dung beetle, *Copris tripartitus*. *Int. J. Pept.* 2009:136284. <https://doi.org/10.1155/2009/136284>
106. Ueda K, Imamura M, Saito A, Sato R (2005) Purification and cDNA cloning of an insect defensin from larvae of the longicorn beetle, *Acalolepta luxuriosa*. *Appl Entomol Zool* 40:335–345. <https://doi.org/10.1303/aez.2005.335>
107. Yamauchi H (2001) Two novel insect defensins from larvae of the cupreous chafer, *Anomala cuprea*: purification, amino acid sequences and antibacterial activity. *Insect Biochem Mol Biol* 32:75–84. [https://doi.org/10.1016/S0965-1748\(01\)00082-0](https://doi.org/10.1016/S0965-1748(01)00082-0)
108. Chernysh SI, Gordja NA, Simonenko NP (2000) Diapause and immune response: induction of antimicrobial peptides synthesis in the blowfly, *Calliphora vicina* R-D (Diptera: Calliphoridae). Diapause immune response induction Antimicrob Pept Synth blowfly *Calliphora Vicin* R-D (Diptera Calliphoridae). 3:139–144
109. Fujiwara S, Imai J, Fujiwara M, Yaeshima T, Kawashima T, Kobayashi K (1990) A potent antibacterial protein in royal jelly. Purification and determination of the primary structure of royalisin. *J Biol Chem* 265:11333–11337
110. Cociancich S, Dupont A, Hegy G, Lanot R, Holder F, Hetru C, Hoffmann JA, Bulet P (1994) Novel inducible antibacterial peptides from a hemipteran insect, the sap-sucking bug *Pyrrhocoris*

- apterus. *Biochem J* 300:567–575. <https://doi.org/10.1042/bj3000567>
111. Ishibashi J, Saito-Sakanaka H, Yang J, Sagisaka A, Yamakawa M (1999) Purification, cDNA cloning and modification of a defensin from the coconut rhinoceros beetle, *Oryctes rhinoceros*. *Eur J Biochem* 266:616–623. <https://doi.org/10.1046/j.1432-1327.1999.00906.x>
  112. Hultmark D, Engstrom Å, Bennich H, Kapur R, Boman HG (1982) Insect immunity: isolation and structure of Cecropin D and four minor antibacterial components from *Cecropia Pupae*. *Eur J Biochem* 127:207–217. <https://doi.org/10.1111/j.1432-1033.1982.tb06857.x>
  113. Moore AJ, Beazley WD, Bibby MC, Devine DA (1996) Antimicrobial activity of cecropins. *J Antimicrob Chemother* 37:1077–1089. <https://doi.org/10.1093/jac/37.6.1077>
  114. Andrä J, Berninghausen O, Leippe M (2001) Cecropins, antibacterial peptides from insects and mammals, are potently fungicidal against *Candida albicans*. *Med Microbiol Immunol* 189:169–173. <https://doi.org/10.1007/s430-001-8025-x>
  115. Efimova SS, Medvedev RY, Chulkov EG, Schagina LV, Ostroumova OS (2018) Regulation of the pore-forming activity of *Cecropin A* by local anesthetics. *Cell tissue biol* 12:331–341. <https://doi.org/10.1134/S1990519X18040028>
  116. Lee E, Kim JK, Jeon D, Jeong KW, Shin A, Kim Y (2015) Functional roles of aromatic residues and helices of papiliocin in its antimicrobial and anti-inflammatory activities. *Sci Rep* 5:12048. <https://doi.org/10.1038/srep12048>
  117. Yun J, Lee DG (2016) *Cecropin A*-induced apoptosis is regulated by ion balance and glutathione antioxidant system in *Candida albicans*. *IUBMB Life* 68:652–662. <https://doi.org/10.1002/iub.1527>
  118. Fu H, Björstād Å, Dahlgren C, Bylund J (2004) A bactericidal *Cecropin-A* peptide with a stabilized  $\alpha$ -helical structure possess an increased killing capacity but no proinflammatory activity. *Inflammation* 28:337–343
  119. Lu D, Geng T, Hou C, Huang Y, Qin G, Guo X (2016) *Bombyx mori Cecropin A* has a high antifungal activity to entomopathogenic fungus *Beauveria bassiana*. *Gene* 583:29–35. <https://doi.org/10.1016/j.gene.2016.02.045>
  120. Srisailam S, Arunkumar AI, Wang W, Yu C, Chen HM (2000) Conformational study of a custom antibacterial peptide cecropin B1: implications of the lytic activity. *Biochim. Biophys Acta (BBA) - Protein Struct Mol Enzymol* 1479:275–285. [https://doi.org/10.1016/S0167-4838\(00\)00008-X](https://doi.org/10.1016/S0167-4838(00)00008-X)
  121. Giacometti A, Cirioni O, Ghiselli R, Viticchi C, Mocchegiani F, Riva A, Saba V, Scalise G (2001) Effect of mono-dose intraperitoneal cecropins in experimental septic shock. *Crit Care Med* 29:1666–1669
  122. Lee E, Shin A, Kim Y (2015) Anti-inflammatory activities of *Cecropin A* and its mechanism of action. *Arch Insect Biochem Physiol* 88:31–44
  123. Wang J, Ma K, Ruan M, Wang Y, Li Y, Fu YV, Song Y, Sun H, Wang J (2018) A novel cecropin B-derived peptide with antibacterial and potential anti-inflammatory properties. *PeerJ*. <https://doi.org/10.7717/peerj.5369>
  124. Chen L, Deng H, Cui H, Fang J, Zuo Z, Deng J, Li Y, Wang X, Zhao L (2017) Inflammatory responses and inflammation-associated diseases in organs. *Oncotarget* 9:7204–7218. <https://doi.org/10.18632/oncotarget.23208>
  125. Choi CS, Lee IH, Kim E, Kim SI, Kim HR (2000) Antibacterial properties and partial cDNA sequences of cecropin-like antibacterial peptides from the common cutworm, *Spodoptera litura*. *Comp. Biochem Physiol Part C Pharmacol Toxicol Endocrinol* 125:287–297. [https://doi.org/10.1016/S0742-8413\(99\)00117-6](https://doi.org/10.1016/S0742-8413(99)00117-6)
  126. Boulanger N, Munks RJL, Hamilton JV, Vovelle F, Brun R, Lehane MJ, Bulet P (2002) Epithelial innate immunity: a novel antimicrobial peptide with antiparasitic activity in the blood-sucking insect *stomoxys calcitrans*. *J Biol Chem* 277:49921–49926. <https://doi.org/10.1074/jbc.M206296200>
  127. Liu X, Guo C, Huang Y, Zhang X, Chen Y (2015) Inhibition of porcine reproductive and respiratory syndrome virus by *Cecropin D* in vitro. *Infect Genet Evol* 34:7–16. <https://doi.org/10.1016/j.meegid.2015.06.021>
  128. Kim SR, Hong MY, Park SW, Choi KH, Yun EY, Goo TW, Kang SW, Suh HJ, Kim I, Hwang JS (2010) Characterization and cDNA cloning of a cecropin-like antimicrobial peptide, papiliocin, from the swallowtail butterfly *Papilio xuthus*. *Mol. Cells* 29:419–423. <https://doi.org/10.1007/s10059-010-0050-y>
  129. Qu X, Steiner H, Engstrom A, Bennich H, Boman HG (1982) Insect immunity: isolation and structure of Cecropins B and D from pupae of the chinese oak silk moth, *antheraea pernyi*. *Eur J Biochem* 127:219–224. <https://doi.org/10.1111/j.1432-1033.1982.tb06858.x>
  130. Hedengren M, Borge K, Hultmark D (2000) Expression and evolution of the *Drosophila Attacin/Diptericin* gene family. *Biochem Biophys Res Commun* 279:574–581. <https://doi.org/10.1006/bbrc.2000.3988>
  131. Hultmark D, Engström A, Andersson K, Steiner H, Bennich H, Boman HG (1983) Insect immunity. Attacins, a family of antibacterial proteins from *Hyalophora cecropia*. *EMBO J* 2:571–576. <https://doi.org/10.1002/j.1460-2075.1983.tb01465.x>
  132. Sun S-C, Lindstrom I, Lee J-Y, Faye I (1991) Structure and expression of the attacin genes in *Hyalophora cecropia*. *Eur J Biochem* 196:247–254. <https://doi.org/10.1111/j.1432-1033.1991.tb15811.x>
  133. Dushay MS, Roethele JB, Chaverri JM, Dulek DE, Syed SK, Kitami T, Eldon ED (2000) Two attacin antibacterial genes of *Drosophila melanogaster*. *Gene* 246:49–57. [https://doi.org/10.1016/S0378-1119\(00\)00041-X](https://doi.org/10.1016/S0378-1119(00)00041-X)
  134. Kang D, Lundström A, Steiner H (1996) *Trichoplusia ni* attacin A, a differentially displayed insect gene coding for an antibacterial protein. *Gene* 174:245–249. [https://doi.org/10.1016/0378-1119\(96\)00089-3](https://doi.org/10.1016/0378-1119(96)00089-3)
  135. Kwon YM, Kim HJ, Kim YI, Kang YJ, Lee IH, Jin BR, Han YS, Cheon HM, Ha NG, Seo SJ (2008) Comparative analysis of two attacin genes from *Hyphantria cunea*. *Comp. Biochem Physiol Part B Biochem Mol Biol*. 151:213–220. <https://doi.org/10.1016/j.cbpb.2008.07.002>
  136. Ourth DD, Lockey TD, Renis HE (1994) Induction of cecropin-like and attacin-like antibacterial but Not antiviral activity in *heliiothis virescens* larvae. *Biochem Biophys Res Commun* 200:35–44. <https://doi.org/10.1006/bbrc.1994.1410>
  137. Rao X-J, Yu X-Q (2010) Lipoteichoic acid and lipopolysaccharide can activate antimicrobial peptide expression in the tobacco hornworm *Manduca sexta*. *Dev Comp Immunol* 34:1119–1128. <https://doi.org/10.1016/j.dci.2010.06.007>
  138. Bang K, Park S, Yoo JY, Cho S (2012) Characterization and expression of attacin, an antibacterial protein-encoding gene, from the beet armyworm, *Spodoptera exigua* (Hübner) (Insecta: Lepidoptera: Noctuidae). *Mol Biol Rep* 39:5151–5159. <https://doi.org/10.1007/s11033-011-1311-3>
  139. Carlsson A, Engström P, Palva ET, Bennich H (1991) Attacin, an antibacterial protein from *Hyalophora cecropia*, inhibits synthesis of outer membrane proteins in *Escherichia coli* by interfering with omp gene transcription. *Infect Immun* 59:3040–3045
  140. Xu X-X, Zhong X, Yi H-Y, Yu X-Q (2012) *Manduca sexta* gloverin binds microbial components and is active against bacteria and fungi. *Dev Comp Immunol* 38:275–284. <https://doi.org/10.1016/j.dci.2012.06.012>
  141. Axen A, Carlsson A, Engstrom A, Bennich H (1997) Gloverin, an antibacterial protein from the immune hemolymph of

- hyalophora* pupae. Eur J Biochem 247:614–619. <https://doi.org/10.1111/j.1432-1033.1997.00614.x>
142. Mrinal N, Nagaraju J (2008) Intron loss is associated with gain of function in the evolution of the gloverin family of antibacterial genes in *Bombyx mori*. J Biol Chem 283:23376–23387. <https://doi.org/10.1074/jbc.M801080200>
  143. Dimarcq J-L, Keppi E, Dunbar B, Lambert J, Reichhart J-M, Hoffmann D, Rankine SM, Fothergill JE, Hoffmann JA (1988) Insect immunity: purification and characterization of a family of novel inducible antibacterial proteins from immunized larvae of the dipteran *Phormia terranova* and complete amino acid sequence of the predominant member, *dip-tericin A*. Eur J Biochem 171:17–22. <https://doi.org/10.1111/j.1432-1033.1988.tb13752.x>
  144. Ishikawa M, Kubo T, Natori S (1992) Purification and characterization of a dip-tericin homologue from *Sarcophaga peregrina* (flesh fly). Biochem J 287:573–578. <https://doi.org/10.1042/bj2870573>
  145. Reichhart JM, Meister M, Dimarcq JL, Zachary D, Hoffmann D, Ruiz C, Richards G, Hoffmann JA (1992) Insect immunity: developmental and inducible activity of the *Drosophila dip-tericin* promoter. EMBO J 11:1469–1477
  146. Hara S, Yamakawa M (1995) A novel antibacterial peptide family isolated from the silkworm. *Bombyx mori*. Biochem. J. 310(2):651–656. <https://doi.org/10.1042/bj3100651>
  147. Bulet P, Dimarcq J-L, Hetru C, Lagueux M, Charlet M, Hegy G, Van Dorsselaer A, Hoffmann JA (1993) A novel inducible antibacterial peptide of *Drosophila* carries an O-glycosylated substitution. J Biol Chem 268:14893–14897
  148. Gobbo M, Biondi L, Filira F, Gennaro R, Benincasa M, Scolaro B, Rocchi R (2002) Antimicrobial peptides: synthesis and antibacterial activity of linear and cyclic drosocin and apidaecin 1b analogues. J Med Chem 45:4494–4504. <https://doi.org/10.1021/jm020861d>
  149. Levashina EA, Ohresser S, Bulet P, Reichhart J-M, Hetru C, Hoffmann JA (1995) Metchnikowin, a novel immune-inducible proline-rich peptide from *Drosophila* with antibacterial and antifungal properties. Eur J Biochem 233:694–700. [https://doi.org/10.1111/j.1432-1033.1995.694\\_2.x](https://doi.org/10.1111/j.1432-1033.1995.694_2.x)
  150. Moghaddam MRB, Gross T, Becker A, Vilcinskas A, Rahnamaeian M (2017) The selective antifungal activity of *Drosophila melanogaster* metchnikowin reflects the species-dependent inhibition of succinate-coenzyme Q reductase. Sci Rep 7:1–9. <https://doi.org/10.1038/s41598-017-08407-x>
  151. Kleino A, Silverman N (2014) The *Drosophila* IMD pathway in the activation of the humoral immune response. Dev Comp Immunol 42:25–35. <https://doi.org/10.1016/j.dci.2013.05.014>
  152. Myllymäki H, Rämét M (2014) JAK/STAT Pathway in *Drosophila* Immunity. Scand J Immunol 79:377–385. <https://doi.org/10.1111/sji.12170>
  153. Valanne S, Wang J-H, Rämét M (2011) The *Drosophila* toll signaling pathway. J Immunol 186:649–656. <https://doi.org/10.4049/jimmunol.1002302>
  154. Ashok Y (2009) *Drosophila* toll pathway: the new model. Sci Signal. <https://doi.org/10.1126/scisignal.252jc1>
  155. Shia AKH, Glittenberg M, Thompson G, Weber AN, Reichhart JM, Ligoxygakis P (2009) Toll-dependent antimicrobial responses in *Drosophila* larval fat body require Spätzle secreted by haemocytes. J Cell Sci 122:4505–4515. <https://doi.org/10.1242/jcs.049155>
  156. Mishima Y, Quintin J, Amanianda V, Kellenberger C, Coste F, Clavaud C, Hetru C, Hoffmann JA, Latgé J-P, Ferrandon D, Rousset A (2009) The N-terminal domain of *Drosophila* Gram-negative binding protein 3 (GNBP3) defines a novel family of fungal pattern recognition receptors. J Biol Chem 284:28687–28697. <https://doi.org/10.1074/jbc.M109.034587>
  157. Wang Y, Jiang H (2006) Interaction of beta-1,3-glucan with its recognition protein activates hemolymph proteinase 14, an initiation enzyme of the prophenoloxidase activation system in *Manduca sexta*. J Biol Chem 281:9271–9278. <https://doi.org/10.1074/jbc.M513797200>
  158. Cherry S, Silverman N (2006) Host-pathogen interactions in *Drosophila*: new tricks from an old friend. Nat Immunol. <https://doi.org/10.1038/ni1388>
  159. Imler JL, Hoffmann JA (2002) Toll receptors in *Drosophila*: A family of molecules regulating development and immunity. Top. Microbiol. Immunol. Curr. [https://doi.org/10.1007/978-3-642-59430-4\\_4](https://doi.org/10.1007/978-3-642-59430-4_4)
  160. Stokes BA, Yadav S, Shokal U, Smith LC, Eleftherianos I (2015) Bacterial and fungal pattern recognition receptors in homologous innate signaling pathways of insects and mammals. Front Microbiol 6:19. <https://doi.org/10.3389/fmicb.2015.00019>
  161. Shokal U, Eleftherianos I (2017) Evolution and function of thioester-containing proteins and the complement system in the innate immune response. Front Immunol 8:759
  162. Kaneko T, Silverman N (2005) Bacterial recognition and signaling by the *Drosophila* IMD pathway. Cell Microbiol 7:461–469. <https://doi.org/10.1111/j.1462-5822.2005.00504.x>
  163. Leulier F, Rodriguez A, Khush RS, Abrams JM, Lemaitre B (2000) The *Drosophila* caspase dredd is required to resist gram-negative bacterial infection. EMBO Rep 1:353–358. <https://doi.org/10.1093/embo-reports/kvd073>
  164. Leulier F, Vidal S, Saigo K, Ueda R, Lemaitre B (2002) Inducible expression of double-stranded RNA reveals a role for dFADD in the regulation of the antibacterial response in *Drosophila* adults. Curr Biol 12:996–1000. [https://doi.org/10.1016/S0960-9822\(02\)00873-4](https://doi.org/10.1016/S0960-9822(02)00873-4)
  165. Ertürk-Hasdemir D, Broemer M, Leulier F, Lane WS, Paquette N, Hwang D, Kim CH, Stöven S, Meier P, Silverman N (2009) Two roles for the *Drosophila* IKK complex in the activation of Relish and the induction of antimicrobial peptide genes. Proc Natl Acad Sci U S A 106:9779–9784. <https://doi.org/10.1073/pnas.0812022106>
  166. O’Shea JJ, Plenge R (2012) JAK and STAT signaling molecules in immunoregulation and immune-mediated disease. Immunity 36:542–550. <https://doi.org/10.1016/j.immuni.2012.03.014>
  167. Kiu H, Nicholson SE (2012) Biology and significance of the JAK/STAT signalling pathways. Growth Factors 30:88–106. <https://doi.org/10.3109/08977194.2012.660936>
  168. Brown S, Hu N, Hombria JCG (2001) Identification of the first invertebrate interleukin JAK/STAT receptor, the *Drosophila* gene domeless. Curr Biol 11:1700–1705. [https://doi.org/10.1016/S0960-9822\(01\)00524-3](https://doi.org/10.1016/S0960-9822(01)00524-3)
  169. Binari R, Perrimon N (1994) Stripe-specific regulation of pair-rule genes by hopscotch, a putative Jak family tyrosine kinase in *Drosophila*. Genes Dev 8:300–312. <https://doi.org/10.1101/gad.8.3.300>
  170. Yan R, Small S, Desplan C, Dearolf CR, Darnell JE (1996) Identification of a Stat gene that functions in *Drosophila* development. Cell 84:421–430. [https://doi.org/10.1016/S0092-8674\(00\)81287-8](https://doi.org/10.1016/S0092-8674(00)81287-8)
  171. Brown KL, Hancock REW (2006) Cationic host defense (antimicrobial) peptides. Curr Opin Immunol 18:24–30. <https://doi.org/10.1016/j.coi.2005.11.004>
  172. Andersson DI, Hughes D, Kubicek-Sutherland JZ (2016) Mechanisms and consequences of bacterial resistance to antimicrobial peptides. Drug Resist Updat. <https://doi.org/10.1016/j.drug.2016.04.002>
  173. Di Somma A, Avitabile C, Cirillo A, Moretta A, Merlino A, Paduano L, Duilio A, Romanelli A (2020a) The antimicrobial peptide *Temporin L* impairs *E.coli* cell division by interacting with FtsZ and the divisome complex. Biochim. Biophys. Acta

- Gen. Subj. 1864(7):129606. <https://doi.org/10.1016/j.bbagen.2020.129606>
174. Rahnamaeian M, Cytryńska M, Zdybicka-Barabas A, Dobszlaff K, Wiesner J, Twyman RM, Zuchner T, Sadd BM, Regoes RR, Schmid-Hempel P, Vilcinskas A (2015) Insect antimicrobial peptides show potentiating functional interactions against Gram-negative bacteria. *Proceedings Biol Sci* 282:20150293. <https://doi.org/10.1098/rspb.2015.0293>
  175. Cociancich S, Ghazi A, Hetru C, Hoffmann JA, Letellier L (1993) Insect defensin, an inducible antibacterial peptide, forms voltage-dependent channels in *Micrococcus luteus*. *J Biol Chem* 268:19239–19245
  176. Maget-Dana R, Ptak M (1997) Penetration of the insect defensin A into phospholipid monolayers and formation of defensin A-lipid complexes. *Biophys J* 73:2527–2533. [https://doi.org/10.1016/S0006-3495\(97\)78281-X](https://doi.org/10.1016/S0006-3495(97)78281-X)
  177. Vizioli J, Richman AM, Uttenweiler-Joseph S, Blass C, Bulet P (2001) The defensin peptide of the malaria vector mosquito *Anopheles gambiae*: antimicrobial activities and expression in adult mosquitoes. *Insect Biochem Mol Biol* 31:241–248. [https://doi.org/10.1016/S0965-1748\(00\)00143-0](https://doi.org/10.1016/S0965-1748(00)00143-0)
  178. Sato H, Feix JB (2006) Peptide–membrane interactions and mechanisms of membrane destruction by amphipathic  $\alpha$ -helical antimicrobial peptides. *Biochim Biophys Acta - Biomembr* 1758:1245–1256. <https://doi.org/10.1016/j.bbame.2006.02.021>
  179. Goyal RK, Mattoo AK (2016) Plant antimicrobial peptides. In: Richard M Epand (eds) *Host defense peptides and their potential as therapeutic agents*. Springer, Cham, pp 111–136. [https://doi.org/https://doi.org/10.1007/978-3-319-32949-9\\_5](https://doi.org/https://doi.org/10.1007/978-3-319-32949-9_5)
  180. Efimova SS, Schagina LV, Ostroumova OS (2014) Channel-forming activity of cecropins in lipid bilayers: effect of agents modifying the membrane dipole potential. *Langmuir* 30:7884–7892. <https://doi.org/10.1021/la501549v>
  181. Travkova OG, Moehwald H, Brezesinski G (2017) The interaction of antimicrobial peptides with membranes. *Adv Colloid Interface Sci*. <https://doi.org/10.1016/j.cis.2017.06.001>
  182. Galdiero E, Lombardi L, Falanga A, Libralato G, Guida M, Carotenuto R (2019) Biofilms: novel strategies based on antimicrobial peptides. *Pharmaceutics*. <https://doi.org/10.3390/pharmaceutics11070322>
  183. Lee H, Lim SI, Shin SH, Lim Y, Koh JW, Yang S (2019) Conjugation of cell-penetrating Peptides to antimicrobial peptides enhances antibacterial activity. *ACS Omega* 4:15694–15701. <https://doi.org/10.1021/acsomega.9b02278>
  184. Sierra JM, Fusté E, Rabanal F, Vinuesa T, Viñas M (2017) An overview of antimicrobial peptides and the latest advances in their development. *Expert Opin Biol Ther*. <https://doi.org/10.1080/14712598.2017.1315402>
  185. Chen J, Guan S-M, Sun W, Fu H (2016) Melittin, the major pain-producing substance of bee venom. *Neurosci Bull* 32:265–272. <https://doi.org/10.1007/s12264-016-0024-y>
  186. Jamasbi E, Lucky SS, Li W, Hossain MA, Gopalakrishnakone P, Separovic F (2018) Effect of dimerized melittin on gastric cancer cells and antibacterial activity. *Amino Acids* 50:1101–1110. <https://doi.org/10.1007/s00726-018-2587-6>
  187. Rady I, Siddiqui IA, Rady M, Mukhtar H (2017) Melittin, a major peptide component of bee venom, and its conjugates in cancer therapy. *Cancer Lett*. <https://doi.org/10.1016/j.canlet.2017.05.010>
  188. Di L (2015) Strategic approaches to optimizing peptide ADME properties. *AAPS J* 17:134–143. <https://doi.org/10.1208/s12248-014-9687-3>
  189. Koehbach J (2017) Structure-activity relationships of insect defensins. *Front Chem*. <https://doi.org/10.3389/fchem.2017.00045>
  190. Vlieghe P, Lisowski V, Martinez J, Khrestchatsky M (2010) Synthetic therapeutic peptides: science and market. *Drug Discov Today* 15:40–56
  191. Knappe D, Cassone M, Inga Nollmann F, Otvos L, Hoffmann R (2014) Hydroxyproline substitutions stabilize non-glycosylated drosocin against serum proteases without challenging its antibacterial activity. *Protein Pept Lett* 21:321–329
  192. Oliva R, Chino M, Pane K, Pistorio V, De Santis A, Pizzo E, D'Errico G, Pavone V, Lombardi A, Del Vecchio P, Notomista E, Natri F, Petraccone L (2018) Exploring the role of unnatural amino acids in antimicrobial peptides. *Sci Rep* 8:1–16. <https://doi.org/10.1038/s41598-018-27231-5>
  193. Amerikova M, Pencheva El-Tibi I, Maslarska V, Bozhanov S, Tachkov K (2019) Antimicrobial activity, mechanism of action, and methods for stabilisation of defensins as new therapeutic agents. *Biotechnol Biotechnol Equip* 33:671–682. <https://doi.org/10.1080/13102818.2019.1611385>
  194. Fosgerau K, Hoffmann T (2015) Peptide therapeutics: Current status and future directions. *Drug Discov Today*. <https://doi.org/10.1016/j.drudis.2014.10.003>
  195. Kumar P, Kizhakkedathu JN, Straus SK (2018) Antimicrobial peptides: diversity, mechanism of action and strategies to improve the activity and biocompatibility in vivo. *Biomolecules*. <https://doi.org/10.3390/biom8010004>
  196. Wang G (2011) Post-translational modifications of natural antimicrobial peptides and strategies for peptide engineering. *Curr Biotechnol* 1:72–79. <https://doi.org/10.2174/2211551x11201010072>
  197. Thorstholm L, Craik DJ (2012) Discovery and applications of naturally occurring cyclic peptides. *Drug Discov Today Technol* 9:e13–e21. <https://doi.org/10.1016/j.ddtec.2011.07.005>
  198. Chen CH, Lu TK (2020) Development and challenges of antimicrobial peptides for therapeutic applications. *Antibiotics*. <https://doi.org/10.3390/antibiotics9010024>
  199. Manteghi R, Pallagi E, Olajos G, Csóka I (2020) Pegylation and formulation strategy of anti-microbial peptide (AMP) according to the quality by design approach. *Eur J Pharm Sci* 144:105197. <https://doi.org/10.1016/j.ejps.2019.105197>
  200. Shao C, Zhu Y, Lai Z, Tan P, Shan A (2019) Antimicrobial peptides with protease stability: progress and perspective. *Future Med Chem* 11:2047–2050. <https://doi.org/10.4155/fmc-2019-0167>
  201. Souza BM, Mendes MA, Santos LD, Marques MR, César LMM, Almeida RNA, Pagnocca FC, Konno K, Palma MS (2005) Structural and functional characterization of two novel peptide toxins isolated from the venom of the social wasp *Polybia paulista*. *Peptides* 26:2157–2164. <https://doi.org/10.1016/j.peptides.2005.04.026>
  202. Zhao Y, Zhang M, Qiu S, Wang J, Peng J, Zhao P, Zhu R, Wang H, Li Y, Wang K, Yan W, Wang R (2016) Antimicrobial activity and stability of the d-amino acid substituted derivatives of antimicrobial peptide polybia-MPI. *AMB Express*. <https://doi.org/10.1186/s13568-016-0295-8>
  203. Jia F, Wang J, Peng J, Zhao P, Kong Z, Wang K, Yan W, Wang R (2017) D-amino acid substitution enhances the stability of antimicrobial peptide polybia-CP. *Acta Biochim Biophys Sin* 49:916–925. [https://doi.org/10.1093/ABBS/GMX091\(\(Shanghai\)\)](https://doi.org/10.1093/ABBS/GMX091((Shanghai)))
  204. Falanga A, Nigro E, De Biasi MG, Daniele A, Morelli G, Galdiero S, Scudiero O (2017) Cyclic peptides as novel therapeutic microbicides: engineering of human defensin mimetics. *Molecules*. <https://doi.org/10.3390/molecules22071217>
  205. Mindt M, Risse JM, Gruß H, Sewald N, Eikmanns BJ, Wendisch VF (2018) One-step process for production of N-methylated amino acids from sugars and methylamine using recombinant

- Corynebacterium glutamicum* as biocatalyst. Sci Rep 8:12895. <https://doi.org/10.1038/s41598-018-31309-5>
206. Liu T, Zhu N, Zhong C, Zhu Y, Gou S, Chang L, Bao H, Liu H, Zhang Y, Ni J (2020) Effect of N-methylated and fatty acid conjugation on analogs of antimicrobial peptide Anoplin. Eur J Pharm Sci. <https://doi.org/10.1016/j.ejps.2020.105453>
  207. Zhong C, Liu T, Gou S, He Y, Zhu N, Zhu Y, Wang L, Liu H, Zhang Y, Yao J, Ni J (2019) Design and synthesis of new N-terminal fatty acid modified-antimicrobial peptide analogues with potent in vitro biological activity. Eur J Med Chem 182:111636. <https://doi.org/10.1016/j.ejmech.2019.111636>
  208. Oguis GK, Gilding EK, Huang YH, Poth AG, Jackson MA, Craik DJ (2020) Insecticidal diversity of butterfly pea (*Clitoria ternatea*) accessions. Ind Crops Prod 147:112214. <https://doi.org/10.1016/j.indcrop.2020.112214>
  209. Koehbach J, Craik DJ (2019) The vast structural diversity of antimicrobial peptides. Trends Pharmacol Sci. <https://doi.org/10.1016/j.tips.2019.04.012>
  210. Gobbo M, Benincasa M, Biondi L, Filira F, Gennaro R, Rocchi R, (2001) Cyclic Analogues of the insect antimicrobial peptides drosocin and apidaecin, In: Peptides: The wave of the future. Springer Netherlands, pp. 776–777. doi:[https://doi.org/10.1007/978-94-010-0464-0\\_363](https://doi.org/10.1007/978-94-010-0464-0_363).
  211. Bulet P, Hetru C, Dimarcq JL, Hoffmann D (1999) Antimicrobial peptides in insects; structure and function. Dev Comp Immunol 23:329–344. [https://doi.org/10.1016/S0145-305X\(99\)00015-4](https://doi.org/10.1016/S0145-305X(99)00015-4)
  212. Cybase [WWW Document], n.d. URL <http://www.cybase.org.au/>. Accessed 16 jul 2020
  213. Bogdanowich-Knipp SJ, Chakrabarti S, Siahaan TJ, Williams TD, Dillman RK (1999) Solution stability of linear vs cyclic RGD peptides. J peptide res. 53(5):530–541
  214. BaAMPs - Home [WWW Document], n.d. URL <http://www.baamps.it/>. Accessed.18 jul 2020
  215. Di Luca M, Maccari G, Maisetta G, Batoni G (2015) BaAMPs: The database of biofilm-active antimicrobial peptides. Biofouling 31:193–199. <https://doi.org/10.1080/08927014.2015.1021340>
  216. Di Somma, A., Moretta, A., Canè, C., Cirillo, A., Duilio, A., (2020b). Inhibition of bacterial biofilm formation, In: Bacterial Biofilms. IntechOpen.
  217. Riool M, de Breij A, Drijfhout JW, Nibbering PH, Zaat SAJ (2017) Antimicrobial peptides in biomedical device manufacturing. Front Chem 5:63. <https://doi.org/10.3389/fchem.2017.00063>
  218. Hwang IS, Hwang JS, Hwang JH, Choi H, Lee E, Kim Y, Lee DG (2013) Synergistic effect and antibiofilm activity between the antimicrobial peptide coprisin and conventional antibiotics against opportunistic bacteria. Curr Microbiol 66:56–60. <https://doi.org/10.1007/s00284-012-0239-8>
  219. Krishnan M, Choi J, Jang A, Kim Y (2020) A novel peptide antibiotic, Pro10-1D, designed from insect defensin shows antibacterial and anti-inflammatory activities in sepsis models. Int J Mol Sci 21:6216. <https://doi.org/10.3390/ijms21176216>
  220. Kalsy M, Tonk M, Hardt M, Dobrindt U, Zdybicka-Barabas A, Cytrynska M, Vilcinskas A, Mukherjee K (2020) The insect antimicrobial peptide cecropin A disrupts uropathogenic *Escherichia coli* biofilms. NPJ biofilms and microbiomes 6(1):1–8. <https://doi.org/10.1038/s41522-020-0116-3>
  221. Gordya N, Yakovlev A, Kruglikova A, Tulin D, Potolitsina E, Suborova T, Bordo D, Rosano C, Chernysh S (2017) Natural antimicrobial peptide complexes in the fighting of antibiotic resistant biofilms: *Calliphora vicina* medicinal maggots. PLoS ONE 12:e0173559. <https://doi.org/10.1371/journal.pone.0173559>
  222. Chernysh S, Gordya N, Tulin D, Yakovlev A (2018) Biofilm infections between Scylla and Charybdis: interplay of host antimicrobial peptides and antibiotics. Infect Drug Resist 11:501–514. <https://doi.org/10.2147/IDR.S157847>
  223. Wu Q, Patočka J, Kuča K (2018) Insect Antimicrobial Peptides, a Mini Review. Toxins. <https://doi.org/10.3390/toxins10110461> ((Basel))
  224. Iwasaki T, Ishibashi J, Tanaka H, Sato M, Asaoka A, Taylor D, Yamakawa M (2009) Selective cancer cell cytotoxicity of enantiomeric 9-mer peptides derived from beetle defensins depends on negatively charged phosphatidylserine on the cell surface. Peptides 30:660–668. <https://doi.org/10.1016/j.peptides.2008.12.019>
  225. Ratcliffe NA, Mello CB, Garcia ES, Butt TM, Azambuja P (2011) Insect natural products and processes: new treatments for human disease. Insect Biochem Mol Biol 41:747–769. <https://doi.org/10.1016/j.ibmb.2011.05.007>
  226. Kono T, Watanabe M, Koyama K, Kishimoto T, Fukushima S, Sugimura T, Wakabayashi K (1999) Cytotoxic activity of pterisin, from the cabbage butterfly, *Pieris rapae*, in various human cancer cell lines. Cancer Lett 137:75–81
  227. Orth JH, Schorch B, Boundy S, Ffrench-Constant R, Kubick S, Aktories K (2011) Cell-free synthesis and characterization of a novel cytotoxic pterisin-like protein from the cabbage butterfly *Pieris rapae*. Toxicon 57:199–207. <https://doi.org/10.1016/j.toxic.2010.11.011>
  228. Mylonakis E, Podsiadlowski L, Muhammed M, Vilcinskas A (2016) Diversity, evolution and medical applications of insect antimicrobial peptides. Philos Trans R Soc Lond B Biol Sci 371:20150290

**Publisher's Note** Springer Nature remains neutral with regard to jurisdictional claims in published maps and institutional affiliations.



# Antimicrobial Peptides: A New Hope in Biomedical and Pharmaceutical Fields

Antonio Moretta<sup>1†</sup>, Carmen Scieuzo<sup>1,2†</sup>, Anna Maria Petrone<sup>1†</sup>, Rosanna Salvia<sup>1,2†</sup>,  
Michele Dario Manniello<sup>1</sup>, Antonio Franco<sup>1,2</sup>, Donatella Lucchetti<sup>3</sup>, Antonio Vassallo<sup>1</sup>,  
Heiko Vogel<sup>4</sup>, Alessandro Sgambato<sup>3,5\*</sup> and Patrizia Falabella<sup>1,2\*</sup>

## OPEN ACCESS

### Edited by:

Francesc Rabanal,  
University of Barcelona, Spain

### Reviewed by:

Surajit Bhattacharjya,  
Nanyang Technological University,  
Singapore  
Clara Balleste,  
Instituto Salud Global Barcelona  
(ISGlobal), Spain

### \*Correspondence:

Patrizia Falabella  
patrizia.falabella@unibas.it  
Alessandro Sgambato  
alessandro.sgambato@crob.it

<sup>†</sup>These authors have contributed  
equally to this work and share  
first authorship

### Specialty section:

This article was submitted to  
Clinical Microbiology,  
a section of the journal  
Frontiers in Cellular and  
Infection Microbiology

**Received:** 16 February 2021

**Accepted:** 10 May 2021

**Published:** 14 June 2021

### Citation:

Moretta A, Scieuzo C, Petrone AM,  
Salvia R, Manniello MD, Franco A,  
Lucchetti D, Vassallo A, Vogel H,  
Sgambato A and Falabella P (2021)  
Antimicrobial Peptides: A New Hope in  
Biomedical and Pharmaceutical Fields.  
*Front. Cell. Infect. Microbiol.* 11:668632.  
doi: 10.3389/fcimb.2021.668632

<sup>1</sup> Department of Sciences, University of Basilicata, Potenza, Italy, <sup>2</sup> Spinoff XFlies s.r.l., University of Basilicata, Potenza, Italy, <sup>3</sup> Department of Translational Medicine and Surgery, Università Cattolica del Sacro Cuore, Rome, Italy, <sup>4</sup> Department of Entomology, Max Planck Institute for Chemical Ecology, Jena, Germany, <sup>5</sup> Centro di Riferimento Oncologico della Basilicata (IRCCS-CROB), Rionero in Vulture, Italy

Antibiotics are essential drugs used to treat pathogenic bacteria, but their prolonged use contributes to the development and spread of drug-resistant microorganisms. Antibiotic resistance is a serious challenge and has led to the need for new alternative molecules less prone to bacterial resistance. Antimicrobial peptides (AMPs) have aroused great interest as potential next-generation antibiotics, since they are bioactive small proteins, naturally produced by all living organisms, and representing the first line of defense against fungi, viruses and bacteria. AMPs are commonly classified according to their sources, which are represented by microorganisms, plants and animals, as well as to their secondary structure, their biosynthesis and their mechanism of action. They find application in different fields such as agriculture, food industry and medicine, on which we focused our attention in this review. Particularly, we examined AMP potential applicability in wound healing, skin infections and metabolic syndrome, considering their ability to act as potential Angiotensin-Converting Enzyme I and pancreatic lipase inhibitory peptides as well as antioxidant peptides. Moreover, we argued about the pharmacokinetic and pharmacodynamic approaches to develop new antibiotics, the drug development strategies and the formulation approaches which need to be taken into account in developing clinically suitable AMP applications.

**Keywords:** drug-resistant microorganisms, antimicrobial peptides, biomedical and pharmacological applications, pharmacokinetics and pharmacodynamics, drug delivery

**Abbreviations:** ACE, Angiotensin-Converting Enzyme I; AMP, Antimicrobial Peptide; APD, Antimicrobial Peptide Database; API, Active pharmaceutical ingredient; DDS, Drug Delivery System; Di-Phe, di-phenylalanine; EGFR, Epidermal Growth Factor Receptor; EPL,  $\epsilon$ -poly-L-lysine; GMO, Glycerol Monooleate; HBBD, HG-Based Burn Dressings; hBD, Human  $\beta$  defensin; HG, Hydrogel; IPTG, Isopropyl  $\beta$ -D-1-Thiogalactopyranoside; LPS, Lipopolysaccharides; MRSA, Methicillin-resistant *Staphylococcus aureus*; PD, Pharmacodynamics; PK, Pharmacokinetics; SARS-CoV-2, Severe Acute Respiratory Syndrome Coronavirus 2; SCID, Severe Combined Immunodeficiency; TLR, Toll-like receptor; WHO, World Health Organization; BPS, block polymeric structure; CB, cubosome; CMC, Critical Micelle Concentration; PA, peptide amphiphiles; SPPS, Solid Phase Peptide Synthesis.



## INTRODUCTION

A wide variety of antimicrobial agents are available today and they are broadly applied to treat different types of human infections. Specifically, antibiotics are powerful drugs used for treatments of pathogenic bacteria (Lei et al., 2019). However, their indiscriminate and prolonged use, especially in developing countries, in both human and veterinary medicine, as well as in agriculture have contributed to the development and spread of drug-resistant microorganisms (Huan et al., 2020). As the World Health Organization (WHO) has extensively announced, the alarming rise globally in resistance towards conventional antimicrobials represents a potential and serious risk to public health (Luong et al., 2020). Therefore, the antibiotic resistance issue has made it urgent to search for alternatives to conventional antibiotics, with novel modes of action and less predisposed to bacterial resistance. In the quest of new antibiotics, the antimicrobial peptides (AMPs), also known as host defense peptides, have recently raised great interest (Haney et al., 2019; Bhattacharjya and Straus, 2020; Mahlapuu et al., 2020). Current research is focused on these natural compounds as innovative anti-infective drugs and novel immunomodulatory candidates (Luong et al., 2020; Mahlapuu et al., 2020).

AMPs are bioactive small proteins, naturally produced by all living organisms as important and indispensable components of their innate immune system, becoming the first-line defense against microbial attacks in Eukaryotes, or produced as a competition strategy in Prokaryotes, to limit the growth of other microorganisms (Lei et al., 2019; Magana et al., 2020). Natural AMPs have potent and broad-spectrum activity against multiple classes of bacteria, yeasts, fungi, viruses and parasites (Huan et al., 2020; Luong et al., 2020), displaying bacteriostatic, microbicidal and cytolytic properties (Pasupuleti et al., 2012). Moreover, the interest in AMPs has recently increased during the Severe Acute Respiratory Syndrome Coronavirus 2 (SARS-CoV-2) pandemic in the search of new antiviral molecules to counteract COVID-19 disease (Kurpe et al., 2020).

AMPs were discovered in 1939, when the microbiologist René Dubos isolated from a soil *Bacillus* strain, an antimicrobial agent, named gramicidin, which was demonstrated to protect mice from pneumococcal infection (Van Epps, 2006). Afterwards, several AMPs have been discovered from both the prokaryotic and eukaryotic kingdom (Boparai and Sharma, 2020), including the tyrocidine, produced by the bacteria *Bacillus brevis*, with activity against bacteria, and the purothionin, identified in the plant *Triticum aestivum*, active against fungi and bacteria (Ohtani et al., 1977). The first described animal-originated AMP is defensin, which was isolated from rabbit leukocytes (Hirsch, 1956); subsequently lactoferrin was identified in cow milk (Groves et al., 1965) and it was demonstrated that lysosomes of human leukocytes (Zeya and Spitznagel, 1966) and human female reproductive tract contain low molecular weight AMPs (Sharma et al., 2011). To date, more than 3,000 AMPs have been discovered, characterized and annotated in the AMP database (APD3) (Huan et al., 2020), just considering that frog skin alone is a reservoir of more than 300 different AMPs (Boparai and Sharma, 2020).

## AMP Properties and Biosynthesis

Natural AMPs are evolutionary conserved gene-encoded molecules with structural and functional diversity, which is responsible for their wide range of activities against different pathogens in various organisms (Zhang and Gallo, 2016). However, although displaying considerable diversity in their physio-chemical and structural properties, origins and mechanisms of action, AMPs share some common features (Moravej et al., 2018). Indeed, they are mostly short molecules (<100 amino acids) (Pasupuleti et al., 2012), typically with a positive net charge (generally ranging from +2 to +11) and a notable proportion of hydrophobic residues (typically 50%) (Haney et al., 2017). They display an amphipathic structure, as they contain both hydrophobic and hydrophilic regions, that enable them to be soluble in aqueous environments (Boparai and Sharma, 2020). A less common class of AMPs is represented by the anionic AMPs, which have a negative net charge ranging from -1 to -7 and have been identified in vertebrates, invertebrates and plants (Harris et al., 2009). They include many negatively charged aspartic and glutamic acid residues, and in animals are found in various vital organs, including the brain, the epidermis, the respiratory and gastrointestinal tracts (Lakshmaiah Narayana and Chen, 2015). They show a different mechanism of action than the cationic ones. In order to facilitate their interaction with the target organism, some anionic AMPs use metal ions to form cationic salt bridges with negatively charged constituents of microbial membranes, allowing their penetration into the cell. When they reach the cytoplasm, they may attach to ribosomes or inhibit ribonuclease activity (Jeżowska-Bojczuk and Stokowa-Sołtys, 2018). Some anionic AMPs, such as theromyzin from *Theromyzom tessulatum* (Tasiemski et al., 2004), require zinc as a functional cofactor and it was found that the complex with zinc has stronger antimicrobial activity (Jiang et al., 2014).

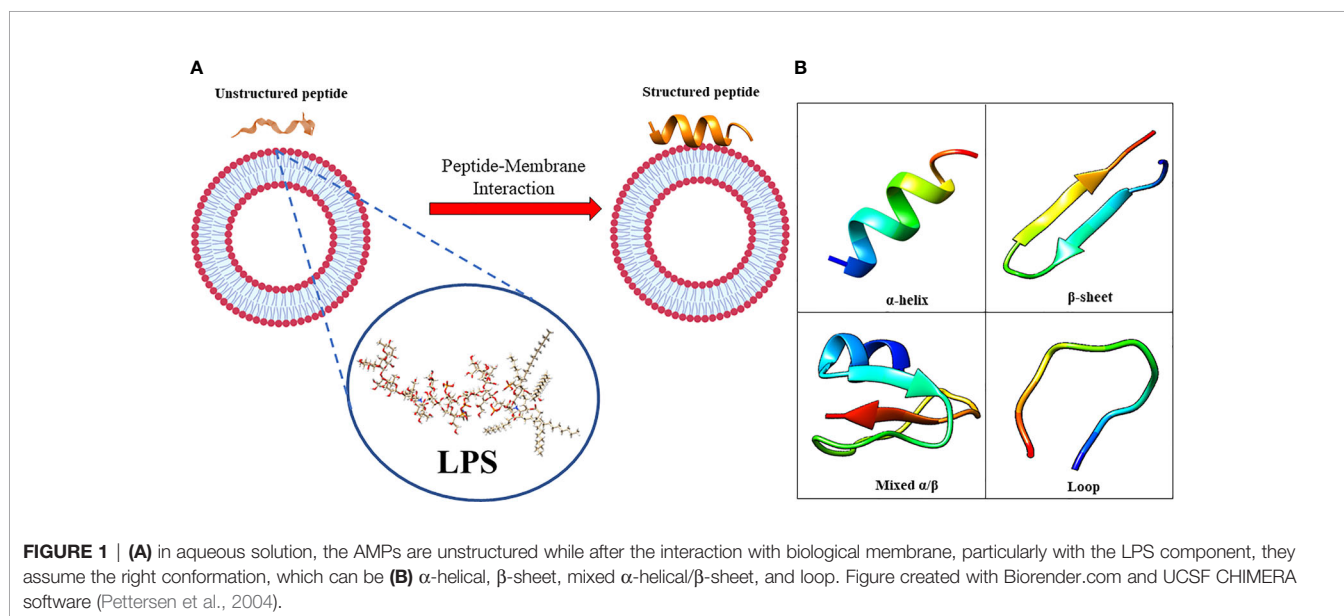
Despite their relative similarity in biophysical characteristics, AMP sequences are rarely similar among closely related or distinct species/organisms (Pasupuleti et al., 2012). However, for some AMPs, a certain degree of identity is found either in the pro-region (the inactive sequence that is deleted by post-translational modifications) or in the amino acid patterns. This event could be due to species adaptation to the unique microbial environment that characterizes the niche occupied by specific species (Pasupuleti et al., 2012).

The amphiphilic nature of the majority of AMPs is responsible for their structural flexibility. AMPs are commonly classified into four categories based on their secondary structure, including linear  $\alpha$ -helical peptides,  $\beta$ -sheet peptides with the presence of 2 or more disulfide bonds,  $\beta$ -hairpin or loop peptides with the presence of a single disulfide bond and/or cyclization of peptide chain, and, finally, extended structures (Boparai and Sharma, 2020). Most AMPs belong to the first two categories.  $\alpha$ -helical peptides display an unstructured conformation in aqueous solution but adopt an amphipathic helical structure in contact with biological membranes. However, a relevant feature is linked to the possible interactions with bacterial structures, such as lipopolysaccharides (LPS), that provoke conformational changes, influencing membrane permeabilization and the correct

passage into the cytosol. Indeed, this interaction could change AMP tertiary structure, and AMP molecules could assume different conformations, such as monomeric helical or helix-loop-helix structures (**Figure 1**) (Bhunia et al., 2011).

For example, the contact with LPS induces oligomerization of specific AMPs, such as temporines, through the interaction among hydrophobic N and C terminal residues, preventing the correct movement throughout the membrane and the correct antimicrobial action (Bhunia et al., 2011). A particular amino acids composition could prevent this oligomerization, enhancing temporin activity. This is the case of temporin-1T1, which is rich in aromatic residues with two positively charged amino acids (Bhunia et al., 2011). The synergy of temporin-1T1 with other temporins (Temporin A and Temporin B), prevent their oligomerization and facilitate the correct crossing of the bacterial membrane (Bhunia et al., 2011). Exceptions are related to some AMPs with particular structural characteristics, including the peptide MSI-594 (an analogue of magainin), that is unstructured in free solution, but have a folded helical hairpin structure when interact with LPS (Bhattacharjya, 2016). The interactions between two helical segments, facilitated by the fifth phenylalanine residue, allows the acquisition of the hairpin structure, implicating its very high activity against bacteria, fungi, and viruses (Domadia et al., 2010; Bhattacharjya, 2016). Another example of change in conformation after the interaction with LPS, is the  $\beta$ -hairpin structures of Tachyplesin I, that becomes more ordered and compact when interacting with LPS (Saravanan et al., 2012; Kushibiki et al., 2014). Another interesting example is linked to the human LL-37 AMP, one of the best studied peptides of this group, present in neutrophils and epithelial cells (Mahlapuu et al., 2016). It has been demonstrated that aromatic-aromatic interactions stabilize protein structure in correlation with lipids (Li et al., 2006) and that LL-37 could undergo a re-orientation depending on the concentration, suggesting also in this case an oligomerization process (Ding et al., 2013). On the contrary,  $\beta$ -sheet peptides are more ordered in aqueous solution because of their rigid

structure and do not undergo radical conformational changes as helical peptides upon membrane interaction (Mahlapuu et al., 2016). It is not easy to clarify the structural conformations of  $\beta$ -sheet AMPs in membranes, because of the potential micelle aggregations; indeed, a recent report on thanatin peptide, isolated from insect *Podisus maculiventris*, showed dimerization of  $\beta$ -sheet structures (Sinha et al., 2017). These dimeric structures could facilitate the bond with LPS molecules, also at the distal ends, fostering bacterial cell associations and agglutination (Sinha et al., 2017). Defensins, a large group of AMPs, which are produced in macrophages, neutrophils and epithelial cells belong to this class (Mahlapuu et al., 2016). It was observed that the right combination of hydrophobicity, charge density and peptide length influence the antimicrobial activity of AMPs. Changing the amino acids position in the peptide chain or increasing the number of positively charged residues affect the secondary structure of AMPs, and consequently their biological activity against pathogens (Wu Q. et al., 2018). Besides the principle that the amino acid sequence determines the function of a peptide, it was found that the amino acid composition (in terms of abundance of residues with specific phyco-chemical properties) also affects AMP activity as clearly documented for a novel class of cationic AMPs known as “cationic intrinsically disordered antimicrobial peptides” or “CIDAMPs” since they are characterized by an intrinsically disordered structure. CIDAMPs have been detected in human skin and other barrier organs (Gerstel et al., 2018; Latendorf et al., 2019) and, carrying a positive net charge, have a low percentage of order-promoting amino acids (mostly hydrophobic residues commonly located within the hydrophobic core of foldable proteins) and a high percentage of disorder-promoting amino acids (mostly charged and polar residues, typically found at the surface of foldable proteins). They show microbicidal activity against several microbes, including *Candida albicans*, *Staphylococcus aureus* and *Pseudomonas aeruginosa* (Gerstel et al., 2018). The protein hornerin, expressed in the cornified epithelium, seems to be the main source of



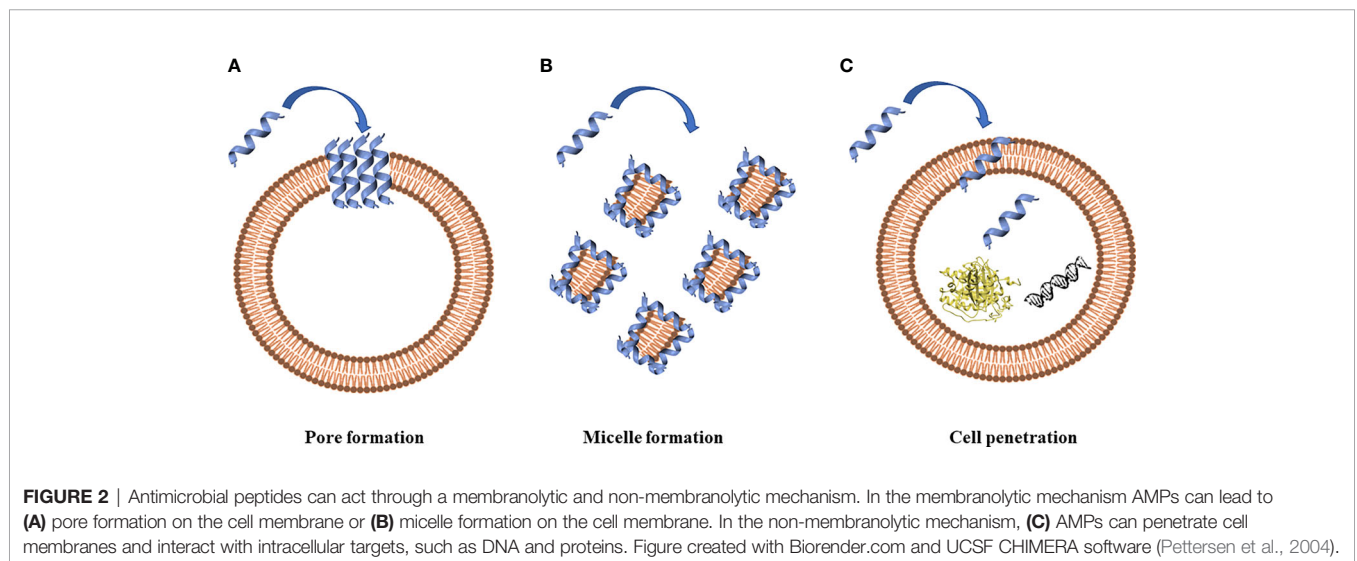
CIDAMPs, which act as disinfectants, helping to keep the surface of healthy skin free of infections (Gerstel et al., 2018).

AMP biosynthesis can occur in three different ways: classical ribosomal synthesis, non-ribosomal synthesis and proteolytic digestion of proteins (Buda De Cesare et al., 2020). Ribosomally synthesized AMPs, such as histatins and human  $\beta$ -defensins, are produced by ribosomal translation of specific mRNAs into the biologically active amino acid sequences in vertebrates, insects, plants, and bacteria. Non-ribosomally synthesized peptides are produced by large enzymes referred to as non-ribosomal peptide synthases, which incorporate non-proteinogenic amino acids into the sequence, and are found in filamentous fungi and bacteria (*Actinomycetes* and *Bacilli*). Finally, some AMPs, called cryptic peptides, are generated by proteolytic cleavage of bigger proteins with other functions. For example, the histone H2A of the Asian toad (*Duttaphrynus melanostictus*) is processed by the enzymatic activity of pepsin C producing buforin I, which in turn is processed by an endopeptidase to generate buforin II (Buda De Cesare et al., 2020). Interestingly, many AMPs are produced as inactive precursors and are active after proteolytic cleavage. Therefore, their activity is not only dependent on their own expression but also on the presence of appropriate proteases (Mahlapuu et al., 2016). The expression of AMPs can be constitutive or inducible by specific external factors (Mahlapuu et al., 2016; Lei et al., 2019). Some AMPs are expressed during the whole cellular lifetime but are stored at high concentration as precursors in granules and are released upon infection in the site of infection or inflammation (Mahlapuu et al., 2016). P9A and P9B are examples of inducible peptides, whose expression can be induced in silkworm (*Bombyx mori*) hemolymph by vaccination with *Enterobacter cloacae*, as demonstrated by Hultmark and colleagues (Hultmark et al., 1980). In addition, Bals et al. (1999) reported that defensin production from epithelial cells of multiple mouse organs increases upon infection with *P. aeruginosa* PAO1.

## Insights Into the Mechanisms of Action of AMPs

The prerequisite to develop efficient AMPs as novel candidate drugs is the understanding of their mode of action. AMPs exert their activity by interaction with microbial cell membranes and this interaction is strongly affected by the lipid composition of biological membranes (Wu Q. et al., 2018). Since microbial membranes are the primary targets of AMPs, it is difficult for bacteria to develop resistance to AMPs as easily as to conventional antibiotics (Boparai and Sharma, 2020). Membrane interactions are mediated by electrostatic forces between positively charged AMPs and negatively charged microbial surfaces. The teichoic acids in the cell wall of Gram-positive bacteria and the LPS in the outer membrane of Gram-negative bacteria supply electronegative charge to the microbial surfaces, strengthening the interaction with AMPs (Boparai and Sharma, 2020). On the contrary, the outer layer of eukaryotic membranes is composed by zwitterionic phosphatidylcholine and sphingomyelin, which do not favor AMP interaction because of their neutral charge at physiological pH. Based on their mode of action, AMPs are divided into “membrane acting peptides”, which destabilize bacterial membranes causing their disruption, and “non-membrane acting peptides”, which are able to translocate across the membranes without damaging them but destabilizing normal cell functions (Boparai and Sharma, 2020) (Figure 2).

Three models have been proposed to explain the permeabilization of bacterial membranes by AMPs: barrel-stave model, toroidal-pore model and carpet model (Raheem and Straus, 2019). Thanks to their positive net charge, AMPs are able to interact with components of bacterial membranes, resulting in the disruption of the lipidic bilayer with cell death. AMP insertion can be perpendicular, as in the barrel-stave model, or perpendicular with the interaction with the head groups of lipids that provokes a deflection in the membrane (toroidal model) (Brogden, 2005). AMPs can also dispose



parallel to the membrane, covering it completely, and forming, at the same time, micelles with the starting broken membranes (carpet model), as proposed by Gazit and colleagues in 1996 (Gazit et al., 1996). Moreover, defensins interact with LPS in Gram-negative bacteria and peptidoglycan in Gram-positive bacteria (Pachón-Ibáñez et al., 2017). Defensins have LPS-neutralizing activity in different bacteria (Lee et al., 2010) despite the chemical structure of LPS varies among them. LPS can self-aggregate forming oligomers above a Critical Micelle Concentration (CMC) because of its amphiphilic nature, a concentration of LPS, or any surfactant, above which it aggregates in micelles. It has been demonstrated that the association of defensin analogues and other peptides, such as gramicidin A, melittin, LL-37 and polymyxin B, with LPS leads to the disintegration of LPS aggregates. Moreover, it was observed that defensins amino acids (such as Arg, Trp, and Tyr) are involved in the stabilization of the peptide-pathogen surface complexes (Zhang et al., 2016).

The interaction with LPS has been demonstrated to be essential for AMPs like gramicidin S and polymyxin B to exert their mechanism of action for bacterial killing (Zhang et al., 2000). Bhunia and colleagues studied the structure of MSI-594 peptide in LPS micelles. They observed that the peptide is unstructured in solution, while it adopts a helix-loop-helix structure in complex with LPS, suggesting how AMPs could overcome the LPS barrier (Bhunia et al., 2009). A mutant form of MSI-594 peptide, substituting Phe5 with Ala amino acid, displays a limited permeabilization through the LPS layer suggesting that peptide conformation is essential to disrupt LPS (Domadia et al., 2010).

Other examples of AMPs acting by perturbation of microbial membrane structure are the fungal peptide alamethicin, the amphibian AMP aurein 1.2, and several defensins (Machado and Ottolini, 2015; Shahmiri et al., 2017; Su et al., 2018) AMPs acting through a non-membranolytic mechanism, thus displaying intracellular activities (such as inhibition of nucleic acids, proteins or cell wall synthesis), include buforin II and indolicidin that bind to DNA (Scocchi et al., 2016), teixobactin that binds to peptidoglycan precursor lipid II (Chiorean et al., 2020), Bac5 that interacts with ribosomes (Mardirossian et al., 2018) and Temporin-L, which binds FtsZ protein inhibiting *Escherichia coli* cell division (Di Somma et al., 2020). A recent study performed by Moura et al. demonstrated that the AMP thanatin interacts with LptC-LptA proteins, which belong to the Lpt complex, involved in the LPS transport, exploiting an inhibitory activity (Moura et al., 2020). Thanatin interaction with Lpt complex prevents LPS translocation to the outer membrane, modifying its stability and permeability and favoring the cell agglutination process (Dash and Bhattacharjya, 2021).

## Sources of AMPs and Their Potential Applications in Clinical Practice

The survival of organisms in an environment where pathogens are widely distributed, solely depends on their defense mechanisms. The inborn immunity of organisms involves endogenous peptides which supply a quick and viable method for safeguard against microbial attacks (Borah et al., 2020) AMPs are universal and

essential components of the defense systems of all life forms, from bacteria to plants and invertebrate and vertebrate species, including mammals (Jenssen et al., 2006; Borah et al., 2020).

They are naturally produced in the body of both lower and higher organisms and their production is cell specific and may be constitutive or inducible in response to pathogenic challenges (Borah et al., 2020). In multicellular organisms, AMPs are mostly localized to specific sites that are normally more exposed to microbes, such as the skin and mucosa epithelia (Jenssen et al., 2006). The primary role of these defense peptides is the killing of invading pathogens; however, in higher organisms they act also as modulators of the innate immune response (Jenssen et al., 2006). AMPs are commonly classified according to their sources, which are represented by microorganisms, plants, and animals.

Below, we give an overview of various naturally occurring AMPs and the potential clinical application of some of them.

### Microorganisms as Source of AMPs

Bacteria and fungi are reservoirs of AMPs (Huan et al., 2020). Among the numerous AMPs, the first isolated and characterized were those produced by bacteria (Jenssen et al., 2006). AMPs from bacteria are not produced for the purpose to protect against infections, but rather as a competition strategy (Jenssen et al., 2006). With their activity they kill other microbes competing for nutrients in the same niches, ensuring the survival of individual bacterial cells (Jenssen et al., 2006). Bacterial AMPs, also called bacteriocins, are represented by a heterogeneous family of small ribosomally synthesized molecules with strong antimicrobial activity at specific concentrations (Soltani et al., 2021). These molecules, produced by Gram-positive and Gram-negative bacteria, are effective against many pathogenic bacteria and are extraordinarily active compared to their eukaryotic counterparts (Jenssen et al., 2006; Soltani et al., 2021). For example, AMPs isolated from *Pseudomonas* spp display activity against several bacterial species, such as *S. aureus*, *E. coli*, *Salmonella*, *Shigella*, showing both general antibacterial and specific antibiofilm activity (Fontoura et al., 2008; Mohammadi-Barzelighi et al., 2019). Mersacidin, isolated by *Bacillus* spp, shows *in vivo* bactericidal activity against Methicillin-resistant *S. aureus* (MRSA) equivalent to that of vancomycin (Jenssen et al., 2006).

AMPs are also produced by human microbiota. Host-microbiota crosstalk is based on AMPs secretion by phagocytic and epithelial cells and microbiota of the human gut, skin, and oral cavity; these peptides contribute to microbial and ecological balance (Magana et al., 2020). An example of these human microbiota AMPs is the thiopeptide lactocillin produced by the vaginal commensal *Lactobacillus gasseri* and acting against Gram-positive bacteria, including *S. aureus* and *Gardnerella vaginalis* (He et al., 2020).

Several filamentous fungi produce AMPs which are similar to plant and animal defensins. Examples of cysteine-rich defensin-like AMPs in ascomycetes are AFP from *Aspergillus giganteus*, PAF from *Penicillium chrysogenum*, ANAFP from *Aspergillus niger*, AcAFP and AcAMP from *Aspergillus clavatus* (Montesinos, 2007; Hegedüs and Marx, 2013). All these fungal peptides have antifungal activity against filamentous ascomycetes, including animal and plant opportunistic and

pathogens, such as *Aspergillus fumigatus*, *Fusarium* sp., and *Botrytis* sp. (Hegedüs and Marx, 2013).

On the basis of their antimicrobial properties and their safety and tolerability, some of these natural AMPs have potential therapeutic applications. The bacteriocin nisin, produced by *Lactococcus lactis*, has been extensively studied being used as food preservative (Soltani et al., 2021). Nisin is the only bacteriocin legally approved as biopreservative and is used in the dairy industry to control contamination from *Listeria* strains (Soltani et al., 2021). Because of its broad-spectrum activity against both Gram-positive and Gram-negative pathogens, nisin is approved for clinical use as an alternative to antibiotics (Dijksteel et al., 2021). Several studies have reported the suitability of nisin in the treatment of several infection diseases, such as mastitis (Cao et al., 2007; Fernández et al., 2008), oral (Shin et al., 2015; Mitra et al., 2019), respiratory (De Kwaadsteniet et al., 2009) and skin (Heunis et al., 2013) infections. Johnson et al. (1978) have been the first to demonstrate that there were fewer numbers of *streptococci* in the dental plaque of monkeys that received nisin in their foods. Moreover, more recent studies support the antimicrobial abilities of nisin against oral pathogenic bacteria relevant to periodontal diseases and caries. Indeed, Tong et al. (2010) showed that nisin A is able to inhibit the growth of cariogenic bacteria. Cao et al. (2007) demonstrated that a nisin-based formulation was effective in the treatment of clinical mastitis in lactating dairy cows caused by different mastitis pathogens. Mastitis is a common inflammatory disease in lactating women, which causes breastfeeding cessation (Foxman et al., 2002). *S. aureus* and *Staphylococcus epidermidis* are two common agents that cause mastitis-associated infections (Foxman et al., 2002). Nisin peptide causes bacterial growth inhibition by membrane pores formation and by interrupting the cell wall biosynthesis through specific lipid II interaction (Prince et al., 2016).

Another example of bacterially derived AMPs used in clinics as alternative to antibiotics is gramicidin, which is a mix of gramicidin A, B and C. They are AMPs naturally produced by *Bacillus brevis*, with activity against several Gram-positive bacteria, inducing membrane depolarization and consequently cell lysis (David and Rajasekaran, 2015; Yang and Yourself, 2018). Gramicidin is a constituent of Neosporin<sup>®</sup>, a triple antibiotic used in ophthalmic and topical preparations (Hallett et al., 1956). Gramicidin S is used in the treatment of wound infection and of the root canal of teeth due to the tetracycline resistant *Enterococcus faecalis* biofilms formation (Berditsch et al., 2016). The bacterium *Streptomyces roseosporus* is a rich source of the anionic AMP daptomycin, which shows bactericidal activity against Gram-positive pathogens (Ball et al., 2004). Daptomycin exerts its bactericidal action by formation of membrane pores, membrane depolarization and inhibition of cell wall synthesis (Taylor and Palmer, 2016). This peptide has been approved and marketed as anionic AMP for the treatment of skin infections caused by Gram-positive bacteria (Wang et al., 2014).

Considering the great variety of AMPs existing in nature, it has to be expected that other novel nature-inspired peptides, pharmacological active, might find clinical applications in the future.

## Plants as Source of AMPs

Bioactive peptides are essential components of plants defense mechanisms, with extraordinary physiological importance, providing fast protection against bacterial and fungal infections (Jenssen et al., 2006; López-Meza et al., 2011; Salas et al., 2015). Plant AMPs not only display microbicide activities but are also involved in cellular signaling (Salas et al., 2015). Several active peptides have been extracted and isolated from roots, flowers, seeds, stems and leaves and are classified based on their amino acids sequence, position and number of cysteine residues involved in the disulfide bridge formation (López-Meza et al., 2011). Ten families of plant AMPs have been described (López-Meza et al., 2011) and the best-studied groups are defensins, thionins and snakins (Jenssen et al., 2006; López-Meza et al., 2011; Huan et al., 2020). The first plant-derived AMP is purothionin, which displays activity against *Corynebacterium fascians*, *Pseudomonas solanacearum*, *Corynebacterium poinsettia* (de Caley et al., 1972). Plant defensins are cysteine-rich AMPs, with four disulphide bridges and a globular structure (Salas et al., 2015); they are basic peptides, composed by 45 to 54 amino acid residues, ubiquitous in the plant kingdom, displaying activities against bacteria and fungi. The PvD1 peptide is a defensin from *Phaseolus vulgaris*, which inhibits growth of yeasts, such as *Candida albicans*, *Candida tropicalis* and *Saccharomyces cerevisiae* (Mello et al., 2011). Thionins, composed by 45 to 47 amino acids, are basic peptides found in several plant tissues, which are toxic to bacteria and phytopathogenic fungi (López-Meza et al., 2011). Snakins are small peptides with 12 cysteine residues forming six disulphide bridges, essential for their biological activity (Meneguetti et al., 2017). Snakin-Z from *Ziziphus jujuba*, composed by 31 amino acids, is more toxic for fungi than bacteria (Meneguetti et al., 2017). Finally, different AMPs have been identified in avocado fruit and in fruits of *Capsicum*, which for their antimicrobial properties could be used in the treatment of infections caused by *S. aureus* and *E. coli* strains (Liu et al., 2006; Guzmán-Rodríguez et al., 2013; Taveira et al., 2014).

Considering their efficiency and broad-spectrum activity, plant AMPs may represent a promising alternative to conventional antibiotics for counteracting infections (da Silva and Machado, 2012).

## Animals as Source of AMPs

Animal AMPs are produced at the sites that are constantly exposed to microbes, such as skin and mucosal barriers (López-Meza et al., 2011). Various AMPs have been isolated from invertebrates and many vertebrate species (including fish, amphibians, and mammals).

In invertebrates the innate immune system is extremely efficient since they lack an adaptive immune system, and in this regard, AMPs play a key role in protection against foreign microbial attacks (Jenssen et al., 2006). Invertebrates can produce a wide range of proteins and peptides which are found in phagocytes, in epithelial cells and in hemolymph (plasma and hemocytes) (Jenssen et al., 2006). The  $\beta$ -hairpin-like peptides tachyplesin (Nakamura et al., 1988) and polyphemusin (Miyata et al., 1989) (from horseshoe crab), and

melittin (from bee venom) (Raghuraman and Chattopadhyay, 2007) are examples of invertebrate AMPs.

A recent study has demonstrated that a pretreatment with Tachyplesin III on mice protects them against *P. aeruginosa* and *Acinetobacter baumannii* infection, reduces the production of pro-inflammatory cytokines (IL-1 $\beta$ , IL-6, and TNF- $\alpha$ ) and induces the macrophage phagocytosis, fundamental to exert bacterial clearance, in a dose-dependent manner (Qi et al., 2019). All these findings must be confirmed in human clinical trials.

More than 200 AMPs have been isolated in insects (Li et al., 2012). The number of these bioactive molecules varies between species. *Hermetia illucens* and *Harmonia axyridis* produce up to 50 AMPs, while they are not found in other species, such as *Acyrtosiphon pisum* (Huan et al., 2020; Moretta et al., 2020). AMPs are produced mainly in the fat body and blood cells (hemocytes) of insects and then are secreted into the hemolymph (Jenssen et al., 2006; Huan et al., 2020). Based on their amino acid sequences and antimicrobial activities, insect AMPs are divided into several groups: cecropins, defensins, proline-rich and glycine-rich peptides (Manniello et al., 2021). Cecropin was the first insect AMP discovered in the hemolymph of the pupae of *Hyalophora cecropia* (Steiner et al., 1981). Cecropins, which are described only in the order *Diptera* and *Lepidoptera*, are linear peptides with  $\alpha$ -helix and without cysteines, composed by around 35 amino acid residues and displaying activity against Gram-positive and Gram-negative bacteria (Wu Q. et al., 2018). Insect defensins are inducible peptides which display strong activity against Gram-positive bacteria and less against Gram-negative bacteria. They are composed by 29-34 amino acid residues and have been isolated from several insect orders, such as Coleoptera, Hemiptera Diptera, Trichoptera, Hymenoptera and Odonata (Bulet et al., 1999). Attacins are an example of glycine-rich AMPs, which show activity against Gram-negative bacteria, including *E. coli* (Carlsson et al., 1991). This group of peptides is heterologous in size, but their common feature is the high content of glycine-residues (10-22%) (Wu Q. et al., 2018), which affect the tertiary structure and consequently their mode of action (Li et al., 2012). Dipterin, Coleopterin, Sarcotoxin IIA are other glycine-rich AMPs isolated from insects (Ando and Natori, 1988; Dimarcq et al., 1988; Sagisaka et al., 2001). Although insect AMPs could be a good alternative to conventional antibiotics, their clinical use is still limited and most of them are just *in vitro* tested (Manniello et al., 2021).

Among them, the melittin peptide is, currently, in clinical use for its antimicrobial potency. Composed by 26 amino acids, melittin is the principal component of venom from the honeybee *Apis mellifera*. Melittin has broad spectrum activity, and its ability to protect *in vivo* against MRSA infections has been demonstrated (Choi et al., 2015). It acts by induction of pore formation following interaction with membrane surfaces (van den Bogaart et al., 2008). Since it also shows anti-inflammatory properties (Lee and Bae, 2016), the Food and Drug Administration (FDA) approved its usage in clinical practice (Dijksteel et al., 2021), for relieving pain associated to tendinitis, arthritis, sclerosis multiple (Park et al., 2004; Son et al., 2007; Yang et al., 2011).

Amphibians, especially frogs, are a rich source of AMPs. Most of the amphibian AMPs have been isolated from the frog skin. These biologically active molecules are released from cutaneous glands and excreted towards the skin surface following pathogen stimulations (Patoocka et al., 2018). The prototypic and the most famous AMP from frogs is the  $\alpha$ -helical magainin (Zasloff, 1987), which is active against yeasts, fungi, bacteria, and viruses (Borah et al., 2020). Esculentins, nigrocin, brevinins, temporins are some of the best characterized peptides produced by frogs of the genus *Rana* (Patoocka et al., 2018). The basic esculentin-1 peptide, composed by 46 amino acid residues and a disulphide bridge, exhibits strong activity against several human pathogens, such as *C. albicans*, *P. aeruginosa*, *E. coli* and *S. aureus* (Patoocka et al., 2018).

Esculentin was *in vitro* tested on human lung epithelium to determine the toxicity, finding a good tolerability in terms of inflammatory effects. Then, it was studied in a mouse model, in which a lung-infection was induced with *P. aeruginosa*: promising results showed a strong reduction in bacterial load not only in lungs but also in spleen, indicating a decrease in systemic spread of bacteria (Chen C. et al., 2017).

Brevinin-2Ta was tested on mice infected with *Klebsiella pneumoniae*. In this study, it was demonstrated that the peptide decreases the bacterial load, altering the microorganism structures in infection sites and it also showed the ability to faster angiogenesis and granulation tissue maturing process, obtaining comparable results to classical antibiotics. For this reason, this peptide is a good candidate for pre-clinical studies, even if some modifications are needed in order to decrease its hemolytic power (Liu et al., 2017). Liu et al. (2017), hypothesized that amino acid substitutions in the primary structure could be the right strategy to reduce the hemolytic activity, improving, at the same time, the antimicrobial one.

Regarding anionic AMPs, the temporin-1Ja, carrying a net charge of -1, has been isolated from the skin secretions of the Japanese frog *Rana japonica* (Isaacson et al., 2002). This anionic peptide revealed moderate activity against *E. coli* and *S. aureus* strains. However, it was found that this peptide synergizes with other temporins, contributing to endotoxin neutralization (Rosenfeld et al., 2006). AMPs can also protect amphibians from ingested pathogens since they are produced in the mucosa of the stomach. The Asian toad peptide buforin and buforin II are the best characterized examples in this regard (Jenssen et al., 2006). Some of these natural AMPs have been used for the production of synthetic peptides, such as the Pexiganan, also known as MSI-78. It is a synthetic 22-amino-acid analogue of magainin-2, which has been tested as a topical cream for treatment of bacterial infections related to diabetic foot ulcers. It showed promising *in vitro* broad-spectrum activity (Ge et al., 1999), but it was rejected by FDA because there was no advantage compared to conventional antibiotics (Koo and Seo, 2019).

Mammalian AMPs have been identified in humans, cattle, sheep and other vertebrates (Huan et al., 2020). Some AMPs from mammals have a second major function inducing chemoattraction and activation of host cells to engage in innate host defense (Yang et al., 2001). AMPs can be stored in phagocytes and epithelial cells and can be released extracellularly

by degranulation in response to different stimuli, becoming available at the site of infection (Yang et al., 2001). For example, cathelicidins are stored within granules of circulating immune cells as inactive propeptides (Jenssen et al., 2006). Cathelicidins and defensins are the main AMPs found in mammals, such as humans, horses, rabbits, sheep and mice. Cathelicidin family comprises heterogeneous peptides which share the N-terminal pro-region but show a variable antibacterial peptide in the C-terminal region, displaying different structures, including  $\beta$ -hairpin,  $\alpha$ -helical, and arginine and proline-rich peptides (Kościuczuk et al., 2012). This structural diversity reflects cathelicidin different functions and their diverse spectrum of antimicrobial and immunomodulatory activities (Jenssen et al., 2006). The  $\alpha$ -helical BMAP-28 is a bovine AMP of the cathelicidin family which is able to permeabilize the membranes of several bacteria and fungi at a moderate concentration *in vitro* (Risso et al., 2002; Benincasa et al., 2006). Only one cathelicidin, the hCAP18 (better known as LL-37), is produced in humans and has been isolated from specific granules of neutrophil granulocytes. A second group of mammalian AMPs are the defensins, which require proteolytic processing to acquire their active form (Selsted and Ouellette, 2005). More than 50 defensins have been identified in mammalian species; some of them are stored in granules of macrophages, neutrophils and Paneth cells, while others are produced by mucosal epithelial cells and keratinocytes (Yang et al., 2001). Defensins production can be constitutive, such as for human  $\beta$ -defensin-1 (hBD1), or inducible, such as for hBD2, whose expression is induced by exposure to bacteria or microbial components, as LPS (Jenssen et al., 2006). Maiti et al. (2014) studied mice mortality after the infection with *Salmonella typhimurium*, demonstrating that the administration of hBD1, hBD2, or a combination of both, lead to an increased mice mortality and a decreased *S. typhimurium* load in peritoneal fluid, liver and spleen.

The anionic peptide Dermcidin, discovered in epithelial and neutrophil granules of humans, is one of the most studied human anionic AMPs. This peptide is proteolytically processed in sweat producing several truncated peptides which display a good spectrum of antimicrobial activity (Schitteck et al., 2001).

There are several examples of mammalian AMPs proposed for clinical applications. The acid-pepsin digestion of bovine lactoferrin results in the release of the peptide lactoferricin, which shows the strongest antimicrobial activity among mammalian lactoferricins (Vorland et al., 1998) and has potent immunological and antitumor properties (Gifford et al., 2005; Yin et al., 2013; Arias et al., 2017). It exerts its bactericidal activity on Gram-positive and Gram-negative bacteria inducing depolarization of the cell membrane, with fusion of negatively charged liposomes and formation of blebs on the cell surface (Ulvatne et al., 2001; Bruni et al., 2016). The bovine lactoferricin displays useful properties for potential applications in human medicine. It has been successfully utilized for treatment of enterohemorrhagic *E. coli* infections (Kühnle et al., 2019). Because of its antimicrobial and anti-inflammatory properties, the bovine lactoferricin can be used for treatment of ocular infections, since it potentiates the effect of conventional

antibiotics against clinical ocular isolates of *P. aeruginosa* and *S. aureus* (Oo et al., 2010). Moreover, it improves diabetic wound healing (Mouritzen et al., 2021) and finds applications in the treatment of osteo-articular diseases (Yan et al., 2013). The saliva of humans and other primates contains various forms of AMPs, among them the histatins, which are small histidine-rich cationic peptides with antifungal properties. Histatin 5, that is the product of histatin 3 proteolytic cleavage, is the most active histatin against several yeasts, such as *Cryptococcus neoformans*, *Candida dubliniensis* and *Candida albicans* (da Costa et al., 2015). Histatins exert their activity by targeting the mitochondria, affecting cell respiration (Kavanagh and Dowd, 2004) and, because of their safety and tolerance, have been successfully tested in topical gels to treat oral fungal infections (Paquette et al., 2002). Several efforts have been made to identify fragments of histatin 5 with pharmaceutical application and have yielded promising results. An example in this regard is the 12-amino acid peptide P113, which was evaluated in phase I and phase II clinical studies as pharmaceutical agent to fight oral candidiasis (Woong et al., 2008; Cheng et al., 2018; Browne et al., 2020).

**Tables 1 and 2** summarize, respectively, naturally occurring AMPs from different sources and those used in clinical practice.

## AMPs: INNATE WEAPONS AGAINST DISEASES

Given the broad spectrum of action of the AMPs, their diversity in sequences and considering the physico-chemical characteristics related to their several sources, they can find application in different fields. Specifically, below we addressed the suitability of AMPs in the biomedical and pharmacological fields, also taking into account the pharmacokinetic and pharmacodynamic approaches to develop new molecules with antimicrobial activity.

The excessive use of antibiotics in clinical treatment has increased pathogens resistance to these compounds (Aminov, 2010). The pharmaceutical industry is trying to solve this problem by looking for new molecules with antibiotic activity or by modifying/improving the existing ones. Nevertheless, pathogens can develop resistance mechanisms that compromise this strategy. Thus, the need to find new active molecules with different mechanisms of action represents one of the most urgent challenges in medicine (Parisien et al., 2008). AMPs are among the most promising alternatives to modern antibiotics and they have already found clinical applications in this field, as previously mentioned, alone or in synergy with existing antibiotics. AMPs are susceptible to proteolysis due to their chemical characteristics and their activity is affected by salts concentration and pH. For this reason, the most promising applications for AMPs in clinical evaluations are those involving topical applications (Hancock and Sahl, 2006). The endogenous production of AMPs is also relevant and worth further studies. For example, sodium butyrate administration has been shown to induce the production of intestinal AMPs, beneficial for the treatment of infectious or inflammatory diseases (Guaní-Guerra et al., 2010).

**TABLE 1** | Overview of AMPs from different sources in nature and the current status of research.

<b>AMPs from Microorganism Class</b>	<b>Source</b>	<b>Peptide Name</b>	<b>Biological activity</b>	<b>Studies</b>	<b>Reference</b>
Bacteriocin	Bacteria <i>Bacillus</i> spp.	Mersacidin	Antibacterial	<i>In vivo</i>	Jenssen et al., 2006 Kruszewska et al., 2004
Bacteriocin	Bacteria <i>Lactobacillus gasseri</i>	Lactocillin	Antibacterial	<i>In vitro</i>	Magana et al., 2020 Donia et al., 2014
Bacteriocin	Bacteria <i>Lactococcus lactis</i>	Nisin	Antibacterial	Clinical practice	Dijksteel et al., 2021
Bacteriocin	Bacteria <i>Bacillus subtilis</i>	Ericin	Antibacterial	<i>In vitro</i>	Sharma et al., 2018
Defensin	Fungi <i>Penicillium chrysogenum</i>	PAF	Antifungal	<i>In vivo</i>	Kaiserer et al., 2003 Barna et al., 2008 Marx, 2004 Palicz et al., 2016
Defensin	Fungi <i>Aspergillus giganteus</i>	AFP	Antifungal	<i>In vitro</i>	Hegedüs and Marx, 2013 Krishnamurthy et al., 2020
<b>AMPs from Plants</b>					
Defensin	<i>Phaseolus vulgaris</i>	PvD1	Antifungal	<i>In vitro</i>	Mello et al., 2011 do Nascimento et al., 2015
Defensin	<i>Persea americana</i>	PaDef	Antibacterial	<i>In vitro</i>	Guzmán-Rodríguez et al., 2013
Thionin	<i>Triticum aestivum</i>	$\alpha$ 1-purothionin	Antibacterial	<i>In vitro</i>	de Caleyá et al., 1972 Oard et al., 2012
Snakin	<i>Ziziphus jujuba</i>	Snakin-Z	Antifungal	<i>In vitro</i>	Daneshmand et al., 2013 Meneguetti et al., 2017
<b>AMPs from Insects</b>					
Cecropin	<i>Hyalophora cecropia</i>	CecA	Antibacterial	<i>In vitro</i>	Wu Q. et al., 2018 Wang et al., 2017
Cecropin	<i>Spodoptera litura</i>	Spodopsin Ia	Antibacterial	Discovery	Choi et al., 1997
Defensin	<i>Drosophila melanogaster</i>	Drosomycin	Antifungal	<i>In vitro</i>	Landon et al., 1997 Fehlbaum et al., 1994
Proline-rich AMPs	<i>Apis mellifera</i>	Abaecin	Antibacterial	<i>In vitro</i>	Casteels et al., 1990 Luiz et al., 2017
Attacin	<i>Hyphantria cunea</i>	Attacin-B	Antibacterial	<i>In vitro</i>	Kwon et al., 2008
Glycine-rich AMPs	<i>Drosophila melanogaster</i>	Diptericin	Antibacterial	<i>In vitro</i>	Verma and Tapadia, 2012 Wicker et al., 1990
<b>AMPs from Animals</b>					
Cathelicidin	Bovine	BMAP-28	Antibacterial	<i>In vivo</i>	Risso et al., 2002 Benincasa et al., 2003
Brevinin	<i>Rana boylei</i>	Brevinin-1BYa	Antifungal	<i>In vivo</i>	Conlon et al., 2003 Liu et al., 2017
Cathelicidin	Pig	Protegrin-1	Antibacterial	<i>In vitro</i>	Soundrarajan et al., 2019 Huynh et al., 2018
<b>AMPs from Humans</b>					
Cathelicidin	Human granulocytes	hCAP18/LL-37	Antibacterial	Clinical trial	Leszczynska et al., 2013
Defensin	Human monocytes	hBD1 hBD2 hBD3	Antibacterial	<i>In vivo</i>	Levón et al., 2015 Maiti et al., 2014
Histatin	Human saliva	Histatin-1	Antibacterial Antifungal	Clinical practice	Khurshid et al., 2017

**TABLE 2** | List of natural AMPs in clinical practice.

<b>Peptide Name</b>	<b>Origin</b>	<b>Mechanism of action</b>	<b>Indication</b>	<b>Reference</b>
Nisin	Bacteria <i>(Lactococcus lactis)</i>	Membrane depolarization	Bacterial infections	Cao et al., 2007 Mittra et al., 2019
Gramicidin	Bacteria <i>(Brevibacillus brevis)</i>	Membrane depolarization/Lysis	Bacterial conjunctivitis	David and Rajasekaran, 2015
Melittin	Insect <i>(Apis mellifera)</i>	Membrane disruption	Anti-inflammatory applications	Lee and Bae, 2016
Daptomycin	Bacteria <i>(Streptomyces roseosporus)</i>	Membrane depolarization/Lysis	Skin infections	Taylor and Palmer, 2016
Lactoferricin	Mammalians	Membrane depolarization	Anti-inflammatory applications	Oo et al., 2010 Yan et al., 2013
Histatin	Humans	Inhibition of respiration	Fungal infections	Paquette et al., 2002



However, AMPs broad spectrum of biological activities suggests other potential clinical benefits such as for the treatment of cancer and viral infections as well as in the immune system modulation (Schweizer, 2009).

## Involvement of AMPs in Respiratory Diseases

Infections in the lower respiratory tract are involved in chronic inflammatory lung disorders such as cystic fibrosis and chronic obstructive pulmonary disease. In cystic fibrosis patients with a *P. aeruginosa* infection, this organism produces AMPs, such as pyocins, which inhibit the growth of its closest competitors. Thus, the same AMPs could be used as a therapeutic agent to minimize the effects of the infection, besides rooting out other susceptible pathogens. Pyocins derived from *P. aeruginosa* strains also have toxic effects on *Haemophilus*, *Neisseria* and *Campylobacter* strains and have been successfully used for the treatment of peritonitis in mice (Scholl and Martin, 2008; Waite and Curtis, 2009).

It is of interest that neutrophils and airway epithelial cells produce AMPs to prevent infection of the respiratory system by pathogens. In cystic fibrosis patients, *P. aeruginosa* induces the secretion of sPLA2-IIA by airways epithelial cells via a Krüppel-like transcription factor (KLF)-2-dependent pathway, that lead to the selective death of *S. aureus* (Rahnamaeian, 2011).

Moreover, the serum level of the human LL-37 peptide is higher in patients with lower respiratory tract infections than in healthy people (Majewski et al., 2018). Recently, it has been reported that the Esculentin peptide (1–21), active on both *P. aeruginosa* planktonic and biofilm forms, has the ability to prolong the survival of mouse models with pulmonary infection. The main AMPs detected in lung tissues and secretions of cystic fibrosis patients are sPLA2-IIA, neutrophil  $\alpha$ -defensins/HNPs, hBDs and LL-37 (Hiemstra et al., 2016).

Similar phenomena have been described in periodontal diseases caused by *Porphyromonas gingivalis* in which the sPLA2-IIA peptide is produced by oral epithelial cells via activation of the Notch-1 receptor and kills oral bacteria (Balestrieri et al., 2009).

## AMPs in Wound Healing and Skin Infections

Skin and soft tissue infections are one the most common microbial infections in humans and AMPs can be a new therapeutic option thanks to their broad-spectrum of biological activities, since skin pathogens include bacteria but also protozoa, fungi and viruses (Sunderkötter and Becker, 2015). Moreover, AMP preparations have the advantage of high concentration at the target site for topical administration because of their low ability to penetrate into the bloodstream. Moreover, AMPs can promote wound healing by modulating cell migration, angiogenesis, chemotaxis, and cytokine release (Ramos et al., 2011).

For example, the hBD2 is induced by the Epidermal Growth Factor Receptor (EGFR) activation and it can increase keratinocyte migration and cytokines production (Sørensen, 2016). Another

peptide highly expressed by keratinocytes at wound sites is represented by hBD3 defensin. It promotes cytokine secretion, cell migration and proliferation by phosphorylating EGFR and STAT proteins (Sørensen et al., 2005). It also speeds up the wound closure when topically applied in a porcine model of infected skin wounds (Hirsch et al., 2009). Moreover, it has been demonstrated that hBD3 exhibits anti-inflammatory activity through the inhibition of TLR (Toll-like receptor) signaling pathways in immune cells leading to a transcriptional repression of the pro-inflammatory genes (Semple et al., 2011).

The expression of skin LL-37 peptide is also increased after wounding (Heilborn et al., 2003), and it seems to be involved in the modulation of angiogenesis. Indeed, LL-37 peptide stimulates endothelial cells proliferation and neovascularization by activating the formyl peptide receptor-like 1 (FPR2/ALX) (Koczulla et al., 2003).

Psoriasis vulgaris is an inflammatory skin disease characterized by abnormal epidermal proliferation and a cellular infiltrate including neutrophils and T cells (Davidovici et al., 2010). Due to the enhanced proliferation rate of psoriatic keratinocytes associated with a reduction of the cell cycle duration, psoriasis has been thought to be an epidermal disease. However, experiments performed with severe combined immunodeficiency (SCID) mice indicated that psoriatic eruptions are induced by CD4+ cells and T cells are believed to play a key role in the pathogenesis of psoriasis (Ellis et al., 1986; Wrone-Smith and Nickoloff, 1996).

The keratinocytes within the epidermis of psoriatic plaques are abnormal and among the abnormalities there is the excessive production of AMPs which, in vertebrates, are believed to modify host inflammatory responses through different mechanisms including regulation of cell proliferation, chemotactic and angiogenic activities (Lai and Gallo, 2009).

HNP1, HNP2, HNP3, hBD2 and hBD3 are defensins identified from lesional psoriatic scale extracts and their presence could help to explain why a hyperproliferative and noninfectious skin disease, such as psoriasis, undergoes less cutaneous infections than it would be expected (Harder et al., 2001; Harder and Schröder, 2005). Studies performed on LL-37 peptide demonstrated that it has both pro-inflammatory and anti-inflammatory activity, can promote chemotaxis, angiogenesis and enhance wound repair (Yang et al., 2000; Koczulla et al., 2003; Braff et al., 2005; Tokumaru et al., 2005; Mookherjee et al., 2006). Frohm et al. were the first to report that cathelicidin/LL-37 expression is upregulated in psoriatic epidermis and suggested that this induction increases the antimicrobial defense ability of the disrupted barrier in the lesions (Frohm et al., 1997). Later, it has been hypothesized that LL-37 could drive inflammation in psoriasis by allowing plasmacytoid dendritic cells (pDCs) to recognize self-DNA through TLR9 (Lande et al., 2007).

## Angiotensin-Converting Enzyme I (ACE) Inhibitory Peptides

The angiotensin-converting enzyme I (ACE) is produced by lung or kidney tissue and the luminal membrane of vascular endothelial

cells. ACE converts inactive decapeptide angiotensin I (ANG I) into vasoconstrictor octapeptide angiotensin II (ANG II). ANG II is involved in several physiological and pathophysiological cardiovascular conditions such as atherosclerosis and hypertension (Wu C. H. et al., 2018). ACE inhibitors are used in hypertension treatment, but they may cause serious side effects, such as cough, rash and edema (Wu C. H. et al., 2018). Hence, it derives the need to identify new and nontoxic ACE inhibitors, whose activity depends on the amount and type of amino acid composition.

It has been observed that the binding to ACE is influenced by hydrophobic amino acids at the peptide C-terminus (Salampessy et al., 2017). Moreover, amino acids like alanine, valine, isoleucine, isoleucine and glycine – which are hydrophobic residues with aliphatic side chains – at the C-terminus have been associated with an increase in the ACE inhibitory activity (Toopcham et al., 2017). SAGGYIW and APATPSFW are two AMPs able to act as ACE inhibitors potentially suitable as antihypertensive peptides. They are produced in wheat gluten hydrolysate by the *P. aeruginosa* protease and contain tryptophan at the C-terminus (Zhang et al., 2020). This observation led to the idea that the presence of a tryptophan at the C-terminus of a peptide could influence the ACE inhibitory activity by blocking the enzyme active site *via* weak interactions, such as electrostatic, hydrophobic and Van Der Waals interactions and hydrogen bonds.

Another example is the VEGY peptide, which was isolated from the marine *Chlorella ellipsoidea* and has been demonstrated to exhibit ACE inhibitory activity and to be stable against gastrointestinal enzymes (Ko et al., 2012). This potential use of AMPs certainly represents a fruitful avenue of pursuit and will likely find clinical applications in the future.

## Pancreatic Lipase Inhibitory Peptides

Obesity and fatty acid metabolism disorders are widespread epidemic. One of the pharmacological strategies to counteract these issues is the dietary lipid inhibition. The pancreatic lipase enzyme hydrolyzes 50–70% of food-derived fat in the human organism and its inhibition is exploited by the Orlistat drug used in obesity treatment. However, in long-term treatment, this strategy can cause side effects, such as pancreatic damage and gastrointestinal toxicity (Cheung et al., 2013). For this reason, the search of new compounds able to inhibit pancreatic lipase, without exerting side effects, represents a still alive need to fight these disorders. Several AMPs have been identified so far that are able to show this activity, which depends on the structure and amino acid composition of the peptide (Hüttel et al., 2013). CQPHPGQTC, EITPEKNPQLR and RKQEEDDEEQRE are three peptides from purified soybean  $\beta$ -conglycinin that have been demonstrated to inhibit the pancreatic lipase (Lunder et al., 2005; Martinez-Villaluenga et al., 2010), and are under investigation for potential clinical applications (Złotek et al., 2020).

## Peptides With Antioxidant Activity

Oxidative stress, caused by an imbalance between production and removal of reactive oxygen species (ROS) in cells and tissues,

can promote diseases like obesity, diabetes, and heart disease (Pizzino et al., 2017). Environmental stressors like pollutants, heavy metals, xenobiotics, high-fat diet and the progression of aging can contribute to an increase in ROS production. Oxidative stress is also involved in several neurological disorders such as Alzheimer's and Parkinson's diseases (Singh et al., 2019).

A growing number of antioxidant AMPs have been identified from different sources, including animals, plants and insects (Balti et al., 2010; Villadóniga and Cantera, 2019; Liang et al., 2020). Peptide antioxidant activity is related to their sequence and amino acid composition. Indeed, it has been suggested that isoleucine, leucine and histidine residues could contribute to the antioxidant activity of fermented anchovy fish extracts (Najafian and Babji, 2019). A study carried out by Wu et al. on the QMDDQ peptide, from a shrimp protein hydrolysate, showed that the antioxidant potency could be related to the high number of active hydrogen sites (Wu et al., 2019). Peptide antioxidant properties are usually expressed as free radical scavenging, metal ion chelation activity and inhibition of lipid peroxidation (Jiang et al., 2020). For example, Zhang et al. showed that the VYLPR peptide has a protective effect on H<sub>2</sub>O<sub>2</sub>-induced cell damage (HEK-293 cells) (Zhang et al., 2019). Moreover, Liang et al. investigated antioxidant peptides deriving from a protein hydrolysate of *Moringa oleifera* seeds and demonstrated their protective effects on Chang liver cells exposed to H<sub>2</sub>O<sub>2</sub> oxidative damage (Liang et al., 2020). Jiang et al. identified four peptides AYI(L) and DREI(L) from Jiuzao protein hydrolysates able to decrease ROS production in HepG2 cells (Jiang et al., 2020).

## AMPs in Intestine Infection and Inflammation

The bacterial microflora is essential for human health and the development of the mucosal immune system. In the small intestine, Paneth cells secrete  $\alpha$ -defensins in response to bacterial antigens including LPS and muramyl dipeptide (Ayabe et al., 2000). Petnicki-Ocwieja et al. showed that the bactericidal activity of crypt secretions of the terminal ileum was compromised by NOD2 gene deletion (Petnicki-Ocwieja et al., 2009). The human NOD2 protein is a cytoplasmic receptor for bacterial molecules principally expressed in Paneth cells (Lala et al., 2003) and it was identified as a susceptibility gene for Crohn's disease (Hugot et al., 2001). Deficient expression of Paneth cell  $\alpha$ -defensins (HD5 and HD6) may contribute to the pathophysiology of Crohn's disease (Bevins, 2006). It has been demonstrated that mice lacking NOD2, fail to express cryptidins, equivalents of human  $\alpha$ -defensins (Kobayashi et al., 2005). Moreover, human  $\alpha$ -defensin expression is reduced in Crohn's disease patients, particularly in those with NOD2 mutations (Wehkamp et al., 2005).

hBD1 was the first defensin identified in the human large intestine and in the not-inflamed colon. It was observed a reduction of hBD1 expression in inflamed mucosa in patients with inflammatory bowel diseases (Wehkamp et al., 2003). hBD1, hBD2, hBD3 and hBD4 expression has been demonstrated to be upregulated in colonic enterocytes in patients with ulcerative colitis (Fahlgren et al., 2004).

Moreover, a lot of interest has been given to the role of AMPs in the stomach, which is easily colonized by *Helicobacter pylori*. Infection by this bacterium leads to the induction of hBD2 (Wehkamp et al., 2003). It has been demonstrated that gastric epithelial cells are induced by *Helicobacter pylori* to upregulate hBD2 production (Grubman et al., 2010).

These observations make defensins very attractive from a pharmacological point of view and can offer a good starting point for future AMP clinical applications.

## PHARMACOKINETIC AND PHARMACODYNAMIC (PK/PD) APPROACH IN THE EVALUATION OF AMP CLINICAL APPLICATIONS

### PK/PD Approach to Determine AMP Antibacterial Efficacy

PK and PD principles that determine response to antimicrobial AMPs can provide clinicians with useful information on the correct dose regimens.

Dosler and colleagues have investigated the *in vitro* activities of AMPs (indolicidin, cecropin [1–7]-melittin A [2–9] amide [CAMA], and nisin), alone and in combination with antibiotics (daptomycin, linezolid, teicoplanin, ciprofloxacin, and azithromycin) against standard and clinical MRSA biofilms, showing that AMPs improve the *in vitro* PK efficacy of traditional antibiotics (Dosler and Mataraci, 2013).

Schmidt and colleagues showed that AMPs (Onc72 and Onc112) reach several organs within 10 min after intravenous and intraperitoneal administration and the PK experiments explain the high *in vivo* efficacies of AMPs indicating their potential use for the treatment of urinary tract infections (Schmidt et al., 2016). However, these data are not sufficient to predict the exact relationship between dose, exposure, and response and translational PK/PD modeling and simulation are used to identify the most suitable dosing regimen in patients. PK/PD modeling can provide useful clues concerning the multifaceted correlation between the selected kind of AMP, the bacterium characteristics, and the reaction of the host organism. Furthermore, complicating factors can also be incorporated into the *in silico* approach thus allowing to carefully predict the right balance between bacterial killing, adverse effects, and appearance of resistance. This practice may, therefore, help to identify and to optimize the dose for novel and established antibacterial agents (Rathi et al., 2016). As previously mentioned, AMPs affect growing bacterial populations differently from antibiotics (ampicillin, ciprofloxacin, gentamicin, kanamycin, neomycin, rifabutin, spectinomycin, and tetracycline), particularly from a PD point of view (Yu et al., 2016). Moreover, Yu and colleagues, analyzing the resistance evolution by predictive model, found that differences in PD and in the mutagenic properties between AMPs and antibiotics produce a much lower probability that resistance will evolve against AMPs (Yu et al., 2018). More experiments with a variety of AMPs are needed to determine if PK/PD characteristics of AMPs can be

generalized and if these characteristics are significantly different from antibiotics. However, all the available data suggest that AMPs are significantly different from antibiotics in terms of PD and mutagenic properties and are good candidates for slowing the evolution of resistance.

### PK/PD Approach to Determine AMP Efficacy in Non-Bacterial Disease

The “right” use of AMPs is imperative, not only in treating bacterial disease but also in other diseases to avoid toxicity and to limit the development of resistance. Few studies have analyzed AMP PK/PD properties in relation to non-bacterial disease. AGPSIVH, FLLPH, and LLCVAV antioxidant peptides were obtained from duck breast protein hydrolysates by Li et al. and beside the nontoxic effects exhibited digestive resistance (Li et al., 2020). Xu and colleagues used *in vitro* and *in vivo* models to study the absorption and potential antioxidant activity and the *in vivo* metabolism, respectively, of WDHHPQLR derived from rapeseed protein (Xu et al., 2018). Koeninger and colleagues showed that hBD2 displays a good tolerability and rapidly enters the bloodstream in a model of experimental colitis after its subcutaneous administration. Thus, besides being well tolerated *in vivo*, it might not only act locally but could also have systemic effects (Koeninger et al., 2020). Several other bioactive peptides have been discovered in recent years, but their PK/PD properties are still unknown. It is therefore necessary to increase the studies to determine the PK/PD efficacy of AMPs also in non-bacterial disease.

## DRUG DEVELOPMENT AND FORMULATION APPROACHES FOR AMP APPLICATIONS

### Production and Costs - Pilot Study vs. Small Industrial Scale

The development of AMPs as APIs (Active pharmaceutical ingredients) has been greatly limited by their high manufacturing costs. Although the chemical synthesis of peptides has high efficiency, it is also complex and expensive. Hence, advanced natural approaches should be considered with the aim to increase the production of alternative molecules. Genetic engineering can be considered one of the most important strategies to obtain higher yields or higher quality of AMPs.

To obtain AMPs, biotechnological approaches involving competent bacteria and yeasts, as well as transgenic plants or animals, should be considered (Sinha and Shukla, 2018). Gaglione and co-workers focused on how to optimize the bacterial culturing using a new composition of culture broth. They basically considered inexpensive as well as readily available components containing well-defined amounts of each nutrient. They also substituted IPTG (isopropyl  $\beta$ -D-1-thiogalactopyranoside) with cheaper and more harmless sugars, such as lactose. Indeed, IPTG use might result in high-cost accumulation for industrial purposes. Altogether, the optimized bacterial culture strategy can contribute to further

development to enhance the manufacturing scalability of AMPs (Gaglione et al., 2019).

However, although bacteria can produce some cyclic peptides, they do not produce disulfide-rich peptides, so that recombinant expression of cyclic peptides might be best performed in yeast- or plant-based recombinant expression systems (Thorsthalm and Craik, 2012; Moridi et al., 2020).

The manufacturing cost of AMPs is estimated to be around \$50-400 per gram of amino acid produced by SPPS (Solid Phase Peptide Synthesis), thus biotechnological engineering or fermentation should give cheaper alternatives. Moreover, the identification, characterization and production of new AMPs also with biotechnology improvement is expensive from many points of view, therefore, it could be useful to perform preliminary *in vitro* screening, to evaluate physio-chemical characteristics, putative modifications in the secondary structure and putative antimicrobial activity (Moretta et al., 2020).

About the peptide drug market in 2018, more than 50 peptide drugs have been commercialized. The annual sales of peptide drugs, including the AMPs, is around 25 billion USD (Koo and Seo, 2019).

## AMP Dosage Forms

Compared to the possible sequence modifications to enhance the molecular stability, the drug delivery platform development has reported a minor attention so far. As described in literature, the dosage forms in ongoing clinical trials encompass topical gel and hydrogel, topical cream, polyvinyl alcohol-based solution for administration in the wound bed, hyaluronic acid-based hydrogel for the administration at the surgical site, oral solutions, and mouth rinse (Mahlapuu et al., 2016).

Concerning dermal administration, burn and chronic wounds can exhibit difficult control, especially in the case of upsurges caused by ESKAPE pathogens (*Enterococcus faecium*, *S. aureus*, *K. pneumoniae*, *A. baumannii*, *P. aeruginosa*, and *Enterobacter* spp). Topical administration of antimicrobials onto the skin provides many advantages since it offers a high local load of the antimicrobial. Moreover, due to the pleiotropic mechanisms of action, AMPs can contribute to fight ESKAPE infections as well as to regulate various mechanisms including the host processes of inflammation and wound healing (Kang et al., 2014; Vassallo et al., 2020). However, AMPs intended to treat chronic skin and soft tissue infections should not (i) be absorbed from the wound or infection site into the systemic circulation; (ii) rouse allergic sensitization. Topical administrations of AMPs have demonstrated to be not free of systemic side effects since the drug transport may also occur *via* skin layers and through hair follicles. Besides, the stability enhancement against enzymatic degradation needs to be assessed when peptides are developed for clinical purposes. Moreover, the membrane border of the epithelial cells includes several peptidases to be considered (e.g., leukocyte elastase, cathepsins B and D, zinc-dependent endopeptidases, interstitial collagenase), since they are characterized by a broad specificity to degrade exogen peptides (Vlieghe et al., 2010; Lam et al., 2018; Pfalzgraff et al., 2018).

## Delivery System

In the context of Drug Delivery System (DDS), peptides are playing an important role as APIs vehicles, due to the intrinsic biodegradability and biocompatibility (Giri et al., 2021). Novel DDS can also help (i) to reduce adverse side-effects, and (ii) to obtain a controlled release of the AMP (Nordström and Malmsten, 2017; Martin-Serrano et al., 2019).

### Hydrogels – Overview and Platform Development for the AMP Dermal and Subdermal Delivery

Hydrogels (HGs) comprise materials constituted by hydrophilic as well as polymeric vehicles to entangle large amounts of water within their three-dimensional (3D) networks (Liu and Hsu, 2018). As reported in the Eur. Pharm 8<sup>th</sup>, gels consist of gelled liquids with suitable gelling agents. Specifically, HGs (i.e., hydrophilic gels) consist of water, glycerol, or propylene glycol-based preparations. These compounds are gelled with starch, cellulose derivatives, poloxamers, carbomers, and magnesium-aluminum silicates (European Pharmacopeia, 2016). HGs exhibit improved bioavailability for applications onto the impaired skin. Moreover, HG-based burn dressings (HBBDD) appear appropriate as they provide a suitable wound covering. Thanks to a cooling sensation that occurs *via* convection and evaporation of the solvent from the wound, HBBDD can also contribute to dissipating the heat that occurs from the concomitant inflammation (Fichman and Gazit, 2014; Goodwin et al., 2016). HGs have also been extensively studied since they exhibit different applicability potentials covering the cell culturing (Caliari and Burdick, 2016), the regenerative medicine (Catoira et al., 2019), and DDS developments.

After chemical interactions, such as the Michael's addition, the Diels–Alder or Schiff base reactions, chemically-crosslinked HGs form the matrix structure (Overstreet et al., 2012) (Figure 3). To obtain a HG that supports the wound closure, Bian and co-workers used modified chitosan with maleic anhydride and a polyethylene glycol derivative, that was modified with benzaldehyde at both ends. *Via* a Schiff-base reaction, the obtained HG showed a shear-thinning behavior. Accordingly, it was intended to be injected/applied into/onto wounds, as it was suitable to adopt the contour as well as to seal the defects of the impaired tissue. Afterwards, the *in situ* HG solidification was promptly realized by using ultraviolet light (Bian et al., 2019).

HG can also be prepared by multiple non-covalent interactions, by which the monomeric building blocks can self-associate in ordered fibrous structures. Also, they are suitable to interact with each other forming the 3D network (Fichman and Gazit, 2014). Moreover, thanks to a self-assembly skill of polymers e.g., *via* changing pH and temperature, the physical cross-linking method favors the formation of weaker and stimuli-responsive HG. Hence, HG can temporarily modify the structure due to the solicitation of external mechanical forces and the shear-thinning behavior (Yan et al., 2010).

Since a substantial change in volume is usually not observed, HGs are also suitable as injectable vehicles (Manna et al., 2019). Moreover, HG can also polymerize *in situ* becoming a shear-

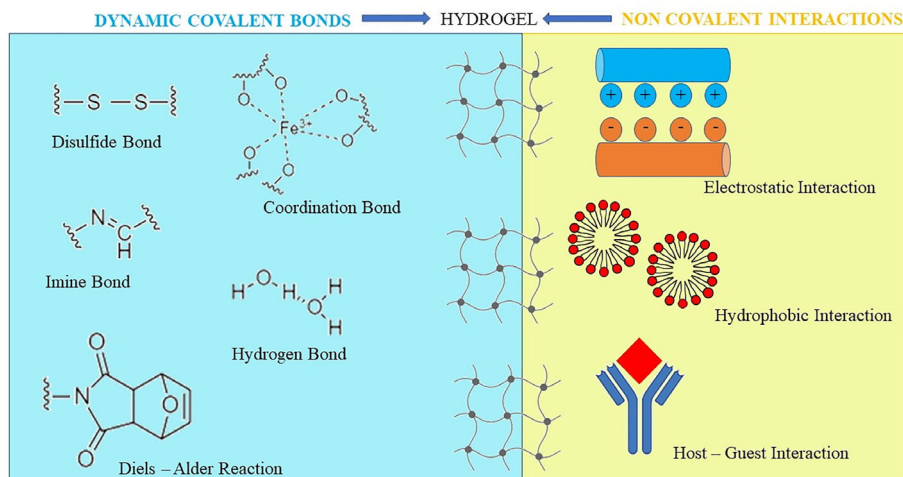


**FIGURE 3** | Chemical and physical bonds to obtain hydrogels. Hydrogels can also be prepared by a hybrid interaction consisting of physical interactions and/or covalent bond formation, exhibiting at the same time reversible mechanical properties and long-term stability.

thinning material after injection, allowing, therefore, AMP delivery. The *in situ* forming HG was demonstrated useful for ophthalmic applications, as well as to support the wound-healing after surgical operations (Travkova et al., 2017). The widely used materials and techniques for surgical closure purposes may contribute to providing some drawbacks. Hence, contaminations by impurities from air or from a fluid leakage can contribute to microbial infection harm (Rajabi et al., 2020). Moreover, medicated HG can release AMPs at the site of action after disruption of the inner matrix by erosion, swelling, or *via* enzyme interactions (Chen M. H. et al., 2017).

Li and co-workers formulated a thermosensitive HG constituted of biodegradable poly (l-lactic acid)-Pluronic L35-poly (l-lactic acid) for cutaneous wound-healing treatment, to investigate whether AMPs encapsulated in this HG formulation demonstrated efficient candidates in wound healing management. They used a type of multifunctional human-derived AMP (i.e., AP-57), with a broad-spectrum antimicrobial activity as well as an immune regulation ability. The AP-57 peptide was enclosed first in biocompatible nanoparticles, named AP-57-NPs. Subsequently, to facilitate their application in cutaneous wound repair, the AP-57-NPs were further encapsulated in a HG matrix (AP-57-NPs-H). As reported, the *in situ* gel-forming system exhibited *in vitro* a low cytotoxicity and a sustained drug release behavior. After applied to the wound, the formulated peptide achieved additional characteristics, such as a non-flowing gel that consequently become a sustained drug depot. Li and co-workers also demonstrated wound-dressing properties of this formulation. The effect of the formulated AMP was then investigated on full-thickness excision wound using the Sprague-Dawley<sup>®</sup> male and albino rat models. At last, the obtained DDS was effective on the wound, and rat models reported a complete wound closure (Li et al., 2015).

A different method to obtain HG in the aqueous phase is the mussel-inspired polydopamine chemistry. A study of Khan and

colleagues reported the use of catechol, instead of dopamine, as a cross-linker with amine-rich polymers to prepare thin films. Catechol is less expensive than dopamine; hence, it was used with  $\epsilon$ -poly-L-lysine (EPL), a natural AMP produced by *Streptomyces albulus*, to fabricate HG with antimicrobial properties. EPL-catechol HG showed *in vitro* antimicrobial and antibiofilm properties against multidrug-resistant *A. baumannii* associated with a good biocompatibility with a mouse myoblast cell line and *in vivo* reduced the bacterial load and improved wound healing when topically applied on the skin of a mouse with a second-degree burn wound also infected with multidrug-resistant *A. baumannii* (Khan et al., 2019). Lee and colleagues engineered nanoparticle-HG corneal implants containing the human AMP LL-37: although *in vivo* studies have not already been carried out, this device could inhibit *in vitro* HSV-1 attack to ocular cells (Lee et al., 2014). An example of insect AMP formulated as HG was recorded from *Lucilia sericata*, in both wound bandages and cosmetics to hinder dermatological pathogens (Mylonakis et al., 2016).

### Cubosome Delivery System

Cubosome represents alternative drug delivery scaffold systems consisting of a curved continuous lipid bilayer that can be realized with amphiphilic molecules. The most common amphiphilic lipid systems can comprise water and glyceryl monooleate (GMO) (2,3-Dihydroxypropyl (9Z)-9-octadecenoate) (1-Oleoyl-rac-glycerol | C<sub>21</sub>H<sub>40</sub>O<sub>4</sub> | ChemSpider). Similar dispersions show several self-assembly dispositions, among which the bicontinuous cubic phases (Figure 4).

Practically, bicontinuous cubic phases can be obtained by dispersing the amphiphilic lipid system into the aqueous phase using e.g., ultrasonication or homogenization. Subsequently, a dispersed gel is obtained, known as cubosome (CB) (Karami and Hamidi, 2016). As a result of the hydrophobic effect,

thermodynamically stable structures with a well-defined disposition of each component (i.e., the cubic liquid crystalline gel) are realized (**Figure 3**). These nanostructures have demonstrated suitability for loading hydrophilic, hydrophobic, as well as amphiphilic cargos.

More importantly, CB can include bioactive compounds, as the structure provides a significantly higher membrane surface area to loading proteins (Barriga et al., 2019).

Anatomically, the stratum corneum represents a strong barrier for the transdermal drug delivery of topically applied drugs, due to the presence of the external and highly organized skin layer. The ability of CB to adhere to the stratum corneum makes CB effectively useful in topical drug delivery for mucosal tissues (Gaballa et al., 2020). The structure and properties of CBs provide a promising vehicle for transdermal drug delivery especially for skin infections (Zeng et al., 2012; Meikle et al., 2019).

AMPs can be adsorbed onto the CB structure that usually shows a slightly negative charge. For instance, Boge and co-workers demonstrated that the GMO based-CB structure contributes to protecting the AMPs from proteolytic degradation, improving their bioavailability after topical administration. Furthermore, they found that AMPs loaded onto CB are highly released in the milieu whether *P. aeruginosa* or human neutrophil elastases are present.

The authors also reported a study investigating CB interaction with both a bacterial membrane model and *E. coli*'s membrane, to further understand how the interaction between AMPs and the membranes can be accomplished. The authors suggested that the bactericidal effect was due to physical interaction between the product and the bacterial membrane and not solely to the release of the peptide. Moreover, they noted that the presence of LL-37, the chosen AMP, constituted of a secondary structure of a linear  $\alpha$ -helix increased the affinity of CB to bacterial membranes (Boge et al., 2017; Boge et al., 2019a; Boge et al., 2019b).

Many papers have reported that the composition of GMO-based CB generally involves the use of stabilizer molecules. The stabilizer avoids the aggregation of hydrophobic portions with the

external aqueous media and consequently helps to reach a thermodynamically stable form (Gaballa et al., 2020). Pluronics, especially poloxamer 407 (F127), represent the most used stabilizing agents. This nonionic copolymer vehicle comprises a central hydrophobic chain of polypropylene oxide with a molecular weight of approximately 12.6 kDa and lateral hydrophilic chains of polyethylene glycol (Barriga et al., 2019). The clinical application of GMO-based CB stabilized by F127 may be limited due to concentration-dependent cytotoxicity. Moreover, F127 may also show hemolytic effect, as well as a poor biodegradability. A novel stabilizer-free antimicrobial nanocarrier was developed by Zabara and co-workers, by dispersing GMO in water using ultrasonication and combining the AMP LL-37 by spontaneous integration in the internal nanostructure. Comparing the new system to the GMO-based CBs stabilized with F127, they found that the stabilizer-free nanocarrier showed cytocompatibility and a higher antimicrobial effect, especially against the tested Gram-negative pathogens, among which *P. aeruginosa* CIP A22 DSMZ 25123 strain (Zabara et al., 2019).

### Other Drug Delivery Systems

Some negative aspects are related to the lipid-based nanocarriers: beside the poor stability, they are also susceptible to aggregation *in vitro* and to esterase activity. This last aspect might also affect the relationship between the *in vitro* and the *in vivo* controlled release of the cargo. Subsequently, materials alternative to lipids have been explored including self-assembled polymeric nanocarriers for preparing both vesicular and bicontinuous systems. Compared to lipids, the block polymeric structures (BPS) can be synthesized from an expansive pool of amphiphilic monomers. Therefore, BPSs, called also polymersomes, have demonstrated high flexibility to functionalization, along with well-defined structures that can be distinguished in both hydrophobic and hydrophilic sections. Hence, the BPS can exhibit substantial rewards involving both mechanical and chemical stability (Allen et al., 2019).

Most AMP formulations in ongoing clinical trials belong to semi-solid preparations for external use (Koebach and Craik, 2019; Koo and Seo, 2019; Sheard et al., 2019). Hence, among the

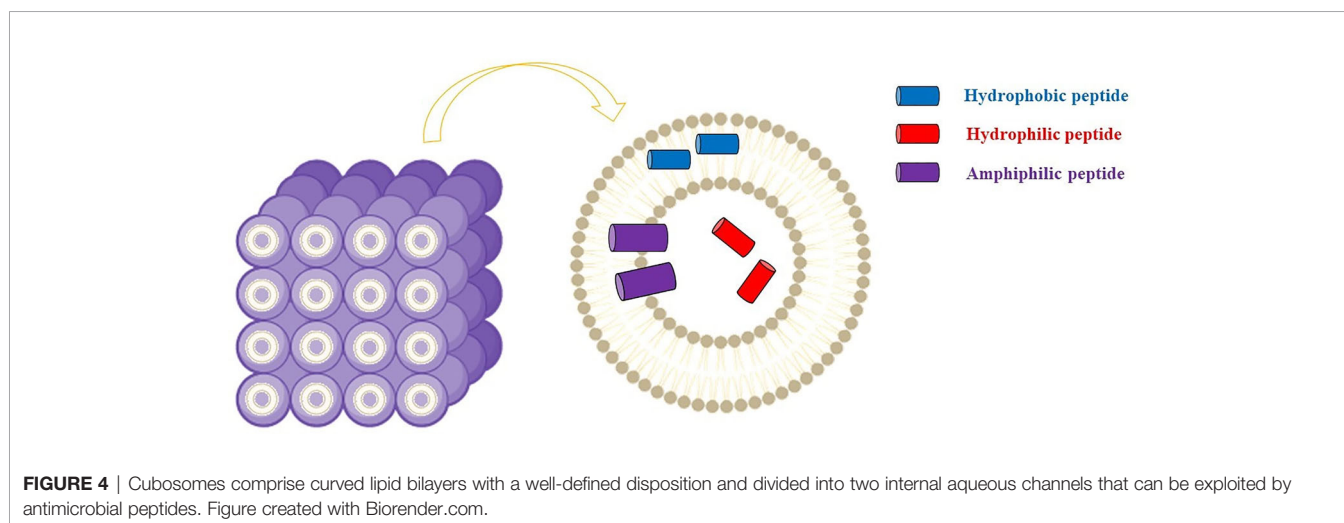


**FIGURE 4** | Cubosomes comprise curved lipid bilayers with a well-defined disposition and divided into two internal aqueous channels that can be exploited by antimicrobial peptides. Figure created with Biorender.com.

topical formulations, topical gel formulations are often mentioned in several research works to treat e.g., chronic skin and soft tissue infections. Moreover, proteins but also longer peptides ranging between 20 to 30 amino acids can also self-assemble naturally to achieve  $\alpha$ -helices or  $\beta$ -sheets motifs. Likewise, two antiparallel  $\beta$ -strands can fold in  $\beta$ -hairpin motif, which contributes to creating higher-ordered fibers and pH-responsive active pharmaceutical ingredient vehicles. Recently, specific functional peptides have been synthesized and utilized as useful nanomaterials. Particularly, important properties have characterized a special group of synthetic peptides called peptide amphiphiles (PAs). They essentially consist of four sequences: (i) a hydrophobic tail (e.g., palmitic acid residue); an internal portion able to form  $\beta$ -sheets, which comprises (ii) an amino acid sequence to promote through hydrogen bond the formation of fibril-like structures; (iii) a spacer containing charged amino acids to allow solubility and cross-linking (Cui et al., 2010); at the opposite end of the structure, (iv) the hydrophilic head can be found that triggers the signaling for the biological response. Due to the molecular organization and the chemical characteristics, PAs can organize spontaneously in a nanostructure using a folding-like behavior to form specific nanostructures, including micelles and microtubes (Figure 5).

Hence, to stabilize the system in a lower energy state, PA molecules can organize the alkyl chains away from the aqueous environment, exposing externally the hydrophilic portion. PAs have attracted special interest as drug carriers due to their (i) advantage of a unique structure of assemblies, (ii) abundant molecular structures, and (iii) ability to give biological functions (Song et al., 2017). Additionally, the self-assembly aptitude of diphenylalanine (Di-Phe) building-blocks can be used to obtain diverse supramolecular nanostructures, such as nanofibrils, or nanowires.

These structures have demonstrated large applicability due to their biocompatibility, high loading capacity and simplicity to obtain the self-assembled nanostructures. Furthermore, as reported by Schnaider and co-workers, nano-assemblies formed by Di-Phe exhibited an intrinsic antibacterial activity (Schnaider et al., 2017).

Such nanostructures can considerably enhance the active pharmaceutical ingredient stability since they become less sensitive towards enzymatic degradation. Likewise, most AMPs forming  $\alpha$ -helices or  $\beta$ -sheets could be inserted into supramolecular nanostructures. This strategy might contribute, therefore, to a suitable delivery of AMPs without using additional vehicles and their molecular stability. Upon contact with the pathogen, the peptide nanostructure is disrupted, especially from peptidases, and releases the AMP.

Also inorganic nanomaterials (metal and metal oxide nanoparticles, silica, nanoclays, and carbon-based nanomaterials) have investigated as AMP delivery systems, because they shield the molecules from degradation and avoid peptide aggregation or conformational changes that could inactivate them (Nordström and Malmsten, 2017). Furthermore, they have the ability to control the drug release (thanks to well-defined pore sizes and forms (Vivero-Escoto et al., 2010)) increasing bioavailability and reducing toxicity (Nordström and Malmsten, 2017). In addition, several nanoparticles have been shown to have antimicrobial properties against both Gram-negative and -positive bacteria, suggesting that the complex AMP-nanoparticle may have a synergistic impact (Hajipour et al., 2012). Another synergistic effect could be achieved by a close interaction between AMP and antibiotics, which can be carried together in mesoporous silica nanoparticles with good chemical stability and biocompatibility, even though it is always important to consider the chemical nature of these nanoparticles, the dosage, and the administration route (Nordström and Malmsten, 2017).

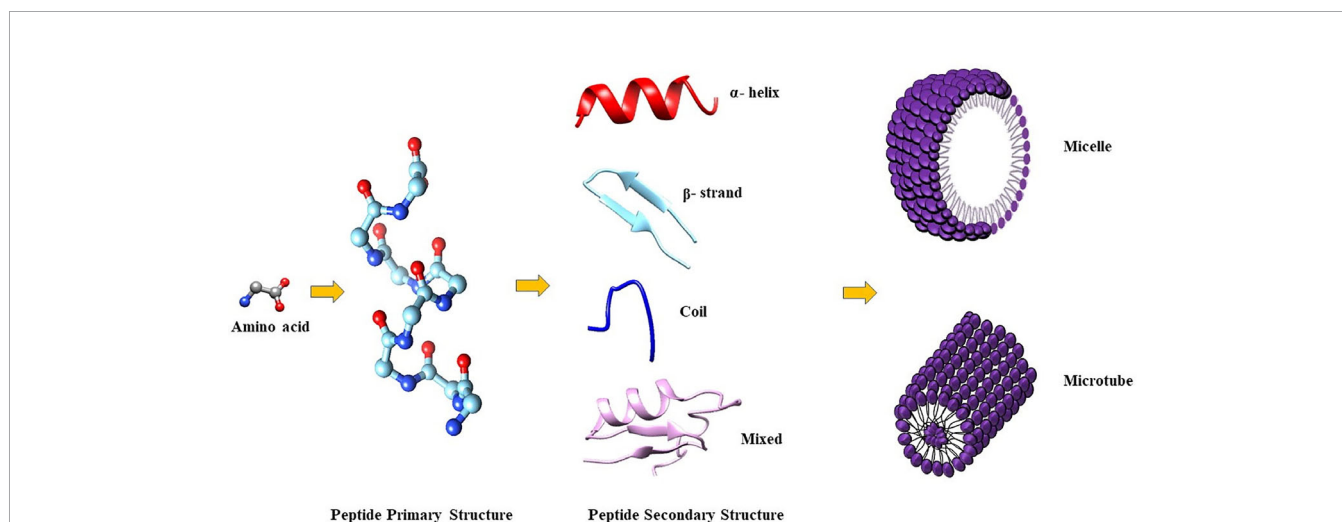


**FIGURE 5** | Arrangement of peptide amphiphiles in self-assembling nanostructures (e.g., micelles and microtubes), which can contain and release APIs. Adapted from Song et al. (2017). Figure created with UCSF CHIMERA software (Pettersen et al., 2004).

## ADMINISTRATION ROUTES

Compared to other routes of administration, the intramuscular, or the subcutaneous routes may not require too much stability of the peptide. Indeed, AMP physicochemical and biological characteristics could be taken into less account in these routes of administration, while size, permeation through gastrointestinal membrane, poor stability to gastric pH and susceptibility to proteolytic enzymes make the oral administration much difficult (Schiffner, 2011).

Hence, injection represents the best route of administration for most of the AMPs (Di, 2015). However, the intravenous administration certainly exposes the peptides to the esterase and peptidase activity present in serum (Vlieghe et al., 2010; Fosgerau and Hoffmann, 2015).

The oral route remains a patient-friendly option, due to the non-invasive and painless administration. However, considering few exceptions, the oral pharmaceutical technologies have not shown radical improvements regarding the AMP formulation to increase their bioavailability. The principal efforts concern the peptide stability due to the presence of pancreatic peptidases, e.g.  $\alpha$ -chymotrypsin, trypsin and pancreatic elastase secreted from the pancreas into the gastrointestinal tract (Vlieghe et al., 2010; Aguirre et al., 2016; Malhaire et al., 2016).

Furthermore, high dosage and low systemic exposure allow minimizing systemic side effects when a drug is formulated for the lung administration. Inhaled medications of peptides have demonstrated superior in terms of rapid onset (Larijani et al., 2005). Peptide macrocycles with antimicrobial effect working as protein epitope mimetics can also be formulated for inhalation, due to appropriate chemical stability. The POL6014, a neutrophil elastase inhibitor (i.e., Murepavadin<sup>®</sup>), can be administered *via* eFlow<sup>®</sup> nebulizer system to treat cystic fibrosis lung infections and it is currently in Phases I/II (NCT03748199, 2018).

In conclusion, as reported above, topical applications involving AMPs loading in nanoparticles, hydrogels, creams, gels and ointments represent the most used and best developed AMP applications and further studies are needed to exploit new suitable administration routes.

## AMPs IN ONGOING CLINICAL TRIALS

We have described several AMPs approved for clinical applications. However, many others, both natural and synthetic, are still under clinical trials (Table 3). Preliminary results suggested that many AMPs could be useful alone or in synergy with common antibiotics

to prevent or treat several diseases, but most of the studies are still ongoing or were stopped because of issues that can be solved, including unfavorable pharmacokinetic profile or unexpected side effects (Browne et al., 2020; Dijksteel et al., 2021).

Below we reported some recent clinical trials, focusing the attention on studies still in progress.

Bacitracin, a natural cyclic AMP from *Bacillus subtilis*, is currently reported in several ongoing studies of phase IV to treat Gram-positive bacterial infections (Bacitracin - ClinicalTrials.gov). These studies are evaluating bacitracin (i) in subjects with minor, second-degree burns, for topical use and in combination with a second ointment of collagenase; (ii) as an ointment to treat skin infections in combination with medical-grade honey; (iii) as an ointment for topical antibiotic therapy after eyelid surgery and to evaluate the use of antibiotic prophylaxis in presence of antibiotic side effects and antibiotic allergy; (iv) as topical antibiotic irrigation to reduce surgical site infections and in combination with neomycin and polymyxin (Neomycin<sup>®</sup>) for postoperative urinary tract infections and to extend the antimicrobial effect to Gram-negative bacteria; (viii) to evaluate the efficacy of preoperative oral antibiotic prophylaxis for preventing surgical site infections in elective colorectal surgery (combination of Bacitracin and the antibiotic Neomycin). Another clinical trial was ongoing to evaluate the topical use of bacitracin to reduce surgical site infections in midfacial fracture surgery, but in April 2020 this trial was closed because of bacitracin toxicity. Other phase IV studies involving bacitracin are aimed to the treatment of (v) facial burns, (vi) in combination with topical tranexamic acid (i.e., 5%, and 25%), and (vii) with polymyxin B (Polysporin<sup>®</sup>) to evaluate the use of Biofine<sup>®</sup> cream on wounds due to cryotherapy for removing actinic keratosis lesions (Bacitracin - ClinicalTrials.gov).

Pexiganan, a linear AMP, is under investigation in four phase III studies for the treatment of diabetic foot ulcers using topical cream formulations (Gottler and Ramamoorthy, 2009).

Omiganan, an indolicidin derivative (Sader et al., 2004), has been tested in a total of sixteen studies and thirteen of them have been completed. Looking at the completed ones, three phase III studies have been reported, among which two were aimed to evaluate the efficacy of AMPs as topical gel formulation to treat rosacea. The third phase III study concerned the treatment of catheter colonization, and prevention of bloodstream infections if applied to the skin surrounding the insertion.

The innate immunity of mammals comprises also the cathelicidins as a distinct class of proteins. Like defensins, although their structural features clearly distinguish them from defensins, cathelicidins act as precursor molecules that can release an AMP after proteolytic cleavage (Dürr et al., 2006).

**TABLE 3** | List of the AMPs in ongoing clinical trials.

AMP	Peptide structural characteristic	Ongoing Clinical Trials
Bacitracin	Natural cyclic peptide	Phase IV
Pexiganan	Natural linear peptide	Phase III
Omiganan	Indolicidin derivative peptide	Phase III
LL-37	Natural $\alpha$ -helical peptide	Phase II
LTX-109	Synthetic Antimicrobial Peptidomimetic	Phase II
Brilacidin	Synthetic peptide	Phase II



The human cathelicidin-derived AMP, named LL-37, belongs to the class of  $\alpha$ -helical AMPs. Currently it can be found on a Phase II clinical trial by Promore Pharma (Promore Pharma AB, Sweden) evaluating LL-37 safety and tolerability in patients with venous leg ulcers (Grönberg et al., 2014; Sierra et al., 2017; Koo and Seo, 2019). It is also under investigation in patients with diabetic foot ulcers (LL-37 - ClinicalTrials.gov).

The synthetic AMP LTX-109 represents a novel class of very short AMPs. It has been described as a synthetic antimicrobial peptidomimetic and has entered the phase II clinical studies (Isaksson et al., 2011) with the aims (i) to assess the clinical and microbiological response of two LTX-109 dosages (i.e., 1%, and 2%) formulated as a topical gel (Lytixar™) for the treatment of non-bullous impetigo; (ii) to evaluate the safety, local tolerability, and efficacy of 1%, 2% and 3% LTX-109 gel formulations for the anterior nares delivery in patients who are carriers of MRSA/MSSA (methicillin-susceptible *S. aureus*); (iii) defining the magnitude of systemic absorption when LTX-109 is applied to the anterior nares as a topical gel; (iv) to evaluate the safety and tolerability of topical Lytixar™ formulation onto uncomplicated skin infections, as well as to investigate both the clinical and microbiological effect of Lytixar™ in patients with uncomplicated skin infection by Gram-positive and to determine the degree of systemic absorption of LTX-109. A further trial in recruiting phase is aimed to demonstrate the safety of a percutaneous application of a 3% gel cream of LTX-109 in *Hidradenitis suppurativa*, to identify the clinical responses and the influences of specific parameters, including age, disease duration, and body mass index (LTX-109 - ClinicalTrials.gov).

Brilacidin is a synthetic AMP, successfully tested in Phase II clinical trials for treatment of acute bacterial skin and skin structure infections. A recent work demonstrated that Brilacidin displays an antiviral activity, inhibiting SARS-CoV2 virus in Vero African green monkey kidney cells and Calu-3 human lung epithelial cells and showing a synergistic inhibitory activity in combination with the antiviral Remdesivir (Bakovic et al., 2021). A Phase II clinical trial is going to start to assess the efficacy and safety of Brilacidin on patients with moderate or severe SARS-CoV-2 infection, hospitalized with respiratory difficulty but not requiring high-level respiratory support (Brilacidin - ClinicalTrials.gov).

## CONCLUSIONS

AMPs can be considered unconventional therapeutic small molecules which have attracted great interest in recent years

## REFERENCES

- 1-Oleoyl-rac-glycerol | C21H40O4 | Chemspider. Available at: <http://www.chemspider.com/Chemical-Structure.4446588.html>.
- Aguirre, T. A. S., Teijeiro-Osorio, D., Rosa, M., Coulter, I. S., Alonso, M. J., and Brayden, D. J. (2016). Current Status of Selected Oral Peptide Technologies in Advanced Preclinical Development and in Clinical Trials. *Adv. Drug Deliv. Rev.* 106, 223–241. doi: 10.1016/j.addr.2016.02.004
- Allen, S. D., Bobbala, S., Karabin, N. B., and Scott, E. A. (2019). On the Advancement of Polymeric Bicontinuous Nanospheres Toward Biomedical Applications. *Nanoscale Horiz.* 4, 321–338. doi: 10.1039/c8nh00300a

because of their promising potential, as they can be used as alternative or complement approaches for treatment of microbial infections. Due to their potency, broad-spectrum activity, different sources available in nature, lack of rapid development of resistance, low accumulation in tissue and rapid killing activity, these peptides show several advantages over conventionally used antibiotics. Moreover, AMPs also display immunomodulatory, antioxidant and anti-inflammatory activities and, for this reason, researchers are devoting considerable efforts to implement the use of AMPs as commercially available drugs. This review examined the features of AMPs, their mechanisms of action and their sources, highlighting their antimicrobial activity against several pathogens involved in human infections. Thus, the efficacy and potentially applicability of AMPs in human diseases has been analyzed. Particularly, we examined the beneficial role of several AMPs in the treatment of skin infections, but we also reviewed their potential use in respiratory diseases and oxidative-stress disorders, such as obesity, diabetes and chronic inflammatory intestinal disorders. Indeed, AMPs display several potential applications in medicine, since they can regulate pro-inflammatory reactions, stimulate cell proliferation, promote wound healing by modulating the cell migration, angiogenesis, chemotaxis and cytokine release. On these bases, pharmaceutical companies are performing great efforts to develop AMPs as therapeutic agents, improving their chemical and metabolic stability, setting up smart and novel formulation strategies, with the aim to improve AMP delivery and, consequently, their activity.

## AUTHOR CONTRIBUTIONS

Conceptualization: PF. Writing - original draft preparation: PF, AMP, AP, CS, RS, MDM. Writing - review and editing: AMP, AP, CS, RS, MDM, AF, DL, AV, HV, AS, PF. Supervision: PF. All authors contributed to the article and approved the submitted version.

## FUNDING

This research was supported by the Italian Ministry of Instruction, University and Research (MIUR) within the frameworks of three projects (PON R&I 2014-2020, protocol ARS01\_00597; PRIN 2017, protocol Prot. 2017AHTCK7; PO FESR BASILICATA 2014-2020 “AAA: SAFE SOS” D.D. 12AF.2020/D.01255-9/11/2020).

- Aminov, R. I. (2010). A Brief History of the Antibiotic Era: Lessons Learned and Challenges for the Future. *Front. Microbiol.* 1, 134. doi: 10.3389/fmicb.2010.00134
- Ando, K., and Natori, S. (1988). Inhibitory Effect of Sarcotoxin IIA, an Antibacterial Protein of *Sarcophaga Peregrina*, on Growth of *Escherichia Coli*. *J. Biochem.* 103, 735–739. doi: 10.1093/oxfordjournals.jbchem.a122337
- Arias, M., Hilchie, A. L., Haney, E. F., Bolscher, J. G. M., Hyndman, M. E., Hancock, R. E. W., et al. (2017). Anticancer Activities of Bovine and Human Lactoferricin-Derived Peptides. *Biochem. Cell Biol.* 95, 91–98. doi: 10.1139/bcb-2016-0175
- Ayabe, T., Satchell, D. P., Wilson, C. L., Parks, W. C., Selsted, M. E., and Ouellette, A. J. (2000). Secretion of Microbicidal  $\alpha$ -Defensins by Intestinal Paneth Cells in Response to Bacteria. *Nat. Immunol.* 1, 113–118. doi: 10.1038/77783

- Bacitracin* - *Clinicaltrials.Gov*. Available at: <https://clinicaltrials.gov/ct2/results?cond=&term=bacitracin&cntry=&state=&city=&dist>.
- Bakovic, A., Risner, K., Bhalla, N., Alem, F., Chang, T. L., Weston, W. K., et al. (2021). Brilacidin Demonstrates Inhibition of SARS-CoV-2 in Cell Culture. *Viruses* 13, 271. doi: 10.3390/v13020271
- Balestrieri, B., Maekawa, A., Xing, W., Gelb, M. H., Katz, H. R., and Arm, J. P. (2009). Group V Secretory Phospholipase A2 Modulates Phagosome Maturation and Regulates the Innate Immune Response Against *Candida Albicans*. *J. Immunol.* 182, 4891–4898. doi: 10.4049/jimmunol.0803776
- Ball, L. J., Goult, C. M., Donarski, J. A., Micklefield, J., and Ramesh, V. (2004). NMR Structure Determination and Calcium Binding Effects of Lipopeptide Antibiotic Daptomycin. *Org. Biomol. Chem.* 2, 1872–1878. doi: 10.1039/B402722A
- Bals, R., Wang, X., Meegalla, R. L., Wattler, S., Weiner, D. J., Nehls, M. C., et al. (1999). Mouse Beta-Defensin 3 is an Inducible Antimicrobial Peptide Expressed in the Epithelia of Multiple Organs. *Infect. Immun.* 67, 3542–3547. doi: 10.1128/IAI.67.7.3542-3547.1999
- Balti, R., Nedjar-Arroume, N., Bougateg, A., Guillochon, D., and Nasri, M. (2010). Three Novel Angiotensin I-converting Enzyme (ACE) Inhibitory Peptides From Cuttlefish (*Sepia Officinalis*) Using Digestive Proteases. *Food. Res. Int.* 43, 1136–1143. doi: 10.1016/j.foodchem.2013.03.091
- Barna, B., Leiter, E., Hegedus, N., Biro, T., and Pocs, I. (2008). Effect of the *Penicillium Chrysogenum* Antifungal Protein (PAF) on Barley Powdery Mildew and Wheat Leaf Rust Pathogens. *J. Basic Microbiol.* 48, 516–520. doi: 10.1002/jobm.200800197
- Barriga, H. M. G., Holme, M. N., and Stevens, M. M. (2019). Cubosomes: The Next Generation of Smart Lipid Nanoparticles? *Angew. Chem. Int. Ed.* 58, 2958–2978. doi: 10.1002/anie.201804067
- Benincasa, M., Scocchi, M., Pacor, S., Tossi, A., Nobili, D., Basaglia, G., et al. (2006). Fungicidal Activity of Five Cathelicidin Peptides Against Clinically Isolated Yeasts. *J. Antimicrob. Chemother.* 58, 950–959. doi: 10.1093/jac/dkl382
- Benincasa, M., Skerlavaj, B., Gennaro, R., Pellegrini, A., and Zanetti, M. (2003). *In Vitro* and *In Vivo* Antimicrobial Activity of Two Alpha-Helical Cathelicidin Peptides and of Their Synthetic Analogs. *Peptides* 24, 1723–1731. doi: 10.1016/j.peptides.2003.07.025
- Berditsch, M., Lux, H., Babii, O., Afonin, S., and Ulrich, A. S. (2016). Therapeutic Potential of Gramicidin S in the Treatment of Root Canal Infections. *Pharmaceuticals* 9 (3), 56. doi: 10.3390/ph9030056
- Bevins, C. L. (2006). Paneth Cell Defensins: Key Effector Molecules of Innate Immunity. *Biochem. Soc. Trans.* 34 (2), 263–266. doi: 10.1042/BST20060263
- Bhattacharjya, S. (2016). NMR Structures and Interactions of Antimicrobial Peptides With Lipopolysaccharide: Connecting Structures to Functions. *Curr. Top. Med. Chem.* 16, 4–15. doi: 10.2174/1568026615666150703121943
- Bhattacharjya, S., and Straus, S. K. (2020). Design, Engineering and Discovery of Novel  $\alpha$ -Helical and  $\beta$ -Boomerang Antimicrobial Peptides Against Drug Resistant Bacteria. *Int. J. Mol. Sci.* 21, 5773. doi: 10.3390/ijms21165773
- Bhunia, A., Ramamoorthy, A., and Bhattacharjya, S. (2009). Helical Hairpin Structure of a Potent Antimicrobial Peptide MSI-594 in Lipopolysaccharide Micelles by NMR Spectroscopy. *Chemistry* 5, 2036–2040. doi: 10.1002/chem.200802635
- Bhunia, A., Saravanan, R., Mohanram, H., Mangoni, M. L., and Bhattacharjya, S. (2011). NMR Structures and Interactions of Temporin-1Tl and Temporin-1Tb With Lipopolysaccharide Micelles: Mechanistic Insights Into Outer Membrane Permeabilization and Synergistic Activity. *J. Biol. Chem.* 286, 24394–24406. doi: 10.1074/jbc.M110.189662
- Bian, S., Zheng, Z., Liu, Y., Ruan, C., Pan, H., and Zhao, X. (2019). A Shear-Thinning Adhesive Hydrogel Reinforced by Photo-Initiated Crosslinking as a Fit-to-Shape Tissue Sealant. *J. Mater. Chem. B* 7, 6488–6499. doi: 10.1039/c9tb01521c
- Boge, L., Browning, K. L., Nordström, R., Campana, M., Damgaard, L. S. E., Seth Caous, J., et al. (2019a). Peptide-Loaded Cubosomes Functioning as an Antimicrobial Unit Against *Escherichia Coli*. *ACS Appl. Mater. Interfaces* 11, 21314–21322. doi: 10.1021/acsami.9b01826
- Boge, L., Hallstenson, K., Ringstad, L., Johansson, J., Andersson, T., Davoudi, M., et al. (2019b). Cubosomes for Topical Delivery of the Antimicrobial Peptide LL-37. *Eur. J. Pharm. Biopharm.* 134, 60–67. doi: 10.1016/j.ejpb.2018.11.009
- Boge, L., Umerska, A., Matougui, N., Bysell, H., Ringstad, L., Davoudi, M., et al. (2017). Cubosomes Post-Loaded With Antimicrobial Peptides: Characterization, Bactericidal Effect and Proteolytic Stability. *Int. J. Pharm.* 526, 400–412. doi: 10.1016/j.ijpharm.2017.04.082
- Boparai, J. K., and Sharma, P. K. (2020). Mini Review on Antimicrobial Peptide, Sources, Mechanism and Recent Applications. *Protein Pept. Lett.* 27, 4–16. doi: 10.2174/0929866526666190822165812
- Borah, A., Deb, B., and Chakraborty, S. (2020). A Crosstalk on Antimicrobial Peptides. *Int. J. Pept. Res. Ther.* 27, 229–244. doi: 10.1007/s10989-020-10075-x
- Braff, M. H., Mi'I, A. H., Di Nardo, A., Lopez-Garcia, B., Howell, M. D., and Wong, C. (2005). Structure-Function Relationships Among Human Cathelicidin Peptides: Dissociation of Antimicrobial Properties From Host Immunostimulatory Activities. *J. Immunol.* 174, 4271–4278. doi: 10.4049/jimmunol.174.7.4271
- Brilacidin* - *Clinicaltrials.Gov*. Available at: <https://clinicaltrials.gov/ct2/results?recrs=&cond=&term=Brilacidin&cntry=&state=&city=&dist>.
- Brogden, K. A. (2005). Antimicrobial Peptides: Pore Formers or Metabolic Inhibitors in Bacteria? *Nat. Rev. Microbiol.* 3, 238–250. doi: 10.1038/nrmicro1098
- Browne, K., Chakraborty, S., Chen, R., Willcox, M. D., Black, D. S., Walsh, W. R., et al. (2020). A New Era of Antibiotics: The Clinical Potential of Antimicrobial Peptides. *Int. J. Mol. Sci.* 21, 7047. doi: 10.3390/ijms21197047
- Bruni, N., Capucchio, M. T., Biasibetti, E., Pessione, E., Cirrincione, S., Giraudo, L., et al. (2016). Antimicrobial Activity of Lactoferrin-Related Peptides and Applications in Human and Veterinary Medicine. *Molecules* 21, 752. doi: 10.3390/molecules21060752
- Buda De Cesare, G., Cristy, S. A., Garsin, D. A., and Lorenz, M. C. (2020). Antimicrobial Peptides: A New Frontier in Antifungal Therapy. *mBio* 11, e02123–e02120. doi: 10.1128/mBio.02123-20
- Bulet, P., Hetru, C., Dimarcq, J. L., and Hoffmann, D. (1999). Antimicrobial Peptides in Insects; Structure and Function. *Dev. Comp. Immunol.* 23, 329–344. doi: 10.1016/s0145-305x(99)00015-4
- Caliari, S. R., and Burdick, J. A. (2016). A Practical Guide to Hydrogels for Cell Culture. *Nat. Methods* 13, 405–414. doi: 10.1038/nmeth.3839
- Cao, L. T., Wu, J. Q., Xie, F., Hu, S. H., and Mo, Y. (2007). Efficacy of Nisin in Treatment of Clinical Mastitis in Lactating Dairy Cows. *J. Dairy Sci.* 90, 3980–3985. doi: 10.3168/jds.2007-0153
- Carlsson, A., Engström, P., Palva, E. T., and Bennich, H. (1991). Attacin, an Antibacterial Protein From *Hyalophora Cecropia*, Inhibits Synthesis of Outer Membrane Proteins in *Escherichia Coli* by Interfering With *Omp* Gene Transcription. *Infect. Immun.* 59, 3040–3045. doi: 10.1128/IAI.59.9.3040-3045.1991
- Casteels, P., Ampe, C., Riviere, L., Van Damme, J., Elicone, C., Fleming, M., et al. (1990). Isolation and Characterization of Abaecin, a Major Antibacterial Response Peptide in the Honeybee (*Apis Mellifera*). *Eur. J. Biochem.* 187, 381–386. doi: 10.1111/j.1432-1033.1990.tb15315.x
- Catoira, M. C., Fusaro, L., Di Francesco, D., Ramella, M., and Boccafoschi, F. (2019). Overview of Naturalhydrogels for Regenerative Medicine Applications. *J. Mater. Sci. Mater. Med.* 30, 115. doi: 10.1007/s10856-019-6318-7
- Cheng, K. T., Wu, C. L., Yip, B. S., Yu, H. Y., Cheng, H. T., Chih, Y. H., et al. (2018). High Level Expression and Purification of the Clinically Active Antimicrobial Peptide P-113 in *Escherichia Coli*. *Molecules* 23, 800. doi: 10.3390/molecules23040800
- Chen, C., Mangoni, M. L., and Di, Y. P. (2017). *In Vivo* Therapeutic Efficacy of Frog Skin-Derived Peptides Against *Pseudomonas Aeruginosa*-Induced Pulmonary Infection. *Sci. Rep.* 7, 8548. doi: 10.1038/s41598-017-08361-8
- Chen, M. H., Wang, L. L., Chung, J. J., Kim, Y. H., Atluri, P., and Burdick, J. A. (2017). Methods to Assess Shear-Thinning Hydrogels for Application as Injectable Biomaterials. *ACS Biomater. Sci. Eng.* 3, 3146–3160. doi: 10.1021/acsbomaterials.7b00734
- Cheung, B. M. Y., Cheung, T. T., and Samaranyake, N. R. (2013). Safety of Antiobesity Drugs. *Ther. Adv. Drug Saf.* 4, 171–181. doi: 10.1177/2042098613489721
- Chiorean, S., Antwi, I., Carney, D. W., Kotsogianni, I., Giltrap, A. M., Alexander, F. M., et al. (2020). Dissecting the Binding Interactions of Teixobactin With the Bacterial Cell-Wall Precursor Lipid II. *Chembiochem* 21, 789–792. doi: 10.1002/cbic.201900504
- Choi, J. H., Jang, A. Y., Lin, S., Lim, S., Kim, D., Park, K., et al. (2015). Melittin, a Honeybee Venom-Derived Antimicrobial Peptide, may Target Methicillin-Resistant *Staphylococcus Aureus*. *Mol. Med. Rep.* 12, 6483–6490. doi: 10.3892/mmr.2015.4275

- Choi, C. S., Yoe, S. M., Kim, E. S., Chae, K. S., and Kim, H. R. (1997). Purification and Characterization of Antibacterial Peptides, Spodopsin Ia and Ib Induced in the Larval Haemolymph of the Common Cutworm, *Spodoptera litura*. *Korean J. Biol. Sci.* 1, 457–462.
- Conlon, J. M., Sonnevend, A., Patel, M., Davidson, C., Nielsen, P. F., and Rollins-Smith, L. A. (2003). Isolation of Peptides of the Brevinin-1 Family With Potent Candidacidal Activity From the Skin Secretions of the Frog *Rana boylei*. *J. Pept. Res.* 62, 207–213. doi: 10.1034/j.1399-3011.2003.00090.x
- Cui, H., Webber, M. J., and Stupp, S. I. (2010). Self-Assembly of Peptide Amphiphiles: From Molecules to Nanostructures to Biomaterials. *Biopolymers* 94, 1–18. doi: 10.1002/bip.21328
- da Costa, J. P., Cova, M., Ferreira, R., and Vitorino, R. (2015). Antimicrobial Peptides: An Alternative for Innovative Medicines? *Appl. Microbiol. Biotechnol.* 99, 2023–2040. doi: 10.1007/s00253-015-6375-x
- Daneshmand, F., Zardini, H. Z., and Ebrahimi, L. (2013). Investigation of the Antimicrobial Activities of Snakin-Z, a New Cationic Peptide Derived From *Zizyphus Jujube* Fruits. *Nat. Prod. Res.* 27, 2292–2296. doi: 10.1080/14786419.2013.827192
- Dash, R., and Bhattacharjya, S. (2021). Thanatin: An Emerging Host Defense Antimicrobial Peptide With Multiple Modes of Action. *Int. J. Mol. Sci.* 22, 1522. doi: 10.3390/ijms22041522
- da Silva, F. P., and Machado, M. C. C. (2012). Antimicrobial Peptides: Clinical Relevance and Therapeutic Implications. *Peptides* 36, 308–314. doi: 10.1016/j.peptides.2012.05.014
- David, J. M., and Rajasekaran, A. K. (2015). Gramicidin A: A New Mission for an Old Antibiotic. *J. Kidney Cancer VHL* 2, 15–24. doi: 10.15586/jkcvhl.2015.21
- Davidovici, B. B., Sattar, N., Jörg, P. C., Puig, L., Emery, P., Barker, J. N., et al. (2010). Psoriasis and Systemic Inflammatory Diseases: Potential Mechanistic Links Between Skin Disease and Co-Morbid Conditions. *J. Invest. Dermatol.* 130, 1785–1796. doi: 10.1038/jid.2010.103
- de Caleyra, R. F., Gonzalez-Pascual, B., Garcia-Olmedo, F., and Carbonero, P. (1972). Susceptibility of Phytopathogenic Bacteria to Wheat Purothionins *In Vitro*. *Appl. Microbiol.* 23, 998–1000. doi: 10.1128/AM.23.5.998-1000.1972
- De Kwaadsteniet, M., Doeschate, K. T., and Dicks, L. M. T. (2009). Nisin F in the Treatment of Respiratory Tract Infections Caused by *Staphylococcus Aureus*. *Lett. Appl. Microbiol.* 48, 65–70. doi: 10.1111/j.1472-765X.2008.02488.x
- Di, L. (2015). Strategic Approaches to Optimizing Peptide ADME Properties. *AAPS J.* 17, 134–143. doi: 10.1208/s12248-014-9687-3
- Dijksteel, G. S., Ulrich, M. M. W., Middelkoop, E., and Boekema, B. K. H. L. (2021). Lessons Learned From Clinical Trials Using Antimicrobial Peptides (AMPs). *Front. Microbiol.* 12, 616979. doi: 10.3389/fmicb.2021.616979
- Dimarcq, J. L., Keppi, E., Dunbar, B., Lambert, J., Reichhart, J. M., Hoffmann, D., et al. (1988). Insect Immunity. Purification and Characterization of a Family of Novel Inducible Antibacterial Proteins From Immunized Larvae of the Dipteran *Phormia Terranova* and Complete Amino-Acid Sequence of the Predominant Member, Dipteracin a. *Eur. J. Biochem.* 171, 17–22. doi: 10.1111/j.1432-1033.1988.tb13752.x
- Ding, B., Soblosky, L., Nguyen, K., Geng, J., Yu, X., Ramamoorthy, A., et al. (2013). Physiologically-Relevant Modes of Membrane Interactions by the Human Antimicrobial Peptide, LL-37, Revealed by SFG Experiments. *Sci. Rep.* 3, 1854. doi: 10.1038/srep01854
- Di Somma, A., Avitabile, C., Cirillo, A., Moretta, A., Merlino, A., Paduano, L., et al. (2020). The Antimicrobial Peptide Temporin L Impairs E. Coli Cell Division by Interacting With FtsZ and the Divisome Complex. *Biochim. Biophys. Acta - Gen. Subj.* 1864, 129606. doi: 10.1016/j.bbagen.2020.129606
- Domadia, P. N., Bhunia, A., Ramamoorthy, A., and Bhattacharjya, S. (2010). Structure, Interactions, and Antibacterial Activities of MSI-594 Derived Mutant Peptide MSI-594F5A in Lipopolysaccharide Micelles: Role of the Helical Hairpin Conformation in Outer-Membrane Permeabilization. *J. Am. Chem. Soc.* 132, 18417–18428. doi: 10.1021/ja1083255
- do Nascimento, V. V., Mello Éde, O., Carvalho, L. P., de Melo, E. J., Carvalho Ade, O., Fernandes, K. V., et al. (2015). PvD1 Defensin, A Plant Antimicrobial Peptide With Inhibitory Activity Against *Leishmania Amazonensis*. *Biosci. Rep.* 35, e00248. doi: 10.1042/BSR20150060
- Donia, M. S., Cimermancic, P., Schulze, C. J., Wieland Brown, L. C., Martin, J., Mitreva, M., et al. (2014). A Systematic Analysis of Biosynthetic Gene Clusters in the Human Microbiome Reveals a Common Family of Antibiotics. *Cell* 158, 1402–1414. doi: 10.1016/j.cell.2014.08.032
- Dosler, S., and Mataraci, E. (2013). *In Vitro* Pharmacokinetics of Antimicrobial Cationic Peptides Alone and in Combination With Antibiotics Against Methicillin Resistant *Staphylococcus Aureus* Biofilms. *Peptides* 49, 53–58. doi: 10.1016/j.peptides.2013.08.008
- Dürr, U. H. N., Sudheendra, U. S., and Ramamoorthy, A. (2006). LL-37, the Only Human Member of the Cathelicidin Family of Antimicrobial Peptides. *Biochim. Biophys. Acta - Biomembr.* 1758, 1408–1425. doi: 10.1016/j.bbamem.2006.03.030
- Ellis, C. N., Gorsulowsky, D. C., Hamilton, T. A., Billings, J. K., Brown, M. D., and Headington, J. T. (1986). Cyclosporine Improves Psoriasis in a Double-Blind Study. *Jama* 256, 3110–3116. doi: 10.1001/jama.1986.03380220076026
- European Pharmacopeia (2016). “Semi-Solid Preparations for Cutaneous Applications,” in *The European Pharmacopeia - Book Version*, EDQM Council of Europe. 808–809.
- Fahlgren, A., Hammarström, S., Danielsson, Å., and Hammarström, M. L. (2004).  $\beta$ -Defensin-3 and-4 in Intestinal Epithelial Cells Display Increased mRNA Expression in Ulcerative Colitis. *Clin. Exp. Immunol.* 137, 379–385. doi: 10.1111/j.1365-2249.2004.02543.x
- Fehlbaum, P., Bulet, P., Michaut, L., Lagueux, M., Broeckart, W., Hetru, C., et al. (1994). Insect Immunity. Septic Injury of *Drosophila* Induces the Synthesis of a Potent Antifungal Peptide With Sequence Homology to Plant Antifungal Peptides. *J. Biol. Chem.* 269, 33159–33163. doi: 10.1016/S0021-9258(20)30111-3
- Fernández, L., Delgado, S., Herrero, H., Maldonado, A., and Rodríguez, J. M. (2008). The Bacteriocin Nisin, an Effective Agent for the Treatment of *Staphylococcal Mastitis* During Lactation. *J. Hum. Lact.* 24, 311–316. doi: 10.1177/0890334408317435
- Fichman, G., and Gazit, E. (2014). Self-Assembly of Short Peptides to Form Hydrogels: Design of Building Blocks, Physical Properties and Technological Applications. *Acta Biomater.* 10, 1671–1682. doi: 10.1016/j.actbio.2013.08.013
- Fontoura, R., Spada, J., Silveira, S., Tsai, S., and Brandelli, A. (2008). Purification and Characterization of an Antimicrobial Peptide Produced by *Pseudomonas* Sp. Strain 4B. *World J. Microbiol. Biotechnol.* 25, 205–213. doi: 10.1007/s11274-008-9882-4
- Fosgerau, K., and Hoffmann, T. (2015). Peptide Therapeutics: Current Status and Future Directions. *Drug Discov. Today.* 20, 122–125. doi: 10.1016/j.drudis.2014.10.003
- Foxman, B., D’Arcy, H., Gillespie, B., Bobo, J. K., and Schwartz, K. (2002). Lactation Mastitis: Occurrence and Medical Management Among 946 Breastfeeding Women in the United States. *Am. J. Epidemiol.* 155, 103–114. doi: 10.1093/aje/155.2.103
- Froh, M., Agerberth, B., Ahangari, G., Stähle-Bäckdahl, M., Lidén, S., Wigzell, H., et al. (1997). The Expression of the Gene Coding for the Antibacterial Peptide LL-37 is Induced in Human Keratinocytes During Inflammatory Disorders. *J. Biol. Chem.* 272, 15258–15263. doi: 10.1074/jbc.272.24.15258
- Gaballa, S., Garhy, O., and Abdelkader, H. (2020). Cubosomes: Composition, Preparation, and Drug Delivery Applications. *J. Adv. Biomed. Pharm. Sci.* 3, 1–9. doi: 10.21608/jabps.2019.16887.1057
- Gaglione, R., Pane, K., Dell’Olmo, E., Cafaro, V., Pizzo, E., Olivieri, G., et al. (2019). Cost-Effective Production of Recombinant Peptides in *Escherichia Coli*. *N. Biotechnol.* 51, 39–48. doi: 10.1016/j.nbt.2019.02.004
- Gazit, E., Miller, I. R., Biggin, P. C., Sansom, M. S. P., and Shai, Y. (1996). Structure and Orientation of the Mammalian Antibacterial Peptide Cecropin P1 Within Phospholipid Membranes. *J. Mol. Biol.* 258, 860–870. doi: 10.1006/jmbi.1996.0293
- Ge, Y., MacDonald, D. L., Holroyd, K. J., Thornsberry, C., Wexler, H., and Zasloff, M. (1999). *In Vitro* Antibacterial Properties of Pexiganan, an Analog of Magainin. *Antimicrob. Agents Chemother.* 43, 782–788. doi: 10.1128/AAC.43.4.782
- Gerstel, U., Latendorf, T., Bartels, J., Becker, A., Tholey, A., and Jens-Michael Schröder, J. M. (2018). Hornerin Contains a Linked Series of Ribosome-Targeting Peptide Antibiotics. *Sci. Rep.* 8, 16158. doi: 10.1038/s41598-018-34467-8
- Gifford, J. L., Hunter, N. H., and Vogel, H. J. (2005). Lactoferricin: A Lactoferrin-Derived Peptide With Antimicrobial, Antiviral, Antitumor and Immunological Properties. *Cell Mol. Life Sci.* 62, 2588–2598. doi: 10.1007/s00018-005-5373-z
- Giri, R. S., Pal, S., Roy, S., Dolai, G., Manne, S. R., Paul, S., et al. (2021). Nanostructures From Protected L/L and D/L Amino Acid Containing Dipeptides. *Pept. Sci.* 113, e24176. doi: 10.1002/pep2.24176

- Glyceryl Monooleate (n.d) *ChemSpider [Www Document]*. Available at: <http://www.chemspider.com/Chemical-Structure.4446588.html>.
- Goodwin, N. S., Spinks, A., and Wasiak, J. (2016). The Efficacy of Hydrogel Dressings as a First Aid Measure for Burn Wound Management in the Pre-Hospital Setting: A Systematic Review of the Literature. *Int. Wound J.* 13, 519–525. doi: 10.1111/iwj.12469
- Gottler, L. M., and Ramamoorthy, A. (2009). Structure, Membrane Orientation, Mechanism, and Function of Pexiganan - A Highly Potent Antimicrobial Peptide Designed From Magainin. *Biochim. Biophys. Acta - Biomembr.* 1788, 1680–1686. doi: 10.1016/j.bbmem.2008.10.009
- Grönberg, A., Mahlapuu, M., Stähle, M., Whately-Smith, C., and Rollman, O. (2014). Treatment With LL-37 is Safe and Effective in Enhancing Healing of Hard-to-Heal Venous Leg Ulcers: A Randomized, Placebo-Controlled Clinical Trial. *Wound Repair Regen.* 22, 613–621. doi: 10.1111/wrr.12211
- Groves, M. L., Peterson, R. F., and Kiddy, C. A. (1965). Polymorphism in the Red Protein Isolated From Milk of Individual Cows. *Nature* 207, 1007–1008. doi: 10.1038/2071007a0
- Grubman, A., Kaparakis, M., Viala, J., Allison, C., Badea, L., Karrar, A., et al. (2010). The Innate Immune Molecule, NOD1, Regulates Direct Killing of *Helicobacter Pylori* by Antimicrobial Peptides. *Cell. Microbiol.* 12, 626–639. doi: 10.1111/j.1462-5822.2009.01421.x
- Guaní-Guerra, E., Santos-Mendoza, T., Lugo-Reyes, S. O., and Terán, L. M. (2010). Antimicrobial Peptides: General Overview and Clinical Implications in Human Health and Disease. *Clin. Immunol.* 135, 1–11. doi: 10.1016/j.clim.2009.12.004
- Guzmán-Rodríguez, J. J., López-Gómez, R., Suárez-Rodríguez, L. M., Salgado-Garciglia, R., Rodríguez-Zapata, L. C., Ochoa-Zarzosa, A., et al. (2013). Antibacterial Activity of Defensin PaDef From Avocado Fruit (*Persea Americana* Var. *Drymifolia*) Expressed in Endothelial Cells Against *Escherichia Coli* and *Staphylococcus Aureus*. *Biomed. Res. Int.* 2013, 986273. doi: 10.1155/2013/986273
- Hajipour, M. J., Fromm, K. M., Ashkarran, A. A., de Aberasturi, D. J., de Larramendi, I. R., Serpooshan, T., et al. (2012). Antibacterial Properties of Nanoparticles. *Trends Biotechnol.* 30, 499–511. doi: 10.1016/j.tibtech.2012.06.004
- Hallett, J. W., Wolkowicz, M. I., and Leopold, I. H. (1956). Ophthalmic Use of Neosporin. *Am. J. Ophthalmol.* 41, 850–853. doi: 10.1016/0002-9394(56)91781-0
- Hancock, R. E., and Sahl, H. G. (2006). Antimicrobial and Host-Defense Peptides as New Anti-Infective Therapeutic Strategies. *Nat. Biotechnol.* 24, 1551–1557. doi: 10.1038/nbt1267
- Haney, E. F., Mansour, S. C., and Hancock, R. E. (2017). Antimicrobial Peptides: An Introduction. *Methods Mol. Biol.* 1548, 3–22. doi: 10.1007/978-1-4939-6737-7\_1
- Haney, E. F., Straus, S. K., and Hancock, R. E. W. (2019). Reassessing the Host Defense Peptide Landscape. *Front. Chem.* 7, 43. doi: 10.3389/fchem.2019.00043
- Harder, J., Bartels, J., Christophers, E., and Schröder, J. M. (2001). Isolation and Characterization of Human  $\mu$ -Defensin-3, a Novel Human Inducible Peptide Antibiotic. *J. Biol. Chem.* 276, 5707–5713. doi: 10.1074/jbc.M008557200
- Harder, J., and Schröder, J. M. (2005). Psoriatic Scales: A Promising Source for the Isolation of Human Skin-Derived Antimicrobial Proteins. *J. Leukoc. Biol.* 77, 476–486. doi: 10.1189/jlb.0704409
- Harris, F., Dennison, S. R., and Phoenix, D. A. (2009). Anionic Antimicrobial Peptides From Eukaryotic Organisms. *Curr. Protein Pept. Sci.* 10, 585–606. doi: 10.2174/138920309789630589
- Hegedüs, N., and Marx, F. (2013). Antifungal Proteins: More Than Antimicrobials? *Fungal Biol. Rev.* 26, 132–145. doi: 10.1016/j.fbr.2012.07.002
- Heilborn, J. D., Nilsson, M. F., Sørensen, O., Stähle-Bäckdahl, M., Kratz, G., Weber, G., et al. (2003). The Cathelicidin Anti-Microbial Peptide LL-37 is Involved in Re-Epithelialization of Human Skin Wounds and is Lacking in Chronic Ulcer Epithelium. *J. Invest. Dermatol.* 120, 379–389. doi: 10.1046/j.1523-1747.2003.12069.x
- He, Y., Niu, X., Wang, B., Na, R., Xiao, B., and Yang, H. (2020). Evaluation of the Inhibitory Effects of *Lactobacillus Gasserii* and *Lactobacillus Crispatus* on the Adhesion of Seven Common Lower Genital Tract Infection-Causing Pathogens to Vaginal Epithelial Cells. *Front. Med.* 7, 284. doi: 10.3389/fmed.2020.00284
- Heunis, T. D., Smith, C., and Dicks, L. M. T. (2013). Evaluation of a Nisin-Eluting Nanofiber Scaffold to Treat *Staphylococcus Aureus*-Induced Skin Infections in Mice. *Antimicrob. Agents Chemother.* 57, 3928–3935. doi: 10.1128/AAC.00622-13
- Hiemstra, P. S., Amatngalim, G. D., van der Does, A. M., and Taube, C. (2016). Antimicrobial Peptides and Innate Lung Defenses: Role in Infectious and Noninfectious Lung Diseases and Therapeutic Applications. *Chest* 149, 545–551. doi: 10.1378/chest.15-1353
- Hirsch, J. G. (1956). Phagocytin: A Bactericidal Substance From Polymorphonuclear Leucocytes. *J. Exp. Med.* 103, 589–611. doi: 10.1084/jem.103.5.589
- Hirsch, T., Spielmann, M., Zuhaili, B., Fossum, M., Metzger, M., Koehler, T., et al. (2009). Human Beta-Defensin-3 Promotes Wound Healing in Infected Diabetic Wounds. *J. Gene Med.* 11, 220–228. doi: 10.1002/jgm.1287
- Home (n.d) *ClinicalTrials.gov [Www Document]*. Available at: <https://clinicaltrials.gov/>.
- Huan, Y., Kong, Q., Mou, H., and Yi, H. (2020). Antimicrobial Peptides: Classification, Design, Application and Research Progress in Multiple Fields. *Front. Microbiol.* 11, 582779. doi: 10.3389/fmicb.2020.582779
- Hugot, J. P., Chamailard, M., Zouali, H., Lesage, S., Cézard, J. P., Belaiche, J., et al. (2001). Association of NOD2 Leucine-Rich Repeat Variants With Susceptibility to Crohn's Disease. *Nature* 411, 599–603. doi: 10.1038/35079107
- Hultmark, D., Steiner, H., Rasmuson, T., and Boman, H. G. (1980). Insectimmunity. Purification and Properties of Three Inducible Bactericidal Proteins From Hemolymph of Immunized Pupae of *Hyalophora Cecropia*. *Eur. J. Biochem.* 106, 7–16. doi: 10.1111/j.1432-1033.1980.tb05991.x
- Hüttel, C., Hettrich, C., Miller, R., Paulke, B. R., Henklein, P., Rawel, H., et al. (2013). Self-Assembled Peptide Amphiphiles Function as Multivalent Binder With Increased Hemagglutinin Affinity. *BMC Biotechnol.* 13, 1–10. doi: 10.1186/1472-6750-13-51
- Huynh, E., Akhtar, N., and Li, J. (2018). Efficient Production of Recombinant Protegrin-1 From *Pichia Pastoris*, and Its Antimicrobial and In Vitro Cell Migration Activity. *Front. Microbiol.* 9, 2300. doi: 10.3389/fmicb.2018.02300
- Isaacson, T., Soto, A., Iwamuro, S., Knoop, F. C., and Conlon, J. M. (2002). Antimicrobial Peptides With Atypical Structural Features From the Skin of the Japanese Brown Frog *Rana Japonica*. *Peptides* 23, 419–425. doi: 10.1016/S0196-9781(01)00634-9
- Isaksson, J., Brandsdal, B. O., Engqvist, M., Flaten, G. E., Svendsen, J. S. M., and Stensen, W. (2011). A Synthetic Antimicrobial Peptidomimetic (LTX 109): Stereochemical Impact on Membrane Disruption. *J. Med. Chem.* 54, 5786–5795. doi: 10.1021/jm200450h
- Jeżowska-Bojczuk, M., and Stokowa-Sołtys, K. (2018). Peptides Having Antimicrobial Activity and Their Complexes With Transition Metal Ions. *Eur. J. Med. Chem.* 143, 997–1009. doi: 10.1016/j.ejmech.2017.11.086
- Jenssen, H., Hamill, P., and Hancock, R. E. (2006). Peptide Antimicrobial Agents. *Clin. Microbiol. Rev.* 19, 491–511. doi: 10.1128/CMR.00056-05
- Jiang, Y., Sun, J., Yin, Z., Li, H., and Zheng, F. (2020). Evaluation of Antioxidant Peptides Generated From Jiuzao (Residue After Baijiu Distillation) Protein Hydrolysates and Their Effect of Enhancing Healthy Value of Chinese Baijiu. *J. Sci. Food. Agric.* 100, 59–73. doi: 10.1002/jsfa.9994
- Jiang, L., Wang, B., Li, B., Wang, C., and Luo, Y. (2014). Preparation and Identification of Peptides and Their Zinc Complexes With Antimicrobial Activities From Silver Carp (*Hypophthalmichthys Molitrix*) Protein Hydrolysates. *Food Res. Int.* 64, 91–98. doi: 10.1016/j.foodres.2014.06.008
- Johnson, I. H., Hayday, H., and Colman, G. (1978). The Effects of Nisin on the Microbial Flora of the Dental Plaque of Monkeys (*Macaca Fascicularis*). *J. Appl. Bacteriol.* 45, 99–109. doi: 10.1111/j.1365-2672.1978.tb04203.x
- Kaiserer, L., Oberparleiter, C., Weiler-Gorz, R., Burgstaller, W., Leiter, E., and Marx, F. (2003). Characterization of the *Penicillium Chrysogenum* Antifungal Protein PAF. *Arch. Microbiol.* 180, 204–210. doi: 10.1007/s00203-003-0578-8
- Kang, S. J., Park, S. J., Mishig-Ochir, T., and Lee, B. J. (2014). Antimicrobial Peptides: Therapeutic Potentials. *Expert Rev. Anti Infect. Ther.* 12, 1477–1486. doi: 10.1586/14787210.2014.976613
- Karami, Z., and Hamidi, M. (2016). Cubosomes: Remarkable Drug Delivery Potential. *Drug Discov. Today* 21, 789–801. doi: 10.1016/j.drudis.2016.01.004
- Kavanagh, K., and Dowd, S. (2004). Histatins: Antimicrobial Peptides With Therapeutic Potential. *Pharm. Pharmacol.* 56, 285–289. doi: 10.1211/0022357022971
- Khan, A., Xu, M., Wang, T., You, C., Wang, X., Ren, H., et al. (2019). Catechol Cross-Linked Antimicrobial Peptide Hydrogels Prevent Multidrug-Resistant Acinetobacter Baumannii Infection in Burn Wounds. *Biosci. Rep.* 39 (6), BSR20190504. doi: 10.1042/BSR20190504

- Khurshid, Z., Najeeb, S., Mali, M., Moin, S. F., Raza, S. Q., Zohaib, S., et al. (2017). Histatin Peptides: Pharmacological Functions and Their Applications in Dentistry. *Saudi Pharm. J.* 25, 25–31. doi: 10.1016/j.jsps.2016.04.027
- Kościuczuk, E. M., Lisowski, P., Jarczак, J., Strzałkowska, N., Józwick, A., Horbańczuk, J., et al. (2012). Cathelicidins: Family of Antimicrobial Peptides. A Review. *Mol. Biol. Rep.* 39, 10957–10970. doi: 10.1007/s11033-012-1997-x
- Kobayashi, K. S., Chamaillard, M., Ogura, Y., Henegariu, O., Inohara, N., Nuñez, G., et al. (2005). Nod2-dependent Regulation of Innate and Adaptive Immunity in the Intestinal Tract. *Science* 307, 731–734. doi: 10.1126/science.1104911
- Koczulla, R., Von, Degenfel, G., Kupatt, C., Krötz, F., Zahler, S., Gloe, T., et al. (2003). An Angiogenic Role for the Human Peptide Antibiotic LL-37/hCAP-18. *J. Clin. Invest.* 111, 1665–1672. doi: 10.1172/JCI17545
- Koehbach, J., and Craik, D. J. (2019). The Vast Structural Diversity of Antimicrobial Peptides. *Trends Pharmacol. Sci.* 40, 517–528. doi: 10.1016/j.tips.2019.04.012
- Koeninger, L., Armbruster, N. S., Brinch, K. S., Kjaerulf, S., Andersen, B., Langnau, C., et al. (2020). Human  $\beta$ -Defensin 2 Mediated Immune Modulation as Treatment for Experimental Colitis. *Front. Immunol.* 11, 93. doi: 10.3389/fimmu.2020.00093
- Ko, S. C., Kang, N., Kim, E. A., Kang, M. C., Lee, S. H., Kang, S. M., et al. (2012). A Novel Angiotensin I-converting Enzyme (ACE) Inhibitory Peptide From a Marine *Chlorella Ellipsoidea* as its Antihypertensive Effect in Spontaneously Hypertensive Rats. *Process Biochem.* 47, 2005–2011. doi: 10.1016/j.procbio.2012.07.015
- Koo, H. B., and Seo, J. (2019). Antimicrobial Peptides Under Clinical Investigation. *Pept. Sci.* 111. doi: 10.1002/pep2.24122
- Krishnamurthy, R., Padma, P., and Dhandapani, K. (2020). Antagonistic Efficiency of *Aspergillus Giganteus* as a Biocontrol Agent Against Aflatoxigenic *Aspergillus Flavus* Infecting Maize. *J. Pure Appl. Microbiol.* 14, 527–539. doi: 10.22207/JPAM.14.1.55
- Kruszewska, D., Sahl, H. G., Bierbaum, G., Pag, U., Hynes, S. O., and Ljungh, Å. (2004). Mersacidin Eradicates Methicillin-Resistant *Staphylococcus Aureus* (MRSA) in a Mouse Rhinitis Model. *J. Antimicrob. Chemother.* 54, 648–653. doi: 10.1093/jac/dkh387
- Kühnle, A., Galuska, C. E., Zlatina, K., and Galuska, S. P. (2019). The Bovine Antimicrobial Peptide Lactoferricin Interacts With Polysialic Acid Without Loss of Its Antimicrobial Activity Against *Escherichia Coli*. *Animals* 10:1. doi: 10.3390/ani10010001
- Kurpe, S. R., Grishin, S. Y., Surin, A. K., Panfilov, A. V., Slizen, M. V., Chowdhury, S. D., et al. (2020). Antimicrobial and Amyloidogenic Activity of Peptides. *can. Antimicrobial. Peptides. Be. Used. Against. SARS-Cov-2? Int. J. Mol. Sci.* 21:9552. doi: 10.3390/ijms21249552
- Kushibiki, T., Kamiya, M., Aizawa, T., Kumaki, Y., Kikukawa, T., Mizuguchi, M., et al. (2014). Interaction Between Tachyplesin I, An Antimicrobial Peptide Derived From Horseshoe Crab, and Lipopolysaccharide. *Biochim. Biophys. Acta* 1844, 527–534. doi: 10.1016/j.bbapap.2013.12.017
- Kwon, Y. M., Kim, H. J., Kim, Y. I., Kang, Y. J., Lee, I. H., Jin, B. R., et al. (2008). Comparative Analysis of Two Attacin Genes From *Hyphantria Cunea*. *Comp. Biochem. Physiol. B Biochem. Mol. Biol.* 151, 213–220. doi: 10.1016/j.cbpb.2008.07.002
- Lai, Y., and Gallo, R. L. (2009). Amped Up Immunity: How Antimicrobial Peptides Have Multiple Roles in Immune Defense. *Trends Immunol.* 30, 131–141. doi: 10.1016/j.it.2008.12.003
- Lakshmaiah Narayana, J., and Chen, J.-Y. (2015). Antimicrobial Peptides: Possible Anti-Infective Agents. *Peptides* 72, 88–94. doi: 10.1016/j.peptides.2015.05.012
- Lala, S., Ogura, Y., Osborne, C., Hor, S. Y., Bromfield, A., Davies, S., et al. (2003). Crohn's Disease and the NOD2 Gene: A Role for Paneth Cells. *Gastroenterology* 125, 47–57. doi: 10.1016/s0016-5085(03)00661-9
- Lam, P. L., Lee, K. K. H., Wong, R. S. M., Cheng, G. Y. M., Bian, Z. X., Chui, C. H., et al. (2018). Recent Advances on Topical Antimicrobials for Skin and Soft Tissue Infections and Their Safety Concerns. *Crit. Rev. Microbiol.* 44, 40–78. doi: 10.1080/1040841X.2017.1313811
- Lande, R., Gregorio, J., Facchinetti, V., Chatterjee, B., Wang, Y. H., Homey, B., et al. (2007). Plasmacytoid Dendritic Cells Sense self-DNA Coupled With Antimicrobial Peptide. *Nature* 449, 564–569. doi: 10.1038/nature06116
- Landon, C., Sodano, P., Hetru, C., Hoffmann, J., and Ptak, M. (1997). Solution Structure of Drosomycin, the First Inducible Antifungal Protein From Insects. *Protein Sci.* 6, 1878–1884. doi: 10.1002/pro.5560060908
- Larijani, B., Tabatabaei, O., Soltani, A., Taheri, E., Pajouhi, M., Bastanagh, M. H., et al. (2005). Comparison of Desmopressin (Ddavn) Tablet and Intranasal Spray in the Treatment of Central Diabetes Insipidus. *DARU J. Pharm. Sci.* 13, 155–159.
- Latendorf, T., Ulrich Gerstel, U., Zhihong Wu, Z., Bartels, J., Becker, A., Tholey, A., et al. (2019). Cationic Intrinsically Disordered Antimicrobial Peptides (CIDAMPs) Represent a New Paradigm of Innate Defense With a Potential for Novel Anti-Infectives. *Sci. Rep.* 9, 3331. doi: 10.1038/s41598-019-39219-w
- Lee, G., and Bae, H. (2016). Anti-Inflammatory Applications of Melittin, a Major Component of Bee Venom: Detailed Mechanism of Action and Adverse Effects. *Molecules* 21, 616. doi: 10.3390/molecules21050616
- Lee, C. J., Buznyk, O., Kuffova, L., Rajendran, V., Forrester, J. V., Phopase, J., et al. (2014). Cathelicidin LL-37 and HSV-1 Corneal Infection: Peptide Versus Gene Therapy. *Transl. Vis. Sci. Technol.* 3, 4. doi: 10.1167/tvst.3.3
- Lee, S. H., Jun, H. K., Lee, H. R., Chung, C. P., and Choi, B. K. (2010). Antibacterial and Lipopolysaccharide (LPS)-Neutralising Activity of Human Cationic Antimicrobial Peptides Against Periodontopathogens. *Int. J. Antimicrob. Agents* 35, 138–145. doi: 10.1016/j.ijantimicag.2009.09.024
- Lei, J., Sun, L., Huang, S., Zhu, C., Li, P., He, J., et al. (2019). The Antimicrobial Peptides and Their Potential Clinical Applications. *Am. J. Transl. Res.* 11, 3919–3931.
- Leszczynska, K., Namiot, D., Byfield, F. J., Cruz, K., Zendzian-Piotrowska, M., Fein, D. E., et al. (2013). Antibacterial Activity of the Human Host Defence Peptide LL-37 and Selected Synthetic Cationic Lipids Against Bacteria Associated With Oral and Upper Respiratory Tract Infections. *J. Antimicrob. Chemother.* 68, 610–618. doi: 10.1093/jac/dks434
- Levón, J., Al-Samadi, A., Mackiewicz, Z., Coer, A., Trebse, R., Waris, E., et al. (2015). Human Beta-Defensin-3 Producing Cells in Septic Implant Loosening. *J. Mater. Sci. Mater. Med.* 26, 98. doi: 10.1007/s10856-015-5440-4
- Liang, L. L., Cai, S. Y., Gao, M., Chu, X. M., Pan, X. Y., and Gong, K. K. (2020). Purification of Antioxidant Peptides of *Moringa Oleifera* Seeds and Their Protective Effects on H<sub>2</sub>O<sub>2</sub> Oxidative Damaged Chang Liver Cells. *J. Funct. Foods* 64, 103698. doi: 10.1016/j.jff.2019.103698
- Liang, W., and Diana, J. (2020). The Dual Role of Antimicrobial Peptides in Autoimmunity. *Front. Immunol.* 11, 2077. doi: 10.3389/fimmu.2020.02077
- Li, X., Fan, R., Tong, A., Yang, M., Deng, J., Zhou, L., et al. (2015). In Situ Gel-Forming AP-57 Peptide Delivery System for Cutaneous Wound Healing. *Int. J. Pharm.* 495, 560–571. doi: 10.1016/j.ijpharm.2015.09.005
- Li, X., Li, Y., Han, H., Miller, D. W., and Wang, G. (2006). Solution Structures of Human LL-37 Fragments and NMR-based Identification of a Minimal Membrane-Targeting Antimicrobial and Anticancer Region. *J. Am. Chem. Soc.* 128, 5776–5785. doi: 10.1021/ja0584875
- Li, T., Shi, C., Zhou, C., Sun, X., Ang, Y., Dong, X., et al. (2020). Purification and Characterization of Novel Antioxidant Peptides From Duck Breast Protein Hydrolysates. *LWT Food Sci. Technol.* 10, 102–108. doi: 10.1016/j.lwt.2020.109215
- Liu, Y. J., Cheng, C. S., Lai, S. M., Hsu, M. P., Chen, C. S., and Lyu, P. C. (2006). Solution Structure of the Plant Defensin VrD1 From Mung Bean and its Possible Role in Insecticidal Activity Against Bruchids. *Proteins* 63, 777–786. doi: 10.1002/prot.20962
- Liu, Y., and Hsu, S. H. (2018). Synthesis and Biomedical Applications of Self-Healing Hydrogels. *Front. Chem.* 6:449. doi: 10.3389/fchem.2018.00449
- Liu, S., Long, Q., Xu, Y., Wang, J., Xu, Z., Wang, L., et al. (2017). Assessment of Antimicrobial and Wound Healing Effects of Brevinin-2Ta Against the Bacterium *Klebsiella Pneumoniae* in Dermal-Wounded Rats. *Oncotarget* 8, 111369–111385. doi: 10.18632/oncotarget.22797
- Li, Y., Xiang, Q., Zhang, Q., Huang, Y., and Su, Z. (2012). Overview on the Recent Study of Antimicrobial Peptides: Origins, Functions, Relative Mechanisms and Application. *Peptides* 37, 207–215. doi: 10.1016/j.peptides.2012.07.001
- LL-37 - *Clinicaltrials.Gov*. Available at: <https://clinicaltrials.gov/ct2/results?recrs=&cond=&term=LL-37&cntry=&state=&city=&dist>.
- López-Meza, J. E., Ochoa-Zarzosa, A., Aguilar, J. A., and Loeza-Lara, P. D. (2011). Antimicrobial Peptides: Diversity and Perspectives for Their Biomedical Application in “Biomedical Engineering, Trends, Research and Technologies”. *IntechOpen*, pp. 275–304. doi: 10.5772/13058
- Ltx-109 - *Clinicaltrials.Gov*. Available at: <https://clinicaltrials.gov/ct2/results?recrs=&cond=&term=LTX-109&cntry=&state=&city=&dist>.
- Luiz, D. P., Almeida, J. F., Goulart, L. R., Nicolau-Junior, N., and Ueira-Vieira, C. (2017). Heterologous Expression of Abacain Peptide From *Apis Mellifera* in *Pichia Pastoris*. *Microb. Cell Fact.* 16, 76. doi: 10.1186/s12934-017-0689-6

- Lunder, M., Bratkovič, T., Kreft, S., and Štrukelj, B. (2005). Peptide Inhibitor of Pancreatic Lipase Selected by Phage Display Using Different Elution Strategies. *J. Lipid. Res.* 46, 1512–1516. doi: 10.1194/jlr.M500048-JLR200
- Luong, H. X., Thanh, T. T., and Tran, T. H. (2020). Antimicrobial Peptides – Advances in Development of Therapeutic Applications. *Life. Sci.* 260, 118407. doi: 10.1016/j.lfs.2020.118407
- Machado, L. R., and Ottolini, B. (2015). An Evolutionary History of Defensins: A Role for Copy Number Variation in Maximizing Host Innate and Adaptive Immune Responses. *Front. Immunol.* 6, 115. doi: 10.3389/fimmu.2015.00115
- Magana, M., Pushpanathan, M., Santos, A. L., Leanse, L., Fernandez, M., Ioannidis, A., et al. (2020). The Value of Antimicrobial Peptides in the Age of Resistance. *Lancet Infect. Dis.* 20, e216–e230. doi: 10.1016/S1473-3099(20)30327-3
- Mahlapuu, M., Björn, C., and Ekblom, J. (2020). Antimicrobial Peptides as Therapeutic Agents: Opportunities and Challenges. *Crit. Rev. Biotechnol.* 40, 978–992. doi: 10.1080/07388551.2020.1796576
- Mahlapuu, M., Håkansson, J., Ringstad, L., and Björn, C. (2016). Antimicrobial Peptides: An Emerging Category of Therapeutic Agents. *Front. Cell. Infect. Microbiol.* 6, 194. doi: 10.3389/fcimb.2016.00194
- Maiti, S., Patro, S., Purohit, S., Jain, S., Senapati, S., and Dey, N. (2014). Effective Control of Salmonella Infections by Employing Combinations of Recombinant Antimicrobial Human Beta-Defensins hBD-1 and hBD-2. *Antimicrob. Agents Chemother.* 58, 6896–6903. doi: 10.1128/AAC.03628-14
- Majewski, K., Kozłowska, E., Żelechowska, P., and Brzezińska-Błaszczyk, E. (2018). Serum Concentrations of Antimicrobial Peptide Cathelicidin LL-37 in Patients With Bacterial Lung Infections. *Cent. Eur. J. Immunol.* 43, 453. doi: 10.5114/cej.2018.81355
- Malhaire, H., Gimel, J. C., Roger, E., Benoît, J. P., and Lagarce, F. (2016). How to Design the Surface of Peptide-Loaded Nanoparticles for Efficient Oral Bioavailability? *Adv. Drug Deliv. Rev.* 106, 320–336. doi: 10.1016/j.addr.2016.03.011
- Manna, S., Ghosh, A. K., and Mandal, S. M. (2019). Curd-Peptide Based Novel Hydrogel Inhibits Biofilm Formation, Quorum Sensing, Swimming Motility of Multi-Antibiotic Resistant Clinical Isolates and Accelerates Wound Healing Activity. *Front. Microbiol.* 10, 951. doi: 10.3389/fmicb.2019.00951
- Manniello, M. D., Moretta, A., Salvia, R., Scieuzo, C., Lucchetti, D., Vogel, H., et al. (2021). Insect Antimicrobial Peptides: Potential Weapons to Counteract the Antibiotic Resistance. *Cell. Mol. Life Sci.* doi: 10.1007/s00018-021-03784-z
- Mardirossian, M., Barriere, Q., Timchenko, T., Müller, C., Pacor, S., Mergaert, P., et al. (2018). Fragments of the Nonlytic Proline-Rich Antimicrobial Peptide Bac5 Kill *Escherichia Coli* Cells by Inhibiting Protein Synthesis. *Antimicrob. Agents Chemother.* 62, e00534–e00518. doi: 10.1128/AAC.00534-18
- Martinez-Villalunga, C., Rupasinghe, S. G., Schuler, M. A., and Gonzalez de Mejia, E. (2010). Peptides From Purified Soybean  $\beta$ -Conglycinin Inhibit Fatty Acid Synthase by Interaction With the Thioesterase Catalytic Domain. *FEBS J.* 277, 1481–1493. doi: 10.1111/j.1742-4658.2010.07577.x
- Martin-Serrano, Á., Gómez, R., Ortega, P., and Mata, F. J. D. (2019). Nanosystems as Vehicles for the Delivery of Antimicrobial Peptides (Amps). *Pharmaceutics* 11, 448. doi: 10.3390/pharmaceutics11090448
- Marx, F. (2004). Small, Basic Antifungal Proteins Secreted From Filamentous Ascomycetes: A Comparative Study Regarding Expression, Structure, Function and Potential Application. *Appl. Microbiol. Biotechnol.* 65, 133–142. doi: 10.1007/s00253-004-1600-z
- Meikle, T. G., Waddington, L. J., and Conn, C. E. (2019). *Inverse Bicontinuous Cubic Phase Nanoparticles for the Delivery of Antimicrobial Peptides*. Available at: <https://www.controlledreleasesociety.org/node/11194>.
- Mello, E. O., Ribeiro, S. F., Carvalho, A. O., Santos, I. S., Da Cunha, M., Santa-Catarina, C., et al. (2011). Antifungal Activity of PvD1 Defensin Involves Plasma Membrane Permeabilization, Inhibition of Medium Acidification, and Induction of ROS in Fungi Cells. *Curr. Microbiol.* 62, 1209–1217. doi: 10.1007/s00284-010-9847-3
- Meneguetti, B. T., Machado, L. D., Oshiro, K. G., Nogueira, M. L., Carvalho, C. M., and Franco, O. L. (2017). Antimicrobial Peptides From Fruits and Their Potential Use as Biotechnological Tools—A Review and Outlook. *Front. Microbiol.* 7, 2136. doi: 10.3389/fmicb.2016.02136
- Mitra, D., Yadav, A., Prithyani, S., John, L. E., Rodrigues, S., and Shah, R. (2019). The Antiplaque Efficacy of Lantibiotic Nisin Extract Mouthrinse. *J. Indian Soc Periodontol.* 23, 31–34. doi: 10.4103/jisp.jisp\_326\_18
- Miyata, T., Tokunaga, F., Yoneya, T., Yoshikawa, K., Iwanaga, S., Niwa, M., et al. (1989). Antimicrobial Peptides, Isolated From Horseshoe Crab Hemocytes, Tachyplesin II, and Polyphemusins I and II: Chemical Structures and Biological Activity. *J. Biochem.* 106, 663–668. doi: 10.1093/oxfordjournals.jbchem.a122913
- Mohammadi-Barzelighi, H., Nasr-Esfahani, B., Bakhshi, B., Daraei, B., Moghim, S., and Fazeli, H. (2019). Analysis of Antibacterial and Antibiofilm Activity of Purified Recombinant Azurin From *Pseudomonas Aeruginosa*. *Iran J. Microbiol.* 11, 166–176. doi: 10.18502/ijm.v11i2.1083
- Montesinos, E. (2007). Antimicrobial Peptides and Plant Disease Control. *FEMS Microbiol. Lett.* 270, 1–11. doi: 10.1111/j.1574-6968.2007.00683.x
- Mookherjee, N., Brown, K. L., Bowdish, D. M., Doria, S., Falsafi, R., Hokamp, K., et al. (2006). Modulation of the TLR-mediated Inflammatory Response by the Endogenous Human Host Defense Peptide LL-37. *J. Immunol.* 176, 2455–2464. doi: 10.4049/jimmunol.176.4.2455
- Moravej, H., Moravej, Z., Yazdanparast, M., Heiat, M., Mirhosseini, A., Moosazadeh Moghaddam, M., et al. (2018). Antimicrobial Peptides: Features, Action, and Their Resistance Mechanisms in Bacteria. *Microb. Drug Resist.* 24, 747–767. doi: 10.1089/mdr.2017.0392
- Moretta, A., Salvia, R., Scieuzo, C., Di Somma, A., Vogel, H., Pucci, P., et al. (2020). A Bioinformatic Study of Antimicrobial Peptides Identified in the Black Soldier Fly (BSF) *Hermetia illucens* (Diptera: Stratiomyidae). *Sci. Rep.* 10, 16875. doi: 10.1038/s41598-020-74017-9
- Moridi, K., Mohammad, H., Eidgahi, M. R. A., Mohsen, M. F., Zare, H., Ghazvini, K., et al. (2020). Construction, Cloning, and Expression of Melittin Antimicrobial Peptide Using *Pichia Pastoris* Expression System. *Gene Rep.* 21, 100900. doi: 10.1016/j.genrep.2020.100900
- Moura, E. C., Baeta, T., Romanelli, A., Laguri, C., Martorana, A. M., Erba, E., et al. (2020). Thanatin Impairs Lipopolysaccharide Transport Complex Assembly by Targeting LptC–LptA Interaction and Decreasing LptA Stability. *Front. Microbiol.* 11, 909. doi: 10.3389/fmicb.2020.00909
- Mouritzen, M. V., Petkovic, M., Qvist, K., Poulsen, S. S., Alarico, S., Leal, E. C., et al. (2021). Improved Diabetic Wound Healing by LFCinB is Associated With Relevant Changes in the Skin Immune Response and Microbiota. *Mol. Ther. Methods Clin. Dev.* 20, 726–739. doi: 10.1016/j.omtm.2021.02.008
- Mylonakis, E., Podsiadlowski, L., Muhammed, M., and Vilcinskis, A. (2016). Diversity, Evolution and Medical Applications of Insect Antimicrobial Peptides. *Philos. Trans. R. Soc Lond. B. Biol. Sci.* 371, 20150290. doi: 10.1098/rstb.2015.0290
- Najafian, L., and Babji, A. S. (2019). Purification and Identification of Antioxidant Peptides From Fermented Fish Sauce (Budu). *J. Aquat. Food. Prod. Technol.* 28, 14–24. doi: 10.1080/10498850.2018.1559903
- Nakamura, T., Furunaka, H., Miyata, T., Tokunaga, F., Muta, T., Iwanaga, S., et al. (1988). Tachyplesin, a Class of Antimicrobial Peptide From the Hemocytes of the Horseshoe Crab (*Tachyplesus Tridentatus*). Isolation and Chemical Structure. *J. Biol. Chem.* 263, 16709–16713. doi: 10.1016/S0021-9258(18)37448-9
- NCT03748199 (2018). *Clinical Study to Investigate Safety, Tolerability, Pharmacokinetics and Pharmacodynamics of POL6014 in Patients With CF - Full Text View - Clinicaltrials.gov*. Available at: <https://clinicaltrials.gov/show/NCT03748199>.
- Nordström, R., and Malmsten, M. (2017). Delivery Systems for Antimicrobial Peptides. *Adv. Colloid Interface Sci.* 242, 17–34. doi: 10.1016/j.cis.2017.01.005
- Oard, S., Ham, J. H., and Cohn, M. (2012). Thionins - Nature's Weapons of Mass Protection, in "Small Wonders: Peptides for Disease Control" vol. 1095. (ACS Symposium Series, Washington, DC: American Chemical Society), 415–443. doi: 10.1021/bk-2012-1095.ch020
- Ohtani, S., Okada, T., Yoshizumi, H., and Kagamiyama, H. (1977). Complete Primary Structures of Two Subunits of Purothionin a, a Lethal Protein for Brewer's Yeast From Wheat Flour. *J. Biochem.* 82, 753–767. doi: 10.1093/oxfordjournals.jbchem.a131752
- Oo, T. Z., Cole, N., Garthwaite, L., Willcox, M. D. P., and Zhu, H. (2010). Evaluation of Synergistic Activity of Bovine Lactoferricin With Antibiotics in Corneal Infection. *J. Antimicrob. Chemother.* 65, 1243–1251. doi: 10.1093/jac/dkq106
- Overstreet, D. J., Dutta, D., Stabenfeldt, S. E., and Vernon, B. L. (2012). Injectable Hydrogels. *J. Polym. Sci. B Polym. Phys.* 50, 881–903. doi: 10.1002/polb.23081
- Pachón-Ibañez, M. E., Smani, Y., Pachón, J., and Sánchez-Céspedes, J. (2017). Perspectives for Clinical Use of Engineered Human Host Defense

- Antimicrobial Peptides. *FEMS Microbiol. Rev.* 41, 323–342. doi: 10.1093/femsre/fux012
- Palicz, Z., Gáll, T., Leiter, É., Kollár, S., Kovács, I., Miszti-Blasius, K., et al. (2016). Application of a Low Molecular Weight Antifungal Protein From *Penicillium Chrysogenum* (PAF) to Treat Pulmonary Aspergillosis in Mice. *Emerg. Microbes Infect.* 5, e114. doi: 10.1038/emi.2016.116
- Paquette, D. W., Simpson, D. M., Friden, P., Braman, V., and Williams, R. C. (2002). Safety and Clinical Effects of Topical Histatin Gels in Humans With Experimental Gingivitis. *J. Clin. Periodontol.* 29, 1051–1058. doi: 10.1034/j.1600-051x.2002.291201.x
- Parisien, A., Allain, B., Zhang, J., Mandeville, R., and Lan, C. Q. (2008). Novel Alternatives to Antibiotics: Bacteriophages, Bacterial Cell Wall Hydrolases, and Antimicrobial Peptides. *J. Appl. Microbiol.* 104, 1–13. doi: 10.1111/j.1365-2672.2007.03498.x
- Park, H. J., Lee, S. H., Son, D. J., Oh, K. W., Kim, K. H., Song, H. S., et al. (2004). Antiarthritic Effect of Bee Venom: Inhibition of Inflammation Mediator Generation by Suppression of NF-kappaB Through Interaction With the p50 Subunit. *Arthritis Rheumatol.* 50, 3504–3515. doi: 10.1002/art.20626
- Pasupuleti, M., Schmidtchen, A., and Malmsten, M. (2012). Antimicrobial Peptides: Key Components of the Innate Immune System. *Crit. Rev. Biotechnol.* 32, 143–171. doi: 10.3109/07388551.2011.594423
- Patockaa, J., Nepovimovab, E., Klimovac, B., Wud, Q., and Kucab, K. (2018). Antimicrobial Peptides: Amphibian Host Defense Peptides. *Curr. Med. Chem.* 25, 1–21. doi: 10.2174/0929867325666180713125314
- Pettersen, E. F., Goddard, T. D., Huang, C. C., Couch, G. S., Greenblatt, D. M., Meng, E. C., et al. (2004). UCSF Chimera—a visualization system for exploratory research and analysis. *J. Comput. Chem.* 25, 1605–1612. doi: 10.1002/jcc.20084
- Petnicki-Ocwieja, T., Hrcncir, T., Liu, Y. J., Biswas, A., Hudcovic, T., Tlaskalova-Hogenova, H., et al. (2009). Nod2 is Required for the Regulation of Commensal Microbiota in the Intestine. *Proc. Natl. Acad. Sci.* 106, 15813–15818. doi: 10.1073/pnas.0907722106
- Pfalzgraff, A., Brandenburg, K., and Weindl, G. (2018). Antimicrobial Peptides and Their Therapeutic Potential for Bacterial Skin Infections and Wounds. *Front. Pharmacol.* 9, 281. doi: 10.3389/fphar.2018.00281
- Pizzino, G., Irrera, N., Cucinotta, M., Pallio, G., Mannino, F., Arcoraci, V., et al. (2017). Oxidative Stress: Harms and Benefits for Human Health. *Oxid. Med. Cell. Longev.* 2017, 8416763. doi: 1155/2017/8416763
- Prince, A., Sandhu, P., Ror, P., Dash, E., Sharma, S., Arakha, M., et al. (2016). Lipid-II Independent Antimicrobial Mechanism of Nisin Depends on its Crowding and Degree of Oligomerization. *Sci Rep.* 6, 37908. doi: 10.1038/srep37908
- Qi, J., Gao, R., Liu, C., Shan, B., Gao, F., He, J., et al. (2019). Potential Role of the Antimicrobial Peptide Tachyplesin III Against Multidrug-Resistant *P. Aeruginosa* and *A. Baumannii* Coinfection in an Animal Model. *Infect. Drug Resist.* 12, 2865–2874. doi: 10.2147/IDR.S217020
- Raghuraman, H., and Chattopadhyay, A. (2007). Melittin: A Membrane-Active Peptide With Diverse Functions. *Biosci. Rep.* 27, 189–223. doi: 10.1007/s10540-006-9030-z
- Raheem, N., and Straus, S. K. (2019). Mechanisms of Action for Antimicrobial Peptides With Antibacterial and Antibiofilm Functions. *Front. Microbiol.* 10, 2866. doi: 10.3389/fmicb.2019.02866
- Rahnamaeian, M. (2011). Antimicrobial Peptides: Modes of Mechanism, Modulation of Defense Responses. *Plant Signal. Behav.* 6, 1325–1332. doi: 10.4161/psb.6.9.16319
- Rajabi, N., Kharaziha, M., Emadi, R., Zarrabi, A., Mokhtari, H., and Salehi, S. (2020). An Adhesive and Injectable Nanocomposite Hydrogel of Thiolatedgelatin/Gelatin Methacrylate/Laponite® as a Potential Surgical Sealant. *J. Colloid Interface Sci.* 564, 155–169. doi: 10.1016/j.jcis.2019.12.048
- Ramos, R., Silva, J. P., Rodrigues, A. C., Costa, R., Guardão, L., Schmitt, F., et al. (2011). Wound Healing Activity of the Human Antimicrobial Peptide LL37. *Peptides* 32, 1469–1476. doi: 10.1016/j.peptides.2011.06.005
- Rathi, C., Lee, R. E., and Meibohm, B. (2016). Translational PK/PD of Anti-Infective Therapeutics. *Drug Discov. Today Technol.* 21–22, 41–49. doi: 10.1016/j.ddtec.2016.08.004
- Risso, A., Braidot, E., Sordano, M. C., Vianello, A., Macri, F., Skerlavaj, B., et al. (2002). BMAP-28, an Antibiotic Peptide of Innate Immunity, Induces Cell Death Through Opening of the Mitochondrial Permeability Transition Pore. *Mol. Cell Biol.* 22, 1926–1935. doi: 10.1128/mcb.22.6.1926-1935.2002
- Rosenfeld, Y., Barra, D., Simmaco, M., Shai, Y., and Mangoni, M. L. (2006). A Synergism Between Temporins Toward Gram-Negative Bacteria Overcomes Resistance Imposed by the Lipopolysaccharide Protective Layer. *J. Biol. Chem.* 281, 28565–28574. doi: 10.1074/jbc.M606031200
- Sørensen, O. E. (2016). “Antimicrobial Peptides in Cutaneous Wound Healing,” in *Antimicrobial Peptides* (Cham: Springer), 1–15. doi: 10.1111/exd.12929
- Sørensen, O. E., Thapa, D. R., Rosenthal, A., Liu, L., Roberts, A. A., and Ganz, T. (2005). Differential Regulation of  $\beta$ -Defensin Expression in Human Skin by Microbial Stimuli. *J. Immunol.* 174, 4870–4879. doi: 10.4049/jimmunol.174.8.4870
- Sader, H. S., Fedler, K. A., Rennie, R. P., Stevens, S., and Jones, R. N. (2004). Omigananpentahydrochloride (MBI 226), a Topical 12-Amino-Acid Cationic Peptide: Spectrum of Antimicrobial Activity and Measurements of Bactericidal Activity. *Antimicrob. Agents Chemother.* 48, 3112–3118. doi: 10.1128/AAC.48.8.3112-3118.2004
- Sagisaka, A., Miyanoishita, A., Ishibashi, J., and Yamakawa, M. (2001). Purification, Characterization and Gene Expression of a Glycine and Proline-Rich Antibacterial Protein Family From Larvae of a Beetle, *Allomyrina Dichotoma*. *Insect Mol. Biol.* 10, 293–302. doi: 10.1046/j.0962-1075.2001.00261.x
- Salampessy, J., Reddy, N., Phillips, M., and Kailasapathy, K. (2017). Isolation and Characterization of Nutraceutically Potential ACE-Inhibitory Peptides From Leatherjacket (Meuschenia Sp.) Protein Hydrolysates. *LWT* 80, 430–436. doi: 10.1016/j.lwt.2017.03.004
- Salas, C. E., Badillo-Corona, J. A., Ramírez-Sotelo, G., and Oliver-Salvador, C. (2015). Biologically Active and Antimicrobial Peptides From Plants. *Biomed. Res. Int.* 2015, 102129. doi: 10.1155/2015/102129
- Saravanan, R., Mohanram, H., Joshi, M., Domadia, P. N., Torres, J., Ruedl, C., et al. (2012). Structure, Activity and Interactions of the Cysteine Deleted Analog of Tachyplesin-1 With Lipopolysaccharide Micelle: Mechanistic Insights Into Outer-Membrane Permeabilization and Endotoxin Neutralization. *Biochim. Biophys. Acta* 1818, 1613–1624. doi: 10.1016/j.bbame.2012.03.015
- Schiffner, H. A. (2011). The Delivery of Drugs—Peptides and Proteins. *Compr. Biotechnol.* 5, 587–604. doi: 10.1016/B978-0-08-088504-9.00338-X
- Schittek, B., Hipfel, R., Sauer, B., Bauer, J., Kalbacher, H., Stevanovic, S., et al. (2001). Dermcidin: A Novel Human Antibiotic Peptide Secreted by Sweat Glands. *Nat. Immunol.* 2, 1133–1137. doi: 10.1038/news011108-3
- Schmidt, R., Ostorházi, E., Wende, E., Knappe, D., and Hoffmann, R. (2016). Pharmacokinetics and *In Vivo* Efficacy of Optimized Oncocin Derivatives. *J. Antimicrob. Chemother.* 71, 1003–1011. doi: 10.1093/jac/dkv454
- Schnaider, L., Brahmachari, S., Schmidt, N. W., Mensa, B., Shaham-Niv, S., Bychenko, D., et al. (2017). Self-Assembling Dipeptide Antibacterial Nanostructures With Membrane Disrupting Activity. *Nat. Commun.* 8, 1–10. doi: 10.1038/s41467-017-01447-x
- Scholl, D., and Martin, D. W. (2008). Antibacterial Efficacy of R-type Pyocins Towards *Pseudomonas Aeruginosa* in a Murine Peritonitis Model. *Antimicrob. Agents Chemother.* 52, 1647–1652. doi: 10.1128/AAC.01479-07
- Schweizer, F. (2009). Cationic Amphiphilic Peptides With Cancer-Selective Toxicity. *Eur. J. Pharmacol.* 625, 190–194. doi: 10.1016/j.ejphar.2009.08.043
- Scocchi, M., Mardrossian, M., Runti, G., and Benincasa, M. (2016). Non-Membrane Permeabilizing Modes of Action of Antimicrobial Peptides on Bacteria. *Curr. Top. Med. Chem.* 16, 76–88. doi: 10.2174/1568026615666150703121009
- Selsted, M. E., and Ouellette, A. J. (2005). Mammalian Defensins in the Antimicrobial Immune Response. *Nat. Immunol.* 6, 551–557. doi: 10.1038/ni1206
- Semple, F., MacPherson, H., Webb, S., Cox, S. L., Mallin, L. J., Tyrrell, C. G. R., et al. (2011). Human  $\beta$ -Defensin 3 Affects the Activity of Pro-Inflammatory Pathways Associated With MyD88 and TRIF. *Eur. J. Immunol.* 41, 3291–3300. doi: 10.1002/eji.201141648
- Shahmiri, M., Cornell, B., and Mechler, A. (2017). Phenylalanine Residues Act as Membrane Anchors in the Antimicrobial Action of Aurein 1.2. *Biointerphases* 12, 05G605. doi: 10.1116/1.4995674
- Sharma, G., Dang, S., Gupta, S., and Gabriani, R. (2018). Antibacterial Activity, Cytotoxicity, and the Mechanism of Action of Bacteriocin From *Bacillus Subtilis* GAS101. *Med. Princ. Pract.* 27, 186–192. doi: 10.1159/000487306
- Sharma, S., Sethi, S., Prasad, R., Samanta, P., Rajwanshi, A., and Malhotra, S. (2011). Characterization of Low Molecular Weight Antimicrobial Peptide

- From Human Female Reproductive Tract. *Indian J. Med. Res.* 134, 679–687. doi: 10.4103/0971-5916.90996
- Sheard, D. E., O'Brien-Simpson, N. M., Wade, J. D., and Separovic, F. (2019). Combating Bacterial Resistance by Combination of Antibiotics With Antimicrobial Peptides. *Pure Appl. Chem.* 91, 199–209. doi: 10.1515/pac-2018-0707
- Shin, J. M., Ateia, I., Paulus, J. R., Liu, H., Fenno, J. C., Rickard, A. H., et al. (2015). Antimicrobial Nisin Acts Against Saliva Derived Multi-Species Biofilms Without Cytotoxicity to Human Oral Cells. *Front. Microbiol.* 6, 617. doi: 10.3389/fmicb.2015.00617
- Sierra, J. M., Fusté, E., Rabanal, F., Vinuesa, T., and Viñas, M. (2017). An Overview of Antimicrobial Peptides and the Latest Advances in Their Development. *Expert Opin. Biol. Ther.* 17, 663–676. doi: 10.1080/14712598.2017.1315402
- Singh, A., Kukreti, R., Saso, L., and Kukreti, S. (2019). Oxidative Stress: A Key Modulator in Neurodegenerative Diseases. *Molecules* 24, 1583. doi: 10.3390/molecules24081583
- Sinha, R., and Shukla, P. (2018). Antimicrobial Peptides: Recent Insights on Biotechnological Interventions and Future Perspectives. *Protein Pept. Lett.* 26, 79–87. doi: 10.2174/0929866525666181026160852
- Sinha, S., Zheng, L., Mu, Y., Ng, W. J., and Bhattacharjya, S. (2017). Structure and Interactions of a Host Defense Antimicrobial Peptide Thanatin in Lipopolysaccharide Micelles Reveal Mechanism of Bacterial Cell Agglutination. *Sci. Rep.* 7, 1–13. doi: 10.1038/s41598-017-18102-6
- Soltani, S., Hammami, R., Cotter, P. D., Rebuffat, S., Said, L. B., Gaudreau, H., et al. (2021). Bacteriocins as a New Generation of Antimicrobials: Toxicity Aspects and Regulations. *FEMS Microbiol. Rev.* 45, fuaa039. doi: 10.1093/femsre/fuua039
- Son, D. J., Lee, J. W., Lee, Y. H., Song, H. S., Lee, C. K., and Hong, J. T. (2007). Therapeutic Application of Anti-Arthritis, Pain-Releasing, and Anti-Cancer Effects of Bee Venom and its Constituent Compounds. *Pharmacol. Ther.* 115, 246–270. doi: 10.1016/j.pharmthera.2007.04.004
- Song, Z., Chen, X., You, X., Huang, K., Dhinakar, A., Gu, Z., et al. (2017). Self-Assembly of Peptide Amphiphiles for Drug Delivery: The Role of Peptide Primary and Secondary Structures. *Biomater. Sci.* 5, 2369–2380. doi: 10.1039/c7bm00730b
- Soundararajan, N., Park, S., Le Van Chanh, Q., Cho, H. S., Raghunathan, G., Ahn, B., et al. (2019). Protegrin-1 Cytotoxicity Towards Mammalian Cells Positively Correlates With the Magnitude of Conformational Changes of the Unfolded Form Upon Cell Interaction. *Sci. Rep.* 9, 11569. doi: 10.1038/s41598-019-47955-2
- Steiner, H., Hultmark, D., Engstrom, A., Bennich, H., and Boman, H. G. (1981). Sequence and Specificity of Two Antibacterial Proteins Involved in Insect Immunity. *Nature* 292, 246–248. doi: 10.1038/292246a0
- Sunderkötter, C., and Becker, K. (2015). Frequent Bacterial Skin and Soft Tissue Infections: Diagnostic Signs and Treatment. *J. Dtsch. Dermatol. Ges.* 13, 501–526. doi: 10.1111/ddg.12721
- Su, Z., Shodiev, M., Leitch, J. J., Abbasi, F., and Lipkowski, J. (2018). Role of Transmembrane Potential and Defects on the Permeabilization of Lipid Bilayers by Alamethicin, an Ion-Channel-Forming Peptide. *Langmuir* 34, 6249–6260. doi: 10.1021/acs.langmuir.8b00928
- Tasiemski, A., Vandenbulke, F., Mitta, G., Lemoine, J., Lefebvre, C., Sautiere, P. E., et al. (2004). Molecular Characterization of Two Novel Antibacterial Peptides Inducible Upon Bacterial Challenge in an Annelid, the Leech *Theromyzon tessulatum*. *J. Biol. Chem.* 279, 30973–30982. doi: 10.1074/jbc.M312156200
- Taveira, G. B., Mathias, L. S., da Motta, O. V., Machado, O. L. T., Rodrigues, R., Carvalho, A. O., et al. (2014). Thionin-like Peptides From Capsicum Annuum Fruits With High Activity Against Human Pathogenic Bacteria and Yeasts. *Biopolymers* 102, 30–39. doi: 10.1002/bip.22351
- Taylor, S., and Palmer, S. (2016). The Action Mechanism of Daptomycin. *Bioorg. Med. Chem.* 24, 6253–6268. doi: 10.1016/j.bmc.2016.05.052
- Thorstholm, L., and Craik, D. J. (2012). Discovery and Applications of Naturally Occurring Cyclic Peptides. *Drug Discov. Today Technol.* 9, e13–e21. doi: 10.1016/j.ddtec.2011.07.005
- Tokumaru, S., Sayama, K., Shirakata, Y., Komatsuzawa, H., Ouhara, K., Hanakawa, Y., et al. (2005). Induction of Keratinocyte Migration Via Transactivation of the Epidermal Growth Factor Receptor by the Antimicrobial Peptide LL-37. *J. Immunol.* 175, 4662–4668. doi: 10.4049/jimmunol.175.7.4662
- Tong, Z., Dong, L., Zhou, L., Tao, R., and Ni, L. (2010). Nisin Inhibits Dental Caries-Associated Microorganism *In Vitro*. *Peptides* 31, 2003–2008. doi: 10.1016/j.peptides.2010.07.016
- Toopcham, T., Mes, J. J., Wichers, H. J., Roytrakul, S., and Yongsawatdigul, J. (2017). Bioavailability of Angiotensin I-Converting Enzyme (ACE) Inhibitory Peptides Derived From *Virgibacillus halodentificans* Sk1-3-7 Proteinases Hydrolyzed Tilapia Muscle Proteins. *Food. Chem.* 220, 190–197. doi: 10.1016/j.foodchem.2016.09.183
- Travkova, O. G., Moehwald, H., and Brezesinski, G. (2017). The Interaction of Antimicrobial Peptides With Membranes. *Adv. Colloid Interface Sci.* 247, 521–532. doi: 10.1016/j.cis.2017.06.001
- Ulvatne, H., Haukland, H. H., Olsvik, O., and Vorland, L. H. (2001). Lactoferricin B Causes Depolarization of the Cytoplasmic Membrane of Escherichia Coli ATCC 25922 and Fusion of Negatively Charged Liposomes. *FEBS Lett.* 492, 62–65. doi: 10.1016/s0014-5793(01)02233-5
- van den Bogaart, G., Guzmán, J. V., Mika, J. T., and Poolman, B. (2008). On the Mechanism of Pore Formation by Melittin. *J. Biol. Chem.* 283, 33854–33857. doi: 10.1074/jbc.M805171200
- Van Epps, H. L. (2006). René Dubos: Unearthing Antibiotics. *J. Exp. Med.* 203, 259. doi: 10.1084/jem.2032fta
- Vassallo, A., Silletti, M. F., Faraone, I., and Milella, L. (2020). Nanoparticulate Antibiotic Systems as Antibacterial Agents and Antibiotic Delivery Platforms to Fight Infections. *J. Nanomater.* 6905631 doi: 10.1155/2020/6905631
- Verma, P., and Tapadia, M. G. (2012). Immune Response and Anti-Microbial Peptides Expression in Malpighian Tubules of Drosophila Melanogaster is Under Developmental Regulation. *PLoS One* 7, e40714. doi: 10.1371/journal.pone.0040714
- Villadóniga, C., and Cantera, A. M. B. (2019). New ACE-Inhibitory Peptides Derived From  $\alpha$ -Lactalbumin Produced by Hydrolysis With *Bromelia antiacantha* Peptidases. *Biocatal. Agric. Biotechnol.* 20, 101258. doi: 10.1016/j.bcab.2019.101258
- Vivero-Escoto, J. L., Slowing, I. I., Trewyn, B. G., and Lin, V. S. (2010). Mesoporous Silica Nanoparticles for Intracellular Controlled Drug Delivery. *Small* 6, 1952–1967. doi: 10.1002/sml.200901789
- Vlieghe, P., Lisowski, V., Martinez, J., and Khrestchatsky, M. (2010). Synthetic Therapeutic Peptides: Science and Market. *Drug Discov. Today* 15, 40–56. doi: 10.1016/j.drudis.2009.10.009
- Vorland, L. H., Ulvatne, H., Andersen, J., Haukland, H., Rekdal, O., Svendsen, J. S., et al. (1998). Lactoferricin of Bovine Origin is More Active Than Lactoferricins of Human, Murine and Caprine Origin. *Scand. J. Infect. Dis.* 30, 513–517. doi: 10.1080/00365549850161557
- Waite, R. D., and Curtis, M. A. (2009). *Pseudomonas Aeruginosa* PAO1 Pyocin Production Affects Population Dynamics Within Mixed-Culture Biofilms. *J. Bacteriol.* 191, 1349–1354. doi: 10.1128/JB.01458-08
- Wang, S. Z., Hu, J. T., Zhang, C., Zhou, W., Chen, X. F., Jiang, L. Y., et al. (2014). The Safety and Efficacy of Daptomycin Versus Other Antibiotics for Skin and Soft-Tissue Infections: A Meta-Analysis of Randomised Controlled Trials. *BMJ Open* 4, e004744. doi: 10.1136/bmjopen-2013-004744
- Wang, M., Huang, M., Zhang, J., Ma, Y., Li, S., and Wang, J. (2017). A Novel Secretion and Online-Cleavage Strategy for Production of Cecropin A in Escherichia Coli. *Sci. Rep.* 7, 7368. doi: 10.1038/s41598-017-07411-5
- Wehkamp, J., Harder, J., Weichenthal, M., Mueller, O., Herrlinger, K. R., Fellermann, et al. (2003). Inducible and Constitutive  $\beta$ -Defensins are Differentially Expressed in Crohn's Disease and Ulcerative Colitis. *Inflamm. Bowel Dis.* 9, 215–223. doi: 10.1097/00054725-200307000-00001
- Wehkamp, J., Salzman, N. H., Porter, E., Nuding, S., Weichenthal, M., Petras, R. E., et al. (2005). Reduced Paneth Cell  $\alpha$ -Defensins in Ileal Crohn's Disease. *Proc. Natl. Acad. Sci.* 102, 18129–18134. doi: 10.1073/pnas.0505256102
- Wicker, C., Reichhart, J. M., Hoffmann, D., Hultmark, D., Samakovlis, C., and Hoffmann, J. A. (1990). Insect Immunity. Characterization of a Drosophila cDNA Encoding a Novel Member of the Dipterocin Family of Immune Peptides. *J. Biol. Chem.* 265, 22493–22498. doi: 10.1016/S0021-9258(18)45732-8
- Woong, S. J., Xuwei, S. L., Sun, J. N., and Edgerton, M. (2008). The P-113 Fragment of Histatin 5 Requires a Specific Peptide Sequence for Intracellular Translocation in *Candida Albicans*, Which is Independent of Cell Wall Binding. *Antimicrob. Agents Chemother.* 52, 497–504. doi: 10.1128/AAC.01199-07



- Wrone-Smith, T., and Nickoloff, B. J. (1996). Dermal Injection of Immunocytes Induces Psoriasis. *J. Clin. Invest.* 98, 1878–1887. doi: 10.1172/JCI118989
- Wu, C. H., Mohammadmoradi, S., Chen, J. Z., Sawada, H., Daugherty, A., and Lu, H. S. (2018). Renin-Angiotensin System and Cardiovascular Functions. *Arterioscler. Thromb. Vasc. Biol.* 38, e108–e116. doi: 10.1038/s41569-019-0244-8
- Wu, Q., Patočka, J., and Kuča, K. (2018). Insect Antimicrobial Peptides, a Mini Review. *Toxins* 10, 461. doi: 10.3390/toxins10110461
- Wu, D., Sun, N., Ding, J., Zhu, B., and Lin, S. (2019). Evaluation and Structure-Activity Relationship Analysis of Antioxidant Shrimp Peptides. *Food. Funct.* 10, 5605–5615. doi: 10.1039/c9fo01280j
- Xu, F., Zhang, J., Wang, Z., Yao, Y., Atungulu, G. G., Ju, X., et al. (2018). Absorption and Metabolism of Peptide Wdhhapqlr Derived From Rapeseed Protein and Inhibition of Huvecs. *J. Agric. Food Chem.* 66, 5178–5189. doi: 10.1021/acs.jafc.8b01620
- Yan, C., Altunbas, A., Yucel, T., Nagarkar, R. P., Schneider, J. P., and Pochan, D. J. (2010). Injectable Solid Hydrogel: Mechanism of Shear-Thinning and Immediate Recovery of Injectable  $\beta$ -Hairpin Peptide Hydrogels. *Soft Matter* 6, 5143–5156. doi: 10.1039/c0sm00642d
- Yan, D., Chen, D., Shen, J., Xiao, G., van Wijnen, A. J., and Im, H. J. (2013). Bovine Lactoferrin is Anti-Inflammatory and Anti-Catabolic in Human Articular Cartilage and Synovium. *J. Cell. Physiol.* 22, 447–456. doi: 10.1002/jcp.24151
- Yang, D., Chen, Q., Schmidt, A. P., Anderson, G. M., Wang, J. M., Wooters, J., et al. (2000). LL-37, the Neutrophil Granule- and Epithelial Cell-Derived Cathelicidin, Utilizes Formyl Peptide Receptor-Like 1 (FPR1) as a Receptor to Chemoattract Human Peripheral Blood Neutrophils, Monocytes, and T Cells. *J. Exp. Med.* 192, 1069–1074. doi: 10.1084/jem.192.7.1069
- Yang, D., Chertov, O., and Oppenheim, J. J. (2001). The Role of Mammalian Antimicrobial Peptides and Proteins in Awakening of Innate Host Defenses and Adaptive Immunity. *Cell. Mol. Life. Sci.* 58, 978–989. doi: 10.1007/PL00000914
- Yang, E. J., Kim, S. H., Yang, S. C., Lee, S. M., and Choi, S. M. (2011). Melittin Restores Proteasome Function in an Animal Model of ALS. *J. Neuroinflammation* 8, 69. doi: 10.1186/1742-2094-8-69
- Yang, X., and Yourself, A. (2018). Antimicrobial Peptides Produced by *Brevibacillus* Spp.: Structure, Classification and Bioactivity: A Mini Review. *World J. Microbiol. Biotechnol.* 34, 57. doi: 10.1007/s11274-018-2437-4
- Yin, C. M., Wong, J. H., Xia, J., and Ng, T. B. (2013). Studies on Anticancer Activities of Lactoferrin and Lactoferricin. *Curr. Protein Pept. Sci.* 14, 492–503. doi: 10.2174/13892037113149990066
- Yu, G., Baeder, D. Y., Regoes, R. R., and Rolff, J. (2016). Combination Effects of Antimicrobial Peptides. *Antimicrob. Agents Chemother.* 60, 1717–1724. doi: 10.1128/AAC.02434-15
- Yu, G., Baeder, D. Y., Regoes, R. R., and Rolff, J. (2018). Predicting Drug Resistance Evolution: Insights From Antimicrobial Peptides and Antibiotics. *Proc. Biol. Sci.* 285, 20172687. doi: 10.1098/rspb.2017.2687
- Zabara, M., Senturk, B., Gontsarik, M., Ren, Q., Rottmar, M., Maniura-Weber, K., et al. (2019). Multifunctional Nano-Biointerfaces: Cytocompatible Antimicrobial Nanocarriers From Stabilizer-Free Cubosomes. *Adv. Funct. Mater.* 29, 1904007. doi: 10.1002/adfm.201904007
- Zasloff, M. (1987). Magainins, a Class of Antimicrobial Peptides From *Xenopus* Skin: Isolation, Characterization of Two Active Forms, and Partial cDNA Sequence of a Precursor. *Proc. Natl. Acad. Sci. U. S. A.* 84, 5449–5453. doi: 10.1073/pnas.84.15.5449
- Zeng, N., Gao, X., Hu, Q., Song, Q., Xia, H., Liu, Z., et al. (2012). Lipid-Based Liquid Crystalline Nanoparticles as Oral Drug Delivery Vehicles for Poorly Water-Soluble Drugs: Cellular Interaction and *In Vivo* Absorption. *Int. J. Nanomedicine* 7, 3703–3718. doi: 10.2147/IJN.S32599
- Zeya, H. I., and Spitznagel, J. K. (1966). Antimicrobial Specificity of Leukocyte Lysosomal Cationic Proteins. *Science* 10154, 1049–1051. doi: 10.1126/science.154.3752.1049
- Zhang, P., Chang, C., Liu, H., Li, B., Yan, Q., and Jiang, Z. (2020). Identification of Novel Angiotensin I-converting Enzyme (ACE) Inhibitory Peptides From Wheat Gluten Hydrolysate by the Protease of *Pseudomonas Aeruginosa*. *J. Funct. Foods* 65, 103751. doi: 10.1016/j.jff.2019.103751
- Zhang, L., Dhillon, P., Yan, H., Farmer, S., and Hancock, R. E. (2000). Interactions of Bacterial Cationic Peptide Antibiotics With Outer and Cytoplasmic Membranes of *Pseudomonas Aeruginosa*. *Antimicrob. Agents Chemother.* 44, 3317–3321. doi: 10.1128/aac.44.12.3317-3321.2000
- Zhang, R., Eckert, T., Lutteke, T., Hanstein, S., Scheidig, A., Bonvin, A. M., et al. (2016). Structure-function Relationships of Antimicrobial Peptides and Proteins With Respect to Contact Molecules on Pathogen Surfaces. *Curr. Top. Med. Chem.* 16, 89–98. doi: 10.2174/1568026615666150703120753
- Zhang, L., and Gallo, R. L. (2016). Antimicrobial Peptides. *Curr. Biol.* 26, 14–19. doi: 10.1016/j.cub.2015.11.017
- Zhang, B., Wang, H., Wang, Y., Yu, Y., Liu, J., Liu, B., et al. (2019). Identification of Antioxidant Peptides Derived From Egg-White Protein and its Protective Effects on H<sub>2</sub>O<sub>2</sub>-induced Cell Damage. *Int. J. Food. Sci. Technol.* 54, 2219–2227. doi: 10.1111/ijfs.14133
- Złotek, U., Jakubczyk, A., Rybczyńska-Tkaczyk, K., Ćwiek, P., Baraniak, B., and Lewicki, S. (2020). Characteristics of New Peptides GQLGEGGAGMG, Gehggagmgggqfpv, EQGFLPGPEESGR, Rlaraglaq, YGNPVGGVGH, and GNPVGGVGHGTTGT as Inhibitors of Enzymes Involved in Metabolic Syndrome and Antimicrobial Potential. *Molecules* 25, 2492. doi: 10.3390/molecules25112492


**Conflict of Interest:** CS, RS, AF and PF were employed by Spinoff XFlies s.r.l.

The remaining authors declare that the research was conducted in the absence of any commercial or financial relationships that could be construed as a potential conflict of interest.

Copyright © 2021 Moretta, Scieuzo, Petrone, Salvia, Manniello, Franco, Lucchetti, Vassallo, Vogel, Sgambato and Falabella. This is an open-access article distributed under the terms of the Creative Commons Attribution License (CC BY). The use, distribution or reproduction in other forums is permitted, provided the original author(s) and the copyright owner(s) are credited and that the original publication in this journal is cited, in accordance with accepted academic practice. No use, distribution or reproduction is permitted which does not comply with these terms.

Article

# Interaction of Temporin-L Analogues with the *E. coli* FtsZ Protein

Angela Di Somma <sup>1</sup>, Carolina Canè <sup>1</sup>, Antonio Moretta <sup>2</sup> and Angela Duilio <sup>1,\*</sup>

<sup>1</sup> Department of Chemical Sciences, Università Federico II di Napoli, 80126 Napoli, Italy; angela.disomma@unina.it (A.D.S.); carolina.cane@unina.it (C.C.)

<sup>2</sup> Department of Science, Università degli Studi della Basilicata, 85100 Potenza, Italy; antonio.moretta@unibas.it

\* Correspondence: angela.duilio@unina.it

**Abstract:** The research of new therapeutic agents to fight bacterial infections has recently focused on the investigation of antimicrobial peptides (AMPs), the most common weapon that all organisms produce to prevent invasion by external pathogens. Among AMPs, the amphibian Temporins constitute a well-known family with high antibacterial properties against Gram-positive and Gram-negative bacteria. In particular, Temporin-L was shown to affect bacterial cell division by inhibiting FtsZ, a tubulin-like protein involved in the crucial step of Z-ring formation at the beginning of the division process. As FtsZ represents a leading target for new antibacterial compounds, in this paper we investigated in detail the interaction of Temporin L with *Escherichia coli* FtsZ and designed two TL analogues in an attempt to increase peptide-protein interactions and to better understand the structural determinants leading to FtsZ inhibition. The results demonstrated that the TL analogues improved their binding to FtsZ, originating stable protein-peptide complexes. Functional studies showed that both peptides were endowed with a high capability of inhibiting both the enzymatic and polymerization activities of the protein. Moreover, the TL analogues were able to inhibit bacterial growth at low micromolar concentrations. These observations may open up the way to the development of novel peptide or peptidomimetic drugs tailored to bind FtsZ, hampering a crucial process of bacterial life that might be proposed for future pharmaceutical applications

**Keywords:** antimicrobial peptide; Temporin-L; FtsZ inhibition; Temporin analogues



**Citation:** Di Somma, A.; Canè, C.; Moretta, A.; Duilio, A. Interaction of Temporin-L Analogues with the *E. coli* FtsZ Protein. *Antibiotics* **2021**, *10*, 704. <https://doi.org/10.3390/antibiotics10060704>

Academic Editor: Jean-Marc Sabatier

Received: 1 May 2021

Accepted: 8 June 2021

Published: 11 June 2021

**Publisher's Note:** MDPI stays neutral with regard to jurisdictional claims in published maps and institutional affiliations.



**Copyright:** © 2021 by the authors. Licensee MDPI, Basel, Switzerland. This article is an open access article distributed under the terms and conditions of the Creative Commons Attribution (CC BY) license (<https://creativecommons.org/licenses/by/4.0/>).

## 1. Introduction

The emergence of resistant bacteria is rising to dangerously high levels worldwide. New resistance mechanisms are emerging and spreading globally, threatening our ability to treat common infectious diseases. Several well-known infections are becoming harder, and sometimes impossible, to treat, as the efficacy of antibiotics is hampered by antimicrobial resistance. The onset of antibiotic resistance is accelerated by the misuse and overuse of antibiotics as these drugs are often overprescribed by health workers and overused by the public [1].

The research and development of new therapeutic agents to fight bacterial infections should then be prioritized. In this respect, growing interest has recently focused on the investigation of antimicrobial peptides (AMPs) as new possible human therapeutics, alone or in combination with current antibiotics. AMPs are produced by several tissues and cell types in a variety of plants and in animal species like insects, amphibians, and vertebrates [2,3]. AMPs are currently considered promising candidates as alternative therapeutic agents because of their broad spectrum of activity against several different microorganisms, their ability to inhibit bacterial growth and decrease the development of bacterial resistance [4,5].

Among AMPs of natural origin, the amphibian Temporins represent one of the largest families with high antibacterial properties against a number of Gram-positive and Gram-

negative bacteria that cause infections such as skin diseases, meningitis and urinary tract infections in human beings [6]. Recently, the mechanism of action of Temporin-L in *E. coli* was completely elucidated, identifying the FtsZ protein as its specific intracellular target [7]. FtsZ belongs to the divisome complex and plays an important role in orchestrating bacterial cell division [8]. Assembly and activation of the divisome machinery are precisely coordinated by the GTPase FtsZ, which polymerizes into a dynamic ring defining the division site, recruiting downstream proteins, and directing peptidoglycan synthesis to drive constriction [9]. Temporin-L is able to specifically bind the FtsZ protein, inhibiting its GTPase activity with a competitive mechanism then hampering cell division.

Since FtsZ is responsible for a crucial biological event of bacterial life and it is absent in humans, this protein might represent a good target for the rational design of new antimicrobial molecules. In this paper, we investigated the interaction of two new Temporin-L analogues with *E. coli* FtsZ. The interaction of native Temporin-L and the two mutated peptides with the protein was evaluated both in silico, through molecular docking analysis, and in vitro by enzymatic and polymerization assays, and the binding parameters were measured by fluorescence analyses. Finally, the antibacterial activity of the two mutated peptides was evaluated by determination of the minimum inhibitory concentration (MIC) compared to native Temporin-L.

Investigation of FtsZ inhibition by antimicrobial peptides might open up the way to the development of new peptide or peptidomimetic drugs able to impair a crucial process of bacterial life by targeting a specific molecule in a reversible way thus avoiding (or slowing down) the onset of antidrug resistance.

## 2. Results

### 2.1. Design of the Mutated Temporin-L Peptides and Molecular Docking Analysis

The antimicrobial peptide Temporin-L (TL) was recently demonstrated to act as a competitive inhibitor toward the *E. coli* FtsZ protein, thus impairing cell division [7]. As FtsZ might represent a good target for the development of new drugs, we were stimulated to investigate this peptide-protein interaction in more detail by docking simulations. FtsZ and TL were modelled using the I-TASSER web server originating the structural models shown in Supplementary Figure S1a,b, respectively. The corresponding model parameters, C-score, TM-score, and RMSD, are listed in Table 1.

**Table 1.** The obtained C-score, TM-score, and RMSD values for the peptides modelled through the I-TASSER server are listed.

Peptide/Protein	C-Score	TM-Score	RMSD (Å)
FtsZ	−0.55	0.64 ± 0.13	7.9 ± 4.4
TL	0.09	0.73 ± 0.11	0.5 ± 0.5
FVKWFKKFLTRIL	0.07	0.72 ± 0.11	0.5 ± 0.5
FVKWFKKFLTRILF	−0.06	0.71 ± 0.12	0.6 ± 0.6

The substituted amino acids are indicated in bold.

Molecular docking experiments were performed to evaluate the FtsZ-TL complexes using the previously obtained models and the PatchDock server; the putative structures were then refined by the FireDock server. Through the PDBsum server, the main interactions at the protein-peptide interface and the involved amino acids could be identified.

Figure 1a,b shows the occurrence of 112 noncovalent interactions and 2 hydrogen bonds involving TL Leu13-FtsZ Gly106 and TL Leu13-FtsZ Thr110 and the putative structure of the complex highlighting the interactions involved at the interface.

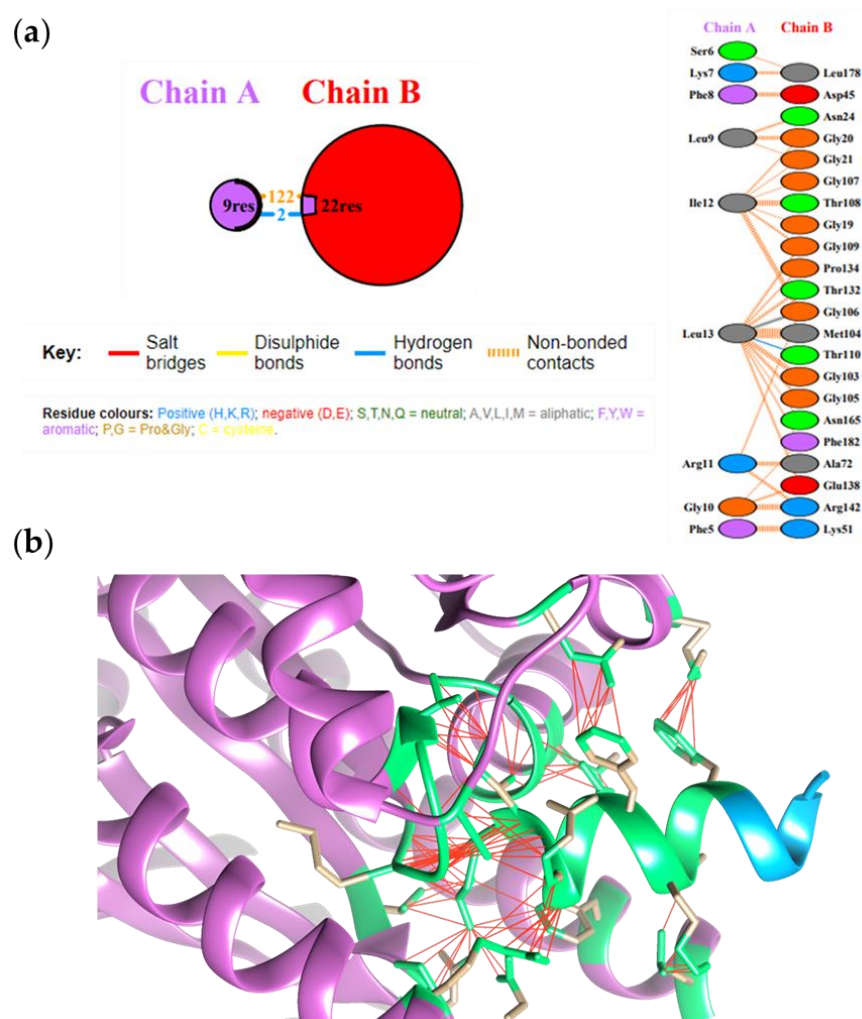


**Figure 1.** (a) Interactions identified at the FtsZ (Chain B)-TL (Chain A) interface. (b) Molecular docking of FtsZ-native TL complex. FtsZ is shown in light magenta, native TL peptide in light blue. The amino acids involved at the peptide-protein interface are in green. Interactions are reported with red lines.

The stability of the complex was evaluated by calculating the global energy, the attractive and repulsive van der Waals forces and the atomic contact energy (ACE). The corresponding values are listed in Table 2 together with the predicted  $\Delta G$  suggesting the formation of a stable peptide-protein complex.

**Table 2.** Global energy, attractive and repulsive van der Waals forces, atomic contact energy, and  $\Delta G$  expressed in Kcal/mol calculated for the FtsZ-TL peptide complexes at 25 °C.

Protein-Peptide Complex	Global Energy (Kcal/mol)	Attractive Van der Waals Forces (KJ/mol)	Repulsive Van der Waals Forces (KJ/mol)
FtsZ-TL	-40.54	-18.63	5.71
FtsZ-TRIL (FVKWFKKFLTRIL)	-26.84	-30.69	18.88
FtsZ-TRILF (FVKWFKKFLTRILF)	-30.99	-46.97	24.35

The substituted amino acids are indicated in bold.

The investigation of the FtsZ-TL complex model suggested by docking simulations prompted us to design specific TL analogues with the aim of improving the peptide–protein interactions and increasing the ability of the peptide to inhibit FtsZ activity. Two mutated Temporin-L peptides were then designed, tailoring the amino acid mutations on the basis of a detailed examination of the docking model and the antibacterial prediction scores calculated by the CAMP (Collection of Antimicrobial Peptides) database. The amino acid sequences of the two mutated TL analogues, TRIL and TRILF are listed in Table 3 together with the prediction scores of their antimicrobial properties generated by using the SVM, DA, RF, and ANN algorithms available in the CAMP database. The data have been compared with those obtained for the native TL.

**Table 3.** Peptide sequences of the designed TL analogs and the corresponding prediction scores generated by four algorithms (SVM, DA, RF, and ANN). Data from native Temporin L are also listed for comparison.

Peptide	SVM	DA	RF	ANN
Native Temporin L FVQWFSKFLGRIL	0.876	0.899	0.9685	AMP
<b>FVKWF</b> KKFLTRIL (TRIL)	0.997	0.981	0.941	AMP
<b>FVKWF</b> KKFLTRILF (TRILF)	0.994	0.973	0.906	AMP

The substituted amino acids are indicated in bold.

A similar or higher putative antibacterial activity for the two TL analogues compared to native TL was predicted by all algorithms.

The models of the two new TL analogues were then built up (Supplementary Figure S1c,d respectively) and their modeling parameters are listed in Table 1. Molecular docking simulations were performed using the same conditions described above and the main interactions at the protein-peptide interface and the involved amino acids identified in both the FtsZ-TRIL and FtsZ-TRILF complexes are shown in Figures 2 and 3, respectively.

A total of 91 noncovalent interactions were detected at the protein-peptide interface for the FtsZ-TRIL complex together with two salt bridges involving TRIL Lys6-FtsZ Asp187 and TRIL Arg11-FtsZ Asp30, and a hydrogen bond between TRIL Lys6 and FtsZ Asp187 (Figure 2).

The FtsZ-TRILF complex model showed 164 noncovalent interactions and the hydrogen bond between TRILF Arg11 and FtsZ Asp45 occurring at the protein-peptide interface (Figure 3).

The stability parameters of both complexes were calculated and are listed in Table 2, together with the predicted  $\Delta G$  values. The *in silico* analyses indicated that both TL analogues were able to form stable peptide-protein complexes with the FtsZ protein suggesting that they were good candidates as inhibitors of its GTPase activity.

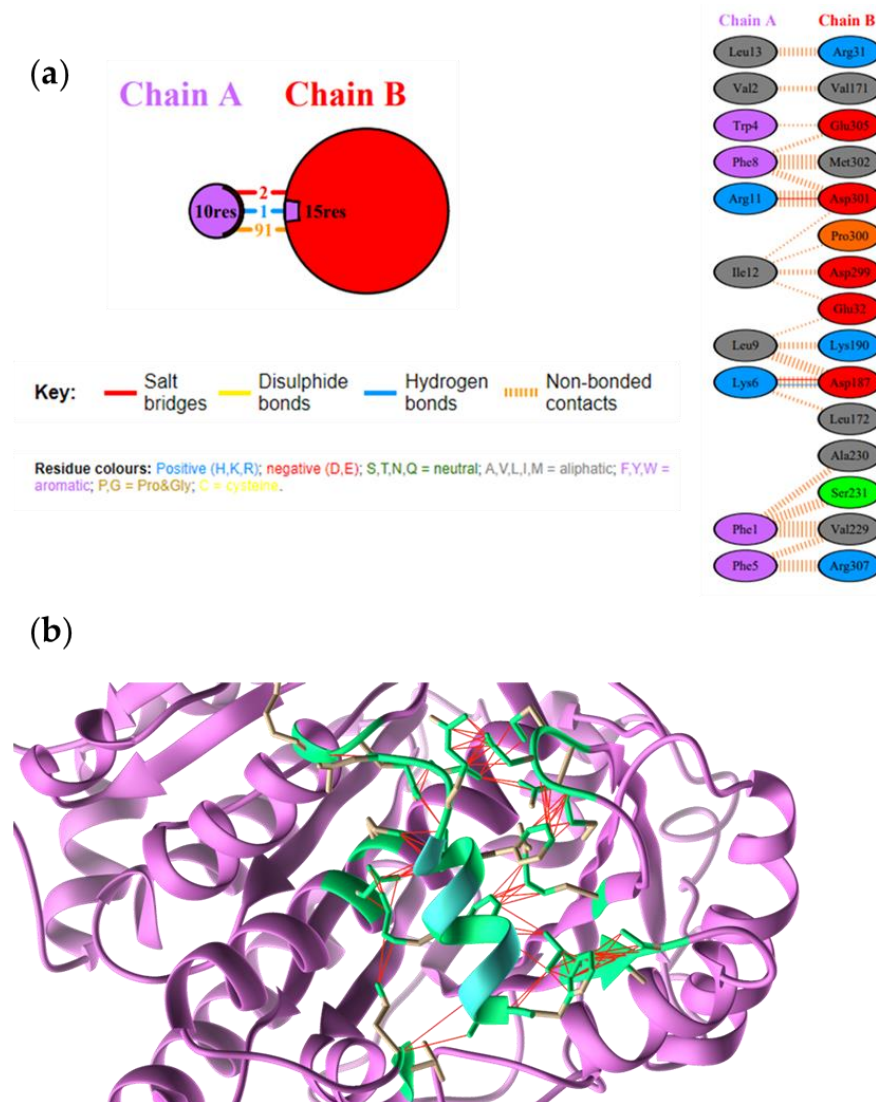


**Figure 2.** (a) Interactions identified at the FtsZ (Chain B)-TRIL (Chain A) interface. (b) Molecular docking of FtsZ–native TRIL complex. FtsZ is shown in light magenta, native TL peptide in light blue. The amino acids involved at the peptide–protein interface are in green. Interactions are reported with red lines.

## 2.2. Binding of the Temporin-L Analogues to FtsZ

As docking calculations suggested the formation of putative FtsZ-TRIL and FtsZ-TRILF complexes, the binding of the two peptides to the FtsZ protein was investigated by fluorescence experiments. A recombinant form of FtsZ was produced in *E. coli*, purified and used in binding and enzymatic assays [7]. A significant decrease of fluorescence intensity of FtsZ with the increased concentrations of antimicrobial peptides was observed in both assays, as shown in Figure 4 where the data from the FtsZ–native TL complex are also reported for comparison.

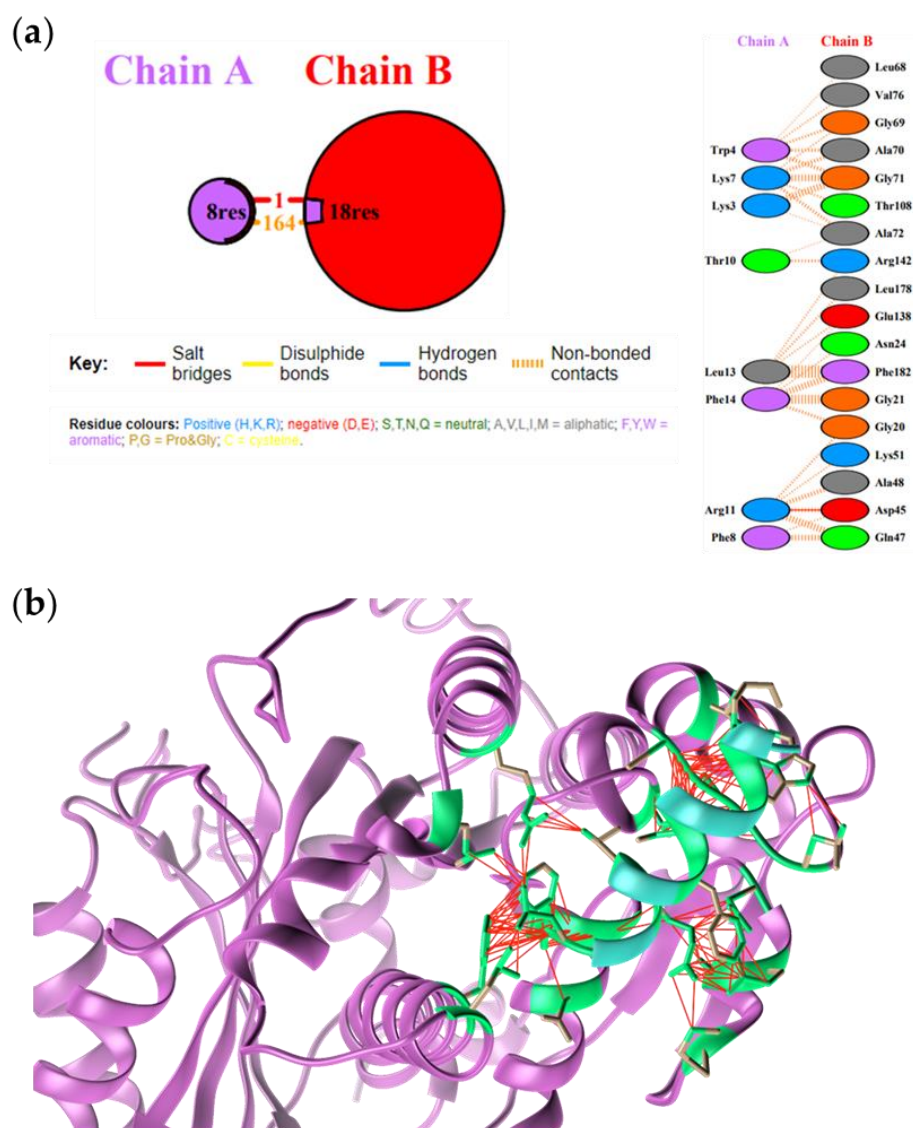


**Figure 3.** (a) Interactions identified at the FtsZ (Chain B)-TRILF (Chain A) interface. (b) Molecular docking of FtsZ–native TRILF complex. FtsZ is shown in light magenta, native TL peptide in light blue. The amino acids involved at the peptide–protein interface are in green. Interactions are reported with red lines.

Moreover, a progressive, although limited, shift from 347 to 340 nm of the maximum emission wavelength could also be detected, demonstrating that the antimicrobial peptides could interact with FtsZ and alter its intrinsic fluorescence.

The dissociation constant of the three complexes were calculated from the fluorescence experiments. The  $K_d$  values for the FtsZ-TL and FtsZ-TRIL complexes were determined as  $11.0 \pm 1.0 \mu\text{M}$  and  $21.4 \pm 1.1 \mu\text{M}$ , respectively, confirming a good interaction between the peptides and the FtsZ protein. Moreover, an even better result was obtained for the FtsZ-TRILF complex whose dissociation constant was measured as  $4.3 \pm 0.2 \mu\text{M}$ , indicating that the insertion of a Phe residue at the C-terminus of TL increased the stability of the interaction with the target protein.

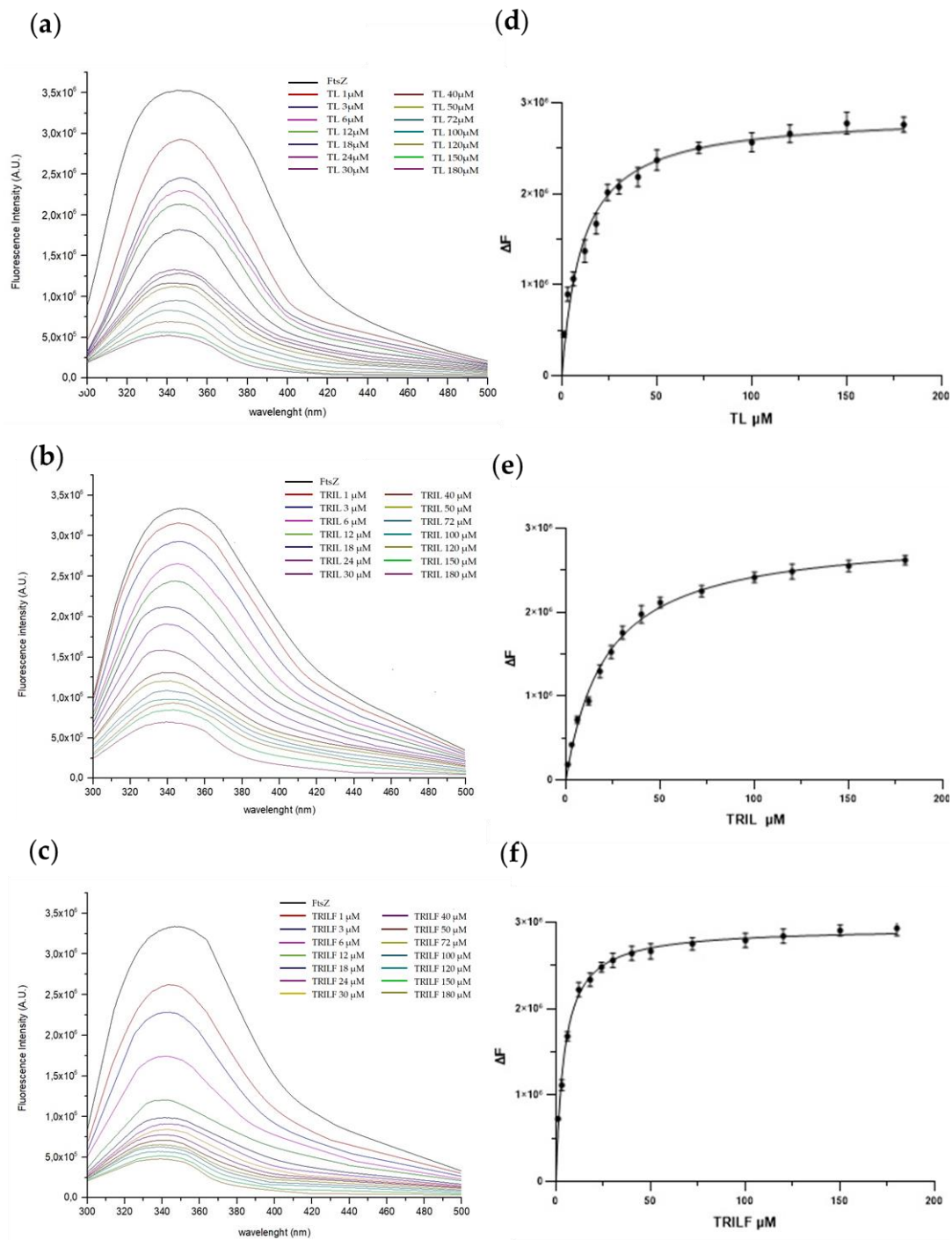


**Figure 4.** Left panel: Spectrofluorimetric titration of FtsZ (12 μM) in complex with native TL (a), TRIL (b) and TRILF (c) from 1 to 180 μM, was performed by monitoring the emissions at 347 nm at 20 °C. Right panel (d–f): Diagram plots extrapolated from fluorescence data. The experiments were performed in duplicate and the standard deviation is reported as error bars.

### 2.3. Effect of TL Analogues on the GTPase Activity of FtsZ

The putative effect of the two TL analogues on FtsZ GTPase activity was evaluated by enzymatic assays. The purified recombinant protein was incubated with GTP in the presence of either TRIL or TRILF peptides (35 μM) and the GTPase activity was monitored in comparison with the untreated protein at different GTP concentrations. The results showed that the FtsZ activity was inhibited by both peptides in a dose-dependent manner, confirming a functional interaction of the antimicrobial peptides with the GTPase. Figure 5



shows the kinetic profiles of the enzymatic assays in the absence and in the presence of the peptides.

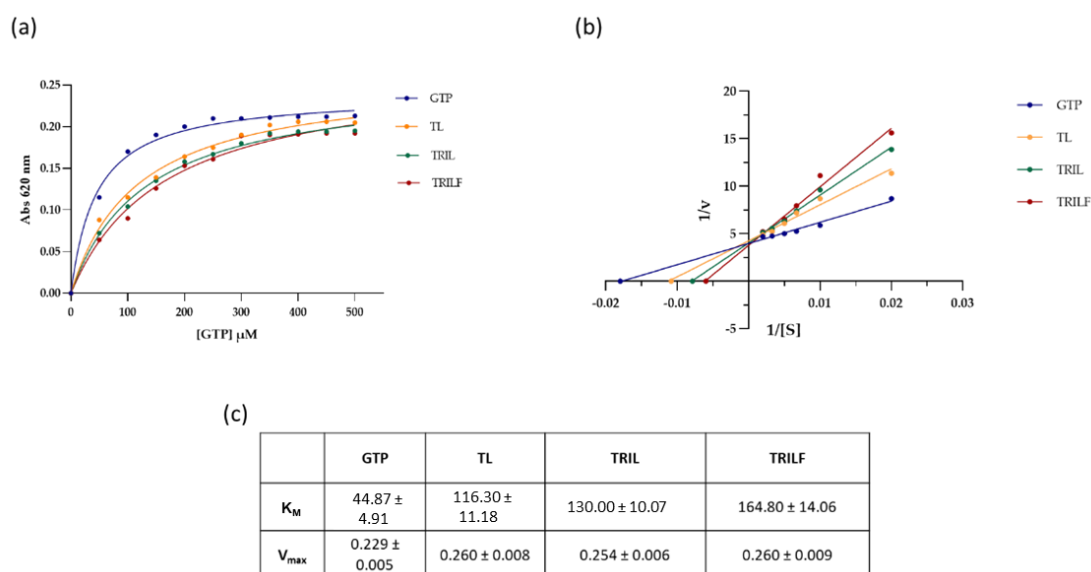


**Figure 5.** (a) Enzymatic activity of recombinant FtsZ (12  $\mu$ M) was performed in 25 mM PIPES/NaOH (pH 6.8), 20 mM  $MgCl_2$ , in the absence (blue line) and in the presence of 35  $\mu$ M TL (yellow line), TRIL (green line) and TRILF (red line) using GTP as substrate. The reaction was performed for 10 min and the  $P_i$  release was determined by measuring the absorbance at 620 nm following 25 min incubation. (b) Lineweaver–Burk plots from which the  $K_M$  constants were calculated. (c) Calculated  $K_M$  constants and  $V_{max}$  for the enzymatic assays. The experiment was performed in duplicate and presented as mean  $\pm$  standard error.

Kinetic parameters were calculated from the Lineweaver-Burk plot (Figure 5b) showing an increase of the apparent  $K_M$  for both peptides,  $130.0 \pm 10.1 \mu$ M for TRIL and  $164.8 \pm 14.1 \mu$ M for TRILF as compared to  $44.9 \pm 4.9 \mu$ M in the absence of the peptides (Figure 5c). These data were compared to the kinetic parameters measured for native TL,  $116.3 \pm 11.2 \mu$ M, indicating that both TRIL and TRILF exerted a stronger inhibitory effect than TL decreasing the affinity of the enzyme for its natural substrate GTP by 65% and 73% respectively. It should be underlined that in all essays, the  $V_{max}$  value remained unchanged, demonstrating that both TL analogues adopted a competitive inhibitory mechanism. The enzymatic activity of FtsZ was also tested in the presence of a different peptide Magainin-2 (Mag-2). Under these conditions, it was clearly demonstrated that this peptide had no effect on the GTP activity since the kinetic parameters were unaltered (Supplementary Figure S2).

#### 2.4. Effect of TL Analogues on the Polymerization of FtsZ

Since FtsZ is known to polymerize into long filaments in the presence of GTP in vitro, we were prompted to investigate the effect of the TL analogues on the polymerization of FtsZ. A simple polymerization assay was then performed by incubating FtsZ with GTP (1 mM) in the absence and in the presence of increasing concentrations of both native TL and the two TL analogues. The FtsZ filaments were purified by centrifugation and analyzed by SDS-PAGE and the amount of protein pelleted was determined by densitometric analysis of the corresponding Coomassie stained gel band.

Figure 6 clearly shows that the amount of polymerized FtsZ decreased when increasing concentrations of either native TL or the two TL analogues were added in the assay. Moreover, FtsZ polymerization was impaired in a dose-dependent manner with TRILF showing the highest inhibition ability, reaching 82% inhibition at 30  $\mu$ M, while TL and TRIL showed 42% and 35% inhibition under the same conditions (Figure 6b).

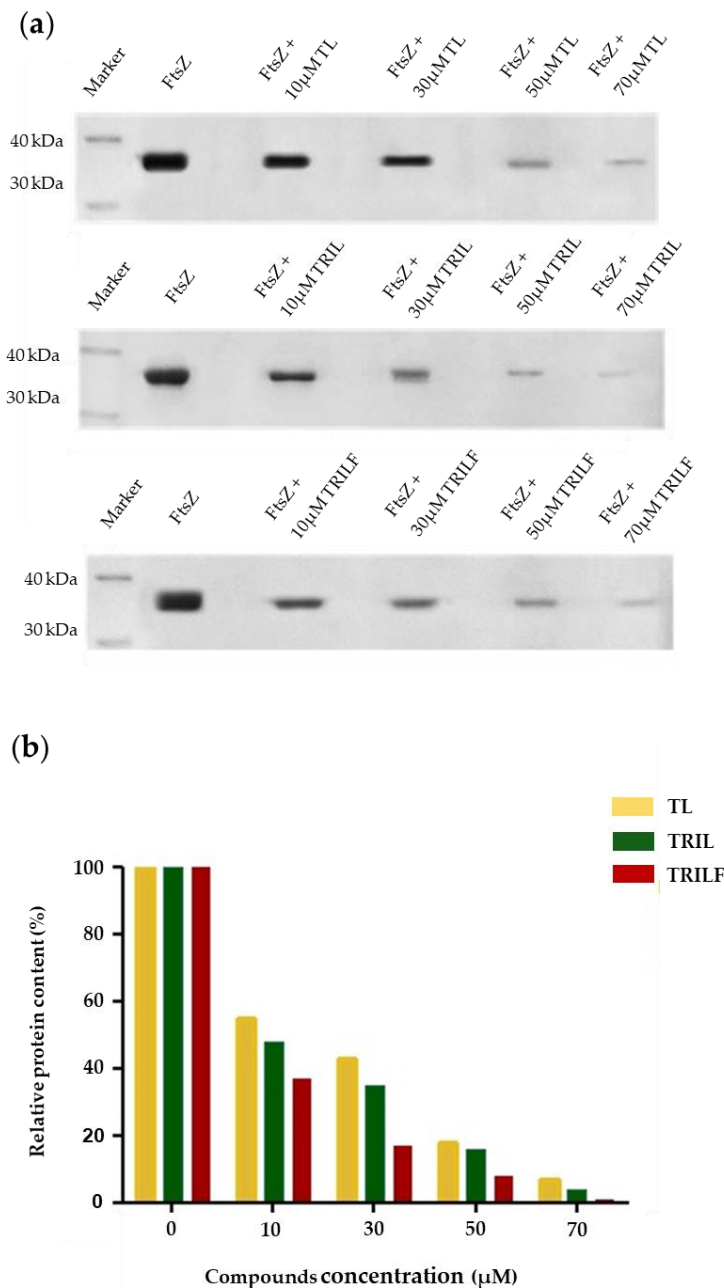


**Figure 6.** Polymerization assay of recombinant FtsZ (12 μM) was carried out in 25 mM PIPES/NaOH, pH 6.8 and 1 mM of GTP in the absence and in the presence of different concentrations of TL, TRIL and TRILF. (a) SDS-PAGE (12.5%) of protein pellet after polymerization reaction. (b) Densitometric analysis of SDS-PAGE in (a), showing the percentage of FtsZ polymerization in the absence and in the presence of TL and TL analogues.

### 2.5. Antimicrobial Activity of TRIL and TRILF

Finally, we evaluated the in vivo antimicrobial activity of TRIL and TRILF on *E. coli* cells. First the minimal inhibitory concentrations (MIC) of both TL analogues were determined by the lowest concentration showing no visible growth after 24 h of incubation, demonstrating that both peptides were highly active against *E. coli* at low micromolar concentrations (MIC = 8 μM).

Next, the growth profile of the *E. coli* cells was evaluated in the presence of different concentrations of the two peptides, as shown in Figure 7.

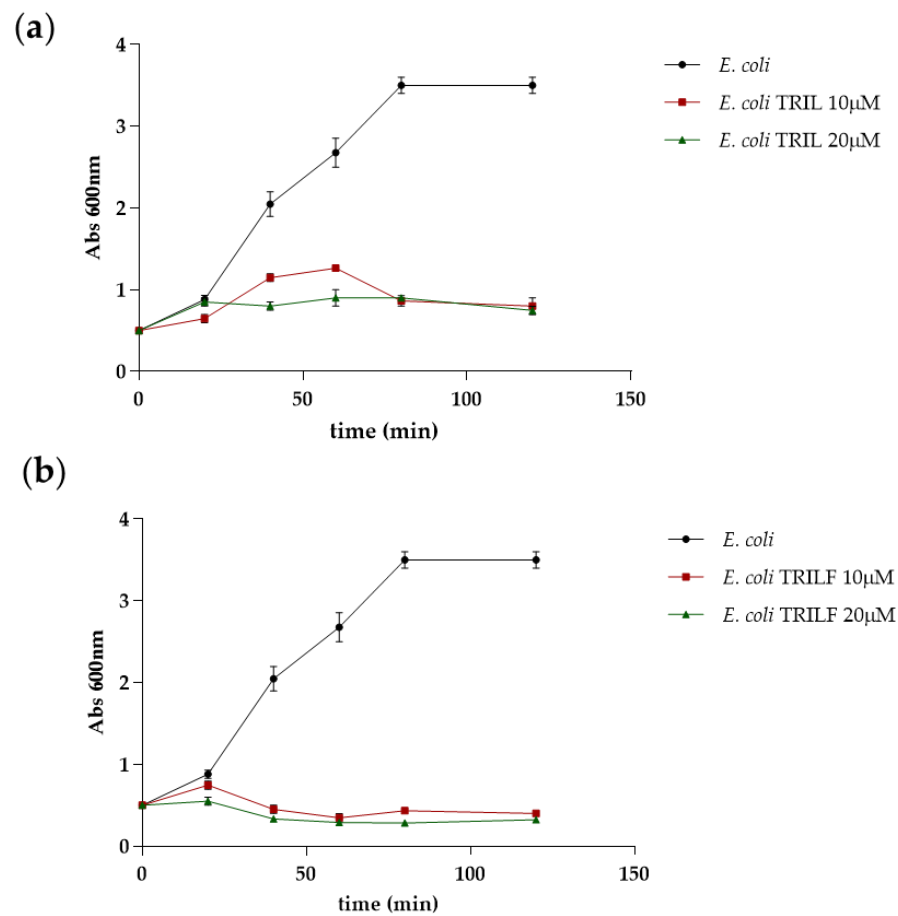


**Figure 7.** Growth profiles of *E. coli* cells in the presence of different concentrations of TRIL (a) and TRILF (b) analogues were obtained by monitoring cells for 120 min at 600 nm. The growth profile in the absence of the peptides is shown for comparison. Experiments were run in duplicate and the standard deviation is reported as error bars.

The growth profiles demonstrated that both peptides are able to inhibit bacterial cell growth with TRILF showing a greater effect being able to totally impair cell growth at 10  $\mu$ M.

In addition, the effect of TRIL and TRILF on *E. coli* was also investigated using a conditional  $\Delta$ ftsZ mutant strain in which the gene coding for FtsZ was silenced when the cells were grown at 42  $^{\circ}$ C.

The growth profile of the  $\Delta$ ftsZ strain was evaluated at 42  $^{\circ}$ C in the absence and in the presence of different concentrations of the two peptides (Figure 8). The growth profiles of the untreated and the treated  $\Delta$ ftsZ mutant strain were almost superimposable, indicating that the two peptides did not exert any effect on the mutant strain. These results suggested that the two TL analogues could affect cell growth only in the presence of FtsZ, confirming this enzyme as their specific target.

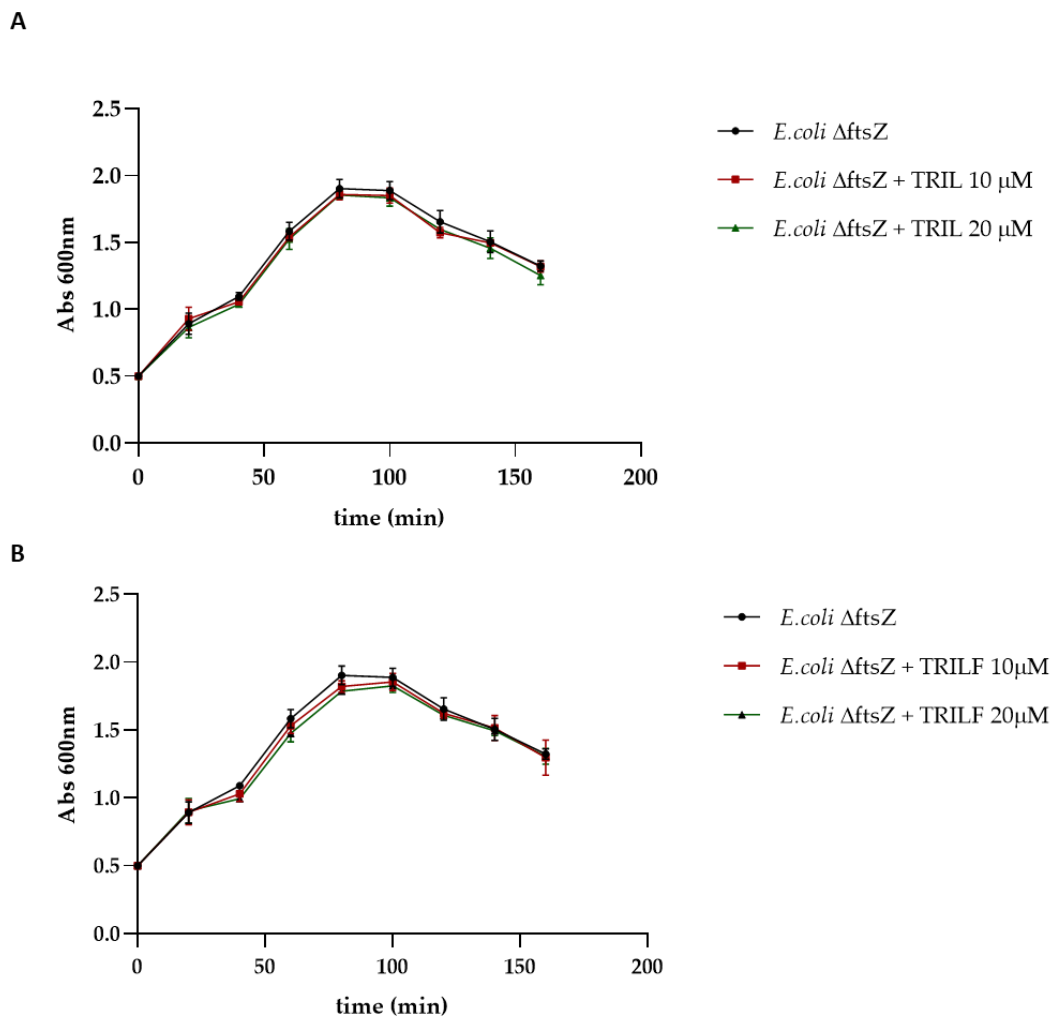


**Figure 8.** Growth profiles of  $\Delta$ ftsZ strain in the absence and in the presence of different concentrations of TRIL (A) and TRILF (B) analogues obtained by monitoring cells for 300 min at 600 nm. Experiments were run in duplicate and the standard deviation is reported as error bars.

### 3. Discussion

Temporin L belongs to a well-known family of small, linear antibiotic peptides with intriguing biological properties and displaying the highest activity among the temporins studied so far, against both bacterial and fungal strains. Since the discovery of temporins in 1996 [10], these peptides have been considered as potential pharmaceutical candidates [11], although their mechanism of action is mostly unknown. In particular, the interaction of Temporin L with both model biomembranes [12], liposomes of different lipid compositions [13] and bacterial membranes [14,15] was carefully examined.

Recently, we investigated the mechanism of action of Temporin L on *E. coli*, showing that the peptide enters the cells interacting with a specific intracellular target, FtsZ, a tubulin-like protein endowed with GTPase activity. FtsZ is a key factor in the divisome complex and inhibition of its GTPase activity by TL impairs cell division [7]. Nowadays, FtsZ is recognized as a leading target in the search for new antibacterial compounds, since it is an essential protein for cell division in most bacteria and is absent in humans [16]. A large number of FtsZ inhibitors, including peptides, natural products, and other synthetic small molecules, have been proposed which might lead to the discovery of novel FtsZ-targeting clinical drugs [17].

On this basis, we were stimulated to examine in more detail the interaction of Temporin L with *E. coli* FtsZ. A model of the peptide-protein complex was then constructed by

docking simulation, showing a good thermodynamic stability, and the main interactions occurring at the complex interface were predicted. Docking calculations suggested that TL interacts with FtsZ close to the GTP binding pocket, making interactions mainly with helices H1, H6, H7 and H8 and strands S4 and S5.

Using the TL-FtsZ model as a guideline, two TL analogues were designed in an attempt to increase peptide-protein interactions and to better understand the structural determinants leading to FtsZ inhibition. Several Temporin L analogues have already been proposed and their properties tested with the aim of increasing the antimicrobial activity of the peptide and decreasing its cytotoxic effects [18]. We focused on TL analogues endowed with higher capability of binding to FtsZ and inhibiting its enzymatic activity.

As suggested by the docking model, all the hydrophobic amino acids have not been replaced because they are involved in a patchwork of hydrophobic interactions with the FtsZ protein. Furthermore, the positively charged residues (Arg and Lys) were left unchanged since they are essential for antibacterial activity, allowing electrostatic interactions with bacterial membranes. Sequence mutations were then introduced at positions 3, 6 and 10 of TL where Lys, Lys and Thr replaced the naturally occurring Gln, Ser and Gly respectively, to ameliorate peptide-protein contacts within the GTP binding site. A further Phe residue was added at the C-terminus of the second TL analogue as the model displayed a sufficiently large cavity to accommodate the hydrophobic ring of the Phe residue.

The TRIL and TRILF analogues were modeled in a complex with *E. coli* FtsZ and the docking calculations predicted an increased stability of both complexes, indicating the correctness of the tailored sequence modifications. Model predictions were then confirmed by investigating the interaction of the two TL analogues with the protein target and their ability to inhibit both FtsZ assembly and GTPase activities on experimental bases.

Fluorescence binding assays performed at different concentrations of TRIL and TRILF analogues demonstrated that both peptides can bind FtsZ, originating stable protein-peptide complexes with dissociation constants in the low micromolar range, thus confirming the docking predictions. A functional investigation of the TL analogues was performed by both enzymatic assays and FtsZ polymerization tests. Both peptides were found to be competitive inhibitors of the GTPase activity of FtsZ, showing a 3–4 times increase in the  $K_M$  of the enzyme for GTP. Moreover, the TL analogues impaired FtsZ polymerization in a dose dependent manner with TRILF showing the highest inhibition capability. Finally, the antibacterial properties of the TL analogues were tested *in vivo* on *E. coli* cells showing that both peptides were able to inhibit bacterial growth at low micromolar concentrations. In Mangoni et al., 2011 [18] different Temporin-L analogues were designed and the authors evaluated their antibacterial activity, obtaining MIC values ranging from 3 to >48  $\mu\text{M}$ . These results indicate that the MIC values obtained for TRIL and TRILF represent a good result, considering that these sequences also show an excellent interaction with the FtsZ protein target.

Our data suggest that a careful inspection of peptide-FtsZ complexes might be instrumental in understanding the main structural determinants leading to enzyme inhibition. Moreover, the competitive inhibitory mechanism exerted by the TL peptides and the  $K_D$  values of the corresponding complexes suggest a reversible mode of action that might impair or delay the onset of bacterial resistance. These observations may open up the way to the development of novel peptide or peptidomimetic drugs tailored to bind FtsZ, exerting a competitive inhibitory activity on this crucial enzyme that might be proposed for future pharmaceutical applications.

## 4. Materials and Methods

### 4.1. Design of the Temporin-L Analogues and Molecular Docking Analyses

The FtsZ protein, native TL and the TL analogues were modelled through the I-TASSER webserver [19,20], which associates to each model a C-score whose value ranges from  $-5$  to  $+2$ . The higher the value, the better the model. The TM-score and RMSD are

known standards for measuring structural similarity between two structures. A TM-score value  $>0.5$  indicates a model of correct topology [21].

The obtained models in .pdb format were exploited to perform the molecular docking analyses using the PatchDock Server [22]. The protein-peptide complexes were then refined with FireDock Server [23], which also gave the global energy, the attractive and repulsive van der Waals (VdW) forces and the atomic contact energy (ACE) values. The PDBsum Server [24,25] was used in order to identify all the interactions and the amino acids involved at the protein-peptide interface. The Gibbs free energy,  $\Delta G$ , and the dissociation constant,  $K_d$ , of the complex have been predicted using the PRODIGY webserver [26]. All the figures have been generated through UCSF CHIMERA software [27].

The two TL analogues were designed on the basis of the FtsZ-native TL complex predicted by docking analysis trying to increase the peptide-protein interactions. Amino acid substitutions were introduced at positions 3 (Q3K), 6 (S6K) and 10 (G10T), leaving all the hydrophobic residues unchanged. Moreover, a Phe residue was added at the C-terminus of the second TL analogous to increase the hydrophobic interaction occurring at the protein-peptide interface as docking simulation showed the occurrence of a large cavity in that area in the FtsZ-TL complex.

The antibacterial activity predictions scores of native TL were calculated by the CAMP (Collection of Antimicrobial Peptides) database [28], which exploits four different machine-learning algorithms: Support Vector Machine (SVM), Discriminant Analysis (DA), Artificial Neural Network (ANN) and Random Forest (RF). The results are given in the form of a numerical score except for the Artificial Neural Network (ANN), where the result is indicated as AMP (antimicrobial) or NAMP (non-antimicrobial).

#### 4.2. Recombinant Production of FtsZ

Recombinant *E. coli* FtsZ was overexpressed and purified from *E. coli* BL21 strain as described previously [7]. The purity of the protein was analyzed by SDS-PAGE 12.5% and its primary structure was validated by MALDI mapping strategy on a 5800 MALDI-TOF/TOF instrument (ABI Sciex, Foster City, CA, USA). The concentration of purified FtsZ was determined by Bradford's method [29], using BSA as a standard. The protein was stored at  $-80\text{ }^{\circ}\text{C}$ .

#### 4.3. Binding Experiment

Fluorescence experiments were performed using a Fluoromax-4 spectrofluorometer from Horiba Scientific, using 1 cm optical path-length quartz cell under controlled temperature conditions (Peltier control system at  $20\text{ }^{\circ}\text{C}$ ). The sample was analyzed, monitoring the fluorescence intensity of aromatic residues with an excitation wavelength of 280 nm. The wavelength range explored was 295–500 nm. FtsZ protein at a concentration of  $12\text{ }\mu\text{M}$  was excited at 280 nm (slit 4 nm) and the emission was monitored at 347 nm (slit 4 nm) without and in the presence of increasing concentrations of TL, TRIL and TRILF (from 1 to  $180\text{ }\mu\text{M}$ ) in a high voltage mode. All experiments were repeated in duplicate. The change in the fluorescence intensity of the reaction set was fitted into "one site-specific binding" equation of GraphPad Prism 5 (GraphPad Software, San Diego, CA, USA).

#### 4.4. GTPase Activity Assay

The amount of Pi released during the assembly of FtsZ was measured using BIOMOL Green phosphate reagent (Biomol, Milan, Italy) as described earlier [7]. Briefly, FtsZ ( $6\text{ }\mu\text{M}$ ) was incubated with different concentrations of GTP, ranging from  $0\text{ }\mu\text{M}$  to  $250\text{ }\mu\text{M}$ , either in the absence or in the presence of  $35\text{ }\mu\text{M}$  TL, TRIL and TRILF in  $25\text{ mM}$  PIPES/NaOH, pH 6.8 for 30 min at  $30\text{ }^{\circ}\text{C}$ . The reaction was performed for 10 min and stopped by addition of  $100\text{ }\mu\text{L}$  BIOMOL Green reagent. The Pi release was determined after incubation at  $25\text{ }^{\circ}\text{C}$  for 25 min by measuring the absorbance at 620 nm. The background was subtracted from all the readings. The experiment was performed in duplicate. Kinetic parameters were fitted by nonlinear regression with GraphPad Prism 4Project.

#### 4.5. Polymerization Assay

Polymerization assays were carried out as described in Zheng et al. [30]. *Escherichia coli* FtsZ protein was diluted at a final concentration of 12  $\mu\text{M}$  in 25 mM PIPES/NaOH, pH 6.8. Different concentrations of TL, TRIL and TRILF (10, 30, 50, 70  $\mu\text{M}$ ) was added to the protein and the polymerization reaction of FtsZ was carried out in the presence of 1 mM GTP at 25 °C for 1 h. Then the reaction was stopped by centrifugation at 14,000 rpm for 60 min and pellets were re-suspended in 25 mM PIPES/NaOH, pH 6.8 and analyzed by 12.5% SDS-PAGE gel. Gels were stained with Coomassie Brilliant Blue and the protein content of bands was measured by densitometric quantification using Quantity One software. Each assay was carried out in triplicates.

#### 4.6. Determination of Antibacterial Activity of TRIL and TRILF

The minimum inhibitory concentration (MIC) of TRIL and TRILF was measured by broth microdilution. The cell strain of *E. coli* BL<sub>21</sub> was incubated overnight in LB at 37 °C. The culture was diluted to obtain a concentration of 0.08 OD<sub>600</sub>/mL in fresh medium and grown at 37 °C for 90 min. At an OD/mL value of 0.5, 50  $\mu\text{L}$  of bacterial suspension was added to ten wells and incubated with serial dilutions of the peptides from an initial concentration of 512  $\mu\text{M}$ . The sterility control well contained 100  $\mu\text{L}$  of LB, while the growth control well contained 100  $\mu\text{L}$  of microbial suspension. The MIC was determined by the lowest concentration showing no visible growth after 24 h of incubation at 37 °C by measuring the Abs at 600 nm. The assay was performed in triplicate.

In addition, *E. coli* cells at 0.5 OD/mL were treated with different concentrations of compounds (1  $\times$  MIC and 2  $\times$  MIC) and the growth was monitored every 20 min reading optical density at 600 nm. The  $\Delta\text{ftsZ}$  cells (a kind gift from Prof. Miguel's group) were grown at 37 °C in LB medium supplemented with 50  $\mu\text{g}/\text{mL}$  kanamycin and subsequently transferred at 42 °C to silence *ftsZ* and treated with different concentrations of compounds. The *ftsZ* thermosensitive mutant has been constructed in which the *ftsZ* gene has been deleted from the *Escherichia coli* chromosome while maintaining a wild-type copy of the gene in a thermosensitive plasmid. [31–33].

**Supplementary Materials:** The following are available online at <https://www.mdpi.com/article/10.3390/antibiotics10060704/s1>, Figure S1: 3D model of FtsZ (a), native Temporin L (b), TRIL analogue (c), and TRILF analogue (d), obtained by ab initio modelling with I-TASSER server. Figure S2: (a) Enzymatic activity of recombinant FtsZ (12  $\mu\text{M}$ ) was performed in 25 mM PIPES/NaOH (pH 6.8), 20mM MgCl<sub>2</sub>, in the absence (blue line) and in the presence of 35 $\mu\text{M}$  of Mag-2 peptide (magenta line), using GTP as substrate. The reaction was performed for 10 min and the Pi release was determined by measuring the absorbance at 620 nm following 25 min incubation. (b) Lineweaver Burk plots from which the KM constants were calculated. (c) Calculated KM constants and Vmax for the enzymatic assays. The experiment was performed in duplicate and presented as mean  $\pm$  standard error.

**Author Contributions:** Conceptualization, A.D.S. and A.D.; validation A.D.S., C.C.; investigation A.D.S., A.M., C.C.; writing—original draft preparation, A.D.S., A.M., C.C., A.D.; writing—review and editing, A.D.; visualization, A.D.S., A.M., C.C., A.D.; All authors have read and agreed to the published version of the manuscript.

**Funding:** This research was funded by MIUR grants ARS01\_00597 Project “NAOCON” and PRIN 2017 “Identification and characterization of novel antitumoral/antimicrobial insect-derived peptides: a multidisciplinary, integrated approach from in silico to in vivo”.

**Data Availability Statement:** Data is contained within the article or Supplementary Material.

**Conflicts of Interest:** The authors declare no conflict of interest.

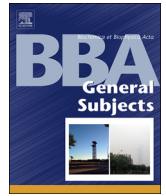
## References

1. Munita, J.M.; Arias, C.A. Mechanisms of Antibiotic Resistance. *Syst. Rev. Pharm.* **2020**, *11*, 817–823.
2. Boparai, J.K.; Sharma, P.K. Mini review on antimicrobial peptides, sources, mechanism and recent applications. *Protein Pept. Lett.* **2020**, *27*, 4–16. [CrossRef]

3. Chen, C.H.; Lu, T.K. Development and challenges of antimicrobial peptides for therapeutic applications. *Antibiotics* **2020**, *9*, 24. [[CrossRef](#)]
4. Lewies, A.; Du Plessis, L.H.; Wentzel, J.F. Antimicrobial peptides: The Achilles' heel of antibiotic resistance. *Probiotics Antimicrob. Proteins* **2019**, *11*, 370–381. [[CrossRef](#)]
5. Datta, S.; Roy, A. Antimicrobial peptides as potential therapeutic agents: A review. *IJPRT* **2021**, *27*, 555–577.
6. Brancaccio, D.; Pizzo, E.; Cafaro, V.; Notomista, E.; De Lise, F.; Bosso, A.; Carotenuto, A. Antimicrobial peptide Temporin-L complexed with anionic cyclodextrins results in a potent and safe agent against sessile bacteria. *Int. J. Pharm.* **2020**, *584*, 119437. [[CrossRef](#)]
7. Di Somma, A.; Avitabile, C.; Cirillo, A.; Moretta, A.; Merlino, A.; Paduano, L.; Duilio, A.; Romanelli, A. The antimicrobial peptide Temporin L impairs *E. Coli* cell division by interacting with FtsZ and the divisome complex. *BBA Gen. Subj.* **2020**, *1864*, 129606. [[CrossRef](#)]
8. Barrows, J.M.; Goley, E.D. FtsZ dynamics in bacterial division: What, how, and why? *Curr. Opin. Cell Biol.* **2021**, *68*, 163–172. [[CrossRef](#)]
9. Baranova, N.; Radler, P.; Hernández-Rocamora, V.M.; Alfonso, C.; López-Pelegrin, M.; Rivas, G.; Loose, M. Diffusion and capture permits dynamic coupling between treadmilling FtsZ filaments and cell division proteins. *Nat. Microbiol.* **2020**, *5*, 407–417. [[CrossRef](#)] [[PubMed](#)]
10. Simmaco, M.; Mignogna, G.; Canofeni, S.; Miele, R.; Mangoni, M.L.; Barra, D. Temporins, antimicrobial peptides from the European red frog *Rana temporaria*. *Eur. J. Biochem.* **1996**, *242*, 788–792. [[CrossRef](#)]
11. Romero, S.M.; Cardillo, A.B.; Martínez Ceron, M.C.; Camperi, S.A.; Giudicessi, S.L. Temporins: An Approach of Potential Pharmaceutical Candidates. *SIS* **2020**, *21*, 309–322. [[CrossRef](#)]
12. Manzo, G.; Ferguson, P.M.; Hind, C.K.; Clifford, M.; Gustilo, V.B.; Ali, H.; Bansal, S.; Bui, T.; Drake, A.F.; Atkinson, R.A.; et al. Temporin L and aurein 2.5 have identical conformations but subtly distinct membrane and antibacterial activities. *Sci. Rep.* **2019**, *9*, 10934. [[CrossRef](#)]
13. Rinaldi, A.C.; Mangoni, M.L.; Rufo, A.; Luzi, C.; Barra, D.; Zhao, H.; Kinnunen, P.K.J.; Bozzi, A.; Di Giulio, A.; Simmaco, M. Temporin L: Antimicrobial, haemolytic and cytotoxic activities, and effects on membrane permeabilization in lipid vesicles. *Biochem. J.* **2002**, *368*, 91–100. [[CrossRef](#)]
14. Mangoni, M.L.; Papo, N.; Barra, D.; Simmaco, M.; Bozzi, A.; Di Giulio, A.; Rinaldi, A.C. Effects of the antimicrobial peptide temporin L on cell morphology, membrane permeability and viability of *Escherichia coli*. *Biochem. J.* **2004**, *380*, 859–865. [[CrossRef](#)]
15. Bellavita, R.; Falanga, A.; Buommino, E.; Merlino, F.; Casciaro, B.; Cappiello, F.; Mangoni, M.L.; Novellino, E.; Catania, M.R.; Polillo, R.; et al. Novel temporin L antimicrobial peptides: Promoting self-assembling by lipidic tags to tackle superbugs. *J. Enzym. Inhib. Med. Chem.* **2020**, *35*, 1751–1764. [[CrossRef](#)]
16. Zorrilla, S.; Monterroso, B.; Robles-Ramos, M.Á.; Margolin, W.; Rivas, G. FtsZ Interactions and Biomolecular Condensates as Potential Targets for New Antibiotics. *Antibiotics* **2021**, *10*, 254. [[CrossRef](#)]
17. Han, H.; Wang, Z.; Li, T.; Teng, D.; Mao, R.; Hao, Y.; Yang, N.; Wang, X.; Wang, J. Recent progress of bacterial FtsZ inhibitors with a focus on peptides. *FEBS J.* **2021**, *288*, 1091–1106. [[CrossRef](#)]
18. Mangoni, M.L.; Carotenuto, A.; Auriemma, L.; Saviello, M.R.; Campiglia, P.; Gomez-Monterrey, I.; Malfi, S.; Marcellini, L.; Barra, D.; Novellino, E.; et al. Structure-activity relationship, conformational and biological studies of temporin L analogues. *J. Med. Chem.* **2011**, *54*, 1298–1307. [[CrossRef](#)]
19. Yang, J.; Yan, R.; Roy, A.; Xu, D.; Poisson, J.; Zhang, Y. The I-TASSER Suite: Protein structure and function prediction. *Nat. Methods* **2015**, *12*, 7–8. [[CrossRef](#)] [[PubMed](#)]
20. Yang, J.; Zhang, Y. I-TASSER server: New development for protein structure and function predictions. *Nucleic Acids Res.* **2015**, *43*, W174–W181. [[CrossRef](#)] [[PubMed](#)]
21. Zhang, Y. I-TASSER server for protein 3D structure prediction. *BMC Bioinform.* **2008**, *9*, 1–8. [[CrossRef](#)]
22. Schneidman-Duhovny, D.; Inbar, Y.; Nussinov, R.; Wolfson, H.J. PatchDock and SymmDock: Servers for rigid and symmetric docking. *Nucleic Acids Res.* **2005**, *33*, W363–W367. [[CrossRef](#)]
23. Mashiaev, E.; Schneidman-Duhovny, D.; Andrusier, N.; Nussinov, R.; Wolfson, H.J. FireDock: A web server for fast interaction refinement in molecular docking. *Nucleic Acids Res.* **2008**, *36*, W229–W232. [[CrossRef](#)]
24. Laskowski, R.A. PDBsum new things. *Nucleic Acids Res.* **2008**, *37*, D355–D359. [[CrossRef](#)]
25. Laskowski, R.A. PDBsum: Summaries and analyses of PDB structures. *Nucleic Acids Res.* **2001**, *29*, 221–222. [[CrossRef](#)]
26. Xue, L.C.; Rodrigues, J.P.; Kastriitis, P.L.; Bonvin, A.M.; Vangone, A. PRODIGY: A web server for predicting the binding affinity of protein–protein complexes. *Bioinformatics* **2016**, *32*, 3676–3678. [[CrossRef](#)]
27. Pettersen, E.F.; Goddard, T.D.; Huang, C.C.; Couch, G.S.; Greenblatt, D.M.; Meng, E.C.; Ferrin, T.E. UCSF Chimera—A visualization system for exploratory research and analysis. *J. Comput. Chem.* **2004**, *25*, 1605–1612. [[CrossRef](#)]
28. Wagh, F.H.; Barai, R.S.; Gurung, P.; Idicula, T.S. CAMPR3: A database on sequences, structures and signatures of antimicrobial peptides. *Nucleic Acids Res.* **2015**, *44*, D1094–D1097. [[CrossRef](#)]
29. Bradford, M.M. A rapid and sensitive method for the quantitation of microgram quantities of protein utilizing the principle of protein-dye binding. *Anal. Biochem.* **1976**, *72*, 248–254. [[CrossRef](#)]
30. Zheng, T.Y.; Du, R.L.; Cai, S.Y.; Liu, Z.H.; Fang, Z.Y.; Liu, T.; Wong, K.Y. Study of benzofuroquinolinium derivatives as a new class of potent antibacterial agent and the mode of inhibition targeting FtsZ. *Front. Microb.* **2018**, *9*, 1937. [[CrossRef](#)]



31. Pazos, M.; Casanova, M.; Palacios, P.; Margolin, W.; Natale, P.; Vicente, M. FtsZ placement in nucleoid-free bacteria. *PLoS ONE* **2014**, *9*, e91984. [[CrossRef](#)] [[PubMed](#)]
32. Pla, J.; Palacios, P.; Sánchez, M.; Garrido, T.; Vicente, M. Stability of components of the Escherichia coli Septator. In *Bacterial Growth and Lysis*; Springer: Boston, MA, USA, 1993; pp. 363–368.
33. Pla, J.; Sanchez, M.; Patacios, P.; Vicente, M.; Aldea, M. Preferential cytoplasmic location of FtsZ, a protein essential for Escherichia coli septation. *Mol. Microbiol.* **1991**, *5*, 1681–1686. [[CrossRef](#)] [[PubMed](#)]



# The antimicrobial peptide Temporin L impairs *E. coli* cell division by interacting with FtsZ and the divisome complex

Angela Di Somma<sup>a,e,\*</sup>, Concetta Avitabile<sup>b,1</sup>, Arianna Cirillo<sup>a</sup>, Antonio Moretta<sup>c</sup>, Antonello Merlino<sup>a</sup>, Luigi Paduano<sup>a</sup>, Angela Duilio<sup>a</sup>, Alessandra Romanelli<sup>d,\*</sup>

<sup>a</sup> Department of Chemical Sciences, University of Naples "Federico II" Via Cinthia 4, 80126 Napoli, Italy

<sup>b</sup> Institute of Biostructures and Bioimaging (CNR), via Mezzocannone 16, 80134 Napoli, Italy

<sup>c</sup> Department of Sciences, University of Basilicata, Potenza, Italy

<sup>d</sup> Department of Pharmaceutical Sciences, University of Milan, Via Venezian 21, 20133 Milan, Italy

<sup>e</sup> National Institute of Biostructures and Biosystems (INBB), Viale Medaglie d'Oro 305, 00136 Roma, Italy

## ARTICLE INFO

### Keywords:

Temporin L  
FtsZ  
Proteomics  
Cell division  
Inhibitor  
Antimicrobial  
Peptide  
Small angle neutron scattering

## ABSTRACT

**Background:** The comprehension of the mechanism of action of antimicrobial peptides is fundamental for the design of new antibiotics. Studies performed looking at the interaction of peptides with bacterial cells offer a faithful picture of what really happens in nature.

**Methods:** In this work we focused on the interaction of the peptide Temporin L with *E. coli* cells, using a variety of biochemical and biophysical techniques that include: functional proteomics, docking, optical microscopy, TEM, DLS, SANS, fluorescence.

**Results:** We identified bacterial proteins specifically interacting with the peptides that belong to the divisome machinery; our data suggest that the GTPase FtsZ is the specific peptide target. Docking experiments supported the FtsZ-TL interaction; binding and enzymatic assays using recombinant FtsZ confirmed this hypothesis and revealed a competitive inhibition mechanism. Optical microscopy and TEM measurements demonstrated that, upon incubation with the peptide, bacterial cells are unable to divide forming long necklace-like cell filaments. Dynamic light scattering studies and Small Angle Neutron Scattering experiments performed on treated and untreated bacterial cells, indicated a change at the nanoscale level of the bacterial membrane.

**Conclusions:** The peptide temporin L acts by a non-membrane-lytic mechanism of action, inhibiting the divisome machinery.

**General significance:** Identification of targets of antimicrobial peptides is pivotal to the tailored design of new antimicrobials.

## 1. Introduction

The growing demand of new antibiotics active against multi-resistant bacteria has encouraged the research of antimicrobial agents from natural sources. Peptides are the most common weapon that organisms from all domains of life produce to prevent the invasion by external pathogens. Antimicrobial peptides (AMPs) are short peptides consisting of 10–50 amino acids, often containing multiple hydrophobic and positively charged residues [1]. Unlike common antibiotics, AMPs, alone and in combination with other antibiotics, are less prone to trigger resistance or transient cross-resistance and mainly act against bacterial cells [2,3].

However, the possible exploitation of AMPs as new antibacterial

drugs is strictly dependent on a clear description of their mechanism of action at the molecular level. Several studies focused on the interaction of antimicrobial peptides with Gram-negative bacterial cells contributed to clarify some details on the mechanism of action of AMP. [4]

These studies indicated the chemical /physical features of bacteria and peptides that are fundamental for their interactions and which pathways, essential for the bacterial cell life, are affected by AMPs. Fluorescence microscopy studies on *E. coli* cells revealed that the kinetic of bacterial cell death is related to the composition of the lipopolysaccharide (LPS) [5]. The interaction of peptides with LPS often triggers the folding of peptides [6,7]. Peptides saturate the outer membrane of bacteria, determining its neutralization, as revealed by Z potential measurements [8,9]. Recently, single cell time-resolved fluorescence

\* Corresponding authors.

E-mail address: [alessandra.romanelli@unimi.it](mailto:alessandra.romanelli@unimi.it) (A. Romanelli).

<sup>1</sup> These authors equally contributed to the work

microscopy studies suggested that cationic AMPs initially permeabilize the outer membrane (OM) enabling a rapid access of the peptide to the periplasm. As the concentration of the peptide in the periplasm grows, the same process occurs to the cytoplasmic membrane, which is permeabilized only after the outer membrane is resealed, allowing AMPs to travel into the cytoplasm and generating a variety of possible damaging events downstream [10].

Protein targets of AMPs are currently deeply investigated, and it is now clear that different peptides may have different targets [11–13]. Processes that have been found to be hampered by AMPs include bacterial cell division and outer membrane biogenesis. Inhibition of cell division is suggested when bacterial cells form elongated structures in the presence of antimicrobial peptides. Studies on the peptide C18G demonstrated that it impairs cell division in *E. coli* by interacting with the transmembrane protein PhoQ that phosphorylates PhoP triggering the over-expression of the protein QueE, that in turn blocks the divisome complex [14]. Inhibition of outer membrane biogenesis yields defects in the architecture of the membrane. A combination of fluorescence microscopy, mass spectrometry and bioinformatics analyses demonstrated that the peptide thanatin affects the LPS transport machinery by interacting with both the periplasmic protein LptA and the outer membrane protein LptD [13].

LptD was also identified as the target of the peptidomimetic L27–11, which is specifically active on *P. aeruginosa* [15]. Furthermore, a 15 amino-acid peptide fragment derived from BamA was demonstrated to have potent antibiotic activity being able to bind BamD, that is part of the complex devoted to the assembly of beta barrel proteins in the outer membrane of *E. coli* [11]. These results suggest that AMPs may interact with either bacterial membrane or specific intracellular protein targets thus affecting cellular mechanisms and that a deeper investigation is essential for the definition of their effect on vital cellular processes.

We investigated the mechanism of action of the peptide Temporin L (TL) a natural peptide secreted from the skin of the European frog *Rana temporaria* active against Gram-positive and Gram-negative bacteria on *E. coli* cells [16]. This peptide interacts with *E. coli* LPS, *in vitro* and *in vivo* [17–19]; however, its mechanism of action has not been clarified. Perturbation of the bacterial membrane that occurs at TL low concentrations is not the lethal event for bacterial cells; this observation leads to the hypothesis that killing of bacterial cells is mediated by the interaction of the peptide with an intracellular target. Functional Proteomic experiments indicated a specific interaction of TL with proteins belonging to the divisome complex. Sequence homology alignment with other AMPs suggested a possible direct interaction with the GTPase FtsZ. Docking experiments supported the FtsZ-TL interaction that was clearly demonstrated by binding and enzymatic assays using recombinant FtsZ revealing a competitive inhibition mechanism. Optical microscopy and TEM measurements demonstrated that, upon incubation with the peptide, bacterial cells are unable to divide forming long necklace-like cell filaments. Finally, the effect of the peptide on the morphology and the structure of bacterial cells at nanoscale level was also investigated by both Ultra Small-Angle Neutron Scattering (USANS) and Small-Angle Neutron Scattering (SANS).

## 2. Materials and methods

The Fmoc amino acids used for the peptide synthesis and 2-(1H-7-Azabenzotriazol-1-yl)-1,1,3,3-tetramethyluronium hexafluorophosphate (HATU) were purchased from IRIS Biotech GMBH. The Rink amide MBHA resin and the activators N-hydroxybenzotriazole (HOBT) and O-benzotriazole-N,N,N',N'-tetramethyl-uronium-hexafluoro-phosphate (HBTU) were purchased from Novabiochem (Gibbstown, NJ, USA). Acetonitrile (ACN) was from Romil, dry N,N-dimethylformamide (DMF), 6-[Fluorescein-5(6)-carboxamido]hexanoic acid, N-(+)-Biotinyl-6-aminoheptanoic acid and all other reagents were from Sigma Aldrich (MERCK).

Purification was carried out on a Phenomenex Jupiter 10  $\mu$  Proteo

90 Å (250  $\times$  10 mm) column. Purification was carried out by RP-HPLC with a Shimadzu LC-8A, equipped with a SPD-M10 AV diode array detector using a Kinetex® 5  $\mu$ m C18 100 Å, AXIA Packed LC Column 50  $\times$  21.2 mm, Ea column with a flow rate of 20 mLmin<sup>-1</sup>. Peptides were obtained with a purity > 95%; yields were calculated based on the amount of peptide obtained after purification.

### 2.1. Peptide synthesis

Peptides were synthesized on solid phase by Fmoc chemistry on the MBHA (0.54 mmol/g) resin by consecutive deprotection, coupling and capping cycle [20].

Biotin-conjugated TL was obtained by removing the amino terminal Fmoc group and coupling the peptide with N-(+)-Biotinyl-6-aminoheptanoic acid in DMF employing the following conditions: 10 equivalents of N-(+)-Biotinyl-6-aminoheptanoic acid + 9.8 equivalents of HATU (0.45 M in DMF) + 14 equivalents of DIPEA; the solution was reacted with the peptide for 3 h at r.t. and double coupling was performed.

Fluorescein conjugated TL was obtained by coupling to the N-terminus amino-acid 6-fluorescein-5(6)-carboxamido]hexanoic acid dissolved in DMF; 5 equivalents of 6-fluorescein-5(6)-carboxamido]hexanoic acid + 4.98 equivalents of HOBT/HBTU (0.45 M in DMF) + 7 equivalents of NMM were incubated with the peptide 3 h at r.t. in the dark. A double coupling was performed. All peptides were cleaved off the resin and deprotected by treatment with TFA/TIS/H<sub>2</sub>O 95/2.5/2.5 v/v/v, 90 min. TFA was concentrated and peptides were precipitated in cold ethyl ether.

Purification of the peptides was performed by semi-preparative RP-HPLC using a gradient of acetonitrile (0.1% TFA) in water (0.1% TFA) from 30 to 85% in 30 min. Products were lyophilized three times and the peptides were characterized by MALDI tandem mass spectrometry (MALDI-MS/MS).

### 2.2. Bacterial cell growth and viability

The minimum inhibitory concentration (MIC) of TL was measured by broth microdilution. The cell strain of *E. coli* BL21 was incubated overnight in *Luria-Bertani* (LB) at 37 °C. The culture was diluted to obtain a concentration of 0.08 OD<sub>600</sub> / mL in fresh medium and grown at 37 °C for 90 min. At an OD/mL value of 0.5, 50  $\mu$ L of bacterial suspension were added to ten wells and incubated with serial dilutions of the TL peptide from an initial concentration of 512  $\mu$ M. The sterility control well contained 100  $\mu$ L of LB, while the growth control well contained 100  $\mu$ L of microbial suspension.

The MIC value of TL on *E. coli* cells was also calculated in the presence of 1 mM GTP. *E. coli* cells were grown as previously described and the MIC was determined by the lowest concentration showing no visible growth after 24 h of incubation at 37 °C by measuring the Abs at 600 nm. The assay was performed in triplicate.

### 2.3. Membrane proteins extraction

*E. coli* cells were inoculated in 10 mL of liquid LB and placed at 37 °C for 16 h under stirring. At the end of the incubation, bacterial cells were grown in 1 L at 37 °C under stirring for 3 h. The pellet was recovered by centrifugation at 4 °C for 15 min at 5,000 rpm and stored at -80 °C.

The cell pellet was resuspended in 5 mL of *Cell Lysis Buffer* (20 mM Tris-HCl pH 8.0500 mM NaCl, 4 mM DTT, 1 mM PMSF) and subjected to mechanical lysis by French Press. The sample was then centrifuged at 4 °C for 30 min at 10,000 rpm in order to remove the cell debris and the supernatant recovered was ultracentrifuged for 2 h at 4 °C at 54,000 rpm. The obtained pellet was resuspended in solubilization buffer (50 mM Tris-HCl pH 8.0, 500 mM NaCl, 10% Glycerol, 4 mM DTT, 1 mM PMSF, 6 mM 3-[(3-Cholamidopropyl)dimethylammonio]-1-

propanesulfonate (CHAPS)) under stirring at 4 °C for 16 h. The sample was again ultracentrifuged for 2 h at 4 °C at 54,000 rpm. The supernatant containing cytosolic proteins was removed, while the membrane proteins were dissolved in solubilization buffer.

#### 2.4. Pull down experiments

The pull-down experiment was performed using 200 µL of dry avidin-conjugated agarose beads. The resin was divided in two portions, one portion was left unmodified and the second was incubated with a solution of 2 mg/mL of biotinylated TL for 30 min at 4 °C under stirring. The supernatant was then removed by centrifugation at 4 °C for 10 min at 3,000 rpm and the resin equilibrated with 5 volumes of binding buffer at 4 °C.

About 2.5 mg of membrane proteins were incubated on free agarose beads at 4 °C for 2 h under stirring to remove possible non-specific binding, according to the pre-cleaning procedure. The supernatant containing the unbound membrane proteins was recovered by centrifugation at 4 °C for 10 min at 3,000 rpm and then incubated on agarose beads with the immobilized peptide for 3 h at 4 °C under stirring. Beads were washed with 5 volumes of binding buffer and the peptide-interacting proteins were released by competitive elution with 500 µL of elution buffer containing an excess of biotin for 1 h at 4 °C under stirring.

TL putative protein interactors were fractionated by SDS-PAGE. Protein bands from sample and control lanes were excised from the gel and subjected to *in situ* hydrolysis with trypsin. The resulting peptide mixtures were analyzed by Liquid Chromatography/Tandem Mass Spectrometry (LC-MS/MS) using a LTQ Orbitrap XL Orbitrap mass spectrometer (Thermo Fisher Scientific, Bremen, Germany) and the data obtained were used to search for a non-redundant protein database using an in house version of the Mascot software leading to identification of the putative AMP protein interactors. The putative peptide interactors were gathered within functional pathways by bioinformatic tools (DAVID, KEGG, STRING).

#### 2.5. Docking calculations

The putative binding site of TL on FtsZ was determined using docking calculations. The structure of FtsZ has been modelled using SwissProt Model Server and the chain A of the structure of the protein from *P. aeruginosa* (2VAW, 60% sequence identity) as starting model [21,22]. The NMR structure of TL was kindly provided by Prof. Bhat-tacharjya [19]. The peptide adopts an  $\alpha$ -helix structure, in good agreement with CD spectra collected in solution [23]. Interestingly, PEP-FOLD3 also predicts a helical structure for this peptide [24].

The model of the FtsZ-TL complex was obtained using FTDOCKs [25]. The structure of the complex was then energy minimized and refined using Flexpeptdock [26]. We have verified that the peptide binding site was predicted also by other docking programs and indeed the peptide binding site was predicted also by PEPDOCK and SWARMDOCK [27,28]. Analysis of the structure was performed using Coot, figures were generated with PyMol ([www.pymol.org](http://www.pymol.org)) [29].

#### 2.6. Expression of *Escherichia coli* FtsZ and enzymatic assay

Untagged *E. coli* FtsZ was expressed from pET28a in BL21 cells. Cells were grown at 37 °C in 200 mL of LB culture media with 50 µg/mL kanamycin and 0.4 mM isopropyl-beta-D-thiogalactopyranoside (IPTG) was added at an optical density of ~0.5 at 600 nm. The culture was grown for 90 min at 37 °C for FtsZ production. Cells were harvested by centrifugation (5,000 rpm, 15 min at 4 °C), and pellets were re-suspended in Tris glycerol buffer (Tris glycerol buffer, 50 mM Tris-HCl, 50 mM KCl, 1 mM EDTA, 10% glycerol, pH 8.0) and were lysed on ice using a sonicator. The soluble fraction, containing the FtsZ protein, was separated from the cell debris by centrifugation (100,000 ×g for 2 h at

4 °C).

The protein from the soluble fraction was precipitated with 30% ammonium sulfate for 16 h. The sample was centrifuged (10,000 rpm for 35 min at 4 °C), and the pellet was resuspended in 5 mL Tris glycerol buffer, pH 8.0 and dialyzed to remove the ammonium sulfate. The sample was purified by anion exchange chromatography using a Mono-Q HR 5/5 column equilibrated with Tris glycerol buffer, pH 8.0. FtsZ was retained on the column and was eluted with a 0–100% gradient of 1 M NaCl in the same buffer [30].

Protein concentration was estimated with Bradford reagent (Bio-Rad protein assay), protein purity was assessed by SDS- polyacrylamide gel electrophoresis (SDS-PAGE) and characterized by mass mapping using MALDI-MS/MS.

The activity of FtsZ on GTP substrate was determined with an enzymatic assay using BIOMOL® Green phosphate reagent (Biomol). Initially, FtsZ (6 µM) was incubated in 25 mM PIPES/NaOH, pH 6.8 for 30 min at 30 °C. The enzyme was then treated with different concentrations of GTP, ranging from 0 µM to 250 µM, either in the absence or in the presence of 35 µM TL. The reaction was performed for 10 min and then stopped by addition of 100 µL BIOMOL® Green reagent and the increase in absorbance at 620 nm was measured following 25 min incubation. The experiment was performed in duplicate. Kinetic parameters were fitted by non-linear regression with GraphPad Prism 4Project. The half-maximal inhibitory concentration (IC<sub>50</sub>) of TL on the GTPase activity of FtsZ was calculated by plotting the percentage of enzymatic activity versus the logarithm of TL concentration.

#### 2.7. Binding experiment

Fluorescence experiments were performed at 25 °C in a 250 µL quartz cuvette (Hellma Germany) on a VARIAN Cary Eclipse Fluorimeter. Titrations were carried out in 50 mM Tris-HCl buffer pH 7.2, 1 M NaCl. Fluo-TL was excited at 440 nm (slit 5 nm) and the emission was monitored at 520 nm (slit 5 nm) without and in the presence of increasing concentrations of FtsZ protein (from 0.003 to 0.121 µM) in a High Voltage mode. The peptide and the protein were dissolved at a 1.5 µM concentration. All experiments were repeated in duplicate. The change in the fluorescence intensity of the reaction set was fit into “one site-specific binding” equation of GraphPad Prism 5 (GraphPad Software).

#### 2.8. Optical microscopy and TEM analyses

*E. coli* cells were inoculated in 10 mL of liquid LB and placed at 37 °C for 16 h under stirring. At the end of the incubation, bacterial cells grown to 0.5 OD/mL were incubated with 20 µM TL and allowed to grow for a further 5 h. A similar bacterial growth was prepared and used as control in the absence of the peptide. Samples of 100 µL were observed by optical microscope using a ZEISS optical microscope for phase contrast and 50× magnifications.

For TEM analysis, *E. coli* cells were treated with sub-MIC concentration of TL for 1 h at 37 °C. After incubation, bacterial cells were centrifugated at 3,000 rpm for 15 min, washed with PBS and re-suspended in PBS containing 2.5% glutaraldehyde to fix the cells. Samples (10 µL) were applied to a glow discharged formvar/carbon film copper mesh grid and led to adsorb for 2 min. The excess liquid was eliminated with water and the sample was stained with 1% uranyl acetate allowing the grids to dry before TEM analyses. TEM analyses were carried out on a JEOL JEM-1400 TEM with an accelerating voltage of 120 kV. Digital images were collected with an EMSIS Xarosa digital camera with Radius software.

#### 2.9. Scattering measurements

*E. coli* cells were grown to 0.5 OD/mL in the presence and in the absence of 20 µM TL up to 1 OD at 600 nm. Cells were then centrifuged

at 5,000 rpm for 15 min, treated with 0.4% paraformaldehyde for 10 min, washed with deuterated PBS1X for three times and the samples were finally resuspended in deuterated PBS1X. Dynamic Light Scattering (DLS) measurements were performed by using a home-made instrument composed by a Photocor compact goniometer, a SMD 6000 Laser Quantum 50 mW light source operating at 532.5 nm, a photomultiplier (PMT-120-OP/B) and a correlator (Flex02-01D) from Correlator.com [31,32]. All measurements were performed at 25 °C with the temperature controlled through the use of a thermostat bath. All the measurements were performed in triplicate at fixed scattering angle of 90°.

Small Angle Neutron Scattering (SANS) measurements were performed at 25 °C with the KWS-2 diffractometer operated by Julich Centre for Neutron Science at the FRMII source located at the Heinz Maier Leibnitz Centre, Garching (Germany). For all the samples, neutrons with a wavelength of 7 Å and  $\Delta\lambda/\lambda \leq 0.1$  were used. A two-dimensional array detector at three different wavelength (W)/collimation (C)/sample-to-detector (D) distance combinations (W 7 Å/C 8 m/D 2 m, W 7 Å/C 8 m/D 8 m, and W 7 Å/C 20 m/D 20 m) measured neutrons scattered from the samples. These configurations allowed collecting data in a range of the scattering vector modulus  $q$  between  $0.002 \text{ \AA}^{-1}$  and  $0.4 \text{ \AA}^{-1}$ .

The USANS measurements were performed on KWS-3 at 25 °C. The sample-to-detector distances was 9.5 m with a wavelengths of 5 Å ( $\Delta\lambda/\lambda = 10\%$ ) and 12.8 Å ( $\Delta\lambda/\lambda = 20\%$ ), respectively. Both in the case of KWS2 and KWS3 measurements a 1 mm Helma quartz cells were used.

### 3. Results

#### 3.1. Effect of Temporin L on *E. coli* cell growth

The antimicrobial activity of TL was verified by monitoring *E. coli* cell growth in the presence of different concentrations of TL. The MIC was calculated to be 32 µM, in agreement with literature data [16]. (Supplementary Fig. 1).

#### 3.2. Pull-down experiment

A detailed investigation of the mechanism of action of TL at the molecular level was pursued by functional proteomics approaches. Biotinylated TL was immobilized onto streptavidin-conjugated agarose beads and incubated with a membrane protein extract from *E. coli* cells. The proteins specifically interacting with the peptide bait were eluted and fractionated by SDS-PAGE. A membrane protein extract was also incubated with streptavidin-conjugated agarose beads lacking the peptide and the eluted proteins were used as control. Protein bands from sample and control lanes were excised from the gel and subjected to *in situ* hydrolysis with trypsin. The resulting peptide mixtures were directly analyzed by LC-MS/MS and the mass spectral data used to search a protein database using an in-house version of the Mascot software leading to protein identification. Proteins that were identified both in the control and in the sample lanes were discarded, whereas those solely occurring in the sample and absent in the control were considered as putative TL interactors.

Fig. 1A and B show the distribution of TL putative protein partners according to their cellular localization and the biological processes they are involved into. A bioinformatic analysis was performed using the String software and the KEGG pathway showing that a large number of proteins gathered within a network involved in cell division and the biosynthesis of peptidoglycan for the production of the division septum (Fig. 1C).

In particular, several proteins belonging to the divisome complex were identified including FtsZ, FtsA, MurG, MukB and MreB.

Among these proteins, FtsZ protein, is a bacterial tubulin homolog and is responsible of the Z ring formation, the first step in the formation of the divisome complex, which implements the cell division. Recently,

FtsZ was reported to be the target of two peptides, CRAMP (16–33) and MciZ [12]. Sequence alignment showed that TL shares a high sequence similarity to the C-terminal portion of both CRAMP (16–33) and MciZ (1–19) (Fig. 2A). This observation urged us to investigate the interaction of TL with FtsZ *in vitro* and *in vivo* and to develop a molecular model of the peptide-protein interaction by docking calculations.

#### 3.3. Docking experiments

The putative structural basis of the binding of TL to FtsZ were investigated by a docking study (Fig. 2B). Calculations reveal that TL may bind the cavity that allows the accommodation of GDP in the structures of FtsZ from *B. subtilis* and *P. aeruginosa* (Fig. 2C), thus suggesting a possible competitive inhibition of the peptide for the GTPase activity of the protein. A detailed analysis of the interactions at the protein/peptide interface suggests the involvement of hydrophobic and coulombic interactions, with Phe and Trp residues of the peptide that pack against residues Gly20, Gly21, Gly71, Ala72, Gly105, Gly106, Gly107 and Phe182 of the protein and with the side chain of the Arg of the peptide that could make a salt bridge with the side chain of Glu138 of Ftsz (Fig. 2D).

#### 3.4. Binding experiments

As docking calculations suggested a possible interaction between TL and FtsZ, we were stimulated to confirm the binding of the peptide TL to the protein FtsZ on experimental basis. A recombinant form of FtsZ was produced in *E. coli*, purified and used in binding and enzymatic assays. Fluorescence experiments were carried out using the peptide labeled at the N-terminus with fluoresceine incubated with increasing concentrations of the protein (Fig. 3A). Data from Fig. 3A allowed us to calculate a Kd value of  $17.4 \pm 0.8 \text{ nM}$ .

#### 3.5. Enzymatic assays

To further validate the docking predictions and to study the effect of TL on FtsZ, the GTPase activity of the recombinant protein was assayed in the absence and in the presence of TL. The purified recombinant protein was incubated with GTP in the presence of the peptide (35 µM) and the GTPase activity of FtsZ was monitored in comparison with the untreated protein at different GTP concentrations. In the presence of TL a decrease in the enzymatic activity of FtsZ was clearly observed confirming a specific interaction of the peptide with FtsZ (Fig. 3B). Kinetic parameters were calculated showing an increase of the apparent  $K_M$  by about 50% (112.0 µM as compared to 56.6 µM in the absence of the peptide) whereas  $V_{max}$  remained unchanged, demonstrating the competitive inhibitory mechanism exerted by TL on FtsZ. The half-maximal inhibitory concentration ( $IC_{50}$ ) of TL on the GTPase activity of FtsZ was also calculated resulting as  $62 \pm 2 \text{ \mu M}$  (Fig. 3C), slightly lower than the  $IC_{50}$  determined for CRAMP (16–33) (16).

#### 3.6. Optical microscopy and TEM analyses

The morphologic effect of FtsZ inhibition by TL on cell division was investigated *in vivo* by both optical microscopy measurements and TEM analyses. on *E. coli* cell cultures grown in the presence and in the absence of the peptide. Optical microscopy images clearly show that in the presence of TL (Fig. 4B) *E. coli* cells form long necklace-like structures containing a large number of *E. coli* cells originated by impairment in cell division that were absent in the control (Fig. 4A). When the same experiment was carried out in the presence of 1 mM GTP, an almost completely rescue of the phenotype was observed as indicated by the large decrease in both the number and the length of the necklace-like structures (Fig. 4C). Accordingly, we evaluated the minimal inhibitory concentration (MIC) of TL on *E. coli* cells in the presence of 1 mM GTP. MIC greasily increased to 256 µM confirming that the presence of GTP

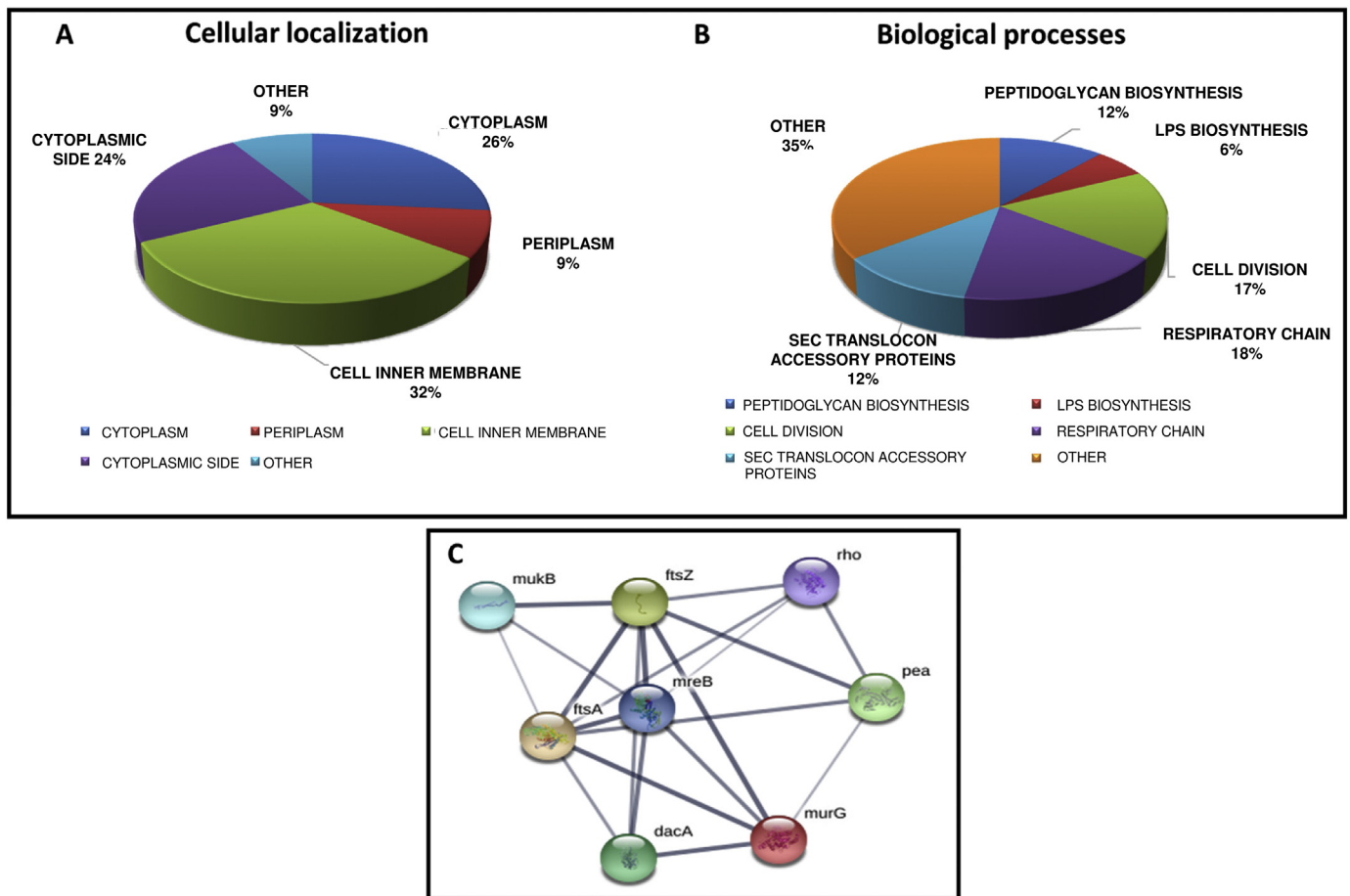


Fig. 1. (A) Distribution of TL putative protein partners identified in the pull-down experiment according to their cellular localization. (B) Distribution of TL putative protein partners according to their biological functions. (C) STRING analysis of the putative TL interactors belonging to the divisome complex showing the occurrence of a network including 8 proteins: FtsZ, FtsA, MurG, MukB, Rho, DacA, pea and MreB.

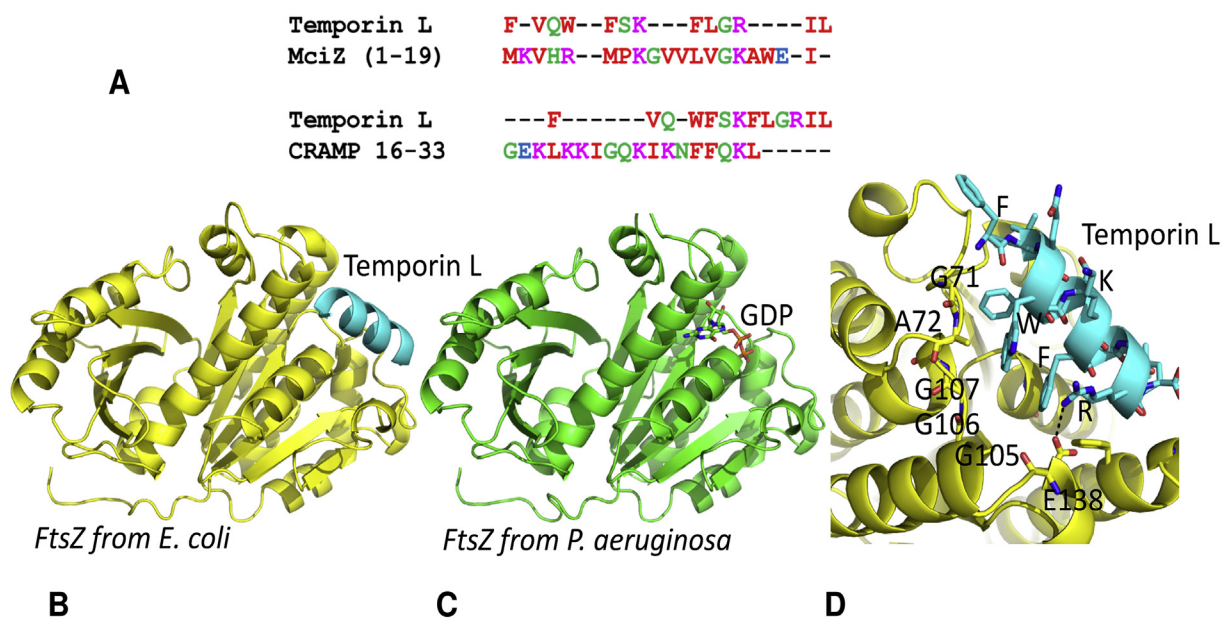
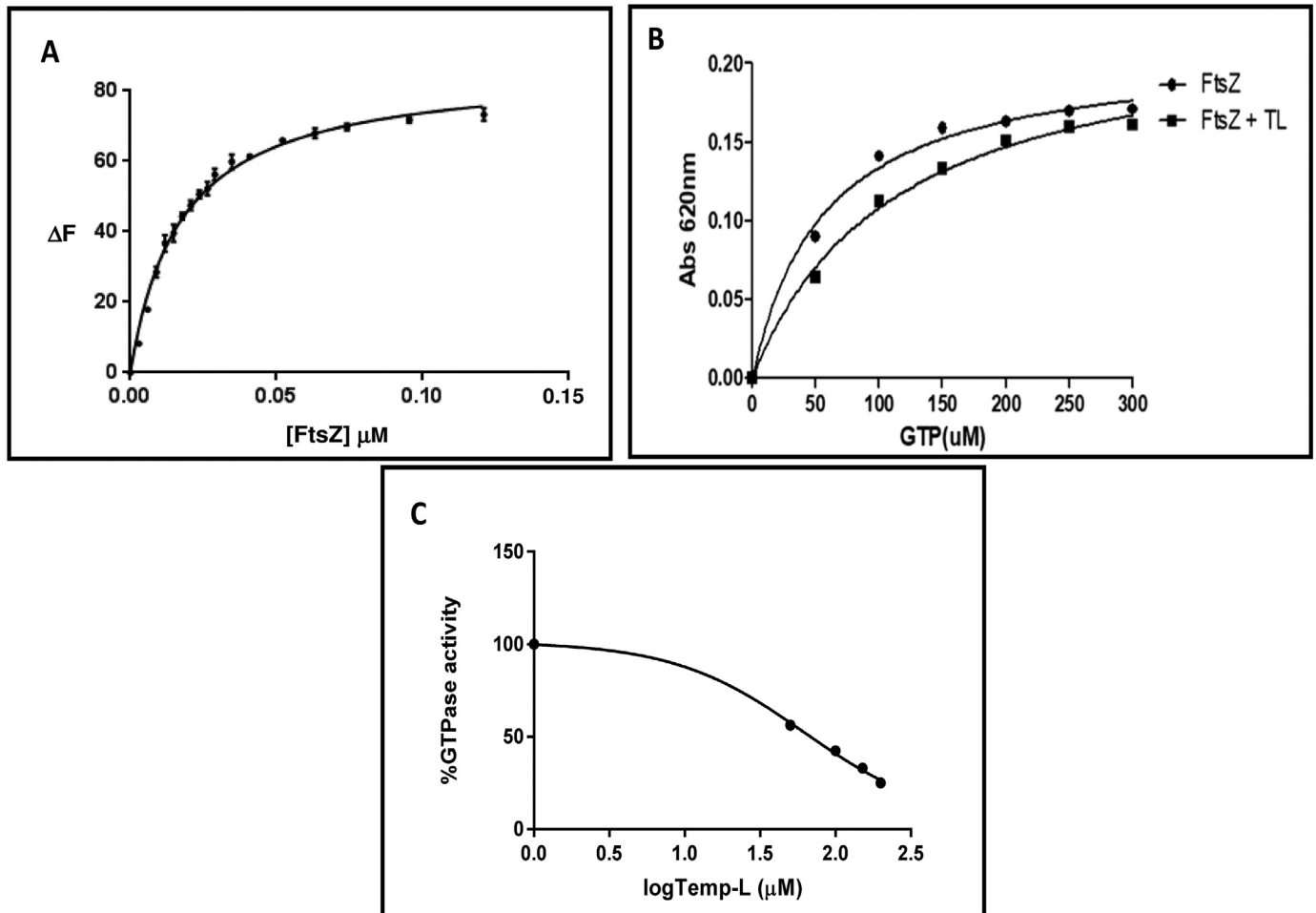
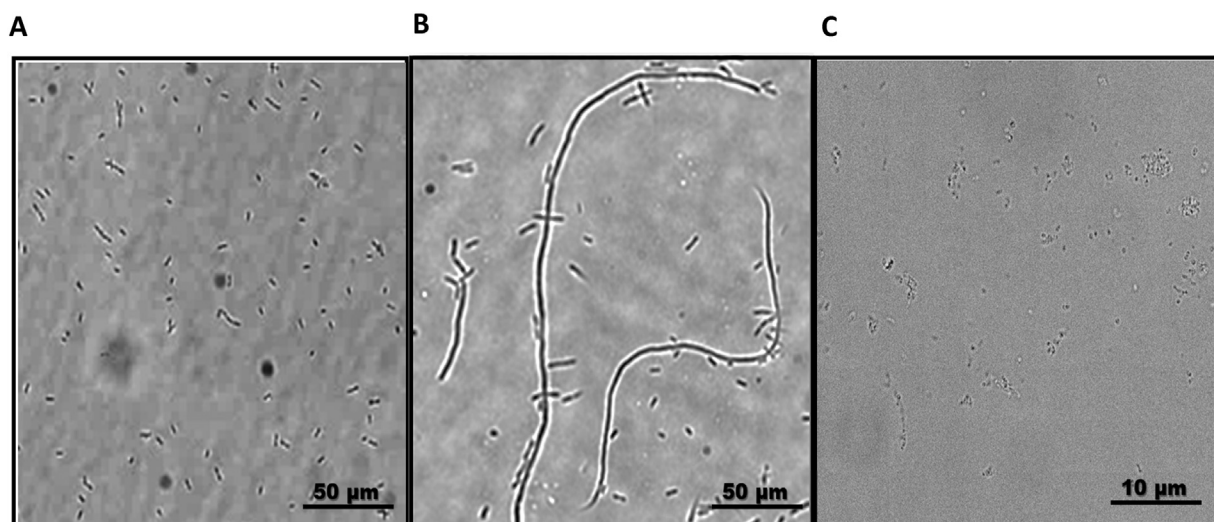


Fig. 2. (A) Sequence alignment of peptides Temporin L, CRAMP 16-33 and MciZ. (B) The predicted structure of the complex between FtsZ (yellow) and TL (cyan). (C) Putative binding site well superimposes to that of GDP in the structures of *B. subtilis* and *P. aeruginosa* FtsZ. (D) Predicted binding site of TL (cyan) on FtsZ structure (yellow).



**Fig. 3.** (A) Binding of TL to FtsZ as determined by fluorescence experiments using N-terminal fluoresceine-labeled TL and recombinant FtsZ. (B) Enzymatic activity of recombinant FtsZ in the absence and in the presence of 35  $\mu\text{M}$  TL using GTP as substrate. (C) Determination of TL  $\text{IC}_{50}$ , i.e. the minimal peptide concentration displaying 50% inhibition of FtsZ GTPase activity.



**Fig. 4.** Optical microscopy images of *E. coli* cells grown in the absence (panel A) and in the presence (panel B) of 20  $\mu\text{M}$  TL. Long necklace-like structures formed by *E. coli* cells were clearly detected in the presence of the peptide confirming the impairment of bacterial cell division. The phenotype was rescued in the presence of 1 mM GTP that restored cell division (panel C).

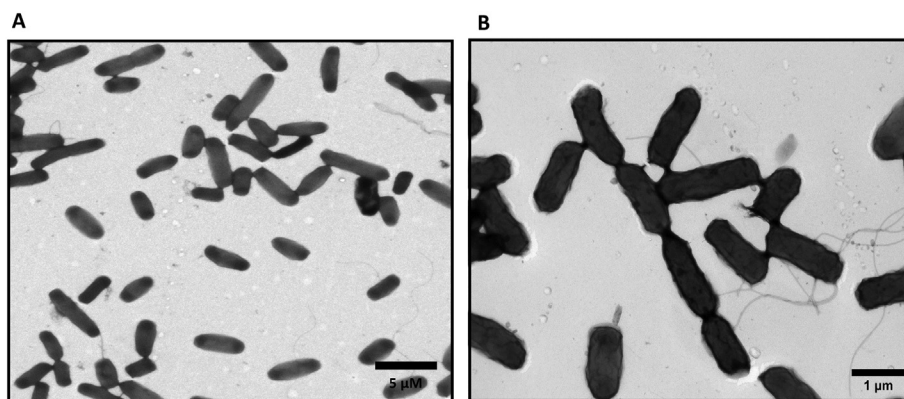


Fig. 5. TEM analysis of *E. coli* cells grown in the absence (panel A) and in the presence (panel B) of 20  $\mu\text{M}$  TL. TEM images further confirmed the occurrence of bacterial cells unable to divide in the presence of TL (panel B) as compared to the control (panel A).

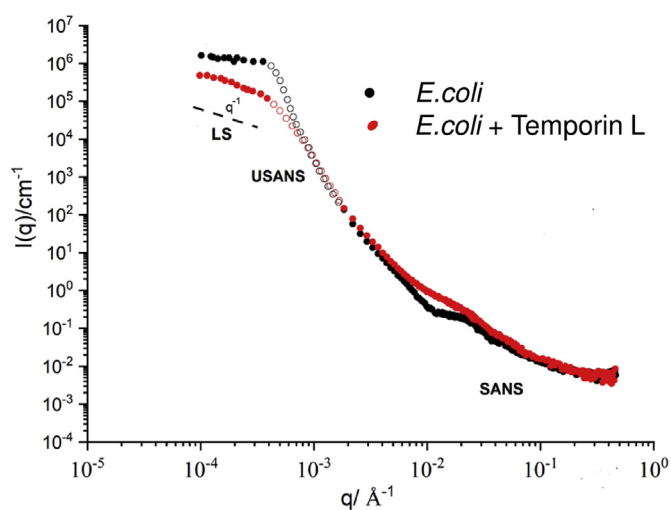


Fig. 6. Dynamic Light Scattering (LS), USANS, and SANS analyses of *E. coli* cells in the absence (black points) and in the presence (red points) of 20  $\mu\text{M}$  TL. LS measurements showed a decrease of the intensity with a  $q^{-1}$  power law for the treated sample, whereas this value remained essentially constant for the untreated sample.

might revert the TL effect.

The TL effect on *E. coli* cells growth was also investigated by TEM analyses. TEM images shown in Fig. 5B confirmed that, following treatment with TL, bacterial cells division was impaired as indicated by several cells bound together and unable to divide when compared to the control (Fig. 5A). No damage of membranes was detected and the cells appeared turgid.

### 3.7. Spectroscopic investigations

The large structures formed by *E. coli* cells upon treatment with TL were further investigated by static light scattering experiments. As shown in Fig. 6, at small values of the scattering vector  $q$ , in the range probed by the LS, the scattering intensity profile decays with a  $q^{-1}$  power law for the sample of *E. coli* cells in the presence of TL, whereas it remains essentially constant for the pure bacteria, *i.e.* for the cells in the absence of the peptide. This suggests that, in the presence of TL, large elongated structures are formed with a length larger than 6000 nm, the limit of LS instrument.

SANS analysis revealed that a significant difference between untreated and treated *E. coli* cells occurs in the range between 20 nm ( $q = 0.001 \text{ \AA}^{-1}$ ) and 60 nm ( $q = 0.003 \text{ \AA}^{-1}$ ). In such range, the profile of the scattering intensity of *E. coli* cells changes drastically upon TL

addition. In the presence of the peptide, the scattering intensity is higher than that collected for the system containing only the bacterial cells. Furthermore, in this later a shoulder in the  $I(q)$  vs  $q$  is present, whereas in the system containing TL the shoulder disappears and the scattering intensity decreases with a greater slope.

## 4. Discussion

Elucidation of the mechanism of action of antimicrobial peptides requires the identification of the peptide targets in bacterial cells. We investigated the mechanism of action of Temporin L by a functional proteomic approach based on pull-down experiments using a biotinylated version of the peptide as a bait to identify its specific protein targets in *E. coli*. It is well known that in the cell many processes are governed by the rapid and transient association of proteins in multi-component functional complexes [33–35]. In bacterial membranes, several proteins are embedded in complexes with cytoplasmic proteins. For example, the protein machine devoted to the transport of LPS spans from the periplasm to the outer membrane. Accordingly, the proteomic experiment led to the identification of several proteins belonging to a multicomponent complex extending from the cytoplasm to all three layers of the cell envelope known as the divisome complex involved in the cell division process.

Among the identified proteins, FtsZ, FtsA, MurG, MukB and MreB are known to assemble into a tightly regulated cellular machinery operating to safely separate the cell into two daughter cells by a two steps mechanism. FtsZ is a bacterial tubulin homolog, expressed in either Gram-positive and Gram-negative cells responsible of the first step in the division of bacterial cells. FtsZ polymerizes in filaments using GTP molecules to generate a ring-like structure, the Z ring, at the site of division, then recruits other proteins to assemble the divisome complex driving the constriction of the cell envelope [12,36]. In *E. coli*, FtsZ is tethered to the membrane through FtsA. MurG is a glycosyltransferase located in the lateral cell wall and at the division site that catalyzes the synthesis of peptidoglycan. Den Blaauween et al. suggested the involvement of MurG in a complex containing several proteins, including FtsA, implicated in cell division [37]. Immunoprecipitation experiments demonstrated that MurG is also associated with MreB. MreB is essential for the maintenance of cell shape and plays a key role in cell division, being recruited to the septum upon direct interaction with FtsZ, an interaction functional to Z ring contraction [38].

Recently, two peptides, namely CRAMP 16–33, an antimicrobial peptide found in multicellular organisms, and MciZ, a peptide expressed during sporulation of *Bacillus subtilis* reported to be the physiological inhibitor of FtsZ, were demonstrated to interact with FtsZ, inhibit its GTPase activity, stop bacterial cell division, causing cell death. Docking experiments show that CRAMP 16–33 binds to the cavity of the T7 loop of FtsZ, whereas MciZ is supposed to compete with



GTP for the same binding site on FtsZ [12]. [39] Sequence alignment showed that TL displays high sequence similarity with CRAMP and also with the N-terminal residues of MciZ. Based on these data, we investigated the possible interaction of TL with FtsZ. Docking simulation revealed that TL may bind FtsZ in the GTP binding site, thus suggesting a possible competitive inhibition mechanism of the peptide for the GTPase activity of the protein, as observed for MciZ. This hypothesis was confirmed by fluorescent binding experiments carried out using recombinant FtsZ in the presence of TL. A high binding affinity was detected for TL toward FtsZ with a  $K_d$  value of  $17.4 \pm 0.8$  nM, supporting the hypothesis that FtsZ is the specific target of the peptide. This value is lower as compared to that reported for MciZ ( $0.3 \pm 0.1$   $\mu$ M), the physiological inhibitor of FtsZ [39].

Functional investigation of the TL effect on FtsZ were then performed both *in vitro* and *in vivo*. Enzymatic assays aimed at measuring the GTPase activity of the FtsZ in the presence of TL confirmed that TL is a competitive inhibitor of the protein, as indicated by the docking simulation. Morphologic investigations of *E. coli* cells in the presence of TL by either optical microscopy measurements or TEM analyses revealed the formation of largely elongated “necklace-like” structures originated by a multitude of bacterial cells, demonstrating that the presence of the peptide hinders *E. coli* cells division. TEM images showed several cells bound together and unable to divide. Consistent with this observation, the results of static light scattering experiments showed the occurrence of elongated structures larger than 6000 nm in the presence of TL.

Analysis of the bacterial cells was also performed by SANS that allows investigation of the morphology and the structure at the nanoscale level. In particular, the atom density distribution of an object is obtained from the analysis of its neutron scattering intensity as function of the scattering vector,  $q$ , when illuminated with a neutron beam. Thus, the scattering profile provides structural information over a size scale,  $d$ , depending on the  $q$  range, according to  $d \sim 2\pi/q$ . In the present paper, SANS was exploited to investigate the effect of TL on *E. coli* cells, focusing on the structure formed in the range of 2 to 300 nm. According to the literature there are only a few papers presenting such investigation on living cells [40].

Neutron scattering measurements discloses a change in the spatial arrangement of the protein involved in the interaction suggesting that a protein underwent a structural change following incubation with the peptide in agreement with the docking calculation. Notably, in the intermediate  $q$  range, *i.e.* the range where structural changes on the membrane would be detectable, SANS analyses clearly showed no differences in the lamellar structure of *E. coli* cells, indicating the absence of a destabilization of the bacteria membrane.

Overall our data depicted the following mechanism of action for Temporin L on *E. coli* cells: the peptide crosses the outer membrane of bacteria and specifically binds FtsZ inhibiting its GTPase activity by a competitive inhibition mechanism. This event impairs bacterial cell division resulting in the formation of long cell filaments, and finally bacterial cell death. Due to its haemolytic activity, Temporin L cannot be considered as an effective alternative to common antibiotics, although optimization of the peptide properties by subtle modification of its chemical structure can reduce its haemolytic activity [18,41]. However, elucidation of the mechanism of action at the molecular level pointed out to FtsZ as a possible good target for the rational design of new antibiotics since this protein is responsible for a crucial biological event of bacterial life and is absent in humans.

## Declaration of Competing Interest

The authors declare that they have no conflicts of interest with the contents of this article.

## Acknowledgments

This work is based upon experiments performed at the KWS2 instrument operated by JCNS at the Heinz Maier-Leibnitz Zentrum (MLZ), Garching, Germany. LP is grateful to MLZ for providing beam time. AD thanks prof. Prof. Miguel Vicente Centro Nacional de Biotecnología, Consejo Superior de Investigaciones Científicas, Madrid, Spain for providing *E. coli* cells for FtsZ production. This work was supported in part by MIUR grants ARS01\_00597 Project “NAOCON” and PRIN 2017 “Identification and characterization of novel antitumoral/antimicrobial insect-derived peptides: a multidisciplinary, integrated approach from *in silico* to *in vivo*”.

## Appendix A. Supplementary data

Supplementary data to this article can be found online at <https://doi.org/10.1016/j.bbagen.2020.129606>.


## References

- [1] C.F. Le, C.M. Fang, S.D. Sekaran, Intracellular targeting mechanisms by antimicrobial peptides, *Antimicrob. Agents Chemother.* 61 (2017).
- [2] A.K. Marr, W.J. Gooderham, R.E. Hancock, Antibacterial peptides for therapeutic use: obstacles and realistic outlook, *Curr. Opin. Pharmacol.* 6 (2006) 468–472.
- [3] A. Lewies, L.H. Du Plessis, J.F. Wentzel, Antimicrobial peptides: the Achilles' heel of antibiotic resistance? *Probiotics Antimicrob. Proteins* 11 (2019) 370–381.
- [4] J.M. Freire, D. Gaspar, A.S. Veiga, M.A. Castanho, Shifting gear in antimicrobial and anticancer peptides biophysical studies: from vesicles to cells, *J. Pept. Sci.* 21 (2015) 178–185.
- [5] A. Agrawal, J.C. Weisshaar, Effects of alterations of the *E. coli* lipopolysaccharide layer on membrane permeabilization events induced by Cecropin A, *Biochim. Biophys. Acta Biomembr.* 1860 (2018) 1470–1479.
- [6] C. Avitabile, L.D. D'Andrea, A. Romanelli, Circular dichroism studies on the interactions of antimicrobial peptides with bacterial cells, *Sci. Rep.* 4 (2014) 4293.
- [7] G. Malgieri, C. Avitabile, M. Palmieri, L.D. D'Andrea, C. Isernia, A. Romanelli, R. Fattorusso, Structural basis of a temporin 1b analogue antimicrobial activity against gram negative bacteria determined by CD and NMR techniques in cellular environment, *ACS Chem. Biol.* 10 (2015) 965–969.
- [8] J.M. Freire, D. Gaspar, B.G. de la Torre, A.S. Veiga, D. Andreu, M.A. Castanho, Monitoring antibacterial permeabilization in real time using time-resolved flow cytometry, *Biochim. Biophys. Acta* 1848 (2015) 554–560.
- [9] C. Avitabile, L.D. D'Andrea, M. Saviano, M. Olivieri, A. Cimmino, A. Romanelli, Binding studies of antimicrobial peptides to *Escherichia coli* cells, *Biochem. Biophys. Res. Co* 478 (2016) 149–153.
- [10] Z. Yang, J.C. Weisshaar, HaloTag assay suggests common mechanism of *E. coli* membrane Permeabilization induced by cationic peptides, *ACS Chem. Biol.* 13 (2018) 2161–2169.
- [11] C.L. Hagan, J.S. Wzorek, D. Kahne, Inhibition of the beta-barrel assembly machine by a peptide that binds BamD, *Proc. Natl. Acad. Sci. U. S. A.* 112 (2015) 2011–2016.
- [12] S. Ray, H.P. Dhaked, D. Panda, Antimicrobial peptide CRAMP (16–33) stalls bacterial cytokinesis by inhibiting FtsZ assembly, *Biochemistry* 53 (2014) 6426–6429.
- [13] S.U. Vetterli, K. Zerbe, M. Muller, M. Urfer, M. Mondal, S.Y. Wang, K. Moehle, O. Zerbe, A. Vitale, G. Pessi, L. Eberl, B. Wollscheid, J.A. Robinson, Thanatin targets the intermembrane protein complex required for lipopolysaccharide transport in *Escherichia coli*, *Sci. Adv.* 4 (2018) eaau2634.
- [14] S.S. Yadavalli, J.N. Carey, R.S. Leibman, A.I. Chen, A.M. Stern, M. Roggiani, A.M. Lippa, M. Goulian, Antimicrobial peptides trigger a division block in *Escherichia coli* through stimulation of a signalling system, *Nat. Commun.* 7 (2016) 12340.
- [15] G. Andolina, L.C. Bencze, K. Zerbe, M. Muller, J. Steinmann, H. Kocherla, M. Mondal, J. Sobek, K. Moehle, G. Malojcic, B. Wollscheid, J.A. Robinson, A Peptidomimetic antibiotic interacts with the periplasmic domain of LptD from *Pseudomonas aeruginosa*, *ACS Chem. Biol.* 13 (2018) 666–675.
- [16] A.C. Rinaldi, M.L. Mangoni, A. Rufo, C. Luzi, D. Barra, H. Zhao, P.K. Kinnunen, A. Bozzi, A. Di Giulio, M. Simmaco, Temporin L: antimicrobial, haemolytic and cytotoxic activities, and effects on membrane permeabilization in lipid vesicles, *Biochem. J.* 368 (2002) 91–100.
- [17] M.L. Mangoni, N. Papo, D. Barra, M. Simmaco, A. Bozzi, A. Di Giulio, A.C. Rinaldi, Effects of the antimicrobial peptide temporin L on cell morphology, membrane permeability and viability of *Escherichia coli*, *Biochem. J.* 380 (2004) 859–865.
- [18] A. Giacometti, O. Cirioni, R. Ghiselli, F. Mochegiani, F. Orlando, C. Silvestri, A. Bozzi, A. Di Giulio, C. Luzi, M.L. Mangoni, D. Barra, V. Saba, G. Scalise, A.C. Rinaldi, Interaction of antimicrobial peptide temporin L with lipopolysaccharide *in vitro* and in experimental rat models of septic shock caused by gram-negative bacteria, *Antimicrob. Agents Chemother.* 50 (2006) 2478–2486.
- [19] A. Bhunia, R. Saravanan, H. Mohanram, M.L. Mangoni, S. Bhattacharjya, NMR structures and interactions of temporin-1T1 and temporin-1Tb with lipopolysaccharide micelles: mechanistic insights into outer membrane permeabilization and synergistic activity, *J. Biol. Chem.* 286 (2011) 24394–24406.
- [20] L. Piras, C. Avitabile, L.D. D'Andrea, M. Saviano, A. Romanelli, Detection of

- oligonucleotides by PNA-peptide conjugates recognizing the biarsenical fluorescein complex FlAsH-EDT2, *Biochem. Biophys. Res. Commun.* 493 (2017) 126–131.
- [21] A. Waterhouse, M. Bertoni, S. Bienert, G. Studer, G. Tauriello, R. Gumienny, F.T. Heer, T.A.P. de Beer, C. Rempfer, L. Bordoli, R. Lepore, T. Schwede, SWISS-MODEL: homology modelling of protein structures and complexes, *Nucleic Acids Res.* 46 (2018) W296–W303.
- [22] M.A. Oliva, D. Trambaiolo, J. Lowe, Structural insights into the conformational variability of FtsZ, *J. Mol. Biol.* 373 (2007) 1229–1242.
- [23] C. Avitabile, L.D. D'Andrea, M. Saviano, A. Romanelli, Determination of the secondary structure of peptides in the presence of gram positive bacterium *S. epidermidis* cells, *RSC Adv.* 6 (2016) 51407–51410.
- [24] Y.M. Shen, J. Maupetit, P. Derreumaux, P. Tuffery, Improved PEP-FOLD approach for peptide and miniprotein structure prediction, *J. Chem. Theory Comput.* 10 (2014) 4745–4758.
- [25] H.A. Gabb, R.M. Jackson, M.J. Sternberg, Modelling protein docking using shape complementarity, electrostatics and biochemical information, *J. Mol. Biol.* 272 (1997) 106–120.
- [26] B. Raveh, N. London, O. Schueler-Furman, Sub-angstrom modeling of complexes between flexible peptides and globular proteins, *Proteins* 78 (2010) 2029–2040.
- [27] H. Lee, L. Heo, M.S. Lee, C. Seok, GalaxyPepDock: a protein-peptide docking tool based on interaction similarity and energy optimization, *Nucleic Acids Res.* 43 (2015) W431–W435.
- [28] M. Torchala, I.H. Moal, R.A. Chaleil, J. Fernandez-Recio, P.A. Bates, SwarmDock: a server for flexible protein-protein docking, *Bioinformatics* 29 (2013) 807–809.
- [29] P. Emsley, B. Lohkamp, W.G. Scott, K. Cowtan, Features and development of coot, *Acta Crystallogr. D Biol. Crystallogr.* 66 (2010) 486–501.
- [30] G. Rivas, A. Lopez, J. Mingorance, M.J. Ferrandiz, S. Zorrilla, A.P. Minton, M. Vicente, J.M. Andreu, Magnesium-induced linear self-association of the FtsZ bacterial cell division protein monomer. The primary steps for FtsZ assembly, *J. Biol. Chem.* 275 (2000) 11740–11749.
- [31] N.F. Della Vecchia, A. Luchini, A. Napolitano, G. D'Errico, G. Vitiello, N. Szekely, M. d'Ischia, L. Paduano, Tris buffer modulates polydopamine growth, aggregation, and paramagnetic properties, *Langmuir* 30 (2014) 9811–9818.
- [32] A. Luchini, C. Irace, R. Santamaria, D. Montesarchio, R.K. Heenan, N. Szekely, A. Flori, L. Menichetti, L. Paduano, Phosphocholine-decorated superparamagnetic iron oxide nanoparticles: defining the structure and probing in vivo applications, *Nanoscale* 8 (2016) 10078–10086.
- [33] M. Monti, M. Cozzolino, F. Cozzolino, G. Vitiello, R. Tedesco, A. Flagiello, P. Pucci, Puzzle of protein complexes in vivo: a present and future challenge for functional proteomics, *Exp. Rev. Proteome* 6 (2009) 159–169.
- [34] G. Chesi, R.N. Hegde, S. Iacobacci, M. Concilli, S. Parashuraman, B.P. Festa, E.V. Polishchuk, G. Di Tullio, A. Carissimo, S. Montefusco, D. Canetti, M. Monti, A. Amoresano, P. Pucci, B. van de Sluis, S. Lutsenko, A. Luini, R.S. Polishchuk, Identification of p38 MAPK and JNK as new targets for correction of Wilson disease-causing ATP7B mutants, *Hepatology* 63 (2016) 1842–1859.
- [35] A. Varone, S. Mariggio, M. Patheja, V. Maione, A. Varriale, M. Vessichelli, D. Spano, F. Formiggini, M. Lo Monte, N. Brancati, M. Frucci, P. Del Vecchio, S. D'Auria, A. Flagiello, C. Iannuzzi, A. Luini, P. Pucci, L. Banci, C. Valente, D. Corda, A signalling cascade involving receptor-activated phospholipase A(2), glycerophosphoinositol 4-phosphate, Shp1 and Src in the activation of cell motility, *Cell Commun. Signal* 17 (2019).
- [36] C.L. Kirkpatrick, P.H. Viollier, New(s) to the (Z)-ring, *Curr. Opin. Microbiol.* 14 (2011) 691–697.
- [37] T. Mohammadi, A. Karczmarek, M. Grouvoisier, A. Bouhss, D. Mengin-Lecreulx, T. den Blaauwen, The essential peptidoglycan glycosyltransferase MurG forms a complex with proteins involved in lateral envelope growth as well as with proteins involved in cell division in *Escherichia coli*, *Mol. Microbiol.* 65 (2007) 1106–1121.
- [38] A.K. Fenton, K. Gerdes, Direct interaction of FtsZ and MreB is required for septum synthesis and cell division in *Escherichia coli*, *EMBO J.* 32 (2013) 1953–1965.
- [39] S. Ray, A. Kumar, D. Panda, GTP regulates the interaction between MciZ and FtsZ: a possible role of MciZ in bacterial cell division, *Biochemistry* 52 (2013) 392–401.
- [40] E.F. Semeraro, J.M. Devos, L. Porcar, V.T. Forsyth, T. Narayanan, In vivo analysis of the *Escherichia coli* ultrastructure by small-angle scattering, *IUCr* 4 (2017) 751–757.
- [41] S.C. Setty, S. Horam, M. Pasupuleti, W. Haq, Modulating the antimicrobial activity of Temporin L through introduction of fluorinated phenylalanine, *Int. J. Pept. Res. Ther.* 23 (2017) 213–225.

Review

# Antimicrobial and Antibiofilm Peptides

Angela Di Somma <sup>1,2</sup> , Antonio Moretta <sup>3</sup>, Carolina Canè <sup>1</sup>, Arianna Cirillo <sup>4</sup> and Angela Duilio <sup>1,\*</sup>

<sup>1</sup> Dipartimento di Scienze Chimiche, Università Federico II, 80126 Naples, Italy; angela.disomma@unina.it (A.D.S.); cane@ceinge.unina.it (C.C.)

<sup>2</sup> Istituto Nazionale Biostrutture e Biosistemi (INBB), 00136 Rome, Italy

<sup>3</sup> Dipartimento di Scienze, Università degli Studi della Basilicata, 85100 Potenza, Italy; antonio.moretta@unibas.it

<sup>4</sup> CEINGE Biotecnologie Avanzate, 80145 Naples, Italy; cirilloa@ceinge.unina.it

\* Correspondence: angela.duilio@unina.it

Received: 27 March 2020; Accepted: 21 April 2020; Published: 23 April 2020



**Abstract:** The increasing onset of multidrug-resistant bacteria has propelled microbiology research towards antimicrobial peptides as new possible antibiotics from natural sources. Antimicrobial peptides are short peptides endowed with a broad range of activity against both Gram-positive and Gram-negative bacteria and are less prone to trigger resistance. Besides their activity against planktonic bacteria, many antimicrobial peptides also show antibiofilm activity. Biofilms are ubiquitous in nature, having the ability to adhere to virtually any surface, either biotic or abiotic, including medical devices, causing chronic infections that are difficult to eradicate. The biofilm matrix protects bacteria from hostile environments, thus contributing to the bacterial resistance to antimicrobial agents. Biofilms are very difficult to treat, with options restricted to the use of large doses of antibiotics or the removal of the infected device. Antimicrobial peptides could represent good candidates to develop new antibiofilm drugs as they can act at different stages of biofilm formation, on disparate molecular targets and with various mechanisms of action. These include inhibition of biofilm formation and adhesion, downregulation of quorum sensing factors, and disruption of the pre-formed biofilm. This review focuses on the properties of antimicrobial and antibiofilm peptides, with a particular emphasis on their mechanism of action, reporting several examples of peptides that over time have been shown to have activity against biofilm.

**Keywords:** antimicrobial peptides; biofilm; mechanism of action; biofilm formation inhibition; resistance

## 1. Introduction

In 1922, Alexander Fleming identified lysozyme from nasal mucus [1], which was considered the first human antimicrobial protein. This discovery was overshadowed when in 1928, Fleming discovered penicillin, which, together with streptomycin, in 1943, led to the beginning of the so-called “Golden Age of Antibiotics”. In the 1940s, along with Howard Florey and Ernst Chain, he brought the therapeutic use of penicillin to fruition, which allowed these scientists to be awarded the Nobel Prize for Medicine in 1945.

With the advent of the “Golden Age of Antibiotics”, there was a loss of interest in the therapeutic potential of natural antimicrobial peptides (AMPs), such as lysozyme [2,3]. However, in the 1960s, due to the increase in the number of multidrug-resistant microbial pathogens, the attention of the scientific community turned to the study of antimicrobial peptides [4–7]. Antimicrobial peptides are small molecules (10–100 amino acids) produced by all living organisms that play an essential role in the innate immunity [8,9]. Since the discovery of the first groups of AMPs, the magainins from the skin of the African clawed frog *Xenopus laevis* by Zasloff et al. [10–12] and the first antimicrobial peptides

isolated from the insect *Hyalophora cecropia* by Boman [13], an ever-increasing number of AMPs have been identified and studied. The Antimicrobial Peptide Database (APD, <http://aps.unmc.edu/AP>), which is constantly updated, contains 3180 antimicrobial peptides from 6 kingdoms: 355 from bacteria, 5 from archaea, 8 from protists, 20 from fungi, 352 from plants, and 2356 from animals, including some synthetic peptides (Figure 1). Cationic AMPs are the largest group even if anionic peptides have also been identified in vertebrates, invertebrates, and plants [9]. Antimicrobial peptides show a broad range of activity against Gram-negative and Gram-positive bacteria, fungi, mycobacteria, and some enveloped viruses [11]. In addition, it has been shown that they might also have cytotoxic effects against cancer cells [14–16].

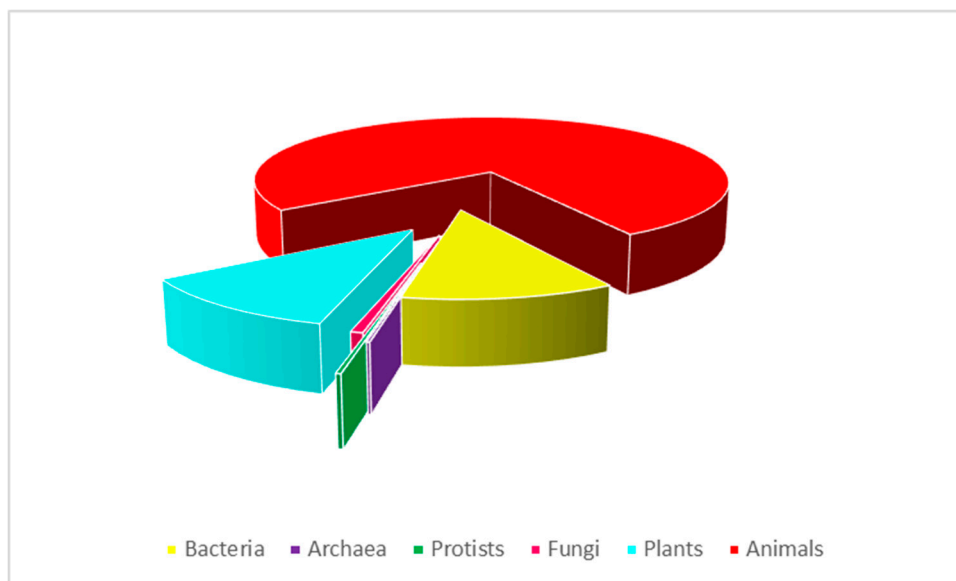


**Figure 1.** Antimicrobial peptides from the Antimicrobial Peptide Database (total of 3180). Data updated to 10th April 2020.

A further aspect of the AMPs activity that has been much investigated in recent years and needs to be more deeply considered is their ability to affect biofilm formation. Biofilms are a complex ensemble of microbial cells irreversibly associated to surfaces and enclosed in an essentially self-produced matrix consisting of polysaccharides, DNA, and proteins. They are ubiquitous in nature, having the ability to adhere to virtually any surface, either biotic or abiotic, including medical devices, causing chronic infections that are difficult to eradicate [17]. The biofilm matrix plays an active role in the development of antimicrobial resistance, protecting bacteria from the host immune system, hostile environmental conditions, and antimicrobial agents, including the majority of antibiotics. Biofilms are very difficult to treat due to their adaptive resistance to antibiotics compared to their planktonic counterparts [17]. Many AMPs show antibiofilm activity against multidrug-resistant bacteria, acting at different stages of biofilm formation, on disparate molecular targets and with various mechanisms.

This review focuses on antimicrobial peptides and their mechanism of action against biofilm formation.

## 2. Antimicrobial Peptides

### 2.1. Structure

AMPs can be classified in four groups according to their secondary structure:  $\alpha$ -helical,  $\beta$ -sheet, loop, and extended peptides [18].  $\alpha$ -helical and  $\beta$ -sheet peptides are more common and AMPs endowed with  $\alpha$ -helical structures are the most studied to date [19].  $\alpha$ -helical AMPs are linear in aqueous solution and will assume amphipathic helical structures when they interact with bacterial

membranes or in the presence of organic solvents [6]. Magainin-2 and LL-37 are examples of peptides that belong to this group (Figure 2a,b) [20,21]. In the  $\alpha$ -helix conformation, the distance between two close amino acids is around 0.15 nm while the angle between them with regard to the center is around 100 degrees from the top view [18].

$\beta$ -sheet peptides are stabilized by at least two disulphide bridges, organized to create an amphipathic structure [19,22,23]. This class includes protegrins (from the cathelicidin family); defensins, the largest group of  $\beta$ -sheet AMPs; and tachyplesins (Figure 2c,d) [24,25]. Due to their rigid structure,  $\beta$ -sheet AMPs are more structured in solution and do not undergo major conformational changes when interacting with a membrane environment [26,27]. Thanatin and lactoferricin B are peptides with a loop structure, stabilized by disulfide, amide, or isopeptide bonds (Figure 2e,f) [19].

The extended AMPs class is populated by peptides that do not show a regular secondary structure. These peptides are rich in arginine, tryptophan, glycine, proline, and histidine residues [19,28]. The 13-residue Arg- and Trp-rich tritrpticin and indolicidin peptides (Figure 2g,h) from porcine and bovine leukocytes, respectively, belong to this group of AMPs [29]. Due to their short length, a simple residue substitution can lead to broad changes in both their structural and functional properties. As an example, replacing Pro residues with Ala in tritrpticin will transform the peptide structure into an  $\alpha$ -helical conformation with improved antimicrobial activity but also with higher cytotoxicity [30].

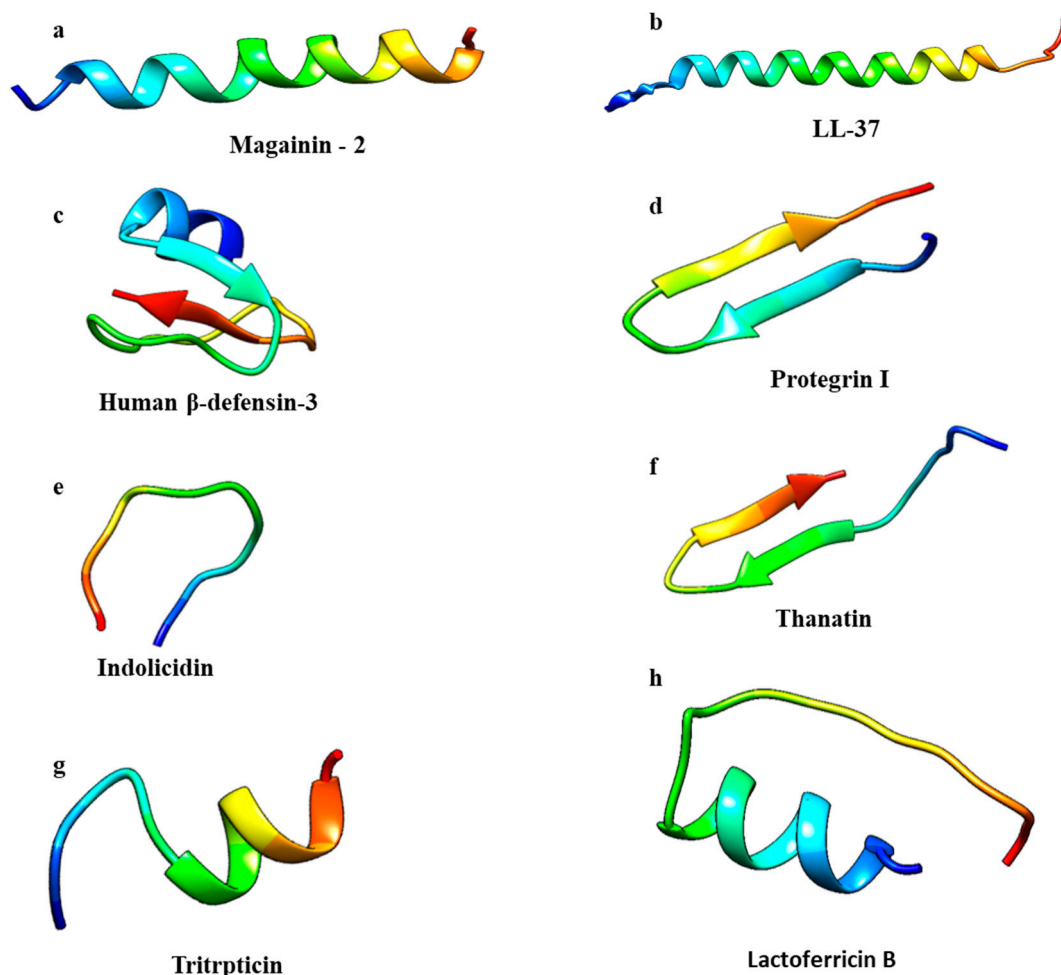


**Figure 2.** Antimicrobial peptide classes:  $\alpha$ -helical,  $\beta$ -sheet, loop, and extended. Structures were generated by CHIMERA software [31]. PDB codes: (a) 2MAG, Magainin-2; (b) 2K6O, LL-37; (c) 1KJ5, Human  $\beta$ -defensin-3; (d) 1PG1, Protegrin I; (e) 1G89, Indolicidin; (f) 5XO3, Thanatin; (g) 1D6X, Tritrpticin; (h) 1LFC, Lactoferricin B.

Antimicrobial peptides have a wide spectrum of action against bacteria, viruses, cancer cells, fungi, and parasites [11,14] as described in the following sections.

## 2.2. Antibacterial Peptides

Antibacterial peptides are among the most studied and are characterized by both hydrophobic and hydrophilic domains. Most of them are cationic and this positive net charge allows these peptides to interact with the negatively charged bacterial membranes [32]. Their mechanism of action has been widely studied. AMPs can lead to bacterial cell death through both membranolytic [33–35] and non-membranolytic mechanisms, interacting with intracellular targets, such as DNA, RNA, and proteins [36–39]. Both Gram-negative and Gram-positive bacteria have molecules on the outer membrane that confer a negative net charge, allowing the electrostatic interaction with cationic peptides [24]. Then, the AMPs accumulate at the surface and, once a certain concentration is reached, they assemble on the bacterial membrane [40].

Three different putative models have been proposed to describe the action of antimicrobial peptides. In the barrel-stave model, peptides perpendicularly insert into the membrane, promoting peptide–peptide lateral interactions. In this mechanism, the AMPs' amphipathic structure plays a significant role because the hydrophilic residues generate the channels' lumen while the hydrophobic side establishes a favorable interaction with membrane lipids [41]. To date, only a few peptides, such as pardaxin and alamethicin, that act through this mechanism have been identified [42,43].

The same event of peptide insertion into the membrane occurs in the toroidal model although the pore formation is not originated by peptide–peptide interactions. In this model, the peptide induces a curvature in the lipid bilayer and the pore is generated by both the peptide and the phospholipid head groups [44]. The essential difference between these two models is the arrangement of the lipid bilayer, as in the toroidal model, the hydrophobic and hydrophilic arrangement of the bilayer is disrupted while it is intact in the barrel-stave model. Many AMPs acting in the toroidal model have been found, including magainin-2 [25], protegrin-1 [45], melittin [46], and lactacin Q [25].

In the carpet model, the AMPs adsorb onto the membrane, covering the entire surface until a threshold concentration is reached [26]. At this stage, a detergent-like effect occurs, leading to the loss of membrane integrity and eventually to disintegration by micelle formation. In this model, specific peptide–peptide interactions are not required, and peptides do not insert into the hydrophobic core to form transmembrane channels [26]. Antimicrobial peptides like LL-37 and cecropin are known to adopt the carpet model mechanism [47,48].

In the non-membranolytic mechanism, peptides can inhibit cell wall and protein synthesis, bacterial cell division, or DNA replication by interacting with specific proteins involved in this biological process. As an example, Di Somma et al. [49] demonstrated that temporin-L (TL) interacts with *E. coli* FtsZ, a protein belonging to the divisome complex, leading to inhibition of the Z-ring formation, thus impairing cell division and causing bacterial death without damaging the cell membrane. Graf et al. reported the subclass of proline-rich AMPs (PrAMPs) that can penetrate the bacterial membrane and kill bacteria by inhibiting protein synthesis [39]. In particular, Mardirossian et al. tested the antimicrobial activity of Bac5 (1–25), an N-terminal fragment of the bovine proline-rich antimicrobial peptide Bac5, on *Escherichia coli*, *Acinetobacter baumannii*, *Klebsiella pneumoniae*, *Staphylococcus aureus*, *Salmonella enterica*, and *Pseudomonas aeruginosa*, showing the inhibition of bacterial protein synthesis [40]. In addition, the synthetic peptide 35409 has been reported to inhibit cell division and induce filamentation, suggesting two different targets within a bacterial cell [41], or the lysine-peptoid hybrid, LP5, binds DNA gyrase and topoisomerase IV, causing inhibition of the replication and ATP leakage from bacterial cells [42].

## 2.3. Anticancer Peptides

Antimicrobial peptides with anticancer activity, also called anticancer peptides (ACPs), are  $\alpha$ -helical or  $\beta$ -sheet peptides and can be divided into two groups. Peptides, such as insect cecropins and frog skin magainins, belong to the first group, characterized by peptides active against both

bacteria and cancer cells but not against normal mammalian cells [50–52]. Peptides toxic to bacteria and both normal and cancer cells, including the bee venom melittin, insect defensins, and the human LL-37 peptide [53,54], belong to the second group. ACPs can lead to cancer cells' death by membranolytic or non-membranolytic mechanisms according to the peptide characteristics and the peculiar target membrane features [55]. Cancer cells differ from normal mammalian cells due to their membrane net negative charge, which is conferred by anionic molecules, such as the phospholipids phosphatidylserine (PS), heparin sulfate, O-glycosylated mucins, and sialylated gangliosides. Differently, mammalian cell membranes are endowed with a zwitterionic character due to the molecules normally present on their membranes [14,45]. In healthy cells, the phosphatidylserine molecules are in the plasma membrane's inner-leaflet, while in cancer cells, the asymmetry between inner and outer membrane leaflets is lost, leading to the presence of PS in the outer leaflet [56,57]. The negative net charge exposed on the cancer outer membrane makes them similar to the bacterial membranes, suggesting that AMPs and ACPs might share similar molecular principles for selectivity and activity [58]. Dermaseptin B2 and B3 have been reported to be active against the proliferation of human prostate, mammary, and lymphoma cancer cells [58]. A study conducted by Lin et al. on the cytotoxic effect of epinecidin-1 on normal and cancer cells showed that this peptide could inhibit the growth of both tumor and normal cell lines. It was also demonstrated that epinecidin-1 induces cytotoxic effects and membrane lysis, perturbing the cancer cell membrane. In addition, this peptide inhibits necrosis in HT1080 cells (highly aggressive fibrosarcoma cell line) by downregulating the necrosis-related genes [59].

#### 2.4. Antiviral Peptides

Because of the emerging resistance of viruses and the limited efficiency of commonly used drugs, antiviral peptides represent good candidates as putative therapeutic agents [60]. Antiviral agents can act at different stages, by inhibiting the activity of viral reverse transcriptase or the pre-integration complex or avoiding the transport of circular viral DNA to the nucleus. Alternatively, they can inhibit the action of viral integrase, impairing viral DNA to integrate into the cellular chromosome. In addition, antiviral compounds may inhibit the viral proteases by blocking the retroviral morphogenesis because, after transcription, the proviral DNA is translated into a polyprotein that requires the activity of viral proteases to generate the proteins needed to assemble the viral capsid [61].

It has been demonstrated that both enveloped RNA and DNA viruses can be targeted by antiviral peptides [62]. AMPs can cause membrane instability by integrating into viral envelopes, thus preventing the viruses from infecting host cells [63]. Melittin, in addition to anticancer activity, has also been reported to have inhibitory activity against enveloped viruses, such as Junin virus (JV), HIV-1, and HSV-2. Melittin was suggested to suppress HSV-1 syncytial mutant-mediated cell fusion, very likely by interfering with the activity of Na<sup>+</sup> K<sup>+</sup> ATPase, a cellular enzyme involved in the membrane fusion process [64]. Some antiviral AMPs can prevent viral particles from entering the host cells by binding specific receptors on mammalian cells. For example, some  $\alpha$ -helical cationic peptides, such as lactoferrin, can prevent HSV infections by binding to heparan sulfate molecules needed for the attachment of HSV viral particles to the host cell surface, thus blocking virus–receptor interactions [65,66].

#### 2.5. Antifungal Peptides

According to their mechanism of action and origin, antifungal peptides can be grouped into membrane-traversing peptides, which can lead to pore formation or act on  $\beta$ -glucan or chitin synthesis, and non-membrane-traversing peptides that interact with the cell membrane and cause cell lysis [67]. Antifungal peptides can lead to fungi death through different mechanisms of action, including inhibition of DNA, RNA, and protein synthesis; induction of apoptotic mechanisms; permeabilization of membranes; inhibition of cell wall synthesis and enzyme activity; or repression of protein folding and metabolic turnover [68,69].

## 2.6. Antiparasitic Peptides

Magainins and cecropins were the first identified antimicrobial peptides that exhibited antiparasitic activity [70]. Although some parasitic microorganisms are multicellular, the mechanism of action of antiparasitic peptides (APPs) is very similar to AMPs, directly interacting with the cell membrane [71]. Scorpine, a peptide deriving from the venom of the scorpion *Pandinus imperator*, is able to inhibit the developmental stages of both the ookinete and gamete of *Plasmodium berghei* [72]. Bombinin H4 was reported to affect the viability of both insect and mammalian forms of *Leishmania* through perturbation of the plasma membranes at micromolar concentrations. The molecular mechanism consists in a rapid depolarization of the plasma membrane and loss of integrity associated with bioenergetic collapse [73]. Cathelicidin is a further example of APP that is able to kill *Caernohabditis elegans* through pore formation on the cell membrane [74].

## 3. Biofilm

Biofilm consists of a mixture of microorganisms embedded in self-produced extracellular polymeric substances (EPSs). The EPS constitutes a structural scaffold for other carbohydrates, proteins, nucleic acids, and lipids to adhere to. The presence of biofilms represents a severe problem in environmental, food, and biomedical fields as these architectures protect bacteria from hostile environments and prevent the effect of antimicrobial agents [75]. The exopolysaccharides' characteristics differ among various bacteria and depend on the growth conditions, medium, and availability of nutrients. In some forms of biofilm, mannose, galactose, and glucose are the most abundant carbohydrates, followed by N-acetyl-glucosamine, galacturonic acid, arabinose, fucose, rhamnose, and xylose, which occur in the composition of the biofilm matrix from *Enterococcus faecalis*, *Staphylococcus aureus*, *Klebsiella pneumoniae*, *Acinetobacter baumannii*, and *Pseudomonas aeruginosa* [76]. Most exopolysaccharides are not biofilm specific, but their production increases following a stress response, such as the production of colanic acid in *Escherichia coli* and the alginate synthesis in *P. aeruginosa* [77].

Biofilm formation and development consist of four different stages: (i) Aggregation or attachment; (ii) microbe adhesion; (iii) biofilm development and maturity; and (iiii) biofilm aging [78]. The aggregation or attachment step is divided into a reversible and irreversible phase. The reversible adhesion begins when the microorganisms come in contact with the target surface. During this event, some weak interactions, including van der Waals and electrostatic forces, and hydrophobic interactions between the molecules occurring on microbial cells and those present on the target surface are established. Afterwards, the irreversible adhesion phase takes place with the formation of covalent interactions and the initial production of exopolysaccharides. In the adhesion step, the formed microcolonies are protected by extracellular polysaccharides or by cellular organelles, such as pili and fimbriae, that allow bacterial cells to survive. During the third stage, the colony grows, acquiring a fungi-like architecture, and cells undergo further adaptation to life in a biofilm. In particular, two properties are often associated with surface-attached bacteria: The increased synthesis of EPSs and the development of antibiotic resistance. These features appear to create a protective environment and cause biofilms to be a tenacious clinical problem. Finally, in the last stage, the biofilm is capable of releasing part of the colonies into the environment and bacterial cells move to further colonize other surfaces in appropriate conditions, thus entering another biofilm cycle. Each stage of the biofilm formation process depends on the microbial genera and species, the characteristics of the attachment surface, the environmental conditions, and the physiological status of the microorganism [79]. Microorganisms' attachment occurs more commonly on surfaces that are hydrophobic, rough, and coated by conditioning films. On the contrary, attachment to surfaces is made more complicated by electrostatic repulsion between the negative organic molecules of surfaces and the bacteria membrane.



### 3.1. Antimicrobial Peptides and Biofilm

The antibiofilm activity of antimicrobial peptides has been less studied than their antimicroorganism capabilities. Moreover, the assessment of a specific ability to impair biofilm formation well apart from their antimicrobial activity is quite difficult to achieve. An AMP can be considered to be antibiofilm if the minimum biofilm inhibitory concentration (MBIC) is below the minimum inhibitory concentration (MIC), with a distinct activity compared to the direct killing antimicrobial capability. Eradication of preformed biofilms is much more difficult than inhibition [80], and the minimum biofilm eradication concentration (MBEC), i.e., the minimum concentration of an antimicrobial agent required to eliminate pre-formed biofilms, is generally larger than MBIC. In all cases, it is fundamental to being able to distinguish between dead and living cells. Recently, Raheem and Straus [81] described many biological assays and biophysical methods and techniques to define the specific antibacterial and antibiofilm functions' peptides. For all these reasons, few peptides endowed with real antibiofilm activity have been identified so far; some of these peptides are listed in Table 1.

**Table 1.** Some of the known antibiofilm peptides. Peptide name, sequence, and source are reported.

Peptide	Sequence	Source	Reference
Protegrin 1	RGGRLCYRRRFCVCGR	leukocytes; Pig, <i>Sus scrofa</i>	[82]
Pleurocidin	GWGSFFKAAHVGKHHVGAALHLYL	skin mucous secretions, Winter flounder, <i>Pleuronectes americanus</i>	[83]
LL-37	LLGDFFRKSKEKIGKEFKRIVQRIKDFLRNLPRTES	neutrophils, monocytes; mast cells; lymphocytes, Mesenchymal Stem Cells; islets; skin, sweat; airway surface liquid, saliva; <i>Homo sapiens</i> ; Also <i>Pan troglodytes</i>	[84]
Indolicidin	ILPWKWPWWPWRR	bovine neutrophils, <i>Bos taurus</i>	[85]
SMAP-29	RGLRRLGRKIAHGVKKGPTVLRIRIAG	sheep leukocytes; <i>Ovis aries</i>	[86]
Human $\beta$ defensin 3	GIINTLQKYCRVRGGRCVAVLSCLPKKEQIGKCSTRGRKCCRKK	skin, tonsils, oral/saliva, <i>Homo sapiens</i>	[87]

Antibiofilm peptides were demonstrated to affect biofilm formation or degradation at different stages and with different mechanisms of action, including inhibition of biofilm formation and adhesion, downregulation of quorum sensing, and killing of pre-formed biofilm [88,89] (Figure 3).

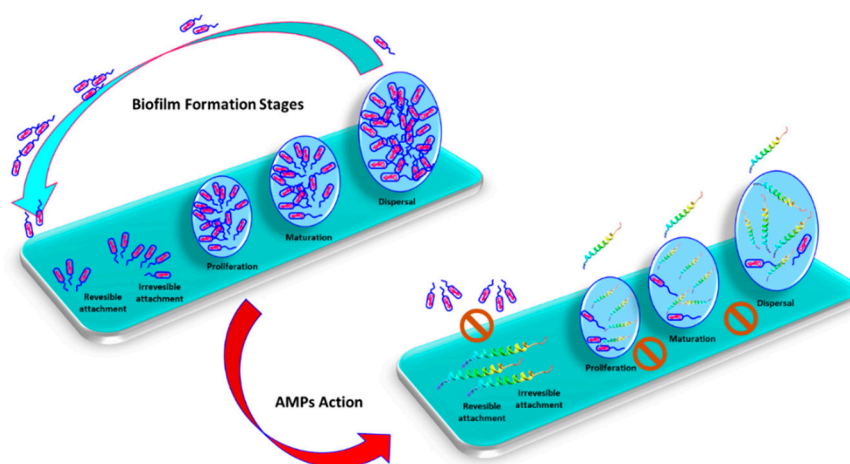


**Figure 3.** Biofilm formation consists on attachment, proliferation, mutation and detachment stages, which can be inhibited by antimicrobial peptides

Nisin A is able to disrupt or degrade the membrane of biofilm-embedded cells of an MRSA strain of *S. aureus*, disturbing the membrane potential [90]. Human cathelicidin LL-37, one of the most studied antibiofilm peptides, is able to affect the bacterial cell signaling system. This peptide can inhibit *P. aeruginosa* biofilm formation at a concentration of 0.5  $\mu\text{g}/\text{mL}$  by downregulating the genes related to the QS system, decreasing the attachment of bacterial cells on the surface and stimulating twitching motility mediated by type IV pili [89,91].

Antimicrobial peptides can also lead to the degradation of the extracellular polymeric matrix of bacterial biofilms. Hepcidin 20 can reduce the extracellular matrix mass of *Staphylococcus epidermidis* and alter its biofilm architecture by targeting the polysaccharide intercellular adhesin (PIA) [92]. Antibiofilm peptides can also target a stringent stress response in both Gram-negative and Gram-positive bacteria or downregulate genes involved in biofilm formation and the transportation of binding proteins [93]. Biofilm formation in staphylococci depends on the synthesis of the polysaccharide intracellular adhesin (PIA), which is encoded by the *icaADBC* locus. Human  $\beta$ -defensin 3 was shown to be able to reduce the expression of the *icaA*, *IcaR*, and *icaD* genes of *S. epidermidis* ATCC 35,984, leading to a reduction of biofilm formation [94].

Gopal et al. [95] reported that NRC-16, a pleurocidin peptide analogue, showed MIC values ranging from 2.17 to 17.4  $\mu\text{g/mL}$  on planktonic bacteria vs. biofilms against different Gram-negative and Gram-positive bacteria, and fungi. It is interesting to note that similar results were obtained with the melittin peptide. For both of them, minimal biofilm inhibitory concentration (MBIC) values ranging from 8 to 35  $\mu\text{g/mL}$  against five clinical strains of *P. aeruginosa* have been obtained [95]. Moreover, Blower et al. [86] demonstrated that the SMAP-29 peptide is able to inhibit biofilm production in *Burkholderia thailandensis* by about 50% at peptide concentrations at or above 3  $\mu\text{g/mL}$ . Anunthawan et al. studied KT2 and RT2, two synthetic tryptophan-rich cationic peptides, which showed activity against multidrug-resistant *E. coli* biofilms at sub-MIC levels [96]. Another peptide known as CRAMP is able to inhibit fungal biofilm formation [97], but surprisingly, it was demonstrated that AS10, a CRAMP shorter fragment, was able to inhibit biofilm growth of *Candida albicans*, *E. coli*, and *P. aeruginosa* [98]. Moreover, IDR-1018 showed antibiofilm activity against several Gram-positive and Gram-negative pathogens [99]. De la Fuente-Núñez et al. studied two synthetic peptides DJK-5 and DJK-6 based on properties associated with IDR-1018, which showed a broad spectrum of antibiofilm activity and the ability to eradicate pre-existing biofilms [100]. Mataraci and Dosler designed the CAMA peptide, a hybrid peptide (cecropin (1-7)–melittin A (2-9) amide) containing the N-terminal region of cecropin A and the N-terminal portion of melittin A. Interestingly, this peptide was able to inhibit methicillin-resistant *Staphylococcus aureus* (MRSA) biofilm formation [101].

### 3.2. Biofilm Resistance to Antimicrobial Peptides

One of the ideas associated to the biofilm resistance to AMPs is related to their interaction with EPS even if the mechanism is still not well understood. Most of the molecules making up EPS have a negative charge, but the exopolymer PIA, composed of poly-N-acetyl glucosamine, is positively charged and it might protect the biofilm from AMPs through electrostatic repulsion with the positively charged peptides [102]. In fact, PIA was demonstrated to defend *S. epidermidis* and *S. aureus* from the LL-37 and the human  $\beta$ -defensin peptides' action [103].

Alginate, made up of the uronic acid D-mannuronate and the C-5 epimer-L guluronate, is an anionic extracellular polysaccharide secreted by Gram-negative bacteria that can interact with positively charged peptides, protecting biofilm-embedded cells. Alginate is able to trap antimicrobial peptides in hydrophobic microdomains consisting of pyranosyl C–H groups, which are inducible when the complexes AMPs–alginate are formed, owing to the charge neutralization between the two species [104,105].

In Gram-positive bacteria, the resistance to AMPs can be mediated by the membrane protein MprF, which is involved in the addition of alanine or lysine to phosphatidylglycerol (PG) to form alanyl-phosphatidylglycerol (APG) and lysyl-phosphatidylglycerol (LPG), respectively, and in the translocation of these compounds to the outer leaflet [106,107]. It was demonstrated that MprF mutants of *S. aureus* were more susceptible to AMPs, suggesting that the addition of lysine or arginine to the membrane could lead to a reduction in the susceptibility to AMPs [108]. An MprF homolog has been found in *P. aeruginosa* involved in the addition of alanine to PG to form APG. This modification led to an increased resistance to antimicrobial agents [109].

In *P. aeruginosa* and *Salmonella enterica*, the PhoP/PhoQ genetic system is able to decrease the LPS net negative charge by adding aminoarabinose to the lipid, conferring AMPs' resistance to bacterial biofilms [110]. In *P. aeruginosa*, a two-component regulatory system pmrA-pmrB has also been found, which regulates resistance to LL-37, polymyxin B, and polymyxin E. This system modifies LPSs in the bacteria's outer membrane, leading to a reduction of the AMPs' interaction with the outer membrane [111]. Moreover, it was found that the addition of an acyl chain to lipid A might contribute to bacterial resistance to AMPs. In *S. enterica Typhimurium*, the PagP enzyme adds additional palmitate (C16:0 acyl chain) to the lipid A moiety. This acylation is thought to be responsible for the increase of the hydrophobic interactions between lipid A and the acyl chains, thus leading to a higher outer membrane fluidity [112]. A higher membrane permeability in response to AMPs was observed in pagP mutants of *S. enterica Typhimurium*, compared to the control strain [113]. It was also demonstrated that deacylation could increase the bacteria's susceptibility to AMPs, thus supporting the finding that lipid A acylation is involved in the bacterial resistance to antimicrobial peptides. The PagL enzyme, located on the outer membrane of several Gram-negative bacteria, is responsible for the deacylation of lipid A, removing R-3-hydroxymyristate from position 3 of some lipid A precursor [114].

The two component systems (TCSs) are used by bacteria to respond to environmental changes. TCSs consist of a membrane sensor, which is able to detect signals from the environment that are transferred by activating a transcriptional response regulator through phosphorylation or de-phosphorylation. The receptor is usually a histidine kinase located in the cytoplasmic membrane that can be activated by environmental signals. The cytoplasmic protein is phosphorylated by the sensor and acts as a transcription factor. The response involves the activation of genes, such as membrane-remodeling genes, ion transporters, and virulence genes, which help Gram-negative and Gram-positive bacteria to better adapt to the environment. Several TCSs systems are known to respond to AMPs, thus helping bacteria to counteract their activity [115–117].

#### 4. Discussion and Future Considerations

The identification of new therapeutic strategies to counteract biofilm-associated infections is among the main challenges in medicine. The high concentrations of antibiotics used in order to disrupt or prevent biofilm formation could be associated with poor prognosis and cytotoxicity. For this reason, a promising strategy might consist in the use of alternative drugs to address biofilm-related infections. Because of their peculiar characteristics, antimicrobial peptides have to be considered as valid candidates in the fight against biofilms. However, AMPs' interaction with EPS components might affect their antimicrobial activity, representing an obstacle for the development of AMPs as antibiofilm drugs. Designed antibiofilm peptides could be used to interfere with signaling pathways involved in the synthesis of EPS components. Otherwise, EPS–AMP interactions could even be used for the design of AMP-based antibiofilm strategies in order to seize essential EPS components, interfering with the biofilm architecture.

The strategy of combining biofilm dispersing agents with conventional antibiotics could also be exploited. Bacterial invasions are often impossible to eradicate by the direct administration of antibiotics due to the protection effect exerted by biofilms, and the use of a high concentration of antibiotics has to be discouraged due to their extreme toxicity. AMP–AMP and AMP–drug combinations induce biofilm matrix degradation, allowing the antibacterial agent to escape protection and to reach bacterial cells, which may be potential areas of future anti-biofilm study and research. Promising combinatorial strategies can then be foreseen consisting in the use of AMPs with compounds able to dissolve the biofilm matrix or antimicrobial peptides in association with drugs used for anti-infective therapy, with anti-inflammatory or mucolytic agents, such as salicylic acid or ibuprofen, or with inhibitors of QS [118].

**Author Contributions:** Conceptualization, A.D.S., A.D.; Writing – original draft, A.D.S., A.M., C.C., A.C., A.D.; Final editing, A.D. All authors have read and agreed to the published version of the manuscript.

**Funding:** This work was supported in part by MIUR grants ARS01\_00597 Project “NAOCON” and PRIN 2017 “Identification and characterization of novel antitumoral/antimicrobial insect-derived peptides: a multidisciplinary, integrated approach from in silico to in vivo”.

**Conflicts of Interest:** The authors declare no conflict of interest.

## Abbreviations

AMPs	Antimicrobial peptides
APD	Antimicrobial Peptide Database
ACPs	Anticancer peptides
MBIC	Minimum Biofilm Inhibitory Concentration
MBEC	Minimum Biofilm Eradication Concentration
MIC	Minimum Inhibitory Concentration
QS	Quorum Sensing
PIA	Polysaccharide Intracellular Adhesin
EPS	Extracellular Polymeric Substances
PS	Phosphatidylserine
PG	Phosphatidylglycerol
APG	Alanyl - Phosphatidylglycerol
LPG	Lysyl - Phosphatidylglycerol
TCS	Two Component Systems

## References

1. Fleming, A. On the antibacterial action of cultures of a penicillium, with special reference to their use in the isolation of *B. influenzae*. *Br. J. Exp. Pathol.* **1929**, *10*, 226. [[CrossRef](#)]
2. Zaffiri, L.; Gardner, J.; Toledo-Pereyra, L.H. History of antibiotics. From salvarsan to cephalosporins. *J. Investig. Surg.* **2012**, *25*, 67–77. [[CrossRef](#)] [[PubMed](#)]
3. Bentley, R. Different roads to discovery; Prontosil (hence sulfa drugs) and penicillin (hence  $\beta$ -lactams). *J. Ind. Microbiol. Biotechnol.* **2009**, *36*, 775–786. [[CrossRef](#)] [[PubMed](#)]
4. Davies, J. Where have all the antibiotics gone? *Can. J. Infect. Dis. Med Microbiol.* **2006**, *17*, 287–290. [[CrossRef](#)] [[PubMed](#)]
5. Katz, M.L.; Mueller, L.V.; Polyakov, M.; Weinstock, S.F. Where have all the antibiotic patents gone? *Nat. Biotechnol.* **2006**, *24*, 1529. [[CrossRef](#)]
6. Mahlapuu, M.; Håkansson, J.; Ringstad, L.; Björn, C. Antimicrobial peptides: An emerging category of therapeutic agents. *Front. Cell. Infect. Microbiol.* **2016**, *6*, 194. [[CrossRef](#)]
7. Guaní-Guerra, E.; Santos-Mendoza, T.; Lugo-Reyes, S.O.; Terán, L.M. Antimicrobial peptides: General overview and clinical implications in human health and disease. *Clin. Immunol.* **2010**, *135*, 1–11. [[CrossRef](#)]
8. Harris, F.; Sarah, R.D.; David, A.P. Anionic antimicrobial peptides from eukaryotic organisms. *Curr. Protein Pept. Sci.* **2009**, *10*, 585–606. [[CrossRef](#)]
9. Malik, E.; Dennison, S.; Harris, F.; Phoenix, D. pH dependent antimicrobial peptides and proteins, their mechanisms of action and potential as therapeutic agents. *Pharmaceuticals* **2016**, *9*, 67. [[CrossRef](#)]
10. Zasloff, M. Magainins, a class of antimicrobial peptides from *Xenopus* skin: Isolation, characterization of two active forms, and partial cDNA sequence of a precursor. *Proc. Natl. Acad. Sci. USA* **1987**, *84*, 5449–5453. [[CrossRef](#)]
11. Zasloff, M. Antimicrobial peptides of multicellular organisms. *Nature* **2002**, *415*, 389. [[CrossRef](#)] [[PubMed](#)]
12. Soravia, E.; Martini, G.; Zasloff, M. Antimicrobial properties of peptides from *Xenopus* granular gland secretions. *FEBS Lett.* **1988**, *228*, 337–340. [[CrossRef](#)]
13. Steiner, H.; Hultmark, D.; Engström, Å.; Bennich, H.; Boman, H.G. Sequence and specificity of two antibacterial proteins involved in insect immunity. *Nature* **1981**, *292*, 246. [[CrossRef](#)] [[PubMed](#)]
14. Hoskin, D.W.; Ramamoorthy, A. Studies on anticancer activities of antimicrobial peptides. *Biochim. Biophys. Acta (BBA)-Biomembr.* **2008**, *1778*, 357–375. [[CrossRef](#)]
15. Kumar, P.; Kizhakkedathu, J.N.; Straus, S.K. Antimicrobial peptides: Diversity, mechanism of action and strategies to improve the activity and biocompatibility in vivo. *Biomolecules* **2018**, *8*, 4. [[CrossRef](#)]

16. Felício, M.R.; Silva, O.N.; Gonçalves, S.; Santos, N.C.; Franco, O.L. Peptides with dual antimicrobial and anticancer activities. *Front. Chem.* **2017**, *5*, 5. [[CrossRef](#)]
17. Jefferson, K.K. What drives bacteria to produce a biofilm? *FEMS Microbiol. Lett.* **2004**, *236*, 163–173. [[CrossRef](#)]
18. Bahar, A.A.; Dacheng, R. Antimicrobial peptides. *Pharmaceuticals* **2013**, *6*, 1543–1575. [[CrossRef](#)]
19. Powers, J.-P.S.; Hancock, R.E. The relationship between peptide structure and antibacterial activity. *Peptides* **2003**, *24*, 1681–1691. [[CrossRef](#)]
20. Huang, Y.B.; Huang, J.F.; Chen, Y.X. Alpha-helical cationic antimicrobial peptides: Relationships of structure and function. *Protein Cell* **2010**, *1*, 143–152. [[CrossRef](#)]
21. Lewies, A.; Wentzel, J.; Jacobs, G.; Du Plessis, L. The potential use of natural and structural analogues of antimicrobial peptides in the fight against neglected tropical diseases. *Molecules* **2015**, *20*, 15392–15433. [[CrossRef](#)] [[PubMed](#)]
22. Yount, N.Y.; Bayer, A.S.; Xiong, Y.Q.; Yeaman, M.R. Advances in antimicrobial peptide immunobiology. *Pept. Sci. Orig. Res. Biomol.* **2006**, *84*, 435–458. [[CrossRef](#)]
23. Bulet, P.; Stöcklin, R.; Menin, L. Anti-microbial peptides: From invertebrates to vertebrates. *Immunol. Rev.* **2004**, *198*, 169–184. [[CrossRef](#)] [[PubMed](#)]
24. Pasupuleti, M.; Schmidtchen, A.; Malmsten, M. Antimicrobial peptides: Key components of the innate immune system. *Crit. Rev. Biotechnol.* **2012**, *32*, 143–171. [[CrossRef](#)] [[PubMed](#)]
25. Lee, T.H.; Hall, K.N.; Aguilar, M.I. Antimicrobial peptide structure and mechanism of action: A focus on the role of membrane structure. *Curr. Top. Med. Chem.* **2016**, *16*, 25–39. [[CrossRef](#)] [[PubMed](#)]
26. Yeaman, M.R.; Yount, N.Y. Mechanisms of antimicrobial peptide action and resistance. *Pharmacol. Rev.* **2003**, *55*, 27–55. [[CrossRef](#)]
27. Dhople, V.; Krukemeyer, A.; Ramamoorthy, A. The human beta-defensin-3, an antibacterial peptide with multiple biological functions. *Biochim. Biophys. Acta (BBA)-Biomembr.* **2006**, *1758*, 1499–1512. [[CrossRef](#)]
28. Nguyen, L.T.; Haney, E.F.; Vogel, H.J. The expanding scope of antimicrobial peptide structures and their modes of action. *Trends Biotechnol.* **2011**, *29*, 464–472. [[CrossRef](#)]
29. Falla, T.J.; Karunaratne, D.N.; Hancock, R.E. Mode of action of the antimicrobial peptide indolicidin. *J. Biol. Chem.* **1996**, *271*, 19298–19303. [[CrossRef](#)]
30. Schibli, D.J.; Nguyen, L.T.; Kernaghan, S.D.; Rekdal, Ø.; Vogel, H.J. Structure-function analysis of tritrypticin analogs: Potential relationships between antimicrobial activities, model membrane interactions, and their micelle-bound NMR structures. *Biophys. J.* **2006**, *91*, 4413–4426. [[CrossRef](#)] [[PubMed](#)]
31. Pettersen, E.F.; Goddard, T.D.; Huang, C.C.; Couch, G.S.; Greenblatt, D.M.; Meng, E.C.; Ferrin, T.E. UCSF Chimera—A visualization system for exploratory research and analysis. *J. Comput. Chem.* **2004**, *25*, 1605–1612. [[CrossRef](#)] [[PubMed](#)]
32. Wieprecht, T.; Apostolov, O.; Seelig, J. Binding of the antibacterial peptide magainin 2 amide to small and large unilamellar vesicles. *Biophys. Chem.* **2000**, *85*, 187–198. [[CrossRef](#)]
33. Haney, E.F.; Straus, S.K.; Hancock, R.E.W. Reassessing the Host Defense Peptide Landscape. *Front. Chem.* **2019**, *7*, 43. [[CrossRef](#)] [[PubMed](#)]
34. Mankoci, S.; Ewing, J.; Dalai, P.; Sahai, N.; Barton, H.A.; Joy, A. Bacterial Membrane Selective Antimicrobial Peptide-Mimetic Polyurethanes: Structure—Property Correlations and Mechanisms of Action. *Biomacromolecules* **2019**, *20*, 4096–4106. [[CrossRef](#)] [[PubMed](#)]
35. Alghalayini, A.; Garcia, A.; Berry, T.; Cranfield, C.G. The Use of Tethered Bilayer Lipid Membranes to Identify the Mechanisms of Antimicrobial Peptide Interactions with Lipid Bilayers. *Antibiotics* **2019**, *8*, 12. [[CrossRef](#)] [[PubMed](#)]
36. Brogden, K.A. Antimicrobial peptides: Pore formers or metabolic inhibitors in bacteria? *Nat. Rev. Microbiol.* **2005**, *3*, 238. [[CrossRef](#)] [[PubMed](#)]
37. Cassone, M.; Frith, N.; Vogiatzi, P.; Wade, J.D.; Otvos, L. Induced resistance to the designer proline-rich antimicrobial peptide A3-APO does not involve changes in the intracellular target DnaK. *Int. J. Pept. Res. Ther.* **2009**, *15*, 121–128. [[CrossRef](#)]
38. Shah, P.; Hsiao, F.S.H.; Ho, Y.H.; Chen, C.S. The proteome targets of intracellular targeting antimicrobial peptides. *Proteomics* **2016**, *16*, 1225–1237. [[CrossRef](#)]
39. Graf, M.; Wilson, D.N. Intracellular Antimicrobial Peptides Targeting the Protein Synthesis Machinery. *Adv. Exp. Med. Biol.* **2019**, *1117*, 73–89. [[CrossRef](#)] [[PubMed](#)]

40. Mardirossian, M.; Sola, R.; Degasperi, M.; Scocchi, M. Search for Shorter Portions of the Proline-Rich Antimicrobial Peptide Fragment Bac5 (1–25) That Retain Antimicrobial Activity by Blocking Protein Synthesis. *ChemMedChem* **2019**, *14*, 343–348. [[CrossRef](#)]
41. Barreto-Santamaría, A.; Curtidor, H.; Arévalo-Pinzón, G.; Herrera, C.; Suárez, D.; Pérez, W.H.; Patarroyo, M.E. A new synthetic peptide having two target of antibacterial action in *E. coli* ML35. *Front. Microbiol.* **2016**, *7*. [[CrossRef](#)] [[PubMed](#)]
42. Gottschalk, S.; Ifrah, D.; Lerche, S.; Gottlieb, C.T.; Cohn, M.T.; Hiasa, H.; Thomsen, L.E. The antimicrobial lysine-peptoid hybrid LP5 inhibits DNA replication and induces the SOS response in *Staphylococcus aureus*. *BMC Microbiol.* **2013**, *13*. [[CrossRef](#)]
43. Rapaport, D.; Shai, Y. Interaction of fluorescently labeled pardaxin and its analogues with lipid bilayers. *J. Biol. Chem.* **1991**, *266*, 23769–23775. [[PubMed](#)]
44. Wimley, W.C. Describing the mechanism of antimicrobial peptide action with the interfacial activity model. *ACS Chem. Biol.* **2010**, *5*, 905–917. [[CrossRef](#)]
45. Yamaguchi, S.; Hong, T.; Waring, A.; Lehrer, R.I.; Hong, M. Solid-state NMR investigations of peptide-lipid interaction and orientation of a  $\beta$ -sheet antimicrobial peptide, protegrin. *Biochemistry* **2002**, *41*, 9852–9862. [[CrossRef](#)] [[PubMed](#)]
46. Henzler Wildman, K.A.; Lee, D.K.; Ramamoorthy, A. Mechanism of lipid bilayer disruption by the human antimicrobial peptide, LL-37. *Biochemistry* **2003**, *42*, 6545–6558. [[CrossRef](#)]
47. Shai, Y. Mode of action of membrane active antimicrobial peptides. *Pept. Sci. Orig. Res. Biomol.* **2002**, *66*, 236–248. [[CrossRef](#)] [[PubMed](#)]
48. Sitaram, N.; Nagaraj, R. Interaction of antimicrobial peptides with biological and model membranes: Structural and charge requirements for activity. *Biochim. Biophys. Acta (BBA)-Biomembr.* **1999**, *1462*, 29–54. [[CrossRef](#)]
49. Di Somma, A.; Avitabile, C.; Cirillo, A.; Moretta, A.; Merlino, A.; Paduano, L.; Duilio, A.; Romanelli, A. The antimicrobial peptide Temporin L impairs *E. coli* cell division by interacting with FtsZ and the divisome complex. *Biochim. Biophys. Acta-Gen. Subj.* **2020**, *1864*, 129606. [[CrossRef](#)] [[PubMed](#)]
50. Baker, M.A.; Maloy, W.L.; Zasloff, M.; Jacob, L.S. Anticancer efficacy of Magainin 2 and analogue peptides. *Cancer Res.* **1993**, *53*, 3052–3057. [[PubMed](#)]
51. Schweizer, F. Cationic amphiphilic peptides with cancer-selective toxicity. *Eur. J. Pharmacol.* **2009**, *625*, 190–194. [[CrossRef](#)] [[PubMed](#)]
52. Papo, N.; Shahar, M.; Eisenbach, L.; Shai, Y. A novel lytic peptide composed of DL-amino acids selectively kills cancer cells in culture and in mice. *J. Biol. Chem.* **2003**, *278*, 21018–21023. [[CrossRef](#)] [[PubMed](#)]
53. Mai, J.C.; Mi, Z.; Kim, S.H.; Ng, B.; Robbins, P.D. A proapoptotic peptide for the treatment of solid tumors. *Cancer Res.* **2001**, *61*, 7709–7712. [[PubMed](#)]
54. Bulet, P.; Hetru, C.; Dimarcq, J.L.; Hoffmann, D. Antimicrobial peptides in insects; structure and function. *Dev. Comp. Immunol.* **1999**, *23*, 329–344. [[CrossRef](#)]
55. Harris, F.; Dennison, S.R.; Singh, J.; Phoenix, D.A. On the selectivity and efficacy of defense peptides with respect to cancer cells. *Med. Res. Rev.* **2013**, *33*, 190–234. [[CrossRef](#)] [[PubMed](#)]
56. Bevers, E.M.; Comfurius, P.; Zwaal, R.F.A. Regulatory mechanisms in maintenance and modulation of transmembrane lipid asymmetry: Pathophysiological implications. *Lupus* **1996**, *5*, 480–487. [[CrossRef](#)] [[PubMed](#)]
57. Utsugi, T.; Schroit, A.J.; Connor, J.; Bucana, C.D.; Fidler, I.J. Elevated expression of phosphatidylserine in the outer membrane leaflet of human tumor cells and recognition by activated human blood monocytes. *Cancer Res.* **1991**, *51*, 3062–3066. [[PubMed](#)]
58. Van Zoggel, H.; Hamma-Kourbali, Y.; Galanth, C.; Ladram, A.; Nicolas, P.; Courty, J.; Amiche, M.; Delbé, J. Antitumor and angiostatic peptides from frog skin secretions. *Amino Acids* **2012**, *42*, 385–395. [[CrossRef](#)]
59. Lin, W.J.; Chien, Y.L.; Pan, C.Y.; Lin, T.L.; Chen, J.Y.; Chiu, S.J.; Hui, C.F. Epinecidin-1, an antimicrobial peptide from fish (*Epinephelus coioides*) which has an antitumor effect like lytic peptides in human fibrosarcoma cells. *Peptides* **2009**, *30*, 283–290. [[CrossRef](#)] [[PubMed](#)]
60. Kołodziej, M.; Joniec, J.; Bartoszcze, M.; Mirski, T.; Gryko, R. Peptides—A new strategy for combating viral infections. *Przegląd Epidemiologiczny* **2011**, *65*, 477–482.
61. Goodsell, D.S. Illustrations of the HIV life cycle. In *The Future of HIV-1 Therapeutics*; Springer: Cham, Switzerland, 2015; pp. 243–252. [[CrossRef](#)]

62. Horne, W.S.; Wiethoff, C.M.; Cui, C.; Wilcoxon, K.M.; Amorin, M.; Ghadiri, M.R.; Nemerow, G.R. Antiviral cyclic d, l- $\alpha$ -peptides: Targeting a general biochemical pathway in virus infections. *Bioorg. Med. Chem.* **2005**, *13*, 5145–5153. [[CrossRef](#)] [[PubMed](#)]
63. Mulder, K.; Lima, L.A.; Miranda, V.; Dias, S.C.; Franco, O.L. Current scenario of peptide-based drugs: The key roles of cationic antitumor and antiviral peptides. *Front. Microbiol.* **2013**, *4*, 321. [[CrossRef](#)] [[PubMed](#)]
64. Matanic, V.C.A.; Castilla, V. Antiviral activity of antimicrobial cationic peptides against *Junin virus* and *herpes simplex virus*. *Int. J. Antimicrob. Agents* **2004**, *23*, 382–389. [[CrossRef](#)] [[PubMed](#)]
65. Andersen, J.H.; Jenssen, H.; Sandvik, K.; Gutteberg, T.J. Anti-HSV activity of lactoferrin and lactoferricin is dependent on the presence of heparan sulphate at the cell surface. *J. Med Virol.* **2004**, *74*, 262–271. [[CrossRef](#)] [[PubMed](#)]
66. Jenssen, H.; Andersen, J.H.; Uhlin-Hansen, L.; Gutteberg, T.J.; Rekdal, Ø. Anti-HSV activity of lactoferricin analogues is only partly related to their affinity for heparan sulfate. *Antivir. Res.* **2004**, *61*, 101–109. [[CrossRef](#)] [[PubMed](#)]
67. Singh, K.; Rani, J. Sequential and structural aspects of antifungal peptides from animals, bacteria and fungi based on bioinformatics tools. *Probiotics Antimicrob. Proteins* **2016**, *8*, 85–101. [[CrossRef](#)]
68. Aoki, W.; Ueda, M. Characterization of antimicrobial peptides toward the development of novel antibiotics. *Pharmaceuticals* **2013**, *6*, 1055–1081. [[CrossRef](#)] [[PubMed](#)]
69. Van der Weerden, N.L.; Bleackley, M.R.; Anderson, M.A. Properties and mechanisms of action of naturally occurring antifungal peptides. *Cell. Mol. Life Sci.* **2013**, *70*, 3545–3570. [[CrossRef](#)] [[PubMed](#)]
70. Gwadz, R.W.; Kaslow, D.; Lee, J.Y.; Maloy, W.L.; Zasloff, M.; Miller, L.H. Effects of magainins and cecropins on the sporogonic development of malaria parasites in mosquitoes. *Infect. Immun.* **1989**, *579*, 2628–2633. [[CrossRef](#)]
71. Dagan, A.; Efron, L.; Gaidukov, L.; Mor, A.; Ginsburg, H. In vitro antiplasmodium effects of dermaseptin S4 derivatives. *Antimicrob. Agents Chemother.* **2002**, *46*, 1059–1066. [[CrossRef](#)]
72. Conde, R.; Zamudio, F.Z.; Rodriguez, M.H.; Possani, L.D. Scorpine, an anti-malaria and anti-bacterial agent purified from scorpion venom. *FEBS Lett.* **2000**, *471*, 165–168. [[CrossRef](#)]
73. Mangoni, M.L.; Papo, N.; Saugar, J.M.; Barra, D.; Shai, Y.; Simmaco, M.; Rivas, L. Effect of natural L-to D-amino acid conversion on the organization, membrane binding, and biological function of the antimicrobial peptides bombinins H. *Biochemistry* **2006**, *45*, 4266–4276. [[CrossRef](#)] [[PubMed](#)]
74. Park, Y.; Jang, S.H.; Lee, D.G.; Hahm, K.S. Antinematodal effect of antimicrobial peptide, PMAP-23, isolated from porcine myeloid against *Caenorhabditis elegans*. *J. Pept. Sci.* **2004**, *10*, 304–311. [[CrossRef](#)] [[PubMed](#)]
75. Maukonen, J.; Mättö, J.; Wirtanen, G.; Raaska, L.; Mattila-Sandholm, T.; Saarela, M. Methodologies for the characterization of microbes in industrial environments: A review. *J. Ind. Microbiol. Biotechnol.* **2003**, *30*, 327–356. [[CrossRef](#)] [[PubMed](#)]
76. López, D.; Vlamakis, H.; Kolter, R. Biofilms. *Cold Spring Harb. Perspect. Biol.* **2010**, *2*, a000398. [[CrossRef](#)] [[PubMed](#)]
77. Rabin, N.; Zheng, Y.; Opoku-Temeng, C.; Du, Y.; Bonsu, E.; Sintim, H.O. Biofilm formation mechanisms and targets for developing antibiofilm agents. *Future Med. Chem.* **2015**, *7*, 493–512. [[CrossRef](#)] [[PubMed](#)]
78. Huang, H.; Ren, H.; Ding, L.; Geng, J.; Xu, K.; Zhang, Y. Aging biofilm from a full-scale moving bed biofilm reactor: Characterization and enzymatic treatment study. *Bioresour. Technol.* **2014**, *154*, 122–130. [[CrossRef](#)] [[PubMed](#)]
79. Davey, M.E.; O’toole, G.A. Microbial biofilms: From ecology to molecular genetics. *Microbiol. Mol. Biol. Rev.* **2000**, *64*, 847–867. [[CrossRef](#)] [[PubMed](#)]
80. Cruz, C.D.; Shah, S.; Tammela, P. Defining conditions for biofilm inhibition and eradication assays for Gram-positive clinical reference strains. *BMC Microbiol.* **2018**, *18*, 1–9. [[CrossRef](#)]
81. Raheem, N.; Strauss, K. Mechanism of action for antimicrobial peptides with antibacterial and antibiofilm functions. *Front. Microbiol.* **2019**, *10*, 2866. [[CrossRef](#)]
82. Morroni, G.; Simonetti, O.; Brenciani, A.; Brescini, L.; Kamysz, W.; Kamysz, E.; Neubauer, D.; Caffarini, M.; Orciani, M.; Giovanetti, E.; et al. In vitro activity of Protegrin-1, alone and in combination with clinically useful antibiotics, against *Acinetobacter baumannii* strains isolated from surgical wounds. *Med Microbiol. Immunol.* **2019**, *208*, 877–883. [[CrossRef](#)] [[PubMed](#)]
83. Tao, R.; Tong, Z.; Lin, Y.; Xue, Y.; Wang, W.; Kuang, R.; Wang, P.; Tian, Y.; Ni, L. Antimicrobial and antibiofilm activity of pleurocidin against cariogenic microorganisms. *Peptides* **2011**, *32*, 1748–1754. [[CrossRef](#)] [[PubMed](#)]

84. Wang, G.; Mishra, B.; Epand, R.F.; Epand, R.M. High-quality 3D structures shine light on antibacterial, anti-biofilm and antiviral activities of human cathelicidin LL-37 and its fragments. *Biochim. Biophys. Acta (BBA)-Biomembr.* **2014**, *1838*, 2160–2172. [[CrossRef](#)]
85. De La Fuente-Núñez, C.; Cardoso, M.H.; De Souza Cândido, E.; Franco, O.L.; Hancock, R.E. Synthetic antibiofilm peptides. *Biochim. Biophys. Acta (BBA)-Biomembr.* **2016**, *1858*, 1061–1069. [[CrossRef](#)] [[PubMed](#)]
86. Blower, R.J.; Barksdale, S.M.; Van Hoek, M.L. Snake cathelicidin NA-CATH and smaller helical antimicrobial peptides are effective against *Burkholderia thailandensis*. *PLoS Negl. Trop. Dis.* **2015**, *9*. [[CrossRef](#)]
87. Sutton, J.M.; Pritts, T.A. Human beta-defensin 3: A novel inhibitor of Staphylococcus-Produced biofilm production. Commentary on Human  $\beta$ -defensin 3 inhibits antibiotic-resistant Staphylococcus biofilm formation. *J. Surg. Res.* **2014**, *186*, 99. [[CrossRef](#)]
88. Arslan, S.Y.; Leung, K.P.; Wu, C.D. The effect of lactoferrin on oral bacterial attachment. *Oral Microbiol. Immunol.* **2009**, *24*, 411–416. [[CrossRef](#)]
89. Overhage, J.; Campisano, A.; Bains, M.; Torfs, E.C.; Rehm, B.H.; Hancock, R.E. Human host defense peptide LL-37 prevents bacterial biofilm formation. *Infect. Immun.* **2008**, *76*, 4176–4182. [[CrossRef](#)]
90. Okuda, K.I.; Zendo, T.; Sugimoto, S.; Iwase, T.; Tajima, A.; Yamada, S.; Sonomoto, K.; Mizunoe, Y. Effects of bacteriocins on methicillin-resistant *Staphylococcus aureus* biofilm. *Antimicrob. Agents Chemother.* **2013**, *57*, 5572–5579. [[CrossRef](#)]
91. Mansour, S.C.; Pena, O.M.; Hancock, R.E. Host defense peptides: Front-line immunomodulators. *Trends Immunol.* **2014**, *35*, 443–450. [[CrossRef](#)]
92. Brancatisano, F.L.; Maisetta, G.; Di Luca, M.; Esin, S.; Bottai, D.; Bizzarri, R.; Campa, M.; Batoni, G. Inhibitory effect of the human liver-derived antimicrobial peptide hepcidin 20 on biofilms of polysaccharide intercellular adhesin (PIA)-positive and PIA-negative strains of *Staphylococcus epidermidis*. *Biofouling* **2014**, *30*, 435–446. [[CrossRef](#)]
93. Pletzer, D.; Coleman, S.R.; Hancock, R.E. Anti-biofilm peptides as a new weapon in antimicrobial warfare. *Curr. Opin. Microbiol.* **2016**, *33*, 35–40. [[CrossRef](#)] [[PubMed](#)]
94. Zhu, C.; Tan, H.; Cheng, T.; Shen, H.; Shao, J.; Guo, Y.; Shi, S.; Zhang, X. Human  $\beta$ -defensin 3 inhibits antibiotic-resistant Staphylococcus biofilm formation. *J. Surg. Res.* **2013**, *183*, 204–213. [[CrossRef](#)] [[PubMed](#)]
95. Gopal, R.; Lee, J.H.; Kim, Y.G.; Kim, M.S.; Seo, C.H.; Park, Y. Anti-microbial, anti-biofilm activities and cell selectivity of the NRC-16 peptide derived from witch flounder, *Glyptocephalus cynoglossus*. *Mar. Drugs* **2013**, *11*, 1836–1852. [[CrossRef](#)]
96. Anunthawan, T.; De La Fuente-Núñez, C.; Hancock, R.E.; Klaynongsruang, S. Cationic amphipathic peptides KT2 and RT2 are taken up into bacterial cells and kill planktonic and biofilm bacteria. *Biochim. Biophys. Acta (BBA)-Biomembr.* **2015**, *1848*, 1352–1358. [[CrossRef](#)]
97. Butts, A.; Krysan, D.J. Antifungal drug discovery: Something old and something new. *PLoS Pathog.* **2012**, *8*. [[CrossRef](#)]
98. De Brucker, K.; Delattin, N.; Robijns, S.; Steenackers, H.; Verstraeten, N.; Landuyt, B.; Luyten, W.; Schoofs, L.; Dogan, B.; Fröhlich, M.; et al. Derivatives of the mouse cathelicidin-related antimicrobial peptide (CRAMP) inhibit fungal and bacterial biofilm formation. *Antimicrob. Agents Chemother.* **2014**, *58*, 5395–5404. [[CrossRef](#)] [[PubMed](#)]
99. Mansour, S.C.; De la Fuente-Núñez, C.; Hancock, R.E.W. Peptide IDR-1018: Modulating the immune system and targeting bacterial biofilms to treat antibiotic-resistant bacterial infections. *J. Pept. Sci.* **2015**, *21*, 323–329. [[CrossRef](#)]
100. De La Fuente-Núñez, C.; Reffuveille, F.; Mansour, S.C.; Reckseidler-Zenteno, S.L.; Hernández, D.; Brackman, G.; Coenye, T.; Hancock, R.E. D-enantiomeric peptides that eradicate wild-type and multidrug-resistant biofilms and protect against lethal *Pseudomonas aeruginosa* infections. *Chem. Biol.* **2015**, *22*, 196–205. [[CrossRef](#)]
101. Mataraci, E.; Dosler, S. In vitro activities of antibiotics and antimicrobial cationic peptides alone and in combination against methicillin-resistant *Staphylococcus aureus* biofilms. *Antimicrob. Agents Chemother.* **2012**, *56*, 6366–6371. [[CrossRef](#)]
102. Otto, M. Bacterial evasion of antimicrobial peptides by biofilm formation. In *Antimicrobial Peptides and Human Disease*; Springer: Berlin/Heidelberg, Germany, 2006; pp. 251–258. [[CrossRef](#)]
103. Vuong, C.; Voyich, J.M.; Fischer, E.R.; Braughton, K.R.; Whitney, A.R.; DeLeo, F.R.; Otto, M. Polysaccharide intercellular adhesin (PIA) protects *Staphylococcus epidermidis* against major components of the human innate immune system. *Cell. Microbiol.* **2004**, *6*, 269–275. [[CrossRef](#)] [[PubMed](#)]



104. Chan, C.; Burrows, L.L.; Deber, C.M. Helix induction in antimicrobial peptides by alginate in biofilms. *J. Biol. Chem.* **2004**, *279*, 38749–38754. [[CrossRef](#)]
105. Kuo, H.H.; Chan, C.; Burrows, L.L.; Deber, C.M. Hydrophobic interactions in complexes of antimicrobial peptides with bacterial polysaccharides. *Chem. Biol. Drug Des.* **2007**, *69*, 405–412. [[CrossRef](#)] [[PubMed](#)]
106. Ernst, C.M.; Kuhn, S.; Slavetinsky, C.J.; Krismer, B.; Heilbronner, S.; Gekeler, C.; Kraus, D.; Peschel, A. The lipid-modifying multiple peptide resistance factor is an oligomer consisting of distinct interacting synthase and flippase subunits. *MBio* **2015**, *6*, e02340-14. [[CrossRef](#)] [[PubMed](#)]
107. Ernst, C.M.; Staubitz, P.; Mishra, N.N.; Yang, S.J.; Hornig, G.; Kalbacher, H.; Bayer, A.S.; Kraus, D.; Peschel, A. The bacterial defensin resistance protein MprF consists of separable domains for lipid lysinylation and antimicrobial peptide repulsion. *PLoS Pathog.* **2009**, *5*, e1000660. [[CrossRef](#)] [[PubMed](#)]
108. Yang, S.J.; Mishra, N.N.; Rubio, A.; Bayer, A.S. Causal role of single nucleotide polymorphisms within the mprF gene of *Staphylococcus aureus* in daptomycin resistance. *Antimicrob. Agents Chemother.* **2013**, *57*, 5658–5664. [[CrossRef](#)]
109. Klein, S.; Lorenzo, C.; Hoffmann, S.; Walther, J.M.; Storbeck, S.; Piekarski, T.; Tindall, B.J.; Wray, V.; Nimtz, M.; Moser, J. Adaptation of *Pseudomonas aeruginosa* to various conditions includes tRNA-dependent formation of alanyl-phosphatidylglycerol. *Mol. Microbiol.* **2009**, *71*, 551–565. [[CrossRef](#)]
110. Ramsey, M.M.; Whiteley, M. *Pseudomonas aeruginosa* attachment and biofilm development in dynamic environments. *Mol. Microbiol.* **2004**, *53*, 1075–1087. [[CrossRef](#)]
111. McPhee, J.B.; Lewenza, S.; Hancock, R.E. Cationic antimicrobial peptides activate a two-component regulatory system, PmrA-PmrB, that regulates resistance to polymyxin B and cationic antimicrobial peptides in *Pseudomonas aeruginosa*. *Mol. Microbiol.* **2003**, *50*, 205–217. [[CrossRef](#)]
112. Dalebroux, Z.D.; Miller, S.I. Salmonellae PhoPQ regulation of the outer membrane to resist innate immunity. *Curr. Opin. Microbiol.* **2014**, *17*, 106–113. [[CrossRef](#)]
113. Guo, L.; Lim, K.B.; Poduje, C.M.; Daniel, M.; Gunn, J.S.; Hackett, M.; Miller, S.I. Lipid A acylation and bacterial resistance against vertebrate antimicrobial peptides. *Cell* **1998**, *95*, 189–198. [[CrossRef](#)]
114. Trent, M.S.; Pabich, W.; Raetz, C.R.; Miller, S.I. A PhoP/PhoQ-induced Lipase (PagL) That Catalyzes 3-O-Deacylation of Lipid A Precursors in Membranes of *Salmonella typhimurium*. *J. Biol. Chem.* **2001**, *276*, 9083–9092. [[CrossRef](#)] [[PubMed](#)]
115. Groisman, E.A.; Kayser, J.; Soncini, F.C. Regulation of polymyxin resistance and adaptation to low-Mg<sup>2+</sup> environments. *J. Bacteriol.* **1997**, *179*, 7040–7045. [[CrossRef](#)] [[PubMed](#)]
116. Macfarlane, E.L.; Kwasnicka, A.; Hancock, R.E. Role of *Pseudomonas aeruginosa* PhoP-PhoQ in resistance to antimicrobial cationic peptides and aminoglycosides. *Microbiology* **2000**, *146*, 2543–2554. [[CrossRef](#)] [[PubMed](#)]
117. Singh, S.; Singh, S.K.; Chowdhury, I.; Singh, R. Understanding the mechanism of bacterial biofilms resistance to antimicrobial agents. *Open Microbiol. J.* **2017**, *11*, 53–62. [[CrossRef](#)]
118. Naves, P.; Del Prado, G.; Huelves, L.; Rodriguez-Cerrato, V.; Ruiz, V.; Ponte, M.C.; Soriano, F. Effects of human serum albumin, ibuprofen and N-acetyl-L-cysteine against biofilm formation by pathogenic *Escherichia coli* strains. *J. Hosp. Infect.* **2010**, *76*, 165–170. [[CrossRef](#)]





Article

# Characterization of the Proteins Involved in the DNA Repair Mechanism in *M. smegmatis*

Angela Di Somma <sup>1,2</sup>, Carolina Canè <sup>1,3</sup>, Antonio Moretta <sup>4</sup>, Arianna Cirillo <sup>3</sup>, Franz Cemič <sup>5</sup> and Angela Duilio <sup>1,\*</sup>

<sup>1</sup> Department of Chemical Sciences, Università Federico II di, 80126 Naples, Italy; angela.disomma@unina.it (A.D.S.); cane@ceinge.unina.it (C.C.)

<sup>2</sup> Istituto Nazionale Biostrutture Biostrumentazioni, INBB, 00136 Rome, Italy

<sup>3</sup> CEINGE Biotecnologie Avanzate, 80145 Naples, Italy; cirilloa@ceinge.unina.it

<sup>4</sup> Department of Science, Università degli Studi della Basilicata, 85100 Potenza, Italy; antonio.moretta@unibas.it

<sup>5</sup> Department of Mathematics, Natural Sciences and Computer Science, University of Applied Sciences Giessen, Wiesenstr. 14, 35390 Giessen, Germany; franz.cemic@mni.thm.de

\* Correspondence: anduilio@unina.it

Received: 18 June 2020; Accepted: 27 July 2020; Published: 29 July 2020



**Abstract:** Several alkylating agents that either occur in the environment or are self-produced can cause DNA-damaging injuries in bacterial cells. Therefore, all microorganisms have developed repair systems that are able to counteract DNA alkylation damage. The adaptive response to alkylation stress in *Escherichia coli* consists of the Ada operon, which has been widely described; however, the homologous system in *Mycobacterium tuberculosis* (MTB) has been shown to have a different genetic organization but it is still largely unknown. In order to describe the defense system of MTB, we first investigated the proteins involved in the repair mechanism in the homologous non-pathogenic mycobacterium *M. smegmatis*. Ogt, Ada-AlkA and FadE8 proteins were recombinantly produced, purified and characterized. The biological role of Ogt was examined using proteomic experiments to identify its protein partners in vivo under stress conditions. Our results suggested the formation of a functional complex between Ogt and Ada-AlkA, which was confirmed both in silico by docking calculations and by gel filtration chromatography. We propose that this stable association allows the complex to fulfill the biological roles exerted by Ada in the homologous *E. coli* system. Finally, FadE8 was demonstrated to be structurally and functionally related to its *E. coli* homologous, AidB.

**Keywords:** alkylating agents; DNA-damaging; adaptive response; *Mycobacterium smegmatis*; molecular docking; gel filtration chromatography

## 1. Introduction

The DNA molecule is a crucial target for several alkylating molecules that either occur in the environment or are self-produced. They can react with nucleophilic sites on DNA bases and cause covalent modifications, cytotoxic damage and impair cell survival [1]. Alkylating agents have electrophilic properties that make them able to directly interact with DNA or RNA, causing mutations during replication and transcription [2]. A number of sites prone to alkylation have been identified on DNA bases including the guanine oxygen site at position 6. Methylation of this oxygen generates O<sup>6</sup>-methylguanine (O<sup>6</sup>-MeG), which prevents the correct base pairing and leads to mutations during DNA replication. Other well-known alkylation products are N<sup>7</sup>-methylguanine (N<sup>7</sup>-MeG), N<sup>3</sup>-methyladenine (N<sup>3</sup>-MeA), N<sup>1</sup>-methyladenine (N<sup>1</sup>-MeA), N<sup>3</sup>-methylcytosine (N<sup>3</sup>-MeC), and O<sup>4</sup>-methylthymine (O<sup>4</sup>-MeT) [3,4].

Bacteria have developed repair systems that are able to counteract DNA alkylation damage and avoid cell death. The adaptive response to alkylation stress in *Escherichia coli* relies on the so-called Ada operon which has been widely described [5,6]. The protein products of this operon provide increased resistance when bacterial cells are exposed to sublethal doses of alkylating agents. The sensor enzyme of the defense mechanism is the Ada protein, a methyltransferase that is able to remove and transfer methyl groups from damaged DNA bases to a cysteine residue in its active site. Following methylation, Ada undergoes conformational changes to become a positive regulator for the expression of the *ada* gene itself and the other repair genes located within the operon, *alkA*, *alkB* and *aidB* and it is involved in the adaptive response [5,7,8].

AlkA is a DNA-glycosylase responsible for the removal of 3-methyl adenine and several other nitrosation products, such as N<sup>7</sup>-methyladenine, N<sup>3</sup>-methylguanine, N<sup>7</sup>-methylguanine, by hydrolyzing their N-glycosidic bonds. The dioxygenase AlkB catalyzes the hydroxylation of the methyl group of methylated DNA bases resulting in the subsequent formation of succinate and CO<sub>2</sub>, and bringing the nitrogen bases back to their original state [9,10]. Finally, the flavoprotein AidB belongs to the family of acyl-Coenzyme A (acyl-CoA) dehydrogenases, which are endowed with unspecific DNA binding properties and weak dehydrogenase activity. This protein has been shown to play a protective role by inactivating alkylating agents before they react with DNA [11,12].

Unlike *E. coli*, the DNA protection system in *Mycobacterium tuberculosis* (MTB) has not been investigated and it is still largely unknown. Recent studies led to the identification of four genes encoding proteins involved in an adaptive response mechanism homologous to the defense system described in *E. coli* but with different gene organization (Figure 1) [13,14]. Exposure of MTB to methylating molecules strongly increases the transcription of *ada-alkA* and *ogt* genes, which demonstrates an inducible response to methylating agents. Moreover, Ogt was identified as a methyltransferase that is homologous to the B domain of the Ada protein in *E. coli* that transfers the O<sup>6</sup>-alkyl group from modified guanines to a strictly conserved cysteine residue (Cys 126) in the protein active site [15,16]. On the basis of sequence homology, Ada-AlkA should consist of the A domain of the *E. coli* Ada protein fused to the AlkA sequence.

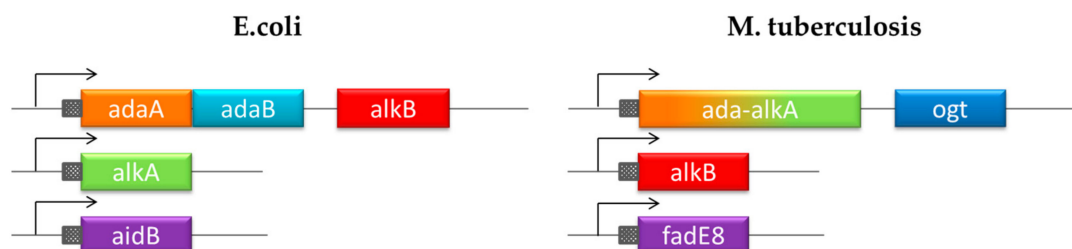


**Figure 1.** Chromosomal organization of the adaptive response to alkylation stress in *E. coli* and *Mycobacterium tuberculosis* (MTB).

With the aim of describing the defense system in MTB, we first investigated the specific role of the proteins involved in the repair mechanism in the homologous non-pathogenic mycobacterium *M. smegmatis*. Most of these proteins were produced in *E. coli* and characterized in terms of structure and function. The biological function of Ogt was elucidated by a functional proteomic approach designed to identify its protein partners in vivo, which suggested a possible interaction with Ada-AlkA. The specific association of these proteins to form a stable complex was validated both in silico and in vitro by docking calculations and gel filtration chromatography using the recombinant forms of Ada-AlkA expressed in *E. coli* and fully characterized. Finally, FadE8, which showed sequence homology with the AidB protein from *E. coli*, was cloned, expressed in *E. coli* and characterized for its FAD binding, dehydrogenase activity and DNA binding capabilities. The investigation of the DNA repair system in *M. smegmatis* allowed us to characterize proteins that are also present in MTB and play key roles in survival and protection mechanisms. Since these proteins are absent in humans, they might represent excellent targets for new potential therapeutic approaches.

## 2. Results and Discussion

The comparing the DNA repair network in MTB with the homologous system in *E. coli*, highlights the uniqueness of the Ogt protein. On the basis of its primary structure, this protein is homologous to the B domain of the *E. coli* protein Ada, whereas the A domain is fused to the DNA-glycosylase AlkA (Figure 1).

Besides its methyltransferase activity, Ada is the sensor protein responsible for the transcription activation of the entire operon following alkylation stress. In a previous paper, Ogt was demonstrated to be a methyltransferase with DNA binding capabilities [15]. This unusual gene organization prompted us to investigate the respective roles of Ogt and Ada-AlkA and the other proteins involved in the repair mechanism in *M. smegmatis*, a non-pathogenic mycobacterium homologous to MTB.

### 2.1. Investigation on the Ogt Protein

The biological role of Ogt under stress conditions was examined by using a functional proteomics approach focused on the identification of its protein partners *in vivo*. The Ogt protein was first produced by recombinant DNA methodologies in *E. coli* cells as glutathione S-transferase (GST)-fused protein. The recombinant protein was purified by a two-step procedure consisting of affinity chromatography on a glutathione-conjugated Sepharose column followed by anionic exchange using a MonoQ column (GE Healthcare). The purity of the protein was assessed by SDS-PAGE and its primary structure validated by MALDI mapping. Ogt was digested with trypsin and the resulting peptide mixture was directly analyzed by MALDI-MS/MS tandem mass spectrometry. The mass signals recorded in the spectra were assigned to the anticipated GST-Ogt sequence on the basis of their molecular mass and the fragmentation spectra (Supplementary Materials, Table S1). Circular dichroism analyses were also carried out to verify the correct folding of the protein. Figure 2 shows the corresponding CD spectrum (blue line) in comparison with native GST (green line), displaying 30%  $\alpha$ -helix, 22%  $\beta$ -sheets and 12% turn in agreement with the literature data [15] and indicating that Ogt is correctly folded.

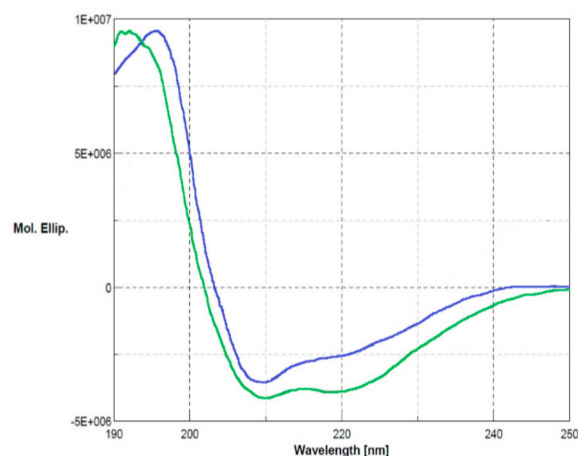


**Figure 2.** Circular dichroism analyses of glutathione S-transferase (GST)-Ogt fused protein (blue line) in comparison with native GST (green line). Secondary structures:  $\alpha$ -helix  $3 \times 10^{-1}$ ,  $\beta$ -sheets  $2.2 \times 10^{-1}$  and turn  $1.2 \times 10^{-1}$ .

Purified recombinant GST-Ogt was then immobilized onto glutathione-conjugated agarose beads to be used as a bait in the functional proteomic experiment. A total *M. smegmatis* cellular extract was then prepared under stress conditions (treatment with 0.03% methyl methane sulfonate (MMS)), and pre-cleaned glutathione-derivatized beads to remove false positive interactors, i.e., proteins with high affinity for the matrix. The unbound proteins were then incubated with the GST-Ogt derivatized agarose beads and the retained interactors were eluted with an excess of reduced GSH. Proteins retained by the beads during the pre-cleaning step were also eluted and used as control.

Proteins eluted from the sample and the control were fractionated by SDS-PAGE and the gel was stained by colloidal blue coomassie. Protein bands from both the control and the sample lanes were excised from the gel, digested in situ with trypsin and the resulting peptide mixtures were directly analyzed by nanoLC-MS/MS. Mass spectral data were used to search a nonredundant protein database using an in-house version of the Mascot software. Proteins occurring in both the sample and in the control were discarded and only those solely present in the sample lane were considered as putative Ogt interactors.

Among the putative Ogt interactors, a number of proteins involved in stress defense and DNA repair mechanisms were identified, including Ada-AlkA. The occurrence of Ada-AlkA within the Ogt putative interactors led to the hypothesis that these two proteins might form a functional complex to fulfill the biological roles exerted by Ada in the homologous *E. coli* system. These considerations prompted us to further investigate the possible interaction between Ogt and Ada-AlkA.

## 2.2. Expression, Purification and Analysis of Ada-AlkA

Since the Ogt protein was already available in a purified form, a recombinant correctly folded form of Ada-AlkA was needed to test the formation of the putative complex. Recombinant Ada-AlkA was produced in *E. coli* as GST-fused protein following the same procedure as reported above. The recombinant protein was purified by affinity chromatography, anionic exchange and gel filtration and analyzed by SDS-PAGE. Structural analyses were carried out by MALDI mapping (Supplementary Materials, Table S2) and circular dichroism in comparison with native GST and confirmed that recombinant Ada-AlkA had the expected primary structure and was correctly folded.

According to the *E. coli* homologous DNA repair system, Ada-AlkA should be a glycosyl hydrolase with the ability to bind DNA. Therefore, we investigated the DNA binding properties of the recombinant protein by using electrophoresis mobility shift assay (EMSA). The biotin-labeled DNA probe, UP35 was incubated with different amounts of the Ada-AlkA protein for 20 min at 25 °C and the protein-DNA complex was separated on 5% native polyacrylamide gel. Figure 3A shows the resulting gel visualized by UV radiation and clearly displaying an Ada-AlkA-dependent shift in the electrophoresis mobility of the DNA-protein complex compared to the isolated probe.

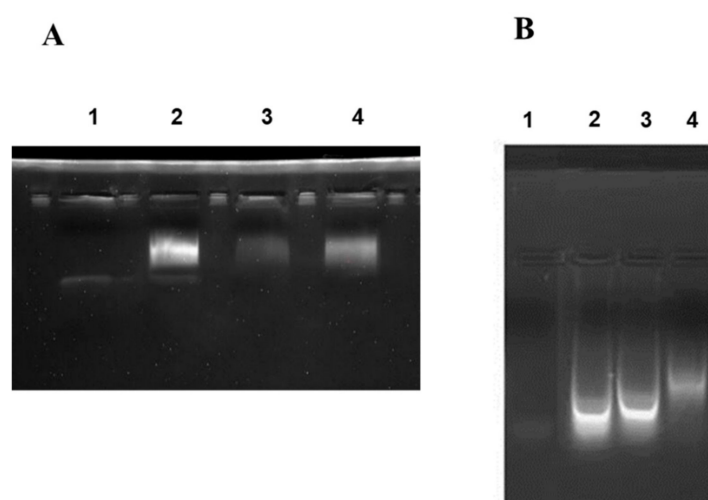


**Figure 3.** Electrophoresis mobility shift assay (EMSA) performed on Ada-AlkA (A) and Ogt (B) proteins. A biotin-labeled DNA probe was incubated with each individual protein for 20 min at 25 °C. Panel A: Lane 1, DNA probe. Lane 2, 3 and 4 DNA-probe incubated with different amounts of Ada-AlkA (40, 20 and 60  $\mu$ M, respectively). Panel B: Lane 1 DNA probe. Lanes 2, 3 and 4 DNA-probe incubated with different amounts of Ogt (10, 50 and 80  $\mu$ M, respectively).

In Lane 2, a low amount of protein was used for the complex, thus leaving a portion of the probe still free, whereas the oligonucleotide probe was completely involved in the complex at higher concentrations of Ada-AlkA.

These data demonstrated that recombinant Ada-AlkA binds DNA with non-sequence specificity. The same EMSA analysis was carried out with recombinant Ogt to confirm previous data on its DNA binding ability using the random probe (Supplementary Materials, Table S3). [15]. The results shown in Figure 3B demonstrated an Ogt dose-dependent shift of the complex compared to the isolated probe.

### 2.3. Ada-AlkA/Ogt Interaction

Since both Ada-AlkA and Ogt retained their correct tertiary structure and their DNA binding capabilities, we pursued a detailed investigation on the possible interaction between the two proteins both in silico and in vitro. A molecular model of the protein–protein interaction was developed by docking calculations and the results were experimentally confirmed by gel filtration chromatography using the recombinant proteins.

Ada-AlkA and Ogt models were obtained through the SwissModel webserver, using the *E. coli* AlkA protein (PDB code 3D4V) as a template for the Ada-AlkA model (Supplementary Materials, Figure S1a) and the MTB H37Rv Ogt protein (PDB code 4WXD) as a template for the Ogt model (Supplementary Materials, Figure S1b).

The putative structural basis of the protein–protein model Ada-AlkA (Chain C)-Ogt (Chain A) were obtained using the PatchDock Server and the structures were refined through the FireDock Server. Calculations revealed that a stable complex might form with a predicted  $\Delta G = -11.5$  Kcal/mol and a dissociation constant,  $K_d = 3.8 \times 10^{-9}$  M (25 °C). A detailed analysis of the interactions at the protein–protein interface suggested the involvement of 197 non-bonded interactions and four hydrogen bonds: Ala132 Chain A with Arg383 Chain C, Ser154 Chain A with Ser440 Chain C, Ser154 Chain A with Leu442 Chain C and Arg155 Chain A with Gln329 Chain C, as shown in Figure 4.

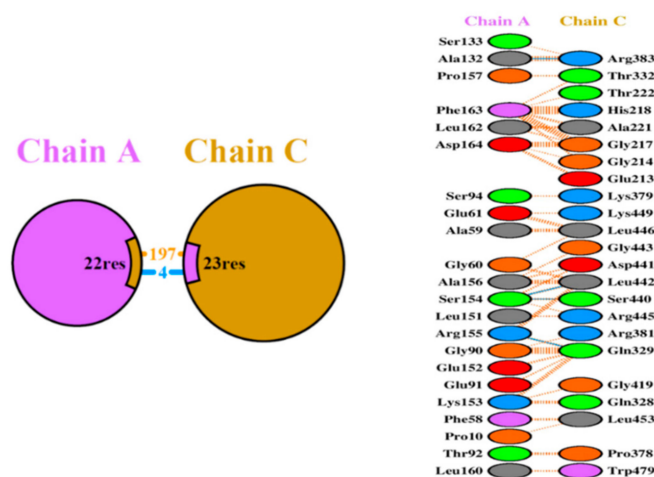


**Figure 4.** Schematic representation of the identified interactions occurring in the Ada-AlkA/Ogt model. Chain A represents Ogt while Chain C is Ada-AlkA.

Figure 5 shows an overview of the Ada-AlkA/Ogt complex model (A) and a detailed description of the interactions occurring at the contact surfaces (B).

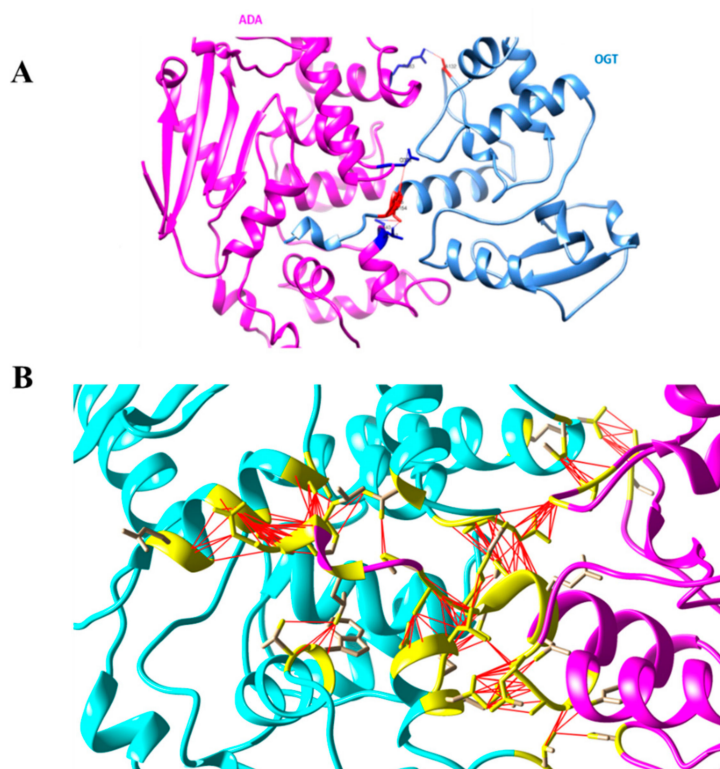


**Figure 5.** (A). Ribbon model of the Ada-AlkA/Ogt complex showing the predicted hydrogen bonds at the protein–protein interface. (B). Detailed description of the Ada-AlkA/Ogt interactions. Residues involved in the interaction are in yellow while the red lines represent the connection between residues. Images were generated by the CHIMERA software.

As the docking calculations suggested a possible interaction between Ada-AlkA and Ogt, we confirmed the complex formation on an experimental basis using the recombinant forms of the two proteins in gel filtration assays. A Superdex<sup>®</sup> 200 column was first calibrated with a mixture of standard proteins and the resulting calibration curve showed a  $R^2$  value of 0.995 and was then used for further analyses. Purified Ogt and Ada-AlkA proteins were individually subjected to gel filtration chromatography to evaluate their individual exclusion volume and to assess their quaternary structure in solution. The Ogt protein was eluted at a volume of 14.8 mL, while Ada-AlkA showed an elution volume of 13.6 mL. Data processing from the calibration curve returned an apparent molecular weight of about 43 kDa and 79 kDa for Ogt and Ada-AlkA respectively, confirming that both proteins have monomeric structure in solution (Figure 6).

Since, the Ada- AlkA preparation showed the presence of some impurities, the Ada- AlkA peak recovered from the gel filtration column (13.6 mL) was incubated with OGT and the putative complex was analyzed by gel filtration chromatography. Ada-AlkA and Ogt coeluted in a single peak with an elution volume of 12.9 mL. This value was processed with the calibration curve resulting in an apparent molecular mass of 120 kDa, thus confirming the formation of the complex. Figure 6A shows the superimposed profiles of the two individual proteins and the complex. In order to demonstrate the presence of both proteins within the complex, the Ada-AlkA/Ogt chromatographic peak was collected and analyzed by 12.5% SDS-PAGE gel in reducing conditions, which showed the occurrence of two protein bands with the expected electrophoretic mobility for Ada-AlkA and Ogt (Figure 6B). The two bands were excised from the gel digested with trypsin and the resulting peptide mixtures directly were analyzed by LC-MS/MS. Mass spectral data were used to search a protein database using the Mascot software, leading to the identification of Ada-AlkA, Swiss Prot code A0R1Z2, and Ogt, Swiss Prot code A0R0A4.

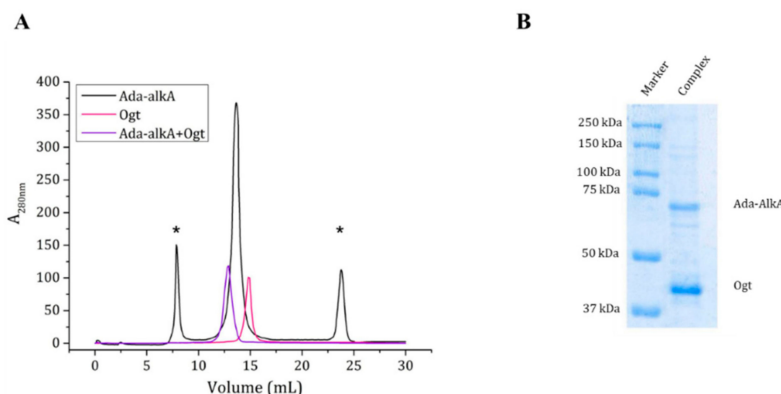


**Figure 6.** (A). Gel filtration chromatography of individual Ada-AlkA (in black) and Ogt (in pink) proteins. Peaks marked with an asterisk represent impurities in the Ada-AlkA preparation. The Ada-AlkA chromatographic peak was recovered, incubated with Ogt and the mixture re-chromatographed (in purple). The chromatogram shows the coelution of Ada-AlkA and Ogt in a single peak. (B). The Ada-AlkA/Ogt chromatographic peak was collected and analyzed on 12.5% SDS-PAGE showing two main protein bands with the expected electrophoretic mobility for Ada-AlkA and Ogt. Identification was confirmed by mass spectrometry.

The chromatographic results confirmed the previous docking calculations and proteomics data, which strongly suggested the association of Ada-AlkA and Ogt in a stable complex. Both Ogt and Ada-AlkA are involved in the adaptive response to alkylation damage in DNA caused by alkylating agents. Ada-AlkA catalyzes the hydrolysis of the deoxyribose N-glycosidic bond to excise a number of different methylated DNA bases. Ogt repairs methylated guanines in DNA by transferring the methyl group to a cysteine residue in the enzyme active site, thus fulfilling the same activity exerted by Ada in the homologous *E. coli* system. However, besides its methyltransferase activity, *E. coli* Ada is a sensor protein that upon methylation is activated as a transcriptional regulator that activates the transcription of its own gene and other alkylation resistance genes, while methylation of Ogt seems to inactivate the enzyme. Therefore, the stable association of Ogt with Ada-AlkA suggests that the complex might exert both methyltransferase and N-glycosyl hydrolase enzymatic activities and have a transcriptional activator role upon methylation.

#### 2.4. Expression, Purification and Structural Analyses of FadE8

Finally, we investigated FadE8, a *M. smegmatis* protein belonging to the adaptive response mechanism homologous to the *E. coli* AidB protein. Recombinant FadE8 was expressed in *E. coli* bearing a N-terminal His tag and purified to homogeneity by affinity chromatography on a Ni-derivatized column. The primary structure of the recombinant protein was verified by MALDI mapping strategy (Supplementary Materials, Table S4) and its correct folding assessed by circular dichroism analyses.

*E. coli* AidB is a flavoprotein belonging to the acyl-Coenzyme A dehydrogenase family, which has shown weak dehydrogenase activity and unspecific DNA binding. A detailed characterization of recombinant FadE8 was then carried out to explore the interaction with flavin adenine dinucleotide (FAD) using docking calculations, the enzymatic activity and the DNA binding capability.

Molecular docking analysis was performed by modeling FadE8 with the I-TASSER Server to obtain the best model with a C-score value of 1.83, an estimated TM-score of  $0.97 \pm 0.05$  and an estimated RMSD score value of  $3.7 \pm 2.5$  Å (Figure 7A). Figure 7B shows the FAD ligand model obtained with the LigParGen Server. The Acyl-CoA dehydrogenase from *Brucella melitensis* in complex with FAD (PDB code 5EZ3 A) was used as a template to model the FadE8-FAD complex. The FadE8-FAD model was obtained using the PatchDock Server and the structures were refined through the FireDock Server. Calculations revealed the occurrence of a stable protein-ligand complex with a Gibbs free energy of  $\Delta G = -7.4$  Kcal/mol was predicted using the PRODIGY webserver (Figure 7C). A detailed analysis of the interactions at the protein/ligand interface suggested the involvement of both hydrophobic



interactions and hydrogen bonds. In particular, Trp36 and Arg107 are involved in hydrophobic interactions with the ligand while Ala101, Ala104, Asp106, Gly109, Lys117, Glu288 and Arg371 residues establish hydrogen bonds with the FAD molecule (Figure 7D).

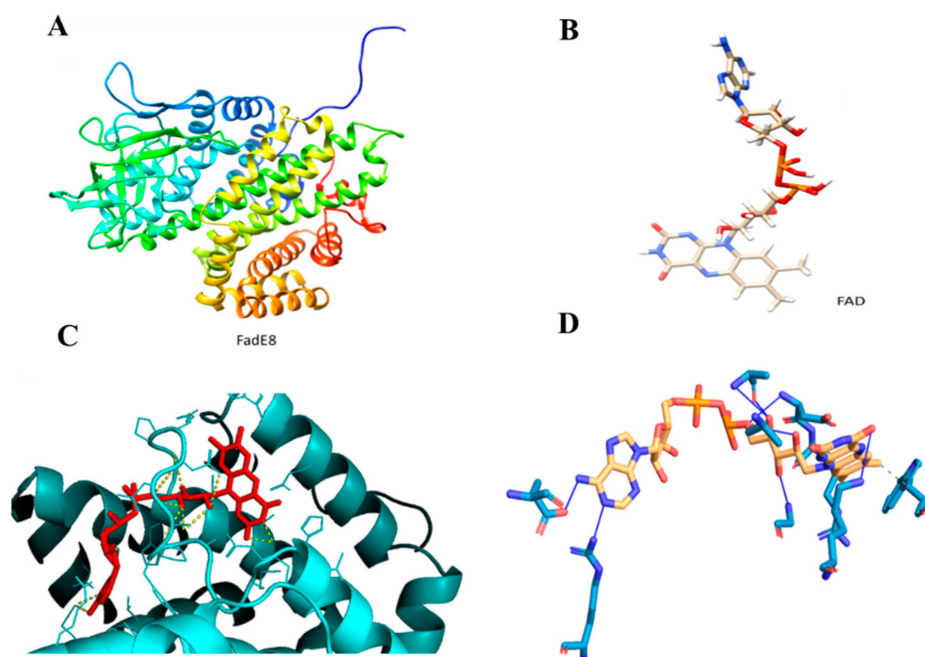


**Figure 7.** (A). FadE8 model obtained with I-TASSER Server. (B). Flavin adenine dinucleotide (FAD) model obtained with the LigParGen Server. (C). Zoom image of the FadE8/FAD model. The protein is shown in cyan while the ligand is shown in red. (D). Predicted interactions between FadE8 and the FAD ligand using the Protein-Ligand Interaction Profiler (PLIP) Server.

As the docking calculations confirmed the interaction of FadE8 with FAD, we tested the dehydrogenase activity of the recombinant protein. FadE8 was incubated in the presence of FAD and isovaleryl-CoA as substrate using 2, 6 dichlorophenolindophenol (DCPIP) as the final electron acceptor. The enzymatic activity was monitored by the change in absorbance at 600 nm over time. Table 1 reports the results obtained compared with human isovaleryl-CoA dehydrogenase and the AidB activity reported in the literature [17].

**Table 1.** Enzymatic activity of recombinant FadE8 in comparison with *E. coli* AidB and human Acyl-CoA dehydrogenase.

Protein	Isovaleryl-CoA Dehydrogenase Activity ( $\mu\text{mol min}^{-1}/\text{mg Protein}$ )
AidB ( <i>E. coli</i> )	$0.12 \pm 0.01$
FadE8 ( <i>M. smegmatis</i> )	$0.30 \pm 0.01$
Human Acyl-CoA dehydrogenase	8.2 to 11.7

As expected, FadE8 displayed weak dehydrogenase activity very similar to AidB and much less than the human enzyme, suggesting that the specific FadE8 substrate might be different from Acyl-CoA molecules as already observed for AidB [11].

Finally, the DNA binding properties of recombinant FadE8 were investigated by EMSA. The biotinylated UP DNA fragment was incubated with the protein for 20 min at 25 °C and the protein-DNA complex was separated on 5% native polyacrylamide gel. A clear retardation shift in the electrophoretic mobility of the DNA-protein complex was observed compared to the free probe (Figure 8).



**Figure 8.** EMSA assay performed on FadE8 protein. A biotin-labeled DNA probe was incubated with the protein for 20 min at 25 °C. Lane 1, DNA probe. Lane 2 DNA-probe incubated with 40 μM FadE8 showing the retardation shift.

These data confirmed that similarly to its homologous AidB, recombinant FadE8 retained its capability to bind DNA with non-sequence specificity.

### 3. Materials and Methods

#### 3.1. Recombinant Production of FadE8, Ogt and Ada-AlkA Proteins

The *fadE8*, *ogt* and *ada-alkA* genes were amplified from *M. smegmatis* genome by polymerase chain reaction (PCR). The *fadE8* gene was cloned into the pET22b-c-myc vector containing the coding sequence for the corresponding recombinant protein fused to a 6-histidine tag at the C-terminus. The *ada-alkA* and *ogt* genes were cloned in pGEX-4T1 vector containing sequences encoding for the corresponding recombinant proteins fused to GST at the N-terminus. Plasmid construction was verified by automated DNA sequencing.

Expression of the recombinant proteins was carried out in BL21 *E. coli* cells, in LB medium at 37 °C with 100 μg/mL kanamycin for FadE8 and 100 μg/mL ampicillin for Ogt and Ada-AlkA in order to select the strain of interest. Expression of recombinant proteins was induced in the exponential phase with isopropyl-thio-β-D-galactoside (IPTG) at a final concentration of 1 mM for FadE8 and 0.1 mM IPTG for Ogt and Ada-AlkA. Cultures were grown at 20 °C for 16 h and cells were then retrieved by centrifugation at 5000× *g* rpm for 20 min at 4 °C.

The cellular pellets were resuspended into two different buffers, 0.1 M Na<sub>2</sub>HPO<sub>4</sub>, 0.15 M NaCl, 1 mM PMSF, pH 7.4 for Ogt and Ada-AlkA and 20 mM Na<sub>2</sub>HPO<sub>4</sub>, 0.5 M NaCl, 20 mM imidazole, 1 mM PMSF, pH 7.4 for FadE8.

Cells were lysed by sonication for 20 min and the sample was centrifuged at 13,000× *g* rpm for 30 min at 4 °C, allowing the separation of the insoluble fraction, which contained inclusion bodies, from the soluble sample. Proteins were purified from the soluble fraction.

His<sub>6</sub>-FadE8 was purified by affinity chromatography on His-Select Nickel Affinity beads (Thermo Fisher, Waltham, Massachusetts, USA) and eluted with 500 mM imidazole in 20 mM Na<sub>2</sub>HPO<sub>4</sub>, 0.5 M NaCl, pH 7.4.

GST-Ogt was purified through two purification steps including affinity chromatography on glutathione agarose beads (Sigma-Aldrich, Darmstadt, Germany) eluted with 1 mM reduced glutathione in 50 mM Tris-HCl pH 9.0, followed by anionic exchange chromatography on a HiTrap Q-HP, 5 mL column (GE Healthcare, Chicago, IL, USA), connected to a fast liquid protein chromatography system. The protein was eluted with 1 M NaCl in 50 mM Tris-HCl pH 8.

Purification of GST-Ada-AlkA was performed through a three-step procedure consisting of affinity chromatography on glutathione agarose beads (Sigma-Aldrich, Darmstadt, Germany) eluted with 10 mM reduced glutathione in 50 mM Tris-HCl pH 9.0, anionic exchange chromatography on HiTrap

Q-HP, 5 mL column (GE Healthcare) eluted with 1 M NaCl in 50 mM Tris-HCl pH 8.0 and gel filtration on a Superdex<sup>®</sup> 200 10/300 GL column connected to a fast liquid protein chromatography system, eluted with 50 mM Tris-HCl pH 8.0, containing 150 mM NaCl.

Protein concentration was determined with the Bradford Reagent from Sigma, using BSA as a standard [18]. Protein purity was verified by SDS-PAGE and their primary structure was validated by MALDI mapping strategy on a 5800 MALDI-TOF/TOF instrument (ABI Sciex, CA, USA) Circular dichroism analyses was performed to verify the correct folding of the proteins using a JASCO J-715 spectropolarimeter equipped with a Peltier thermostatic cell holder (Model PTC-348WI) and a 1 cm optical path-length quartz cell. CD spectra were acquired in the range 190–250 nm, with three accumulations performed for each measurement, at a scanning speed of 50 nm/min and data pitch of 1.0 nm.

The quaternary structure of Ada-alkA and Ogt was assessed by gel filtration chromatography on Superdex<sup>®</sup> 200 10/300 GL eluted with 50 mM Tris-HCl pH 8.0 containing 150 mM NaCl.

### 3.2. Protein-DNA Interaction

The interaction of Ada-alkA, Ogt and FadE8 with DNA was investigated by EMSA experiments using biotin-labeled DNA probes, fragments UP35, UP(Primm) and a random probe (the MALDI-MS spectrum is reported in Supplementary Materials, Figure S2, a kind gift from Dott.ssa Musumeci). Oligonucleotide sequence probes are shown in Supplementary Materials, Table S3).

Sense and antisense oligonucleotides were annealed by incubation at 95 °C for 5 min and then gradual cooling to room temperature. Proteins were incubated with the probes for 20 min at 25 °C in 20 µL of 25 mM HEPES pH 7.6, containing 50 mM KCl, 12.5 mM MgCl<sub>2</sub>, 1 mM DTT, 20% glycerol, and 0.1% triton. Protein–DNA complexes were separated on 5% native polyacrylamide gel (29:1 cross-linking ratio) in 45 mM Tris pH 8.0, containing 45 mM boric acid, 1 mM EDTA at 200 V (20 V/cm) at room temperature. Visualization of DNA samples was carried out using UV radiation.

### 3.3. Isovaleryl-CoA Dehydrogenase Activity of FadE8

The dehydrogenase activity of FadE8 was evaluated by incubation with 2 mM isovaleryl-CoA (Sigma-Aldrich, Darmstadt, Germany) as substrate and 0.1 mM 2, 6 dichlorophenolindophenol (DCPIP) as the terminal electron acceptor in a final volume of 300 µL at room temperature in 200 mM phosphate buffer, pH 8.0. Enzymatic activity was determined by monitoring the change in absorbance at 600 nm using a Beckman DU 7500 spectrophotometer assuming a molar extinction coefficient of 20.6 mM<sup>-1</sup> cm<sup>-1</sup> for DCPIP (13).

### 3.4. FadE8-Flavin Adenine Dinucleotide Molecular Docking Analysis

The ability of FadE8 to bind the flavin adenine dinucleotide (FAD) coenzyme was evaluated by docking analyses. The FadE8 protein was modeled using the I-TASSER Server [19–21]. Each model is associated with a C-score whose value ranges from –5 to +2. The higher this value the better the model. TM-score and RMSD are known standards for measuring structural similarity between two structures. A TM-score value > 0.5 indicates a model of correct topology while a score < 0.17 means a random similarity [22]. FAD model was obtained using the LigParGen Server [23–25] exploiting the Isomeric SMILES Code, Cc1cc2nc3c(nc(=O)[nH]c3=O)n(C[C@H](O)[C@H](O)[C@H](O)CO[P@](O)(=O)O[P@@](O)(=O)OC[C@H]3O[C@H]([C@H](O)[C@@H]3O)n3cnc4c(N)ncnc34) c2cc1C, from the RCSB PDB (Protein DataBase). The protein-ligand model was constructed using the PatchDock Server [26] and the structures were then refined with the FireDock Server [27], which also provided the global energy, the attractive and repulsive Van der Waals (VdW) forces and the atomic contact energy (ACE) values of the complex. The Protein-Ligand Interaction Profiler (PLIP) Server [28] was used to define the interactions between the FadE8 protein and the ligand. Finally, the ΔG<sub>noelec</sub> binding affinity of the complex was predicted using the PRODIGY webserver using the

“No Electrostatics Prediction” protocol [29]. All the figures were generated through UCSF CHIMERA software [30] and the PyMOL Molecular Graphics System, Version 1.2r3pre, Schrödinger, LLC.

### 3.5. Isolation of Ogt Complexes in *Mycobacterium smegmatis*

The GST-Ogt fused protein was produced in *E. coli*, and purified according to the procedure described above. The purified recombinant protein was immobilized on glutathione-derivatized agarose beads.

A total *M. smegmatis* cellular extract was prepared by growing mycobacterial cells in LB medium containing 100 µg/mL ampicillin and 0.05% tween 80. At a value of 0.4 OD/mL the culture was treated with sub-inhibitory concentrations (0.03%) of the alkylating agent methyl methane sulfonate (MMS). After 3 h, cells were recovered by centrifugation at 4000× g rpm at 4 °C for 15 min and the pellets were solubilized in 50 mM Na<sub>2</sub>HPO<sub>4</sub> pH 7.4 containing 150 mM NaCl and 1 mM PMSF. Cells were disrupted by French press and centrifuged at 14,000× g rpm for 30 min at 4 °C. *M. smegmatis* protein extract was pre-cleaned by incubation with reduced glutathione-agarose beads to remove non-specific binding proteins. The unbound proteins were incubated with the GST-Ogt derivatized beads for 2 h at 25 °C. After extensive washing with 50 mM Na<sub>2</sub>HPO<sub>4</sub> containing 150 mM NaCl and 1% Triton, the proteins specifically bound to the GST-Ogt bait were eluted with 20 mM Tris-HCl buffer pH 8.0 containing 1 mM reduced glutathione-proteins from the pre-cleaning step were also eluted and used as control.

Proteins from the sample and the control were fractionated by 10% SDS-PAGE and the gel bands were digested in situ with trypsin. The resulting peptide mixtures were directly analyzed by liquid chromatography/tandem mass spectrometry (LC-MS/MS) on a LTQ Orbitrap XL system (Thermo Fisher, Waltham, Massachusetts, USA) equipped with a nano-LC. The elution was accomplished with 95% acetonitrile, 5% water and 0.1% formic acid as eluent. Mass spectral data were used for database search by an in-house version of the Mascot software leading to the identification of the proteins. Proteins that occurred in both the sample and the control were discarded and those found solely in the sample were considered as putative Ogt interactors.

### 3.6. Ada-AlkA and Ogt Molecular Docking Analysis

The putative interaction between Ogt and on Ada-AlkA was determined by molecular docking calculations. Both proteins were modeled using the SWISS MODEL Server [31] and the model of the Ada-AlkA-Ogt complex was obtained using the PatchDock Server [26]. The structure was refined with the FireDock Server [27], which also provided the global energy, the attractive and repulsive Van der Waals (VdW) forces and the atomic contact energy (ACE) values of the complex. The amino acids occurring at the protein interface and the molecular interactions were identified by the PDBsum Server [32–34]. The Gibbs free energy, ΔG, and the dissociation constant, K<sub>d</sub>, of the complex were predicted using the PRODIGY webserver [35,36]. All the figures were generated by the UCSF CHIMERA software [30].

### 3.7. Validation of Ada-AlkA and Ogt Complex

The formation of the Ada-AlkA/Ogt complex was evaluated by gel filtration chromatography. The two purified proteins were incubated in 1:1 ratio in 50 mM Tris-HCl pH 8.0 containing 20 mM NaCl for 2 h at 25 °C and the complex was chromatographed on a Superdex<sup>®</sup> 200 10/300 GL column. Calibration of the column was performed using thyroglobulin (669 kDa), apoferritin (443 kDa), β-amylase (200 kDa), albumin (66 kDa) and carbonic anhydrase (29 kDa) as molecular mass markers. The collected fractions were analyzed by SDS-PAGE and the bands corresponding to Ada-AlkA and Ogt proteins were digested in situ with trypsin and identified by LC-MS/MS using an HPLC-Chip/Q-TOF 6520 (Agilent Technologies, Santa Clara, CA, USA) to confirm the identity of the two proteins.

#### 4. Conclusions

This work focused on investigating the specific role of proteins involved in the DNA repair mechanism in *M. smegmatis*, a non-pathogenic mycobacterium. Although this mechanism has been widely described in *E. coli*, it is still pretty unknown in mycobacteria, which show a different genetic organization. With the aim of describing the DNA repair mechanism in mycobacteria, we first investigated the protein components of the *M. smegmatis* system. Ogt, Ada-AlkA and FadE8 proteins were cloned and expressed in *E. coli* and validated for their amino acid sequence and the correct folding.

The functional proteomics experiment was aimed at identifying the Ogt protein partners and the results suggested that this protein specifically interacts with Ada-AlkA. Formation of the Ogt/Ada-AlkA complex was then confirmed by docking calculations and gel filtration experiments. Since Ogt is homologous to the B domain of *E. coli* Ada protein, its specific association with Ada-AlkA might restore the same functional activity shown by the Ada protein in *E. coli*, even though they are part of different genes. Therefore, the presence of Ogt and Ada-AlkA in the complex might provide the complex with multiple biological functions that enable it to bind DNA and to exert both methyltransferase and N-glycosidase enzymatic activities. Moreover, it can be expected that the Ada-AlkA moiety is converted to a sensor protein that acts as a positive transcriptional regulator for the other genes involved in the adaptive response to DNA alkylation damage in *M. smegmatis*. However, further genetic investigations are needed to confirm this hypothesis.

Finally, we were able to outline a structural and functional analysis of FadE8 protein and to determine that this protein and its *E. coli* homologous AidB are not only structurally but also functionally related. We demonstrated that FadE8 is able to bind the FAD coenzyme, thus showing a dehydrogenase activity similar to AidB and it is endowed with a specific DNA binding capability.

The investigation of the DNA repair system in *M. smegmatis* allowed us to characterize proteins that are also present in MTB and play key roles in survival and protection mechanisms. Since these proteins are absent in humans, they might represent excellent targets for possible new therapeutic approaches.

**Supplementary Materials:** The following are available online at <http://www.mdpi.com/1422-0067/21/15/5391/s1>, Figure S1: Ada and Ogt protein models; Figure S2: MALDI-MS spectrum. MALDI-MS spectrum of the Random oligonucleotide probe in the linear mode showing the expected mass value (7632.21 Da). Table S1: Peptide mapping of the GST-Ogt fused protein by MALDI-TOF; Table S2: Peptide mapping of the GST-Ada-AlkA fused protein by MALDI-TOF; Table S3: Oligonucleotide probes used in the EMSA experiments; Table S4: Peptide mapping of the FadE8 protein by MALDI-TOF.

**Author Contributions:** Conceptualization, A.D.S. and A.D.; investigation, A.D.S., A.M., C.C.; methodology, A.D.S. and A.M.; validation, A.D.S., A.M., C.C., A.C.; visualization, A.D.S., A.M., C.C., A.C., A.D.; writing—original draft preparation, A.D.S., A.M., C.C., A.D.; writing—review and editing, A.D., F.C. All authors have read and agreed to the published version of the manuscript.

**Funding:** This research was funded by the MIUR grants ARS01\_00597 Project “NAOCON” and PRIN 2017 “Identification and characterization of novel antitumoral/antimicrobial insect-derived peptides: a multidisciplinary, integrated approach from in silico to in vivo”.

**Conflicts of Interest:** The authors declare no conflict of interest.

#### Abbreviations

O <sup>6</sup> -MeG	O <sup>6</sup> -methylguanine
N <sup>7</sup> -MeG	N <sup>7</sup> -methylguanine
N <sup>3</sup> -MeA	N <sup>3</sup> -methyladenine
N <sup>1</sup> -MeA	N <sup>1</sup> -methyladenine
N <sup>3</sup> -MeC	N <sup>3</sup> -methylcytosine
O <sup>4</sup> -MeT	O <sup>4</sup> -methylthymine
DCPIP	2,6 dichlorophenolindophenol
MTB	Mycobacterium tuberculosis
GST	Glutathione S-transferase
GSH	Glutathione
EMSA	Electrophoretic mobility shift assay

CD	Circular dichroism
PDB	Protein Data Bank
FAD	Flavin adenine dinucleotide
PCR	Polymerase chain reaction
IPTG	Isopropyl-thio- $\beta$ -D-galactoside
LC-MS/MS	Liquid chromatography/tandem mass spectrometry

## References

1. Sturla, S.J. DNA adduct profiles: Chemical approaches to addressing the biological impact of DNA damage from small molecules. *Curr. Opin. Chem. Biol.* **2007**, *11*, 293–299. [[CrossRef](#)] [[PubMed](#)]
2. Di Pasquale, P.; Caterino, M.; Di Somma, A.; Squillace, M.; Rossi, E.; Landini, P.; Iebba, V.; Schippa, S.; Papa, R.; Selan, L.; et al. *E. coli* to DNA-Methylating Agents Impairs Biofilm Formation and Invasion of Eukaryotic Cells via Down Regulation of the N-Acetylneuraminase Lyase NanA. *Front. Microbiol.* **2016**, *7*, 147. [[CrossRef](#)]
3. Hu, C.W.; Chen, C.M.; Ho, H.H.; Chao, M.R. Simultaneous quantification of methylated purines in DNA by isotope dilution LC-MS/MS coupled with automated solid-phase extraction. *Anal. Bioanal. Chem.* **2012**, *402*, 1199–1208. [[CrossRef](#)] [[PubMed](#)]
4. Drabløs, F.; Feyzi, E.; Aas, P.A.; Vaagbø, C.B.; Kavli, B.; Bratlie, M.S.; Pena-Diaz, J.; Otterlei, M.; Slupphaug, G.; Krokan, H.E. Alkylation damage in DNA and RNA-repair mechanisms and medical significance. *DNA Rep.* **2004**, *3*, 1389–1407. [[CrossRef](#)] [[PubMed](#)]
5. Landini, P.; Volkert, M.R. Regulatory responses of the adaptive response to alkylation damage: A simple regulon with complex regulatory features. *J. Bacteriol.* **2000**, *182*, 6543–6549. [[CrossRef](#)]
6. Rippa, V.; Amoresano, A.; Esposito, C.; Landini, P.; Volkert, M.; Duilio, A. Specific DNA binding and regulation of its own expression by the AidB protein in *Escherichia coli*. *J. Bacteriol.* **2010**, *192*, 6136–6142. [[CrossRef](#)]
7. Nieminuszczy, J.; Grzesiuk, E. Bacterial DNA repair genes and their eukaryotic homologues: 3. AlkB dioxygenase and Ada methyltransferase in the direct repair of alkylated DNA. *Acta Biochim. Pol.* **2007**, *54*, 459–468. [[CrossRef](#)]
8. Sedgwick, B.; Lindahl, T. Recent progress on the Ada response for inducible repair of DNA alkylation damage. *Oncogene* **2002**, *21*, 8886–8894. [[CrossRef](#)]
9. Mielecki, D.; Grzesiuk, E. Ada response—a strategy for repair of alkylated DNA in bacteria. *FEMS Microbiol.* **2014**, *1*, 1–11. [[CrossRef](#)]
10. Delaney, J.C.; Essigmann, J.M. Mutagenesis, genotoxicity, and repair of 1-methyladenine, 3-alkylcytosines, 1-methylguanine, and 3-methylthymine in alkB *Escherichia coli*. *Proc. Natl. Acad. Sci. USA* **2004**, *101*, 14051–14056. [[CrossRef](#)]
11. Rippa, V.; Duilio, A.; di Pasquale, P.; Amoresano, A.; Landini, P.; Volkert, M.R. Preferential DNA damage prevention by the *E. coli* AidB gene: A new mechanism for the protection of specific genes. *DNA Repair* **2011**, *10*, 934–941. [[CrossRef](#)] [[PubMed](#)]
12. Hamill, M.J.; Jost, M.; Wong, C.; Bene, N.C.; Drennan, C.L.; Elliott, S.J. Electrochemical characterization of *Escherichia coli* adaptive response protein AidB. *Int. J. Mol. Sci.* **2012**, *13*, 16899–16915. [[CrossRef](#)]
13. Yang, M.; Aamodt, R.M.; Dalhus, B.; Balasingham, S.; Helle, I.; Andersen, P.; Tønjum, T.; Alseth, I.; Rognes, T.; Bjørås, M. The ada operon of *Mycobacterium tuberculosis* encodes two DNA methyltransferases for inducible repair of DNA alkylation damage. *DNA Repair* **2011**, *10*, 595–602. [[CrossRef](#)]
14. Singh, A. Guardians of the mycobacterial genome: A review on DNA repair systems in *Mycobacterium tuberculosis*. *Microbiology* **2017**, *163*, 1740–1758. [[CrossRef](#)]
15. Miggiano, R.; Casazza, V.; Garavaglia, S.; Ciaramella, M.; Perugino, G.; Rizzi, M.; Rossia, F. Biochemical and Structural Studies of the *Mycobacterium tuberculosis* O6-Methylguanine Methyltransferase and Mutated Variants. *J. Bacteriol.* **2013**, *195*, 2728. [[CrossRef](#)] [[PubMed](#)]
16. Mattossovich, R.; Merlo, R.; Miggiano, R.; Valenti, A.; Perugino, G. O6-alkylguanine-DNA Alkyltransferases in Microbes Living on the Edge: From Stability to Applicability. Review. *Int. J. Mol. Sci.* **2020**, *21*, 2878. [[CrossRef](#)] [[PubMed](#)]

17. Bradford, M.M. A rapid and sensitive method for the quantitation of microgram quantities of protein utilizing the principle of protein-dye binding. *Anal. Biochem.* **1976**, *72*, 248. [[CrossRef](#)]
18. Roy, A.; Kucukural, A.; Zhang, Y. I-TASSER: A unified platform for automated protein structure and function prediction. *Nat. Protoc.* **2010**, *5*, 725. [[CrossRef](#)]
19. Yang, J.; Yan, R.; Roy, A.; Xu, D.; Poisson, J.; Zhang, Y. The I-TASSER Suite: Protein structure and function prediction. *Nat. Methods* **2015**, *12*, 7. [[CrossRef](#)]
20. Yang, J.; Zhang, Y. I-TASSER server: New development for protein structure and function predictions. *Nucleic Acids Res.* **2015**, *43*, W174–W181. [[CrossRef](#)]
21. Zhang, Y. I-TASSER server for protein 3D structure prediction. *BMC Bioinform.* **2008**, *9*, 40. [[CrossRef](#)]
22. Jorgensen, W.L.; Tirado-Rives, J. Potential energy functions for atomic-level simulations of water and organic and biomolecular systems. *Proc. Natl. Acad. Sci. USA* **2005**, *102*, 6665–6670. [[CrossRef](#)] [[PubMed](#)]
23. Dodda, L.S.; Vilseck, J.Z.; Tirado-Rives, J.; Jorgensen, W.L. 1.14\* CM1A-LBCC: Localized bond-charge corrected CM1A charges for condensed-phase simulations. *J. Phys. Chem. B* **2017**, *121*, 3864–3870. [[CrossRef](#)] [[PubMed](#)]
24. Dodda, L.S.; Cabeza de Vaca, I.; Tirado-Rives, J.; Jorgensen, W.L. LigParGen web server: An automatic OPLS-AA parameter generator for organic ligands. *Nucleic Acids Res.* **2017**, *45*, W331–W336. [[CrossRef](#)] [[PubMed](#)]
25. Schneidman-Duhovny, D.; Inbar, Y.; Nussinov, R.; Wolfson, H.J. PatchDock and SymmDock: Servers for rigid and symmetric docking. *Nucleic Acids Res.* **2005**, *33*, W363–W367. [[CrossRef](#)] [[PubMed](#)]
26. Mashiach, E.; Schneidman-Duhovny, D.; Andrusier, N.; Nussinov, R.; Wolfson, H.J. FireDock: A web server for fast interaction refinement in molecular docking. *Nucleic Acids Res.* **2008**, *36*, W229–W232. [[CrossRef](#)]
27. Salentin, S.; Schreiber, S.; Haupt, V.J.; Adasme, M.F.; Schroeder, M. PLIP: Fully automated protein–ligand interaction profiler. *Nucleic Acids Res.* **2015**, *43*, W443–W447. [[CrossRef](#)]
28. Kurkcuoglu, Z.; Koukos, P.I.; Citro, N.; Trellet, M.E.; Rodrigues, J.P.G.L.M.; Moreira, I.S.; Roel-Touris, J.; Melquiond, A.S.J.; Geng, C.; Schaarschmidt, J.; et al. Performance of HADDOCK and a simple contact-based protein–ligand binding affinity predictor in the D3R Grand Challenge 2. *J. Comput. Aid. Mol. Des.* **2018**, *32*, 175–185. [[CrossRef](#)]
29. Pettersen, E.F.; Goddard, T.D.; Huang, C.C.; Couch, G.S.; Greenblatt, D.M.; Meng, E.C.; Ferrin, T.E. UCSF Chimera—A visualization system for exploratory research and analysis. *J. Comput. Chem.* **2004**, *25*, 1605–1612. [[CrossRef](#)]
30. Waterhouse, A.; Bertoni, M.; Bienert, S.; Studer, G.; Tauriello, G.; Gumienny, R.; Heer, F.T.; de Beer, T.A.P.; Rempfer, C.; Bordoli, L.; et al. SWISS-MODEL: Homology modelling of protein structures and complexes. *Nucleic Acids Res.* **2018**, *46*, W296–W303. [[CrossRef](#)]
31. Laskowski, R.A. PDBsum new things. *Nucleic Acids Res.* **2008**, *37* (Suppl. 1), D355–D359. [[CrossRef](#)] [[PubMed](#)]
32. De Beer, T.A.; Berka, K.; Thornton, J.M.; Laskowski, R.A. PDBsum additions. *Nucleic Acids Res.* **2013**, *42*, D292–D296. [[CrossRef](#)] [[PubMed](#)]
33. Laskowski, R.A. PDBsum: Summaries and analyses of PDB structures. *Nucleic Acids Res.* **2001**, *29*, 221–222. [[CrossRef](#)]
34. Vangone, A.; Bonvin, A.M. Contacts-based prediction of binding affinity in protein–protein complexes. *Elife* **2015**, *4*, e07454. [[CrossRef](#)] [[PubMed](#)]
35. Xue, L.C.; Rodrigues, J.P.; Kastritis, P.L.; Bonvin, A.M.; Vangone, A. PRODIGY: A web server for predicting the binding affinity of protein–protein complexes. *Bioinformatics* **2016**, *32*, 3676–3678. [[CrossRef](#)]
36. Caterino, M.; Corbo, C.; Imperlini, E.; Armiraglio, M.; Pavesi, E.; Aspesi, A.; Loreni, F.; Dianzani, I.; Ruoppolo, M. Differential proteomic analysis in human cells subjected to ribosomal stress. *Proteomics* **2013**, *13*, 1220–1227. [[CrossRef](#)]



## Article

# Role of Ovarian Proteins Secreted by *Toxoneuron nigriceps* (Viereck) (Hymenoptera, Braconidae) in the Early Suppression of Host Immune Response

Rosanna Salvia <sup>1,2</sup>, Carmen Scieuzo <sup>1,2</sup>, Annalisa Grimaldi <sup>3</sup> , Paolo Fanti <sup>1</sup>, Antonio Moretta <sup>1</sup> , Antonio Franco <sup>1,2</sup>, Paola Varricchio <sup>4</sup>, S. Bradleigh Vinson <sup>5</sup> and Patrizia Falabella <sup>1,2,\*</sup> 

<sup>1</sup> Department of Sciences, University of Basilicata, Via dell'Ateneo Lucano 10, 85100 Potenza, Italy; r.salvia@unibas.it (R.S.); carmen.scieuzo@unibas.it (C.S.); paolo.fanti@unibas.it (P.F.); antonio.moretta@unibas.it (A.M.); antonio.franco@unibas.it (A.F.)

<sup>2</sup> Spinoff XFlies s.r.l, University of Basilicata, Via dell'Ateneo Lucano 10, 85100 Potenza, Italy

<sup>3</sup> Department of Biotechnology and Life Science, University of Insubria, Via J.H. Dunant 3, 21100 Varese, Italy; Annalisa.Grimaldi@uninsubria.it

<sup>4</sup> Department of Agricultural Sciences, University of Naples "Federico II", 80055 Portici, Italy; paolavarricchio9599@gmail.com

<sup>5</sup> Department of Entomology, Texas A&M University, 370 Olsen Blvd, College Station, TX 77843-2475, USA; bvinson@tamu.edu

\* Correspondence: patrizia.falabella@unibas.it



**Citation:** Salvia, R.; Scieuzo, C.; Grimaldi, A.; Fanti, P.; Moretta, A.; Franco, A.; Varricchio, P.; Vinson, S.B.; Falabella, P. Role of Ovarian Proteins Secreted by *Toxoneuron nigriceps* (Viereck) (Hymenoptera, Braconidae) in the Early Suppression of Host Immune Response. *Insects* **2021**, *12*, 33. <https://doi.org/10.3390/insects12010033>

Received: 10 December 2020

Accepted: 31 December 2020

Published: 5 January 2021

**Publisher's Note:** MDPI stays neutral with regard to jurisdictional claims in published maps and institutional affiliations.



**Copyright:** © 2021 by the authors. Licensee MDPI, Basel, Switzerland. This article is an open access article distributed under the terms and conditions of the Creative Commons Attribution (CC BY) license (<https://creativecommons.org/licenses/by/4.0/>).

**Simple Summary:** *Toxoneuron nigriceps* is an endoparasitoid of the tobacco budworm *Heliothis virescens*. Parasitoid strategies to survive involve different regulating factors that are injected into the host body together with the egg: the venom and the calyx fluid, containing a Polydnavirus (PDV) and Ovarian Proteins (OPs). The combination of these factors increases the success of parasitism. Although many studies have been reported on venom protein components and the knowledge on PDVs is increasing, little is known on OPs. These secretions are able to interfere early with the host cellular immune response, acting specifically on host haemocytes, cells involved in immune response. Our results show that OPs induce several alterations on haemocytes, including cellular oxidative stress condition and modifications of actin cytoskeleton, so inducing both a loss of haemocyte functionality and cell death. Overall, in synergy with PDV and venom, OPs positively contribute to the evasion of the host immune response by *T. nigriceps*.

**Abstract:** *Toxoneuron nigriceps* (Viereck) (Hymenoptera, Braconidae) is an endophagous parasitoid of the larval stages of the tobacco budworm, *Heliothis virescens* (Fabricius) (Lepidoptera, Noctuidae). During oviposition, *T. nigriceps* injects into the host body, along with the egg, the venom, the calyx fluid, which contains a Polydnavirus (*T. nigriceps* BracoVirus: *TnBV*), and the Ovarian Proteins (OPs). Although viral gene expression in the host reaches detectable levels after a few hours, a precocious disruption of the host metabolism and immune system is observed right after parasitization. This alteration appears to be induced by female secretions including *TnBV* venom and OPs. OPs, originating from the ovarian calyx cells, are involved in the induction of precocious symptoms in the host immune system alteration. It is known that OPs in braconid and ichneumonid wasps can interfere with the cellular immune response before Polydnavirus infects and expresses its genes in the host tissues. Here we show that *T. nigriceps* OPs induce several alterations on host haemocytes that trigger cell death. The OP injection induces an extensive oxidative stress and a disorganization of actin cytoskeleton and these alterations can explain the high-level of haemocyte mortality, the loss of haemocyte functionality, and so the reduction in encapsulation ability by the host.

**Keywords:** Ovarian Proteins; host-parasitoid interaction; *Heliothis virescens*; *Toxoneuron nigriceps*



## 1. Introduction

Parasitoid insects have developed in some species a great variety of adaptations in terms of physiological integration which make them similar to parasites, which constitute the most specialized forms of zoophagy [1]. Parasitoids belong to different insect orders, such as Diptera, Coleoptera, Lepidoptera, Trichoptera, and Neuroptera but they are common above all among the Hymenoptera [2]. Parasitoids develop at the expense of a single victim, the host, killing it [3]. They can be classified by different parameters, such as the number of deposited eggs per host and the parasitization mode [3]. Their host can be an egg, a larva, a pupa or, rarely, adult insects. Parasitoids are generally defined as ectoparasitoids when the juvenile stages feed on the host from the outside of the body and endoparasitoids when the development of the parasitoid takes place inside the host body [4].

During evolution, insects have developed many defense mechanisms as a result of frequent attacks by pathogens and parasites. They have an innate immunity defense, capable of recognizing and identifying a large class of foreign organisms and responding selectively and effectively to attacks [5–8]. The non-self-recognition by insects is due to the molecular interaction between the non-self-molecules and the specific receptors distributed on the host cell surface [9,10]. When the receptors recognize and bind to the proper ligands (non-self-molecules), a signal cascade is activated into the cell, promoting the immune response through the production of antimicrobial peptides (AMPs) and the melanization process [11,12].

To overcome the immune defenses of the host, the parasitoids have developed several strategies that are generally classified as active and passive [13]. The parasitic factor responsible for the active immune suppression in the host include maternal factors such as the venom and the ovarian calyx fluid, which contain the Ovarian Proteins (OPs) and in some cases Polydnavirus (PDV) or virus-like particles (VLP), and embryonic factors such as teratocytes [4,14–17].

PDVs belong to a Polydnaviridae family with unique biological traits, whose members are divided in two groups, Ichnovirus and Bracovirus, all associated with endophagous parasitoids of lepidopteran larvae [18–20]. Several genes expressed, even at an early stage of infection, by PDVs in different tissues of the host, including the haemocytes, have been shown to be implicated in the active suppression of the host immune response [21–27]. The expression of the viral gene in the host tissues does not guarantee an escape of the immune response in the early hours following oviposition. This problem is overcome by some parasitoids by injecting (together with the egg and the venom) the OPs, produced by epithelial cells of the female parasitoid reproductive traits [28,29]. The OPs have not been investigated as exhaustively as the other parasitoid maternal factors.

In this work we investigated the role of OPs of the endophagous parasitoid, the Hymenoptera Braconidae *Toxoneuron nigriceps* (Viereck) on its natural host, the noctuid moth *Heliothis virescens* (Fabricius). The parasitoid is able to lay the egg in all the larval stages of its host which, while reaching the mature larval stage, shows a slowed development, and the inability to pupate [30,31]. This alteration of the host development that allows the development of the parasitoid larva, is due to changes in the neuroendocrine equilibrium, to the redirection of the host biochemical and metabolic processes, in a condition of severe alteration of the host's immune response [32–34]. This regulation of the host physiology is induced by both maternal (fluid of the calyx and venom) and embryonic (teratocytes) factors of parasitic origin [35,36]. The expression of *T. nigriceps* BracoVirus (*TnBV*) genes into host cells determines the functional inactivation of the prothoracic glands in the mature larvae [33–38] and induces apoptosis in haemocytes [26,39]. The teratocytes, cells derived from the embryonic serosal membrane [40] contribute to the arrest of the host development [41] inducing the transformation of 20-hydroxyecdysone into inactive polar metabolites [31,32,42–44]. Among the factors of maternal origin, *TnBV* and venom have been the most studied factors [15,24,26,44]. The virus infects different tissues like the fat body, the haemocytes and the prothoracic glands, in which it actively expresses

its genes. Among the viral genes, *TnBV1* [45,46] and *TnBVank1* [24,26] seem to play an important role in the suppression of the immune response. In the parasitized host a decrease in the number of haemocytes has been observed as early as 2 h up to 24 h after the oviposition, with the lower number of haemocytes observed after 4 h [39]. Two hours after parasitization *H. virescens* haemolymph showed a high number of apoptotic cells and a very low level of cell proliferation [39]. Furthermore, as a result of parasitization, the remaining haemocytes showed strong morphological and structural changes, losing the ability to adhere to external objects and to encapsulate invading microorganisms [39]. The expression of the identified *TnBV* genes, that are responsible for morphological alterations and apoptosis in haemocytes, always occurs at least after 3–4 h [24,26]. We hypothesize that the very early suppression of the host immune response after oviposition is correlated to both a passive mechanism, due to the presence of a fibrous layer on the egg surface, and an active mechanism, due to the action of the possible synergic effect of the venom and OP mixture [47–49]. The venom composition was elucidated by using a combined transcriptomic and proteomic approach [15] and several proteins putatively involved in the alteration of the immune system of the parasitized host identified.

Currently, nothing is known about the function of OPs of *T. nigriceps* and their role in the alterations of the immune system of the host *H. virescens*. Here we present research we did on this aspect. In particular, we believe that OPs can interfere with the cellular immune response before *TnBV* infects and expresses its genes in the host tissues.

## 2. Materials and Methods

### 2.1. Insect Rearing

*Toxoneuron nigriceps* parasitoid was reared according to the methodology described by Vinson et al. [50]. The larvae of the host *Heliothis virescens* were reared on an artificial diet developed by Vanderzant et al. [51] (Corn Earworm Diet, Bioserve, Frenchtown, NJ, USA). The breeding temperature was maintained at  $29\text{ }^{\circ}\text{C} \pm 1\text{ }^{\circ}\text{C}$ , both for non-parasitized and parasitized *H. virescens* larvae. *Toxoneuron nigriceps* adults were bred at a temperature of  $25\text{ }^{\circ}\text{C} \pm 1\text{ }^{\circ}\text{C}$ . In both cases a photoperiod of 16 h of light and 8 h of darkness was set with a relative humidity of  $70\% \pm 5\%$ . For the following analysis *H. virescens* larvae parasitized at day one of the last instar were used.

### 2.2. Calyx Fluid Collection and Ovarian Protein Purification

About 80–100 adult females of *T. nigriceps*, two weeks old, previously anesthetized on ice for 10–15 min, were used for the collection of the calyx fluid, containing *T. nigriceps* BracoVirus (*TnBV*) and Ovarian Protein (OPs). From each female, immersed in a physiological solution of  $1\times$  Phosphate-Buffered Saline (PBS), the entire reproductive apparatus was removed, pulling away the ovipositor with a pair of forceps. The isolated ovaries, explanted by one or two females, were placed in a drop of  $20\text{ }\mu\text{L}$  of  $1\times$  PBS (1 or 2 equivalent females) at  $4\text{ }^{\circ}\text{C}$  and the ovarian calyx were dissected to allow the flow of the calyx fluid. The collected liquid was transferred into a  $1.5\text{ mL}$  tube (Eppendorf, Hamburg, DE, catalogue number 0030120.086) and centrifuged at  $2000\times g$  for 5 min at  $4\text{ }^{\circ}\text{C}$  to remove the eggs and the calyx tissues and any other debris. The supernatant, containing OPs and *TnBV*, was further purified with  $0.45\text{ }\mu\text{m}$  Millex PVDF filters (Millipore, Burlington, MA, USA, catalogue number SLHVM33RS) followed by washing 3 times with  $1\text{ mL}$  of  $1\times$  PBS. To separate *TnBV* a centrifugation was carried out at  $30,000\times g$  for 1 h at  $4\text{ }^{\circ}\text{C}$  and subsequently the supernatant containing the OPs was concentrated by ultrafiltration in a column with cut-off 3000 (Millipore, Burlington, MA, USA, catalogue number UFC900308), by centrifuging the sample at  $3000\times g$  until a volume of around  $500\text{ }\mu\text{L}$  was obtained. The resulting filtrate was stored at  $-80\text{ }^{\circ}\text{C}$  for subsequent uses (Protocol S1).

### 2.3. Collection of Haemocytes from Larvae of *H. virescens*

Larvae of *H. virescens* on the third day of the last instar were anesthetized in water, sterilized in 70% ethanol (*v/v*) and subsequently washed in sterile deionized water. The

first pair of legs was cut and the hemolymph from the wound was collected and transferred to a centrifuge tube containing 1 mL of MEAD pre-cooled solution in ice [39]. The sample was centrifuged at  $400\times g$  for 7 min at 4 °C. The precipitate was washed twice with a MEAD-PBS solution (1:1). Finally, the haemocytes were gently resuspended in 1 mL of Grace Insect Medium (Sigma Aldrich, St. Louis, MO, USA, catalogue number, G8142) containing FBS (Gibco, Gaithersburg, MD, USA, catalogue number A4766801) 10% and antibiotic-antimycotic 1% (Gibco, Gaithersburg, MD, USA, catalogue number 15240062).

An amount of  $1 \times 10^6$  haemocyte cells per well were inoculated in 24-well culture plates (Corning Incorporated, New York, NY, USA, catalogue number CLS3527-100EA). OPs (deriving from 1 or 2 equivalent females) or  $1 \times$  PBS (as control) collected as described above were added to the haemocytes in the culture medium and incubated at 27 °C.

#### 2.4. Cells Viability

To evaluate cell viability after the treatment with OPs, and to compare the effect of parasitization and OPs alone, trypan blue staining (Sigma Aldrich, St Louis, MO, USA, catalogue number T8154) was used on haemocytes, collected from parasitized and non-parasitized larvae. OPs (obtained from 1 or 2 equivalent females) or  $1 \times$  PBS (as control) were added to the haemocytes collected from non-parasitized larvae in the culture medium and incubated at 27 °C for 24 h. Trypan blue staining was added to the cell suspension at a final concentration of 0.04% and then haemocytes were counted by Neubauer's chamber under microscopy (Eclipse 80i, Nikon, Tokyo, Japan).

#### 2.5. Light Microscopy Haemocyte Observations

The haemocytes incubated with OPs (deriving from 2 equivalent females) at different time (30 min, 1 h and 2 h) or with  $1 \times$  PBS (negative control) were detached from the well transferred on slides and subjected to different staining methodologies: May Grünwald GIEMSA (Sigma Aldrich, St Louis, MO, USA, catalogue number MG500 and GS500), 2,7 dichlorodihydrofluorescein acetate ( $H_2DCFDA$ ) (Thermo Fisher Scientific, Waltham, MA, USA, catalogue number D399), and tetramethylrhodamine isothiocyanate (TRITC)-conjugated phalloidin (Sigma Aldrich, St Louis, MO, USA, catalogue number P1951) dyes. For each analyzed parameter, evaluation was performed considering five random fields in three independent replicates in which cells with alteration were counted on the total number of cells.

Haemocytes were fixed with 4% paraformaldehyde for 10 min, washed with  $1 \times$  PBS, and stained with May–Grünwald dye for 15 min followed by 30 min in 5% Giemsa stain. The cells were washed three times with  $1 \times$  PBS and the slides were mounted with glycerol (Sigma Aldrich, St Louis, MO, USA, catalogue number G5516) for morphologic observation.

For  $H_2DCFDA$  staining, after fixing on slides, cells were incubated in the dark with  $H_2DCFDA$  10  $\mu$ M for 30 min at room temperature. After washing three times in  $1 \times$  PBS, the slides were mounted with glycerol.

A further staining was carried out using TRITC-conjugated phalloidin staining, the haemocytes fixed on slides, were incubated with TRITC-conjugated phalloidin diluted 50  $\mu$ g/mL in 1% BSA (Sigma Aldrich St Louis, MO, USA, catalogue number 05470) for 2 h at room temperature in dark conditions and then, after three washes with  $1 \times$  PBS, the slides were mounted with glycerol.

For all staining methodologies, the slides were observed microscopically with Nikon Eclipse 80i equipped with a Nikon Plan Fluor 100 $\times$ /0.5–1.3 Oil Iris objective and the images, five random fields obtained in three independent replicates, were recorded with a Nikon Digital Sight DS-U1 camera, and the percentage of stained/fluorescent cells was counted on the total number of cells.

#### 2.6. Chromatographic Sphere Staining

Sephadex Fine G50 chromatographic beads (Cytiva, Little Chalfont, England, GB catalogue number 17004202) were stained with the Congo Red dye (Sigma Aldrich, St Louis,

MO, USA, catalogue number 75768). The beads were autoclaved in 1 mL of 1× PBS at 121 °C for 20 min and centrifuged at 13,000× *g* for 5 min. The supernatant was removed and 500 µL of a 1× PBS solution containing 20 mg/mL of Congo Red was added. The beads were autoclaved again at 121 °C for 20 min, centrifuged at 13,000× *g* for 5 min and repeatedly washed with 1× PBS to remove excess of dye.

### 2.7. Encapsulation Measurement

Before testing the effect of OPs on encapsulation, we defined the minimum time needed in *H. virescens* to obtain an adequate level of encapsulation. To assess this time we performed an assay, injecting 30 beads into 5 larvae for each, at 3 different dissection times after injection (10 min, 3 h, 6 h) for 3 replicates. The level of encapsulation reached after 6 h was found to be adequate to see the encapsulation effect in subsequent experiments. All the recovered beads were observed under the microscope (Eclipse 80i, Nikon, Tokyo, Japan).

### 2.8. Injections of OPs and Chromatographic Spheres in *H. virescens* Larvae and Evaluation of In Vivo Encapsulation Degree

The injections were performed on larvae of *H. virescens*, on the first day of the fifth instar larva. The larvae were anesthetized in water, sterilized in 70% ethanol (Sigma Aldrich St Louis, MO, USA, catalogue number 51976) (*v/v*) and subsequently washed in deionized water. Then, they were dried and placed on a Petri dish. Injection of the Sephadex Fine G 50 (50–150 µm) chromatographic beads was performed in the neck membrane, using a Hamilton syringe (Sigma-Aldrich, St Louis, MO, USA, catalogue number HAM80075-1EA) having a needle with 0.13 mm internal diameter and 0.47 mm outer diameter. The chromatographic spheres were injected at different times (10 min, 1 h or 3 h) after OPs injections or 5 µL of 1× PBS. After 6 h from the injection of the spheres, the time necessary for the formation of a complete haemocyte capsule (Figure S1), the larvae were anesthetized in water, sterilized in ethanol 70% (*v/v*) and washed in deionized water. Subsequently they were dried and placed in a drop of 1× PBS solution. The dissection was performed by cutting the head and longitudinally cutting in the ventral position. The chromatographic spheres attached to the tissues were collected and counted. The spheres were classified according to the degree of encapsulation as: 0 = unencapsulated (no haemocytes layer); 1 = the thickness of capsule is one or more than one layer, but less than a half of the bead's radius; 2 = the thickness of capsule is equal or more than a half of the bead's radius. We considered encapsulated the beads that showed after 6 h case 2, and not encapsulated when the beads showed case 0 or 1.

### 2.9. Statistical Analysis of Data

Statistical analysis was performed with one-way ANOVA (analysis of variance) and Bonferroni or Tukey post-hoc tests. Statistical differences were analyzed both among all treatments and between control and treated samples at the same experimental time. For the encapsulation assay we first verified that there was no statistical difference among the experimental groups in the percent of recovered beads after the dissection and then we compared the percent of encapsulated beads on the number of recovered beads.

## 3. Results

### 3.1. Cell Viability of the Haemocytes after Treatment with Ovarian Proteins

The extracted haemocytes from non-parasitized *H. virescens* larvae (control) showed 85% of cell viability. The haemocytes extracted from larvae of *H. virescens* after 24 h from the parasitization showed only 30% of cell viability. The cell viability of haemocytes cultured in the presence of *T. nigriceps* Ovarian Proteins (OPs) for 24 h did not vary according to their concentration. The cell viability percentages equal to 34% and 38% referred to, respectively, samples treated with OPs deriving from 1 or 2 equivalent *T. nigriceps* females. Table S1 and Figure 1 show the obtained results.

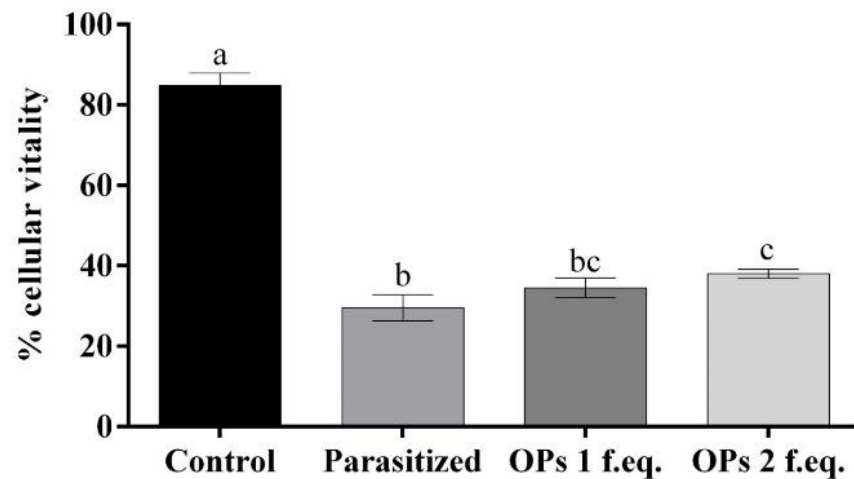


**Figure 1.** Percentage of haemocyte viability incubated with  $1\times$  PBS (control), haemocytes extracted from larvae 24 h after parasitization, haemocytes incubated with Ovarian Proteins (OPs) deriving from 1 or 2 equivalent females. Data are presented as means  $\pm$  SD ( $n = 3$  replicates). Statistical analysis was performed with one-way ANOVA and Tukey post-hoc test. Different letters indicate significant differences ( $p$  value  $< 0.0001$ ).

### 3.2. Haemocyte Staining

#### 3.2.1. May Grunwald–Giemsa Staining

The haemocytes, treated with OPs deriving from 2 equivalent females at different incubation times (30 min, 1 h and 2 h) were observed after May Grunwald–Giemsa (MGG) staining. The cells showed a different staining as a function of the cytoplasmic pH and this allowed the different cell populations to be counted in the three different examined samples (Figure 2). The percentage of cells with acidophilic cytoplasm and massive vacuolization was greater than control and increased in relation to the different times of OP exposure (Table S2, Figure 3).

Figure 3 shows that after 30 min of incubation the percentage of cells with acidophilic cytoplasm was 27%. After 1 h the percentage was raised to 34% compared to the relative control and after 2 h the percentage reached 41%.

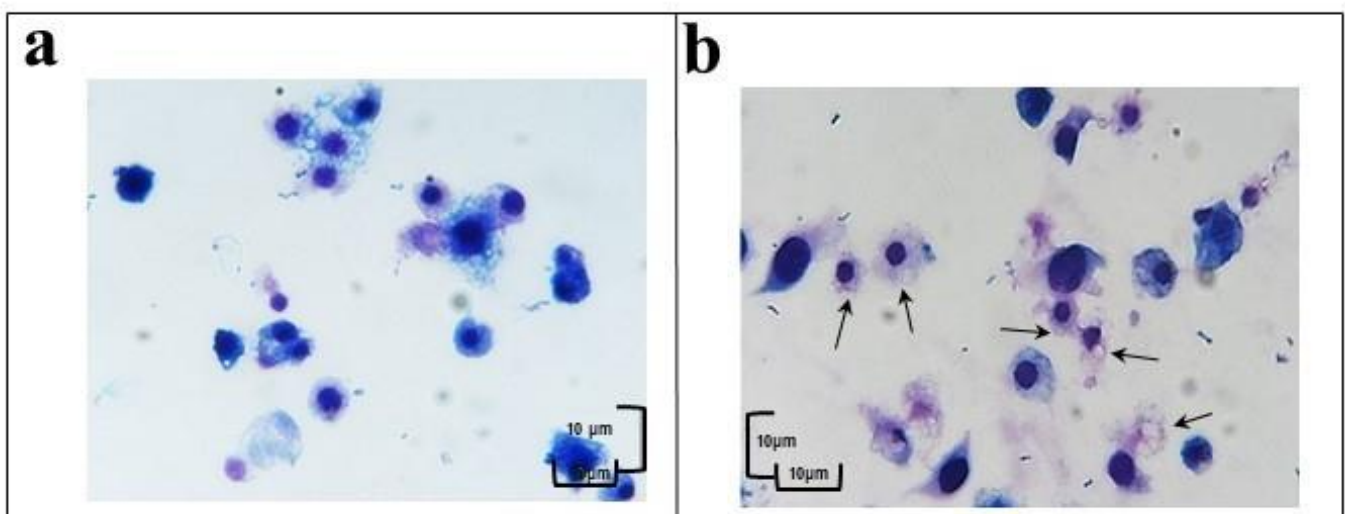


**Figure 2.** Haemocytes treated with  $1\times$  PBS (a) or with OPs for 2 h (b) stained with May Grunwald–Giemsa dye. Scale bar 10  $\mu$ m. Arrows indicate vacuolization process.

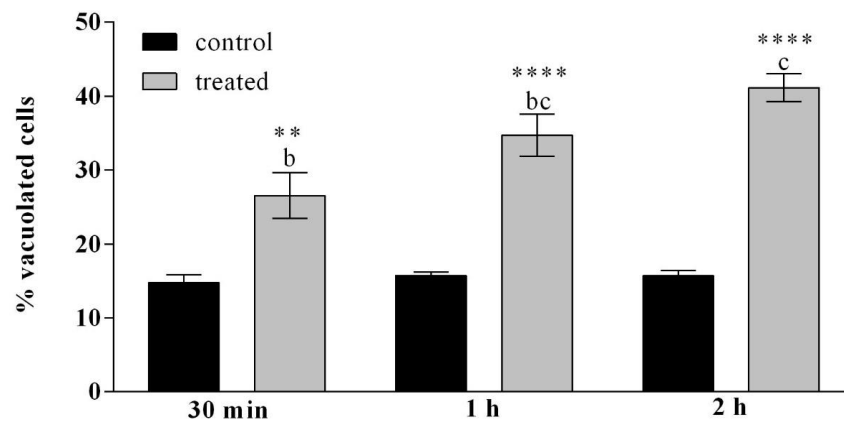
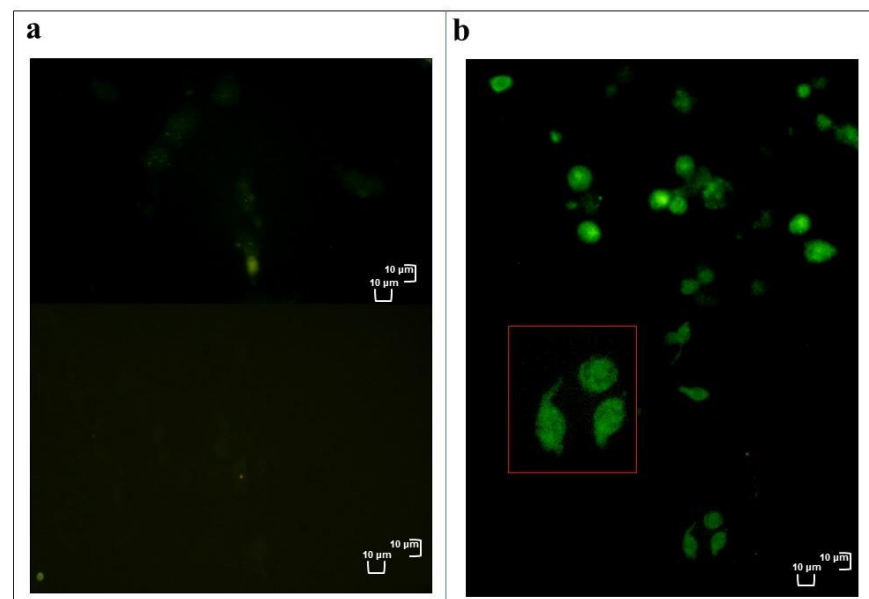


**Figure 3.** Percentage of haemocytes showing vacuolization, after treatment with OPs deriving from 2 equivalent females at different incubation times (30 min, 1 h and 2 h) and observed after May Grunwald–Giemsa (MGG) staining. Data are presented as means  $\pm$  SD ( $n = 3$  replicates). Statistical analysis was performed with one-way ANOVA and Bonferroni (for control vs. treatment analysis) and Tukey post-hoc test (for all sample analysis). Different letters indicate significant differences among all treatments ( $p$  value  $< 0.0001$ ), asterisks indicate significant differences between control and treated samples at the same experimental time (\*\*  $p$  value  $< 0.01$ ; \*\*\*\*  $p$  value  $< 0.0001$ ).

### 3.2.2. H<sub>2</sub>DCFDA Staining

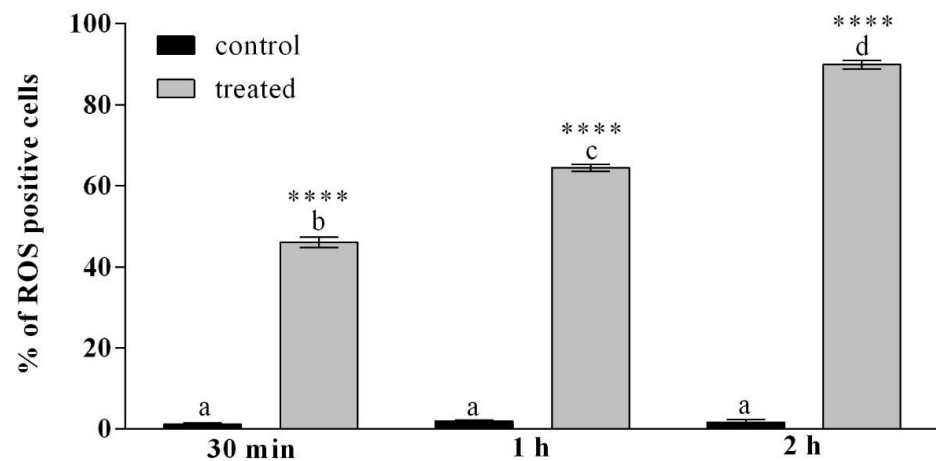
Haemocytes treated with OPs (2 equivalent females) at different times (30 min, 1 h and 2 h) were stained with 2,7 dichlorodihydrofluorescein acetate (H<sub>2</sub>DCFDA). H<sub>2</sub>DCFDA after entering into the cells, were converted into dichlorodihydrofluorescein (H<sub>2</sub>DCF) by intracellular esterases, H<sub>2</sub>DCF is rapidly oxidized to a highly fluorescent compound, 2,7-dichlorofluorescein (DCF), only in the presence of reactive oxygen species (ROS).

Figure 4 and Figure S2 show a strong fluorescent signal indicative of high oxidative stress in cells incubated for 2 h with OPs and a very weak fluorescent signal that could constitute the background experiment and/or could be indicative of cell physiological presence of ROS at low concentrations in control cells.



**Figure 4.** Healthy in vitro haemocytes (a) or treated with OPs for 2 h (b) and stained with 2,7 dichlorodihydrofluorescein acetate (H<sub>2</sub>DCFDA). Red box = enlargement of cells below. Scale bar 10  $\mu$ m.

Table S3 and Figure 5 report the percentage of haemocytes showing a strong fluorescent signal indicative of oxidative stress, after incubation with OPs at different times. After 30 min of incubation with OPs, 46% of haemocytes were strongly fluorescent, after 1 h of treatment 64% of cells were fluorescent, after 2 h of incubation with OPs, almost the totality of the haemocytes (90%) showed oxidative stress.



**Figure 5.** Percentage of haemocytes stained with H<sub>2</sub>DCFDA showing oxidative stress, after treatment with OPs deriving from 2 equivalent females at different times of exposure (30 min, 1 h and 2 h). Data are presented as mean  $\pm$  SD ( $n = 3$ ). Statistical analysis was performed with one-way ANOVA and Bonferroni (for control vs. treatment analysis) and Tukey post-hoc test (for all sample analysis). Different letters indicate significant differences among all treatments ( $p$  value  $< 0.0001$ ), asterisks indicate significant differences between control and treated samples at the same experimental time ( $p$  value  $< 0.0001$ ).

### 3.2.3. TRITC-Conjugated Phalloidin Staining

Actin filaments were detected using TRITC-Conjugated phalloidin staining in healthy haemocytes (control) or treated with OPs at different times (30 min, 1 h and 2 h) and stained with phalloidin. Figure 6 shows in the treated cells a weak and fragmented signal localized near the nucleus and along the plasma membrane while a strong and homogeneously distributed fluorescent signal is observed in control cells.

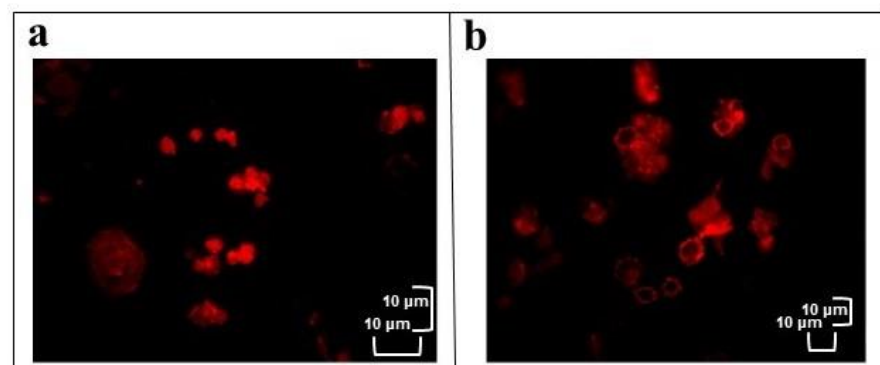


**Figure 6.** In vitro healthy haemocytes (a) or treated with OPs for 2 h (b) and stained with TRITC-Conjugated phalloidin. Scale bar 10  $\mu$ m.

In Figure 7 and in Table S4 the percentage of cells that show cytoskeletal damage on the total number of cells is reported. After 30 min of incubation with OPs the percentage of cells with cytoskeletal damage was equal to 31% of the total haemocytes, while no damage to actin filaments was observed in control cells. After 1 h the percentage rose to 70% for the treated cells. After 2 h 80% of the treated cells showed cytoskeletal damage.

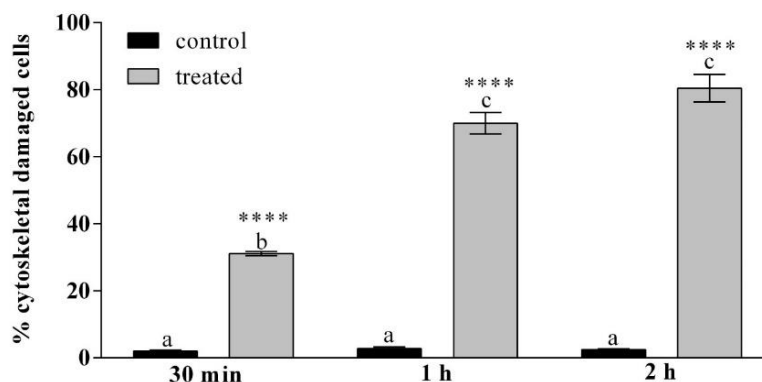


**Figure 7.** Percentage of haemocytes stained with phalloidin showing cytoskeletal damage, after treatment with OPs deriving from 2 equivalent females at different times of exposure (30 min, 1 h and 2 h). Data are presented as mean ± SD ( $n = 3$ ). Statistical analysis was performed with one-way ANOVA and Bonferroni (for control vs. treatment analysis) and Tukey post-hoc test (for all sample analysis). Different letters indicate significant differences among all treatments ( $p$  value < 0.0001), asterisks indicate significant differences between control and treated samples at the same experimental time ( $p$  value < 0.0001).

### 3.3. In Vivo Encapsulation

To assess whether the alterations induced by OPs influenced the ability of the haemocytes to recognize and encapsulate foreign intruders, a test was performed by injecting OPs (2 females equivalent) or 1 × PBS into *H. virescens* larvae at different times (10 min, 1 h and 3 h) before injection of chromatographic spheres used as non-self-material. Chromatographic spheres were injected also in *H. virescens* parasitized larvae. The spheres were classified according to the level of encapsulation as: 0 = unencapsulated (no haemocytes layer); 1 = the thickness of capsule is one or more than one layer, but less than a half of the bead’s radius; 2 = the thickness of capsule is equal or more than a half of the bead’s radius. We considered encapsulated exclusively the spheres of type 2 (Figure S1). Figure 8 and Table S5 show a strong reduction in the encapsulation capacity in the different treatments.

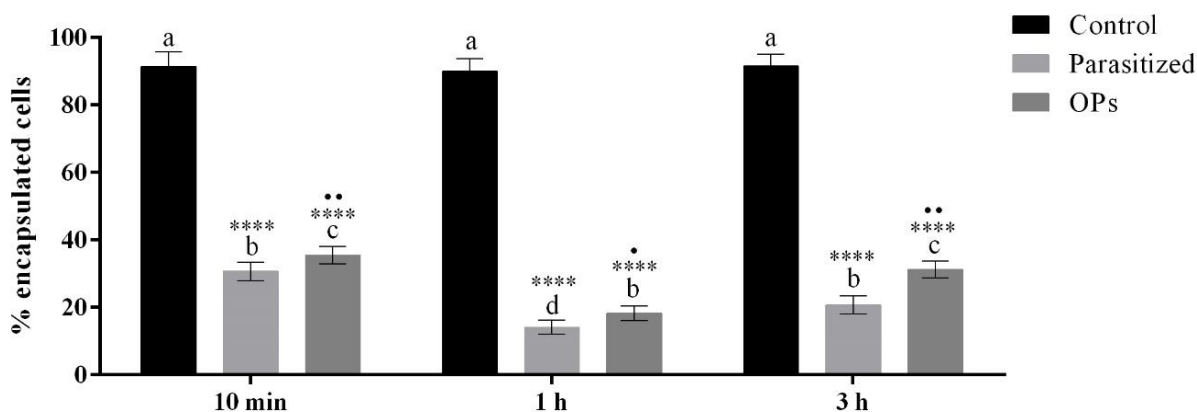


**Figure 8.** Percentage of encapsulation of chromatographic spheres extracted after 6 h from larvae injected with 1 × PBS (control), after parasitization or OP treatment at 10 min, 1 h or 3 h before injection of spheres. Data are presented as mean ± SD ( $n = 3$ ). Statistical analysis was performed with one-way ANOVA and Bonferroni (for control vs. treatment and parasitized vs. OPs analysis) and Tukey post-hoc test (for all sample analysis). Different letters indicate significant differences among all treatments ( $p$  value < 0.0001), asterisks indicate significant differences between control and treated samples at the same experimental time ( $p$  value < 0.0001), dots indicate significant differences between parasitized and OP treatment at the same experimental time (••  $p$  value < 0.01, •  $p$  value < 0.05).



#### 4. Discussion

Endoparasitoid insects have developed, during evolution, mechanisms capable to alter the physiology and biochemistry of the host, and they are able to create an environment suitable for the development of their progeny [4,27,39,52]. Such alterations imply the manipulation of the host's immune system. The suppression of the immune reaction in hosts parasitized by endophagous hymenopterans is a very complex syndrome, characterized by several molecular mechanisms integrating each other [39,43,53]. The maternal factors, introduced into the host during the oviposition, are the main protagonists of the physiological alterations observed in the parasitized hosts [54,55]. These factors include venom proteins, symbiotic Polydnavirus (PDV), virus-like particles (VLP) and ovarian proteins (OPs) [4,15,16,49,52,56,57]. Among these, the PDVs have received a great interest over the years as an important source of useful genes [19]. PDVs are associated exclusively with endoparasitoid wasps of lepidopteran larvae [43,58]. PDVs replicate only in the cells of the wasp ovarian calyces and are released in the lumen of the oviduct [28,29]. Once introduced into the host, PDVs infect tissues and actively express their genes [59]. The products of these genes induce a wide range of alterations to the neuroendocrine and immune system [27]. Many genes of viral origin have been isolated and characterized [4,24,26,38,44,45,60–65], but their expression requires several hours to be able to perform the immunosuppressive effect. Because the insect's immune system is already functioning within minutes of recognizing the parasitoid, the parasitoid needs to alter its defense mechanisms in a short time [66]. Therefore, other maternal factors, such as OPs [28,49,67] and venom [15,56,68–71], or the proteins that cover and protect the parasitoid egg [72–75] must necessarily set to mediate immune-suppression in the early stages of parasitization. Luckhart and Webb [76] demonstrated the immunosuppressive intervention of OPs after 30 min from parasitization in *Campoletis sonorensis*. As already showed by Ferrarese et al. [39], there is a reduction of the haemocyte titer in the haemolymph following parasitization, probably due also to the action of the venom and/or OPs that induce, after few hours, a high cellular mortality. The molecular mechanisms that induce such alterations have not been clarified yet.

In this study we focused on the role of OPs in the host-parasitoid system *Heliothis virescens-Toxoneuron nigriceps*. OPs seem to interfere with the cell-mediated immune system in the minutes following parasitization, before *T. nigriceps* BracoVirus (*TnBV*) infects host tissues and expresses its genes. The OPs induce a series of alterations affecting the haemocytes and carrying the cell to death.

In haemocytes treated with OPs many alterations are recorded, including mitochondrial alterations accompanied by ATP depletion, loss of transmembrane potential and the consequent increase in reactive oxygen species (ROS) in the cytoplasm. Mitochondria, therefore, can be a very important target in the attempt to alter cellular function. A similar picture has been described as one of the different manifestations of cell death [77]. Furthermore, several studies suggest that the alteration of the actin cytoskeleton is strongly linked to the increase in intracellular ROS levels and apoptosis [78,79]. ROS are physiologically present in cells at low concentrations and increase considerably in the case of severe mitochondrial damage [80,81]. In our system, haemocytes treated with OPs show that oxidative stress often occurs with cytoskeletal damage to actin filaments; these changes may explain the high levels of haemocyte mortality. The vacuolization observed in the haemocytes already after 30 min from exposure to OPs, confirms the observations reported by Ferrarese et al. [39] on haemocytes extracted from parasitized larvae. These high levels of oxidizing agents, together with a change in pH, probably linked to the increase of ROS, can negatively affect survival and cellular functionality [82,83]. All the observed alterations induce a loss of functionality in the haemocytes. In fact, by injecting OPs and chromatographic spheres into the larval haemocoel, a loss of encapsulation capacity by the haemocytes was observed. We observed a strong reduction of encapsulation both in parasitized larvae and when treated with OPs, as already reported for the endoparasitoid *Macrocentrus cingulum* in which OP treatment inhibited the encapsulation in a

dose-dependent manner [84]. A *T. nigriceps* OP stronger effect was recorded at 1 h. This allowed the hypothesis in that the inhibition of haemocyte's encapsulation capacity is caused not only by OPs but also by venom and *TnBV*. Indeed, a previous study [15], among *T. nigriceps* venom proteins, identified the Calreticulin protein, whose role in inhibition of encapsulation has been reported in several parasitoids [85–88]. On the contrary in *M. cingulum* the mix of venom and OPs did not have a different effect compared to OPs alone, suggesting that, in this case, there are no synergic effect of venom and OPs in suppressing the encapsulation by *Ostrinia furnacalis* haemocytes [84]. Moreover, we observed a higher percentage of unencapsulated beads in larvae parasitized 3 h before injection of beads compared to larvae treated with OPs. This could be due to the expression of *TnBV* genes that act on the host immune system [24,26].

The present work confirms the hypothesis that OPs have short-term immunosuppressive activity also in the host-parasitoid system *H. virescens*-*T. nigriceps*, as reported in other host-parasitoid system, such as *Chilo suppressalis*-*Cotesia chilonis* [89]. To guarantee the success of parasitization a synergic action of all parasitic factors is required. Several *TnBV* genes have been reported to be responsible for morphological alterations and apoptosis in haemocytes, but their expression occurs at least after 3–4 h [24,26]. The fibrous layer on the *T. nigriceps* egg surface [47] venom proteins [15] and OPs ensure an escape from host cellular immune responses immediately after oviposition.

Knowledge of the sequence of biologically active proteins will probably allow us to understand the mechanisms by which they act.

## 5. Conclusions

Little information on the role of Ovarian Proteins (OPs) is available in the literature. Most of the studies concerning host-parasitoid systems, and in particular the parasitic factors, focus on Polydnavirus (PDV), if they are present, and venom. With this study we provide valuable information on possible functions of these secretions on host haemocytes, in the host-parasitoid system *Heliothis virescens*-*Toxoneuron nigriceps*. Experiments performed on haemocytes treated with OPs showed many alterations, including the increase of reactive oxygen species (ROS) in the cytoplasm and actin cytoskeleton disruption. These changes provoke both reduction in haemocyte functionality, losing encapsulation capacity, and increasing cellular death. Our study shows that OPs have a significant action, especially regarding the functional alteration of haemocytes, the cells of the host immune response. Overall OPs, together with other maternal factors (venom and PDV) actively contribute to suppress the host immune response, supporting the development of the parasitoid larva and the success of the parasitism.

This study underlines the importance of OPs and suggests further in-depth analysis to characterize the entire protein profile of this mixture of parasitic origin, and also specific analysis to identify the active proteins responsible for the described effects.

**Supplementary Materials:** The following are available online at <https://www.mdpi.com/2075-4450/12/1/33/s1>, Protocol S1: Extraction and purification of *Toxoneuron nigriceps* Ovarian Proteins (OPs), Table S1: Data obtained counting haemocytes incubated with 1×PBS solution (control), haemocytes extracted from larvae 24 h after parasitization and OPs derived from 1 or 2 equivalent females, Table S2: Data obtained from the counts of healthy cells or treated with OPs at different times (30 min, 1 h and 2 h) showing vacuolization, Table S3: Data obtained from counting healthy cell or treated with OPs at different times (30 min, 1 h and 2 h) showing ROS positive cells, Table S4: Data obtained from haemocytes stained with phalloidin showing cytoskeletal damage, after OPs treatment at different exposure times (30 min, 1 h and 2 h), Table S5: Data obtained from haemocytes after injection of chromatographic spheres and after OPs treatment at different exposure times (30 min, 1 h and 2 h) or parasitization, Figure S1: Chromatographic spheres extracted from 5 larvae for each time (10 min (a), 3 h (b) and 6 h (c) after OP injection, Figure S2: Healthy haemocytes or treated with OPs for 2 h and stained with DAPI and H<sub>2</sub>DCFDA.

**Author Contributions:** Conceptualization, P.F. (Patrizia Falabella); methodology, R.S., A.G., C.S.; data curation, P.F. (Paolo Fanti), P.V., R.S.; writing—original draft preparation, P.F. (Patrizia Falabella); writing—review and editing, R.S., C.S., A.G., P.F. (Paolo Fanti), A.M., A.F., P.V., S.B.V., P.F. (Patrizia Falabella); supervision, P.F. (Patrizia Falabella). All authors have read and agreed to the published version of the manuscript.

**Funding:** This research was funded by University of Basilicata.

**Data Availability Statement:** Data is contained within this article and the supplementary material.

**Conflicts of Interest:** The authors declare no conflict of interest.

## References

1. Quicke, D.L.J. *Parasitic Wasps*; Chapman & Hall: London, UK, 1997.
2. Heraty, J. Parasitoid Biodiversity and Insect Pest Management. In *Insect Biodiversity: Science and Society*, 2nd ed.; Footitt, R.G., Adler, P.H., Eds.; John Wiley & Sons: Hoboken, NJ, USA, 2017; pp. 603–625.
3. Godfray, H.C.J. Parasitoids. In *Encyclopedia of Biodiversity*, 2nd ed.; Levin, S.A., Ed.; Elsevier: Amsterdam, The Netherlands, 2007; pp. 1–13.
4. Pennacchio, F.; Strand, M.R. Evolution of developmental strategies in parasitic Hymenoptera. *Annu. Rev. Entomol.* **2006**, *51*, 233–258. [[CrossRef](#)] [[PubMed](#)]
5. Schmidt, O.; Theopold, U.; Strand, M.R. Innate immunity and evasion by insect parasitoids. *BioEssays* **2001**, *23*, 344–351. [[CrossRef](#)] [[PubMed](#)]
6. Bangham, J.; Jiggins, F.; Lemaitre, B. Insect immunity: The post-genomic era. *Immunity* **2006**, *25*, 1–5. [[CrossRef](#)] [[PubMed](#)]
7. Sheehan, G.; Garvey, A.; Croke, M.; Kavanagh, K. Innate humoral immune defences in mammals and insects: The same, with differences? *Virulence* **2018**, *9*, 1625–1639. [[CrossRef](#)]
8. Brivio, M.F.; Mastore, M. When Appearance Misleads: The Role of the Entomopathogen Surface in the Relationship with Its Host. *Insects* **2020**, *11*, 387. [[CrossRef](#)]
9. Welchman, D.P.; Aksoy, S.; Jiggins, F.; Lemaitre, B. Insect immunity: From pattern recognition to symbiont-mediated host defense. *Cell Host Microbe* **2009**, *6*, 107–114. [[CrossRef](#)] [[PubMed](#)]
10. Wang, X.; Zhang, Y.; Zhang, R.; Zhang, J. The diversity of pattern recognition receptors (PRRs) involved with insect defense against pathogens. *Curr. Opin. Insect Sci.* **2019**, *33*, 105–110. [[CrossRef](#)] [[PubMed](#)]
11. Sheehan, G.; Farrell, G.; Kavanagh, K. Immune priming: The secret weapon of the insect world. *Virulence* **2020**, *11*, 238–246. [[CrossRef](#)]
12. Nakhleh, J.; Moussawi, L.E.; Osta, M.A. Chapter Three—The Melanization Response in Insect Immunity. *Adv. Insect Physiol.* **2017**, *52*, 83–109.
13. Asgari, S. Venoms from Endoparasitoids. In *Parasitoid Viruses*; Beckage, N.E., Drezen, J.M., Eds.; Academic Press: Cambridge, MA, USA, 2012; pp. 217–231.
14. Strand, M.R. Teratocytes and their functions in parasitoids. *Curr. Opin. Insect Sci.* **2014**, *6*, 68–73. [[CrossRef](#)]
15. Laurino, S.; Grossi, G.; Pucci, P.; Flagiello, A.; Bufo, S.A.; Bianco, G.; Salvia, R.; Vinson, S.B.; Vogel, H.; Falabella, P. Identification of major *Toxoneuron nigriceps* venom proteins using an integrated transcriptomic/proteomic approach. *Insect Biochem. Mol. Biol.* **2016**, *76*, 49–61. [[CrossRef](#)] [[PubMed](#)]
16. Leobold, M.; Bézier, A.; Pichon, A.; Herniou, E.A.; Volkoff, A.N.; Drezen, J.M. The domestication of a large DNA virus by the wasp *Venturia canescens* involves targeted genome reduction through pseudogenization. *Genome Biol. Evol.* **2018**, *10*, 1745–1764. [[CrossRef](#)] [[PubMed](#)]
17. Salvia, R.; Grimaldi, A.; Girardello, R.; Scieuzo, C.; Scala, A.; Bufo, S.A.; Vogel, H.; Falabella, P. *Aphidius ervi* Teratocytes Release Enolase and Fatty Acid Binding Protein Through Exosomal Vesicles. *Front. Physiol.* **2019**, *10*, 715. [[CrossRef](#)]
18. Fath-Goodin, A.; Webb, B.A. Polydnviruses: General Features. In *Encyclopedia of Virology*, 3rd ed.; Mahy, B.W.J., Van Regenmortel, M.H.V., Eds.; Academic Press: Cambridge, MA, USA, 2008; pp. 256–261.
19. Strand, M.R.; Burke, G.R. Polydnviruses: From discovery to current insights. *Virology* **2015**, *479–480*, 393–402. [[CrossRef](#)] [[PubMed](#)]
20. Volkoff, A.N.; Hugué, E. Polydnviruses (Polydnviridae, Bracovirus, and Ichnovirus). In *Reference Module in Life Sciences*; Elsevier: Amsterdam, The Netherlands, 2020.
21. Lovallo, N.C.; McPherson, B.A.; Cox-Foster, D.L. Effects of the polydnvirus of *Cotesia congregata* on the immune system and development of non-habitual hosts of the parasitoid. *J. Insect Physiol.* **2002**, *48*, 517–526. [[CrossRef](#)]
22. Yin, L.; Zhang, C.; Qin, J.; Wang, C. Polydnvirus of *Campoplex chloridae*: Characterization and temporal effect on host *Helicoverpa armigera* cellular immune response. *Arch. Insect Biochem. Physiol.* **2003**, *52*, 104–113. [[CrossRef](#)] [[PubMed](#)]
23. Barat-Houari, M.; Hilliou, F.; Jousset, F.X.; Sofer, L.; Deleury, E.; Rocher, J.; Ravallec, M.; Galibert, L.; Delobel, P.; Feyereisen, R.; et al. Gene expression profiling of *Spodoptera frugiperda* hemocytes and fat body using cDNA microarray reveals polydnvirus-associated variations in lepidopteran host genes transcript levels. *BMC Genom.* **2006**, *7*, 160. [[CrossRef](#)]

24. Falabella, P.; Varricchio, P.; Provost, B.; Espagne, E.; Ferrarese, R.; Grimaldi, A.; de Eguileor, M.; Fimiani, G.; Ursini, M.V.; Malva, C.; et al. Characterization of the IkappaB-like gene family in polydnviruses associated with wasps belonging to different Braconid subfamilies. *J. Gen. Virol.* **2007**, *88*, 92–104. [[CrossRef](#)]
25. Gueguen, G.; Kalamarz, M.E.; Ramroop, J.; Uribe, J.; Govind, S. Polydnviral Ankyrin Proteins Aid Parasitic Wasp Survival by Coordinate and Selective Inhibition of Hematopoietic and Immune NF-kappa B Signaling in Insect Hosts. *PLoS Pathog.* **2013**, *9*, e1003580. [[CrossRef](#)]
26. Salvia, R.; Grossi, G.; Amoresano, A.; Scieuzo, C.; Nardiello, M.; Giangrande, C.; Laurenzana, I.; Ruggieri, V.; Bufo, S.A.; Vinson, S.B.; et al. The multifunctional polydnvirus TnBVANK1 protein: Impact on host apoptotic pathway. *Sci. Rep.* **2017**, *7*, 11775. [[CrossRef](#)]
27. Ye, X.Q.; Shi, M.; Huang, J.H.; Chen, X.X. Parasitoid polydnviruses and immune interaction with secondary hosts. *Dev. Comp. Immunol.* **2018**, *83*, 124–129. [[CrossRef](#)] [[PubMed](#)]
28. Tanaka, K.; Matsumoto, H.; Hayakawa, Y. Analysis in the course of polydnvirus replication in ovarian calyx cells of the parasitoid wasp, *Cotesia kariyai* (Hymenoptera: Braconidae). *Appl. Entomol. Zool.* **2002**, *37*, 323–328. [[CrossRef](#)]
29. Park, B.; Yonggyun, K. Polydnvirus replication at ovarian calyx in *Cotesia plutellae* and endocrine impact. *Korean J. Appl. Entomol.* **2010**, *43*, 225–231.
30. Lewis, W.J.; Vinson, S.B. Egg and larval development of *Cardiochiles nigriceps*. *Ann. Entomol. Soc. Am.* **1968**, *61*, 561–565. [[CrossRef](#)]
31. Pennacchio, F.; Vinson, S.B.; Tremblay, E. Growth and development of *Cardiochiles nigriceps* Viereck (Hymenoptera, Braconidae) larvae and their synchronization with some changes of the hemolymph composition of their host, *Heliothis virescens* (F.) (Lepidoptera, Noctuidae). *Arch. Insect Biochem. Physiol.* **1993**, *24*, 65–77. [[CrossRef](#)]
32. Pennacchio, F.; Vinson, S.B.; Tremblay, E.; Tanaka, T. Biochemical and developmental alterations of *Heliothis virescens* (F.) (Lepidoptera, Noctuidae) larvae induced by the endophagous parasitoid *Cardiochiles nigriceps* (Hymenoptera, Braconidae). *Arch. Insect Biochem. Physiol.* **1994**, *26*, 211–233. [[CrossRef](#)]
33. Pennacchio, F.; Sordetti, R.; Falabella, P.; Vinson, S.B. Biochemical and ultrastructural alterations in prothoracic glands of *Heliothis virescens* (F.) (Lepidoptera: Noctuidae) last instar larvae parasitized by *Cardiochiles nigriceps* Viereck (Hymenoptera: Braconidae). *Insect Biochem. Molec. Biol.* **1997**, *27*, 439–450. [[CrossRef](#)]
34. Pennacchio, F.; Falabella, P.; Sordetti, R.; Varricchio, P.; Malva, C.; Vinson, S.B. Prothoracic gland inactivation in *Heliothis virescens* (F.) (Lepidoptera: Noctuidae) larvae parasitized by *Cardiochiles nigriceps* Viereck (Hymenoptera: Braconidae). *J. Insect Physiol.* **1998**, *44*, 845–857. [[CrossRef](#)]
35. Tanaka, T.; Vinson, S.B. Depression of prothoracic gland activity of *Heliothis virescens* by venom and calix fluid from the parasitoid, *Cardiochiles nigriceps*. *J. Insect Physiol.* **1991**, *37*, 139–144. [[CrossRef](#)]
36. Pennacchio, F.; Vinson, S.B.; Tremblay, E.; Ostuni, A. Alteration of ecdysone metabolism in *Heliothis virescens* (F.) (Lepidoptera: Noctuidae) larvae induced by *Cardiochiles nigriceps* Viereck (Hymenoptera: Braconidae) teratocytes. *Insect Biochem. Mol. Biol.* **1994**, *24*, 383–394. [[CrossRef](#)]
37. Falabella, P.; Caccialupi, P.; Varricchio, P.; Malva, C.; Pennacchio, F. Protein Tyrosine Phosphatases of *Toxoneuron nigriceps* bracovirus as potential disrupters of host prothoracic glands. *Arch. Insect Biochem. Physiol.* **2006**, *61*, 157–169. [[CrossRef](#)] [[PubMed](#)]
38. Salvia, R.; Nardiello, M.; Scieuzo, C.; Scala, A.; Bufo, S.A.; Rao, A.; Vogel, H.; Falabella, P. Novel Factors of Viral Origin Inhibit TOR Pathway Gene Expression. *Front Physiol.* **2018**, *9*, 1678. [[CrossRef](#)]
39. Ferrarese, R.; Brivio, M.; Congiu, T.; Falabella, P.; Grimaldi, A.; Mastore, M.; Perletti, G.; Pennacchio, F.; Sciacca, L.; Tettamanti, G.; et al. Early suppression of immune response in *Heliothis virescens* larvae by the endophagous parasitoid *Toxoneuron nigriceps*. *Invert. Surv. J.* **2005**, *2*, 60–68.
40. Pennacchio, F.; Vinson, S.B.; Tremblay, E. Morphology and ultrastructure of the serosal cells (teratocytes) in *Cardiochiles nigriceps* Viereck (Hymenoptera: Braconidae) embryos. *Int. J. Insect Morphol. Embryol.* **1994**, *23*, 93–104. [[CrossRef](#)]
41. Pennacchio, F.; Vinson, S.B.; Tremblay, E. Host regulation effects of *Heliothis virescens* (F.) larvae induced by teratocytes of *Cardiochiles nigriceps* Viereck (Lepidoptera, Noctuidae—Hymenoptera, Braconidae). *Arch. Insect Biochem. Physiol.* **1992**, *19*, 177–192. [[CrossRef](#)]
42. Pennacchio, F.; Vinson, S.B.; Malva, C. Regulation of host endocrine system by the endophagous braconid *Cardiochiles nigriceps* and its polydnvirus. In *Endocrine Interactions of Insect Parasites and Pathogens*; Edwards, J.P., Weaver, R.J., Eds.; BIOS Scientific Publishers: Oxford, UK, 2001; pp. 123–132.
43. Grimaldi, A.; Caccia, S.; Congiu, T.; Ferrarese, R.; Tettamanti, G.; Rivas-Pena, M.; Perletti, G.; Valvassori, R.; Giordana, B.; Falabella, P.; et al. Structure and function of the extraembryonic membrane persisting around the larvae of the parasitoid *Toxoneuron nigriceps*. *J. Insect Physiol.* **2006**, *52*, 870–880. [[CrossRef](#)] [[PubMed](#)]
44. Falabella, P. The mechanism utilized by *Toxoneuron nigriceps* in inhibiting the host immune system. *Invert. Surviv. J.* **2018**, *15*, 240–255.
45. Varricchio, P.; Falabella, P.; Sordetti, R.; Graziani, F.; Malva, C.; Pennacchio, F. *Cardiochiles nigriceps* polydnvirus: Molecular characterization and gene expression in parasitized *Heliothis virescens* larvae. *Insect Biochem. Mol. Biol.* **1999**, *29*, 1087–1096. [[CrossRef](#)]
46. Lapointe, R.; Wilson, R.; Vilaplana, L.; O'reilly, D.R.; Falabella, P.; Douris, V.; Bernier-Cardou, M.; Pennacchio, F.; Iatrou, K.; Malva, C.; et al. Expression of a *Toxoneuron nigriceps* polydnvirus-encoded protein causes apoptosis-like programmed cell death in lepidopteran insect cells. *J. Gen. Virol.* **2005**, *86*, 963–971. [[CrossRef](#)]

47. Davies, D.H.; Vinson, S.B. Passive evasion by eggs of braconid parasitoid *Cardiochiles nigriceps* of encapsulation in vitro by hemocytes of host *Heliothis virescens*. Possible role for fibrous layer in immunity. *J. Insect Physiol.* **1986**, *32*, 1003–1010. [[CrossRef](#)]
48. Hu, J.; Zhu, X.X.; Fu, W.J. Passive evasion of encapsulation in *Macrocentrus cingulum* Brischke (Hymenoptera: Braconidae), a polyembryonic parasitoid of *Ostrinia furnacalis* Guenee (Lepidoptera: Pyralidae). *J. Insect Physiol.* **2003**, *49*, 367–375. [[CrossRef](#)]
49. Teng, Z.; Wu, H.; Ye, X.; Xiong, S.; Xu, G.; Wang, F.; Fang, Q.; Ye, G. An Ovarian Protein Involved in Passive Avoidance of an Endoparasitoid to Evade Its Host Immune Response. *J. Proteome Res.* **2019**, *18*, 2695–2705. [[CrossRef](#)] [[PubMed](#)]
50. Vinson, S.B.; Guillot, F.S.; Hays, D.B. Rearing of *Cardiochiles nigriceps* in the laboratory, with *Heliothis virescens* as hosts. *Ann. Entomol. Soc. Am.* **1973**, *66*, 1170–1172. [[CrossRef](#)]
51. Vanderzant, E.S.; Richardson, C.D.; Fort, S.W., Jr. Rearing of the bollworm on artificial diet. *J. Econ. Entomol.* **1962**, *55*, 140. [[CrossRef](#)]
52. Beckage, N.E.; Gelman, D.B. Wasp parasitoid disruption of host development: Implication for new biologically based strategies for insect control. *Annu. Rev. Entomol.* **2004**, *49*, 299–330. [[CrossRef](#)] [[PubMed](#)]
53. Schmidt, O. Insect Immune Recognition and Suppression. In *Insect Immunology*; Beckage, N.E., Ed.; Academic Press: Cambridge, MA, USA, 2008; pp. 271–294.
54. Mrinalini; Werren, J.H. Parasitoid Wasps and Their Venoms. In *Evolution of Venomous Animals and Their Toxins*; Gopalakrishnakone, P., Malhotra, A., Eds.; Toxinology; Springer: Berlin/Heidelberg, Germany, 2015; pp. 1–26.
55. Moreau, S.J.; Asgari, S. Venom Proteins from Parasitoid Wasps and Their Biological Functions. *Toxins* **2015**, *7*, 2385–2412. [[CrossRef](#)] [[PubMed](#)]
56. Teng, Z.W.; Xiong, S.J.; Xu, G.; Gan, S.Y.; Chen, X.; Stanley, D.; Yan, Z.C.; Ye, G.Y.; Fang, Q. Protein Discovery: Combined Transcriptomic and Proteomic Analyses of Venom from the Endoparasitoid *Cotesia chilonis* (Hymenoptera: Braconidae). *Toxins* **2017**, *9*, 135. [[CrossRef](#)]
57. Volkoff, A.N.; Cusson, M. The Unconventional Viruses of Ichneumonid Parasitoid Wasps. *Viruses* **2020**, *12*, 1170. [[CrossRef](#)]
58. Strand, M.R. Chapter 12—Polydnvirus Gene Products that Interact with the Host Immune System. In *Parasitoid Viruses*; Beckage, N.E., Drezen, J.M., Eds.; Academic Press: Cambridge, MA, USA, 2012; pp. 149–161.
59. Bitra, K.; Zhang, S.; Strand, M.R. Transcriptomic profiling of *Microplitis demolitor* bracovirus reveals host, tissue and stage-specific patterns of activity. *J. Gen. Virol.* **2011**, *92*, 2060–2071. [[CrossRef](#)]
60. Johner, A.; Lanzrein, B. Characterization of two genes of the polydnvirus of *Chelonus inanitus* and their stage-specific expression in the host *Spodoptera littoralis*. *J. Gen. Virol.* **2002**, *83*, 1075–1085. [[CrossRef](#)]
61. Falabella, P.; Varricchio, P.; Gigliotti, S.; Tranfaglia, A.; Pennacchio, F.; Malva, C. *Toxoneuron nigriceps* polydnvirus encodes a putative aspartyl protease highly expressed in parasitised host larvae. *Insect Mol. Biol.* **2003**, *12*, 9–17. [[CrossRef](#)] [[PubMed](#)]
62. Provost, B.; Varricchio, P.; Arana, E.; Espagne, E.; Falabella, P.; Huguet, E.; La Scaleia, R.; Cattolico, L.; Poirié, M.; Malva, C.; et al. Bracovirus contain a large multigene family coding for a protein tyrosine phosphatase. *J. Virol.* **2004**, *78*, 13090–13103. [[CrossRef](#)] [[PubMed](#)]
63. Dupas, S.; Wanjiru Gitau, C.; Branca, A.; Le Rü, B.P.; Silvain, J.F. Evolution of a Polydnvirus Gene in Relation to Parasitoid–Host Species Immune Resistance. *J. Hered.* **2008**, *99*, 491–499. [[CrossRef](#)] [[PubMed](#)]
64. Desjardins, C.A.; Gundersen-Rindal, D.E.; Hostetler, J.B.; Tallon, L.J.; Fadrosch, D.W.; Fuester, R.W.; Pedroni, M.J.; Haas, B.J.; Schatz, M.C.; Jones, K.M.; et al. Comparative genomics of mutualistic viruses of *Glyptapanteles* parasitic wasps. *Genome Biol.* **2008**, *9*, R183. [[CrossRef](#)]
65. Legeai, F.; Santos, B.; Robin, S.; Bretaudeau, A.; Dikow, R.; Lemaitre, C.; Jouan, V.; Ravallec, M.; Drezen, J.M.; Tagu, D.; et al. Conserved and specific genomic features of endogenous polydnviruses revealed by whole genome sequencing of two ichneumonid wasps. *bioRxiv* **2019**, in press. [[CrossRef](#)]
66. Carton, Y.; Poirié, M.; Nappi, A. Insect immune resistance to parasitoids. *Insect Science* **2008**, *15*, 67–87. [[CrossRef](#)]
67. Webb, B.A.; Luckhart, S. Evidence for an early immunosuppressive role for related *Campoletis sonorensis* venom and ovarian proteins in *Heliothis virescens*. *Arch. Insect Biochem. Physiol.* **1994**, *26*, 147–163. [[CrossRef](#)]
68. Vincent, B.; Kaeslin, M.; Roth, T.; Heller, M.; Poulain, J.; Cousserans, F.; Schaller, J.; Poirié, M.; Lanzrein, B.; Drezen, J.; et al. The venom composition of the parasitic wasp *Chelonus inanitus* resolved by combined expressed sequence tags analysis and proteomic approach. *BMC Genom.* **2010**, *11*, 693. [[CrossRef](#)]
69. Goecks, J.; Mortimer, N.T.; Mobley, J.A.; Bowersock, G.J.; Taylor, J.; Schlenke, T.A. Integrative approach reveals composition of endoparasitoid wasp venoms. *PLoS ONE* **2013**, *8*, e64125. [[CrossRef](#)]
70. Yan, Z.C.; Fang, Q.; Wang, L.; Liu, J.; Zhu, Y.; Wang, F.; Li, F.; Werren, J.H.; Ye, G. Insights into the venom composition and evolution of an endoparasitoid wasp by combining proteomic and transcriptomic analyses. *Sci. Rep.* **2016**, *6*, 19604. [[CrossRef](#)]
71. Yang, L.; Lin, Z.; Fang, Q.; Wang, J.; Yan, Z.; Zou, Z.; Song, Q.; Ye, G. Identification and characterization of serine protease inhibitors in a parasitic wasp, *Pteromalus puparum*. *Sci. Rep.* **2017**, *7*, 15755. [[CrossRef](#)] [[PubMed](#)]
72. Asgari, S.; Schmidt, O. Passive protection of eggs from parasitoid, *Cotesia rubecula*, in the host *Pieris rapae*. *J. Insect Physiol.* **1994**, *40*, 789–795. [[CrossRef](#)]
73. Beckage, N.E. Parasitoids and polydnviruses. *Bioscience* **1998**, *48*, 305–311. [[CrossRef](#)]
74. Han, L.B.; Yin, L.H.; Huang, L.Q.; Wang, C.Z. Differential immunosuppression by *Campoletis chloridae* eggs and ichnovirus in larvae of *Helicoverpa armigera* and *Spodoptera exigua*. *J. Invertebr. Pathol.* **2015**, *130*, 88–96. [[CrossRef](#)]

75. Yin, C.; Li, M.; Hu, J.; Lang, K.; Chen, Q.; Liu, J.; Guo, D.; He, K.; Dong, Y.; Luo, J.; et al. The genomic features of parasitism, Polyembryony and immune evasion in the endoparasitic wasp *Macrocentrus cingulum*. *BMC Genom.* **2018**, *19*, 420. [[CrossRef](#)] [[PubMed](#)]
76. Luckhart, S.; Webb, B.A. Interaction of a wasp ovarian protein and polydnavirus in host immune suppression. *Dev. Comp. Immunol.* **1996**, *20*, 1–21. [[CrossRef](#)]
77. Bras, M.; Queenan, B.; Susin, S.A. Programmed Cell Death via Mitochondria: Different Modes of Dying. *Biochemistry* **2005**, *70*, 231–239. [[CrossRef](#)]
78. Gourlay, C.W.; Ayscough, K.R. A Role for Actin in Aging and Apoptosis. *Biochem. Soc. Trans.* **2005**, *33*, 1260–1264. [[CrossRef](#)]
79. Redza-Dutordoir, M.; Averill-Bates, D.A. Activation of apoptosis signalling pathways by reactive oxygen species. *Biochim. Biophys. Acta.* **2016**, *1863*, 2977–2992. [[CrossRef](#)]
80. Li, T.S.; Marbán, E. Physiological levels of reactive oxygen species are required to maintain genomic stability in stem cells. *Stem Cells* **2010**, *28*, 1178–1185. [[CrossRef](#)]
81. Chen, Y.; Zhou, Z.; Min, W. Mitochondria, Oxidative Stress and Innate Immunity. *Front. Physiol.* **2018**, *9*, 1487. [[CrossRef](#)] [[PubMed](#)]
82. Stefani, M.; Dobson, C.M. Protein aggregation and aggregate toxicity: New insights into protein folding, misfolding diseases and biological evolution. *J. Mol. Med.* **2003**, *81*, 678–699. [[CrossRef](#)] [[PubMed](#)]
83. Milkovic, L.; Cipak, G.A.; Cindric, M.; Mouthuy, P.A.; Zarkovic, N. Short Overview of ROS as Cell Function Regulators and Their Implications in Therapy Concepts. *Cells* **2019**, *8*, 793. [[CrossRef](#)] [[PubMed](#)]
84. Li, Y.; Lu, J.F.; Feng, C.J.; Ke, X.; Fu, W.J. Role of venom and ovarian proteins in immune suppression of *Ostrinia furnacalis* (Lepidoptera: Pyralidae) larvae parasitized by *Macrocentrus cingulum* (Hymenoptera: Braconidae), a polyembryonic parasitoid. *Insect Sci.* **2007**, *14*, 93–100. [[CrossRef](#)]
85. Choi, J.Y.; Whitten, M.M.; Cho, M.Y.; Lee, K.Y.; Kim, M.S.; Ratcliffe, N.A.; Lee, B.L. Calreticulin enriched as an early-stage encapsulation protein in wax moth *Galleria mellonella* larvae. *Dev. Comp. Immunol.* **2002**, *26*, 335–343. [[CrossRef](#)]
86. Asgari, S.; Schmidt, O. Is cell surface calreticulin involved in phagocytosis by insect hemocytes? *J. Insect. Physiol.* **2003**, *49*, 545–550. [[CrossRef](#)]
87. Zhu, J.Y.; Fang, Q.; Wang, L.; Hu, C.; Ye, G.Y. Proteomic analysis of the venom from the endoparasitoid wasp *Pteromalus puparum* (Hymenoptera: Pteromalidae). *Arch. Insect Biochem. Physiol.* **2010**, *75*, 28–44. [[CrossRef](#)]
88. Wang, L.; Fang, Q.; Qian, C.; Wang, F.; Yu, X.Q.; Ye, G. Inhibition of host cell encapsulation through inhibiting immune gene expression by the parasitic wasp venom calreticulin. *Insect Biochem. Mol. Biol.* **2013**, *43*, 936–946. [[CrossRef](#)]
89. Teng, Z.W.; Xu, G.; Gan, S.Y.; Chen, X.; Fang, Q.; Ye, G.Y. Effects of the endoparasitoid *Cotesia chilonis* (Hymenoptera: Braconidae) parasitism, venom, and calyx fluid on cellular and humoral immunity of its host *Chilo suppressalis* (Lepidoptera: Crambidae) larvae. *J. Insect Physiol.* **2016**, *85*, 46–56. [[CrossRef](#)]

# We are IntechOpen, the world's leading publisher of Open Access books Built by scientists, for scientists

4,800

Open access books available

122,000

International authors and editors

135M

Downloads

Our authors are among the

154

Countries delivered to

TOP 1%

most cited scientists

12.2%

Contributors from top 500 universities



WEB OF SCIENCE™

Selection of our books indexed in the Book Citation Index  
in Web of Science™ Core Collection (BKCI)

Interested in publishing with us?  
Contact [book.department@intechopen.com](mailto:book.department@intechopen.com)

Numbers displayed above are based on latest data collected.  
For more information visit [www.intechopen.com](http://www.intechopen.com)



# Inhibition of Bacterial Biofilm Formation

*Angela Di Somma, Antonio Moretta, Carolina Canè,  
Arianna Cirillo and Angela Duilio*

## Abstract

Biofilm is a complex matrix consisting of extracellular polysaccharides, DNA, and proteins that protect bacteria from a variety of physical, chemical, and biological stresses allowing them to survive in hostile environments. Biofilm formation requires three different stages: cell attachment to a solid substrate, adhesion, and growth. The inhibition of one of these steps by small molecules, such as antimicrobial peptides, or their action on specific targets will leave pathogens armless against classical antibiotics. Any drug impairing crucial processes for bacterial life will inevitably lead to the development of drug-resistant strains, whereas the inhibition of biofilm formation might prevent the onset of bacterial resistance. In this section, we will focus on proteins involved in biofilm formation as useful targets for the development of new drugs that can effectively and specifically impair biofilm formation with slight effects on cell survival, thus avoiding the generation of drug-resistant strains.

**Keywords:** bacterial biofilms, biofilm inhibition, antimicrobial peptides, protein target, mechanism of action

## 1. Introduction

Microorganisms have the extraordinary ability to live in almost all environments and to protect themselves from external agents through sophisticated survival mechanisms. Bacteria can be found in planktonic form or in specific conditions, as sessile aggregates on both biotic and abiotic surfaces originating complex structures known as biofilm.

Biofilms are an ensemble of microbial cells irreversibly associated with a surface and enclosed in an essentially self-produced matrix. The biofilm matrix consists of polysaccharides, proteins, and DNA and constitutes a stubborn source that protects bacteria from a variety of physical, chemical, and biological stresses. One of its characteristics is the capability to impair antimicrobial molecules to spread through the polymer matrix or the ability of the matrix material to inactivate antibacterial molecules. Today, the increase and spread of antibiotic resistance among microorganisms (bacteria, fungi, viruses, and parasites) represent one of the greatest emergencies for human health worldwide [1]. Based on these characteristics, biofilm plays crucial roles in humans and nonhuman infections and represents the most important adaptive mechanism closely related to pathogenicity.



An antibiofilm agent must display several specific characteristics to target the biofilm lifestyle. First, due to the temporal biofilm heterogeneity, it must show a rapid killing ability to face a changing entity and to target cells before their entry into the biofilm community; it must be able to act in different environmental niches and to target different growth rate cells. The cells located in the periphery of biofilm are directly in contact with nutrients and oxygen, while those placed deepest in the biofilm layers may undergo lack of nutrients, anoxia, and acidic conditions. In this way, a metabolic and spatial heterogeneity is generated including both rapidly and slowly growing cells. In particular, due to environmental conditions, inside the biofilm, it is possible to find the so-called persister, dormant, quiescent cells characterized by a low rate of cell division that are believed to play an essential role in the biofilm resistance to antibiotics [2]. Other important characteristics for a good antimicrobial candidate are the ability to interfere with the production of the extracellular matrix and the possibility to penetrate the biofilm architecture. This matrix consists for 90% of EPS, whose principal components are proteins, polysaccharides, lipids, and extracellular DNA, and it is involved into the biofilm architecture maintenance. An antibiofilm agent should also be able to interfere with bacterial cell communication machinery.

This chapter aims to investigate and clarify in detail the inhibition of biofilm formation by different approaches.

Other additional aspects to consider the identification of potential antimicrobial agents are the ability to recruit immune cells and/or modulate the host immune response and the synergy with other conventional and unconventional antimicrobial compounds [3, 4].

Biofilms are very dynamic and spatially heterogeneous structures originating gradients of oxygen, nutrients, and pH, and their formation occurs through three phases: adhesion, maturation, and dispersal phase as described earlier.

## **2. Small molecules capable to inhibit biofilm formation**

The inhibition or prevention of biofilm formation has been a subject of study for a long time. The first important action against biofilm formation is to prevent bacterial adhesion to surfaces and host tissues to reduce infection [5]. Preventing bacterial adhesion is an attractive target [6] for hampering bacterial infection, and several different strategies have been proposed including hindering cellular receptors from recognizing adhesion surfaces or inhibiting the process of bacterial adhesion. Blocking the primary colonizers can prevent initial biofilm colonization and the subsequent infection produced by planktonic cells released from the biofilm itself.

The adhesion process consists of various distinct steps. In the first step, bacterial cell establishes reversible adhesion interactions on host surfaces [7], while in the second step, a stronger type of adhesion is carried out, which involves specific molecules that bind in a complementary manner [5]. In particular, in Gram-negative bacteria, adhesion is mediated by special proteins known as adhesins associated with cell surface structures such as fimbriae or pili [8, 9]. Initial adhesion is then followed by a complex colonization process that offers a number of advantages to bacteria, including increased protection against dislocation by hydrokinetic forces from fluid surfaces or better access to nutrients released by the host cells [10]. Finally, in these favorable conditions, the development of the elaborate biofilm structures can take place.

For a long time, the first strategies used to inhibit the adhesion process were focused on the use of adhesin analogues that bind to the receptor and competitively

block bacterial adhesion [5]. However, this strategy resulted unpractical because adhesin proteins are not readily available, and they become toxic at the relatively high concentrations that had to be used. An attempt to overcome this problem consisted in the design and use of synthetic peptides mimicking the sequence of cell surface adhesins. For example, the small peptide p1025 inhibits *Streptococcus mutans* binding to dental surfaces [11]. Analogously, a fragment of the fimbrillin adhesin was found to inhibit the adhesion of *Porphyromonas gingivalis* to hydroxyapatite [12]. However, this approach showed several drawbacks as different adhesins usually mediate the adhesion process and the expression of carbohydrates or cell surface ligands may vary depending on environmental conditions, originating a large number of variables and making this approach more difficult and not very applicable.

A novel and interesting approach to inhibit bacterial adhesion consists in the use of cell coatings with antimicrobial peptides that alter the chemical properties of the surface [13, 14], thus interfering with bacterial adhesion and preventing surface binding. Although “passive,” this method is rather attractive and may serve as a novel approach to address the biofilm problem on artificial medical devices. However, limited successes have been achieved so far due to attachment variability among different bacterial strains. Recently, many active polymeric coatings were designed to bind the surface and release a variety of antimicrobial molecules such as antibiotics, bacteriocins, and metal ions [15–18]. A significant reduction in biofilm formation of *Staphylococcus epidermidis* on hydrogel-coated and serum/hydrogel-coated silicone catheters was observed following the release of bacteriophage factors from the polymer with and without supplemental divalent cations [19]. Similarly, treatment of piperacillin-tazobactam coated tympanostomy tubes reduces biofilm infection of ciprofloxacin-resistant *Pseudomonas aeruginosa* (CRPA) [20]. The negative aspect of this approach might be the continuous release of high concentration of antimicrobials in a short time by the active polymer often higher than the MIC values without a specific target. However, target release polymer can be foreseen as the new era of biofilm treatments in industrial food safety and packaging [21].

Recently, great attention was paid to a different approach addressed to killing planktonic cells for prevention and treatment of biofilms. The new catheter lock solution C/MB/P (citrate, methylene blue, and parabens) was able to act against planktonic and sessile bacteria within a biofilm preventing bacterial colonization of hemodialysis catheters [22]. Killing planktonic cells might represent a good approach, but this strategy cannot be carried out on long term because any drug targeting crucial processes for bacterial life will unavoidably lead to the development of resistant strains.

An effective and positive control of biofilm formation might be obtained by interfering with specific cellular process crucial for biofilm formation. Biofilm formation is often associated with the phenomenon of quorum sensing (QS), in which bacterial cells communicate with each other by small diffusible signal molecules [23]. Moreover, bacterial gene expression has to be synchronized to form biofilms, and to achieve this goal, the quorum-sensing (QS) mechanism is used by bacteria, producing and responding to a several intra and intercellular signals called autoinducers [24]. At low-cell densities, the autoinducer is present in the extracellular media in a small amount that is too dilute to be detected. When the cell density increases, the autoinducer concentration reaches a threshold, and the autoinducer-receptor complex (the regulatory protein) acts to induce or repress the expression of target genes. The QS controls some physiological processes such as secretion of virulence factors, biofilm formation, and antibiotic resistance in several bacterial species [25, 26]. Investigation and elucidation of

the molecular mechanisms underlying the QS effects on biofilms including the production of virulence factors may help to control bacterial infection. More than 70 species of Gram-negative bacteria communicate and control their population density and mobility via N-acyl homoserine lactones (AHLs) mediated QS and represented one of the primary scaffolds studied for the design of potential biofilm inhibitors [27]. N-butanoylhomoserine lactone 1 (C4-AHL, for the rhl system) and 3-oxo-C12-AHL 5 (for the las system) are among the most important AHLs involved in QS (REF Small molecule control of bacterial biofilms). In *P. aeruginosa*, one of the most important bacteria involved in human infections, different antibiofilm molecules focused on AHL analogues were designed to develop new strategies to impair biofilm formation. The Blackwell et al. identified, designed, and synthesized several different AHLs capable to significantly reduce biofilm formation and virulence factor production in *P. aeruginosa* [28, 29].

A different approach consisted in the use of the synthetic halogenated furanone produced by secondary metabolism of the Australian macroalga *Delisea pulchra*, which is able to penetrate the biofilm matrix and to alter its architecture in flow chambers [30, 31]. Furthermore, T315, an integrin-linked kinase inhibitor previously identified as a potential therapeutic agent against chronic lymphocytic leukemia [32], was shown to selectively inhibit biofilm formation in both *Salmonella typhi* and *Salmonella Typhimurium* at early stages of biofilm development without affecting bacterial viability. T315 was also demonstrated to reduce biofilm formation in *Acinetobacter baumannii* but had no effect on *P. aeruginosa* suggesting a bacterial specificity [33].

### 3. Biofilm inhibition by antimicrobial peptides

Antimicrobial peptides (AMPs) are small molecules (10–100 amino acids) widespread in nature that play an essential role in the innate immunity. Recently, much attention has been paid to AMPs as they exert a broad spectrum of action, exploiting different activities as antibacterial, antifungal, antiparasites, anticancer, and antibiofilm factors [34]. This paragraph will focus on the ability of some antimicrobial peptides to inhibit biofilm formation.

The use of antimicrobial peptides to impair biofilm formation is attracting great interest, and many peptides have already been tested on different bacterial biofilms. In particular, the molecular mechanism of biofilm inhibition by AMPs is very much under investigation. The AMPs tested on biofilms so far derive from different natural sources, such as humans, mammals, bacteria, plants, and amphibians, but many synthetic peptides have also been studied. For example, it was demonstrated that the human cathelicidin LL-37 and indolicidin peptides could prevent biofilm formation of *P. aeruginosa* by downregulating the transcription of Las and Rhl, two quorum-sensing systems [35]. Moreover, AMPs could inhibit biofilm formation by increasing twitching motility in *P. aeruginosa* through the stimulation of the expression of genes needed for type IV pili biosynthesis and function. Type IV pili has the main function to increase bacteria movement on surfaces, which could facilitate cell removal [35]. The synthetic antimicrobial peptide meta-phenylene ethynylene (mPE), based on magainin, was active against biofilms of *Streptococcus mutans*, both as an intracellular antibiotic by binding to DNA and as a membrane-active molecule inhibiting lipopolysaccharides (LPSs), similar to magainin action [36].

In addition, the LL-37 peptide can also inhibit initial biofilm attachment. In *Pseudomonas aeruginosa*, this peptide downregulates the expression of genes associated with the assembly of flagella involved in the process of initial adherence [37]. Antiadhesion could be one of the major AMPs antibiofilm properties leading

to their potential use as an effective pretreatment strategy. For example, the nisin peptide, which interferes with cell wall synthesis and is capable to form membrane pores, delays biofilm formation, but it does not inhibit the *Staphylococcus aureus* growth when it is immobilized in multiwalled carbon nanotubes [38].

AMPs can also cause biofilm matrix disruption. The human liver-derived hepcidin 20 peptide can reduce the mass of extracellular matrix and can alter the *S. epidermidis* biofilm architecture by targeting polysaccharide intercellular adhesin (PIA). Being endowed with nucleosidase activity, the fish-derived piscidin-3 peptide can degrade *P. aeruginosa* extracellular DNA by coordinating with  $\text{Cu}^{2+}$  through its N-terminus [39, 40].

Although several antimicrobial peptides have nowadays been studied for the inhibition of biofilm formation, a further aspect needs to be considered. Several biofilms have developed defense mechanisms to protect themselves from antimicrobial agents. The interaction with EPS is thought to be the principal reason of biofilm resistance to AMPs even if the exact mechanism is not well understood. Gram-negative bacteria, such as *P. aeruginosa*, can secrete alginate, an anionic extracellular polysaccharide consisting of uronic acid D-mannuronate and C-5 epimer-L-guluronate. Alginate can interact with cationic AMPs and protect *P. aeruginosa* biofilm from the effect of the antimicrobial peptides [41]. Moreover, the peptide sensing system known as aps, first recognized in *S. epidermidis*, can protect Gram-positive bacteria from AMP action. This system upregulates the D-alanylation of teichoic acid and increases the expression of putative AMP efflux pumps. It was demonstrated that *Enterococcus faecalis* D-alanine deficient mutant is more resistant to AMPs than the wild type even if they produce less biofilm [42].

#### 4. Biofilm inhibition by protein targets

Planktonic bacteria can adhere to different cells or tissues starting biofilm formation via production of a multitude of proteins, which act at different stages of biofilm formation. Some proteins contribute to biofilm accumulation, while others are involved into the mediation of primary attachment to surfaces [43, 44]. For this reason, the formation and the development of bacterial biofilm can be associated with the production of specific proteins, which play essential roles in the bacterial biofilm formation and development. Strategies leading to the identification of these proteins are fundamental as they could represent interesting targets to inhibit biofilm formation, allowing the development of new antibiofilm agents and procedures [45]. In this paragraph, we will focus on some target proteins involved in the production of biofilms in different bacteria: the N-acetylneuraminase lyase (NanA) in *Escherichia coli*, the bifunctional enzyme N-acetyl-D-glucosamine-1-phosphate acetyltransferase (GlmU) in *Mycobacterium smegmatis*, and the surface protein G (SasG) in *S. aureus*.

The NanA protein of *E. coli* is an enzyme able to recognize the sialic acid, a molecule essential to a number of critical biological processes, such as cell recognition, adhesion, and immune system evasion. NanA catalyzes the transformation of sialic acid into pyruvate and N-acetyl-D-mannosamine [46, 47], favoring cell-cell adhesion. Therefore, NanA plays a fundamental role in the adhesion development of host cells a process of great importance in the formation of biofilm. This enzyme is then considered an important target for developing molecules able to reduce biofilm accumulation. Recently, a relationship between methylation stress in *E. coli* and the reduction of bacterial adhesion properties thus decreasing its ability to form biofilm was reported. This phenomenon was associated with a drastic reduction in the expression levels of the NanA protein, suggesting a possible role of NanA in

biofilm formation and bacteria host interactions. Using a null NanA mutant and DANA, a substrate analog acting as competitive inhibitor, it was demonstrated that the downregulation of NanA or inhibition of its enzymatic activity affects biofilm formation and adhesion properties of *E. coli* [48, 49].

Another important protein target is GlmU, a bifunctional enzyme with acetyltransferase activity involved in the biosynthesis of Uridine diphosphate N-acetylglucosamine (UDP-GlcNAc), a key precursor of  $\beta$ -1,6-N-acetyl-D-glucosamine polysaccharide adhesin required for biofilm formation [50, 51]. GlmU is a possible factor involved in biofilm production in *M. smegmatis*, a nonpathogenic bacterium homologous to the pathogenic *M. tuberculosis*. The response of *M. smegmatis* to alkylating stress is different from *E. coli*, resulting in an increase in biofilm formation possibly due to a very strong defense mechanism. In this contest, GlmU has an important role in the process of biofilm production in *M. smegmatis*, being its expression highly upregulated when the bacterium needs to activate defense mechanisms [52]. Experiments with both conditional deletion and overexpressing glmU mutants demonstrated that the downregulation of GlmU decreased *M. smegmatis* capabilities to produce biofilm, whereas the overexpression of enzyme increased biofilm formation. These results were supported by inhibition of GlmU acetyltransferase activity with two different inhibitors, suggesting the involvement of this enzyme in the *M. smegmatis* defense mechanisms. Focusing on the inhibition of GlmU might then be an efficient method to disable the bacterium defense mechanism.

*S. aureus* is a common pathogen responsible for nosocomial and community infections being able to colonize the squamous epithelium of the anterior nares. One of the adhesins likely to be responsible for this ability is the *S. aureus* surface protein G (SasG), which promotes cellular aggregation leading to biofilm formation [53, 54]. SasG comprises an N-terminal A domain and repeated B domains with only the B domain required for the accumulation of biofilm. Expression of SasG does not increase the adherence of bacteria, and it is not involved in primary attachment but plays a role in the accumulation phase of biofilm formation [55]. For different aspects and playing different roles, NanA, GlmU, and SasG may all represent interesting targets to address the inhibition of biofilm production.

## 5. Conclusions

Currently, biofilm infections constitute a serious medical problem, and their treatment is far from being satisfactory. Biofilm formation inhibitors have several potential therapeutic applications as coatings in medical devices or in the prophylaxis of implanted surgery. In this respect, the identification of new strategies to counteract biofilm formation is a broad subject of study. The antibiofilm activity of many molecules such as proteins, peptides, and small organic molecules is currently under investigation. Each of these molecules is endowed with specific characteristics and can exert its ability to inhibit bacterial biofilm formation with different mechanisms. Antibiofilm agents are able to act both at the initial stages of biofilm formation, such as bacterial adhesion to the host surface, and on preformed biofilm, leading to the disruption of the EPS architecture. Many small organic molecules are able to interfere with the bacterial QS system, but their lack of activity in *in vivo* models and the high toxicity make these molecules of limited use in clinical applications.

As antimicrobial peptides show a broad spectrum of action, exploiting different activities including antibiofilm capabilities, these molecules might be considered as new promising factors to impair biofilm formation that exploit different mechanisms to hamper biofilms at different stages.

The administration of a single antibiotic is often not enough to eradicate bacterial invasions, and a high concentration of the antibiotic can be extremely toxic. A possible solution might be the coadministration of antibiotics with antibiofilm peptides that allow the use of low antibiotic concentrations. This strategy can be tuned to affect biofilms without killing bacteria, thus avoiding the emergence of drug-resistant populations through synergy with existing antibiotics.

## Acknowledgements

This work was supported in part by MIUR grants ARS01\_00597 Project “NAOCON” and PRIN 2017 “Identification and characterization of novel anti-tumoral/antimicrobial insect-derived peptides: a multidisciplinary, integrated approach from *in silico* to *in vivo*.”

## Conflict of Interest

The authors declare no conflict of interest.

## Author details

Angela Di Somma<sup>1\*</sup>, Antonio Moretta<sup>2</sup>, Carolina Canè<sup>3</sup>, Arianna Cirillo<sup>3</sup> and Angela Duilio<sup>1</sup>

1 Department of Chemical Sciences, Federico II University, Naples, Italy

2 Department of Science, University of Basilicata, Potenza, Italy

3 CEINGE Biotecnologie Avanzate, Naples, Italy

\*Address all correspondence to: [angela.disomma@unina.it](mailto:angela.disomma@unina.it)

## IntechOpen

© 2019 The Author(s). Licensee IntechOpen. This chapter is distributed under the terms of the Creative Commons Attribution License (<http://creativecommons.org/licenses/by/3.0>), which permits unrestricted use, distribution, and reproduction in any medium, provided the original work is properly cited. 

## References

- [1] Cepas V, López Y, Munoz E, Rolo D, Ardanuy C, Martí S, et al. Relationship between biofilm formation and antimicrobial resistance in gram-negative bacteria. *Microbial Drug Resistance*. 2019;**25**(1):72-79
- [2] Lebeaux D, Ghigo JM, Beloin C. Biofilm-related infections: Bridging the gap between clinical management and fundamental aspects of recalcitrance toward antibiotics. *Microbiology and Molecular Biology Reviews*. 2014;**78**(3):510-543
- [3] Anderson JM, Patel JD. Biomaterial-dependent characteristics of the foreign body response and *S. epidermidis* biofilm interactions. In: *Biomaterials Associated Infection*. New York, NY: Springer; 2013. pp. 119-149
- [4] Beloin C, Renard S, Ghigo JM, Lebeaux D. Novel approaches to combat bacterial biofilms. *Current Opinion in Pharmacology*. 2014;**18**:61-68
- [5] Ofek I, Hasty DL, Sharon N. Anti-adhesion therapy of bacterial diseases: Prospects and problems. *FEMS Immunology and Medical Microbiology*. 2003;**38**(3):181-191
- [6] Bavington C, Page C. Stopping bacterial adhesion: A novel approach to treating infections. *Respiration*. 2005;**72**(4):335-344
- [7] Hasty DL, Ofek I, Courtney HS, Doyle RJ. Multiple adhesins of streptococci. *Infection and Immunity*. 1992;**60**(6):2147
- [8] Krogfelt KA. Bacterial adhesion: Genetics, biogenesis, and role in pathogenesis of fimbrial adhesins of *Escherichia coli*. *Reviews of Infectious Diseases*. 1991;**13**(4):721-735
- [9] Kline KA, Fälker S, Dahlberg S, Normark S, Henriques-Normark B. Bacterial adhesins in host-microbe interactions. *Cell Host & Microbe*. 2009;**5**(6):580-592
- [10] Zafriri D, Oron Y, Eisenstein BI, Ofek I. Growth advantage and enhanced toxicity of *Escherichia coli* adherent to tissue culture cells due to restricted diffusion of products secreted by the cells. *The Journal of Clinical Investigation*. 1987;**79**(4):1210-1216
- [11] Kelly CG, Younson JS, Hikmat BY, Todryk SM, Czisch M, Haris PI, et al. A synthetic peptide adhesion epitope as a novel antimicrobial agent. *Nature Biotechnology*. 1999;**17**(1):42
- [12] Lee JY, Sojar HT, Bedi GS, Genco RJ. Synthetic peptides analogous to the fimbriin sequence inhibit adherence of *Porphyromonas gingivalis*. *Infection and Immunity*. 1992;**60**(4):1662-1670
- [13] Hetrick EM, Schoenfisch MH. Reducing implant-related infections: Active release strategies. *Chemical Society Reviews*. 2006;**35**(9):780-789
- [14] Tamilvanan S, Venkateshan N, Ludwig A. The potential of lipid- and polymer-based drug delivery carriers for eradicating biofilm consortia on device-related nosocomial infections. *Journal of Controlled Release*. 2008;**128**(1):2-22
- [15] La AS, Ercolini D, Marinello F, Mauriello G. Characterization of bacteriocin-coated antimicrobial polyethylene films by atomic force microscopy. *Journal of Food Science*. 2008;**73**(4):T48-T54
- [16] Ruggeri V, Francolini I, Donelli G, Piozzi A. Synthesis, characterization, and *in vitro* activity of antibiotic releasing polyurethanes to prevent bacterial resistance. *Journal of biomedical materials research part a: An official journal of the Society for Biomaterials, the Japanese Society for*

- Biomaterials, and the Australian Society for Biomaterials and the Korean society for Biomaterials. 2007;**81**(2):287-298
- [17] Xu Q, Czernuszka JT. Controlled release of amoxicillin from hydroxyapatite-coated poly (lactic-co-glycolic acid) microspheres. *Journal of Controlled Release*. 2008;**127**(2):146-153
- [18] Taylor EN, Webster TJ. The use of superparamagnetic nanoparticles for prosthetic biofilm prevention. *International Journal of Nanomedicine*. 2009;**4**:145
- [19] Curtin JJ, Donlan RM. Using bacteriophages to reduce formation of catheter-associated biofilms by *Staphylococcus epidermidis*. *Antimicrobial Agents and Chemotherapy*. 2006;**50**(4):1268-1275
- [20] Jang CH, Park H, Cho YB, Choi CH, Park IY. The use of piperacillin-tazobactam coated tympanostomy tubes against ciprofloxacin-resistant *Pseudomonas* biofilm formation: An *in vitro* study. *International Journal of Pediatric Otorhinolaryngology*. 2009;**73**(2):295-299
- [21] Balasubramanian A, Rosenberg LE, Yam KIT, Chikindas ML. Antimicrobial packaging: Potential vs. reality—A review. *The Journal of Applied Packaging Research*. 2009;**3**(4):193-221
- [22] Steczko J, Ash SR, Nivens DE, Brewer L, Winger RK. Microbial inactivation properties of a new antimicrobial/antithrombotic catheter lock solution (citrate/methylene blue/ parabens). *Nephrology, Dialysis, Transplantation*. 2009;**24**(6):1937-1945
- [23] Li YH, Tian X. Quorum sensing and bacterial social interactions in biofilms. *Sensors*. 2012;**12**(3):2519-2538
- [24] Camilli A, Bassler BL. Bacterial small-molecule signaling pathways. *Science*. 2006;**311**(5764):1113-1116
- [25] Miller MB, Bassler BL. Quorum sensing in bacteria. *Annual Review of Microbiology*. 2001;**55**(1):165-199
- [26] Irie Y, Parsek MR. Quorum sensing and microbial biofilms. In: *Bacterial Biofilms*. Berlin, Heidelberg: Springer; 2008. pp. 67-84
- [27] Worthington RJ, Richards JJ, Melander C. Small molecule control of bacterial biofilms. *Organic & Biomolecular Chemistry*. 2012;**10**(37):7457-7474
- [28] Geske GD, Wezeman RJ, Siegel AP, Blackwell HE. Small molecule inhibitors of bacterial quorum sensing and biofilm formation. *Journal of the American Chemical Society*. 2005;**127**(37):12762-12763
- [29] Geske GD, O'Neill JC, Miller DM, Wezeman RJ, Mattmann ME, Lin Q, et al. Comparative analyses of N-acylated homoserine lactones reveal unique structural features that dictate their ability to activate or inhibit quorum sensing. *Chembiochem*. 2008;**9**(3):389-400
- [30] Hentzer M, Riedel K, Rasmussen TB, Heydorn A, Andersen JB, Parsek MR, et al. Inhibition of quorum sensing in *Pseudomonas aeruginosa* biofilm bacteria by a halogenated furanone compound. *Microbiology*. 2002;**148**(1):87-102
- [31] Roy R, Tiwari M, Donelli G, Tiwari V. Strategies for combating bacterial biofilms: A focus on anti-biofilm agents and their mechanisms of action. *Virulence*. 2018;**9**(1):522-554
- [32] Lee SL, Hsu EC, Chou CC, Chuang HC, Bai LY, Kulp SK, et al. Identification and characterization of a novel integrin-linked kinase inhibitor. *Journal of Medicinal Chemistry*. 2011;**54**(18):6364-6374
- [33] Moshiri J, Kaur D, Hambira CM, Sandala JL, Koopman JA, Fuchs JR,



- et al. Identification of a small molecule anti-biofilm agent against *Salmonella enterica*. *Frontiers in Microbiology*. 2018;**9**:2804
- [34] Malik E, Dennison S, Harris F, Phoenix D. pH dependent antimicrobial peptides and proteins, their mechanisms of action and potential as therapeutic agents. *Pharmaceuticals*. 2016;**9**(4):67
- [35] Overhage J, Campisano A, Bains M, Torfs EC, Rehm BH, Hancock RE. Human host defense peptide LL-37 prevents bacterial biofilm formation. *Infection and Immunity*. 2008;**76**(9):4176-4182
- [36] Beckloff N, Laube D, Castro T, Furgang D, Park S, Perlin D, et al. Activity of an antimicrobial peptide mimetic against planktonic and biofilm cultures of oral pathogens. *Antimicrobial Agents and Chemotherapy*. 2007;**51**(11):4125-4132
- [37] Dean SN, Bishop BM, Van Hoek ML. Susceptibility of *Pseudomonas aeruginosa* biofilm to alpha-helical peptides: D-enantiomer of LL-37. *Frontiers in Microbiology*. 2011;**2**:128
- [38] Qi X, Poernomo G, Wang K, Chen Y, Chan-Park MB, Xu R, et al. Covalent immobilization of nisin on multi-walled carbon nanotubes: Superior antimicrobial and anti-biofilm properties. *Nanoscale*. 2011;**3**(4):1874-1880
- [39] Brancatisano FL, Maisetta G, Di Luca M, Esin S, Bottai D, Bizzarri R, et al. Inhibitory effect of the human liver-derived antimicrobial peptide hepcidin 20 on biofilms of polysaccharide intercellular adhesin (PIA)-positive and PIA-negative strains of *Staphylococcus epidermidis*. *Biofouling*. 2014;**30**(4):435-446
- [40] Libardo MDJ, Bahar AA, Ma B, Fu R, McCormick LE, Zhao J, et al. Nuclease activity gives an edge to host-defense peptide piscidin 3 over piscidin 1, rendering it more effective against persisters and biofilms. *The FEBS Journal*. 2017;**284**(21):3662-3683
- [41] Chan C, Burrows LL, Deber CM. Helix induction in antimicrobial peptides by alginate in biofilms. *Journal of Biological Chemistry*. 2004;**279**(37):38749-38754
- [42] Fabretti F, Theilacker C, Baldassarri L, Kaczynski Z, Kropec A, Holst O, et al. Alanine esters of enterococcal lipoteichoic acid play a role in biofilm formation and resistance to antimicrobial peptides. *Infection and Immunity*. 2006;**74**(7):4164-4171
- [43] Pizarro-Cerdá J, Cossart P. Bacterial adhesion and entry into host cells. *Cell*. 2006;**124**(4):715-727
- [44] Speziale P, Pietrocola G, Foster TJ, Geoghegan JA. Protein-based biofilm matrices in staphylococci. *Frontiers in Cellular and Infection Microbiology*. 2014;**4**:171
- [45] Sintim HO, Smith JA, Wang J, Nakayama S, Yan L. Paradigm shift in discovering next-generation anti-infective agents: Targeting quorum sensing, c-di-GMP signaling and biofilm formation in bacteria with small molecules. *Future Medicinal Chemistry*. 2010;**2**(6):1005-1035
- [46] Daniels AD, Campeotto I, van der Kamp MW, Bolt AH, Trinh CH, Phillips SE, et al. Reaction mechanism of N-acetylneuraminic acid lyase revealed by a combination of crystallography, QM/MM simulation, and mutagenesis. *ACS Chemical Biology*. 2014;**9**(4):1025-1032
- [47] Uchida Y, Tsukada Y, Sugimori T. Purification and properties of N-acetylneuraminidase from *Escherichia coli*. *The Journal of Biochemistry*. 1984;**96**(2):507-522

[48] Di Pasquale P, Caterino M, Di Somma A, Squillace M, Rossi E, Landini P, et al. Exposure of *E. coli* to DNA-methylating agents impairs biofilm formation and invasion of eukaryotic cells via down regulation of the N-acetylneuraminase lyase NanA. *Frontiers in Microbiology*. 2016;**7**:147

[49] Volkert MR, Landini P. Transcriptional responses to DNA damage. *Current Opinion in Microbiology*. 2001;**4**(2):178-185

[50] Burton E, Gawande PV, Yakandawala N, LoVetri K, Zhanel GG, Romeo T, et al. Antibiofilm activity of GlmU enzyme inhibitors against catheter-associated uropathogens. *Antimicrobial Agents and Chemotherapy*. 2006;**50**(5):1835-1840

[51] Itoh Y, Wang X, Hinnebusch BJ, Preston JF, Romeo T. Depolymerization of  $\beta$ -1, 6-N-acetyl-d-glucosamine disrupts the integrity of diverse bacterial biofilms. *Journal of Bacteriology*. 2005;**187**(1):382-387

[52] Di Somma A, Caterino M, Soni V, Agarwal M, di Pasquale P, Zanetti S, et al. The bifunctional protein GlmU is a key factor in biofilm formation induced by alkylating stress in *Mycobacterium smegmatis*. *Research in Microbiology*. 2019;**170**:171-181

[53] Corrigan RM, Rigby D, Handley P, Foster TJ. The role of *Staphylococcus aureus* surface protein SasG in adherence and biofilm formation. *Microbiology*. 2007;**153**(8):2435-2446

[54] Roche FM, Meehan M, Foster TJ. The *Staphylococcus aureus* surface protein SasG and its homologues promote bacterial adherence to human desquamated nasal epithelial cells. *Microbiology*. 2003;**149**(10):2759-2767

[55] Geoghegan JA, Corrigan RM, Gruszka DT, Speziale P, O'Gara JP,

Potts JR, et al. Role of surface protein SasG in biofilm formation by *Staphylococcus aureus*. *Journal of Bacteriology*. 2010;**192**(21):5663-5673